Comparative Pharmacokinetics

Comparative Pharmacokinetics: Principles, Techniques, and Applications, Second Edition. Jim E. Riviere.
 ISBN: 978-0-813-82993-7

Comparative Pharmacokinetics

Principles, Techniques, and Applications

Second Edition

Jim E. Riviere

WILEY-BLACKWELL

A John Wiley & Sons, Inc., Publication

Blackwell Publishing was acquired by John Wiley & Sons in February 2007. Blackwell's publishing program has been merged with Wiley's global Scientific, Technical and Medical business to form Wiley-Blackwell.

Registered office: John Wiley & Sons, Ltd, The Atrium, Southern Gate, Chichester, West Sussex, PO19 8SQ, UK

Editorial offices: 2121 State Avenue, Ames, Iowa 50014-8300, USA
The Atrium, Southern Gate, Chichester, West Sussex, PO19 8SQ, UK
9600 Garsington Road, Oxford, OX4 2DQ, UK

For details of our global editorial offices, for customer services and for information about how to apply for permission to reuse the copyright material in this book please see our website at www.wiley.com/wiley-blackwell.

Library of Congress Cataloging-in-Publication Data

Riviere, Jim E. (Jim Edmond), author.
Comparative pharmacokinetics / Jim E. Riviere, North Carolina State University, Raleigh, North Carolina. – 2nd Edition.
p. ; cm.
Includes bibliographical references and index.
ISBN 978-0-8138-2993-7 (pbk. : alk. paper)
1. Pharmacokinetics. 2. Veterinary pharmacology. I. Title.
[DNLM: 1. Pharmacokinetics. QV 38]
RM301.5.R58 2011
636.089′578–dc22

2010047729

A catalogue record for this book is available from the British Library.

Set in 10/12pt Times by Toppan Best-set Premedia Limited

1 2011

Contents

Coauthors

The numbers in parentheses indicate chapters coauthored with Dr. Jim E. Riviere.

Ronald Baynes (7)
Center for Chemical Toxicology Research and Pharmacokinetics
Department of Population Health and Pathobiology
College of Veterinary Medicine
North Carolina State University
Raleigh, NC, USA
Ronald_Baynes@ncsu.edu

James Brooks (Illustrator)
Center for Chemical Toxicology Research and Pharmacokinetics
Department of Population Health and Pathobiology
College of Veterinary Medicine
North Carolina State University
Raleigh, NC, USA
Jim_Brooks@ncsu.edu

Jennifer Buur (5)
College of Veterinary Medicine
Western University of Health Sciences
Pomona, CA, USA
jbuur@westernu.edu

Jason Chittenden (14 and 16)
Center for Chemical Toxicology Research and Pharmacokinetics
College of Veterinary Medicine
North Carolina State University
Raleigh, NC, USA

Pharsight, Inc.
Cary, NC, USA
Jason.Chittenden@certara.com

Jennifer Davis (17)
Department of Clinical Sciences
College of Veterinary Medicine
North Carolina State University
Raleigh, NC, USA
Jennifer_Davis@ncsu.edu

Teresa Leavens (11)
Center for Chemical Toxicology Research and Pharmacokinetics
Department of Population Health and Pathobiology
College of Veterinary Medicine
North Carolina State University
Raleigh, NC, USA
Teresa_Leavens@ncsu.edu

Sharon Mason (19)
Department of Biological Sciences
Campbell University
Buies Creek, NC, USA
MasonS@Campbell.edu

Marilyn Martinez (15)
Center for Veterinary Medicine
US Food and Drug Administration
Rockville, MD, USA
Marilyn.Martinez@fda.hhs.gov

Jim E. Riviere
Center for Chemical Toxicology Research and Pharmacokinetics
Department of Population Health and Pathobiology
College of Veterinary Medicine
North Carolina State University
Raleigh, NC, USA
Jim_Riviere@ncsu.edu

Pierre-Louis Toutain (13)
UMR181 Physiopathologie et Toxicologie Expérimentales INRA
Ecole Nationale Vétérinaire de Toulouse-23
Chemin des Capelles–31076
Toulouse, France
pl.toutain@envt.fr

Xin-Rui Xia (3)
Center for Chemical Toxicology Research and Pharmacokinetics
Department of Population Health and Pathobiology
College of Veterinary Medicine
North Carolina State University
Raleigh, NC, USA
Summer_Xia@ncsu.edu

Preface

The second edition of *Comparative Pharmacokinetics* follows the first edition's goals of providing the conceptual basis of pharmacokinetics as a tool for quantifying biological processes encountered in comparative medicine.

The organization of this book remains the same whereby the basic principles of physiology are introduced for systems involved in the absorption, distribution, metabolism, and elimination (ADME) of chemicals and drugs in the body. This is followed by chapters developing the primary approaches used in pharmacokinetic modeling today, namely compartmental, noncompartmental, population, and physiological approaches. Chapters on nonlinear processes, dosage regimen construction, and statistical aspects of data analysis are presented, followed by overviews of pharmacokinetic–pharmacodynamic (PK-PD) modeling and specific applications on bioequivalence, disease effects, interspecies extrapolations, and drug residues in food-producing animals.

As in the first edition, this author has authored or coauthored all chapters for consistency. New additions to this text include extensive revisions of the Distribution chapter coauthored by Jennifer Buur, the Hepatic Biotransformation chapter by Ronald Baynes, and the Physiological Models chapter by Teresa Leavens. Chapters on Study Design and Population Modeling by Jason Chittenden, Dosage Adjustment in Disease by Jennifer Davis, and Tissue Residues by Sharon Mason have been expanded and revised. Pierre-Louis Toutain comprehensively rewrote the PK-PD chapter as PK-PD modeling has become widespread in comparative medicine. A new chapter on Quantitative Structure–Permeability Relationships coauthored with Xin-Rui Xia has been added to illustrate how molecular properties of chemicals and drugs are correlated to membrane transport, the basis of most pharmacokinetic processes. Also, this chapter introduces basic statistical concepts of regression analysis and study validation that are expounded upon later in the book. Finally, the Bioequivalence chapter by Marilyn Martinez of the U.S. Food and Drug Administration offers a complete regulatory perspective on determining product bioequivalence. This chapter demonstrates many of the pharmacokinetic principles introduced in the earlier chapters and adds in the requirements for statistical rigor needed for a regulatory approval. All the remaining chapters have been revised and updated. In addition, cross-referencing topics across all chapters has been expanded to help the reader to make important conceptual linkages between theory and applications.

This comparative and veterinary pharmacokinetics textbook serves as an introduction to this discipline from the perspectives of physiology and medicine. The wide availability

of economic but powerful computers with comprehensive software packages can make pharmacokinetic analysis seem automatic. A primary goal of this book is to ensure that studies are properly designed before being conducted, that the proper models are used for the end points in mind, and that resulting pharmacokinetic parameters are interpreted correctly.

Jim E. Riviere

1 Introduction

Pharmacokinetics is best defined as the use of mathematical models to quantitate the time course of drug absorption and disposition in man and animals. With the tremendous advances in medicine and analytical chemistry, coupled with the almost universal availability of computers, what was once an arcane science has now entered the mainstream of most fields of human and veterinary medicine. This discipline has allowed dosages of drugs to be tailored to individuals or groups to optimize therapeutic effectiveness, minimize toxicity, and avoid violative tissue residues in the case of food-producing animals.

What differentiates this discipline from other fields of pharmacology and medicine is its focus on quantitating biological phenomena using various mathematical models and restricting its purview to the movement of drugs and chemicals into, through, and out of the body. The subsequent effects of these drugs on biological processes fall in the realm of pharmacodynamics (PD), which is beyond the scope of the present pharmacokinetic text but is extensively reviewed in Chapter 13 when linkage to pharmacokinetic models is developed. There are numerous applications of pharmacokinetics in clinical practice, some of them unknown to the practitioner as actually being pharmacokinetic modeling exercises since the terminology has become embedded into the lexicon of general medicine.

Since the publication of the first comparative pharmacokinetics text by Desmond Baggot in 1977, there has been explosive growth in all aspects of this discipline. This growth has continued after the publication of the first edition of the present text in 1999 and the release in 2004 of the pivotal UK "PK and PK-PD in Veterinary Medicine" workshop (Lees, 2004). The continued integration of pharmacokinetic concepts into global veterinary drug regulations further fuels this growth, a development that can be appreciated by reading Chapter 15 on regulatory aspects of drug product bioequivalence.

The primary pharmacokinetic models originally utilized by comparative and veterinary pharmacokineticists were the classic open compartmental models. These models, first clearly elucidated by Teorell in 1937, have been the mainstay of pharmacokinetics for much of the last decade. However, the use of noncompartmental models, especially those based on statistical moment analyses, has recently expanded across multiple areas. This popularity can be linked in part to a superb suitability for analysis by digital computers. Paradoxically, many of the properties that make the analysis of serum pharmacokinetic data amenable to exponential equations result from a few mathematical peculiarities in the solution of these compartmental models. Newer noncompartmental approaches to

Comparative Pharmacokinetics: Principles, Techniques, and Applications, Second Edition. Jim E. Riviere.
 ISBN: 978-0-813-82993-7

data analysis share many of these attributes and thus also share the same limitations of the classic modeling approaches. These intricacies will be completely explored in this text.

In the last decade, there has been a greatly increased use of so-called population pharmacokinetic approaches. This growth has been facilitated by the availability of user-friendly software and the implicit recognition that interindividual variability in the physiology underlying pharmacokinetic parameters may overshadow drug-specific parameters. Quantitating this variability using stochastic techniques is becoming widespread.

Pharmacokinetic principles have become widespread in the discipline of toxicology, an application termed toxicokinetics. There are no fundamental differences between pharmacokinetic and toxicokinetic principles except that the latter often deal with higher doses of chemicals, which may saturate metabolizing enzymes and in some cases may damage eliminating organs, thereby altering the disposition of the toxin. However, the principles involved are identical, and the concepts presented in this text are applicable to both fields.

Physiologically based pharmacokinetic (PBPK) models have become routine in many fields of pharmacology and toxicology. These models, unlike the others mentioned, build on the basis of sound anatomical and physiological principles and, although data-intensive, may allow the best opportunity for true mechanism-based interspecies pharmacokinetic extrapolations. Individual organ function is easily scaled across species and *in vitro* data may be extrapolated to the whole animal. This modeling approach has been increasingly applied to the problem of drug and chemical residues in food-producing animals.

The goal of quantitative pharmacology is always to extrapolate the drug concentration profile in the simpler *in vitro* experimental environment to that which actually exists in the cells or tissues of whole animals. Such an extrapolation (albeit very crude) is made daily with the use of minimum inhibitory concentrations (MICs) to estimate the efficacy of an antimicrobial drug against a specific bacteria in a human or animal patient. Recent work has focused on quantifying *in vitro*-to-*in vivo* correlations, one flavor of which termed IVIVC focuses on predicting oral absorption from *in vitro* dissolution studies. *In vitro* studies may be conducted with very simple subcellular, single-cell, or tissue culture systems or more complex perfused organ preparations (also referred to as *ex vivo* models).

In drug development and biochemical toxicology laboratories, extrapolation is often from a simple receptor or subcellular fraction assay, which detects drug or toxin binding, to the dose of drug that would be required to achieve this effective concentration *in vivo*. Alternatively, DNA binding or cytotoxicity screens may detect potential adverse events associated with a specific chemical. This defines a hazard in the risk assessment process. However, sufficient exposure in the intact organism is still required for this hazard to be realized as a risk. Pharmacokinetics is often the bridge in this extrapolation. In fact, sophisticated concentration–response relationships, obtained from *in vitro* bioassay systems, may be defined and then linked to the *in vivo* dose–response profile using integrated pharmacokinetic–pharmacodynamic (PK-PD) modeling techniques. PBPK models also provide the framework for tying drug delivery to cells in modern systems biology schemes that attempt to model the cellular responses seen after chemical exposure using the tools of genomics, proteomics, and metabonomics.

Work has also exploded in the field of quantitative structure–activity relationships (QSARs) that relates molecular properties to biological activity. From its application to pharmacokinetics, progress has been made to use such techniques to predict oral bioavailability or transdermal delivery. A new chapter in this edition introduces these concepts.

The extrapolation of pharmacokinetic parameters across species is a major focus of research. This is true in laboratory animal medicine and especially so in exotic animal and zoo animal medicine. Many "classic" compartmental pharmacokinetic studies conducted in multiple animal species have been extrapolated using the techniques of allometry. This is often employed when laboratory animal toxicology data must be extended to humans to put into perspective the relationship between the expected toxic dose and therapeutically useful doses. This later concept of a "therapeutic window" framed by a minimal effective therapeutic dose or resultant concentration and maximally safe toxic threshold is found in many areas of medicine and is implicitly based in pharmacokinetic methodology.

The fields of clinical pharmacology have grown in both human and veterinary medicine. Subpopulations of patients based on age or disease processes are routinely defined and dosages of drug appropriately altered. Part of the growth of this discipline was facilitated by the routine application of pharmacokinetics in clinical patients. This was facilitated by the development of population pharmacokinetic approaches mentioned earlier, which merge the estimation of pharmacokinetic parameters with simultaneous clinical estimates of physiological parameters and population variability. Its application to defining disease-induced changes in drug disposition and probing the nature of pharmacokinetic variance are widespread. In veterinary medicine, these same principles are needed to extrapolate dosage regimens for extralabel drug use.

This proliferation of pharmacokinetics throughout these diverse fields has been propelled by the explosive growth in analytical methodologies using principles of both chromatography (high-performance liquid and gas chromatography) and immunology (radioimmunoassay, enzyme-linked immunosorbent assay [ELISA]). Not only has the cost per sample of these procedures plummeted but their availability and sensitivity have also increased tremendously. For many drugs, simple disposable card-type assays are being developed that will provide the clinician instantly with estimates of drug concentrations. In veterinary medicine, such assays are available to monitor milk and urine for the presence of violative drug residues.

With the drug concentration data now readily available, complex mathematical modeling that was once restricted to the esoteric and truly "user-unfriendly" and even "user-adverse" mainframe computers can now be routinely done on nearly any available personal computer using one of a myriad of simple-to-use pharmacokinetic software packages including Win-Nonlin and other packages (e.g., CONSAAM and SAAM, PK-Analyst, P-Pharm). In fact, the proliferation of these automated software packages is one of the developments that highlighted the need for this text because, parallel to this proliferation of tools to conduct pharmacokinetic analyses, many workers have failed to study its basic principles and often inappropriately apply models to experimental and clinical situations.

1.1 OBJECTIVES AND PHILOSOPHY

The purpose of this book is to provide an introduction of the discipline of pharmacokinetics for the student, researcher, and comparative medicine clinician. The text presents an overview of the basic processes of drug absorption and disposition and then details how these processes can be quantitated using different pharmacokinetic approaches. The book is directed toward both the individual responsible for doing the analysis and the user of the pharmacokinetic information generated. To properly employ pharmacokinetic information, the limitations of the specific model that generated the pharmacokinetic parameter esti-

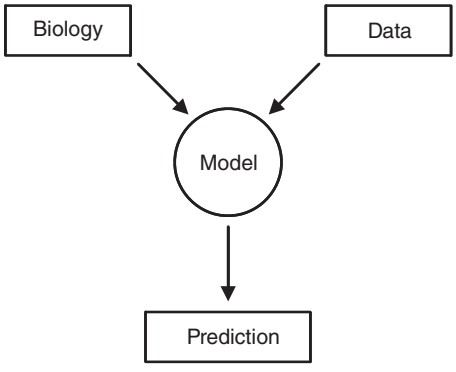

Fig. 1.1 Conceptual framework of how a pharmacokinetic model links the observed data to the underlying biology controlling drug disposition.

mates must be appreciated. Are the parameters compatible with the model in which it will be used to make predictions? Many pharmacokinetic parameters are model-dependent, and serious errors may occur if the inappropriate parameters are used. A pharmacokinetic model is simply an artificial mathematical link to the underlying interaction of a drug's pharmacology with an animal's physiology (Fig. 1.1). The nature of the link will determine the types of parameters calculated.

A common misconception is that if one specific model fails to adequately predict the data or experimental scenario, then the process being studied is assumed to not be amenable to pharmacokinetic analysis. Often, the fault is that insufficient data have been collected to properly define the model and its so-called inference space. The "links" were not properly constructed. In other cases, incomplete understanding of the disposition processes involved resulted in construction of a woefully inadequate model in the first place. The limitations of specific models and techniques must be appreciated before extrapolations can be made.

This book is also written for the individual who never plans on actually doing a pharmacokinetic study but desires to understand more about the time course of drug movement throughout the body. The primary goal of pharmacokinetics is to generate parameters that are mathematical abstractions that quantitate physiological processes as an aid to better understanding drug disposition. Mathematical modeling generates parameters that may vary as the physiology varies as a result of disease, age, sex, or drug-induced toxicity. The parameters are mathematical constructs that reflect changes in underlying physiology. There is no absolute value of any parameter that exists independent of the model; parameters are defined by the model and reflect the nature of the mathematical links to the physiology.

Models may be classified as mechanistic (e.g., compartmental and physiological), which represent some abstraction of the underlying physiologic reality, or as empirical (e.g., noncompartmental, neural-net analysis), which are restricted to predicting observed data. Alternatively, models may be classified as deterministic and thus purport to have exact predictability; or stochastic, which incorporate a level of statistical uncertainty in the predictions. An understanding of how models and links are derived is necessary for a thorough understanding of drug disposition and, ultimately, drug efficacy or toxicity.

There are many misconceptions as to what a pharmacokinetic study actually entails. Many workers in veterinary medicine believe that measuring drug concentrations in plasma or blood and plotting the resulting concentration–time profile comprises such a study.

Similarly, some feel that if parameters such as peak concentration (C_{max}), time to peak concentration, and the area under the concentration–time curve (AUC) are recorded, a pharmacokinetic analysis has been performed. In fact, to determine product bioequivalence, this does comprise a complete study. A new Chapter 15 has been added to this edition to overview the use of such approaches and present appropriate statistical techniques used in determining product bioequivalence by regulatory authorities. As will be stressed throughout this book, the problem with such analyses is that they are descriptive only for the experiment performed and are difficult to use for extrapolation to another animal or clinical conditions.

A pharmacokinetic study in the context of this book is defined as an experiment in which some type of mathematical model is fitted to the drug concentration–time profile in blood, tissue, and/or excreta. This opens the possibility of correlating model parameters to physiological processes or using them for interspecies extrapolation. In these types of analyses, parameters such as half-life ($T_{½}$), volume of distribution (Vd), and clearance (Cl) are calculated in addition to the descriptive parameters mentioned above. A separate chapter will be devoted to the physiology underlying each type of parameter. Similarly, the major types of modeling paradigms adopted will be developed and compared. Whatever type of model is employed (linear vs. nonlinear, compartmental vs. noncompartmental), a model is only a tool to estimate drug concentrations and generate parameters that are useful for further analyses and quantitating the biological process under investigation. Models are neither correct nor incorrect, but should be judged only as to how accurately drug concentrations are predicted under new exposure conditions.

The selection of a model relative to its use for prediction of future events is an important decision. Fig. 1.2 depicts how three radically different mathematical models may fit the same limited data set. The three models are statistically equivalent in terms of their ability to describe the observed data, and thus all are mathematically appropriate. However, only the exponential model has a relatively direct link to biological reality. All three predict very different drug concentrations for times beyond the actual data collected. Within the observed time interval, all models accurately interpolate drug concentrations at times between collections. This is defined as the inference space of the model. However, extrapolation outside

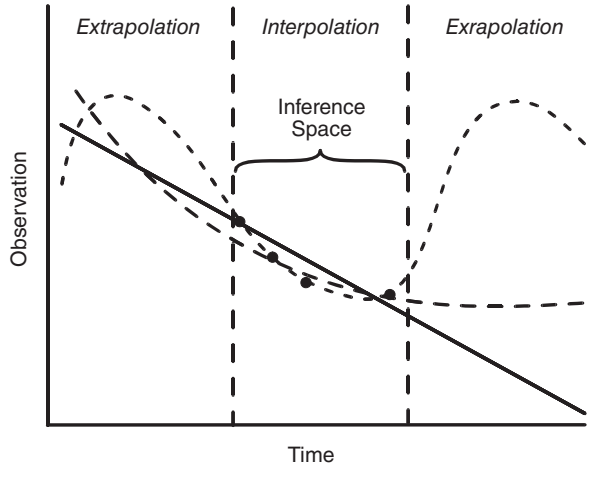

Fig. 1.2 Illustration of how three very diverse mathematical models may adequately describe the same limited set of data yet result in very different values when predictions are extrapolated beyond the models' inference space. Linear (—); sinusoidal (– –); exponential (— — —).

of the observed time window requires knowledge that the model has biological reality at these time points. Collection of as few as one or two additional data points would expand the model's inference space and help select the more predictive model. It is surprising how often this simple limitation of fitting equations to data is overlooked.

Completely independent of the model selected, it is the fitting of the model to the data, for the purposes of the investigator, that must be optimized. This is where statistics interfaces with pharmacokinetics. For example, three different approaches and sets of sampling intervals are used in studies to estimate a peak drug plasma concentration, to determine a dosing interval for chronic treatment, or to estimate the tissue residue withdrawal time in a food-producing animal. Although the underlying models may be very similar, or even identical, these three cases require optimizing estimates of different components of the model, and thus the experimental time frame may be very different, ranging from minutes to hours to days. The drug concentration ranges for these three applications are also likely to differ by three to four orders of magnitude. Failure to select a specific model appropriate to the proper experimental frame of reference may lead to serious errors in extrapolation. These aspects of experimental design and data analysis will be extensively reviewed at the end of the text.

Semantics plays a very important role in this interface between statistics and pharmacokinetics. Serious errors have occurred when the same term in both disciplines refers to two different items. Examples include the use of the Greek letter β, which in statistics may refer to the probability of a type II statistical error or the slope of a regression line, but in pharmacokinetics may specifically refers to the terminal exponential slope of the plasma drug concentration versus time data from a two-compartment model following intravenous drug administration. Standard practices for fitting mathematical models to the same data set in both disciplines may be very different. For example, the modeling approaches used in pharmacokinetics often are based on additive exponential functions simply because the resulting parameters then have physiological meaning; that is, they can be linked back to the animal. Such exponential functions are but a subset of those available to the statistician and may not even be the best for fitting to a specific curve. Nevertheless, they are used because they are interpretable and have physiological meaning, and thus can be incorporated into models that physiologically and pharmacologically make sense. Even if exponential equations are used by both disciplines, pharmacokinetic analysis often employs the principle of superposition and thus curve "stripping" to analyze the data, a restriction not present in a pure statistical model. Neither approach is right or wrong as each has its merits. Problems arise only when parameters from one model are mistakenly used as input into another.

Recent advances in *in vitro* technology and the ease of conducting large-scale pharmacokinetic trials have resulted in a plethora of readily available data that would appear to span all levels of biological organization. This is especially true in comparative pharmacology and risk assessment. The combination of such diverse data requires that certain assumptions be fulfilled and the limits of the mathematical bridges employed to link the data sets be strictly defined. Even when done properly, some combinations of diverse *in vitro* and *in vivo* model systems result in the generation of so-called emergent properties, the hallmark of complex system behavior. In other cases, nonlinear systems dynamics or "chaotic behavior" may take hold, making extrapolations possible but difficult unless the behavior is clearly understood. Thus, as will become evident throughout this text, pharmacokinetics and other forms of mathematical extrapolations may be used in many scenarios, but they must be applied in the proper context and the assumptions and defining rules inherent to each system closely tested and followed.

1.2 TARGET AUDIENCE AND APPLICATIONS

The focus of this book is to present the basic concepts of pharmacokinetic principles to the scientist or practitioner with a strong biological background. The mathematics should be tolerable to such an individual as it will not go much beyond what he or she has already encountered in related disciplines. The most obvious user of pharmacokinetic principles is the basic scientist studying drug or chemical disposition in animals. Simple pharmacokinetic studies are often used to describe the blood or tissue concentrations seen after drug administration. These parameters provide the basis for determining differences in the rate and extent of drug absorption, distribution, or elimination, as well as permitting the calculation of safe and efficacious dosage regimens. They allow for the development of simple mathematical models to interpret the time-dependent nature of numerous biological phenomena. These strategies will be completely developed.

Pharmaceutical scientists use pharmacokinetics in many industrial and regulatory settings. Parameters are derived to define the shape of an efficacious drug's blood concentration versus time profile (AUC, C_{max}) so that other products may be formulated to "copy" this profile or, in pharmacokinetic jargon, to be "bioequivalent." Similarly, drug absorption is assessed in simple model systems to select candidate drugs for development and determine the purity of a drug formulation. Pharmacokinetic parameters are calculated to extrapolate from preclinical and clinical trial results. Toxicologists in these environments must use pharmacokinetic principles to interpret the dose that produces a toxicological "event" in an animal study relative to its potential to do the same in a clinical setting at therapeutic doses. Many practices of risk assessment use similar extrapolations.

The field of pharmacokinetics and its concepts has become especially important as a consequence of the dramatic and almost radical changes that are presently occurring relative to the regulations surrounding drug use in veterinary medicine. For most of the recent past, the operative concept was that a single dose of drug listed on a product label was optimal for all therapeutic uses. The legal concept of "flexible or professional labeling" and the passage by the US Congress in 1994 of the Animal Medicinal Drug Use Clarification Act (AMDUCA) legalizing extralabel drug use forever eradicated this fallacious ideal of a single optimal dose. The veterinarian must now select a drug dose based on numerous factors inherent to the therapeutic scenario at hand to maximize therapeutic efficacy and minimize the likelihood of drug-induced toxicity or induction of microbial resistance. Unlike human medicine and companion animal practices, food animal veterinarians face the further restriction that proper withdrawal times must be determined to ensure that drug residues do not persist in the edible tissues or by-products (milk, eggs) of treated animals long after they have left the care of the veterinarian (Fig. 1.3). As will be demonstrated, the withdrawal time is in reality a pure pharmacokinetic parameter since it can be calculated solely from knowledge of the legal tissue tolerance and the drug's half-life or rate of decay in that tissue.

Yet it is not only the food animal veterinarian who faces these challenges. The laboratory animal and exotic/zoo animal worker must often extrapolate drug dosages across species with widely differing body sizes and physiology since there are very few approved drugs for the treatment of such animals. Pharmacokinetic principles and techniques are ideally suited for this application. Practitioners are often faced with disease processes (e.g., renal failure) that are known to affect the disposition of a drug. Knowledge of how such a pathological process affects a drug's clearance or volume of distribution is sufficient to adapt a dosage regimen appropriate for this condition.

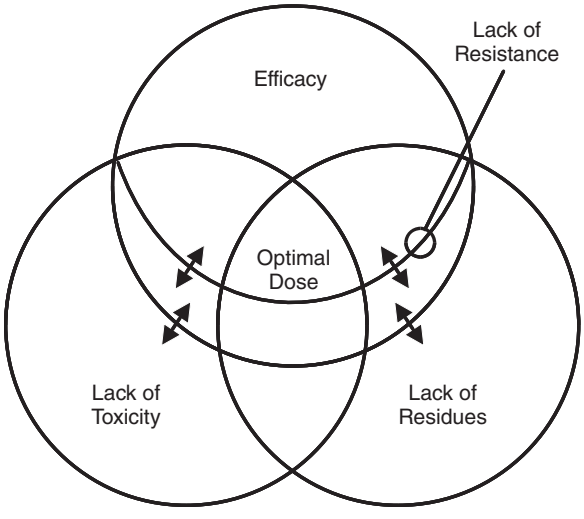

Fig. 1.3 Illustration of the food animal veterinarian's dilemma in optimizing the dose of a therapeutic drug.

Other scientists who deal with drugs in both *in vitro* and *in vivo* systems may not be interested in constructing complex pharmacokinetic models but rather in the relationship between the administered dose and the effect. The link between dose and effect, however, is the drug concentration at the site of action (the so-called biophase), which is the essence of a pharmacokinetic study. These data are necessary to link these different systems in order to determine whether a drug concentration threshold exists for drug action or toxicity, or to study the time course of drug effect. Pharmacokinetics provides the parameters to serve as experimental end points and to extrapolate beyond the individual experiment to the target population.

To pursue these varied goals, this book starts with the biology and progresses to the presentation of the different modeling approaches used in pharmacokinetics. The book concludes with elements of experimental design and data analysis, followed by some specific applications to select fields.

BIBLIOGRAPHY

Baggot, J.D. 1977. *Principles of Drug Disposition in Domestic Animals: The Basis of Veterinary Clinical Pharmacology*. Philadelphia: W.B. Saunders Co.

Bar-Yam, Y. 1992. *Dynamics of Complex Systems*. Reading, MA: Addison Wesley.

Bourne, D.W.A. 1995. *Mathematical Modeling of Pharmacokinetic Data*. Lancaster, PA: Technomic Publishing Co.

Boxenbaum, H. 1992. Pharmacokinetics: philosophy of modeling. *Drug Metabolism Reviews*. 24:89–120.

DiStefano, J.J., and Landaw, E.M. 1984. Multiexponential, multicompartmental, and non-compartmental modeling. I. Methodological limitations and physiological interpretations. *American Journal of Physiology*. 246:R651–R664.

Edelstein-Keshet, L. 2005. *Mathematical Models in Biology*. Philadelphia: SIAM Classics in Applied Mathematics.

Ette, E.I., and Williams, P.J. 2007. *Pharmacometrics The Science of Quantitative Pharmacology*. Hoboken, NJ: Wiley.

Gabrielsson, J., and Weiner, D. 2007. *Pharmacokinetic and Pharmacodynamic Data Analysis: Concepts and Applications*, 4th Ed. Stockholm: Swedish Pharmaceutic.

Gaines, P.E. 1988. *Linear Stochastic Systems*. New York: John Wiley & Sons.

Gibaldi, M., and Perrier, D. 1982. *Pharmacokinetics*, 2nd Ed. New York: Marcel Dekker.

Lees, P. (ed.) 2004. Special reviews issue: PK and PK-PD in veterinary medicine. *Journal of Veterinary Pharmacology and Therapeutics.* 27:395–535.

Patterson, S., and Jones, B. 2006. *Bioequivalence and Statistics in Clinical Pharmacology*. Boca Raton, FL: Chapman and Hall/CRC.

Reddy, M.B., Yang, R.S.H., Clewell, H.J., and Andersen, M.E. 2005. *Physiological Based Pharmacokinetic Modeling*. New York: Wiley Interscience.

Riviere, J.E. 2009. Pharmacokinetics of nanomaterials: an overview of carbon nanotubes, fullerenes and quantum dots. *Wiley Interdisciplinary Review of Nanomedicine and Nanobiotechnology*. 1:26–34.

Rowland, M., and Tozer, T.N. 1995. *Clinical Pharmacokinetics*, 3rd Ed. Philadelphia: Lippincott Williams & Wilkins.

Teorell, T. 1937. Kinetics of distribution of substances administered to the body. *Archives International Pharmacodynamics*. 57:205–240.

Wagner, J.G. 1975. *Fundamentals of Clinical Pharmacokinetics*. Lancaster, PA: Technomic Publishing Co.

2 Principles of Drug Movement in the Body

Pharmacokinetics is the study of the time course of drug concentrations in the body. It provides a means of quantitating absorption, distribution, metabolism, and elimination (ADME), the four key physiological processes that govern the time course of drug fate. It is a crucial tool to providing quantitative and experimentally testable end points for many aspects of drug discovery, as well as providing a bridge between early safety and efficacy studies conducted in different species. In the premarketing phase of drug development, it is an essential component in establishing effective yet safe dosage forms and regimens. When applied to a clinical situation, pharmacokinetics provides the practitioner with a useful tool to design optimally beneficial drug dosage schedules for each individual patient. Alternatively, an understanding of pharmacokinetic principles allows more rational therapeutic decisions to be made. In food animals, pharmacokinetics provides the conceptual underpinnings for understanding and utilizing the withdrawal time to prevent violative drug residues from persisting in the edible tissues of food-producing animals. Finally, a comprehensive study of this discipline provides the framework upon which many aspects of pharmacology can be integrated into a rational plan for drug usage.

2.1 AN OVERVIEW OF DRUG DISPOSITION

In order to fully appreciate the processes governing the fate of drugs in animals, the various steps involved must be defined and ultimately quantitated. The processes relevant to a discussion of the absorption and disposition of a drug administered by the intravenous (IV), intramuscular (IM), subcutaneous (SC), oral (PO), topical (TOP), or inhalational (IN) route are illustrated in Fig. 2.1. The normal reference point for pharmacokinetic analysis is the concentration of free, nonprotein-bound drug dissolved in the serum (or plasma) because this is the body fluid that carries the drug throughout the body and from which samples for drug analysis can be readily and repeatedly collected. Additionally, for the majority of drugs used, drug in the systemic circulation is in equilibrium with the extracellular fluid of well-perfused tissues; thus, serum or plasma drug concentrations generally reflect extracellular fluid drug concentrations. *A drug must generally be present at its site of action in a tissue at a sufficient concentration for a specific period of time to produce a pharmacological effect.* Since tissue concentrations of drugs are reflected by extracellular

Comparative Pharmacokinetics: Principles, Techniques, and Applications, Second Edition. Jim E. Riviere.
 ISBN: 978-0-813-82993-7

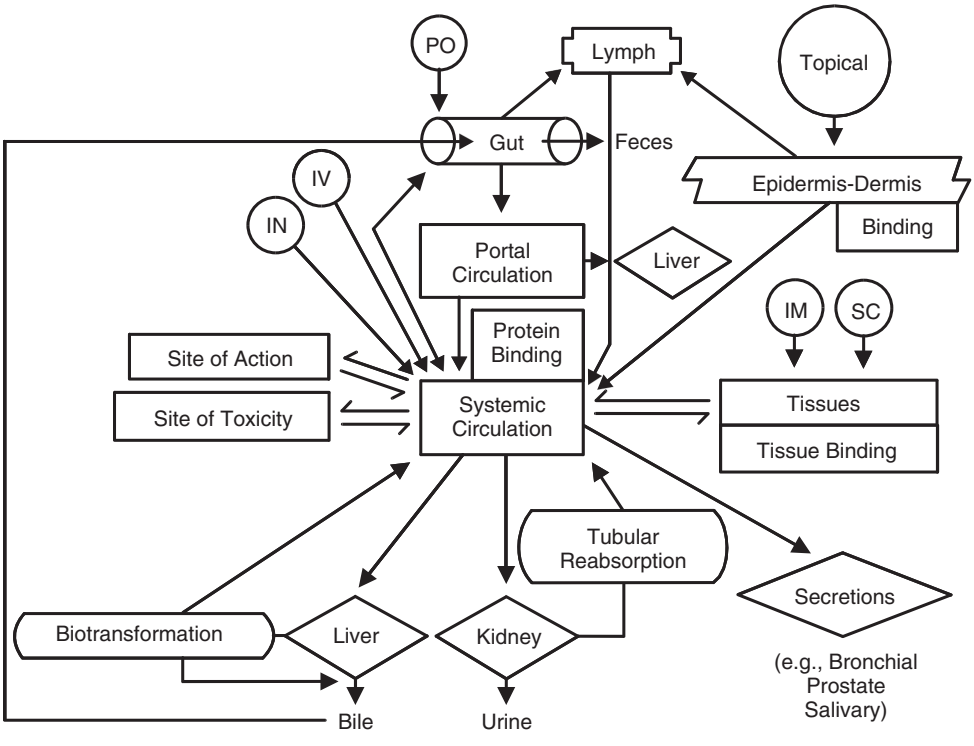

Fig. 2.1 Basic schema illustrates how drug is absorbed, distributed, metabolized, and excreted from the body. These processes are those that form the basis for developing pharmacokinetic models. Sites of action and toxicity are effect compartments developed in Chapter 13.

fluid and thus serum drug concentrations, a pharmacokinetic analysis of the disposition of drugs in the scheme outlined in Fig. 2.1 is useful to assess the activity of a drug in the *in vivo* setting.

Blood concentration monitoring does not immediately reflect the movement of very lipophilic drugs or particles in the lymphatic system, a parallel "circulatory system" whose importance to the biodistribution of certain drugs is only now being appreciated. Although much of the material in lymph finally returns to the blood circulation via the thoracic duct, some material may get filtered and trapped in regional lymph nodes after oral, topical, or inhalational dosing and not be detected in studies based on blood sampling.

The conceptualization in Fig. 2.1 is especially important in veterinary medicine because species differences in any of these processes may affect the extent and/or time course of drug absorption and disposition in the body. By dividing the overall process of drug fate into specific phases, this relatively complex situation can be more easily handled. It is the purpose of this chapter to present an overview of the physiological basis of absorption, distribution, biotransformation, and excretion. This discussion will then provide a groundwork for the subsequent chapters that deal with approaches to quantify these processes.

One must realize that such conceptual schemes are created to solve practical problems in pharmacology or therapeutics. The concentration of a drug achieved in a tissue can be described using pharmacokinetic techniques. However, the interpretation of this drug concentration is defined by the user of the data. If a drug is being targeted to a specific tissue (e.g., liver), the liver becomes the site of action. In contrast, if the toxicity of a drug is

primarily expressed in the liver, the same organ now becomes the site of toxicity. Finally, the site of action and toxicity may be in different tissues, yet the liver may be the tissue of concern for residues in a food animal. In all three cases, the pharmacokinetic model describing the time course of drug concentration in the liver may be similar; only the interpretive value associated with the drug concentration is different. This is not a function of the mathematical model describing the drug concentration; rather it is dependent on the use to which the information is put. In other cases, the parameters of the pharmacokinetic model describing chemical in liver may be very applicable to three different concentrations (e.g., 100, 10, 1 µg/mL for toxicity, activity, residues) or three different time scales (hours, days, weeks). *A pharmacokinetic model must be interpreted in the context of the experiment from which it was created.* This relativity in the interpretation of pharmacokinetic data will continue to be stressed throughout this book.

2.2 THE IMPORTANCE OF MEMBRANE BARRIERS

Despite the myriad of anatomical and physiological differences among animals, the biology of drug absorption and distribution, and in some cases even elimination, is very similar in that it involves drug molecules crossing a series of barriers made from different biological membranes. As illustrated in Fig. 2.2, these barriers may be associated with either several layers of cells (tissue) or a single cell, and both living and dead protoplasm may be involved. Despite the different biochemical and morphological attributes of each of these membranes, a unifying concept of biology is the basic similarity of all membranes; tissue, cell, or organelle. Although the specific biochemical components may vary, the fundamental organization is similar. This fact provides a simple construct to understand the major determinants of drug absorption, distribution, and excretion.

Membrane barriers, and the resistance they offer to drug movement, often define the nature of compartments or other structural units in pharmacokinetic models. Biological spaces are defined by the restrictions of these barriers. The most effective barriers are those that protect the organism from the external environment. These include the skin as well as various segments of the gastrointestinal and respiratory tracts, which also protect the internal physiological milieu from the damaging external environment. The interstitial fluid is a common compartment through which any drug must transit either after absorption on route to the blood stream or after delivery by blood to tissue on route to a cellular target.

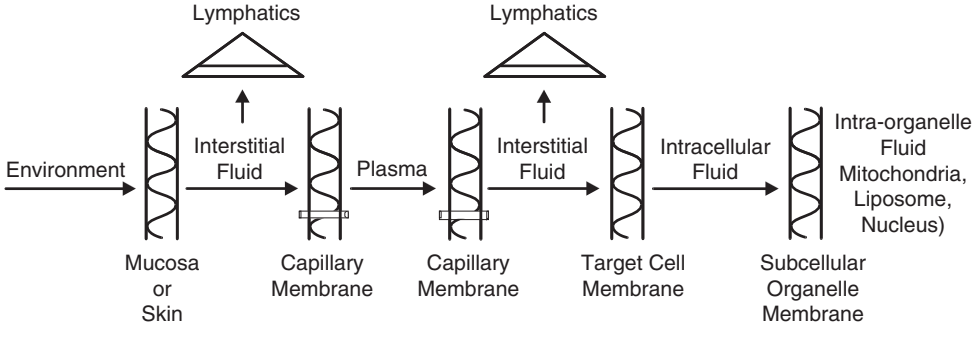

Fig. 2.2 Illustration of how absorption, distribution, and excretion essentially constitute a journey of drug through various lipoidal membrane barriers. Note the continuity of interstitial fluid with the lymphatic system as well as the pores present in capillary membranes representing "leaky" junctions.

The continuity of this space has recently been taken advantage of in pharmacokinetic studies through the use of implantable microdialysis probes and microfiltration catheters that allow direct sampling of interstitial fluid. The lymphatic system also maps onto the interstitial space and has received considerable attention lately relative to transport of very lipophilic substances, particulate matter including nanoparticles, as well as cellular components of the immune system.

Membranes define homogeneous tissue compartments, and membranes must be traversed in all processes of drug absorption and disposition. The capillary membranes delimiting the vascular from interstitial spaces are relatively "leaky" to larger molecules due to fenestrations in their walls. The mechanisms by which chemicals cross these ubiquitous membrane barriers often determine the type of pharmacokinetic models appropriate to quantitate the movement of specific drugs.

The basic model of the cellular membrane as originally postulated by Davson and Danielli in 1935 is still the most generally accepted description for the structure of cellular membranes. The major modification is in the increased fluidity of the lipid components, with the resulting fluid mosaic model proposed by Singer and Nicholson (1972) depicted in Fig. 2.3. A large body of microscopic and biochemical data has now confirmed and expanded this insightful model (Engelman, 2005). All cellular membranes appear to be bimolecular lipid leaflets closely associated with globular proteins and glycoproteins that may reside on either surface (intracellular or extracellular) or traverse the entire structure. The lipid leaflets are arranged with hydrophilic (polar) head groups on the surface and hydrophobic (nonpolar) tails forming the interior. Several types of lipids are found in biological membranes, with phospholipids, sphingolipids, and cholesterol predominating. Packing of these phospholipids is relatively loose, hence contributing to membrane fluidity. In contrast, sphingolipid packing is tight, forming a more gel-like consistency. Cholesterol further modifies these properties due to its tendency to cause more order (less fluidity) in lipid packing. These different lipid properties result in heterogeneous regions of the membrane showing different properties dependent on the local lipid environment, as well as inconsistencies in membrane thickness. Recent data also suggests that such membrane

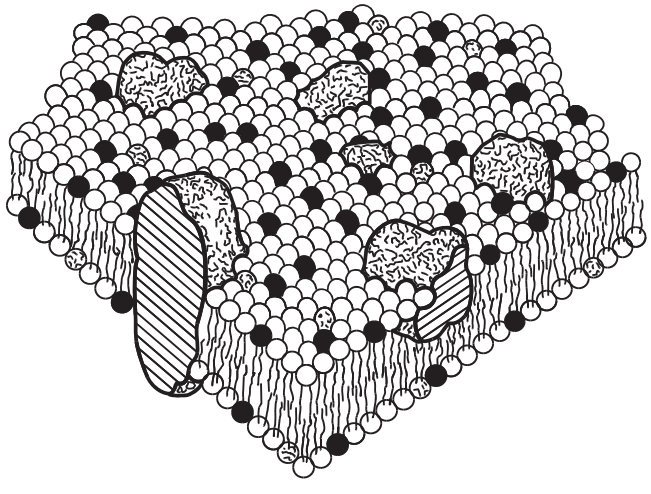

Fig. 2.3 Fluid mosaic model of a bilayer lipid membrane.

compartments may even be stabilized by elements of the cell's cytoskeleton as well as transmembrane proteins. The specific lipid composition of these membranes varies widely across different tissues and levels of biological organization.

The most recent concept of membrane organization suggest that the membrane environment is more complex than originally thought with some level of microstructure occurring in the lipid environment that further modulates both location and function of membrane proteins. In addition to the heterogeneity imposed on membrane structure from different degrees of lipid order, so-called cholesterol- and sphingolipid-rich "lipid or membrane rafts" may also form and interact with proteins, which both stabilize some structures in the membrane and also allow for lateral movement inside the membrane. These systems manifest themselves in the function of various physiological processes important to drug transport and activity, including signal transduction (calveolae maintain receptor couplings to other molecules) and transmembrane vesicular trafficking, the latter involved in the movement of some drugs across membranes.

The location of the proteins in the lipid matrix is primarily a consequence of their hydrophobic regions residing in the lipid interior and their hydrophilic and ionic regions occupying the surface. This is the thermodynamically most stable configuration. This location is greatly affected by the lipid microenvironment described above. In addition, some membrane proteins are anchored by microfilaments to the cytoskeleton of the cell. The primary force responsible for maintaining structural integrity of both the lipids and proteins are hydrophobic, and to a lesser extent, electrostatic intermolecular interactions. Changes in the fluidity of the lipids or their organization alter protein conformations, which then may modulate their activity. These complex protein–protein, protein–lipid, and lipid–lipid interactions results in a significant "patchiness" to the localization of transport structures in the membrane, which modify the nature and kinetics of drug transport.

Aqueous channels may exist within integral proteins that traverse the membrane. In other cases, integral proteins may actually be enzymatic transport proteins that function as active or facilitative transport systems. As will be discussed later in this chapter, compounds handled by active transport systems will have different pharmacokinetic properties than those whose rate is determined by movement through lipid domains. Finally, some membranes possess "reverse transport systems" that effectively pump drugs that were absorbed across the membrane back outside of the cell, the classic example being P-glycoprotein (Pgp). Despite this level of membrane complexity, the primary pathway for most drugs to cross lipid membranes has been repeatedly shown to be passive diffusion through the lipid environment.

Thus, for a drug to be absorbed or distributed throughout the body, it must be able to pass through a lipid membrane on some part of its sojourn through the body. In some protected sites of the body (e.g., brain, cerebral spinal fluid), additional membranes (e.g., glial cells) may have to be traversed before a drug arrives at its target site. These specialized membranes could be considered a general adaptation to further shelter susceptible tissues from hostile lipophilic chemicals. Similarly, drug characteristics that promote transmembrane diffusion would favor drug action and effect (again, unless specific transport systems intervene).

This general phenomenon of the enhanced absorption and distribution of lipophilic compounds is a unifying tenet that runs throughout the study of drug fate. The body's elimination organs can also be viewed as operating according to a somewhat similar principle. The primary mechanism by which a chemical can be excreted from the body is by becoming less lipophilic and more hydrophilic, the latter property being required for

excretion in the aqueous fluids of the urinary or biliary system, although amphipathic drugs (having both lipophilic and polar properties) are preferentially excreted in the bile. When a hydrophilic or polar drug is injected into the blood stream, it will be minimally distributed and rapidly excreted by one of these routes. However, if a compound's lipophilicity evades this easy excretion, the liver and other organs may metabolize it to less lipophilic and more hydrophilic metabolites that have a restricted distribution (and thus reduced access to sites for activity) in the body and can be more readily excreted. This basic tenet runs through all aspects of pharmacology.

2.3 DRUG PASSAGE ACROSS MEMBRANES BY DIFFUSION

Considerable evidence indicates that lipid-based membranes are permeable to nonpolar lipid-soluble compounds and polar water-soluble compounds with sufficient lipid solubility to diffuse through the hydrophobic lipid regions of the membrane. The rate of diffusion of a compound across a membrane is directly proportional to its concentration gradient across the membrane, lipid:water partition coefficient, and diffusion coefficient. This can be summarized by Fick's law of diffusion in the equation

$$\text{Rate of diffusion}(\text{mg/s}) = \frac{D(\text{cm/s}) \cdot P}{h(\text{cm})}(X_1 - X_2)(\text{mg}), \tag{2.1}$$

where D is the diffusion coefficient for the specific penetrant (nonionized moiety) in the membrane being studied, P is the partition coefficient for the penetrant between the membrane and the external medium, h is the thickness or actual length of the path by which the drug diffuses through the membrane, and $X_1 - X_2$ is the concentration gradient (ΔX) across the membrane. The diffusional coefficient of the drug is a function of its molecular size, molecular conformation, and solubility in the membrane milieu. The partition coefficient is the relative solubility of the compound in lipid and water, which reflects the ability of the penetrant to gain access to the lipid membrane. Depending on the membrane, there is a functional molecular size and/or weight cutoff that prevents very large molecules from being passively absorbed across any membrane. As will be demonstrated in Chapter 8, when the rate of a process is dependent on a rate constant (in this case $[D{\cdot}P/h]$, often referred to as the permeability coefficient K_p) and a concentration gradient, a linear or first-order kinetic process will be operative. In membrane transfer studies, the total flux of a drug across a membrane is dependent on the area of membrane exposed; thus, the rate above is often expressed in terms of cm^2. This relationship holds well *in vitro*, but is only an approximation *in vivo* since in many barriers, penetration is slow, and a long period of time is required to achieve steady state. When steady state is not achieved, Fick's second law of diffusion may be used to estimate instantaneous fluxes, a discussion of which is beyond the scope of the present chapter.

If the lipid:water partition coefficient is too great, depending on the specific membrane, the compound may be sequestered in the membrane rather than traverse it. Thus, some fraction of X will actually not be available for diffusion through the system. This could be modeled using compartmental schemes similar to that presented in Chapter 8, in which the sequestered portion of the drug is considered to be a separate compartment. However, in general, passage through membranes correlate with various lipid:water partition coeffi-

cients. The fluid phase most often used for its determination is octanol:water, resulting in log $K_{o/w}$ being used as a surrogate for K_p. In some cases in which the specific lipid composition of the membrane is known, a slurry of the actual lipids may be employed. This is becoming more sophisticated with the advent of advanced organ culture techniques in which, for example, with skin, lipid membranes very similar in composition, structure, and function to those *in vivo* can be routinely prepared in culture and used to study drug transport. Chapter 3 present modeling approaches used to correlate membrane permeability (K_p).

2.4 EFFECTS OF pH ON MEMBRANE TRANSPORT

Evidence also indicates that membranes are more permeable to the nonionized than the ionized form of weak organic acids and bases. If the nonionized moiety has a lipid:water partition coefficient favorable for membrane penetration, then it will ultimately reach equilibrium on both sides of the membrane. The ionized form of the drug is completely prevented from crossing the membrane because of its low lipid solubility. The amount of the drug in the ionized or nonionized form depends on the pK_a (negative logarithm of the acidic dissociation constant) of the drug and the pH of the medium on either side of the membrane (e.g., intracellular vs. extracellular fluid; gastrointestinal vs. extracellular fluid; topical formulation vs. skin). Protonated weak acids are nonionized (e.g., COOH), while protonated weak bases are ionized (e.g., NH_3^+). If the drug has a fixed charge at all pH levels encountered inside and outside of the body (e.g., quaternary amines, aminoglycoside antibiotics), they will never cross lipid membranes by diffusion. This would restrict both their absorption and their distribution and generally lead to an enhanced rate of elimination. It is the unionized form of the drug that is governed by Fick's law of diffusion and described by Equation 2.1. For this equation to predict the movement of a drug across membrane systems *in vivo*, the relevant pH level of each compartment must be considered relative to the compound's pK_a, otherwise erroneous predictions will be made.

When the pH of the medium is equal to the pK_a of the dissolved drug, 50% of the drug exists in the ionized state and 50% in the nonionized, lipid-soluble state. The ratio of nonionized to ionized drug is given by the Henderson–Hasselbalch equation.

For acids:

$$\mathrm{p}K_a - \mathrm{pH} = \log[(\mathrm{H\ Acid})^\circ/(\mathrm{Acid})] \tag{2.2}$$

For bases:

$$\mathrm{p}K_a - \mathrm{pH} = \log[(\mathrm{H\ Base})/(\mathrm{Base})^\circ] \tag{2.3}$$

These equations are identical as they involve the ratio of protonated (H) to nonprotonated moieties. The only difference is that for an acid, the protonated form $(\mathrm{H\ Acid})^\circ$ is neutral, and for a base, the protonated form $(\mathrm{H\ Base})^+$ is ionized.

As can be seen by these equations, when the pH is one unit less or one unit more than the pK_a for weak bases or acids, respectively, the ratio of ionized to nonionized forms is 10. Thus, each unit of pH away from the pK_a results in a 10-fold change in this ratio. This phenomenon allows for a drug to be differentially distributed across a membrane in the presence of a pH gradient. The side of the membrane with the pH favoring ionized drug (high pH for an acidic drug; low pH for an alkaline drug) will tend to have higher total

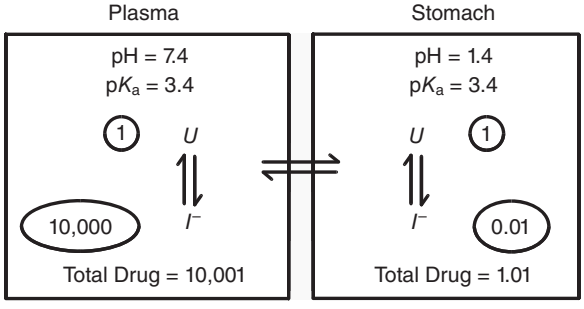

Fig. 2.4 Phenomenon of pH partitioning and ion trapping of a weak acid.

(ionized plus nonionized) drug concentrations. This pH partitioning results in a phenomenon termed "ion trapping" in the area where ionized drug predominates. Fig. 2.4 illustrates this concept with an organic acid of $pK_a = 3.4$ partitioning between gastric contents of pH = 1.4 and plasma of pH = 7.4. Assuming that the nonionized form of the drug (U) is in equilibrium across the membrane, then according to Equation 2.2, there will be a 100-fold (log 2; 3.4 – 1.4) difference on the gastric side and a 10,000-fold (log 4; 7.4 – 3.4) difference on the plasma side of the membrane, for a transmembrane concentration gradient of total drug ($U + I$) equal to 10,001/1.01, where I is the ionized form of the drug. Note that the unionized concentration on both sides of the membrane is in equilibrium. It is the total drug concentrations that are different. In this case, the gradient is generated by the difference in pH across an ion-impermeable barrier generated by the local milieu.

Such a gradient would greatly favor the absorption of this weak acid across the gastrointestinal tract into plasma. This is the situation that exists for weak acids, such as penicillin, aspirin, and phenylbutazone. In contrast, a weak base would tend to be trapped in this environment, and thus minimal absorption would occur. Examples of such weak bases are morphine, phenothiazine, and ketamine. This is toxicologically significant with the weakly basic strychnine. If strychnine were placed into the strongly acidic stomach, no systemic toxicity would be observed. However, if the stomach was then infused with alkali, most of this base would become nonionized, readily absorbed, and lethal. In summary, weak acids are readily absorbed from an acid environment and sequestered in an alkaline medium. In contrast, weak bases are absorbed in an alkaline environment and trapped in an acidic environment.

This pH partitioning phenomenon is important not only for understanding absorption (as illustrated above) but also in any situation in which the pH values of fluid compartments across a biological membrane are different (see Fig. 2.2). It will occur for a drug distributing from plasma (pH = 7.4) to milk (pH = 6.5–6.8), to cerebrospinal fluid (pH = 7.3), to the rumen (pH = 5.5–6.5), or to intracellular sites (pH = 7.0). Thus, weakly acidic drugs will tend not to distribute into the milk after systemic distribution (e.g., penicillin), while weakly basic drugs (e.g., erythromycin) will. If a disease process alters the pH of one compartment (e.g., mastitis), the normal equilibrium ratio will also be perturbed. In mastitis, in which the pH level may increase almost one unit, this preferential distribution of basic antibiotics will be lost. The relatively acidic pH of cells relative to plasma is responsible for the relatively large tissue distribution seen with many weakly basic drugs (e.g., morphine, amphetamine). Similarly, in the ruminant, many basic drugs tend to distribute into the rumen, resulting in distribution volumes much larger than those in monogastric

animals. In fact, a drug that distributes into this organ may then undergo microbial degradation, resulting in its elimination from the body.

There are a number of mathematical transformations that can be made to these basic equations to facilitate the calculation of concentration gradients. For example, to calculate the equilibrium ratio (R) of two compounds across a membrane, the following equations could be used.

For two acids (a and b):

$$R(\text{a/b}) = \frac{1+10^{(\text{pH(a)-p}K_a)}}{1+10^{(\text{pH(b)-p}K_a)}} \tag{2.4}$$

For two bases (a and b):

$$R(\text{a/b}) = \frac{1+10^{(\text{p}K_a\text{-pH(a)})}}{1+10^{(\text{p}K_a\text{-pH(b)})}} \tag{2.5}$$

These pH effects have also been directly incorporated into partition coefficients such as log $K_{o/w}$ by determining what its value is as a function of different pH. The resulting parameter is called log D_{pH} and may be more useful to describe a compound's permeability from solutions of acids or bases of specific pH. Log $K_{o/w}$ is normally tabulated at a pH of 7.4.

This phenomenon is also very important for the passive tubular reabsorption of weak acids and bases being excreted by the kidney. For carnivores with acidic urine relative to plasma, weak acids tend to be reabsorbed from the tubules into the plasma, while weak bases tend to be preferentially excreted. This principle has been applied to the treatment of salicylate (weak acid) intoxication in dogs in which alkaline diuresis promotes ion trapping of the drug in the urine, hence its more rapid excretion. Disease-induced changes in urine pH will likewise alter the disposition of drugs sensitive to this phenomenon.

2.5 PATHWAYS FOR MEMBRANE TRANSPORT

One can appreciate that many of the principles that govern diffusion of a drug across biological membranes are applicable to many phases of drug disposition. However, there are several specialized membranes that possess specific transport systems. In these cases, the laws of diffusion and pH partitioning do not govern transmembrane flux of drugs. These specializations in transport can be best appreciated as mechanisms by which the body can exert control and selectivity over the chemicals that are allowed to enter the protected domain of specific organs, cells, or organelles. Such transport systems can be rather nonspecific as are those of the kidney and liver, which excrete charged waste products. A similar situation occurs in the gastrointestinal tract, where relatively nonspecific transport systems allow for the absorption, and thus entrance to the body, of essential nutrients that do not have sufficient lipophilicity to cross membranes by diffusion. In specific tissues, they allow for select molecules to enter cells depending on cellular needs, or allow compounds that circulate throughout the body to only have a biological response in a tissue possessing the correct transport receptor. Particulate matter may be absorbed by these different mechanisms.

Up to this point, we have concentrated our discussion on drug movement by passive diffusion across membranes. However, the structure of both cellular and tissue membranes

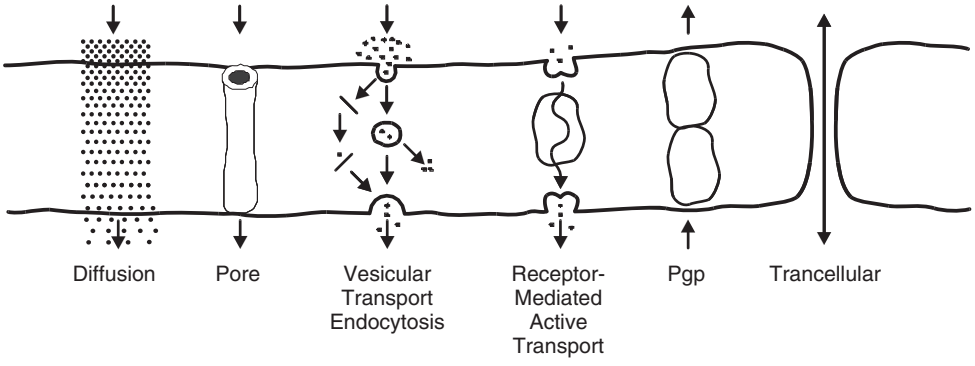

Fig. 2.5 Schematic representation of potential routes of compound movement across membranes.

are heterogeneous and offer other mechanism for movement across membranes. Fig. 2.5 summarizes the potential pathways across membranes that may be involved in drug transport.

The primary example is the protein carrier-mediated processes of active transport or facilitated diffusion. These systems are characterized by specificity and saturability. In the case of active transport, biological energy is utilized to move the drug against its concentration gradient. In facilitated diffusion, the carrier protein binds to the drug and carries it across the membrane down its concentration gradient, facilitating entry of hydrophilic or charged compounds that normally cannot cross the membrane by passive diffusion because they are not lipophilic. These systems are important for the gastrointestinal absorption of many essential nutrients, for cellular uptake of many compounds (e.g., glucose), for the removal of drugs from the cerebral spinal fluid through the choroid plexus, and for the biliary and renal excretion of numerous drugs.

The precise molecular mechanisms behind facilitated and active transport systems are beyond the scope of a pharmacokinetic book such as this. Texts in biochemistry or cellular physiology should be consulted for more detail. For most drugs, the principle of passive diffusion suffices for constructing pharmacokinetic models. Active transport systems are primarily encountered in processes of elimination, which will be dealt with in Chapters 6 and 7. As discussed above, Pgp transport systems also exist, which removes a drug that has already entered a cell or crossed a tissue membrane barrier (e.g., blood–brain barrier).

Active transport processes may dramatically alter the pharmacokinetics of a compound when the process is saturated at concentrations attainable in the body. At this point, unlike with diffusion, drug flux across a membrane is no longer directly proportional to concentration as was described by Equation 2.1. This scenario is depicted in Fig. 2.6. In pharmacokinetic terminology, concentration dependence is termed linear or first-order and is an assumption made in most generally applicable pharmacokinetic models, be they compartmental, noncompartmental, physiological, or population based. When the telltale plateauing of a saturable process is detected, so called nonlinear or zero-order processes are involved, and specific models must be employed to handle them. The development of such models, which are also encountered in drug protein binding and biotransformation, will be introduced in the chapters discussing these concepts. The incorporation of these processes into pharmacokinetic models will be formally presented in Chapter 10 on nonlinear models.

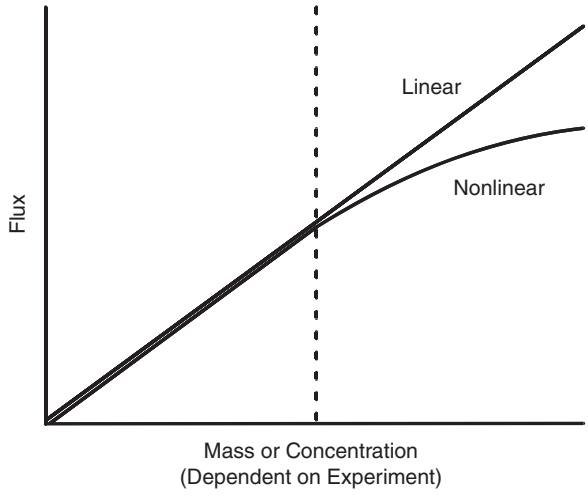

Fig. 2.6 Relationship of compound flux to concentration illustrating linear and nonlinear kinetics.

There are other transport processes important for certain drugs. Some membranes have pores or fenestrae, which allow filtration to occur. In these cases, relatively small molecules (molecular weights <1000) can pass through independent of their lipid solubility, but larger molecules are excluded. This phenomenon is very important in excretory processes. The primary route of excretion for most compounds is the kidney, which possesses just such a porous endothelium in its glomerular basement membrane. Thus, hydrophilic drugs in solution in the aqueous plasma are readily excreted into the glomerular filtrate. In addition, most capillaries in the body have "leaky" cell–cell junctions, which allow compounds in solution in the plasma to enter the extracellular fluids. However, unless inflammation is present, which increases capillary permeability, proteins are excluded.

In all of these scenarios, drugs move through these tissues as a solute dissolved in water and essentially are transported wherever the water goes. This process is termed bulk flow and is dependent on the concentration of drug dissolved in the plasma or tissue fluid. This is a linear process and thus is easily modeled by most pharmacokinetic systems. Exceptions are few (e.g., Donnan exclusion principle in glomerular filtration) and will be dealt with where appropriate. The only general exception that may affect the structure of some models is limitation of molecular size, which is generally encountered only in disposition of proteins, oligonucleotides, nanomaterials, or synthetic polymers.

In some tissues, cells may absorb drugs by endocytosis or macro- and micropinocytosis, processes in which a compound binds to the surface of the membrane, which then invaginates and interiorizes the compound through a number of diverse mechanisms. This is not a primary mechanism of transmembrane passage for most small therapeutic drugs; however, it could be important for proteins and nanomaterials. Such systems are well described for uptake into renal tubules (e.g., uptake of charged peptides and aminoglycoside antibiotics), but they are also present in a myriad of other cell types, including phagocytic cells as well as keratinocytes. There is a large literature developing on different mechanisms behind endocytosis, including clathrin-mediated and membrane raft systems (Ungewickell and Hinrichsen, 2007; Patel et al., 2008). Cell-penetrating peptides have been described that are capable of carrying small molecules to large protein complexes across membranes

relatively rapidly (minutes to hours) by processes not dependent on endocytosis (Zorko and Langel, 2005). Some of these systems are being targeted to facilitate cellular drug transport, and thus are being described by pharmacokinetic approaches.

Finally, most inorganic ions, such as sodium and chloride, are sufficiently small that they easily can cross aqueous membrane pores and channels. The movement of these charged substances is generally governed by the transmembrane electrical potential maintained by active ion pumps. Again, drugs and chemicals commonly modeled in pharmacokinetic studies do not have these properties and thus are not relevant to the scope of this text.

2.6 INTEGRATION OF MEMBRANE TRANSPORT CONCEPTS

The principles governing the translocation of drugs across membranes and distribution throughout the body are based on the physical-chemical properties of the drug, which affects its interactions with the molecular components of the body. From the perspective of pharmacokinetics, the major processes that determine drug absorption and disposition, and the ones that are quantitated using mathematical models, are related to the mass movement of drugs across biological barriers. Energy is required to move any chemical across these barriers. This energy is usually related to a physical-chemical concept called thermodynamic activity, which reflects the energy ultimately responsible for moving a compound across membranes via diffusion or bulk flow. This holds for most processes (except those mediated by active biological pumps) encountered in pharmacokinetics that are responsible for movement of drugs into, through, and out of the body.

The best way to increase or create diffusion-driven transport is to create a concentration gradient, or increase the potential energy by creating a large driving force on only one side of a membrane. This can be accomplished by increasing dose or by asymmetrical mechanisms such as ion trapping, which produce the same result. Whatever the source, most linear pharmacokinetic processes are driven by concentration gradients ultimately related to the administered dose.

It is the nature and relative rate of drug movements across these membranes, and drug distribution in the spaces defined by these multiple barriers, that provide for the subtle changes in drug concentration that allow pharmacokinetic models to be constructed. As will be developed in later chapters, differences in the rate and extent of drug movement across different barriers (natural or synthetic as in the case of slow-release drug delivery formulations) allow models to be constructed that provide mathematical links to these events and thus give one the ability to predict the concentration achieved over time after administering specific doses.

A crucial concept related to dose available for membrane uptake versus actual transport relates to the relative rate of drug delivery to a tissue and its permeability across the tissue. Fig. 2.7 illustrates the two extremes possible in this scenario, one where membrane permeability is high but delivery is low and the second where delivery is high but membrane permeability is low. These scenarios are respectively termed “perfusion limited” versus “permeability limited.” Permeability-limited uptake occurs when multiple membranes are encountered or when more hydrophilic drugs not capable of diffusing through a lipid membrane are studied. Perfusion-limited uptake is often seen in areas of low blood perfusion or when high rates of drug transport occur through active transport systems. These phenomena will be revisited when discussing intestinal drug absorption, hepatic elimination, and in building physiological-based pharmacokinetic models.

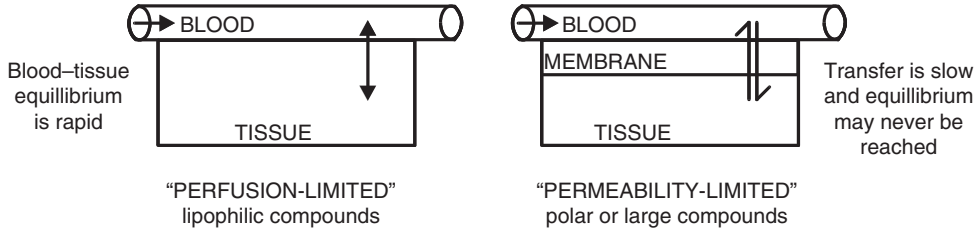

Fig. 2.7 Permeability- versus perfusion rate-limited processes.

In conclusion, an understanding of the processes that govern the movement of drugs across lipid-based biological membranes is important to the study of drug absorption, distribution, and excretion. Lipid-soluble drugs are easily absorbed into the body and well distributed throughout the tissues. In contrast, hydrophilic drugs are not well absorbed but are easily eliminated. If membranes separate areas of different pH levels, concentration gradients may form due to pH partitioning or ion trapping. The precise nature of the kinetic models needed to describe trafficking of a compound across a membrane will be dependent on the specific mechanism of transport (diffusion, active, pore, endocytosis). All of these principles will be repeatedly encountered in the study of drug disposition presented in the remaining chapters of this text.

BIBLIOGRAPHY

Alberts, B., Bray, D., Lewis, J., Raff, M., Roberts, K., and Watson, J.D. 1989. *Molecular Biology of the Cell*, 2nd Ed. New York: Garland Publishing Co.

Brodie, B.B., Gillette, J.R., and Ackerman, H.S. 1971. *Handbook of Experimental Pharmacology, Vol. 28, Part I, Concepts in Biochemical Pharmacology*. Berlin: Springer.

Davson, H., and Danielli, J.F. 1952. *Permeability of Natural Membranes*, 2nd Ed. London: Cambridge University Press.

Engelman, D.M. 2005. Membranes are more mosaic than fluid. *Nature*. 438:578–580.

Patel, H.H., Murray, F., and Insel, P.A. 2008. Caveolae as organizers of pharmacologically relevant signal transduction molecules. *Annual Review of Pharmacology and Toxicology*. 48:359–391.

Pratt, W.B., and Taylor, P. 1990. *Principles of Drug Action*, 3rd Ed. New York: Churchill Livingstone.

Singer, S.J., and Nicholson, G.L. 1972. The fluid mosaic model of the structure of cell membranes. *Science*. 175:720–731.

Ungewickell, E.J., and Hinrichsen, L. 2007. Endocytosis: clathrin-mediated membrane budding. *Current Opinion Cell Biology*. 19:417–425.

Zorko, M., and Langel, U. 2005. Cell-penetrating peptides: mechanism and kinetics of cargo delivery. *Advanced Drug Delivery Reviews*. 57:529–545.

3 Quantitative Structure–Permeability Relationships

with Xin-Rui Xia

The transport of drug molecules across various biological membranes is an essential biological process governing their pharmacokinetic properties. As developed in the previous chapter and illustrated in Fig. 2.2, a drug must cross several semipermeable membranes in its journey through the body. In the process of absorption through skin or the gastrointestinal tract, distribution to different organ tissues, and during elimination through excretory organs, drugs must cross membranes.

Since membrane transport is central to all pharmacokinetic models, this chapter will use this phenomenon as an example of how mathematical models can be applied to analyze biological data. In the process, the reader will also become more familiar with basic modeling techniques that will be applied throughout the text, as well as better understand the molecular determinants of chemical transport through membranes.

The ability of a molecule to pass through a membrane is described by its permeability. The membrane permeability is determined by the physicochemical properties of the drug and the physicochemical and biological properties of the membrane. As illustrated in Figs. 2.3 and 2.5, biological membranes are composed primarily of a lipid matrix. Various globular proteins may embed in the matrix and function as transporters across the membrane. These physicochemical and biological factors govern the membrane permeability characteristics. Drugs may cross biological membranes by passive diffusion, facilitated passive diffusion, or active transport.

As we have learned in Chapter 2, passive diffusion is a universal transport mechanism for all molecules, drugs or toxins alike, describing the substances moving/diffusing from a more concentrated environment to a less concentrated environment. Equation 2.1 demonstrated that the driving force of passive transport is the concentration gradient ($X_1 - X_2$ or ΔX), allowing drugs to diffuse across a biological membrane from a compartment of high to low concentration. Diffusion rate is directly proportional to this gradient, but it also depends on the physicochemical properties of the substance (lipophilic or hydrophilic, neutral or ionizable), the physicochemical and biological properties of the membrane, its thickness (h), and the area of absorptive surface. The properties of this *drug–membrane system* is reflected in the value of the diffusion coefficient (D) and partition coefficient (P), specific for the drug–membrane being modeled.

Because the biological membrane is lipoidal, lipid-soluble drugs diffuse most rapidly. Small molecules tend to penetrate membranes more rapidly than larger ones. Many drugs

Comparative Pharmacokinetics: Principles, Techniques, and Applications, Second Edition. Jim E. Riviere.
 ISBN: 978-0-813-82993-7

are weak organic acids or bases, which could dissociate to ionic forms in an aqueous environment. The ratio of ionized and neutral forms is dependent on the pH of the environment, and can be quantitated using the Henderson–Hasslebach equations (Eqs. 2.2 and 2.3) previously presented in Chapter 2. Recall that the neutral form is usually lipid soluble (lipophilic) and diffuses readily across biological membranes, while the ionized form is prohibited from transport across the lipid membrane. Depending on structural characteristics and physicochemical properties, other molecules may be transported by one of the other molecular-mediated transport systems discussed. For the purpose of our discussion, we will restrict our focus to passive diffusion to illustrate how these physicochemical properties that determine membrane permeability can be described and quantitated using quantitative structure–permeability relationships (QSPeRs).

As presented in Chapter 2, Fick's law of diffusion at steady state (Eq. 2.1) can be rewritten in terms of the permeability coefficient (K_p) that characterizes the membrane permeability:

$$K_p = (D \cdot P)/h. \tag{3.1}$$

When the steady-state flux (J_{ss}) at donor concentration (C_d) and receptor concentration (C_r) across a membrane of area (A) are measured experimentally, the permeability coefficient can be obtained as

$$K_p = J_{ss}/[(C_d - C_r)A]. \tag{3.2}$$

Chapter 4 will present the experimental techniques used to determine K_p across gastrointestinal (Fig. 4.4) and skin (Fig. 4.11) membranes. The permeability coefficient is the primary quantitative measure of membrane permeability, and as will be extensively developed in Chapter 8, forms the basis of first-order linear rate constants used in pharmacokinetic modeling.

The problem is that determination of K_p for all drugs and chemicals in all membrane systems across multiple species is overwhelming from an experimental perspective. *Experimental measurement of permeability is a time-consuming and costly practice. The throughput of experimental measurements is limited and requires that analytical techniques be available for all matrices.* A solution to this dilemma is to use QSPeR to predict K_p's based on fundamental physicochemical properties.

The European Union has formally acknowledged this by establishing the REACH (Registration, Evaluation and Authorisation of Chemicals, EC1907/2006) program, which is based on developing robust quantitative structure–activity relationships (QSARs) to predict the absorption, distribution, metabolism, and elimination (ADME) properties that form the basis of pharmacokinetic practice. QSPeR is a subset of QSAR models focused on determining membrane permeability coefficients. REACH has accelerated research in this area. In addition to the regulatory benefits and potential to drastically decrease animal usage, QSPeR studies have taught us about the physicochemical determinants of membrane permeability. It allows us to probe anatomical and species differences in K_p as a function of chemical properties such as molecular weight (MW), charge, and solubility. This forms the basis for developing more mechanistic models of drug disposition based on basic molecular properties.

The QSPeR approach has been applied in many disciplines, including drug discovery and occupational and environmental risk assessment. QSPeR modeling, first widely practiced by Hansch in the 1970s, is extensively used to predict the membrane permeability of

chemicals and toxins in different matrices (pharmaceuticals, cosmetics, and occupational and environmental media) in risk assessment. In drug discovery and development process, QSPeR is used by pharmaceutical companies to predict membrane permeability and bioavailability of new drug candidates. If the candidate agents are predicted to lack the desired pharmacokinetic properties, the agents could be eliminated from further costly clinical experiments. Combinatorial library design often uses diversity analysis and QSPeR to select chemicals for synthesis and testing. The predictive model could provide critical information in the chemical library design–combinatorial synthesis–high-throughput screening (HTS) cycle. Data culminating from the HTS assays are then available to build more robust QSPeR models that can be used to guide more refined lead discovery, optimization, and development.

The techniques to be briefly overviewed in this chapter are also applicable to link drug and chemical molecular properties to other pharmacokinetic and pharmacodynamic parameters developed throughout the remainder of this text.

3.1 QSPeR MODELING

QSPeR modeling is an attempt to correlate structural or chemical property descriptors of compounds with the membrane permeability of the compounds. After the permeability coefficients of a number of compounds (n) have been experimentally measured for a specific membrane, a quantitative relationship between the membrane permeability and the physicochemical descriptors of the compounds can be established via QSPeR modeling. Once a QSPeR model is established and validated, it can be used to predict the membrane permeability for new compounds.

The fundamental assumption of QSPeR is that variations in the membrane permeability of a series of chemicals sharing a common transport mechanism are correlated with variations in their structural and physicochemical properties. These physicochemical descriptors accounting for hydrophobicity, topology, electronic properties, and steric effects can be obtained from experimental measurement, empirical derivation, or computation. Several sets of molecular descriptors have been developed that can be used for QSPeR model development (Karelson, 2000). A validated predictive model can be used to predict the membrane permeability of new chemicals to save substantial time, money, and human resources in lieu of the time-consuming and labor-intensive processes of chemical synthesis and subsequent biological evaluation. However, QSPeR modeling cannot exist in isolation of real-world data. It is developed from experimental data, and must be validated with experimental data. QSPeR modeling coupled to experimental measurements form a synergistic relationship. One does not replace the other. QSPeR provides direction for more effective experimental measurements; in turn, the new experimental data can be used to develop new models or refine original models.

There are four steps in QSPeR model development:

1. Collection of experimental data
2. Selection of molecular descriptors that can properly relate chemical structure to the membrane permeability of interest
3. Application of statistical methods that correlate changes in structure with changes in permeability
4. Model validation

3.1.1 Data collection

For predictive model development, K_p data should ideally come from the same experimental assay protocol, and care should be taken to avoid interlaboratory variability. This is one of the primary challenges facing development of precise QSPeR models, and is a major issue when these techniques are applied to veterinary medicine.

At present, most model development depends on data mining. Much data have been generated over decades of scientific research, with much of this data never having been fully utilized. Development of computer-based computational programs, coupled with the expansion of the Internet and availability of powerful search engines, now make data mining more productive. Many data sets have already been published in review and QSAR manuscripts, books, and databases, allowing them to be incorporated into QSPeR analyses.

The quality of data is crucial for successful QSPeR model development. If possible, data should come from the same assay protocol so that individual laboratory variability is not a factor. Measurement errors could be introduced in many experimental procedures, particularly when animals and biological samples are involved. Variations brought into the data set by the use of measurements from different laboratories across different animals and protocols increases experimental error and decrease the statistical validity of the model. These issues are fully developed in Chapters 14, 15, and 16 from the perspective of pharmacokinetic modeling. They are just as applicable to QSPeR studies.

An example of a well-studied QSPeR data set is that of 97 permeability coefficients for 94 compounds collected *in vitro* through human skin, gathered by Flynn in 1990. This provided the first large database of skin permeability values measured in a single species. These data were a compilation from 15 different literature sources. These data are expected to contain a high degree of experimental error due to interlaboratory variability, particularly variability arising from the use of skin from different sources and location on the body. In attempts to develop QSPeR models using the data set, steroids were considered outliers and not included in the predictive model developments (Potts and Guy, 1992; Cronin et al., 1999). It was postulated that the steroids may penetrate the skin by a different mechanism from other molecules. A more recent study (Johnson et al., 1995) indicated that the steroid data in Flynn's data set were substantially different from those found in a range of other literature sources, and concluded that they may be erroneous. Moss and Cronin (2002) reanalyzed the refined database by replacing erroneous steroid data with new data (Johnson et al., 1995; Degim et al., 1998) and obtained a QSPeR model with improved statistical correlation. This data set, now consisting of 119 compounds with K_p, log octanol/water partition coefficient (log $K_{o/w}$), and MW was used here to illustrate QSPeR model development.

3.1.2 Descriptor selection

The predictivity of a QSPeR model is dependent not only on the original data set but also on how well the selected molecular descriptors can encode the variation of the biological activity of the membrane system being studied with chemical structure. Knowing the transport mechanisms at the molecular level is the key to select among the wide variety and types of specific molecular descriptors. Many types of chemical structure descriptors are available from commercial software packages which often also include statistical tools to help in evaluating which descriptors best encode structure–activity variation.

For the skin penetration data set, the primary barrier to absorption is the stratum corneum, which for the purpose of this QSPeR exercise is a lipid membrane. The reader

should consult Chapter 4 and Figs. 4.5 and 4.6 for a more extensive biological description of the skin barrier. For the present demonstration of the QSPeR model development, Equation 3.1 relates K_p to partition coefficient and diffusivity. The two major molecular descriptors that will be used in the following analysis are the log $K_{o/w}$, representing a hydrophobicity descriptor predictive of the partition coefficient into a lipid membrane, and MW, representing the molecular size descriptor that modulates diffusivity. The log $K_{o/w}$ could be considered a surrogate metric for a skin partition coefficient.

3.1.3 Statistical methods

A statistical method is used to establish a quantitative relationship between the collected data and molecular descriptors. Although the relationship between a molecular descriptor and biological activity may be linear or nonlinear, it remains common practice to use linear approaches such as multiple linear regression (MLR) or partial least squares (PLS) regression analysis to construct the QSPeR model. For nonlinear modeling, the polynomial neural network (PNN) offers an alternative that combines the best features of artificial neural networks (ANNs) and MLR/PLS by providing the inherent nonlinearity of the ANN with the desired analytical regression equation furnished by MLR and PLS (Tetko et al., 2000). The selection of a statistical method is dependent on the complexity of the transport mechanisms, data availability, and molecular descriptor selection. These decisions would ultimately determine the application range of the established model and prediction robustness of the model. (Chapter 14 can be consulted for application of regression analyses to pharmacokinetic modeling; however, unlike QSPeR studies, pharmacokinetic models are constrained by the type of mathematical functions used [e.g., polyexponentials], and thus the range of techniques available are likewise reduced.)

When MLR analysis was used to analyze the skin permeability data using log $K_{o/w}$ and MW as descriptors, a quantitative correlation was established as follows:

$$\text{Log}\,(K_p)_i = a(\log\ K_{o/w})_i + b(\text{MW})_i + c;\ i = 1,2,3,\ldots,n \tag{3.3}$$

where a, b, and c are the regression coefficients obtained from the regression analysis; $(K_p)_i$, $(\log\ K_{o/w})_i$, and $(\text{MW})_i$ are the skin permeability, octanol/water partition coefficient, and MW of the i^{th} compounds, respectively; and n is the number of compounds.

The data set was divided into a training set and external validation set following random selection through activity sampling as described below. The skin permeability model established from the database was

$$\text{Log}\,K_p = 0.75\ \log\ K_{o/w} - 0.0089\ \text{MW} - 2.47 \tag{3.4}$$
$$(n = 86,\ R^2 = 0.84,\ F = 210;\ Q^2_{\text{LOO}} = 0.82,\ Q^2_{\text{LMO25\%}} = 0.82).$$

Fig. 3.1 illustrates the observed versus predicted K_p. The statistical goodness-of-fit parameters used to describe this model are introduced and described in detail below.

3.1.4 Model validation

In QSPeR model development, it is critical to insure that any model developed is applicable to a broad-based data set. Any model has its own restricted application ranges depending on the original data, its molecular descriptors, and the statistical methods used.

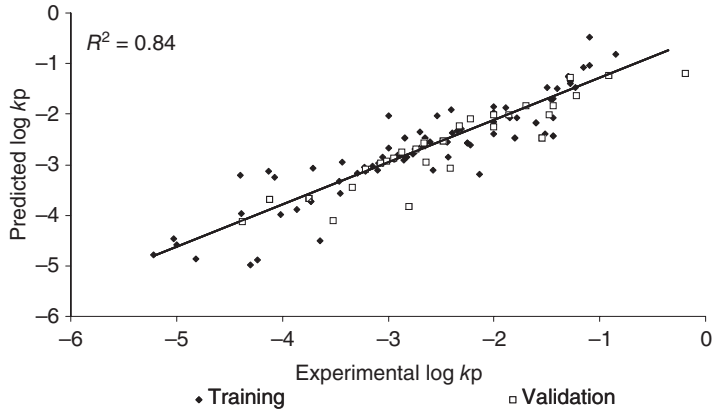

Fig. 3.1 Regression plot of experimental versus predicted log K_p in skin.

The goodness of fit of a model is measured by the coefficient of determination, R^2, which is the most widely used measure of the ability of a QSPeR model to fit the data in the training set. The *F*-test provides a measure of statistical significance of the regression function. (See Chapter 14 and Equations 14.5 and 14.6 for a definition of these statistics and a further perspective on curve fitting.) In regression, the R^2 coefficient of determination is a statistical measure of how well the regression line approximates the real data points. An R^2 of 1.0 indicates that the regression line perfectly fits the data. The R^2 does not tell us about the robustness and predictivity of the model applied to other chemicals.

There are several approaches to estimate model predictivity using internal validation. Cross-validation metrics are the most commonly used technique. They are a statistical method in which different proportions of chemicals are iteratively removed from the training set used for model development and then "predicted" as new values by the model developed using this reduced set. This verifies "internal predictivity." Parameters used include Q^2_{LOO} (leave-one-out), Q^2_{LMO} (leave-many-out), or the $Q^2_{\mathrm{LMO25\%}}$ or Q^2_{25} (leave-a-random 25%-out).

The value of Q^2 is derived from a cross-validation procedure in which a fraction of chemicals in the training set are excluded and then predicted by the model generated from the remaining chemicals. When each chemical is left out one at a time and the process repeated for each chemical, this is known as leave-one-out (LOO) cross-validation. If many of the training compounds are left out (e.g., 25% of the compounds are left out), the process is known as leave-many-out (LMO) cross-validation. Both LOO and LMO methods test the stability of the model through perturbation of the regression coefficients by consecutively omitting chemicals during the model generation procedure. LMO cross-validation is stronger than LOO cross-validation. It is suggested that internal cross-validations with $Q^2_{\mathrm{LOO}} > 0.7$ indicate models with high robustness and internal predictive ability (Gramatica, 2007). However, this internal validation criterion is only a necessary condition, but not a sufficient condition, for robustness and predictivity of the model against new external chemicals that have not been used in the training set. It could give an overly optimistic estimate of model predictivity for some external chemicals.

For the skin permeability data set, after removal of the outliers, the internal cross-validation output was $Q^2_{\mathrm{LOO}} = 0.82$ and $Q^2_{\mathrm{LMO25\%}} = 0.82$. Both of the Q^2_{LOO} and $Q^2_{\mathrm{LMO25\%}}$

values are higher than 0.7, indicating that the predictive model Equation 3.4 is robust for internal prediction.

3.1.5 External validation

Even if the model is validated as high quality by internal cross-validation, uncertainty will remain regarding its ability to predict chemicals not in the training set. To address this question, external validation data sets are required. The external cross-validation can be conducted in two distinct approaches: using new experimental data or splitting the data set.

3.1.5.1 *External validation using new experimental measurement data*

The most straightforward method is to validate the developed predictive model using a new set of experimental data. After the predictive model is established, new experiments are conducted for a new set of validation compounds under the same experimental protocols from which the training data set was generated. The new data is then used to cross-validate the predictive model. This ideal approach requires high-throughput methods to provide high-quality data.

3.1.5.2 *Data set splitting approach*

In current practice, it is difficult to obtain a new set of data for external cross-validation due to the limited throughput of experimental methods. An alternative data set splitting approach is commonly used in the absence of additional experimental data. This approach is to split the original data set into training set and validation set before the model development phase; the training set will be used for model development and the validation set will be used for external cross-validation. This splitting approach is appreciated because the validation set has never been used for model development and is therefore considered external compounds.

How to split the original data set into training set and validation set is of crucial importance. The best splitting must guarantee that the training and validation sets are scattered over the whole area occupied by representative points in the descriptor space (representative activity) and that the training set is distributed over the entire area occupied by representative points for the whole data set (diversity). A widely used splitting method is the random selection through activity sampling, in which all compounds in the original data set are ordered in descending values of the biological activity (Gramatica et al., 2007). The two compounds having the highest and lowest values are selected and every fourth compound is selected as the validation set. This splitting ensures that 25% of the total data set is used as a validation set and the rest of the compounds are used as the training set. The splitting could be performed using more advanced methodologies based on similarity analysis (e.g., D-optimal distance, Kohonen map—ANN or self-organizing map) (Gramatica, 2007).

This curve-fitting approach used in chemical structure-based QSPeR is very different from the approach used to model individual animal pharmacokinetic data presented throughout the rest of this text since all concentration–time data points are generally used in a pharmacokinetic analysis. However, as will be developed in Chapter 16 when population models are introduced, training and external validation data sets are used when large populations of individual data are available.

The predictive power of the regression model developed on the selected training set is estimated on the predicted values of prediction set chemicals by the external Q^2 that is defined as (Cramer et al., 1988):

$$Q^2_{\text{ext}} = 1 - \frac{\sum_{i=1}^{i=29} (y_i - \hat{y}_i)^2}{\sum_{i=1}^{i=29} (y_i - \overline{y}_{\text{tr}})^2}, \tag{3.5}$$

where y_i and $\hat{y}_i$ are measured log K_p values and the predicted log K_p values by Equation 3.4 of the 29 external validation compounds, and $\overline{y}_{\text{tr}}$ the averaged value of the measured log K_p values of the training probe compounds; the summations cover all the 29 validation compounds. The $Q^2_{\text{ext}} = 0.823$ for the skin permeability model revealed that the predictive model (Eq. 3.4) has robust predictivity for external compounds.

3.2 APPLICABILITY DOMAIN

The final step in a formal QSPeR modeling exercise is the definition of the applicability domain of a QSPeR model. Even a robust, significant, and validated QSPeR model cannot be expected to reliably predict the modeled property for the entire universe of chemicals. In fact, only the predictions for chemicals falling within a chemical-space domain defined by the training set of chemicals used to define the QSPeR model could be considered reliable. The applicability domain is a theoretical region in chemical space, defined by the model descriptors and modeled response, constrained by the nature of the chemicals in the training set. Extrapolation beyond this applicability domain should not be considered reliable.

The general discussion of inference space and interpolation versus extrapolation in Chapter 1, illustrated in Fig. 1.2, should be revisited. The application of these terms to QSPeR analysis is parallel but more complex since multiple molecular descriptors define a multidimensional applicability domain in a QSPeR analysis, rather than the two-dimensional inference space (defined simply by time and concentration) in a pharmacokinetic analysis. In reality, all mathematical, and thus pharmacokinetic, models have this constraint since their use is restricted to the nature of the data used to define them.

A leverage approach is used to verify whether a new chemical will lie within the structural model domain or outside the domain (Atkinson, 1985). The Williams plot can be used to visualize the applicable domain of a QSAR model, which is a plot of standardized cross-validated residuals (R) versus leverage (Hat diagonal) values (h). Compounds with cross-validated standardized residuals greater than three standard deviation units ($>3\sigma$) are considered as outliers. Prediction should be considered unreliable for compounds having leverage values higher than a critical leverage value (i.e., $h > h^*$), the critical value being $h^* = 3(m + 1)/n$, where m is the number of variables in the model and n is the number of compounds in the training set. When the leverage value of a compound is lower than the critical value, the prediction is reliable. Thus, the applicability domain is defined as $0 - h^*$ (x-axis) and $\pm 3\sigma$ (y-axis).

One of the important applications of the applicability domain is to identify outliers and high-leverage compounds in the data set. Taking the skin permeability data set as an example, the original data set has 119 compounds; after splitting, the training set has 88

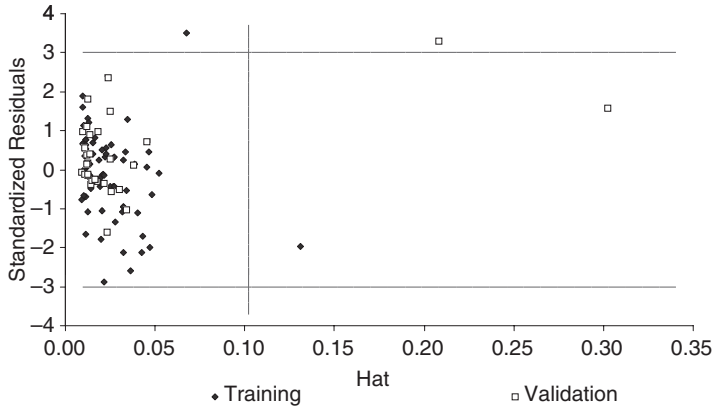

Fig. 3.2 Williams plot showing applicability domain for QSPeR model.

compounds and the validation set has 31 compounds. The Williams plot defined by the data set is given in Fig. 3.2. It shows that there are two outliers (one in the training set and one in the validation set) having standardized residuals higher than 3, and there are two high-leverage compounds having a leverage higher than 0.102 (one in the training set and one in the validation set). These outliers and high-leverage compounds can be removed from the data set for model development, resulting in a training set of 86 and validation set of 29 compounds used in the previous analysis.

3.3 OTHER MODELS AND APPLICATIONS

The focus of this chapter was to briefly introduce the reader to QSPeR analysis as an example of how pharmacokinetic parameters that will be developed in future chapters can be correlated to physical chemical properties. It is also the technique used to define physicochemical determinants of specific rate processes. Finally, it also nicely illustrates an application of mathematical modeling to a well-defined problem in biological membrane transport.

Relative to skin, there have been a number of more complex QSPeR models applied to predict K_p that provide for a richer range of molecular diversity and potential membrane interactions. A widely used model in both skin and other biological membrane transport (e.g., distribution) is the linear free energy relationship developed by Abraham and Martins (2004) expressed as

$$\text{Log}\, K_p = c + a\Sigma\alpha_2^H + b\Sigma\beta_2^H + s\pi_2^H + rR_2 + vV_x, \tag{3.6}$$

where $\Sigma\alpha_2^H$ is the hydrogen bond donor acidity, $\Sigma\beta_2^H$ is the hydrogen bond acceptor basicity, π_2^H is dipolarity/polarizability, R_2 represents the excess molar refractivity, and V_x is the McGowan volume. The parameters a, b, s, r, and v are strength coefficients coupling the molecular descriptors of each chemical to skin permeability in a specific experimental system (e.g., skin, vehicle or formulation), reflecting stratum corneum interactions. The predictability of drug penetration through skin is much better using this type of model than those parameterized solely with log $K_{o/w}$ and MW.

Our laboratory also explored methods to assess how formulation or vehicles affect K_p (Riviere and Brooks, 2005, 2007). In the discussion to this point, we have defined K_p specifically for a molecule in a specific experimental system. The skin K_p data used above was defined using water as a vehicle. However, most environmental and occupational exposures occur in complex chemical mixtures, and all topical drugs are formulated in vehicles. As can be seen in Fig. 3.3a, when the model in Equation 3.2 was fit to pig skin, vertical

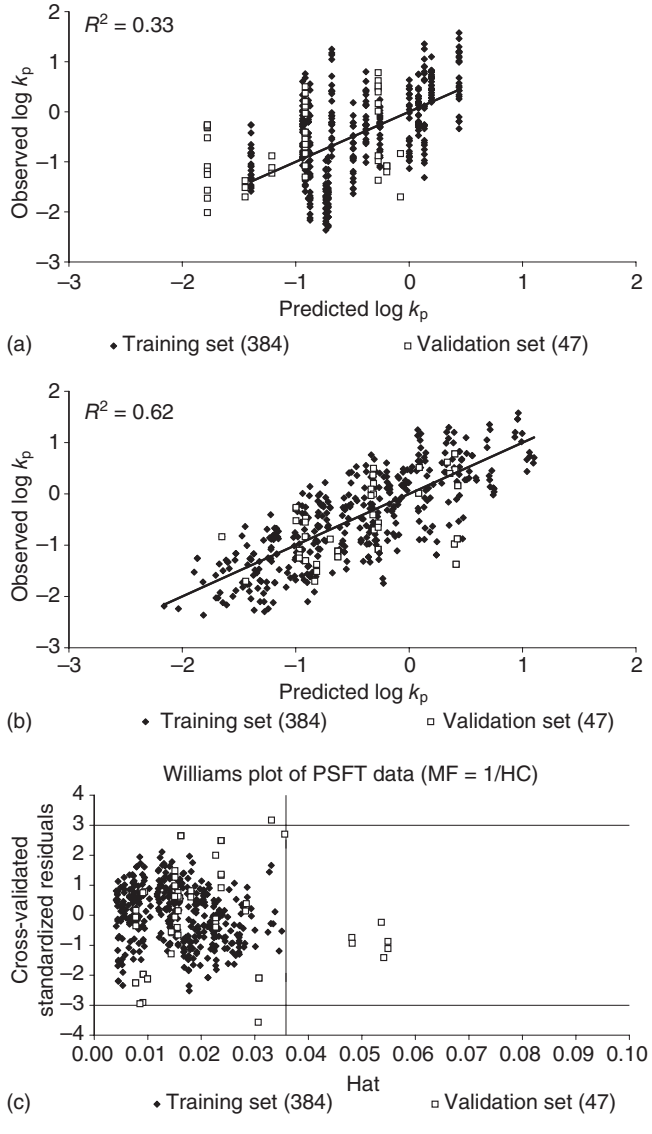

Fig. 3.3 Predicted versus observed K_p of a series of chemicals in porcine skin administered in different vehicles. QSPeR models: (a) ignoring applied vehicle; (b) taking into account vehicle composition using a mixture factor; and (c) the applicability domain for model with mixture factor. Note that in this example, a number of treatments in the validation set are outside of the applicability domain (c), suggesting that prediction of their behavior should not be attempted using this model. PSFT, porcine skin flow-through diffusion cell; MF, mixture factor.

columns arise, which are related to vehicle effects not accounted for in the QSPeR model. When a mixture factor is computed to account for the application vehicle, an improved fit results as seen in Fig. 3.3b. The applicability domain for this model is also depicted in Fig. 3.3c. In this case, a number of compounds in the validation set fall outside of the applicability domain.

A great deal of work has been done on QSPeR analyses of gastrointestinal permeability. In fact, QSPeR models were used to define drug properties needed for efficient absorption that will be presented in Chapter 4. "Lipinsky's rule of five," defining the properties needed for oral absorption, is the result of a QSPeR analyses. Finally, this chapter has focused on using QSPeR models as illustrative of the QSAR process in general since membrane transport is central to pharmacokinetic modeling. However, QSAR is a much broader discipline and has been used to relate a wide variety of molecular properties to a number of biological end points including drug receptor binding and activity, chemical and drug toxicity, and drug interaction with all levels of the genome. We have recently applied a QSAR approach to define the potential biological activity of the surface of diverse nanoparticles to predict subsequent interactions of a nanoparticle with the body (Xia et al., 2010).

QSPeR analysis shows the power of using mathematical models to probe interactions between drugs and biological systems. The focus of pharmacokinetics is to analyze animal systems in order to generate quantitative metrics that can be used to predict drug disposition in the body or define a drug–animal interaction so tools such as QSPeR can be used to relate them to fundamental chemical properties.

BIBLIOGRAPHY

Abraham, M.H. 1993. Scales of solute hydrogen-bonding: their construction and application to physicochemical and biochemical processes. *Chemical Society Review*. 22:73–83.

Abraham, M., and Martins, F. 2004. Human skin permeation and partitioning: general linear free energy relationship analysis. *Journal of Pharmaceutical Sciences*. 93:1508–1523.

Atkinson, A.C. 1985. *Plots, Transformations and Regression*. Oxford: Clarendon Press.

Cramer, R.D., Patterson, D.E., and Bunce, J.D. 1988. Comparative molecular field analysis (CoMFA). 1. Effect of shape on binding of steroids to carrier proteins. *Journal of the American Chemical Society*. 110:5959–5967.

Cronin, M.T.D., Dearden, J.C., Moss, G.P., and Murray-Dickson, G. 1999. Investigation of the mechanism of flux across human skin in vitro by quantitative structure–permeability relationships. *European Journal of Pharmaceutical Sciences*. 7:325–330.

Degim, I.T., Pugh, W.J., and Hadgraft, J. 1998. Skin permeability data: anomalous results. *International Journal of Pharmaceutics*. 170:129–133.

Ette, E.I., and Williams, P.J. 2007. *Pharmacometrics: The Science of Quantitative Pharmacology*. Hoboken, NJ: Wiley.

Flynn, G.L. 1990. Physicochemical determinants of skin absorption. In: Gerrity, T.R., and Henry, C.J. (eds.), *Principles of Route-to-Route Extrapolation for Risk Assessment*. New York: Elsevier, pp. 93–127.

Gramatica, P. 2007. Principles of QSAR models validation: internal and external. *QSAR Combinatorial Science*. 26:694–701.

Gramatica, P., Giani, E., and Papa, E. 2007. Statistical external validation and consensus modeling: a QSPR case study for Koc prediction. *Journal of Molecular Graphing and Modelling*. 25:755–766.

Hansch, C., and Dunn, W.J. 1972. Linear relationships between lipophilic character and biological activity of drugs. *Journal of Pharmaceutical Sciences*. 61:1–19.

Johnson, M., and Maggiora, G.M. 1990. *Concepts and Applications of Molecular Similarity*. New York: John Wiley & Sons.

Johnson, M.E., Blankschtein, D., and Langer, R. 1995. Permeation of steroids through human skin. *Journal of Pharmaceutical Sciences*. 84:1144–1146.

Karelson, M. 2000. *Molecular Descriptors in QSAR/QSPR*. New York: John Wiley & Sons.

Moss, G.P., and Cronin, M.T.D. 2002. Quantitative structure–permeability relationships for percutaneous absorption: re-analysis of steroid data. *International Journal of Pharmaceutics*. 238:105–109.

Perkins, R., Fang, H., Tong, W., and Welsh, W.J. 2003. Quantitative structure-activity relationship methods: perspectives on drug discovery and toxicology. *Environmental Toxicology and Chemistry*. 22:1666–1679.

Potts, R.O., and Guy, R.H. 1992. Predicting skin permeability. *Pharmaceutical Research*. 9:663–669.

Potts, R.O., and Guy, R.H. 1995. A predictive algorithm for skin permeability: the effects of molecular size and hydrogen bond activity. *Pharmaceutical Research*. 12:1628–1633.

Riviere, J.E., and Brooks, J.D. 2005. Predicting skin permeability from complex chemical mixtures. *Toxicology and Applied Pharmacology*. 208:99–110.

Riviere, J.E., and Brooks, J.D. 2007. Prediction of dermal absorption from complex chemical mixtures: incorporation of vehicle effects and interactions into a QSPR framework. *SAR and QSAR Environmental Research*. 18:31–44.

Tetko, I.V., Aksenova, T.I., Volkovich, V.V., Kasheva, T.N., Filipov, D.V., Welsh, W.J., Livingstone, D.J., and Villa, A.E.P. 2000. Polynomial neural network for linear and nonlinear model selection in quantitative- structure activity relationship studies on the Internet. *SAR QSAR Environmental Research*. 11:263–280.

Vijay, V., Baynes, R.E., Young, S.S., and Riviere, J.E. 2010. Selection of appropriate training sets of chemicals for modeling dermal permeability using uniform coverage design. *QSAR Combinatorial Science*. 28:1478–1486.

Xia, X.R., Baynes, R.E., Monteiro-Riviere, N.A., and Riviere, J.E. 2007. A system coefficient approach for quantitative assessment of the solvent effects on membrane absorption from chemical mixtures. *SAR and QSAR Environmental Research*. 18:579–593.

Xia, X.R., Monteiro-Riviere, N.A., and Riviere, J.E. 2010. An index for characterization of nanomaterials in biological systems. *Nature Nanotechnology*. 5:671–675.

4 Absorption

Absorption is the movement of drug from the site of administration into the blood. There are a number of methods available for administering drugs to animals. The primary routes of drug absorption from environmental exposure in mammals are gastrointestinal, dermal, and respiratory. The first two are also used as routes of drug administration for systemic effects, with additional routes including intramuscular (IM), subcutaneous (SC), or intraperitoneal injection, as well as intravenous administration. Other variations on gastrointestinal absorption include intrarumenal, sublingual, and rectal drug delivery. Many techniques are available for localized therapy, which may result in systemic drug absorption as a side effect. Among others, these include topical, intramammary, intra-articular, subconjunctival, and spinal fluid injections.

4.1 GASTROINTESTINAL ABSORPTION

One of the primary routes of drug administration is oral ingestion of a pill or tablet that is designed for drug delivery to cross the gastrointestinal mucosa. The common factor in all forms of oral drug administration is the delivery of a drug such that it gets into solution in the gastrointestinal fluids, from which it can then be absorbed across the mucosa and ultimately reach the submucosal capillaries and the systemic circulation. Examples of oral drug delivery systems include solutions (aqueous solutions, elixirs) and suspensions, pills, tablets, boluses for food animals, capsules, pellets, and sustained-release mechanical devices for ruminants.

The major obstacle encountered in comparative and veterinary medicine is the enormous interspecies diversity in comparative gastrointestinal anatomy and physiology, which results in major species differences in strategies for and efficiency of oral drug administration. This is often appreciated but overlooked when laboratory animal data are extrapolated to humans. Rats and rabbits are widely utilized in preclinical disposition and toxicology studies, although many investigators fail to appreciate that these animals' gastrointestinal tracts are very different from one another and from those of humans and common veterinary species.

From a pharmacologist's perspective, the gastrointestinal tract of all species can be simply presented as diagrammed in Fig. 4.1. As discussed in Chapter 2, the gastrointestinal tract is

Comparative Pharmacokinetics: Principles, Techniques, and Applications, Second Edition. Jim E. Riviere.
 ISBN: 978-0-813-82993-7

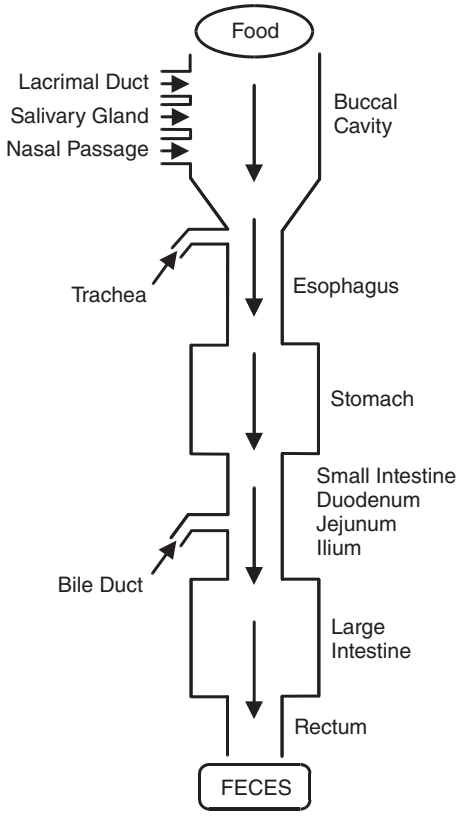

Fig. 4.1 Functional structure of the gastrointestinal tract.

best conceptualized as actually being part of the external environment, which, in contrast to the skin, is protected and whose microenvironment is closely regulated by the organism. Because of its central role in digestion and nutrient absorption, there are many evolutionary adaptations to this basically simple mucosa structure that allow for physical, chemical, enzymatic, and microbial breakdown of potential food for liberation and ultimate absorption of nutrients. This tract is further adapted such that these digestive processes do not harm the organism's own tissues, which in carnivores may be identical to the food being eaten.

The gastrointestinal tract presents a significant degree of heterogeneity relative to morphology and physiology, which translates to great regional variations in drug absorption. In the oral cavity, where food is masticated, some absorption may occur in sublingual areas. In fact, this site is actually utilized as a route for systemic drug (e.g., nitroglycerin) and nicotine (e.g., oral tobacco) delivery. The esophagus and cranial portion of the stomach is lined by cornified epithelium, which provides an effective barrier and often decreases the chance of absorption for drugs formulated for intestinal drug delivery. The structure and function of this cornified epithelium is actually similar to that of skin described later, except for the presence of mucosal glands. A great deal of recent research has been focused on developing new transbuccal drug delivery systems. As mentioned, the prototype example was sublingual nitroglycerin tablets. Newer systems use novel adhesive technology, which allows actual polymer patches to adhere to the buccal mucosa. Oral sprays and dissolving tapes also target this mucosa. This route is a comparatively more permeable barrier than

skin. Additionally, compared with oral gastrointestinal absorption, it bypasses the portal vein and thus eliminates the potential for first-pass hepatic biotransformation.

The simple mucosal lining of the stomach allows absorption; however, the presence of surface mucus, which protects the epithelium from self-digestion secondary to acid and enzyme secretion, may be a barrier for some drugs. The acidity and motility of the stomach also creates a hostile environment for drugs and even influences the absorption of drugs farther down the tract. For oral drug absorption to be successful, the drug must be capable of surviving this relatively harsh environment. For some drugs (e.g., penicillin G) susceptible to acid hydrolysis, minimal absorption by the oral route will occur unless they are administered in a formulation that protects them in an acid environment but liberates them in the more alkaline environment of the intestines. There are significant species differences in gastric anatomy and physiology that can be utilized to optimize species-specific drug formulations as discussed later in this chapter.

The primary site for most drug absorption is the small intestine, with over 99% of oral administered drugs being absorbed here. In this region of the gastrointestinal tract, the pH levels of the contents are more alkaline, and the epithelial lining is conducive to drug absorption. The blood flow to this region is also much greater than to the stomach. The small intestine is lined by simple columnar epithelium resting on a basement membrane and a submucosal tissue bed that is very well perfused by an extensive capillary and lymphatic network. This capillary bed drains into the hepatic portal vein. One of the major anatomical adaptations for absorption in this region is the presence of microvilli that increase the surface area of the small intestine some 600-fold over that of a simple tube. The second anatomical adaptation is that of the villi of the intestine, which can be easily appreciated by examining a cross section (Fig. 4.2). Drug absorption across the intestinal barrier occurs either via transcellular or paracellular routes. Since diffusion is the

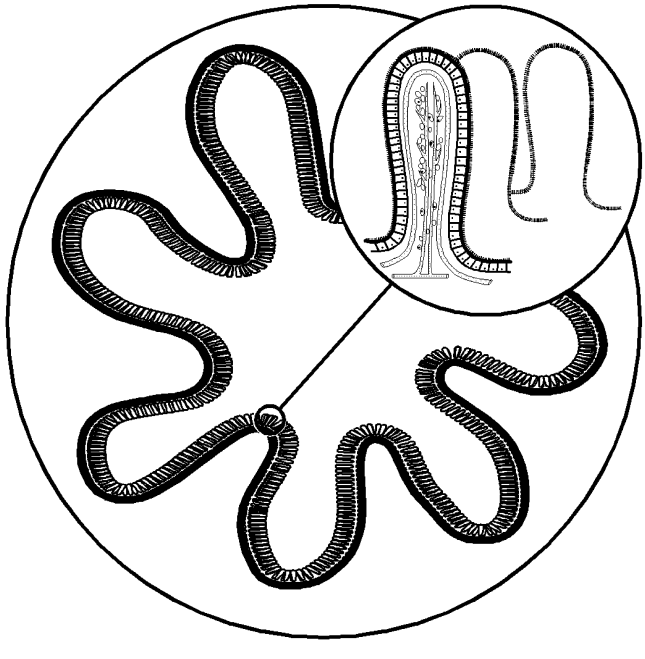

Fig. 4.2 Cross section of the small intestine showing villi adaptations, which increase surface area available for absorption.

primary mechanism for transcellular drug absorption, the increase in area due to these two anatomical configurations significantly increases absorption, as can be seen by realizing that Equation 2.1 is expressed per unit surface area. These transport mechanisms are also highly developed for ion and glucose transport, and can be regulated by multiple systems. Disease often alters their properties.

The viable epithelial cells of the intestines are also endowed with the necessary enzymes for drug metabolism, which contributes to a second first-pass effect. Recent research has also indicated that the mechanism and extent of absorption, and the magnitude of local intestinal metabolism, vary between the tips and crypts of the villi. The final determinant of a drug's tortuous journey through the gastrointestinal tract is the resident microbial population that inhabits the intestinal contents. Many bacteria are capable of metabolizing specific drugs, resulting in a third component of the first-pass effect. This epithelial and bacterial biotransformation is generally categorized as "presystemic" metabolism to differentiate it from the metabolism that occurs following portal vein delivery of drug to the liver. However, from the perspective of pharmacokinetic analysis of plasma drug concentrations following oral drug administration, all three components are indistinguishable and become combined in the aggregate process of oral absorption assessed by the pharmacokinetic rate constant K_a.

There are also specific active transport systems present within the intestinal mucosa of the microvilli that are responsible for transcellular nutrient (e.g., amino acids, peptides, anions, metals) absorption. However, these systems have a very high capacity, and if a specific drug or toxicant has the proper molecular configuration to be transported, saturation and its accompanying nonlinearity is unlikely. There is some evidence that select therapeutic drugs (e.g., ampicillin) may be absorbed by active transport systems in the small intestine. These drugs behave as if their absorption were linear and, from a pharmacokinetic perspective, they can be modeled using the same first-order rate constants as passively absorbed drugs unless nonlinear behavior is clearly evident. These modeling techniques will be presented in much greater detail in later chapters. For drugs that are actively transported, their permeability would be greater than for passive absorbed drugs. However, the drug would still have to be soluble in the aqueous gastrointestinal contents to bind to the luminal receptors for subsequent transport.

4.1.1 Disintegration, dissolution, diffusion, and other transport phenomena

In order for a drug to be absorbed across the intestinal mucosa, the drug must first be dissolved in the aqueous intestinal fluid. Two steps—disintegration and dissolution—may be required for this to occur. Disintegration is the process whereby a solid dosage form (e.g., tablet) physically disperses so that its constituent particles can be exposed to the gastrointestinal fluid. Dissolution occurs when the drug molecules then enter into solution. This component of the process is technically termed the pharmaceutical phase and is controlled by the interaction of the formulation with the intestinal contents. This is often studied in well regulated and controlled *in vitro* dissolution studies. To achieve the same dissolution rate *in vitro* and *in vivo*, saturation solubility in the test medium should be comparable with the *in vivo* situation. These systems (e.g., U.S. Pharmacopeia [USP] apparatus) are usually configured to model human dosage-form dissolution (e.g., 500-mL vessel volumes) and may not be appropriate for species with significantly smaller or larger stomachs or gastrointestinal fluids of different pH or viscosity.

Table 4.1 Biopharmaceutics Classification System (BCS) relating absorption as a function of permeability and solubility.

Class 1	**Class 2**
Rapid dissolution	HIGH permeability
HIGH permeability	LOW solubility
HIGH solubility	
Class 3	**Class 4**
LOW permeability	LOW solubility
HIGH solubility	LOW permeability

It is the drug's solubility, compared with rate and extent of absorption as reflected in a drug's permeability through the gastrointestinal mucosa, that determines the ultimate ability of an oral drug to be given for systemic effects. Independent of formulation, these factors determine how "sensitive" a drug may be to its environment relative to absorptive potential. This is nicely captured in the Biopharmaceutics Classification System (BCS) depicted in Table 4.1 that attempts to classify drugs according to relative solubility and membrane permeability (Amidon et al., 1995). For a drug to be optimally absorbed, it must be soluble in the primarily aqueous gastrointestinal fluids as well as have sufficient permeability (lipophilic, not charged) across the mucosa. Class I drugs are relatively easy to both formulate and deliver since once dissolution occurs, the drug is soluble and capable of being absorbed. In contrast, class IV drugs, even when released from a formulation, may have difficulty dissolving and then transporting across the mucosa. Class I drugs are easy to study *in vitro*, while class IV drugs require *in vivo* testing due to their sensitivity to the absorption environment. This solubility-versus-permeability dichotomy is crucial to understand drug absorption after oral and, as we will see later, dermal absorption, as knowledge of each alone is not sufficient to predict a drug's absorption.

This scheme above is conceptually similar to the perfusion- versus permeability-limited tissue distribution discussed and depicted in Fig. 2.7 in the previous chapter. When permeability is not rate limiting, movement into a tissue is a function of its rate of delivery. In an oral absorption scenario, this would equate to dissolution and solubility. In contrast, for a drug with low intrinsic permeability, absorption or movement into tissue will not be dependent on the mass available for transfer, its solubility in an oral absorption context, but rather its permeability will dictate amount absorbed. Both these scenarios illustrate rate-limiting processes involved in drug disposition and, as will be seen, are major determinants of the pharmacokinetic properties of a drug and/or its formulation. This topic is more fully discussed in Chapter 15 where these techniques are used to assess drug bioequivalence.

Important physical chemical factors of a specific drug that determine solubility and permeability include size, ionization, salt form, number of hydrogen bonding donors and acceptors, polar surface areas, partition coefficient, dissolution rate, and molecular stability in the gastrointestinal milieu. In addition to the molecular properties of a specific drug molecule, a drug in a formulation may exist in either a crystalline, noncrystalline (amorphous), or a mixed state called polymorphs. Although chemically identical, polymorphs differ in their solubility, dissolution rate, melting points, and other physical characteristics crucial to producing a stable and controlled formulation. Polymorphs occur by crystallizing drug under different conditions (temperature, solvents, hydration states) and can be characterized using tools such as crystallography, X-ray diffraction, and scanning calorimetry.

These drug-specific parameters may independently impact dissolution, solubility, and permeability.

4.1.2 Formulation factors

The pharmaceutical literature is replete with formulation factors that may influence the dissolution and absorption of a drug preparation, assuming in the first place that one has an active component of known purity and potency. The issue then becomes, what are the potential interactions that can occur between the active ingredients and the excipients that make up the formulation? Additionally, what are the effects of the practitioner's compounding techniques (materials used, mixing efficacy, etc.) on the amount of active ingredients ultimately appearing in the formulation? Although this discussion is the focus of a biopharmaceutics text, the strategies are often encountered in pharmacokinetics as they may affect the parameters estimated after oral administration. A number of these issues will be expanded upon when they impact the formal determination of bioequivalence in Chapter 15.

Table 4.2 lists the pharmaceutical processes involved in absorption that may be affected by formulation. Following oral administration of tablets, disintegration must first occur. The speed and efficacy of this process will determine how much drug is actually available for subsequent steps. The resulting particle size (and hence surface area) is an important determinant for the next dissolution phase, in which the drug enters solution, an absolute prerequisite for diffusion across the mucosal barrier. Dissolution also involves diffusion across the liquid boundary layers, which are an interface between the particles and the absorption milieu. Many pharmaceutical factors may affect the efficiency of the disintegration and dissolution processes. For tablets, the nature and homogeneity of the excipients become important considerations. Buffers must be included to ensure that all of the drug particles adequately and rapidly dissolve. These factors are the primary determinants of differences in efficacy between so-called pioneer and generic drug products. Once the drug is in solution, then binding or complexation to inert filler ingredients may occur. It is important to remember that all of this is happening while the particles are in transit through the gastrointestinal tract. Thus, if the formulation results in a decreased rate of disintegration or dissolution, the rate and extent of absorption may be decreased. These processes are competing kinetic events and thus are sensitive to all of the rate processes involved.

Table 4.2 Pharmaceutical factors affecting absorption.

Disintegration
Excipients
Compaction pressure
Enteric coatings, capsules
Homogeneity
Dissolution
Crystalline state of drug
Particle size/surface area
Binding
Local pH, buffers
Boundary layers in different regions of gastrointestinal tract
Barrier diffusion
Solubility/permeability factors (BCS)
Transit time

Similar factors are involved with oral capsules and even liquid dosage forms, in which case the drug may interact with the vehicle. In fact, these scenarios are probably most pertinent to practitioner compounding. For capsules, the breakdown of the capsule replaces tablet disintegration as the initial rate-determining step. After release of the capsule contents, all of the above factors come into play. It cannot be overstated that such pharmaceutical factors are critical determinants of the extent and rate of subsequent drug absorption.

Some dosage forms, such as capsules and lozenges, may not be designed to disintegrate, but rather to allow drug to slowly elute from their surface. Dissolution is often the rate-limiting step controlling the absorption process and can be enhanced by formulating the drug in salt form (e.g., sodium or hydrochloride salts), buffering the preparation (e.g., buffered aspirin), or decreasing dispersed particle size (micronization) so as to maximize exposed surface area. Alternatively, disintegration and dissolution can be decreased so as to deliberately provide slow release of drug. This strategy is used in so-called extended-release or slow-release dosage forms and involves complex pharmaceutical formulations that produce differential rates of dissolution. This may be accomplished by dispersing the dosage form into particles with different rates of dissolution or by using multilaminated dosage forms, which delays release of the drug until its layer is exposed. All of these strategies decrease the overall rate of absorption.

Similar strategies can also be used to target drugs to the distal segments of the gastrointestinal tract by using delayed-release enteric coatings, which dissolve only at specific pH ranges, thereby preventing dissolution until the drug is in the region targeted. This strategy has been applied for colonic delivery of drugs in humans for treatment of Crohn's disease. Colonic treatment of drug often is variable due to variance in gastrointestinal transit times affecting delivery of drug to this region, as well as variance in water content throughout the colon that results in uneven dissolution of a formulation.

In extended-release formulations, the end result is that absorption becomes slower than all other distribution and elimination processes, making the pharmaceutical phase the rate-limiting or rate-controlling step in the subsequent absorption and disposition of the drug. When this occurs, as will be seen in the pharmacokinetic modeling chapters that follow, the rate of absorption controls the rate of apparent drug elimination from the body, and a so-called flip-flop scenario becomes operative.

4.1.3 pH Effects

After the drug is in solution, it must still be in a nonionized, relatively lipid-soluble form to be absorbed across the lipid membranes that make up the intestinal mucosa. For orally administered products, the pH of the gastrointestinal contents becomes very important, as is evident from the earlier discussion on pH partitioning in Chapter 2. Specifically, a weak acid would tend to be preferentially absorbed in the more acidic environment of the stomach since a larger fraction would be in the nonionized form. However, the much larger surface area and blood flow available for absorption in the more alkaline intestine may, coupled with a relatively acidic pH (5.5) at the apical membrane's mucous layer, override this effect. It is important to mention why a weak acid such as aspirin is better absorbed in a bicarbonate buffered form, which would tend to increase the ionized fraction and thus decrease membrane passage. The paradox is that dissolution, a process favored by the ionized form of the drug, must first occur. Only the dissolved ionized aspirin is available to the partitioning phenomenon described in Chapter 2. Thus, when more aspirin is dis-

solved in the buffered microenvironment, more is available for partitioning and diffusion across the mucosa. It is a misconception that the very small amount of buffering activity in the tablet actually increases gastric pH. In contrast to the situation of a weak acid, a weak base tends to be better absorbed in the more alkaline environment. However, it must be repeated that the very large surface area available in the intestines, coupled with high blood flow and a pH of approximately 5.3 in the immediate area of the mucosal surface, makes it the primary site of absorption for most drugs (weak acids with $pK_a > 3$ and weak bases with $pK_a < 7.8$). An obstacle to absorption is that the compound must also be structurally stable against chemical or enzymatic attack. Finally, compounds with a fixed charge and/or very low (or very high) lipid solubility for the uncharged moiety may not be significantly absorbed after oral administration. Examples include the polar aminoglycoside antibiotics, the so-called enteric sulfonamides, quaternary ammonium drugs, and many class IV BCS drugs.

4.1.4 Absorption of lipids and particles

The discussion of potential absorption pathways across the intestinal mucosa parallels the scheme depicted in Fig. 2.5. For small drug molecules, the transcellular pathways of diffusion, pores, active transport systems, as well as paracellular transport all fit well into the biopharmaceutical discussions concerning oral absorption.

In contrast, the movement of very lipid soluble drugs and particles across endocytotic pathways in the gastrointestinal mucosa are fundamentally different than small molecule transport pathways. This alternative mechanism of transport exists to allow the body to absorb dietary fats and fat-soluble vitamins. Bile, discussed below in the context of enterohepatic circulation, also serves the function of emulsifying fatty substances that are not capable of solubilizing in the primarily aqueous environment of the intestines. The result of this detergent-like action of bile is the formation of large surface area micelles that have a hydrophilic surface and hydrophobic interior. These act as transport vehicles to deliver fat-soluble drugs to the intestinal brush border surface for passage across the lipid membrane into the cell via endocytotic mechanisms. Without bile, fat-soluble molecules would not be able to overcome the so-called "dissolution barrier." Once in the cell, metabolism occurs and the lipid content is packaged in chylomicrons, which then pass through the basolateral membrane of the enterocyte and enter the lymphatic vessels to ultimately be transported to the thoracic duct and enter the circulation.

This unique mechanism for micelle absorption and chylomicron lymphatic transport has been also been described as the mechanism for absorption of micron, submicron, and nanosized particles. Pharmaceutical scientists have formulated drugs in micelles so as to be able to be absorbed via this mechanism. There are two primary advantages for using this approach; the first being protecting the drug encapsulated in the micelle from destruction by gastric acid (labile peptides such as insulin), and the second serving a mechanism to target lymphatic delivery after oral administration. Significant research is being conducted in this area. The absorptive kinetics of drugs handled by this process is only now being studied.

In contrast to most drugs, compounds that are absorbed by this route often must be administered with a meal to promote bile acid secretion and associated micelle formation. Food effects are thus significant for such fat-soluble drugs. This effect is mechanistically different than that described below where food modulates gastric emptying times and delivery of soluble drugs to the absorptive sites in the small intestines.

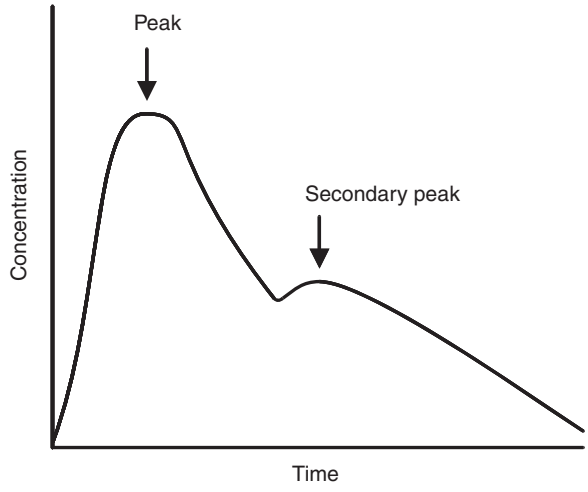

Fig. 4.3 Profile of concentration versus time demonstrates a secondary peak that could result from enterohepatic recycling.

4.1.5 Enterohepatic recycling

The gastrointestinal tract has also evolved into an excretory organ for elimination of non-absorbed solid wastes and other metabolic by-products excreted in the bile. The bile duct drains into the upper small intestine. For some drugs, this results in a phenomenon called enterohepatic recycling, whereby a drug from the systemic circulation is excreted into the bile and is reabsorbed from the small intestine back into the blood stream. In many cases, drugs that are metabolized by phase II conjugation reactions are "unconjugated" by resident bacterial flora, which generates free drug for reabsorption. Thus compounds that are excreted into the bile may have a prolonged sojourn in the body because of the continuous opportunity for intestinal reabsorption. The cardinal sign of this process is a "hump" in the plasma drug concentration–time profile after administration (Fig. 4.3). Chapter 7 should be consulted for an in-depth discussion of biliary secretory processes.

Complex absorption profiles (e.g., nonconstant or biphasic K_a) may also be seen for drugs absorbed in multiple sites of the gastrointestinal tract since absorption rates may not be constant across all areas. Such drugs are also marked by significant interindividual variability since dietary or environmental influences on transit times proximal to the absorptive sites results in different rates of drug delivery. This profile may also be seen in animals engaging in coprophagy and licking topical dose sites, scenarios discussed later in this chapter.

4.1.6 Intestinal P-glycoprotein transporters

The focus up to this point in the discussion has been absorption of drugs from the gastrointestinal lumen to the vascular or lymphatic system. However, as depicted in Fig. 2.5, drug movement can also occur in the opposite direction, effectively returning absorbed drug back into the gastrointestinal lumen. This phenomenon is mediated by a series of

transport proteins termed the ATP-binding cassette superfamily of efflux transporters that includes P-glycoprotein, the multidrug resistance protein (MDRP1), and a multidrug organic ion transporter. Most work has been conducted on the P-glycoprotein transporter whose substrates include many drugs, xenobiotics, and dietary compounds (e.g., flavonoids from grapefruit juice) with little structural similarities. In veterinary medicine, compounds reported to be transported by this system include cyclosporine, ciprofloxacin, verapamil, and avermectins.

What makes studying the clinical impact of such transporters difficult is that these systems confound interpretation of transport data moving drug into the body when substrate specificity overlaps between systems. Second, many P-glycoprotein substrates are also substrates of cytochrome p450 drug metabolizing enzymes (e.g., CYP3A), which further confounds data modeling since both processes reduces the amount of active parent drug absorbed into the body. As seen with other transport systems, this system shows competition between substrates as well as genetic polymorphisms (e.g., Collie dogs deficient) and species specificity. When drugs are transported by multiple systems such as these, correlation between physiochemical parameters or simple *in vitro* systems to *in vivo* absorption are complex and often unsuccessful.

4.1.7 Species effects on gastrointestinal transit time and food interactions

Food may also interact with other aspects of oral drug absorption besides promoting bile release, and may have opposite effects for more hydrophilic drugs compared with the micellar fat solubilization pathway discussed above. Depending on the physicochemical properties of the specific drug, administration with food may significantly decrease absorption for some drugs. Such effects are not only drug dependent but also are species dependent due to the continuous foraging behavior of ruminants and some other omnivores compared with the periodic feeding habits of predatory carnivores. These variables are difficult to incorporate into formal pharmacokinetic models, yet they add to the variability in parameters derived from these studies.

The first potential interaction relates to the rate of drug delivery to the small intestine, which is governed by the rate of drug release from the stomach, the so-called gastric emptying time. This process is dependent on the eating habits of the species. Continuous foraging animals (e.g., herbivores such as horses and ruminants) have a steady input of drug and a relatively stable gastric pH compared with periodic eaters (e.g., carnivores such as dogs and cats and omnivores such as pigs), which have more variable eating patterns and large swings in gastric pH depending on the presence or absence of food. In addition, the drug may directly interact with the ingested food, as is the case of chelation of tetracyclines with divalent cations such as Mg^{++} in antacids or Ca^{++} in milk products. Thus, the decision to administer a compound with or without food is species and drug dependent and may significantly alter the bioavailability (rate and extent of absorption) of the drug.

Recent workers have also reported significant differences between the anatomy and physiology of small animal companion species (dog, cat) and humans, relative to both the strength of gastric contractions that impact formulation integrity, as well as the diameter of the pyloric valve, which controls gastric emptying into the small intestines. In addition to cats having relatively small stomach volumes compared with dogs and humans, cats also possess the smallest pyloric opening (1–2 mm), with dogs intermediate (2–4 mm) followed

by the relatively large pylorus in humans (3–7 mm). This difference results in retention of tablets in the feline and canine stomachs that would normally be released in humans. This sieving phenomenon has a significant effect on the gastric emptying time of particulate formulations, a knowledge of which has also led to the development of species-specific dosage formulations that are retained for longer periods of time in the gastric environment. An additional formulation factor that results in gastric retention is the ability of flocculant material to escape emptying in species with larger stomachs.

The unique physiology of the equine and ruminant gastrointestinal tract deserves further discussion. Both species have significant anatomical adaptations to allow for microbial digestion of polysaccharides. An obvious problem could arise from the use of microcellulose-based, sustained-release tablet formulations designed for humans. Administered to a herbivore, such tablets would be digested and the drug quickly absorbed rather than the tablet remaining intact as they do in a monogastric animal. Absorption would be dramatically decreased if the drug were metabolized by endogenous microbes. In contrast, if the drug is an antimicrobial, it may disturb this microflora and alter digestive processes.

The forestomachs of a ruminant provide a major obstacle to the delivery of an oral dosage form to the true stomach (abomasum) for ultimate release to the intestines, although a significant amount of drug absorption may occur from this site. The rumen is essentially a large fermentation vat (>50 L in cattle, 5 L in sheep) lined by stratified squamous epithelium, buffered at a pH of approximately 6 by extensive input of saliva, which maintains it in a fluid to soft consistency designed primarily for the absorption of volatile fatty acids. If drugs dissolve in this medium and remain intact, they undergo tremendous dilution, which decreases their rate of absorption. They then are pumped from the rumen and reticulum through the omasum for a rather steady input of drug into the true stomach. In preruminant calves, drug may bypass the rumen entirely through the rumen-reticulo groove and essentially behave as if administered to a monogastric animal. In contrast, fermentation in the horse occurs after drug absorption by the small intestine and thus has less impact than in ruminants. However, a nonabsorbed drug that reaches the equine large intestines and cecum, the site of fermentation, may have disastrous effects (e.g., colic) if digestive flora or function is perturbed. As alluded to earlier, a similar strategy is used to target drugs to the human colon. In addition to extended-release or delayed-release enteric coatings, prodrug approaches have been used that inhibit drug absorption until specific enzymes are encountered in the distal gastrointestinal tract. These enzymes liberate the active moiety from the prodrug (e.g., azo reduction).

4.1.8 Unique oral drug delivery systems in animal species

Because of the wide variety of species differences in gastrointestinal anatomy and physiology, unique strategies for development of species-specific drug delivery devices arise. An understanding of ruminant physiology has allowed for the development of some innovative mechanical drug delivery technologies termed rumen retention systems. These essentially are encapsulated pumps that "sink" to the bottom of the rumen and become trapped, as do many unwanted objects (e.g., nails and wire in hardware disease) when ingested by a ruminant. These submarine-like devices then slowly release drug into the ruminal fluid for a true sustained-release preparation. They may be reservoir based or powered by osmotic pumps. Chewable tablets are often used in dogs and cats as are oral pastes. This area has recently been reviewed by Brayden et al. (2010).

4.1.9 First-pass metabolism

A unique aspect of oral drug absorption is the fate of the absorbed drug once it enters the submucosal capillaries. Drug absorbed distal to the oral cavity and proximal to the rectum in most species enters the portal circulation and is transported directly to the liver, where biotransformation may occur. This can be appreciated in Figs. 2.1 and 4.1 and is the major cause for differences in a drug's ultimate disposition compared with all other routes of administration. This may result in a significant "first-pass" biotransformation of the absorbed compound. Some of the more complex pharmacokinetic models are needed to quantitate drugs with a significant first-pass effect. Finally, some drugs that are too polar to be absorbed across the gastrointestinal wall are formulated as ester conjugates to increase lipid solubility and enhance absorption. Once the drug crosses the gastrointestinal epithelium in this form, subsequent first-pass hepatic biotransformation enzymes and circulating blood and mucosal esterases cleave off the ester moiety, releasing free drug into the systemic circulation. Chapter 7 on biotransformation should be consulted for more details on drug metabolism by the liver.

As discussed earlier, for some drugs, there is also a significant loss secondary to P-glycoprotein transport, gastric acid hydrolysis or metabolism by enzymes in the brush border of intestinal mucosal cells. This severely restricts the absorption of protein, peptide, and oligonucleotide (e.g., antisense) drugs administered orally. This presystemic intestinal breakdown of peptides deserves further comment. Peptidases are located in the microvilli epithelium, which is present to digest protein and peptides into their constituent amino acids. Proteases from the pancreas complete the process of digestion of proteins that were not completely hydrolyzed by stomach acids. Protein digests and peptides are then efficiently broken down into amino acids to allow for absorption. Despite substantial pharmaceutical research efforts over the past decade to overcome this obstacle to the delivery of these products of the modern biotechnology industry, little progress has been made, and administering peptide drugs orally only contributes to the extent of the caloric value of the amino acid constituents. Encapsulation strategies to mimic chylomicron transport appear to be the only promising strategy.

The use of selected drug administration sites prevents first-pass hepatic metabolism by allowing absorption through gastrointestinal tract segments not drained by the portal vein. These include the oral cavity, buccal, and rectal routes of drug administration. As discussed earlier, the keratinized buccal mucosa is very similar to skin. Rectal drug administration is accomplished with suppositories and formulations (e.g., diazepam), which allow retention and adhesion of drug to the distal rectum. There is some debate as to whether this pathway is truly available in the dog. Drug absorption by this route is by passive diffusion and obeys the diffusion principles discussed previously.

4.1.10 Coprophagy

Another potential complication unique to veterinary medicine is coprophagy, which is the consumption of feces by animals. Although experimental design often prevents this in a laboratory study, it does occur in the field situation. This may result in drug transfer between animals (allocoprophagy) in a herd or home environment, or drug recycling in an individual ingesting its own feces (autocoprophagy). Rabbits routinely ingest fresh feces twice daily for nutritional purposes, which would result in drug profiles similar to twice-daily dosing or recycling (e.g., Fig. 4.3) despite a single daily dose administration.

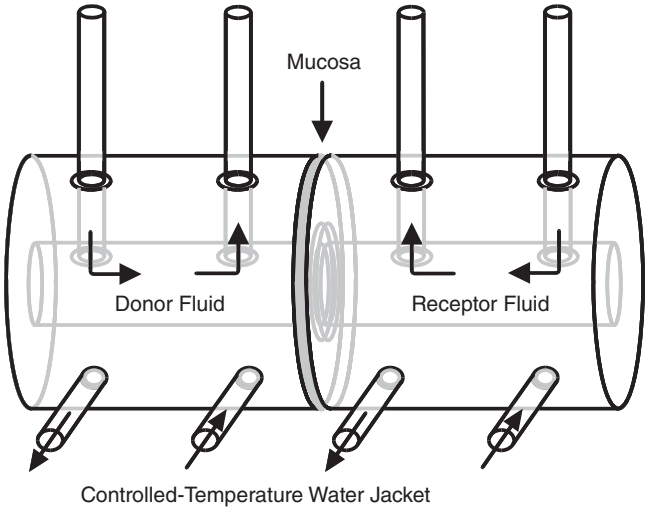

Fig. 4.4 *In vitro* chamber used to assess absorption across gastrointestinal membranes.

4.1.11 Absorption models

It must be stressed that the de facto standard for assessing oral absorption is based on the use of intact animals. The design of such bioavailability and bioequivalence studies is often driven by regulatory guidelines. Chapter 15 deals with the design and interpretation of these studies in more detail.

There are also a number of *in vitro* methodologies available. The simplest, classic technique is the use of *in vitro* diffusion cells (water jacketed to control temperature), whereby a piece of gastrointestinal mucosa is clamped between two chambers (Fig. 4.4). An intestinal membrane may be grown using cell culture techniques. The most widely used system is the Caco model derived from a human intestinal carcinoma cell line. However, its use has recently been challenged on the grounds that metabolism in these transformed cells may be different from that in normal human intestinal cells, and total protein functions may not be the same as intact nontransformed enterocyte cell lines. Depending on the purpose of the study, drug is placed in solution in the donor chamber, and the appearance of drug is monitored in the receptor chamber. This technique has also been extensively used to study the biophysics and bioenergetics of active transport processes and in quantitative structure–permeability relationship (QSPeR) analyses introduced in Chapter 3.

More sophisticated models acknowledge the complexity of the *in vivo* setting and study drugs by using *in situ* intestinal flap preparations or isolated perfused intestinal segments, a technique facilitated by the arcuate vascular distribution to discrete intestinal segments. In these situations, drugs are placed in the intestinal contents, and the appearance of the drug is monitored in the venous drainage or perfusate. Finally, the most sophisticated techniques available are conducted in conscious, nonmedicated animals or humans and use remote-controlled microprocessor-embedded drug devices administered orally. The passage of these submarine-like devices is monitored by fluoroscopy, and when the capsule reaches a specific segment of the gastrointestinal tract, the device is activated and drug released. Drug absorption is then monitored by assaying blood samples. In all of these cases, the

pharmacokinetic models discussed in subsequent chapters are then used to derive parameters to quantitate absorption.

In conclusion, oral drug dosing is the most convenient but most species-specific and variable method for drug administration by the veterinarian. The quantitative estimate of the rate and extent of drug absorption, termed bioavailability, will be introduced at the end of this chapter and fully discussed later. Factors that modify oral absorption of drugs in animals are extensively discussed in Chapter 15 on bioequivalence once the pharmacokinetic parameters that quantitate the rate and extent of absorption have been fully developed.

4.2 TOPICAL AND PERCUTANEOUS ABSORPTION

The skin is a complex, multilayered tissue comprising 18,000 cm^2 of surface in an average human male. The quantitative prediction of the rate and extent of percutaneous penetration (into skin) and absorption (through skin) of topically applied chemicals is complicated by the biological variability inherent in skin. Mammalian skin is a dynamic organ with a myriad of biological functions. The most obvious is its barrier property, which is of primary concern in the absorption problem. Another major function is thermoregulation, which is achieved and regulated by three mechanisms: thermal insulation provided by pelage and hair, sweating, and alteration of cutaneous blood flow. Other functions of the skin include mechanical support, neurosensory reception, endocrinology, immunology, and glandular secretion. These additional biological roles lead to functional and structural adaptations that affect the skin's barrier properties and thus the rate and extent of percutaneous absorption.

The skin is generally considered to be an efficient barrier, preventing absorption (and thus systemic exposure) of most topically administered compounds. It is a membrane that is relatively impermeable to aqueous solutions and most ions. It is, however, permeable in varying degrees to a large number of solid, liquid, and gaseous xenobiotics. Although one tends to think of most cases of poisoning as occurring through the oral or, less frequently, the respiratory route, the widespread use of organic chemicals has enhanced exposure to many toxicants that can penetrate the dermal barrier. An example is the large number of agricultural workers who have experienced acute dermal poisoning from direct exposure to parathion (dermal LD_{50} = 20 mg/kg) during field application or from more casual exposure, such as contact with vegetation previously treated with such insecticides. Similar situations often occur in veterinary species.

The gross features of mammalian skin are illustrated in Fig. 4.5. Compared with most routes of drug absorption, the skin is by far the most diverse across species (e.g., sheep vs. pig) and body sites (e.g., human forearm vs. scalp). Three distinct layers and a number of associated appendages make up this heterogeneous organ. The epidermis is a multilayered tissue varying in thickness in humans, from 0.15 mm (eyelids) to 0.8 mm (palms). The primary cell type found in the epidermis is the keratinocyte. Proliferative layers of the basal keratinocyte (stratum germinativum) differentiate and gradually replace the surface cells as they deteriorate and are sloughed from the epidermis. A number of other cell types are also found interspersed in the epidermis, including the pigmented melanocytes; Merkel cells, which may play a sensory role; and Langerhans cells, which probably play a role in cutaneous immunology. These cells are not important contributors to the skin's barrier properties. The basal keratinocyte layer consists of nucleated cuboidal to columnar cells.

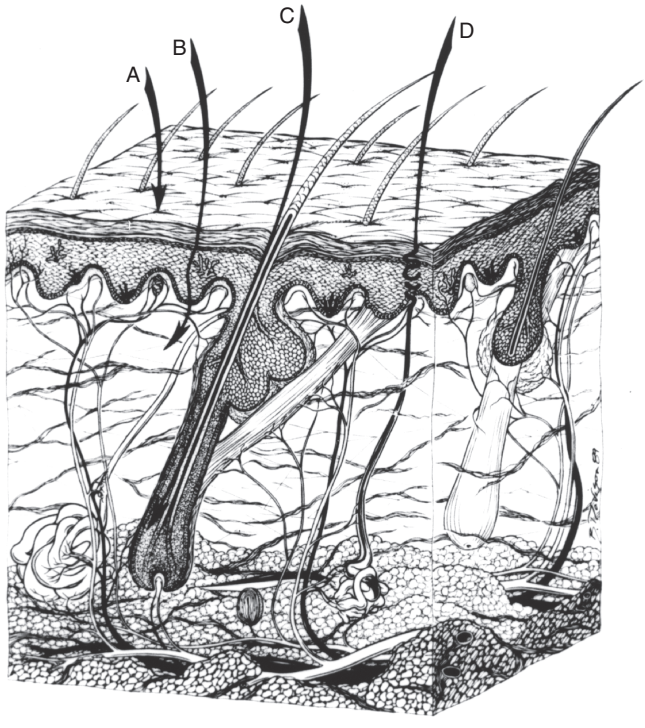

Fig. 4.5 Microstructure of mammalian skin showing potential routes of penetration. A: intercellular; B: transcellular; C: intrafollicular; D: via sweat ducts.
Source: Riviere and Monteiro-Riviere (1991) (Reproduced with permission).

As these cells move toward the surface, they lose their shape, becoming rounded and ultimately flattened. Three loosely defined layers—the stratum spinosum, stratum granulosum, and stratum lucidum—are areas of considerable morphological and biochemical change, and although variable, their width is several times that of the final surface layer.

The primary morphological changes that occur as the keratinocytes progressively die are that they become greatly flattened, and the nuclei become progressively less obvious. In respect to penetration, the primary biochemical change is the production of fibrous, insoluble keratin that fills the cells, and a sulfur-rich amorphous protein that comprises the cell matrix and thickened cell membrane. In addition, the keratinocytes synthesize a variety of lipids that form the distinguishing granules in the stratum granulosum and release their contents into the intercellular spaces. The result in the stratum corneum is dead proteinaceous keratinocytes embedded in an extracellular lipid matrix, a structure referred to by Elias as the "brick-and-mortar" model depicted in Fig. 4.6. The intercellular lipid composition is not homogenous in all layers of the epidermis, making the lipid topography complex. Species differences (lipid composition) also occur.

4.2.1 The stratum corneum barrier

It is the final layer, the stratum corneum, that provides the primary barrier to the penetration of foreign compounds. This barrier consists of 8–16 layers of flattened, stratified, highly

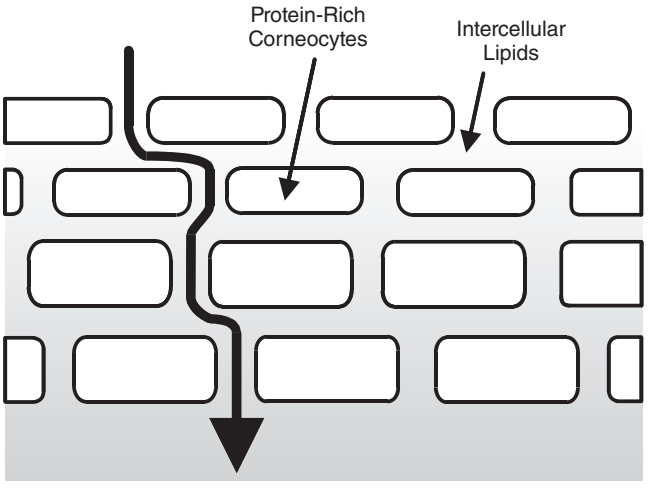

Fig. 4.6 Conceptual "brick-and-mortar" model of the stratum corneum demonstrating predominant intercellular pathway for topically applied compounds.

keratinized cells embedded in a lipid matrix composed primarily of sterols, other neutral lipids, and ceramides. These cells are approximately 25–40-μm wide, lie tangential to the skin surface, and are oriented as relatively impermeable shingles to form a layer approximately 10-μm thick. The sequence of events from basal cell to stratum corneum formation requires about 4 weeks. Although highly water retarding, the dead, keratinized cells are highly water absorbent (hydrophilic), a property that keeps the skin supple and soft. A natural oil covering the skin, the sebum, appears to maintain the water-holding capacity of the epidermis but has no appreciable role in retarding the penetration of xenobiotics.

Disruption of the stratum corneum removes all but a superficial deterrent to penetration. One line of evidence utilizes "tape-stripping" experiments, in which an adhesive (cellophane tape) is placed on the skin repeatedly, removing progressive sections of the corneum. The skin continuously loses its ability to retard penetration, and compound flux increases greatly. This can be noninvasively assessed by measuring the skin's ability to prevent insensible water loss from the body to the environment by using water as a marker of molecular transport across the cutaneous barrier. This is performed by measuring transepidermal water loss (TEWL). This value increases greatly when the stratum corneum is either stripped away using adhesive tape (Fig. 4.7) or removed by extracting the intercellular barrier lipids.

For many compounds, the stratum corneum has been calculated to afford 1000 times the resistance to penetration as the layers beneath it. Exceptions to this rule are extremely lipid-soluble compounds with tissue:water partition coefficients greater than 400. As in most other epithelial tissues, the two deeper layers of the skin (dermis and SC tissue) generally offer little resistance to penetration, and once a substance has penetrated the outer epithelium, these tissues are rapidly traversed. For the highly lipid-soluble compounds, this may not be true, and the dermis may function as a barrier preventing a chemical that has penetrated the epidermis from being absorbed into the blood.

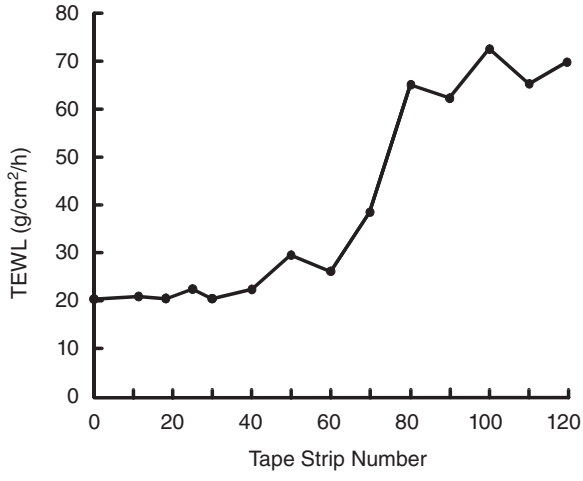

Fig. 4.7 Increase in transepidermal water loss (TEWL) in porcine skin as a function of stratum corneum barrier removal with cellophane tape stripping.

4.2.2 Dermis and appendages

The dermis is a highly vascular area, providing ready access for drug distribution once the epithelial barrier has been passed. The blood supply in the dermis is under complex, interacting neural and local humoral influences whose temperature-regulating function can have an effect on distribution by altering blood supply to this area. This function of mammalian skin is different from that of the other epithelial tissues discussed and offers another variable for predicting transdermal drug delivery. The absorption of a chemical possessing vasoactive properties would be affected through its action on the dermal vasculature; vasoconstriction would retard absorption and increase the size of a dermal depot, while vasodilation may enhance absorption and minimize any local dermal depot formation.

The appendages of the skin are found in the dermis and extend through the epidermis, as can readily be appreciated from examining Fig. 4.5. The primary appendages are the sweat glands (eccrine and apocrine), hair, and sebaceous glands. Since these structures extend to the outer surface, they play a role in the penetration of certain compounds. Sweat glands also provide for excretion of sebum, which some consider to be a vehicle for lateral diffusion of topical substances on the surface of the skin (e.g., certain topical flea products such as fiprinil). In sheep, sebum heavily concentrated with lanolin provides a continuous layer of lipid over the surface of the skin. Finally, the orifice of both hair ducts and sweat glands may trap particulate drug formulations, which then function as extended-release depots to the surface of the skin.

4.2.3 Topical drug delivery and the definition of dose

From the perspective of pharmacokinetic models of transdermal and topical drug delivery systems, there are significant differences from other routes of administration (e.g., oral, injection) as to what constitutes a dose. Dermatological preparations target drugs to the skin (penetration is important), whereas transdermal preparations target drugs to the

Table 4.3 Percutaneous absorption of parathion and paraoxon.

Dose	4 μg/cm²	40 μg/cm²	400 μg/cm²
Parathion	0.32 ± 0.02	0.77 ± 0.11	1.86 ± 0.14
	7.91 ± 0.38%	1.91 ± 0.28%	0.46 ± 0.04%
Paraoxon	0.61 ± 0.18	3.93 ± 1.16	10.12 ± 1.71
	15.52 ± 4.42%	9.38 ± 2.90%	2.53 ± 0.43%

Source: Adapted from Chang, S.K., Dauterman, W.C., and Riviere, J.E. 1994. Percutaneous absorption of parathion and its metabolites paraoxon and p-nitrophenol administered alone or in combination: *in vitro* flow through diffusion cell system. *Pesticide Biochemistry and Physiology*. 48:56–62.
Flux in μg/cm²/h using *in vitro* porcine skin; second row is % dose.

systemic circulation (absorption is important). In veterinary medicine, many pour-on pesticides are in fact transdermal delivery systems. For most exposures, the concentration applied to the surface of the skin exceeds the absorption capacity. Thus, application of higher doses results in a decreased fraction of dose absorbed but an increase in actual drug flux (Table 4.3). However, for therapeutic transdermal patches with a fixed concentration of drug and rate-controlled release properties (much like the oral extended-release formulations discussed earlier), it is the contact surface area that more accurately reflects dose, and thus dose is expressed not, for example, in mg/kg but in mg/cm^2 of dosing area. This surface area dependence also holds for any topical application even if absorption capacity is superseded.

Yet another source of nonlinearity results are secondary to the effects of occlusive (water-impermeable) drug vehicle or patches. As the skin hydrates, a threshold is reached at which transdermal flux dramatically increases (approximately 80% relative humidity), as with the topical parathion studies in Fig. 4.8. When the skin becomes completely hydrated under occlusive conditions, flux can be dramatically increased. Therefore, dose alone is often not a sufficient metric to describe topical doses, and application method and surface area become controlling factors. Hydration can also markedly affect the pH of the skin, which varies between 4.2 and 7.3, with an effective barrier pH of 6 in porcine skin. For drugs or chemicals with pK_a levels in this range, the principles embedded in the Henderson–Hasselbalch Equations 2.2 and 2.3 become important. The unionized fraction may change as a function of skin pH, thereby further modulating percutaneous absorption.

4.2.4 Pathways for and modeling of dermal absorption

Anatomically, percutaneous absorption might occur through several routes. The current consensus is that the majority of nonionized, lipid-soluble toxicants appear to move through the intercellular lipid pathway between the cells of the stratum corneum, the rate-limiting barrier of the skin. It was previously thought that the primary route was transcellular (through the cells), but recent work has discredited this view. A third possible route is through the appendages, such as hair follicles or sweat ducts. Very small and/or polar molecules appear to have more favorable penetration through appendages or other diffusion shunts, but only a small fraction of drugs are represented by these molecules. Initial penetration particularly may be aided by appendages. In addition, the epidermal surface area is 100–1000 times the surface area of the skin appendages. Passage through the skin is passive, there being no evidence for active transport. Simple diffusion seems to account for penetration through the skin, whether by gases, ions, or nonelectrolytes. Polar sub-

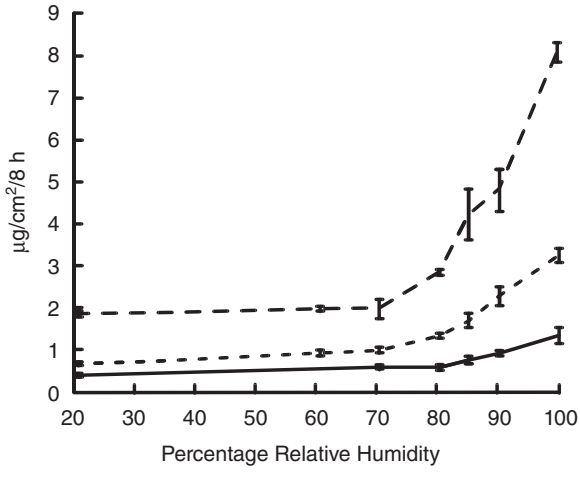

Fig. 4.8 Increase in parathion percutaneous absorption as a function of increasing relative humidity. Applied doses: 4 µg/cm^2 (—); 40 µg/cm^2 (– –); 400 µg/cm^2 (— — —).

stances, in addition to movement through shunts, may diffuse through the outer surface of the protein filaments of the hydrated stratum corneum, while nonpolar molecules dissolve in and diffuse through the nonaqueous lipid matrix between the protein filaments.

The rate of percutaneous absorption through this intercellular lipid pathway is correlated to the partition coefficient of the penetrant. This has resulted in numerous studies correlating the extent of percutaneous absorption with a drug's lipid:water partition coefficient, typified by Fig. 4.9. However, similar to what occurs with gastrointestinal permeability, the solubility of the topically applied drug in the dosing vehicle determines the total of drug available for diffusion, the X_1 in the diffusion model presented in Equation 2.1.

In skin absorption studies, the rate of drug flux across the skin is expressed using the permeability coefficient, K_p, defined as $D{\cdot}P/h$ from the diffusion Equation 2.1. This results in absorptive flux being a function of K_p and available (soluble) drug in solution on the surface of skin:

$$\text{Flux (mass/time)} = K_p(1/\text{time}) \cdot C(\text{mass}). \tag{4.1}$$

An assessment of K_p alone may be misleading when predicting drug absorption. For example, a very lipophilic drug (high partition coefficient) would have a high dermal permeability. However, if dosed in a formulation where it was sparingly soluble, only a small amount of drug would be available for partitioning and diffusion. Thus, a better end point for the potential for topical delivery would be to obtain maximum flux that occurs when both solubility and partitioning are optimal. This is often the end point for pharmaceutical formulation studies.

Some workers further correlated skin penetration to molecular size and other indices of potential interaction between the penetrating molecule and the skin that are not reflected in the partition coefficient. These QSPeR models are discussed as examples in Chapter 3, where Equation 3.3 and Fig. 3.1 related K_p to log $K_{o/w}$ and molecular weight (MW) with log $K_{o/w}$ being a primary predictor of partition coefficient. For most purposes, dermal penetration is often correlated to this partition coefficient. If lipid solubility is too great, then

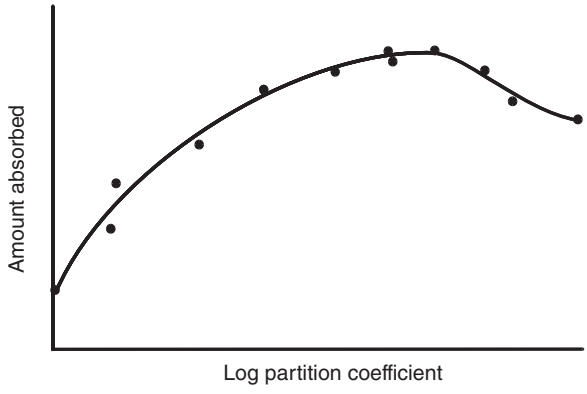

Fig. 4.9 Relation between log partition coefficient and amount absorbed.

compounds that penetrate the stratum corneum may remain there and form a reservoir, evidenced by a plateauing in extent of absorption versus partition coefficient plots (Fig. 4.9). Alternatively, penetrated compounds may also form a reservoir in the dermis. For such compounds, slow release from these depots may result in a prolonged absorption half-life. Conditions that alter the composition of the lipid (harsh delipidizing solvents, dietary lipid restrictions, disease) may alter the rate of compound penetration by changing its partitioning behavior.

Recent studies have demonstrated that the skin may also be responsible for metabolizing topically applied compounds. Both phase I and phase II metabolic pathways have been identified. For some compounds, the extent of cutaneous metabolism influences the overall fraction of a topically applied compound that is absorbed, making this process function as an alternative absorption pathway. Cutaneous biotransformation is used to promote the absorption of some topical drugs that normally would not penetrate the skin. Prodrugs, consisting of the more lipid-soluble ester analogues, penetrate the stratum corneum, and then the active drugs are liberated through the action of cutaneous or blood esterases. Cutaneous metabolism may also be important for certain aspects of skin toxicology when nontoxic parent compounds are bioactivated within the epidermis, such as benzo[a]pyrene to an epoxide. Finally, resident bacteria on the surface of the skin may also metabolize topical drugs, as demonstrated with pentachlorophenol absorption in pig skin dosed in soil with and without antibiotics (Fig. 4.10). This effect is potentiated under warm and wet occlusive dosing conditions, which both promote bacterial growth and reduce skin barrier properties.

4.2.5 Variations in species and body region

Penetration of drugs varies through different body regions. In humans, the rate of penetration of most nonionized toxicants is generally in the following order: scrotal > forehead > axilla = scalp > back = abdomen > palm and plantar. The palmar and plantar regions are highly cornified, producing a much greater thickness (100–400 times that of other regions) that introduces an overall lag time in diffusion. In addition to thickness, the actual size of corneocytes may be important. Differences in hair follicle density may affect absorption of more polar molecules. The scalp should thus be considered in a different

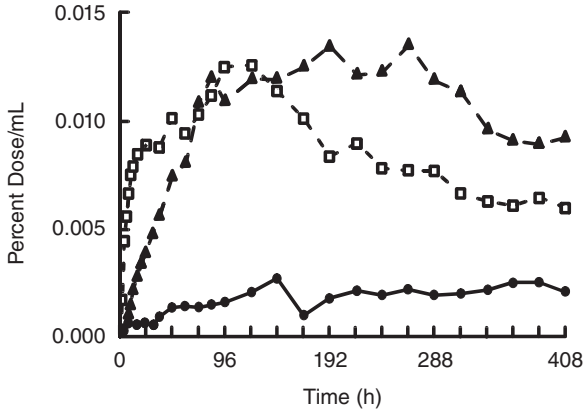

Fig. 4.10 Application vehicle effects on the percutaneous absorption of topically dosed pentachlorophenol (40 µg/cm^2) on *in vivo* pigs. Nonoccluded soil (•••); occluded soil (□); occluded soil with antimicrobials (▲).

light from the rest of the body. Finally, differences in cutaneous blood flow that have been documented in different body regions may be an additional variable to consider in predicting the rate of percutaneous absorption. These factors are also important in animals.

Although generalizations are tenuous at best, human skin appears to be more impermeable than, or at least as impermeable as, the skin of the cat, dog, rat, mouse, or guinea pig. The skin of pigs and some primates serve as useful approximation to human skin, but only after a comparison has been made for each specific substance. The major known determinants of species differences are thickness, hair density, lipid composition, and cutaneous blood flow.

4.2.6 Factors that modulate absorption

Soaps and detergents are perhaps the most damaging substances routinely applied to skin. Whereas organic solvents must be applied in high concentrations to damage the skin and increase the penetration of solute through human epidermis, only 1% aqueous solutions of detergents are required to achieve the same effect. Alteration of the stratum corneum appears to be the cause of increased penetration. Organic solvents can be divided into damaging and nondamaging categories relative to their effects on the barrier properties of skin. The damaging category includes methanol, acetone, ether, hexane, and mixed solvents such as chloroform:methanol or ether:ethanol. These solvents and mixtures are able to extract lipids and proteolipids from tissues and thereby alter drug permeability by removing its lipid barrier. Another mechanism for this solvent effect is that the solvents themselves may partition into the intercellular lipid pathway, changing its lipophilicity and barrier property. Use of more polar or amphoteric solvents may enhance the penetration of polar molecules. In contrast, solvents such as higher alcohols, esters, and olive oil do not appear to damage skin appreciably.

The penetration rate of solutes dissolved in any solvent may often be modulated from effects on solubility and partition coefficient. This is best explained by partitioning of the penetrant into the nonabsorbed solvent, preventing release of the chemical into the stratum corneum. Such vehicle effects were quantitated in Chapter 3, Fig. 3.3. The vertical heights

of the columns representing an individual chemical dosed in different vehicles was greater than the slope of the line relating the chemical's K_p to its molecular descriptors, clearly illustrating how vehicle effects may dominate inherent K_p. This is very similar to the strategies used to formulate injectable depot preparations using insoluble additives that retain drug at the injection site.

For a specific chemical, rate of penetration can be drastically modified by the solvent system used. In transdermal patches, specific chemical enhancers (e.g., solvents such as ethanol; other lipid-interacting moieties) are included in the formulation to reversibly increase skin permeability and enhance drug delivery. Alternatively, drug release is formulated to be rate limiting from the patch system (membranes, microencapsulation, etc.) so that a constant (zero-order) release from the patch occurs, thereby providing controlled drug delivery. This provides an interesting issue when attempting to use a transdermal patch (e.g. fentanyl) developed for human skin permeability in a different species whose skin permeability may be less than that of humans, and thus become rate limiting.

In environmental exposures, the chemical may come into contact with the skin as a mixture or in contaminated soil. In mixtures, other components may function as solvents and modulate the rate of absorption. Other components may retard absorption through surface chemical interactions. In soil, a large fraction of the toxicant may remain bound to soil constituents, thereby reducing the fraction absorbed. Similarly as just discussed, metabolism by soil bacteria may further modify absorption profiles. Not surprisingly, lipid-soluble toxicants may be markedly resistant to removal by washing within a short time after application due to depot formation. For example, 15 min after application, a substantial portion of parathion cannot be removed from exposed skin by soap and water.

In veterinary medicine, another potential modifying factor is the tendency for animals to either lick themselves or other animals. This could either reduce dose or increase absorption secondary to oral delivery. This phenomenon has been well documented by Laffont et al. (2001) with topical ivermectin in cattle and probably occurs with topical ectoparasiticides in cats. The specific pharmacokinetic model used to account for licking with subsequent oral absorption is discussed in Chapter 8 and depicted in Fig. 8.26. For many topical ectoparasiticides applied to veterinary species, only formulations that retain drug on the skin or restrict their penetration to the stratum corneum or sebaceous gland reservoirs are used since the targeted pests are on the surface of the skin and high systemic blood concentrations could lead to toxicity.

Another strategy for transdermal delivery is to overcome the cutaneous barrier by using heat, electrical (iontophoresis) or ultrasonic (phonophoresis) energy, or microneedles rather than the concentration gradient in passive diffusion to drive drug through the skin. These techniques hold the most promise for delivering peptides and oligonucleotide drugs that now can be administered only by injection. In these cases, dose is based on the surface area of application and the amount of energy required to actively deliver the drug across skin. In iontophoresis, this amounts to a dose being expressed in $\mu A/cm^2$. Formulation factors are also very different since many of the excipients used are also delivered by the applied electrical current in molar proportion to the active drug. A recent but related strategy is to use very short-duration high-voltage electrical pulses (electroporation) to reversibly break down the stratum corneum barrier, allowing larger peptides and possibly even small proteins to be systemically delivered. Finally, microneedles are being developed, which penetrate just the stratum corneum and allow drugs to be released (needles dissolve) or infused into the dermis. From the perspective of pharmacokinetic modeling, the classic models to be presented in subsequent chapters are then used to quantitate disposition. The

only difference is that the dose is now expressed in terms of applied electrical current rather than drug mass, which is used when a chemical gradient provides the driving force.

4.2.7 Experimental models

Before leaving the subject of dermal penetration, it is important to consider briefly the experimental techniques used to assess percutaneous absorption. Whole-animal *in vivo* studies generally assess the fraction of the applied dose that is absorbed using techniques to be discussed later. There are many *in vitro* approaches to assess topical penetration. Most employ diffusion cell systems, which sandwich skin of various thicknesses between a donor and a receiver reservoir, the same systems used to assess gastrointestinal transport (Fig. 4.4). The chemical is placed in the donor side (epidermis), and appearance of compound in the receiver (dermal) is monitored over time. This system can use a variety of "skin" sources ranging from full-thickness specimens (epidermis and dermis), to epidermis alone, to various "artificial" membranes such as lipid layers. In most skin studies, unlike other mucosa, the donor reservoir is usually left open to the ambient environment. This basic diffusion cell (Fig. 4.11) in which the receiver solution is a fixed volume is called a static

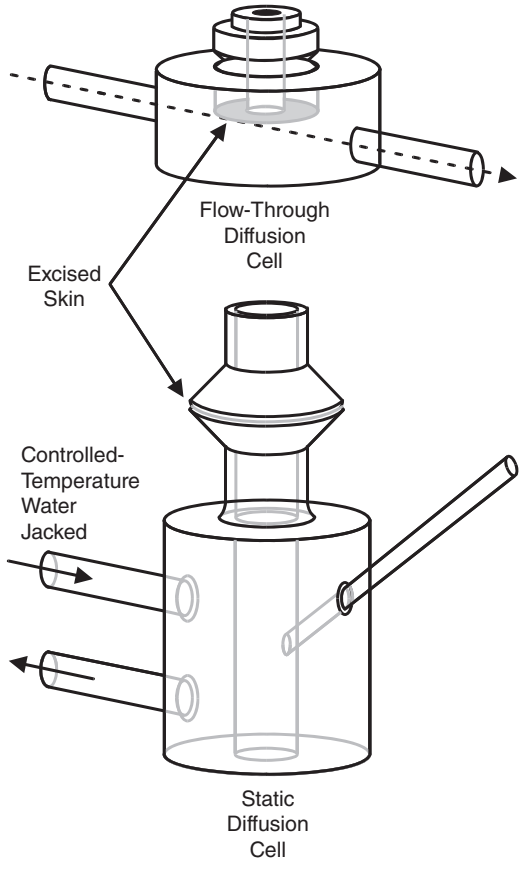

Fig. 4.11 Flow-through and static diffusion cells used to assess *in vitro* percutaneous absorption.

cell. If, instead, the receiver solution is continuously pumped through the dermal reservoir of the cell, a "flow-through" system results that mimics the *in vivo* setting in which blood continuously removes absorbed compound. Various cell and organ culture approaches have also been developed that assess absorption across cultured epidermal and/or dermal membranes. All of these systems have also been used to assess cutaneous metabolism.

The next level of complexity in an *in vitro* system is the use of isolated perfused skin flap preparations that employ surgically prepared vascularized skin flaps harvested from animals and then transferred to an isolated organ perfusion chamber. This model, developed in the author's laboratory, allows absorption to be assessed in skin that is viable, is anatomically intact, and has a functional microcirculation.

4.3 RESPIRATORY ABSORPTION

The third major route for systemic exposure to drugs and toxicants is the respiratory system. Since this system's primary function is gas exchange (O_2, CO_2), it is always in direct contact with environmental air as an unavoidable part of breathing. A number of toxicants are in gaseous (CO, NO_2, formaldehyde), vapor (benzene, CCl_4), or aerosol (lead from automobile exhaust, silica, asbestos, manufactured nanomaterials) forms and are potential candidates for entry via the respiratory system. Each of these modes of inhalational exposure results in a different mechanism of compound absorption and, for the purposes of this text, a different definition of dose. A textbook of anesthesiology should be consulted for more details on disposition and absorption of gases in humans and animals.

Opportunities for systemic absorption are excellent through the respiratory route since the cells lining the alveoli are very thin and profusely bathed by capillaries. The surface area of the lung is large (50–100 m^2), some 50 times the area of the skin. Based on these properties and the diffusion equation presented earlier (Eq. 2.1), the large surface area, the small diffusion distance, and high level of blood perfusion maximize the rate and extent of passive absorption driven by gaseous diffusion.

At the alveoli (site of gas exchange), the epithelial membranes are exceedingly thin and have an intimate association with the capillary walls of the vascular system. There is minimal interstitial space for an absorbed chemical to traverse. During each passage through the lung, blood cells must pass single file in immediate proximity to the site of gas exchange. The distance from the vasculature to the "outside" membrane is only about 1.5 µm for the alveoli. This enables an exceedingly rapidly exchange of gases, approximately 5 s in the case of CO_2 and 1/5 s for O_2. A thin film of fluid wetting the alveolar membrane aids in the initial absorption of toxicants from the alveolar air by providing an easy mechanism for entry into solution. However, in some cases, the phospholipids of the surfactant monolayer may interact with more lipophilic compounds to retard uptake.

The process of respiration involves the movement and exchange of air through several interrelated passages, including the nose, mouth, pharynx, trachea, bronchi, and successive smaller airways terminating in the alveoli, where gaseous exchange occurs. All of these anatomical modifications protect the internal environment of the air passages from the harsh outside environment by warming and humidifying the inspired air. The passages also provide numerous obstacles and baffles to prevent the inhalation of particulate and aerosol droplets. Thus, the absorption of particulate and aerosolized liquids is fundamentally different from that of gases. As will be developed, the absorption of such impacted solids and

liquids along the respiratory tract has much more in common with oral and topical absorption, with the critical caveat that the precise dose of compound finally available for absorption is very difficult to determine.

The volume of the respiratory tree where gaseous exchange does not occur results in a residual volume, which is the amount of air retained by the lung despite maximal expiratory effort. Toxicants in the respiratory air may not be cleared immediately because of slow release from this volume. Although the dynamics of air exchange that occurs during inhalation and expiration cycles is beyond the scope of this chapter, this must be considered should a precise estimate of inhalational exposure be desired.

Another unique aspect of respiratory exposure is the fact that the pulmonary blood circulation is in series with the systemic circulation. Thus, in contrast to topical or oral exposure, compounds absorbed in the lung will enter the oxygenated pulmonary veins, which drain to the systemic arterial circulation. Compared with oral administration, this reduces first-pass hepatic metabolism.

4.3.1 Vapors and gases

Since the rate of entry of vapor-phase toxicants is controlled by the alveolar ventilation rate, the toxicant is presented to the alveoli in an interrupted manner, whose frequency is equal to the rate of breathing; about 20 times per minute. The diffusion coefficient of a gaseous toxicant in the fluids of, and associated with, pulmonary membranes is an important consideration, but doses are more appropriately discussed in terms of the partial pressure of the gas in the inspired air. Upon inhalation of a constant tension of a toxic gas, arterial plasma tension of the gas approaches its tension in the expired air. The rate of entry is then determined by the blood solubility of the toxicant. If there is a high blood:gas partition coefficient, a larger amount must be dissolved in the blood to raise the partial pressure. Gases with a high blood:gas partition coefficient require a longer period to approach the same tension in the blood as in inspired air than it takes for less soluble gases. Similarly, a longer period of time is required for blood concentrations of such a gas to be eliminated, thus prolonging detoxification. Simple diffusion accounts for the somewhat complex series of events in the lung regarding gas absorption.

Another important point to consider in determining how much of an inhaled gas is absorbed into the systemic circulation is the relation of the fraction of lung ventilated to the fraction perfused. Increased perfusion of the lung will favor a more rapid achievement of blood–gas equilibrium. Decreased perfusion will decrease the absorption of toxicants, even those that reach the alveoli. Various ventilation–perfusion "mismatches" may alter the amount of an inhaled gas that is systemically absorbed. Similarly, pulmonary diseases that thicken the alveoli or obstruct the airways may also affect overall absorption.

4.3.2 Aerosols and particulates

The absorption of aerosols and particulates is affected by a number of physiological factors specifically designed to preclude access to the alveoli. The upper respiratory tract, beginning with the nose and continuing down its tubular elements, is a very efficient filtering system for excluding particulate matter (solids, liquid droplets). A coal miner is subject to an inhalation of 6000 g of coal dust particles during the occupational lifetime, but only 100 g are found postmortem; it is therefore obvious that the protective filtering mechanism is an effective one. The parameters of air velocity and directional air changes favor

Table 4.4 Percent retention of inhaled aerosol particles in various regions of the human respiratory tract (450 cm^2 tidal air).

Region	Percent retention of indicated particle sizes				
	20 μm	**6 μm**	**2 μm**	**0.6 μm**	**0.2 μm**
Mouth	15	0	0	0	0
Pharynx	8	0	0	0	0
Trachea	10	1	0	0	0
Pulmonary bronchi	12	2	0	0	0
Secondary bronchi	19	4	1	0	0
Tertiary bronchi	17	9	2	0	0
Quaternary bronchi	6	7	2	1	1
Terminal bronchioles	6	19	6	4	6
Respiratory bronchioles	0	11	5	3	4
Alveolar ducts	0	25	25	8	11
Alveolar sacs	0	5	0	0	0
Total	93	83	41	16	22

Source: Adapted from Hatch and Gross (1964).

impaction of particles in the upper respiratory system. Particle characteristics such as size, coagulation, sedimentation, electrical charge, and diffusion are important to retention, absorption, or expulsion of airborne particles. In addition to these characteristics, a mucous blanket propelled by ciliary action clears the tract of particles by directing them to the gastrointestinal system (via the glottis) or to the mouth for expectoration. This system is responsible for 80% of toxicant lung clearance. The deposition of various particle sizes in different respiratory regions is summarized in Table 4.4; particles larger than 6 μm do not reach the alveolus. Renewed interest has surfaced in this area secondary to the realization that inhalational exposure is an important mechanism seen after occupational exposure to manufactured nanomaterials (e.g., fullerenes, carbon nanotubes).

Phagocytosis is very active in the respiratory tract, both coupled to the directed mucosal route and via penetration through interstitial tissues of the lung and migration to the lymph, where phagocytes may remain stored for long periods in lymph nodes. Ninety percent of material deposited in the respiratory tract may be cleared in less than 1 h. Compared with absorption in the alveoli, absorption through the upper respiratory tract is quantitatively of less importance. However, inhaled toxicants that become deposited on the mucous layer can be absorbed into the myriad of cells lining the respiratory tract and exert a direct toxicological response. This route of exposure is often used to deliver pharmaceutics by aerosol. If a compound is extremely potent, systemic effects may occur.

The end result of this extremely efficient filtering mechanism is that most inhaled drugs deposited in nasal or buccal mucus ultimately enter the gastrointestinal tract. This can best be appreciated by examining the respiratory drainages depicted in Fig. 4.1. Therefore, the disposition of aerosols and particulates largely mirrors that of orally administered drugs. This is an important consideration when interpreting inhalational exposures in which the end points are metabolism, pharmacokinetics, or systemic toxicity. Except for drug that is locally absorbed into the epithelium underlying this ubiquitous mucous blanket, or for that small fraction of drug that actually penetrates into the alveoli, most drug ultimately presented to the gastrointestinal tract for absorption. This fraction of drug undergoes a first-pass hepatic biotransformation and thus shares a metabolic fate with drug orally

administered. The disposition patterns are thus often mixed and must be compared with both parenteral and oral routes for the complete process to be understood.

Nasal administration is a preferred route for many inhalant medications. It recently was employed to deliver insulin in a metered fashion. In these cases, great care is made to deliver aerosols of the specific size for deposition on the nasal mucosa and upper respiratory tract. The bioavailability of these compounds is assessed using the techniques developed for other routes, although a local effect is often desired. The problems with this strategy are the attainment of an accurately delivered dose and the inactivation and binding of administered drug by the thick mucous blanket. A great deal of effort has been focused on using metered nasal delivery for peptide drugs such as insulin; however, the inherent variability makes the delivery of a precise dose very difficult. Drugs delivered by this route usually have a wide therapeutic window and large safety index.

The direct penetration of airborne toxicants at alveolar surfaces or in the upper respiratory tract is not the only action of toxicological importance. Both vapors and particulates may accumulate in upper respiratory passages to produce irritant effects. Despite the effectiveness of ciliary movement and phagocytosis, the cumulative effects of silica, asbestos, or coal dust ultimately cause important chronic fibrosis even though direct absorption is of minor importance. Thus, phagocytosis prevents acute damage but may contribute to chronic toxicity.

There is little evidence for active transport in the respiratory system (phenol red and disodium chromoglycate are notable exceptions), although pinocytosis may be of importance for penetration. The lung is an area of extensive metabolic activity, although detoxification mechanisms do not appear to be of major importance. Perhaps less well appreciated is the fact that the lung is also an excretory route for ethanol, forming the scientific basis for the breath analyzer test for alcohol intoxication.

The final point to consider relates to some specific peculiarities of nasal absorption. In the region of the olfactory epithelium, there exists a direct path for inhaled compounds to be absorbed directly into the olfactory neural tissue and central nervous system, thereby bypassing both the systemic circulation and the blood–brain barrier. The mass of drugs involved in this uptake process is very small and thus would not affect a pharmacokinetic analysis. However, this route has obvious toxicological significance and is being explored as a potential biological mechanism for some aspects of the putative multiple chemical sensitivity syndrome.

4.4 OTHER ROUTES OF ADMINISTRATION

In order to make this discussion of absorption complete, it is important to realize that other extravascular drug administration routes are often encountered. Relative to pharmacokinetic analysis, these are dealt with in the same fashion as the primary routes discussed above. The important difference is that in all cases, the barrier to absorption is less than that encountered in oral or topical delivery. Second, all of these routes involve an invasive procedure to inject drug into an internal body tissue, thereby bypassing the epithelial barriers of the skin and gastrointestinal tract. They are relevant to therapeutic drug administration, but not to toxicology, since they are an invasive technique.

The primary therapeutic routes of drug administration are SC (or SQ) and IM. In these cases, the total dose of drug is known and is injected into tissue that is well perfused by systemic capillaries that drain into the central venous circulation. Recently, implantable

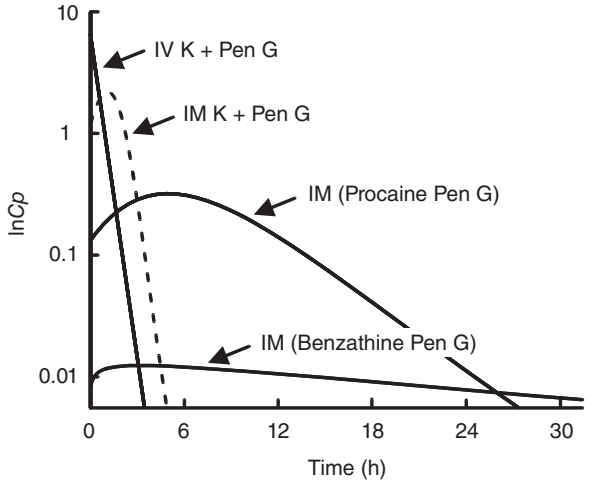

Fig. 4.12 Effects of formulation and route of administration on the plasma concentration-versus-time profiles of penicillin G.

osmotic pumps have been used to deliver defined dosage rates. Both of these routes as well as intravenous administration are termed parenteral to contrast primarily with oral (enteral) and topical dosing, which are classified as nonparenteral routes of drug administration. A primary difference is that parenteral routes bypass all of the body's defensive mechanisms. Parenteral dosage forms are manufactured under strict aseptic guidelines that eliminate microbial and particulate contamination, resulting in sterile preparations that must be administered using aseptic techniques. This restriction does not apply to oral or topical dosage forms. As with all methods of drug administration, there are numerous variables associated with SC and IM dosing, which can be conveniently classified into pharmaceutical and biological categories.

By far, the dosing form has the greatest influence on the rate and extent of absorption of parenteral drugs. The classic examples are potassium, procaine, and benzathine penicillin G (Fig. 4.12). The formulation strategy is to complex the active drug (e.g., penicillin G) with a moiety that delays its release to the surrounding capillary beds by modulating the drug's solubility. A pharmaceutics text should be consulted for the chemistry of these processes. The result is that the rate of release of the compound from the dosing formulation becomes slower than that of the drug's elimination and, as with the slow-release oral and transdermal patches discussed earlier, this release becomes rate limiting.

The potential problems with these strategies are twofold. If one considers antimicrobial therapy, for bacteria with very high therapeutic thresholds (e.g., minimum inhibitory concentrations [MICs]), the prolonged release formulations may never provide therapeutic drug concentrations. In fact, prolonged subtherapeutic concentrations may select for antimicrobial resistance. Second, such so-called depot preparations in food animals may result in persistent drug concentrations in tissues, thereby prolonging the withdrawal time (see Chapter 19). Furthermore, drug depots at injection sites may persist much longer than effective blood concentrations do and be easily detected at slaughter. One must exhibit care to differentiate drug tissue concentrations at injection sites from those achieved after absorption and systemic distribution. This scenario also nicely illustrates the reason that

knowledge of both the extent and rate of drug absorption are needed to adequately describe the absorption of a drug.

The development of depot preparations has received a lot of attention from pharmaceutical companies. Some contraceptives in humans achieve monthly dosing intervals through injection in the SC tissue of insoluble tablets that result in very slow drug release, the best example being the use of levonorgestrel implanted capsules (Norplant®). Similar strategies have been employed in veterinary medicine for the administration of growth promotants. These include estradiol formulated in rubber implants (Cornpudose®), progesterone and estradiol pellets (Implant-C®), and zeranol (Ralgro®). These formulations stress the necessity of knowing the dosage form used when conducting any pharmacokinetic analysis as it is the rate-controlling factor in drug disposition. These considerations will be discussed in more detail in Chapter 8 when the required pharmacokinetic techniques will be presented.

The second major variable concerning parenteral injections relates to the physiology of the injection site. For a drug to be adequately absorbed from a depot preparation, there must be access to the perfusing capillaries and an adequate rate of tissue perfusion. A major source of variability is the muscle into which IM injections are made. Studies have elegantly demonstrated in horses that if the injection is made in between the fascial tissue bundles of a muscle group, less systemic absorption will occur than if the injection is made in the muscle mass. Similarly, if the muscle group or, more likely, the SC injection site, has poor blood perfusion, then less absorption may occur. If the injection results in a local tissue reaction, subsequent inflammation and fibrosis may "wall off" the drug formulation, preventing absorption. Changes in ambient temperature, with compensatory changes in skin blood perfusion, may modulate absorption rate. There are numerous variables in these processes, and it is often only through the use of careful pharmacokinetic analyses that their influence on drug absorption can be ascertained.

Finally, other routes of drug administration are occasionally employed that require absorption for activity. Administration of drugs by intraperitoneal injection is often used in toxicology studies in rodents since larger volumes can be administered. Peritoneal absorption is very efficient, provided adequate "mixing" of the injection with the peritoneal fluid is achieved. Most of the drug absorbed after intraperitoneal administration enters the portal vein and thus may undergo first-pass hepatic metabolism. The disposition of intraperitoneal drug thus mirrors that of oral administration.

Some drugs are administered by conjunctival, intravaginal, or intramammary routes. In these cases, achievement of effective systemic concentrations is often not required for what is an essentially local therapeutic effect. Some relatively sophisticated drug delivery strategies have been employed that take advantage of the unique anatomy of some veterinary species. Prolonged absorption from these sites may result in persistent tissue residues in food-producing animals if the analytical sensitivity of the monitoring assay is sufficiently low. The systemic absorption of these dosage forms is quantitated using procedures identical to those employed for other routes of administration.

4.5 BIOAVAILABILITY

The final topic to consider is the assessment of the extent and rate of absorption after oral, topical, or inhalational drug administration. The extent of drug absorption is defined as absolute systemic availability and is denoted in pharmacokinetic equations as the fraction

of an applied dose absorbed into the body (F). Although this topic will also be discussed extensively in the subsequent modeling chapters of this text when distribution and elimination principles and bioequivalence techniques have been presented, it is important and convenient at this juncture to introduce the basic concepts so as to complete the discussion of drug absorption.

If one is estimating the extent of drug absorption by measuring the resultant concentrations in either blood or excreta, one must have an estimate of how much drug normally would be found if the entire dose were absorbed. To estimate this, an intravenous dose is required since this is the only route of administration that guarantees that 100% of the dose is systemically available ($F = 1.0$) and the pattern of disposition and metabolism can be quantitated. Parameters used to measure systemic availability are thus calculated as a ratio relative to the intravenous dose. The only problems encountered using intravenous data as a benchmark for extent of absorption arise if precipitation occurs after dosing and, paradoxically, the intravenous dose is not completely available. This is a rare event and is dealt with using various injectable vehicle strategies.

For most therapeutic drug studies, systemic absorption is assessed by measuring blood concentrations. In contrast, for pesticides and other toxicants that may be very lipophilic and thus produce very low blood concentrations, urine and feces are often collected to reflect systemic exposure. In both cases, the amount of drug collected after administration by the route under study is divided by that collected after intravenous administration. When drug concentrations in blood (or serum or plasma) are assayed, total absorption is assessed by measuring the area under the (concentration–time) curve (AUC), as shown in Fig. 4.13 using the trapezoidal method to be fully developed in Chapters 9 and 15. This is a geometrical technique that breaks the AUC into corresponding trapezoids based on the number of samples assayed. The terminal area beyond the last data point (a triangle) is estimated and added together with the previous trapezoidal areas. Absolute systemic availability then is calculated as

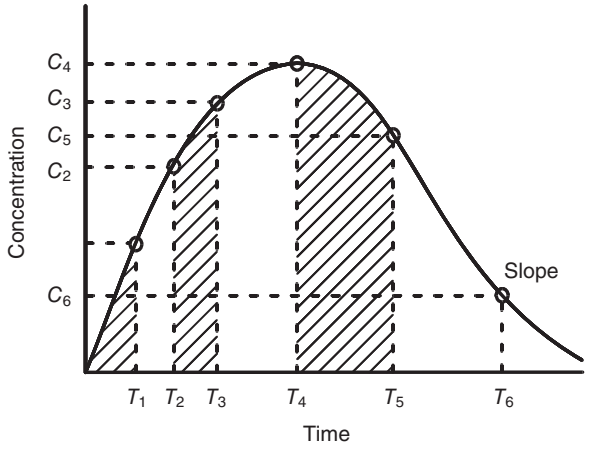

Fig. 4.13 Breakdown of a plasma concentration-versus-time curve into trapezoids used to calculate the area under the curve.

$$F(\%) = \frac{[\text{Urine} + \text{Feces}]_{\text{ROUTE}} \cdot \text{Dose}_{\text{IV}}}{[\text{Urine} + \text{Feces}]_{\text{IV}} \cdot \text{Dose}_{\text{ROUTE}}} \tag{4.2}$$

$$F(\%) = \frac{[\text{AUC}]_{\text{ROUTE}} \cdot \text{Dose}_{\text{IV}}}{[\text{AUC}]_{\text{IV}} \cdot \text{Dose}_{\text{ROUTE}}} \tag{4.3}$$

The selection of which technique to use is dependent on the nature of the compound studied. There are further mathematical limitations to these techniques (e.g., best method to extrapolate the terminal triangle, problems with slow-release dosage formulations), which can be overcome using some of the pharmacokinetic techniques presented in Chapters 9 and 15. Additionally, calculation of F only provides an estimate of the extent, and not rate, of drug absorption. To calculate rate, embodied by the rate constant K_a, pharmacokinetic techniques are required; these are presented in Chapter 8.

Finally, so-called relative systemic availability may be calculated for two nonintravenous formulations in which the data for the reference product are in the denominator, and the test formulation is in the numerator. In many instances, for environmental chemicals and pesticides, urine is more readily accessible and analytically preferred for assessing exposure, although complete urine collections are required. Collection of random urine voids can be independently assessed by simultaneously measuring creatinine concentrations in urine since creatinine is produced at a relatively constant rate and will normalize the data to compensate for incomplete collections.

Topical bioavailability is often determined by measuring drug directly in skin. One approach, termed dermatopharmacokinetics, measures drug in stratum corneum tape strips reflecting the amount of compound that has partitioned into the stratum corneum and is driving diffusion. Other approaches use biopsies to measure drug in the epidermis or dermis.

In summary, knowledge of the biological principles involved in drug absorption by any route is important to the proper application of pharmacokinetics to therapeutic and toxicological problems. The unique biology associated with any specific route must often be taken into consideration when constructing models and sampling strategies, especially when data from such studies are extrapolated to the real world. Assumptions used in building models must be based on the relevant biology of the animal being studied. This chapter provides a brief foray into the biological factors that form the basis for the data to which pharmacokinetic models will be applied.

BIBLIOGRAPHY

Ahmed, I., and Kasrarian, K. 2002. Pharmaceutical challenges in veterinary product development. *Advanced Drug Delivery Reviews*. 54:871–882.

Amidon, G.L., Lennernas, H., Shah, V.P., and Crison, J.R. 1995. A theoretical basis for a biopharmaeutics drug classification system: the correlation of *in vitro* drug product dissolution and *in vivo* bioavailability. *Pharmaceutical Research*. 12:413–420.

Barry, B.W. 1983. *Percutaneous Absorption*. New York: Marcel Dekker.

Borchardt, R.T., Smith, P.L., and Wilson, G. 1996. *Models for Assessing Drug Absorption and Metabolism*. New York: Plenum Press.

Brayden, D.J., Oudet, E.J.M., and Baird, A.W. 2010. Drug delivery systems in domestic animals species. In: Cunningham, F., Elliott, J., and Lees, P. (eds.), *Comparative and Veterinary Pharmacology*. Heidelberg: Springer, pp. 79–112.

Bronaugh, R.L., and Maibach, H.I. 1989. *Percutaneous Absorption*, 2nd Ed. New York: Marcel Dekker.
Bronaugh, R.L., and Maibach, H.I. 1991. *In Vitro Percutaneous Absorption-Principles, Fundamentals and Applications*. Boca Raton, FL: CRC Press.
Csáky, T.Z. 1984. *Handbook of Experimental Pharmacology, Vol. 70, Parts I and II, Pharmacology of Intestinal Permeation*. Berlin: Springer-Verlag.
Custodio, J.M., Wu, C.-Y., and Benet, L.Z. 2008. Predicting drug disposition, absorption/elimination/transporter interplay and the role of food on drug absorption. *Advanced Drug Delivery Reviews*. 60:717–733.
Edman, P., and Björk, E. 1992. Routes of delivery: case studies. (1) Nasal delivery of peptide drugs. *Advanced Drug Delivery Reviews*. 8:165–177.
Feingold, K.R. 2007. The role of epidermal lipids in cutaneous permeability barrier homeostasis. *Journal of Lipid Research*. 48:2531–2546.
Firth, E.G., Nouws, J.F.M., Driessenss, F., Schmaetz, P., Peperkamp, K., and Klein, W.R. 1986. Effect of injection site on the pharmacokinetics of procaine penicillin G in horses. *American Journal of Veterinary Research*. 47:2380–2384.
Fressman, J.B., and Lennernäs, H. 2000. *Oral Drug Absorption*. New York: Marcel Dekker.
Gibson, M. 2004. *Pharmaceutical Preformulation and Formulation*. Boca Raton, FL: CRC Press.
Gizurarson, S. 1990. Animal models for intranasal drug delivery studies. *Acta Pharmaceutica Nordica*. 2:105–122.
Hardee, G.E., and Baggot, J.D. 1998. *Development and Formulation of Veterinary Dosage Forms*, 2nd Ed. New York: Marcel Dekker.
Harrison, A.P., Erlwanger, K.H., Elbrønd, V.S., Andersen, N.K., and Unmack, M.A. 2004. Gastrointestinal-tract models and techniques for use in safety pharmacology. *Journal of Pharmacological and Toxicological Methods*. 49:187–199.
Hatch, T.F., and Gross, P. 1964. *Pulmonary Deposition and Retention of Inhaled Aerosols*. New York: Academic Press.
Hayes, A.W. 1994. *Principles and Methods of Toxicology*, 3rd Ed. New York: Raven Press.
Klaasen, C.D. 1996. *Casarett and Doull's Toxicology: The Basic Science of Poisons*. New York: McGraw-Hill.
Kunta, J.R., and Sinko, P.J. 2004. Intestinal drug transporters: *in vivo* function and clinical relevance. *Current Drug Metabolism*. 5:109–124.
Laffont, C.M., Alvinerie, M., Bousquet-Mélou, A., and Toutain, P.L. 2001. Licking behaviors and environmental contamination arising from pour-on ivermectin for cattle. *International Journal of Parasitology*. 31:1687–1692.
Lee, V.H.L., and Yamamoto, A. 1990. Penetration and enzymatic barriers to peptide and protein absorption. *Advanced Drug Delivery Reviews*. 4:171–207.
Lennernäs, H. 2003. Intestinal drug absorption and bioavailability: beyond involvement of single transport function. *Journal of Pharmacy and Pharmacology*. 55:429–433.
Martanto, W., Davis, S.P., Holiday, N.R., Wang, J., Gill, H.S., and Prausnitz, M.R. 2004. Transdermal delivery of insulin using microneedles *in vivo*. *Pharmaceutical Research*. 21:947–952.
Martinez, M.N., and Riviere, J.E. 1994. Review of the 1993 Veterinary Drug Bioequivalence Workshop. *Journal of Veterinary Pharmacology and Therapeutics*. 17:85–119.
Martinez, M.N., Amidon, G., Clark, L., Jones, W.W., Mitra, A., and Riviere, J.E. 2002. Applying the Biopharmaceutics Classification System to veterinary pharmaceutical products. Part II. Physiological considerations. *Advanced Drug Delivery Reviews*. 54:825–850.
Martinez, M.N., Papich, M.G., and Riviere, J.E. 2004. Veterinary application of *in vitro* dissolution data and the Biopharmaceutics Classification System. *Pharmacopeial Forum*. 30:2295–2303.
McClellan, R.O., Medinsky, M.A., and Snipes, M.B. 2006. Inhalational toxicology. In: Riviere, J.E. (ed.), *Biological Concepts and Techniques in Toxicology*. New York: Taylor and Francis, pp. 297–364.
Mitragotri, S. 2003. Modeling skin permeability to hydrophilic and hydrophobic solutes based on four permeation pathways. *Journal of Controlled Release*. 86:69–92.
Monteiro-Riviere, N.A., Bristol, D.G., Manning, T.O., Rogers, R.A., and Riviere, J.E. 1990. Interspecies and interegional analysis of the comparative histological thickness and laser Doppler blood flow measurements at five cutaneous sites in nine species. *Journal of Investigative Dermatology*. 95:582–586.
Ott, W.R., Steinemann, A.C., and Wallace, L.A. 2007. *Exposure Analysis*. New York: Taylor and Francis.
Patton, J.S., and Platz, R.M. 1992. Routes of delivery: case studies. (2) Pulmonary delivery of peptides and proteins for systemic action. *Advanced Drug Delivery Reviews*. 8:179–196.

Qiao, G.L., and Riviere, J.E. 1997. Pentachlorophenol dermal absorption and disposition from soil in swine: effects of occlusion and skin microorganism inhibition. *Toxicology and Applied Pharmacology*. 147:234–246.

Read, N.W., and Sugden, K. 1987. Gastrointestinal dynamics and pharmacology for the optimum design of controlled release oral dosage forms. *Critical Reviews of Therapeutic Drug Carrier Systems*. 3:221–262.

Riviere, J.E. 1994. Influence of compounding on bioavailability. *Journal of the American Veterinary Medical Association*. 205:226–231.

Riviere, J.E. 2006. *Dermal Absorption Models in Toxicology and Pharmacology*. Boca Raton, FL: Taylor Francis/CRC Press.

Riviere, J.E. 2007. The future of veterinary therapeutics: a glimpse towards 2030. *The Veterinary Journal*. 174:462–471.

Riviere, J.E., and Brooks, J.D. 2005. Predicting skin permeability from complex chemical mixtures. *Toxicology and Applied Pharmacology*. 208:99–110.

Riviere, J.E., and Heit, M.C. 1997. Electrically assisted transdermal drug delivery. *Pharmaceutical Research*. 14:691–701.

Riviere, J.E., and Monteiro-Riviere, N.A. 1991. The isolated perfused porcine skin flap as an *in vitro* model for percutaneous absorption and cutaneous toxicology. *Critical Reviews in Toxicology*. 21:330.

Riviere, J.E., and Papich, M. 2001. Potential and problems of developing transdermal patches for veterinary applications. *Advanced Drug Delivery Reviews*. 50:175–203.

Riviere, J.E., Monteiro-Riviere, N.A., and Williams, P.L. 1995. Isolated perfused porcine skin flap as an *in vitro* model for predicting transdermal pharmacokinetics. *European Journal of Pharmacy and Biopharmaceutics*. 41:152–162.

Roth, W.L., Freeman, R.A., and Wilson, A.G.E. 1993. A physiological based model for gastrointestinal absorption and excretion of chemicals carried by lipids. *Risk Analysis*. 13:531–543.

Stevens, C.E., and Humes, I.D. 1995. *Comparative Physiology of the Vertebrate Digestive System*, 2nd Ed. New York: Cambridge University Press.

Thombre, A.G. 2004. Oral delivery of medications to companion animals: palatability considerations. *Advanced Drug Delivery Reviews*. 56:1399–1413.

Toutain, P.L., and Koritz, G.D. 1997. Veterinary drug bioequivalence determination. *Journal of Veterinary Pharmacology and Therapeutics*. 20:79–90.

Traver, D.S., and Riviere, J.E. 1981. Penicillin and ampicillin therapy in horses. *Journal of the American Veterinary Medical Association*. 178:1186–1189.

Traver, D.S., and Riviere, J.E. 1982. Ampicillin in mares: a comparison of intramuscular sodium ampicillin or sodium ampicillin-ampicillin trihydrate injection. *American Journal of Veterinary Research*. 43:402–404.

United States Pharmacopeia 23rd Edition/National Formulary 18th Edition. 1995. Rockville, MD: United States Pharmacopeial Convention, Inc.

Wang, R.G.M., Knaak, J.B., and Maibach, H.I. 1993. *Health Risk Assessment: Dermal and Inhalational Exposure and Absorption of Toxicants*. Boca Raton, FL: CRC Press.

5 Distribution

with Jennifer Buur

A xenobiotic absorbed into the systemic circulation following any route of administration must reach its site of action at a high enough concentration for a sufficient period of time to elicit a biological response. Distribution processes determine this outcome. Fig. 2.1 (see Chapter 2) should be consulted to assess how distribution processes need to be understood in the context of predicting drug disposition.

Distribution of chemicals to peripheral tissues is dependent on four factors: (1) the physiochemical properties of the compound; (2) the concentration gradient established between the blood and tissue; (3) the ratio of blood flow to tissue mass; and (4) the affinity of the chemical for tissue constituents.

The physiochemical properties of the chemical (pK_a, lipid solubility, molecular weight) are most important in determining its propensity to distribute to a specific tissue. For most molecules, distribution out of the blood into tissue is by simple diffusion down a concentration gradient; hence, distribution is generally described by first-order rate constants. The principles discussed in Chapter 2 for movement of compounds across diffusion barriers also apply here, as one could consider distribution as "absorption" into the tissues from the blood. The complicating factors are that the driving concentration is now dependent on blood flow, the surface area for absorption into tissues is dependent on tissue mass and capillary density, the relevant partition coefficient is the blood–tissue ratio, and plasma/tissue protein binding complicates the picture. An understanding of distribution is a prerequisite to predicting pharmacological response.

5.1 PHYSIOLOGICAL DETERMINANTS OF DISTRIBUTION

Body fluids are distributed among three primary compartments; only one of which, vascular fluid, is thought to have an important role in the distribution of most compounds throughout the body. Human plasma amounts to about 4% of the total body weight and 53% of the total blood volume. By comparison, the interstitial tissue fluids account for 13% and intracellular fluids 41% of body weight. Use of microdialysis and ultrafiltration probes, catheters, and tissue cages allows the concentration of drug to be directly monitored in the interstitial fluid and thus further opens the window for pharmacokinetic analysis. The concentration that a compound may achieve in the blood following exposure depends in

Comparative Pharmacokinetics: Principles, Techniques, and Applications, Second Edition. Jim E. Riviere.
 ISBN: 978-0-813-82993-7

part on its apparent volume of distribution. If the xenobiotic is distributed only in the plasma (low apparent volume of distribution), a high concentration of the xenobiotic could be achieved in the vascular system. In contrast, the plasma concentration would be markedly lower if the same quantity of xenobiotic were distributed to a larger pool, including the interstitial water and/or cellular fluids as is seen with xenobiotics with a high apparent volume of distribution.

The next important consideration is the relative blood flow to different tissues. Two factors will favor chemical accumulation into a tissue: high blood flow per unit mass of tissue and a large tissue mass. Tissues with a high blood flow–mass ratio include the brain, heart, liver, kidney, and endocrine glands. Tissues with an intermediate ratio include muscle and skin, while tissues with a low ratio (indicative of poor systemic perfusion) include adipose tissue and bone. These ratios are generalizations, and some tissues may actually be categorized in two disparate groups. An excellent example is the kidney, where the renal cortex receives some 25% of cardiac output and thus has a very high blood flow–mass ratio. However, the renal medulla receives only a small fraction of this blood flow and thus could be categorized in the intermediate to low group.

If the affinity of the chemical for the tissue is high, then the chemical will still accumulate in poorly perfused tissues (such as fat). It will, however, take a relatively longer period of time to "load" or "deplete" these tissues. A relatively low blood flow–mass ratio is a major physiological explanation for depot formation.

Differences in perfusion and affinity have therapeutic and toxicological implications. Fig. 5.1 depicts the relative tissue concentrations in pigs of the environmental contaminant pentachlorophenol (PCP) dosed topically in soil (relevant environmental exposure conditions) for 3 weeks with the skin either occluded or exposed to air. Two trends can be immediately noted. Higher accumulation of PCP occurred in well-perfused tissues such as liver, lung, kidney, and ovary. Also, as discussed in Chapter 4, occlusion of the dosing site increased the absorbed dose and thus tissue concentrations (recall Fig. 4.10). Many antimicrobial agents used in comparative medicine show preferential distribution to liver and kidney over muscle and other tissues, an important consideration in food animal medicine.

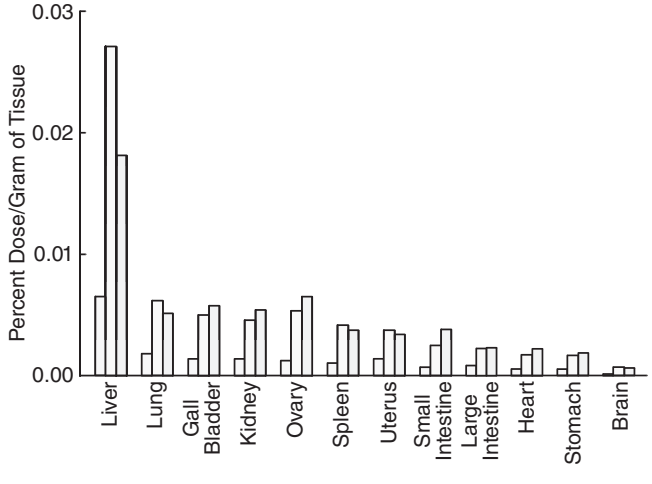

Fig. 5.1 Comparative tissue distribution at 17 days after topical pentachlorophenol dosing (300 mg) in soil on pigs. Histograms represent (nonoccluded/occluded/occluded with antimicrobials) dosing conditions. Note the predominant distribution to liver.

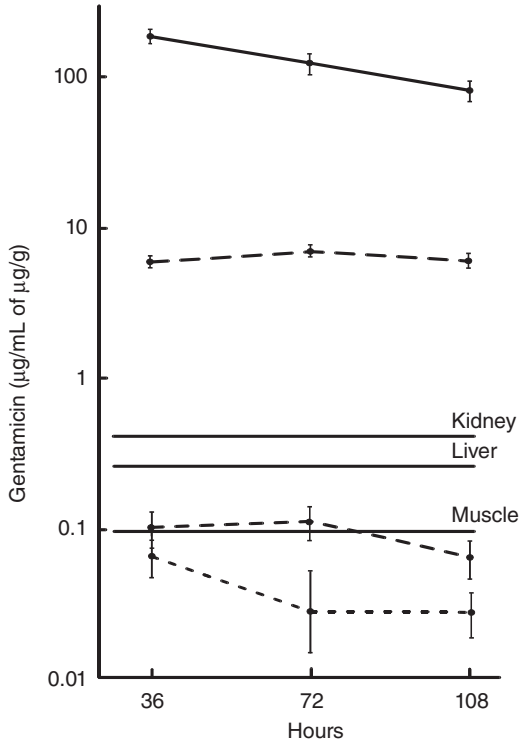

Fig. 5.2 Mean (±standard error of the mean [SEM]) gentamicin concentrations in pigs after a multiple dosage regimen shows predominant distribution to kidney and liver. Renal cortex (———); liver (– – –); muscle (- - -); plasma11 (···). Horizontal lines are legal tissue tolerances putting tissue concentrations in perspective for veterinary usage in food animals.

This is shown in Fig. 5.2, which depicts the tissue depletion for intravenous gentamicin in pigs relative to simultaneous plasma concentrations. Numerous examples of similar relative tissue distributions can be seen throughout the literature for many classes of compounds including nanoparticles, reinforcing the general principle of organ flow-dependent diffusion. This topic will be revisited in Chapter 19 in which the pharmacokinetics of tissue residue depletion is presented.

The data above required no pharmacokinetic analysis as only comparative tissue concentrations were employed. However, in some cases, performing very simple manipulations of the data, using the concept of the *a*rea *u*nder the concentration–time *c*urve (AUC) presented in Chapter 4, may shed more light on the problem at hand and simplify interpretation of the data. Studies designed to induce changes in the distribution of systemic blood flow by using systemic hyperthermia have demonstrated blood flow shunting using imaging and microsphere techniques. Similarly, the same strategy has been used to target peripheral tissues with the chemotherapeutic drug cisplatin while simultaneously shunting flow away from the kidney, where drug toxicity may occur. Cisplatin covalently binds to tissue sites, and thus tissue concentrations largely reflect total exposure. The observed blood AUCs were linearly related to infusion dose over three different doses, indicating that saturation of any disposition process did not occur. Because of this linearity, observed tissue concentrations were also dose dependent, and thus tissue concentration should be normalized to

Table 5.1 Comparison of hyperthermic (42°C) and normothermic (37°C) tissue distribution of cisplatin administered in three 1-h infusions (20, 50, and 80 mg/m^2).

Tissue	Ratio[a]
Lung	2.3 ± 0.4
Ileum	2.0 ± 0.2
Adrenal	1.8 ± 0.1
Pyloric stomach	1.7 ± 0.2
Colon	1.6 ± 0.2
Duodenum	1.6 ± 0.1
Spleen	1.5 ± 0.2
Pancreas	1.5 ± 0.2
Outer renal cortex	1.5 ± 0.1
Rectum	1.4 ± 0.2
Jejunum	1.4 ± 0.2
Heart	1.4 ± 0.3
Esophagus	1.3 ± 0.1
Ovary	1.2 ± 0.2
Thyroid	1.2 ± 0.2
Cardiac stomach	1.2 ± 0.1
Inner renal cortex	1.2 ± 0.1
Uterus	1.2 ± 0.1
Muscle	1.1 ± 0.3
Fat	1.0 ± 0.3
Bone marrow	0.96 ± 0.32
Renal medulla	0.79 ± 0.08
Skin	0.79 ± 0.13
Cervical lymph node	0.64 ± 0.11

[a] $\text{Ratio}\,(\pm\text{SEM}) = \dfrac{[\text{Platinum}]_{42} / \text{AUC}}{[\text{Platinum}]_{37} / \text{AUC}}$.

AUC, a metric representing blood–tissue partitioning, as an indicator of systemic exposure. When the ratio of these normalized tissue concentrations in hyperthermic animals (42°C) were compared with those of normal dogs (37°C), statistically significant differences in tissue ratios were observed (Table 5.1). A ratio of 1.0 would indicate no preferential tissue accumulation with hyperthermia. The liver, lung, and several gastrointestinal tissues tended to accumulate drugs, while the renal medulla, lymph nodes, and skin had lower ratios, indicating restricted distribution. These differences are significant for a drug such as cisplatin with a low therapeutic index, as doses may be reduced to avoid kidney toxicity while still maintaining effective concentrations in target tissues such as the lung.

5.2 TISSUE BARRIERS TO DISTRIBUTION

Some organs have unique anatomical barriers to xenobiotic penetration. The classic and most studied example is the blood-brain barrier, which has a glial cell layer interposed between the capillary endothelium and the nervous tissue. In the membrane scheme depicted in Fig. 2.2 (see Chapter 2), this amounts to an additional lipid membrane between the capillary and target tissue. Only nonionized lipid-soluble compounds can penetrate this

Table 5.2 Select list of therapeutics known to be substrates of P-glycoprotein.

Amitriptyline
Cyclosporine
Digoxin
Doxorubicin
Erythromycin
Ivermectin
Ketoconazole
Loperamide
Verapamil
Vincristine

barrier. Similar considerations apply to ocular, prostatic, testicular, synovial, mammary gland, and placental xenobiotic distribution. Chemicals may also distribute into transcellular fluid compartments, which are also demarcated by an epithelial cell layer. These include cerebrospinal, intraocular, synovial, pericardial, pleural, peritoneal, and cochlear perilymph fluid compartments.

A few tissues possess selective transport mechanisms that accumulate specific chemicals against concentration gradients. For example, the blood–brain barrier possesses glucose, L-amino acid, and transferrin transporters. If the xenobiotic resembles an endogenous transport substrate, then it may preferentially concentrate in a particular tissue. Likewise, some tissues possess selective efflux transport processes that remove chemicals from certain protected sites. Renal specific organic anion transports (OATs) and amino acid transporters play important roles in the redistribution of molecules from the proximal renal tubules. Similar processes and transport systems for peptides and other compounds are also found in other organs.

P-glycoprotein is one of the best understood efflux transporters. It is encoded by the MDR1 (also known as ABCB1) gene and is a member of the ATP-binding cassette superfamily of transporters that also includes the cystic fibrosis transmembrane regulator and the sulfonylurea-sensitive ATP-dependent potassium channel. P-glycoprotein is normally expressed in the intestinal tract, brain, biliary canaliculi, placenta, testes, and proximal renal tubules. While P-glycoprotein has wide substrate specificity, drugs that have the proper physiochemical characteristics (high lipophilicity) to enter tissues such as the brain do not achieve effective concentrations because of this active efflux mechanism. Table 5.2 gives a short list of P-glycoprotein substrates.

A specific genetic mutation leading to nonfunctional proteins in some dogs produces neurotoxicosis from standard doses of therapeutics such as avermectins and loperamide. In addition, increased expression of P-glycoprotein contributes to drug resistance in both neoplasia and microorganisms including *Plasmodium falciparum*, the causative agent of malaria. Therefore, knowledge and understanding of these mechanisms and how they are altered in diseased states contributes to both drug selection and dosing regimen design.

In addition to physical barriers and active transport mechanisms, ion trapping (see Chapter 2) plays a role in the tissue distribution of xenobiotics. Tissues such as cerebral spinal fluid or milk have a lower pH level than the circulating blood plasma. This results in the accumulation of weak bases into these sites. Disease states can change the pH of tissues and alter distribution of therapeutics.

5.3 PLASMA PROTEIN BINDING

Following entry into the circulatory system, a chemical is distributed throughout the body and may accumulate at the site of action, be transferred to a storage depot, or be transported to organs that will detoxify, activate, or eliminate the compound. Although many xenobiotics have sufficient solubility in the aqueous component of blood to account for simple solution as a means of distribution, the primary distribution mechanism for insoluble xenobiotics is in association with plasma proteins. Although cellular components (e.g., red blood cells) may also be responsible for transport of drugs, such transport is seldom the major route. The transport of compounds by lymph is usually of little quantitative importance, except for certain proteins and nanoparticles that are primarily transported by this mechanism. It must be recognized, however, that both erythrocytes and lymph also play roles in the transport of some lipophilic drugs and toxins, in some instances to an important extent.

Studies of plasma proteins have shown albumin to be particularly important in the binding of drugs. This is especially true for weak acids, with weak bases often binding to α1-acid glycoproteins. For certain hormones, specific high-affinity transport proteins are present and there is evidence of a significant binding/partitioning role for lipoproteins in carrying very lipophilic chemicals in the blood; an example being the transport of cholesterol by low- and high-density lipoproteins. Additionally, lipoproteins can preferentially enter certain cells due to cellular recognition proteins located on the outer core of the lipoprotein, a process being used to target drugs to specific cells by association with nanocarriers. This phenomenon facilitates transport across cell membranes and can lead to increased xenobiotic concentrations in specific tissues similar to the active transport systems discussed previously.

Since binding properties alter not only distribution but other pharmacokinetic processes such as metabolism and elimination, they are often exploited in the design of unique formulations including lipid-based vehicles such as liposomal formulations of amphotericin B or griseofulvin. Current investigation into the alteration of binding properties has demonstrated the possibility of selective and enhanced distribution into neoplastic tissue secondary to a variety of encapsulation techniques.

5.3.1 Ligand–protein interactions

An interesting aspect of disposition is the apparent contradiction that, although many xenobiotics are "unreactive" in a strictly chemical sense, they can be reversibly bound to a variety of biological constituents. In the case of most ligand–protein interactions, reversible binding follows the law of mass action and provides a remarkably efficient means whereby xenobiotics can be transported to various tissues. The xenobiotic–protein interaction may be simply described according to the law of mass action as

$$[X]_F + [\text{Free sites}] \underset{K_2}{\overset{K_1}{\rightleftharpoons}} [X]_B, \tag{5.1}$$

where $[X]_F$ and $[X]_B$ are free (ultrafilterable) and bound xenobiotic molecules, respectively, and K_1 and K_2 are the specific rate constants for association and dissociation. It is important to stress that K_2 dictates the rate of xenobiotic release to a site of action, inaction, or storage. The ratio K_2/K_1 is identical to the dissociation constant, K_{diss}. Among a group of binding sites on proteins, those with the smallest K_{diss} value for a given xenobiotic will bind it most tightly. In contrast to reversible binding seen with most therapeutic drugs, agents such as

cisplatin, and some potentially carcinogenic metabolites that are formed from chlorinated hydrocarbons (such as CCl_4), are covalently bound to tissue proteins. In this case, there is no true distribution of the ligand, as K_2 is nonexistent; thus, there is no opportunity for dissociation.

Once a molecule binds to a plasma protein, it moves throughout the circulation until it dissociates, usually for attachment to another large molecule. Dissociation occurs when the affinity for another biomolecule or tissue component is greater than that for the plasma protein to which the xenobiotic was originally bound. Thus, forces of association must be strong enough to establish an initial interaction, and they must also be weak enough such that a change in the physical or chemical environment can lead to dissociation. Dissociation could occur by binding to proteins of greater affinity (lower K_{diss} values); binding with a higher concentration of proteins of lower affinity; or changes in K_{diss} associated with alterations in ionic strength, pH, temperature, or conformational changes in the binding site induced by binding of other molecules.

Ligand–protein interactions are dynamic and in constant flux. As long as binding is reversible, redistribution will occur whenever the concentration of one pool (i.e., blood or tissue) is diminished. Redistribution must occur when the concentration is diminished in order to reestablish equilibrium. Disease states, fasting status, body temperature, and interactions with endogenous and exogenous compounds all contribute to the constantly changing pools of free and bound molecules.

5.3.2 Covalent binding

Proteins complex with ligands by a variety of mechanisms. Covalent binding may have a profound direct effect on an organism due to modification of an essential molecule. However, this usually accounts for a minor portion of the total dose and is of no importance in further distribution of xenobiotics since such compounds cannot dissociate. As previously mentioned, when metabolites of some compounds are covalently bound to proteins, there may be no opportunity for subsequent release of the ligand apart from release upon breakdown of the protein itself (e.g., intracellular metabolism). The cancer chemotherapeutic drug cisplatin covalently binds to albumin through an aquation reaction. In incubation studies, "aging" occurs after a short period of time independent of drug concentration, and the majority of circulating cisplatin is covalently bound (Fig. 5.3). Hyperthermia thermodynamically accelerates this process and thus reduces effective filterable (and thus diffusible) drug concentrations even sooner. However, cisplatin may also bind to lower-molecular-weight nucleophiles (e.g., peptides, amino acids) and be distributed to tissues in association with these more mobile molecules. Once in the cell, the free cisplatin is regenerated, which can then exert its effect. Similar types of reactive interactions may also occur with certain nanomaterials.

5.3.3 Noncovalent binding

Noncovalent binding is of primary importance with respect to distribution because of the opportunities to dissociate after transport. In rare cases, the noncovalent bond may be so tight (K_{diss} extremely small) that a compound remains in the blood for very lengthy periods. For example, 3-hydroxy-2,4,4-triiodo-α-ethyl hydrocinnamic acid has a half-life of about 1 year with respect to its binding to plasma albumin. Types of interactions that lead to noncovalent binding include the following.

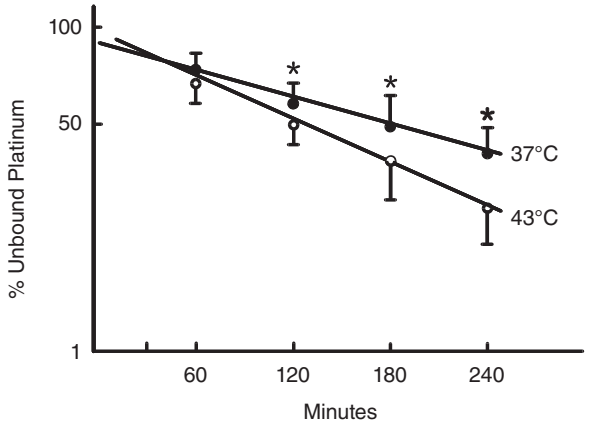

Fig. 5.3 Percent ultrafilterable (unbound, free) cisplatin in canine serum incubated at 37 and 43°C demonstrating increased rate of covalent binding at elevated temperatures.

5.3.3.1 *Ionic binding*

Charged drugs may be bound to plasma proteins by ionic interactions. Electrostatic attraction occurs between two oppositely charged ions on a drug and a protein. Proteins are capable of binding charged metal ions. The degree of binding varies with the chemical nature of each compound and the net charge. Dissociation of ionic bonds usually occurs readily, but some members of the transition group of metals exhibit high association constants (low K_{diss} values), and exchange is slow. Ionic interactions may also contribute to binding of alkaloids with ionizable nitrogenous groups and other ionizable xenobiotics.

5.3.3.2 *Hydrogen binding*

Hydrogen bonds arise when a hydrogen atom, covalently bound to one electronegative atom, is "shared" to a significant degree with a second electronegative atom. As a rule, only the most electronegative atoms (O, N, and F) form stable hydrogen bonds. Protein side chains containing hydroxyl, amino, carboxyl, imidazole, and carbamyl groups can form hydrogen bonds, as can the N and O atoms of peptide bonds themselves. Hydrogen bonding plays an important role in the structural configuration of proteins and nucleic acids. While generally stronger than weak interactions produced by van der Waals forces, hydrogen bonding is significantly weaker than ionic bonding.

5.3.3.3 *Weak interactions*

Van der Waals forces produce weak interactions that act between the nucleus of one atom and the electrons of another atom; that is, between dipoles and induced dipoles. The attractive forces arise from slight distortions induced in the electron clouds surrounding each nucleus as two atoms are brought close together. The binding force is critically dependent on the proximity of interacting atoms and diminishes rapidly with distance. However, when these forces are summed over a large number of interacting atoms that "fit" together spatially, they can play a significant role in determining specificity of xenobiotic–protein interactions.

5.3.3.4 *Hydrophobic interactions*

A final mechanism of binding is based on hydrophobic interactions. When two nonpolar groups come together, they exclude the water between them, and this mutual repulsion of water results in a hydrophobic interaction. In the aggregate, they present the least possible disruption of interactions among polar water molecules and thus can lead to thermodynamically stable complexes. Some authorities consider this a special case involving van der Waals forces. The minimization of thermodynamically unfavorable contact of a polar grouping with water molecules provides the major stabilizing effect in hydrophobic interactions.

5.3.4 Methods for quantification of protein binding

A number of *in vitro* and *in vivo* methods have been employed to study ligand–protein interactions. *In vivo* techniques such as microdialysis, ultrafiltration, or tissue cages concentrate on quantification of unbound xenobiotics within plasma or tissues at times of equilibrium. *In vitro* techniques include ultrafiltration, electrophoresis, equilibrium dialysis, radioligand binding, ultracentrifugation, fluorescence or nuclear magnetic resonance (NMR) spectroscopy, gel filtration, high-performance affinity chromatography, and automated sequential trace enrichment of dialysate. Saturation binding studies focus on the physiochemical characterization of the protein binding and the direct assessment of molecular binding properties such as maximal binding (B_{max}), as well as the equilibrium dissociation constant (K_{diss}). Alternately, these techniques can also be used to quantify the percent of xenobiotic bound at various plasma concentrations. The most widely used techniques are radioligand binding studies, ultrafiltration, and equilibrium dialysis.

No matter the technique, the basic concept is the same. A semipermeable membrane is used to restrict passage of protein but allow unbound drug to cross the barrier. Bound drug is placed on one side of the membrane, and samples are collected from the protein-free side. Ultrafiltration allows rapid protein–drug separation, while equilibrium dialysis requires time for the separation to occur. The fraction of free drug is then calculated based on the difference between total drug used and free drug measured from the appropriate filtrate as is described in Equation 5.2:

$$[X]_T = [X]_B + [X]_F, \tag{5.2}$$

where $[X]_T$, $[X]_B$, and $[X]_F$ are the concentration of total, bound, and free xenobiotic molecules. The ratio of $[X]_F/[X]_T$ is the fraction unbound, f_u, which is incorporated in many pharmacokinetic equations throughout this text. Almost all techniques assume that no adsorption of drug to the membrane occurs, the drug–protein binding is at equilibrium, the binding equilibrium does not change with altered concentrations of protein, and there is no leakage of bound proteins through the membrane. Volume shifting and sample dilution are other aspects of study design that can confound analysis using these techniques.

5.3.5 Interpretation of ligand–protein interactions

A characteristic of ligand–protein interactions is the great number of binding possibilities for attachment of a small molecule (xenobiotic) to a large molecule (protein). Although highly specific (high-affinity, low-capacity) binding is known to occur with a number of

drugs, examples of specific binding for toxicants are limited. In most cases, low-affinity, high-capacity binding describes the interactions. Often, the number of binding sites cannot be accurately determined because of the nonspecific nature of the interactions.

To understand the physiochemical and biological significance of xenobiotic binding to a protein, several factors must be considered. The maximal number of molecules bound per protein molecule, B_{max}, and the maximum number of binding sites, n, are important considerations as they comprise the definitive binding capacity of the protein. Another consideration is the binding affinity, $K_{binding}$ (or $1/K_{diss}$). If the protein has but one binding site for the xenobiotic, a single value of K_{diss} (or $K_{binding}$) describes the strength of the interaction. More usually, the value of the binding constant will vary when more than one binding site is present, each site having its intrinsic association constant, K_1, K_2, and so on. This is especially true in the case of those xenobiotics for which van der Waals forces and hydrophobic binding appear to contribute to binding of a nonspecific, low-affinity nature. Of course, the chemical nature of the binding site is of critical importance in determining the binding characteristics.

The environment of the protein, the three-dimensional molecular structure of the binding site, the general location in the overall protein molecule, cooperativity, and allosteric effects are all factors that influence binding. Fig. 5.4 illustrates the effect of storage on the binding properties of sulfamethazine in porcine plasma. Both B_{max} and K_{diss} in fresh porcine plasma were significantly different from when the same study was performed using frozen porcine plasma. Thus, even sample storage and the processing of the protein used in the experiments must be taken into account when interpreting data.

Studies have not generally provided an adequate elucidation of these factors; that is, binding is usually too complex to be accurately described by any one set of equations. The complexity also makes it difficult to predict the *in vivo* effects of ligand–ligand interactions such as displacement.

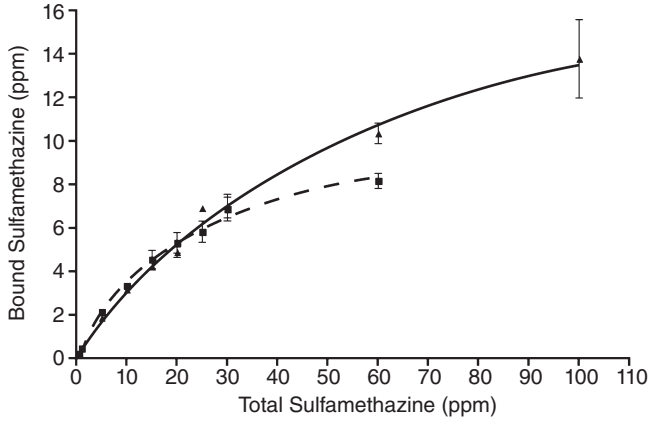

Fig. 5.4 Alteration of protein-binding characteristics of sulfamethazine in fresh and frozen porcine plasma. Data points represent averages from seven experiments, with each experiment having three replicates and using plasma pooled from a minimum of three different pigs. Solid line represents fresh plasma; dashed line represents frozen plasma.

5.3.6 Analysis of protein binding

Methods for analyzing binding phenomena are legion, and all possess unique terminology depending on the roots of their disciplines (e.g., biochemistry vs. physiology vs. pharmacology). Classic techniques for data analysis, such as Scatchard plots, double reciprocal plots, and Rosenthal plots, require transformation to linearize the data. The transformation process distorts error and violates assumptions of linear regression by altering the relationship between the values on the *x*- and *y*-axis. These methods have been abandoned since nonlinear regression can be performed using common software packages. Nonlinear techniques are considered better than classic techniques since they do not require the transformation of data and provide more accurate parameter estimations. These techniques are also used to describe other saturable processes. Many of these essentially nonlinear pharmacokinetic interactions will be dealt with more extensively in Chapter 10 using a terminology consistent with pharmacokinetic models.

Chemical–protein complexes that are held together by relatively weak bonds (energies of the order of hydrogen bonds or less) readily associate and dissociate at physiological temperature. In these circumstances, a state of thermodynamic equilibrium can be readily attained. The law of mass action can be applied as follows:

$$K_{\text{binding}} = \frac{[XP]}{[X]\cdot[P]} = \frac{1}{K_{\text{diss}}}, \tag{5.3}$$

where K_{binding} is the equilibrium constant for association, $[XP]$ is the concentration of chemical–protein bound complex, $[X]$ is the concentration of free chemical, and $[P]$ is the concentration of total protein. This equation does not describe the binding sites or binding affinity. Evaluation of parameters $B_{\max}$ or K_{diss} requires nonlinear regression of saturation studies. If there is a single specific binding site, then the data can be fit to a one site binding hyperbolic equation,

$$[X]_{\text{B}} = \frac{B_{\max}\cdot[X]_{\text{T}}}{K_{\text{diss}} + [X]_{\text{T}}}, \tag{5.4}$$

where $[X]_{\text{T}}$ and $[X]_{\text{B}}$ are the concentration of total and bound xenobiotic molecules, $B_{\max}$ is maximal binding capacity, and K_{diss} is the dissociation constant for that ligand–protein interaction. Fig. 5.4 illustrates the specific one site binding saturation study of sulfamethazine presumably to albumin in porcine plasma derived using ultrafiltration. Additional binding equations exist for other situations including multiple binding sites, cooperative binding, nonsaturable processes, and competitive binding.

Xenobiotic–protein binding may be defined as (1) specific, high affinity, low capacity, and (2) nonspecific, low affinity, high capacity. The term high affinity implies an affinity constant (K_{binding}) of the order of $100\,\text{M}^{-1}$ or greater, while low affinity implies a K_{binding} of the order of $10\,\text{M}^{-1}$ or less. Nonspecific, low-affinity binding appears to be most characteristic of nonpolar compounds.

Hydrophobic binding of highly lipid xenobiotics (many environmental contaminants) is probably not limited to a single plasma protein. The comparative binding of dichlorodiphenyltrichloroethane (DDT) to five human plasma proteins was strongest for albumin and lipoprotein fractions, although binding to any of three other proteins could adequately explain transport of DDT in the blood. Similar results have been reported for dieldrin, parathion, and carbaryl.

Protein binding data are frequently expressed in terms of percent of ligand bound. Although useful, the limitations should be recognized, for as ligand concentration is lowered, the percentage of binding increases. When a compound has a high affinity for a protein (e.g., albumin), percent binding falls sharply when the total ligand concentration exceeds a certain value that saturates the binding sites available. This topic will be revisited in greater detail when nonlinear pharmacokinetic models are developed in Chapter 10. A basic text in biochemistry should be consulted for more details on the analysis of ligand–protein interactions.

5.3.7 Displacement

If a xenobiotic is administered after binding sites on a protein are occupied by another chemical, competition for the site occurs. Toxic effects or enhanced activity may be noted due to a higher concentration of free xenobiotic. However, the clinical implications of such an interaction are limited since other pharmacokinetic mechanisms such as clearance also contribute to free xenobiotic concentrations. A clinical study looking at the interaction between sulfamethazine and flunixin meglumine in pigs demonstrates this scenario (Buur et al., 2009). Sulfamethazine was given by constant rate infusion such that the free concentration of sulfamethazine was held steady. Flunixin meglumine was subsequently given as a bolus dose and free sulfamethazine concentrations were monitored. Fig. 5.5 illustrates that while an increase concentration of free sulfamethazine did occur ($\uparrow f_u$), the concentration spike was short lived as other mechanisms worked quickly to reestablish equilibrium. Mercury has a greater affinity for metallothionein than has cadmium and displaces cadmium from the protein *in vitro*. The displacing substance may also be an endogenous ligand. In renal disease, accumulation of so-called uremic toxins may occur, which displaces administered drugs and results in enhanced toxicity, as is discussed in Chapter 17. This disease-induced increase in a compound's free fraction may be responsible for disease-induced increases in a xenobiotic's distribution volume.

Competition for the same site on plasma proteins may have especially important consequences when one of the potentially toxic ligands has a very high affinity. If compound A has low fractional binding (e.g., 30%), and compound B displaces 10% of A from the protein, the net increase of free A is from 70 to 73%, a negligible increase. However, if A is 98% bound and 10% is displaced, the amount of free A increases from 2 to 12%, a sixfold increase in free compound, which could result in a severe toxicological reaction. Once again, it is important to remember that *in vitro* interactions do not take into account the milieu of multiple processes that occur *in vivo* (e.g., increased clearance of free drug) such that the effects of alteration in one area may be mitigated by processes of other mechanisms within the body. The classic example of displacement resulting in clinical effects was once believed to be between phenylbutazone and warfarin. While displacement of warfarin does occur in this situation, it is now accepted that the clinical manifestation of this interaction is due to inhibition of warfarin metabolism by phenylbutazone rather than by binding displacement.

Competitive binding for very nonpolar compounds with infinite binding sites would be unlikely to occur at physiological concentrations. A change in binding may also occur when a second ligand produces an allosteric effect resulting in altered affinity of the protein for the originally bound compound (noncompetitive binding).

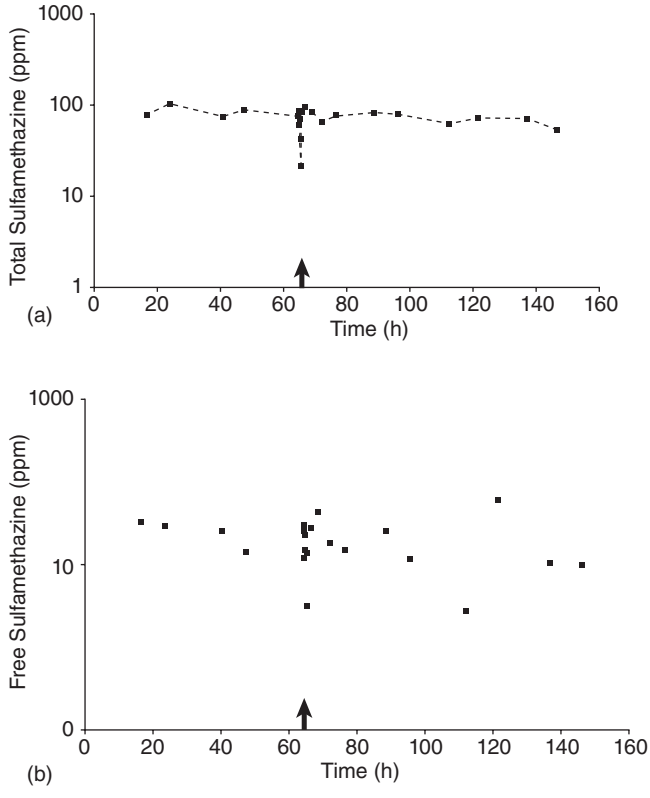

Fig. 5.5 Concentration of total (a) and free (b) sulfamethazine in porcine plasma in a single representative pig. Arrow represents the timing of a single IV bolus of flunixin meglumine.

Most pharmacokinetic models in the human and comparative medical literature only assess total drug concentrations. When the extent of protein binding differs dramatically among species, inappropriate extrapolations often occur, as will be seen with doxycycline in Chapter 18. Similarly, interpretation of the extent of tissue distribution when the extent of protein binding is not known may be misleading. The most precise predictions can often be made when the free fraction of drug is known over the concentration ranges of the study being conducted or when free drug concentration is directly quantitated *in vivo* using techniques such as microdialysis or tissue cages.

5.4 OTHER FACTORS AFFECTING DISTRIBUTION

Among the factors that affect distribution, apart from binding to blood macromolecules per se, are the route of administration, molecular weight, rate of metabolism, polarity and stereochemistry of the parent compound or metabolic products, and rate of excretion. Molecular weight, charge, and/or polarity have been discussed. Stereoselectivity in the disposition of a drug is an often-ignored phenomenon that could influence many studies. Its impact on metabolism is obvious; however, any receptor-mediated binding or transport

process, including high-specificity protein binding, could be affected. Propranolol and ibuprofen have been shown to demonstrate stereoselective distribution.

5.4.1 Tissue binding

A major factor determining distribution is the extent of tissue binding. This is a process identical to that of serum protein binding except that the results on drug disposition are opposite, and a greater diversity of proteins exist in various tissues. Tissue binding is governed by the same mechanisms as discussed above and tends to increase a drug's distribution, although not necessarily activity as the drug may be sequestered away from active drug receptors or target microorganisms. Covalent binding also occurs and is relevant to toxicology and tissue residue depletion.

Depending on the pharmacokinetic model employed, irreversible covalent tissue binding may actually be mathematically detected as an increase in the drug's elimination if only blood samples are used in the analysis since there is no redistribution of drug back into the blood. For distribution to be quantitated, the basic assumption in most modeling systems is that the process is reversible, and thus an equilibrium will ultimately be achieved between drug movement into and out of tissue. When irreversible binding occurs, compound is extracted from blood, and when excretory output (e.g., urine, feces, expired air) is not monitored, this is interpreted in many models as elimination. These model assumptions are often ignored. The quantification of tissue binding and its effects on pharmacokinetic parameters will be covered in Chapters 8 and 10.

5.4.2 Other considerations

Route of administration may affect the extent of distribution. Gastrointestinal and intraperitoneal absorption provide immediate passage of a compound to the liver via the portal system, whereas the dermal and respiratory routes provide at least one passage through the systemic circulation prior to reaching the liver and thus extending the time prior to presentation for metabolism. The metabolism of most xenobiotics results in products that are more polar and thus more readily excreted (than the parent molecule). Therefore, the rate of metabolism is a critical determinant in the distribution of a compound since those compounds that are readily metabolized are usually readily excreted, and their reduced hydrophobicity makes them proportionally less prone to distribute to and accumulate in the tissues. This effect would not be seen if the analytical method used could not distinguish metabolites from parent compound. The same principle holds for polarity, since the greater the polarity, the more readily a xenobiotic may be excreted but be less able to cross membrane barriers and distribute to tissues.

The role of pharmacogenomics in all aspects of pharmacokinetics has been firmly established over the past few years. Pharmocogenomics has established a relationship between genetic markers and xenobiotic distribution phenotypes. Genetic subpopulations have been identified and will continue to be identified explaining interindividual variability in tissue distribution to genes variations in protein binding, efflux pumps, and metabolism. The most comprehensive information is on the variety of cytochrome P450 enzyme variants found within human and animal population. As will be discussed more thoroughly in Chapter 7, variations in these enzymes can widely alter the metabolism of xenobiotics. This can result in alteration of free drug concentrations available for tissue distribution. As discussed earlier in the chapter, genetic variation in the MDR1 gene leads to increased concentrations

of xenobiotics within the central nervous system (CNS). With the elucidation of multiple mammalian genomes, new information regarding genetic subpopulations and the roles various genes play in the distribution of xenobiotics will undoubtedly continue to alter our thinking about the determinants of distribution.

As can be appreciated from this discussion, there are numerous factors that could affect distribution of a compound to tissues. Another factor is the methodology used to assess tissue distribution. Autoradiography and imaging techniques are excellent approaches to anatomically localize distributed drug to the level of organs, cells, and even subcellular components. However, most pharmacokinetic studies rely on analytical techniques. When a tissue sample is collected from an animal, the sample is actually a homogenate of cells, extracellular fluid, and blood. The concentration measured cannot be uniquely assigned to any specific tissue or body fluid compartment. The use of microdialysis and ultrafiltration probes provides a direct estimate of extracellular and interstitial fluid concentrations. There are many techniques available to separate tissue from fluid components; however, the investigator must be sure that drug diffusion does not occur during the procedures and again confound results. Furthermore, most analytical studies quantitate total xenobiotic concentration rather than focusing on free xenobiotic concentration. Care must be taken to take all of these factors into account when analyzing and interpreting distribution data.

5.5 CONSEQUENCES OF DISTRIBUTION

There are numerous tissues to which a chemical may be distributed, some of them capable of eliciting a pharmacological or toxicological (intended vs. unintended) response, while others serve only as a "sink" or "depot" for the chemical. Sinks may also be formed as a result of chemical binding to tissue or plasma proteins. The physiological significance of such sinks is that chemicals will be distributed to, and in some cases stored in, these tissues and only slowly be released back into the systemic circulation for ultimate elimination. Such tissue binding may actually protect against acute adverse effects by providing an "inert" site for xenobiotic localization.

Storage may, however, prolong the overall residence time of a compound in the body and promote accumulation during chronic exposure; two processes that would potentiate chronic toxicity. Thus, when a toxicant is stored in a depot removed from the site of action (such as polychlorinated biphenyls in fat or lead in bone), no adverse effect may be manifested immediately, although the potential for toxicity exists. For example, lead stored in bone is not thought to cause harm, but it has the potential for mobilization into soft tissues, whereupon toxic symptoms may appear. As the toxicant in storage depots is in equilibrium with the free toxicant in plasma, mobilization is constant, and exposure to the target organ is constant (although at a low level). Thus, the opportunity for chronic effects (positive and negative) is always present. In fact, it is possible that the mechanism of toxicity for a compound may be solely related to its ability to mobilize a second bound toxicant from its site of storage and thereby elicit a toxicological effect not directly associated with the compound itself. Finally, this phenomenon may be used to therapeutic advantage by administering compounds that can redistribute harmful chemicals from storage sites and promote elimination. This is the rationale for using systemic chelation therapy to mobilize stored metals. Additionally, formulations of therapeutics have also been designed to take advantage of low levels of chronic exposure leading to prolonged clinical effects.

If the animal is a food-producing species, such tissue storage may result in residues in the edible meat products. Tissue concentrations thus become an end point in themselves, devoid of a biological or toxicological relevance in the tissue in which they are found. The relevance of such tissue levels is set by regulations that legally establish safe tissue tolerances or maximum residue levels for specific tissues and species. Fig. 5.2 illustrates this relationship between tissue accumulation and legal tolerances. These are based on extrapolations of safety to the consuming human population and food consumption patterns. Interpretation is limited when tissue concentration data are presented independent of the context of their use. Tissue depletion data collected in the very low concentration ranges appropriate for tissue residue studies are not appropriate to be used to estimate therapeutic efficacy against a tissue-residing bacterium or as an indicator of tissue distribution. As will be seen, the pharmacokinetic techniques used to describe these two different scenarios may be similar, although the resulting parameters may be very different.

All of these factors are important considerations when selecting the proper pharmacokinetic model. Many of these factors are implicit, especially when physiological pharmacokinetic models are employed. However, they strongly affect the interpretation of the primary parameter that quantitates distribution, the volume of distribution (*Vd*). As will be seen throughout the text, *Vd* is a proportionality factor that relates the mass of drug in a compartment (or dose) to the volume into which it is diluted, yielding a concentration

$$Vd\ (\text{mL}) = \text{Mass (mg)}/\text{Concentration (mg/mL)}. \tag{5.5}$$

Vd appears in equations that relate drug concentration to pharmacokinetic or physiological variables. It relates the total amount of drug present in the body to the concentration in the sampled body fluid, usually plasma. The calculation of its value will be dependent on the modeling scheme adopted. It is the physiological and protein-binding properties discussed above that change the nature of the concentration profile being modeled and thus will change the value of *Vd* obtained. The actual *Vd* as a function of plasma and tissue binding can be expressed as

$$Vd = V_{\text{plasma}} + V_{\text{tissue}} \cdot [f_u(\text{plasma})/f_u(\text{tissue})], \tag{5.6}$$

where V_{plasma} and V_{tissue} are plasma and tissue volumes and f_u are the unbound (free) fractions of drug in plasma and tissue, respectively. In many cases, *Vd* will be calculated using a number of different pharmacokinetic approaches that may not be sensitive to these physiological variables. However, as will be repeatedly stressed, *Vd* is a primary pharmacokinetic parameter whose precise estimation is central to any model used.

BIBLIOGRAPHY

Ariens, E.J., Soudijn, W., and Timmermans, P.B.M.W.M. 1983. *Stereochemistry and Biological Activity of Drugs*. Oxford: Blackwell Scientific Press.

Bai, S.A., Walle, U.K., Wilson, M.J., and Walle, T. 1983. Stereoselective binding of the (–)enantiomer of propranolol to plasma and extravascular binding sites in the dog. *Drug Metabolism and Disposition*. 11:394–395.

Barza, M. 1981. Principles of tissue penetration of antibiotics. *Journal of Antimicrobial Chemotherapy, Supplement C*. 8:7–28.

Beer, J., Wagner, C.C., and Zeitlinger, M. 2009. Protein binding of antimicrobials: methods of quantification and for investigation of its impact on bacterial killing. *AAPS Journal*. 11:1–12.

Benet, L.Z., and Hoener, B.A. 2002. Changes in plasma protein binding have little clinical relevance. *Clinical Pharmacology and Therapeutics*. 71:115–121.

Bidgood, T., and Papich, M.G. 2002. Plasma pharmacokinetics and tissue fluid concentrations of meropenem after intravenous and subcutaneous administration in dogs. *American Journal of Veterinary Research*. 63:1622–1628.

Buur, J.L., Baynes, R.E., Smith, G.W., and Riviere, J.E. 2009. A physiologically based pharmacokinetic model linking plasma protein binding interactions with drug disposition. *Research in Veterinary Science*. 86:293–301.

Elmquist, W.E., and Sawchuck, R.J. 1997. Application of microdialysis in pharmacokinetic studies. *Pharmaceutical Research*. 14:267–288.

Kenakin, T.P. 1987. *Pharmacologic Analysis of Drug Receptor Interaction*. New York: Raven Press.

Khan, A.Z., and Aarons, L. 1989. Design and analysis of protein binding experiments. *Journal of Theoretical Biology*. 140:145–166.

Koch-Weser, J., and Sellers, E.M. 1976. Binding of drugs to serum albumin. *New England Journal of Medicine*. 294:311–316, 526–531.

LeBlanc, P.P. 1988. Drug distribution in the body. *General Pharmacology*. 3:357–360.

Mammarlund-Udenaes, M., Paalzow, L.K., and deLange, E.C.M. 1997. Drug equilibration across the blood-brain barrier: pharmacokinetic considerations based on the microdialysis method. *Pharmaceutical Research*. 14:128–134.

Mealey, K.L. 2004. Therapeutic implications of the MDR-1 gene. *Journal of Veterinary Pharmacology and Therapuetics*. 27:257–264.

Meijer, D.K.F., and van der Sluijs, P. 1989. Covalent and noncovalent protein binding of drugs: implications for hepatic clearance, storage, and cell-specific drug delivery. *Pharmaceutical Research*. 6:105–118.

Notarianni, L.J. 1990. Plasma protein binding of drugs in pregnancy and in neonates. *Clinical Pharmacokinetics*. 18:20–36.

Peterson, L.R., and Gerding, D. 1980. Influence of protein binding of antibiotics on serum pharmacokinetics and extravascular penetration: clinically useful concepts. *Reviews of Infectious Diseases*. 2:340–348.

Poulin, P., and Krishnan, K. 1995. A biologically based algorithm for predicting human tissue: blood partition coefficients of organic chemicals. *Human and Experimental Toxicology*. 14:273–280.

Putnam, F.W. 1975. *The Plasma Proteins: Structure, Function and Genetic Control*. New York: Academic Press.

Riond, J.L., and Riviere, J.E. 1988. Multiple intravenous dose pharmacokinetics and residue depletion profile of gentamicin in pigs. *Journal of Veterinary Pharmacology and Therapeutics*. 11:210–214.

Riond, J.L., and Riviere, J.E. 1989. Doxycycline binding to plasma albumin of several species. *Journal of Veterinary Pharmacology and Therapeutics*. 12:253–260.

Riviere, J.E., Page, R.L., Dewhirst, M.W., Tyczkowska, K., and Thrall, D.E. 1986. Effect of hyperthermia on cisplatin pharmacokinetics in normal dogs. *International Journal of Hyperthermia*. 2:351–358.

Riviere, J.E., Page, R.L., Rogers, R.A., Chang, S.K., Dewhirst, M.W., and Thrall, D.E. 1990. Non-uniform alteration of cis-diammine dichioroplatinum (II) tissue distribution in dogs with whole body hyperthermia. *Cancer Research*. 50:2075–2080.

Schmidt, S., Gonzalez, D., and Derendorf, H. 2010. Significance of protein binding in pharmacokinetics and pharmacodynamics. *Journal of Pharmaceutical Science*. 99:1107–1122.

Toutain, P.L., and Bousquet-Mélou, A. 2002. Free drug fraction vs. free drug concentration: a matter of frequent confusion. *Journal of Veterinary Pharmacology and Therapeutics*. 25:460–463.

Toutain, P.L., and Bousquet-Mélou, A. 2004. Volumes of distribution. *Journal of Veterinary Pharmacology and Therapeutics*. 27:441–453.

Tozer, T.N. 1981. Concepts basic to pharmacokinetics. *Pharmacology Therapeutics*. 12:109–131.

Upton, R.N. 1990. Regional pharmacokinetics I. Physiological and physiological basis. *Biopharmaceutics and Drug Disposition*. 11:647–662.

Upton, R.N. 1990. Regional pharmacokinetics II. Experimental methods. *Biopharmaceutics and Drug Disposition*. 11:741–752.

Wasan, K.M., Brocks, D.R., Lee, S.D., Sachs-Barrable, K., and Thronton, S.J. 2008. Impact of lipoproteins on the biological activity and disposition of hydrophobic drugs: implications for drug discovery. *Nature Reviews: Drug Discovery*. 7:84–99.

Williams, K., Day, R., Knihinicki, R., and Duffield, A. 1986. The stereoselective uptake of ibuprofen enantiomers into adipose tissue. *Biochemical Pharmacology*. 35:3403–3405.

Yamaoka, T., Tabata, Y., and Ikada, Y. 1994. Distribution and tissue uptake of poly(ethylene glycol) with different molecular weights after intravenous administration to mice. *Journal of Pharmaceutical Sciences*. 83:601–606.

6 Renal Elimination

A primary route for drug elimination from the body is the kidney. Drugs can also be eliminated in bile, sweat, saliva, tears, milk, and expired air; however, for most therapeutic drugs, these routes are generally not quantitatively important as mechanisms for reducing total body burden of drug. The degree of lipid solubility and extent of ionization in blood determines how much drug will be excreted by the kidney. For drugs that are first biotransformed by the liver, the more water-soluble metabolites are then ultimately excreted through the kidney in the urine. The kidney has also been the most widely studied excretory organ because of the accessibility of urine to collection and analysis. Many of the principles utilized by pharmacologists in quantitating excretory organ function, especially clearance, were originally developed by renal physiologists to noninvasively assess kidney function. Smith's (1956) classic reference on renal physiology is still instructive for the determination of renal clearance. What has changed over the ensuing six decades is that we now know the molecular structure and pharmacogenomics of the transport processes involved.

There are two components relevant to any discussion of renal drug excretion; physiology and quantitation. This chapter will introduce the physiology and expand on the perspective developed earlier. Renal drug excretion can be considered using the same principles of membrane transport, except in this case, the movement is from the vascular system to outside the body. Generally, only drugs that are either dissolved in the plasma or bound to circulating blood proteins are available for excretion. Many of the methods routinely used in pharmacokinetics to quantitate drug excretion are dependent on the specific modeling techniques employed. However, the final parameter estimated by most of these approaches is the renal clearance of the drug. The concept of clearance, deeply rooted in renal physiology, will be extensively developed here and expanded on in the next chapter (on hepatic drug elimination). Precise and practical methods for its experimental determination will be introduced; however, full development must wait until the basic pharmacokinetic models have been presented in later chapters.

6.1 RENAL PHYSIOLOGY RELEVANT TO CLEARANCE OF DRUGS

For a perspective of drug excretion, the kidney should be considered as an excretory organ designed to remove foreign compounds (e.g., drugs) and metabolic by-products (e.g.,

Comparative Pharmacokinetics: Principles, Techniques, and Applications, Second Edition. Jim E. Riviere.
 ISBN: 978-0-813-82993-7

creatinine, urea) from the blood. As will become evident, the major clinical indices of renal function, such as blood urea nitrogen (BUN), serum creatinine (SCR), and creatinine clearance, are actually pharmacokinetic parameters of creatinine and urea excretion.

As discussed relative to distribution in the last chapter, the kidney receives approximately 25% of the cardiac output and thus processes a prodigious amount of blood. The kidney functions in a two-step manner to accomplish its tasks. The first step is passage through a filtering unit to retain formed cellular elements (e.g., erythrocytes, white blood cells) and proteins in the blood, only allowing the passage of plasma fluid into the remainder of the kidney. The second step utilizes a system of anatomically and physiologically segmented tubules to further modify the contents of the filtered fluid depending on a host of physiological needs including but not limited to fluid, electrolyte, and acid–base balance and the regulation of systemic blood pressure.

The primary functional unit of the kidney is the nephron depicted in Fig. 6.1. Depending on the species, there may be 500,000 nephrons per kidney. The sum of their individual function is the observed organ function. Their specific anatomical arrangement is species dependent, often determined by the evolutionary adaptation of the animal to its environment relative to the need to conserve body fluids. The filtration unit is the glomerulus, while the

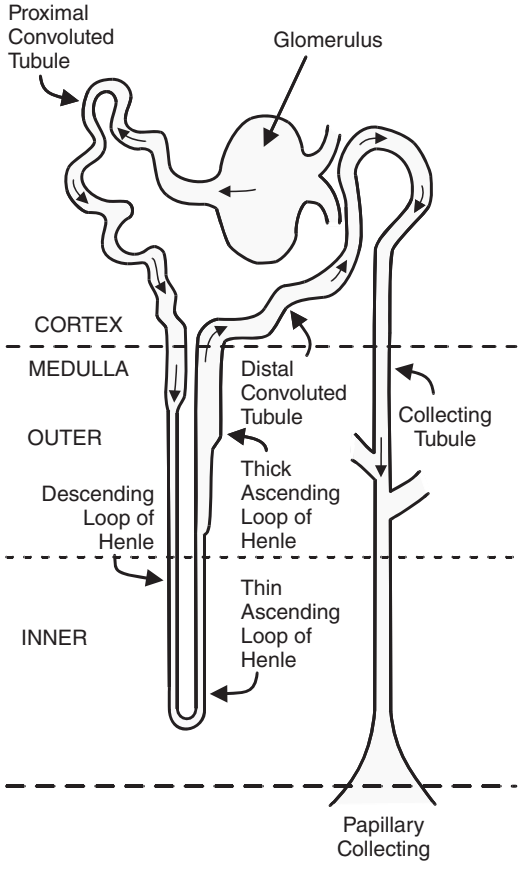

Fig. 6.1 Structure of a nephron.

remainder of the fluid processing is accomplished by the extensive tubular system, whose segments are named in relation to their relative distance (proximal vs. distal) measured through the tubules from the glomerulus. The junction between these is a unique anatomical adaptation called the loop of Henle, which is designed to use countercurrent exchangers to efficiently produce a concentrated urine since most of the water that is filtered by the glomerulus must be reabsorbed back into the body. The loop of Henle also forces the distal tubules to return toward the surface of the kidney to interact with the glomeruli. Grossly, the region of the kidney containing the glomeruli as well as the proximal and returning distal tubules is on the outside toward the surface and comprises the renal cortex. This region of the kidney is very well perfused by blood and is primarily characterized by oxidative metabolic processes. The interior region is the medulla, which is occupied by the penetrating loops of Henle; it is poorly perfused and is characterized by anaerobic metabolism.

The reabsorption of sodium, chloride, and urea produces osmotic gradients for the subsequent reabsorption of water. This is facilitated by the very low medullary blood flow, which maintains a hyperosmotic (relative to blood) environment characterized by high sodium chloride and urea tonicity. The tubular segments involved in this reabsorption (primarily the proximal tubule and loop of Henle) are the primary targets for diuretic drugs that function by blocking sodium or chloride reabsorption. As fluid moves from the proximal to distal segments, the fluid contents become more concentrated as water is reabsorbed. Filtrate in the distal tubules from individual nephrons then drains into the collecting ducts for excretion from the body as urine. The distal nephron is the final control point for the ultimate volume of urine produced. Urine volume is regulated by antidiuretic hormone (ADH, vasopressin), which alters the permeability of the collecting ducts exposed to the hyperosmotic medulla, through which the tubules penetrate. When permeable, water is reabsorbed back into the medulla, the urine is more concentrated, and diuresis is reduced (hence antidiuretic).

The amount of tubular fluid filtered by the glomeruli is thus acted upon by the various nephron segments to reabsorb wanted materials (primarily water and sodium) back into the blood and to let the remainder be excreted into the urine. Most of these processes are regulated by neural and hormonal systems whose function is control of fluid homeostasis and blood pressure. Because of the role of fluid balance in maintaining systemic blood pressure, there are additional anatomical adaptations that allow for this regulation. The primary one is that the distal tubules of nephrons course back up to the glomeruli at the point that the arterial blood supply enters, forming the juxtaglomerular apparatus. Different nephron segments may associate with different glomeruli, which results in the gross kidney averaging of individual nephron function, an anatomical arrangement that introduces a certain degree of heterogeneity and thus variability in any renal excretory process. This anatomical adaptation is the major manifestation that allows for the operation of the renin–angiotensin system to regulate blood pressure. Part of the function of this system is modulated by changing nephron blood flow, which secondarily may alter the ability of the kidney to excrete drugs. Finally, the kidney is also the site where acid–base balance is metabolically tuned by controlling acid and base excretion. Some of these processes are coupled to electrolyte secretion (e.g., potassium and sodium) and thus are further modulated by hormones, such as aldosterone. These nephron functions may inadvertently alter the amount of drug eliminated in the tubules by changing tubular fluid pH and consequently the ionized fraction of weak acids and bases according to the Henderson–Hasselbalch equation presented in Chapter 2. This modification in tubular fluid may affect the value of renal clearance determined in pharmacokinetic studies.

There are specific tubular transport systems that excrete products directly into the tubular fluid, which are not filterable because of plasma protein binding. Other transport systems reabsorb essential nutrients (e.g., glucose) back into the blood that were filtered into the tubular fluid. Drugs are also processed by these same transport systems, making drug excretion dependent on the physiological status of the animal. This is especially true when a drug biochemically resembles an endogenous substrate. As is similar to all transport processes, saturation and competition may occur, and as will be developed in subsequent chapters, nonlinear behavior may become detectable.

A full discussion of these varied functions of the kidney would take multiple books to adequately cover, and in fact, many multivolume references in renal physiology and nephrology admirably accomplish this task and should be consulted for further details. The purpose of this brief review is to present sufficient anatomy, physiology, and transport system molecular biology so that the process of drug excretion is intelligible. Some select aspects of renal physiology in disease states will also be presented in Chapter 17 when the effects of renal disease on drug disposition are taken into account. Now, effort will be focused on demonstrating how different methods for determining renal function are derived and relate to similar pharmacokinetic parameters.

6.2 MECHANISMS OF RENAL DRUG EXCRETION

Drugs are normally excreted by the kidney through the processes of (1) glomerular filtration, (2) active tubular secretion and/or reabsorption, and/or (3) passive, flow-dependent, nonionic back diffusion. These processes can be considered as vectorial quantities, each possessing magnitude and direction relative to transport between tubular fluid and blood. Their sum determines the ultimate elimination of a specific drug by the kidney as illustrated in Fig. 6.2. *The total renal excretion of a drug equals its rate of filtration plus secretion*

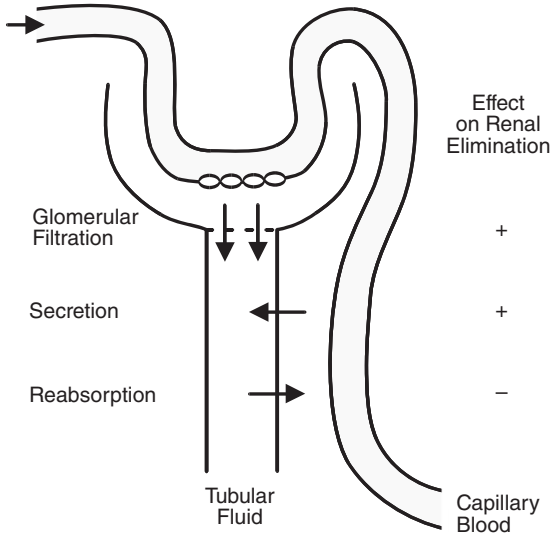

Fig. 6.2 Vectorial processes of nephron function and their net effect on overall renal drug elimination.

minus reabsorption. If a drug is reabsorbed back from the tubular fluid into the blood, its net renal excretion will be reduced. In contrast, if a drug is secreted from the blood into the tubular fluid, its net excretion will be increased. These events will be subsequently quantitated.

6.2.1 Glomerular filtration

Excretion by this process is unidirectional with drug removal from the blood by bulk flow. Only nonprotein-bound drugs are eliminated by this process since only neutral molecules with a diameter of less than 75–80 Å may be efficiently filtered (smaller for charged molecules). However, some larger molecules may be filtered to some extent as illustrated by recent findings that neutral globular proteins and nanoparticles with hydrodynamic radii up to 5–6 nm may be excreted by the kidney. The rate of drug filtration is dependent on both the extent of drug protein binding and the glomerular filtration rate (GFR), whose calculation will be developed below.

Glomerular filtration is essentially ultrafiltration through the relatively permeable glomerular filtration barrier, which consists of the epithelial cells of Bowman's capsule, the glomerular basement membrane, and the slit pores formed from juxtaposing epithelial foot processes (Fig. 6.3). These possess a fixed negative charge that is a major contributor to the rate-limiting aspect of this barrier. When damaged, filtration selectivity is impaired, and proteins may pass into tubular fluid. This is the primary manifestation of glomerular diseases that affects drug excretion. The anionic nature of the glomerular membrane pores also further restricts excretion of cationic molecules due to a Donnan exclusion effect. This factor can generally be ignored when calculating drug clearances, although in very carefully designed studies with drugs such as polyamines and aminoglycosides, its contribution can be quantitated relative to the filtration of similarly sized uncharged molecules.

The rate of glomerular filtration is dependent not only on the efficiency of the filtration barrier but also on the net filtration pressure (approximately 17 mm Hg). Filtration pressure is a function of blood flow and the balance of hydrostatic pressure (primarily arterial blood pressure) promoting filtration, countered by the nonfiltered glomerular oncotic pressure generated by the tendency of nonfiltered albumin to retain water in the glomerular capillaries. This process is not saturable, and thus a constant fraction of drug presented to the glomeruli will be filtered. Because of the dependency on drug concentration in blood, renal

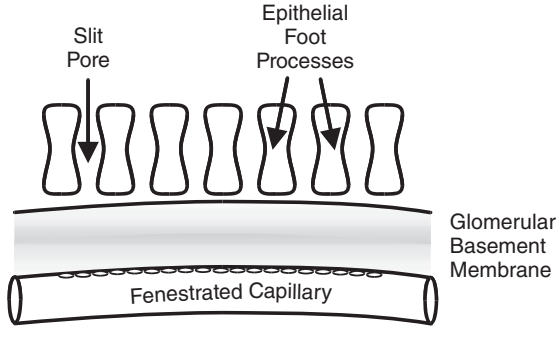

Fig. 6.3 The glomerular filtration barrier.

drug excretion due to glomerular filtration is a linear first-order kinetic rate process. Each nephron contributes to the overall ability of the kidney to filter drugs, with the total glomerular filtration capacity being the sum of single nephron filtrations. This has a major influence in renal disease processes marked by loss of nephrons and is the prime contributing factor to reduced glomerular filtration in renal disease. Finally, changes in renal blood flow will also decrease glomerular filtration, and thus vasoactive drugs that cause renal arterial constriction may decrease their own clearance. Drugs that alter the modulators of intrarenal blood flow (e.g., inhibitors of prostaglandins, angiotensin, kinins) may also alter their own excretion as a result of changes in the distribution of renal blood flow to the glomeruli. The fraction of plasma that is ultimately filtered through the glomeruli and presented to the tubules for further action is termed the filtered load.

6.2.2 Active tubular secretion and reabsorption

The magnitude of these processes is not affected by the extent of plasma drug protein binding. These saturable, carrier-mediated processes are energy dependent and described by the laws of Michaelis–Menten enzyme kinetics fully presented in Chapter 9. In order to promote absorption from the tubular filtrate into blood, tubule cells have microvilli, much like the intestinal mucosal cells presented in Chapter 4, that maximize the surface area to cell volume ratio presented to the tubule. For secretion from the interstitial space into the tubule lumen, the basolateral surfaces of these cells (side facing the capillaries) have intensive membrane invaginations that also increase the surface area for interaction with the perfusing capillaries to facilitate active secretion. To provide the energy to drive these processes, proximal tubule cells have high mitochondrial densities to generate adenosine triphosphate (ATP), which fuels the Na/K adenosine triphosphatase (ATPase)-coupled transport systems. This high level of oxidative metabolism is the primary reason for the sensitivity of the kidney to hypoxic or anoxic conditions, which results in renal damage if blood perfusion is interrupted even for short periods of time.

These active systems are now known to belong to the organic anion transporters (OATs) and organic cation transporters (OCTs) of the SLC22A, and the organic anion transporting polypeptides (OATPs) of the SLCO superfamilies of drug transporters, as well as the ATP-binding cassette (ABC) transporters previously discussed in Chapter 5. Their structure and genetic control has been extensively characterized using cloning techniques. Based on their preferential substrate selectivity, these systems have been generally discussed as being weak acid or base transport systems, the convention used in this text.

The cellular structure of transport systems across tubule cells involves two separate pairs of transporters, which create an overall "polarity" of tubule cell function relative to the interstitial fluid and tubular lumen (Fig. 6.4). One set is located in the brush border of the interface with tubular fluid and the other is located in the basolateral membrane. Energy coupling with ATP generally occurs in the basal portion of the cell (proximity to mitochondria), which, in secretion, builds up intracellular drug concentrations, which are then transported to the tubular fluid by concentration-driven facilitated transport carriers. In reabsorption, the reverse occurs as the basolateral active "pumps" create low intracellular drug concentrations that promote facilitated carrier-mediated reabsorption through the brush border tubular membrane. Most transport systems are also stoichiometrically coupled to the transport of an electrolyte (e.g., Na, K, Cl, H), which ensures electrical neutrality and provides a mechanism for modulating the systemic concentrations of these elements.

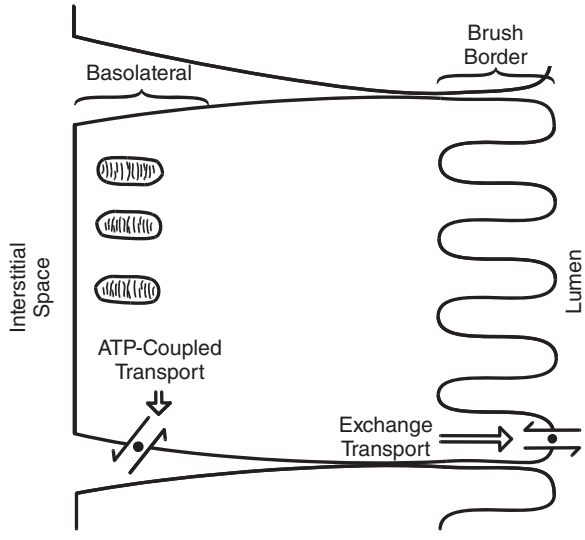

Fig. 6.4 Schematic of a renal tubular cell illustrating the location of active and exchange transport systems. The interstitial space is bathed by postglomerular capillaries and the luminal side contributes to the final makeup of the tubular fluid.

The primary ion that drives these transporters and regulates overall renal function is sodium. Thus, all drug transport systems are usually coupled to a Na ATPase transmembrane system whose structure and polarity will determine the nature and direction of drug movement. The identical motif exists in other organs; thus, similar mechanisms will be encountered when we discuss biliary transport systems in Chapter 7. The major difference between renal and hepatic cellular transport mechanisms is that in the kidney, cells are specialized as to the substrates being transported in relation to their location in different nephron segments. In the liver, regional specialization does not occur, and all cells involved in hepatobiliary transport have similar structure and function. In addition, the renal and hepatic transporters have different substrate specificities, which contributes to drugs being selectively excreted by renal or hepatobiliary processes. In general, small ($<\approx$200 MW) and hydrophilic organic drugs are excreted by the kidney while large and amphipathic drugs are excreted by the liver.

This two-membrane transport process is the mechanism of toxicity of some compounds. The classic example is the antibiotic cephaloridine, which, unlike other cephalosporins, is actively transported into proximal tubular cells but does not possess a brush border transport system to allow drug efflux into the tubular fluid. High concentrations of drug thus accumulate in the tubular cells, which results in nephrotoxicity. A similar phenomenon occurs in some liver cells involved in hepatobiliary secretion.

There are two distinct secretory pathways in the later sections of the proximal renal tubule that are relevant to a discussion of drug and toxicant excretion: one for acids and one for bases; the organic anion and cation transporters, respectively, discussed above. The primary orientation of this system is from blood to tubular filtrate, removing drugs and/or metabolite conjugates from the blood that were not removed by glomerular filtration. Table 6.1 lists some drugs that are actively secreted by the tubules. Active reabsorption systems are also present that act on drug already present in the filtered load. These systems are

Table 6.1 Renal tubular handling of drugs.

Acids	Bases
Acetazolamide (A, P)	Amphetamine (P)
p-Aminohippurate (A)	Chioroquine (P)
Chlorothiazide (A, P)	Diphenhydramine (P)
Chiorpropamide (A)	Dopamine (A)
Cephaloridine (A)	Ephedrine (P)
Dapsone (A)	Fenfluramine (P)
Diodrast (A)	Hexamethonium (A)
Ethacrynic acid (A)	Histamine (A)
Furosemide (A)	Isoproterenol (A, P)
Glucuronides (A)	Morphine (A)
Hippurates (A)	Neostigmine (A)
Indomethacin (A)	Opiates (P)
Mersalyl (A)	Phenothiazine (P)
Methotrexate (A)	Procainamide (A, P)
Nitrofurantoin (P)	Procaine (A)
Penicillin (A, P)	Quinidine (A, P)
Phenolsulfonphthalein (A, P)	Tetraethylammonium (A)
Phenylbutazone (A, P)	Thiamine (A)
Probenecid (A, P)	Trimethoprim (A, P)
Salicylic acid (A, P)	
Spironolactone (A)	
Sulfonamides (A, P)	

A: active tubular secretion or reabsorption; P: passive tubular reabsorption (nonionic back diffusion).

generally present to recover essential nutrients (e.g., glucose) that have been filtered by the glomerulus. Some drugs reach their target sites by this mechanism, making their tubular fluid concentration more important for predicting activity than their blood concentrations. An excellent example is the diuretic furosemide, which is first secreted by the tubules into the tubular fluid and is then actively reabsorbed back into the tubular cells, gaining access to its receptors for activity. Thus, the best concentration–time profile to predict the diuretic action of furosemide is that of the urine rather than blood. This phenomenon is further discussed in Chapter 13 when pharmacokinetic–pharmacodynamic (PK-PD) models for such compounds are considered.

Drugs (and other endogenous substrates) may compete for tubular transport sites, thereby functioning as reversible, competitive inhibitors. This interaction has been classically studied with the organic acid transport system. Weak acids such as probenecid or phenylbutazone will inhibit secretion of the weak acid penicillin, thereby prolonging penicillin blood concentrations. Thus, when two or more drugs in the same ionic class are administered, their rate and extent of renal excretion will be affected. Many drug metabolites are conjugates (e.g., glucuronides) produced by phase II biotransformation reactions and secreted by the transport system for weak acids, which may further complicate the pattern of drug excretion. In addition, agents secreted by the acid transport system may produce biphasic effects, inhibiting secretion at low doses and reabsorption at high doses. Salicylate inhibition of uric acid secretion follows this pattern. Damage to renal tubules from toxins, interstitial nephritis, and hypercalcemic nephropathy will impair the renal secretion of drugs and conjugates by active tubular processes.

There are direct pharmacokinetic implications to the carrier-mediated mechanism of renal tubular drug secretion. The limited capacity of carrier-mediated processes means that above certain blood drug concentrations, transport will proceed at a maximal rate independent of concentration in blood; that is, so-called nonlinear zero-order kinetics will become controlling, which will have adverse affects on the utility of normal linear pharmacokinetic models. These factors may become more important in renal disease states in which renal capacity is already diminished. Under these circumstances, drug renal clearance will approach the GFR, as additional drug concentrations in blood will not now be secreted into the urine. At subsaturation concentrations, renal clearance of an actively secreted substance is dependent on and limited by renal plasma flow. Thus, flow-limited mechanisms discussed below, and more extensively in the hepatic elimination chapter, will become important considerations.

6.2.3 Passive tubular reabsorption

The final determinant of a drug's renal disposition is the mechanism of nonionic passive tubular reabsorption, or back diffusion, a process dependent on urine flow rate, lipid solubility of the nonionized drug moiety, and urine pH. At low urine flow rates, there is greater opportunity for diffusion of drug from the distal tubular fluid back into the blood. Diffusion is facilitated by the high concentration of drug in the tubular fluid. Polar compounds having low lipid solubility, such as many drug metabolites, are not reabsorbed since they cannot cross the lipid membrane. In contrast, lipid-soluble, nonionized drugs are reabsorbed into the blood. This is the identical process discussed for passive drug absorption in Chapters 2 and 4, except that in these cases, the "outside of the body" is now the filtered tubular fluid. The ratio of ionized to nonionized molecules determines the concentration gradient that drives the drug into the fluid. Table 6.1 also lists drugs passively reabsorbed by renal tubules. The extent of reabsorption is a function of the drug's pK_a and the pH of the tubular fluid as described by the Henderson–Hasselbalch equations (see Chapter 2, Eqs. 2.2–2.5). The pH of the urine can undergo drastic changes as a function of diet and coadministered drugs (e.g., urine acidifiers and alkalizers). Tubular reabsorption of organic acids occurs with pK_a values between 3.0 and 7.5 and for basic drugs with pK_a values between 7.5 and 10.5. Weak acids thus are reabsorbed at low urinary pH (acidic), while weak bases are reabsorbed at high urinary pH (alkaline). Therefore, the renal excretion of an acidic drug decreases in acidic urine but increases in alkaline urine.

This principle is employed in treating salicylate intoxication in dogs. A brisk, alkaline diuresis is induced to decrease salicylate reabsorption into the blood and hasten excretion into the urine by trapping the salicylic acid in an ionized form in the alkaline urine. Reabsorption is further decreased by the elevated urinary flow rate. In contrast, induction of an alkaline diuresis will enhance the toxicity of basic drugs by increasing the amount of tubular reabsorption. Drugs often employed in critical care situations, such as procainamide or quinidine, have increased reabsorption and thus systemic activity in this alkaline state.

Species differences in urinary pH can have a major influence on the rate of renal excretion of ionizable drugs. Carnivores tend to have more acidic (pH 5.5–7.0) urine than herbivores (pH 7.0–8.0). Thus, with all other disposition factors being equal, a weakly acidic drug will have a higher renal excretion in herbivores than in carnivores, and a weakly basic drug will have a greater renal excretion in carnivores than in herbivores. In healthy animals,

small changes in urinary pH or urine flow rate do not significantly contribute to altered drug clearance. However, with decreased function in renal disease, there is a decreased tubular load of drug. Altered urinary pH theoretically could further decrease overall drug clearance. Conditions such as renal tubular acidosis and the Fanconi syndrome modify drug elimination by enhancing reabsorption of acidic drugs and decreasing reabsorption of basic drugs.

6.2.4 Pinocytosis

There are other peculiarities of renal tubular transport that must be reviewed before discussing how to quantitate these processes. Some drugs are reabsorbed into the tubules by pinocytosis. This occurs by interaction of filtered drug in the tubular fluid with the brush border membrane (Fig. 6.5). This is a very low-capacity and slow process that is easily saturated. Pinocytozed drug is then transferred to lysosomes and generally digested in the cell (e.g., peptides and filtered proteins such as β_2 microglobulin). However, for some compounds, such as the aminoglycosides, enzymatic breakdown does not occur, and the drug is essentially stored in the kidney. Therefore, although the drug is reabsorbed from the tubular fluid, it is not transported through the cell into the blood.

Thus, unlike other tubular reabsorption processes, reabsorption with storage or metabolism can decrease elimination of drug from the body. This is important when considering the meaning of a clearance calculated from pharmacokinetic parameters determined from blood alone. Reabsorption into the renal parenchyma will generally not be detected from blood-centered systemic pharmacokinetic models because any return flux back to the blood is at very low rates. Urine drug concentrations must be included in the analysis for pinocytotic absorption to be detected. However, such reabsorption has toxicological significance because the drug does accumulate in the tubular cells and could produce an adverse effect. Finally, this phenomenon has a significant influence on the prediction of tissue

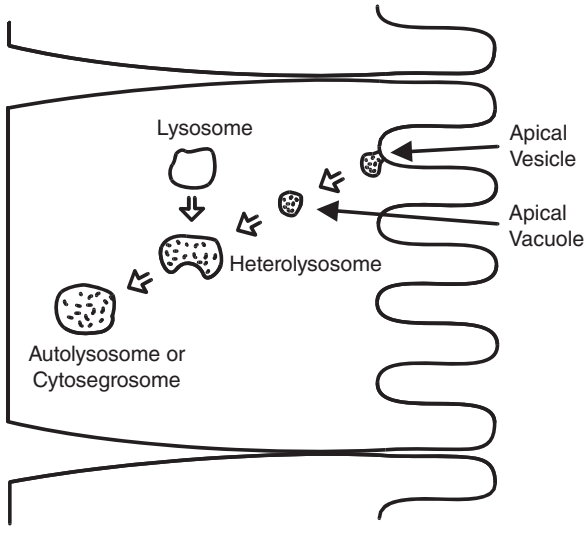

Fig. 6.5 Schematic of pinocytotic reabsorption in a tubule cell.

residue profiles in the kidney resulting from drugs with prolonged elimination half-lives (e.g., aminoglycosides).

6.2.5 Renal drug metabolism

The final confounding influence on determination of renal drug clearance occurs when drug is metabolized by the kidney. Most of the phase I and phase II enzymatic systems presented in detail in Chapter 7 also exist in the kidney, although different isozymes may be expressed. Oxidative processes generally occur within the proximal tubule cells. Two scenarios may occur. The first is when drug is metabolized solely by the kidney and not the liver, or a combination of both processes occurs. The second is when *relay* metabolism occurs, and the kidney further metabolizes a drug previously biotransformed by the liver. A toxicologically relevant example of this is the metabolism of hexachlorobutadiene by the liver to its glutathione conjugate. In the kidney, β-lyase then cleaves the conjugate with release of free drug into the renal tubule cells. Finally, hepatic metabolites may induce renal enzymes to further metabolize a drug. These interactions are complex and often are of toxicological significance.

Similar to the discussion above, compound that is metabolized by the kidney is lost to the systemic circulation since parent drug would not be detected, even in the urine. To quantitate this, one must use radiolabeled drug and/or know the specificity of the analytical method relative to separating parent drug and metabolite concentrations. This process contributes to the overall renal elimination of drug from the body and can be easily studied using many of the pharmacokinetic modeling techniques presented in later chapters. Renal drug biotransformation may also occur in the medulla by anaerobic metabolic processes (e.g., prostaglandin endoperoxide synthetase). This process is small relative to reducing overall body burden because only 1% of renal blood flow delivers compounds to this region but has toxicological significance to the renal medulla where drug and/or metabolite may accumulate. Finally, brush border enzymes are present that metabolize peptides in the filtered tubular load to amino acids for reabsorption.

A great deal of effort is spent on studying the toxicological significance of renal drug metabolism because lethal synthesis may occur where a nontoxic parent drug is metabolically activated within the renal tubular cells into a toxic metabolite. The classic example of renal cortical drug activation is chloroform to toxic phosgene and carbon tetrachloride to its toxic trichloromethyl free radical. In the medulla, prostaglandin endoperoxide synthetase metabolizes acetaminophen to a toxic free radical that produces interstitial nephritis after chronic treatment and activates benzidine to a carcinogenic metabolite. The biochemical mechanisms of metabolism will be presented in Chapter 7. Stereoselectivity in both active tubular secretion and metabolism in the kidney may occur with specific drugs (e.g., quinidine). The implications to assessment of renal drug excretion are similar to that of drugs metabolized by the kidney and are usually not taken into account.

This is a limited introduction of the wide range of processes that occur in the kidney and may affect renal drug elimination. A complete assessment of the renal mechanisms requires that both blood and urine data be collected to fully describe these events. If the drug is metabolized, assays must differentiate parent drug from metabolites. Numerous pharmacokinetic strategies will be presented in later chapters to specifically quantitate these processes. When simple blood-based models are used, these mechanisms may be obscured and aberrant predictions made.

6.3 THE CONCEPT OF CLEARANCE AND ITS CALCULATION

Urine analysis is required for any detailed study of drug disposition. The problem with simply measuring the concentration of drug in urine as an index of its renal excretion is that the kidney also modulates the volume of urine produced in association with its primary mission of regulating fluid balance. Thus, the concentration of drug alone may be higher or lower depending on the ultimate urine volume. To accurately assess how much drug is eliminated, the product of volume of urine produced and the concentration of drug in urine (mass/volume) must be determined to provide the amount excreted (mass). If timed urine samples are collected, then an excretion rate (mass/time) is determined. Similarly, to assess how efficient this process is, one must know how much drug is actually presented to the kidney for excretion. This is related to the concentration of drug in the arterial blood. As alluded to above, this is especially important when renal disease lowers the extent of glomerular filtration and reduces the filtered load of drug.

The physiological concept of clearance was developed by early workers to generate a parameter that measured the efficiency of renal excretion processes by assessing the total mass of compound ultimately excreted and relating it to the concentration of drug presented to the kidney for excretion. As will be stressed, *the net clearance of a substance is the vectorial sum of glomerular filtration, tubular secretion, tubular reabsorption, and renal metabolism.*

6.3.1 Definition of clearance

With this background in renal physiology, the task at hand is to establish parameters that are useful to quantitate drug or xenobiotic elimination by the kidney. The parameter that is used throughout physiology and pharmacokinetics to quantitate drug elimination through an organ, and by extension out of the body, is clearance (*Cl*). The relevant equation defining the whole-body clearance (Cl_B) of a drug is the sum of all elimination clearances:

$$Cl_B = Cl_{renal} + Cl_{hepatic} + Cl_{other}. \tag{6.1}$$

This equation illustrates the elegance of using Cl_B as the prime estimate of drug elimination since contributory organ function, when expressed as clearances, is simply additive. The only exception to this rule is for a drug eliminated through the lung since the pulmonary circulation is in series with the systemic circulation and receives the total cardiac output. Calculation of Cl_B provides an efficient strategy for estimating how a drug or toxicant is eliminated from the body as it indirectly compares systemic clearance with renal and hepatic clearances. It is also the primary parameter used to construct clinical dosage regimens. Because of the historical role of renal physiology in defining clearance and the easy accessibility of the kidney's excretory product (urine) for collection and analysis, the concept of clearance and simple methods for its determination will be developed in this chapter. However, Cl_B will be revisited in Chapter 7 when $Cl_{hepatic}$ becomes the parameter of interest.

6.3.2 Renal clearance (Cl_{renal})

The first definition of renal clearance is the *volume of blood cleared of a substance by the kidney per unit of time or, alternatively, the volume of blood required to contain the quantity*

of drug removed by the kidney during a specific time interval. As will be developed shortly, it is a physiologically based parameter that relates drug excretion directly to a measurable estimate of renal function. This is very important for calculating dosage regimens for patients with renal disease.

Recall from the previous discussion of renal physiology that the actual value for a drug's renal clearance is the vectorial sum of filtration + tubular secretion – tubular reabsorption, making it a parameter that estimates the entire contribution of the kidney to drug elimination. Similarly, any change in renal drug processing will be reflected in renal clearance if it is not compensated for by more distal components of the renal tubules.

Two types of data are needed to calculate clearance: (1) an estimate of blood drug concentration presented to the kidney; and (2) the amount of drug removed by the kidney. The latter can be estimated by either measuring the amount of drug excreted by the urine or comparing the difference between the renal arterial and venous drug concentrations to assess how much drug was extracted while passing through the organ.

To begin, we will use the classic approach, which directly measures extraction, based on Fick's law:

$$Cl\ (\mathrm{mL/min}) = Q \cdot E = Q \cdot [(C_{\mathrm{art}} - C_{\mathrm{ven}})/(C_{\mathrm{art}})], \tag{6.2}$$

where Q is renal arterial blood flow, E is the extraction ratio, and C_{art} and C_{ven} are arterial and venous blood concentrations, respectively. As will be presented in Chapter 11, this approach is also the basis for many organ-specific clearances used in building physiologically based pharmacokinetic models. The obvious difficulty with this approach is that arterial and venous blood samples must be collected. However, renal physiologists realized that this approach could be modified to more easily assess renal function.

This equation also illustrates that *the maximal rate of clearance for any drug is controlled by the blood flow to the respective clearing organ (e.g., kidney, liver) when complete extraction (E = 1) occurs*. The maximal clearance for any compound completely extracted from the blood would be the cardiac output for that species. Complete extraction could occur via combination of kidney and liver metabolism or complete inactivation through the lung. This allows one to estimate maximum clearances of drugs in different species based on knowledge of cardiac output and renal or hepatic drug clearances if the eliminating organ is known. These concepts will be further discussed when physiologically based models linked by blood flow are discussed in Chapter 11.

The amount of substance removed or extracted by the kidney is equivalent to the amount excreted into the urine. If one makes a timed collection of urine and measures the urine concentration and volume, then the amount (X) of drug extracted by the kidney over a specific time interval, that is, its rate of renal excretion, denoted ($\Delta X/\Delta t$) (the origin of the Δ terminology defined as "change in" will be presented in Chapter 8), is

$$\Delta X/\Delta t\ (\mathrm{mg/min}) = [U(\mathrm{mg/mL})] \cdot [V(\mathrm{mL/min})], \tag{6.3}$$

where U is the concentration of drug in urine and V is the urine production. Now, the only component needed is the concentration presented to the kidney. Because renal function fluctuates and urine sampling requires relatively long intervals to collect sufficient samples for analysis, blood concentrations should be relatively constant to ensure that the measured values do not change throughout a sampling interval. This is in contrast to using Equation 6.2, where short sampling intervals can be employed since simultaneous arterial and venous

blood samples may be collected. When urine is collected, fluctuating blood concentrations may bias the results. Thus, workers used constant-rate intravenous infusion of chemicals to ensure that so-called steady-state blood concentrations were achieved. With this experimental design, the renal clearance of substance *X* is calculated as

$$Cl_{\text{renal}}\,(\text{mL/min}) = (\Delta X/\Delta t)/C_{\text{art}} = (U_x \cdot V)/C_{\text{art}}. \tag{6.4}$$

This expression also provides the second widely used definition for clearance, which is *the rate of drug excretion relative to its plasma concentration.* It is the proportionality constant linking the rate of drug elimination to a specific plasma concentration. This expression will serve as the basis for many of the pharmacokinetic techniques to be developed in subsequent chapters.

Some minor discrepancies may result when drug clearances are calculated by use of blood or plasma data alone versus techniques such as this, which employ urine collection. As discussed earlier in this chapter, even for a drug that is excreted solely by the kidney, tubular reabsorption with storage (e.g., aminoglycoside antibiotics) will result in a lower Cl_{renal} calculated from urine data rather than blood-based methods since, as can be seen from Equation 6.2, tubular reabsorption would not be reflected in the venous blood concentrations since the substance is now trapped in the tubular cells. A similar discrepancy may occur with intrarenal drug metabolism since, like renal storage, this process does not return parent drug to venous blood. In a research setting, the difference is often used as conclusive evidence that either of these two phenomena actually occur. This issue will be revisited in Chapter 8.

6.3.3 Estimates of GFR

The original perspective of the renal physiologists was to develop an estimate of renal GFR. In order for Cl_{renal} to accurately measure GFR, a chemical that is solely cleared by glomerular filtration is required so that the kinetics are linear and thus do not change with varying blood concentrations; that is, the more variable processes of tubular reabsorption and secretion will not confound the estimate. The classic GFR marker, the biologically inert polysaccharide inulin, is not bound to plasma proteins and is only filtered by the glomerulus. Thus, the clearance of inulin reflected the maximum amount of a compound that could be excreted by filtration alone since all of the inulin presented is free and available for filtration. Finally, in order to provide a reasonably straightforward technique, plasma or serum venous inulin concentrations are used since arterial samples are difficult to obtain. Although this results in a constant overestimation of clearance since C_{ven} is less than C_{art}, it has become a standard practice. Additionally, the inulin concentrations employed are high relative to the amount extracted, and thus the arteriovenous difference is not important as long as the sampling protocols used are the same. GFR is thus commonly calculated as

$$\text{GFR}\,(\text{mL/min}) = Cl_{\text{inulin}} = (U_{\text{inulin}} \cdot V)/Cp_{\text{inulin}}, \tag{6.5}$$

where *Cp* is the common nomenclature in pharmacokinetics to denote plasma concentration. GFR estimates are commonly normalized to body weight to adjust for different individual body sizes and then expressed in units of mL/(min-kg), that is, mL/min/kg. Table 6.2 lists Cl_{inulin} across species ranging from cows to rats. Recently, the radiolabeled GFR markers ^{125}I-iothalamate and Cr-ethylenediaminetetraacetic acid (EDTA) have been employed to facilitate the assay.

Table 6.2 Glomerular filtration rates (mL/min/kg) in select species as assessed by inulin clearance.

Cow	1.8
Horse	1.7
Human	1.8
Goat	2.2
Sheep	2.0
Dog	4.0
Rat	10.0

If one compares GFR measured as Cl_{inulin} with the renal clearance of a study drug or toxicant, then the ratio of clearances gives some insight into how the kidney excretes this compound relative to the processes of glomerular filtration, tubular secretion, and tubular reabsorption. This ratio, termed the *fractional clearance*, is calculated as

$$\text{Fractional clearance}(X) = \frac{(U_x \cdot V)/Cp_x}{(U_{\text{inulin}} \cdot V)/Cp_{\text{inulin}}} \tag{6.6}$$

However, one notes that V appears in both the numerator and denominator and thus cancels out. Rearrangement of terms yields

$$\text{Fractional clearance}(X) = \frac{U_x \cdot Cp_{\text{inulin}}}{U_{\text{inulin}} \cdot Cp_x} \tag{6.7}$$

Therefore, timed urine collections are not required, and only urine and plasma samples of inulin and the chemical of interest need be assayed in any urine sample. Fractional clearance <1 implies tubular reabsorption, ≈1 implies only glomerular filtration, and >1 implies tubular secretion.

Two endogenous substances produced at a constant rate as metabolic products of systemic metabolism have a fractional clearance close to unity. The closest, plasma (or serum) creatinine, is produced secondary to muscle metabolism of creatine phosphate. The second, urea, is produced as a by-product of protein metabolism. Creatinine, which is easily assayed in both urine and serum by spectrophotometric techniques, became an excellent surrogate for inulin since the body's metabolic processes provided the constant-rate infusion. Creatinine clearance is the standard clinical test for estimating GFR within the method embodied in Equation 6.5. It has also been extensively used in pharmacokinetics as an independent estimate of GFR. Creatinine clearance is superior to urea clearance because urea is reabsorbed in the distal tubules as part of the countercurrent mechanism to concentrate urine and may vary depending on the hydration status of the animal. Additionally, ruminants metabolically handle urea differently than other species, which confounds its use in certain disease conditions. In some species (e.g., dogs), the fractional clearance of creatinine to inulin approaches a value of 1.1, suggesting some tubular secretion of creatinine. However, its ease of measurement and endogenous production overshadows this relatively minor error.

The final estimate of GFR is based on monitoring only SCR or serum urine nitrogen (SUN), commonly called BUN, as a rough estimate of GFR. It is instructive to consider how this relationship is derived. When the production of creatinine or urea is constant under

normal steady-state conditions, all of the compound produced by the body is excreted by the kidney. A steady state can only be achieved, and in fact is defined, when the rate of input (muscle production of creatinine, protein catabolism to urea) equals its rate of output (excretion), which we defined in Equation 6.4 as $\Delta X/\Delta t$. If we rewrite this equation in terms of creatinine (X = CR),

$$Cl_{cr} \approx \text{GFR} = (\Delta\text{CR}/\Delta t)/\text{SCR}, \text{ rearranged yielding } (\text{SCR})\ (\text{GFR}) = \Delta\text{CR}/\Delta t. \quad (6.8)$$

This suggests that if $\Delta\text{CR}/\Delta t$ remains constant, then the product of SCR and GFR will be constant, or for two different levels of GFR (1 and 2),

$$(\text{SCR}_1)\ (\text{GFR}_1) = (\text{SCR}_2)\ (\text{GFR}_2). \quad (6.9)$$

The ratio of two SCRs is therefore inversely proportional to the ratio of the respective GFRs. Normal SCR is 1 mg/dL when GFR is normal, thus 1/SCR reflects the ratio of normal to abnormal GFR. If GFR is reduced by 50%, SCR doubles. If GFR is reduced to 75% of normal, SCR will increase fourfold, and so on. Because the rate of creatinine production is constant and related to muscle mass, clinicians have developed nomograms to adjust SCR to reflect gender differences in muscle mass. This inverse relation (hyperbolic) also explains why, with a decrease in renal function, SCR and SUN dramatically increase in renal disease, while GFR only decreases linearly.

This constant daily excretion of metabolic by-products into the urine allows urine concentrations to be used to normalize the excretion of other chemicals in a manner analogous to fractional clearance. In some toxicology and field monitoring protocols in which drug or chemical excretion into urine is assessed, urine concentrations will often be adjusted by urine creatinine concentrations to correct for differences in urine volumes between study subjects. This provides an internal standard as to the length of the urine collection and ensures that adequate urine volume has been collected. This approach is particularly useful when chemical excretion into the urine is used as a field indicator or biomarker of chemical exposure and collection of timed or even complete urine samples cannot be guaranteed. By using urine creatinine concentration as a normalizing factor, urinary toxicant concentrations can be adjusted by creatinine concentrations to compensate for differences in dilution between individuals.

6.4 NONLINEARITY OF TUBULAR SECRETION AND REABSORPTION

The discussion thus far has been limited to determining clearances of substances that are primarily eliminated through glomerular filtration. The pharmacokinetics of this process is linear since saturation does not occur, and only nonprotein-bound drugs are filtered through the glomerular basement membrane complex. When the renal clearance of a drug eliminated by glomerular filtration is estimated, only the filtration of the free or unbound drug is assessed; thus, changes in protein binding will change the net excretion of drug. Drugs and toxicants that undergo passive tubular reabsorption obey Fick's law of diffusion since concentration gradients described again by linear first-order rate constants provide the driving force across the tubular epithelium. In contrast, compounds that are actively secreted

from postglomerular capillaries across the renal tubules and into the tubular fluid show saturation at high concentrations, competition with drugs secreted by the same pathways, and dependence on the magnitude of renal blood flow—all hallmarks of nonlinear pharmacokinetic behavior. For such compounds, clearance will not be constant but rather will be dependent on the concentration of drug presented to the kidney.

As discussed earlier in the physiology section, as tubular secretory pathways become saturated, the ratio of clearance to GFR (e.g., the fractional clearance of Eq. 6.6) will decrease. To develop this concept, we will revisit our definition of a drug cleared by GFR and acknowledge that only the free or unbound drug concentration ($C_f = Cp \cdot f_u$) is eliminated by glomerular filtration. Protein-bound drug (C_b) cannot be filtered. (A review of protein binding in Chapter 5 may be helpful at this juncture.) The rate of renal excretion ($\Delta X/\Delta t$) can be expressed as simply

$$(\Delta X/\Delta t) = C_f \cdot \text{GFR}. \tag{6.10}$$

As C_f becomes greater, $\Delta X/\Delta t$ will increase in direct proportion (e.g., linearly). However, recalling Equation 6.4, its clearance will be $\Delta X/\Delta t$ divided by C_{art}. In this case, C_{art} is the total blood concentration presented to the kidney ($C_f + C_b$). Clearance thus equals

$$Cl_{renal} = (\Delta X/\Delta t)/C_{art} = (\Delta X/\Delta t)/(C_f + C_b). \tag{6.11}$$

These relations have two implications. The first is that as total blood concentrations of drug increase (C_{art}), so does $\Delta X/\Delta t$; however, Cl_{renal} remains constant

$$Cl_{renal} = (C_f \cdot \text{GFR})/(C_{art}) \tag{6.12}$$

since C_{art} will increase in direct proportion to $C_f + C_b$ as long as the fraction bound does not change.

However, if only the extent of protein binding of a drug is increased ($C_f\downarrow$, $C_b\uparrow$), its rate of renal excretion $\Delta X/\Delta t$ will decrease (Eq. 6.10) as will its clearance since the C_{art} ($C_f + C_b$) will be constant. If the extent of protein binding is decreased (as discussed in Chapter 5 when displacement occurs), then C_f will increase as will Cl_{renal}, ultimately resulting in a reduction of free and active drug concentrations.

Therefore, drugs cleared by filtration have constant clearance with changing total drug concentrations but are sensitive to the extent of protein binding. As will be seen in Chapter 7, this is characteristic of low-extraction clearance processes. For such a drug with high protein binding, only the small fraction presented for filtration can ever be extracted and cleared by the kidney. Since the total renal clearance of a compound is the sum of filtration plus secretion, a drug solely cleared by filtration will have a relatively low clearance compared with one that is also actively secreted. If one considers this in terms of the extraction ratio (E) defined in Equation 6.2, Cl_B will always be less than the renal blood flow (Q) since the extraction ratio is less than 1 and dependent on the glomerular filtration fraction. Such drugs are termed *low-extraction drugs*, and their Cl_{renal} will be sensitive to the extent of protein binding. Examples of such drugs include inulin, aminoglycosides, antibiotics, tetracyclines, and digoxin.

In contrast, consider a drug that also undergoes active tubular secretion. In this case, even a drug that is protein bound ($\uparrow C_b$) or distributed into red blood cells will be secreted

into the urine since the affinity for specific tubular transport proteins will be greater than that for the relatively nonspecific protein-binding sites or partitioning in erythrocytes. The extraction ratio will thus approach 1.0, and Cl_{renal} will approach the renal blood flow Q. Such drugs are termed *high-extraction or perfusion-limited* to acknowledge the relationship of clearance to blood flow. The classic example is para-aminohippurate (PAH), which is almost completely extracted as it passes through the kidney, making its clearance almost equal to renal plasma flow. In fact, PAH renal clearance was often calculated in clinical situations using Equation 6.4 to estimate renal blood flow. Other such drugs include many of the β-lactam antibiotics (e.g., penicillin) and many sulfate and glucuronide conjugate products of hepatic drug biotransformation. These concepts are developed further in Chapter 7 where low- and high-extraction drugs cleared by the liver are discussed in detail.

The final implication of active tubular secretion is that at sufficiently high concentrations, saturation of the secretory pathways may occur. The point at which this occurs is termed the maximum tubular transport (T_m). At concentrations well below saturation, clearance will remain relatively constant since the rate of secretion will be dependent on the concentration, much as it is with filtered drugs. However, as T_m is approached, the rate of secretion $\Delta X/\Delta t$ will decrease until it reaches the maximal rate ($Q \cdot T_m$) and from that point on will be constant and independent of blood concentration. Since $\Delta X/\Delta t$ decreases and C_{art} increases, Equation 6.4 suggests that Cl_{renal} will also reach a maximal plateau. Since the total renal clearance of a drug is the sum of glomerular filtration plus tubular secretion, the rate of excretion for a drug versus its plasma concentration will have a shape characteristic of its renal elimination pathway, as seen in Fig. 6.6. Similarly, if another drug or endogenous compound that competes for tubular secretion is also present (e.g., probenecid coadministered with penicillin), $\Delta X/\Delta t$ and Cl_{renal} will decrease.

The final complication occurs when a drug undergoes passive tubular reabsorption. The dependency of this process on urinary pH has already been discussed. In this case, C_{art} will be constant, but $\Delta X/\Delta t$ and thus Cl_{renal} will vary depending on the urinary pH. Since this is an equilibrium process, time is required for this diffusion to occur. Thus, if the renal clearance of a drug is dependent on urine flow, it is presumed to undergo passive tubular

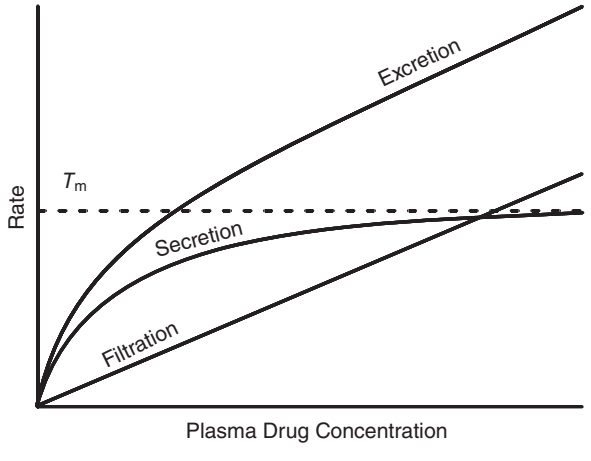

Fig. 6.6 Decomposition of the rate of drug excretion into components of glomerular filtration and tubular secretion.

reabsorption. When high tubular loads are presented, reabsorption is overloaded as equilibrium cannot be achieved and nonreabsorbed drug is eliminated into the urine.

Using the principles presented in the above paragraphs, one can now examine the dependence of the rate of drug excretion $\Delta X/\Delta t$ and Cl_{renal} on the plasma drug concentration for drugs secreted by these different mechanisms, as shown in Figs. 6.7 and 6.8. $\Delta X/\Delta t$ will generally increase with increasing concentrations; however, secretion and reabsorption will make these curves deviate from the linearity seen with solely filtered drugs at high concentrations. In contrast, and more instructive, clearance for a filtered drug is constant and is the value approached by both secreted and reabsorbed drugs at high concentrations.

A final complication arises depending on whether plasma, serum or blood concentrations are measured. As the reader can appreciate from most of the discussions in this text, terms are often used interchangeably in the literature as the difference is usually very small.

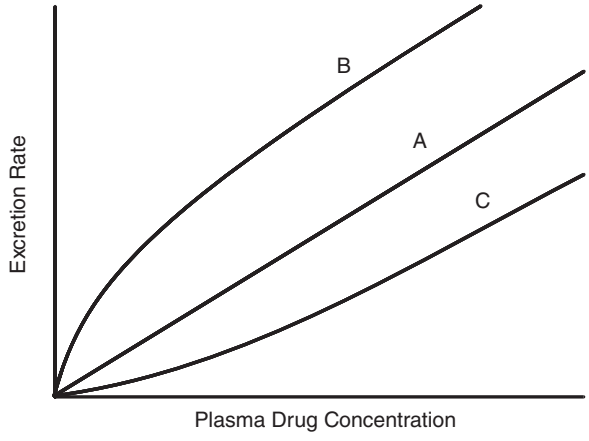

Fig. 6.7 Comparison of rate of renal excretion ($\Delta X/\Delta t$) versus plasma drug concentration for a drug eliminated in the kidney by glomerular filtration (A), tubular secretion (B), or tubular reabsorption (C).

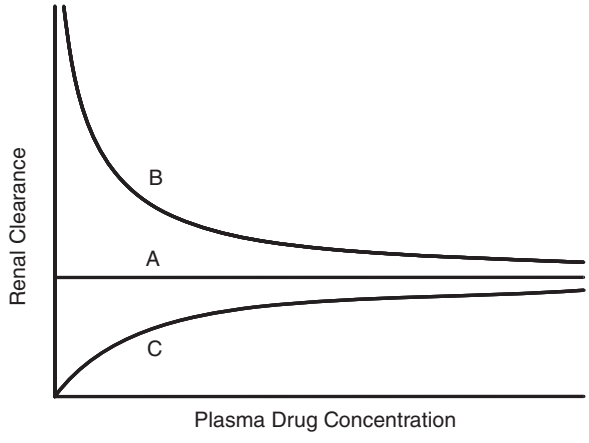

Fig. 6.8 Renal clearance versus plasma drug concentration of a drug handled by glomerular filtration (A), tubular secretion (B), or tubular reabsorption (C).

However, from a theoretical perspective relative to renal clearance, if an exact value of a renal extraction ratio is desired, only blood concentrations should be used since concentrations of drug in red blood cells are available for active tubular secretion despite not being filtered at the glomerulus.

6.5 SUMMARY

Unfortunately, it is not as easy to assess the function of other organs as it is for the kidney since their excretory fluids are not easily experimentally accessible as urine. Techniques used to assess organ clearance require some additional pharmacokinetic techniques that build on the clearance principles developed above. These concepts will be revisited in the pharmacokinetic modeling chapters, in which various strategies for calculating drug clearances will be presented. For example, the best method for calculating Cl_B is based on using steady-state drug infusions with a formula similar to Equation 6.4. Techniques will also be presented to deal with nonsteady-state drug concentrations, some of which have been developed into rapid tests for estimating GFR. In most cases, such pharmacokinetic approaches are now used to clinically assess renal function.

BIBLIOGRAPHY

Caldwell, J., Winter, S.M., and Hutt, A.J. 1988. The pharmacological and toxicological significance of the stereochemistry of drug disposition. *Xenobiotica*. 18(Suppl. 1):59–70.

Dresser, M.J., Leabman, M.K., and Giacomini, K.M. 2001. Transporters involved in the elimination of drugs in the kidney" organic anion transporters and organic cation transporters. *Journal of Pharmaceutical Sciences*. 90:397–421.

Garrett, E.R. 1978. Pharmacokinetics and clearances related to renal processes. *International Journal of Clinical Pharmacology*. 16:155–172.

Hagenbuch, B. 2010. Drug uptake systems in liver and kidney: a historic perspective. *Clinical Pharmacology and Therapeutics*. 87:39–47.

Hayes, A.W. 1994. *Principles and Methods of Toxicology*, 3rd Ed. New York: Raven Press.

Inui, K.I., Masuda, S., and Saito, H. 2000. Cellular and molecular aspects of drug transport in the kidney. *Kidney International*. 58:944–958.

Keller, F., and Scholle, J. 1983. Criticism of pharmacokinetic clearance concepts. *International Journal of Clinical Pharmacology, Therapy and Toxicology*. 21:563–568.

Klaasen, C.D. 2008. *Casarett and Doull's Toxicology: The Basic Science of Poisons*, 7th Ed. New York: McGraw-Hill.

Lee, W., and Kim, R.B. 2004. Transporters and renal drug elimination. *Annual Review of Pharmacology and Toxicology*. 44:137–166.

Osborne, C.A., and Finco, D.R. 1995. *Canine and Feline Nephrology and Urology*. Baltimore, MD: Williams & Wilkins.

Pritchard, J.B., and Miller, D.S. 1993. Mechanism mediating renal secretion or organic anions and cations. *Physiological Reviews*. 73:765–796.

Riviere, J.E. 1982. Limitation on the physiologic interpretation of aminoglycoside body clearance derived from pharmacokinetic studies. *Research Communications in Chemical Pathology and Pharmacology*. 38:31–42.

Riviere, J.E., Bowman, K.F., and Rogers, R.A. 1985. Decreased fractional renal excretion of gentamicin in subtotal nephrectomized dogs. *Journal of Pharmacology and Experimental Therapeutics*. 234:90–93.

Rowland, M., Benet, L.Z., and Graham, G.G. 1973. Clearance concepts in pharmacokinetics. *Journal of Pharmacokinetics and Biopharmaceutics*. 1:123–136.

Seldin, D.W., and Giebisch, G. 1985. *The Kidney: Physiology and Pathophysiology*. New York: Raven Press.
Smith, H.W. 1956. *Principles of Renal Physiology*. New York: Oxford University Press.
Tarloff, J.B., and Lash, L.H. 2005. *Toxicology of the Kidney*, 3rd Ed. Boca Raton, FL: CRC Press.
Toutain, P.L., and Bousquet-Mélou, A. 2004. Plasma clearance. *Journal of Veterinary Pharmacology and Therapeutics*. 27:415–425.
Tozer, T.N. 1981. Concepts basic to pharmacokinetics. *Pharmacology and Therapeutics*. 12:109–131.

7 Hepatic Biotransformation and Biliary Excretion

with Ronald Baynes

Hepatic disposition is one of the final keys in the absorption, distribution, metabolism, and elimination (ADME) scheme needed to describe disposition of drugs and chemicals in the body. The liver is responsible for both biotransformation and biliary excretion as well as enterohepatic recycling. In many ways, the liver should be considered as two separate organs—one encompassing metabolism and the other biliary excretion.

Drug localization and biotransformation in the liver are dependent on many factors associated with both the biological system and drug itself. These include biological properties of the liver (chemical composition, relative activity of major drug metabolism enzymes, hepatic volume/perfusion rate, and drug accessibility to and extraction by hepatic metabolic sites) as well as physicochemical properties of the drug (pK_a, lipid solubility, molecular weight). If single large or multiple doses of a drug are given, hepatic drug binding and metabolic sites may become saturated, which facilitates drug distribution to other metabolic sites, including the blood, kidney, skin, gastrointestinal tract (including the gut flora), lung, brain, placenta, and other organs. Despite this caveat, the liver is quantitatively the major drug metabolism organ in the body.

Drug metabolism studies in animals are easier to conduct than in humans due to practical and ethical considerations, including the accessibility of special tissue collection and homogeneity of subject population. However, inter- and intraspecies differences in drug metabolic rate are, in most cases, the primary source of variation in drug disposition and therefore in drug activity or toxicity. Extrapolation of metabolism data between animal species is difficult primarily because of the diversity in drug metabolizing enzymes, which will be discussed in more detail later in this chapter. Much of our understanding of drug metabolism is based on *in vitro* metabolic experiments, which sometimes can be difficult to correlate with metabolic data from *in vivo* pharmacokinetic studies. Even with a single species, as has been demonstrated in human populations, genetic polymorphism (>1% difference in DNA sequence) can lead to differences in metabolism that can have significant adverse clinical responses following drug exposure.

Recalling our discussion in Chapter 2 about the phenomenological role of metabolism in drug distribution and excretion, it would be hard to imagine what would happen in biological systems without xenobiotic metabolism. Absorbed compounds would stay in the body for a much longer period of time and have prolonged activity, tissue accumulation, and potentially, toxicity. Metabolism is necessary for the animal or human body to rid itself

Comparative Pharmacokinetics: Principles, Techniques, and Applications, Second Edition. Jim E. Riviere.
 ISBN: 978-0-813-82993-7

of lipophilic xenobiotics as an effective defense mechanism against adverse effects. In general, the intensity of drug action is proportional to the concentration of the drug and/or its active metabolite(s) at the target site. On the other hand, drug-associated toxicity is also dependent on the chemical form (active or inactive) and concentration at the same or other relevant target site. Therefore, any process or factor that modifies the drug's metabolite concentration at a target site will cause an altered activity or toxicity profile.

Drug metabolism may often result in metabolite(s) with altered chemical structures that change the receptor type affected, drug-receptor affinity, or pharmacological effect. Most parent drugs can be deactivated to inactive metabolites. In contrast, some drugs can also be activated either from an inactive form (prodrug) to an active drug or from an active form (e.g., meperidine) to an active metabolite (normeperidine) with similar activity/toxicity. Therefore, drug metabolism can either reduce or enhance the parent drug's effect, create another activity, or even elicit toxicity, depending on both the drug and the biological system in question.

The pharmacological and pharmacokinetic properties of a drug can be changed by metabolism in one or several of the following ways: pharmacological activation or deactivation, change in disposition kinetics of drug uptake (absorption from application site), distribution, and excretion (e.g., bile excretion, enterohepatic circulation, and renal excretion). For most drugs and toxicants, the liver is the major metabolic organ, which, in addition to its role in biliary excretion, makes an understanding of its function central to a knowledge of drug disposition. This chapter will focus on hepatic metabolism and drug hepatobiliary excretion in animal species and introduce some basic biochemical and pharmacokinetic concepts relevant to this role. Although these discussions are focused on the liver, the principles elucidated may also be applicable to extrahepatic sites of drug biotransformation.

7.1 PHASE I AND PHASE II REACTIONS

Various metabolic pathways are involved in drug metabolism, including oxidation, reduction, hydrolysis, hydration, and conjunction. These processes can be divided into phase I and phase II reactions (Table 7.1). Some workers have also defined so-called phase III reactions, although this concept has not been well accepted. Phase I includes reactions introducing functional groups to drug molecules necessary for the phase II reactions, which primarily involve conjugation. In other words, phase I products act as substrates for phase II processes, resulting in conjugation with endogenous compounds, which further increases their water solubility and polarity, thus retarding tissue distribution and facilitating drug excretion from

Table 7.1 Drug metabolism reactions.

Phase I	Phase II
Oxidation	Glucuronidation/glucosidation
Cyt P450 dependent	Sulfation
Others	Methylation
Reduction	Acetylation
Hydrolysis	Amino acid conjugation
Hydration	Glutathione conjugation
Dethioacetylation	Fatty acid conjugation
Isomerization	

the body. The biochemical mechanisms to be presented are also applicable to metabolism in other body sites (e.g., kidney and skin, discussed in earlier chapters). Interested readers should consult standard texts on drug metabolism or biochemical pharmacology/toxicology for specific detailed examples illustrating the chemistry of these processes.

Our knowledge regarding the molecular mechanisms of drug metabolism has been predominately gained from studies on the liver at different experimental levels, including *in vivo* intact animals, *ex vivo* liver perfusion, and *in vitro* liver slices, hepatocyte cell cultures, isolated/purified subcellular hepatocyte organelles, and isolated enzyme or enzyme components. The later *in vitro* systems are particularly suited for studies with human tissue. Two subcellular organelles are quantitatively the most important: the endoplasmic reticulum (ER; isolated in the microsome fraction) and the cytosol (isolated in the soluble cell-sap fraction). Phase I oxidation enzymes are almost exclusively localized in the ER, along with the phase II enzyme of glucuronyl transferase. In contrast, other phase II enzymes are mainly present in the cytoplasm. Microsomal fractions of the hepatocyte retain most, if not all, of the enzymatic activity in drug metabolism.

7.1.1 Phase I metabolism

Phase I metabolism includes four major pathways: oxidation, reduction, hydrolysis, and hydration, of which oxidation is the most important. Some specific phase I reactions with examples are illustrated in Tables 7.2–7.4. Special attention should be given to oxidation mediated by the microsomal mixed-function oxidase (MFO) system. This system is also termed monooxygenases, which infers that this enzyme system incorporates one atom of molecular oxygen into the substrate (drug) and one atom into water. The monooxygenations of drugs can be catalyzed either by cytochrome P450 monooxygenase (CYP) and thus called CYP-dependent monooxygenase system, or by flavin-containing monooxygenases

Table 7.2 Oxidation reactions.

Reaction/enzymes	Example of substrate
Reaction by MFO systems	
Alcohol oxidation	Ethanol
Aromatic hydroxylation	Lidocaine
Aliphatic hydroxylation	Pentobarbitone
Dehalogenation	Halothane
N-dealkylation	Diazepam
O-dealkylation	Codeine
S-dealkylation	*S*-Methylthiopurine
Epoxidation	Benzo[a]pyrene
Oxidative deamination	Amphetamine
N-oxidation	3-Methylpyridine
	2-Acetylaminofluorene
S-oxidation	Chlorpromazine
Phosphothionate oxidation	Parathion
Non-MFO enzymes	
Alcohol dehydrogenase	Ethanol
Aldehyde dehydrogenase	Acetaldehyde
Alkyihydrazine oxidase	Carbidopa
Amine oxidases	Imipramine
Aromatases	Cyclohexane carboxylic acid CoA
Xanthine oxidase	Theophylline

Table 7.3 Hydrolysis reactions.

Substrate	Enzyme
Esters	Plasma: nonspecific acetylcholinesterases, pseudocholinesterases, other esterases
	Liver: specific esterases for particular groups of chemicals
Amides	Liver: amidases
	Plasma: nonspecific esterases
Hydrazides, carbamates	Less common
Peptides, proteins	Enzyme in gut secretions

Table 7.4 Additional reactions involved in drug metabolism.

Reaction	Compound
Hydration	Epoxides (benzo[a]pyrene-4,5-epoxide)
Ring cyclization	Proguanil
N-carboxylation	Tocainide
Transamidation	Propiram
Isomerization	α-Methylfluorene-2-acetic acid
Decarboxylation	L-DOPA
Dethioacetylation	Spironolactone

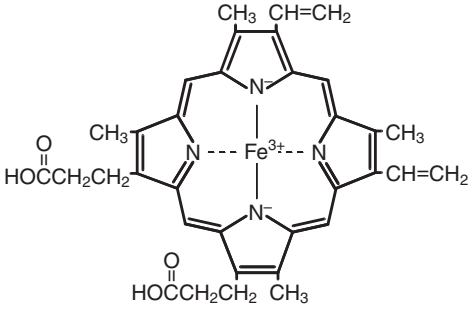

Fig. 7.1 Structure of ferriprotoporphyrin-9 that forms the core Cyt P450.

(FMOs). The "cytochrome" in the former system infers that CYP enzymes have a heme structure that is known as ferriprotoporphyrin-9 (F-9), which is the core of the enzyme (Fig. 7.1). This F-9 structure is basically the same for all CYP enzymes described below. These enzymes are also named P450 as they absorb UV light at 450 nm when reduced and bound to carbon monoxide. Many research articles will refer to these enzymes as "CYPs" or "P450s."

7.1.2 CYP nomenclature

With the advent of gene cloning and sequencing, and the application of molecular biology techniques to CYP structure analysis, tremendous progress was made in the last decade in the isolation and sequencing of the cDNAs encoding multiple forms of the hemoprotein. The rapid determination of full-length CYP amino acid sequences enabled the development

of a coherent nomenclature system describing the different and unique isoforms. CYPs were first discovered in 1958 and they are currently classified according to their amino acid sequence homology. As of 2010, there are over 7500 animal CYP isoforms in 781 gene families where genomic and protein sequences known. In order to keep up with recent findings in this continually expanding database, the reader is encouraged to access via the Internet the P450 Gene Superfamily Nomenclature Committee (http://drnelson.uthsc.edu/cytochromeP450.html).

CYPs with 40% homology belong to the same family and thus far, more than 70 CYP families have been discovered, with 17 families (e.g., CYP1, CYP2, CYP3) found in humans. CYPs with 55% homology are grouped into some 44 subfamilies (e.g., CYP1A, CYP2A, CYP2D), and there are isoforms that originate from a single gene (e.g., CYP1A1; CYP2D6, CYP3A4). About 95% of the drugs used in human clinical situations are metabolized by members of families CYP1, CYP2, and CYP3 (e.g., CYP1A2, CYP2C9, CYP2C19, CYP2D6, and CYP3A4) in liver (Williams et al., 2003; Hodgson, 2010). CYP nomenclature will often include mention of "orphan" P450s, which is to designate relatively recently identified CYPs for humans or other species and for which there is very little available information (Guengerich et al., 2010). Orphan P450s may not play a major role in drug metabolism but could play a major role in activation of carcinogens and protoxicants.

7.1.3 CYP genetic polymorphism

Genetic variability of these CYP enzymes in humans have been extensively evaluated, and the reported genetic polymorphisms identified in most CYP genes explain the sometimes observed interindividual differences in enzyme activity that manifest itself in interindividual differences in drug disposition. Again, the genetic polymorphism is often seen in CYP1, CYP2, and CYP3 family members that represent the major genes in pharmacogenetics (Yang et al., 2010). CYP 2D6 polymorphism is the often quoted example of genetic polymorphism in humans where a small percentage (e.g., 10% in some populations) are "poor metabolizers" (hydroxylation) of the drug debrisquinone. This landmark discovery in the mid-1970s and its scientific and clinical impact are elegantly reviewed by Smith (2001), who first identified this genetic polymorphism that spawned the growth of modern pharmacogenetics. Beyond the genetic polymorphism at the gene level, the reader should be aware that there are regulatory mechanisms at the transcriptional, translational, and posttranslational levels that contribute to variability in CYP activities within the human population (Lim and Huang, 2008). While gender differences in CYP activity have been extensively reported for rodent species (Yang et al., 2006), sexual dimorphism has not been consistently been observed in humans (Yang et al., 2010) and has not been completely examined in veterinary species and even within breeds of animals (Fink-Gremmels, 2008).

There is some evidence that gender differences in CYP2D and CYP3A expression in cats may explain why bufuralol-1-hydroxylation and midazolam-4-hydroxylation, respectively, is significantly greater in one sex over the other (Shah et al., 2007). There is also evidence that within the beagle breed of dogs, there are subpopulations in beagle dogs' ability to metabolize celecoxib. About 45% of the population (from a colony of 242 beagle laboratory dogs) is capable of extensively metabolizing this drug and CYP2D15 polymorphism has been proposed as a possible reason, although only 14% of canine lines carry this unique canine isoenzyme (Paulson et al., 1999). The reader can obtain more detailed information on genetic polymorphism in dogs, cats, horses, rabbits, rats, and mice from an excellent review paper by Mosher and Court (2010).

7.1.4 CYP species comparisons

Comparisons in CYP activity within and across animal species is, however, very difficult, especially when CYPs in veterinary species are not as well characterized as in humans. Some knowledge of this comparative activity across veterinary species is important for the following reasons: (1) drugs are used across various veterinary species in a label and extralabel manner; and (2) veterinary species (e.g., dogs, pigs) are often used in the preclinical phases of the development of human drugs. In these two scenarios, comparative CYP data will be useful to help predict drug clearance, efficacy, and potential toxicosis. Much of the species comparisons to date have focused on the use of liver microsomal fractions, yet we know that there are other interactions that could influence the final bioavailability of the drug.

There are rather consistent trends for CYP activity across different laboratory species; for example, CYP2E1 > CYP1A2 and CYP4A > CYP2D (Guengerich, 1997). There are also species differences in levels of CYP activity. For example, the level of activity diclonfenac-4-hydroxylase for CYP2C is in the following order of activity: human > monkey, rat > rabbit > mouse > dog, while the order for 7-ethoxy-4-trifluor-methyl-coumarin-O-dealkylation for CYP1A2 is dog >> rabbit, monkey > human > mouse > rat. These species comparisons strongly suggest that use of dogs in preclinical trials to assess hepatic clearance of coumarin and diclofenac would have either overestimated or underestimated the clearance and bioavailability of these drugs in humans. This is critically important for drugs with narrow therapeutic windows (e.g., coumarin). Fink-Gremmels (2008) provides a list of unique canine CYP isoenzymes (e.g., CYP2B11, 2C41, 2D15) with human CYP homologies, and although orthologous CYPs metabolize one substrate (e.g., CYP2D6 in humans and CYP2D15 in canine metabolize dextrometorphan), it is not predictive of substrate specificity. CYP2D has other clinical relevance as it is necessary for the demethylation of an important ionophore coccidiostat, monensin, in several veterinary species. However, horses have the lowest CYP2D catalytic efficiency to demethylate monensin, which explains why accidental or intentional mixing of this ionophore with horse feed often causes fatal cardiomyopathy.

Another animal species that is often used in preclinical trials as an animal model for human drug development is the pig. While there are various pig models available such as the conventional pig as those used in animal production systems, there are minipigs and micropigs whose CYP activity can be many order of magnitude higher than the conventional pig, which coincidentally is similar to that of humans (Nebbia et al., 2003). CYP3A4 is the major CYP in humans as well as the major CYP in pigs, suggesting that the pig may have some value in preclinical evaluation of drugs for humans, although pigs are recognized as being relatively poor at sulfate conjugation (see phase II discussion).

7.1.5 Basic CYP MFO reactions

Some CYPs may be located in the mitochondrial inner membrane, and some are located in the ER; both types are membrane-bound proteins and can result in two different kinds of electron transfer chains. As a general rule, the CYP oxidation reactions require the presence of molecular oxygen (O_2), reduced nicotinamide adenine dinucleotide phosphate (NADPH), and NADPH-cytochrome P450 reductase that is closely associated with CYP. The NADPH-cytochrome P450 reductase is a protein with a monomeric molecular weight of 78 kDa and is closely associated with CYP in the ER membrane. It is found in most

tissues but predominantly found in the liver, whose expression is under the influence of the active thyroid hormone triiodothyronine (T_3). This reductase enzyme is a flavoprotein that consists of 1 mole of flavin adenine dinucleotide (FAD) and 1 mole of flavin mononucleotide (FMN), and is different from other flavoproteins, as usually, only one FAD or FMN can be found as the prosthetic group in the flavoproteins.

Studies have demonstrated that a heat-stable lipid is essential for MFO activity in drug oxidation. The lipid may function in substrate binding, facilitation of electron transfer, or providing a "template" for the interaction of CYPs and NADPH-Cyt P450 reductase. Readers should recall that NADPH is the product of the pentose phosphate pathway in the cytoplasm. The NADPH reductase uses the NADPH to "fuel" the two electrons necessary for cycling of CYP. In essence, two electrons from NADPH migrate from FAD to FMN and then to CYP heme iron as shown in the electron transport chain below:

$$\text{NADPH} \Rightarrow \text{FAD} \Rightarrow \text{FMN} \Rightarrow \text{CYP}.$$

The reactions are initiated by insertion of a single oxygen atom into the drug molecule and are usually followed by rearrangement and/or decomposition of the product to yield an oxidized metabolite, which may be subject to further metabolism. The MFO reaction conforms to the following stoichiometry:

$$\text{NADPH} + \text{H}^+ + \text{O}_2 + \text{Drug} \xrightarrow{\text{CYP}} \text{NADP}^+ + \text{H}_2\text{O} + \text{Drug-OH},$$

where Drug-OH is the hydroxylated drug metabolite generated as an oxidation product. The overall reaction is catalyzed by the enzyme CYP, which also catalyzes the *N*-, *O*-, and *S*-dealkylation reactions of many drugs. These heteroatom dealkylation reactions can be considered as a special form of hydroxylation in which the initial event is a carbon hydroxylation (Table 7.2). The above reaction sequences should be recognized as an oversimplification of the catalytic cycle for CYP reactions. The system is dynamic and the steps described above may not be in a linear order, and we know that the CYP structures undergo major conformational changes with ligand binding (Ekroos and Sjogren, 2006). These authors for example demonstrated an increase in the active site volume by >80% when erythromycin and ketaconazole were bound to CYP3A4. The heme component of the ligand (RH) CYP complex can exist in well-recognized states (e.g., Fe^{2+}-RH; Fe^{3+}-RH) and others forms (e.g., FeO^{2+}; FeO^{3+}) that remain controversial. Many of the oxidation reactions have the potential for dismutation that result in reactive oxygen species that can cause oxidative damage to tissue, especially the liver. There are well-documented studies of these oxygenation reactions associated with various CYPs (1A, 2A, 2B, 2E, 3A, and 4A); however, almost all of the work has been conducted *in vitro* with either microsomes or cultured cells and the biomarkers used to demonstrate oxidative damage *in vivo* are not well validated.

Compounds can also undergoing reduction by hepatic microsomes catalyzed by CYP and can include azo- and nitrocompounds, epoxides, halogenated hydrocarbons, and heterocyclic ring compounds. Mammalian cells have limited ability to reduce azo bonds, but intestinal microflora may play a more significant role in this reduction reaction.

While the enzyme reactions described in this chapter are focused on CYP catalytic reactions, there are several other oxidation reactions and hydrolysis reactions (Tables 7.2 and 7.3) that do not require CYP. Good examples of these nonmicrosomal oxidations include alcohol dehydrogenase catalysis of alcohols to aldehydes and ketones with further oxida-

tion of the aldehydes to acids. The latter is deemed a detoxification step as the aldehydes are toxic and not readily excreted because of their lipophilicity.

7.1.6 Phase II metabolism

Phase II conjugating enzymes (Table 7.5) play a very important role in the deactivation of the phase I metabolites of many drugs containing functional groups such as hydroxyl, amino, carboxyl, epoxide, or halogen that can now undergo conjugation reactions with endogenous substances such as sugars, amino acids, glutathione (GSH), and sulfates. Phase II reactions can occur by direct deactivation of some parent compounds when their specific structure does not require phase I modification. For example, the analgesic drug paracetamol (acetaminophen) can be deactivated directly by phase II reactions using glutathione, glucuronide, and sulfate conjugation mechanisms. Phase II deactivation can be achieved both by gross chemical modification of the drug, thereby decreasing their receptor affinity, and by enhancement of excretion from the body, often via the kidney. These phase II reactions also result in a larger molecular weight drug metabolite, which may also be eliminated by active secretion into the bile. Genetic polymorphism has also been identified with phase II enzymes, and this includes uridine diphosphate glucuronosyl transferase (UGT), GSH-transferases, the methylases, and acetyltransferases. Only UGT and *N*-acetyltransferase (NAT) polymorphism in humans and veterinary species will be described here in more detail as adverse drug reactions have been associated with these species.

Slow NATs in humans has been associated with adverse reactions to amine drugs such as sulfonamides, isoniazid, dapsone, and procainamide (Sim et al., 2008). Dogs are known to completely lack the NAT genes; cats have only one (NAT1), humans two (NAT1 and NAT2), and rodents have three NAT genes. Fast and slow acetylators have been identified in various rodent strains, and the following database (www.mbg.duth.gr/non-humannatnomenclature/) is available online for the NAT allelic variants in many nonhuman species. Aromatic amine-based drugs such as sulfonamides can be substrates for NAT2 where an acetylated sulfonamide is formed and eliminated in the urine. The drug is also a substrate for CYP2C9, which results in formation of hydroxylamines, which are then eliminated by glucuronide and/or sulfate conjugation. In slow acetylator populations where there is limited NAT2 for a single-step clearance of the sulfonamide, the drug's only choice of elimination is through the above oxidative pathway, which can sometimes result in enough cytotoxic hydroxylamines that can cause the adverse reactions observed in slow acetylators of sulfonamides. Because dogs fail to express NAT and are thus poor acetyl-

Table 7.5 Phase II conjugation reactions.

Reaction	Enzyme	Functional group
Glucuronidation	UDP-glucuronyltransferase	–OH; –COOH; $–NH_2$; –SH
Glycosidation	UDP-glycosyltransferase	–OH; –COOH; –SH
Sulfation	Sulfotransferase	$–NH_2$; $–SO_2$; $–SO_2NH_2$; –OH
Methylation	Methyltransferase	–OH; $–NH_2$
Acetylation	Acetyltransferase	$–NH_2$; $–SO_2NH_2$; –OH
Amino acid conjugation		–COOH
Glutathione conjugation	Glutathione-*S*-transferase	Epoxide, organic halide
Fatty acid conjugation		–OH
Condensation		Various

ators, they are often susceptible to sulfonamide toxicity sometimes presented as conjunctivitis sicca.

Glucuronidation is one of the major metabolic pathways for elimination of lipophilic drugs and this reaction often involved the conjugation of functional groups from the drug (e.g., R-OH, R-NH_2, R-COOH) with the sugar derivative, uridine 5′-diphosphoglucuronic acid. This reaction is catalyzed by UGT, which are represented by 35 different UGT gene products in different animals species and more than 350 substrates have been identified to date. The UGT1 and UGT2 gene families have been described in humans, and genetic polymorphism has been associated with various disease states and adverse drug reactions. Hyperbilirubinemia associated with failure to conjugate bilirubin via glucuronidation has been linked to mutant UGT1A1 alleles or UGT1A1 promoter polymorphism. Cats and other felines are known to be very sensitive to phenolics and acetaminophen, and it has been historically attributed to low glucuronidation capacity. Recent studies have demonstrated that mutation of UGT1A6 gene is associated with the adverse drug reaction in cats (Court and Greenblatt, 2000).

7.1.7 Impact of metabolism

A variety of phase I and phase II reactions can take place simultaneously or sequentially in the body. For example, parathion can be catalyzed by Cyt P450 to an intermediate, which in turn can be either further oxidized to paraoxon or hydrolyzed to *p*-nitrophenol followed by conjugation reactions (Fig. 7.2). This complicated metabolic profile has been observed in the pig and will serve as the primary example illustrating a number of topics in this text. As discussed in Chapter 6, a compound metabolized in the liver may be subsequently metabolized in the kidney prior to excretion.

Stereochemistry also plays a major role in drug metabolism since most enzyme systems can be stereoselective. Examples include the enantiomers of amphetamine, 2-arylproprionic acid nonsteroidal anti-inflammatory drugs (NSAIDs) (e.g. carprofen, ketoprofen, vedaprofen), cyclophosphamide, pentobarbitone, permethrin, phenytoin, verapamil, and warfarin. In veterinary medicine, this had impact in interpreting pharmacokinetic studies of NSAIDs in which assays were not sensitive to stereochemistry (e.g. immunoassay vs. high performance liquid chromatography [HPLC]).

In summary, phase I metabolism is primarily responsible for drug deactivation, although phase II plays an important role in deactivation of some drugs. Phase I reactions prepare drugs or toxicants for phase II metabolism; that is, phase I modifies the drug molecule by introducing a chemically reactive group on which the phase II reactions can be carried out for the final deactivation and excretion. It should be noted that that not all drugs have to go through phase I and then phase II metabolism for elimination from the body. Some drugs as described in Table 7.2 can be cleared by phase I only without conjugation reactions. Recall in Chapter 2 that, generally, only lipophilic compounds are capable of crossing biological membranes, including access to drug metabolism enzymes, which produce more hydrophilic metabolites. This increased water solubility restricts drug/metabolite distribution to extracellular fluids, thereby enhancing excretion. Since many phase I and phase II reactions can occur on the same drug molecule, there is a possibility of interaction among various metabolic routes in terms of competing reactions for the same substrate (drug, toxicant, or its metabolite). Finally, some species are deficient in phase II conjugation reactions. Cats are poor in their ability to glucuronidate drugs, pigs are deficient in sulfate conjugation, and dogs are relatively poor acetylators. In addition to these known species differences, the role of CYPs in idiosyncratic drug adverse reactions should not be underestimated, and it

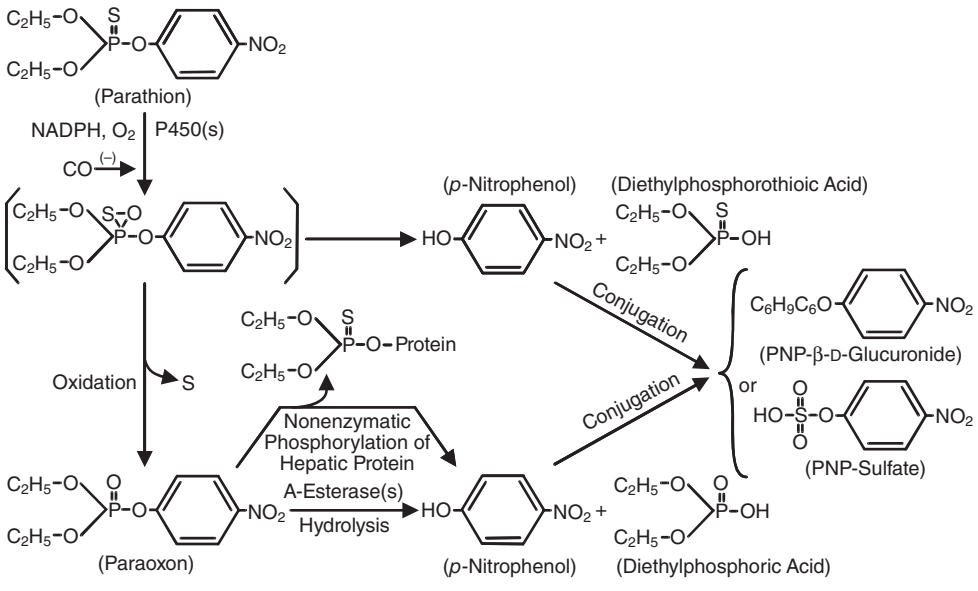

Fig. 7.2 Proposed metabolic pathways of parathion in mammals.

may be erroneous to simply assume that idiosyncratic drug responses are dose independent. Predicting metabolism is still very difficult as available crystal structure in CYPs have deficiencies (e.g., energy of different substrate bonds) that make predictions difficult even with modern computational tools. For example, very few of the ligand-bound CYPs accurately predict the regioselectivity of warfarin oxidation in humans (Williams et al., 2003).

7.2 METABOLISM INDUCTION AND INHIBITION

Drug metabolism is substantially influenced from enzyme induction or inhibition that occurs secondary to the deliberate or passive intake of a number of chemicals that humans and animals are increasingly exposed to in the environment, for medical reasons, or simply as a result of individual lifestyle (smoking, alcohol consumption, etc.). In laboratory animals, contaminants and natural constituents of diet have been shown to affect the pattern of drug metabolism observed. In many cases, the compound itself may alter its own metabolic fate by induction or inhibition.

7.2.1 Metabolic induction

Many currently used drugs, food additives, household chemicals, and environmental contaminants (including pesticides) possessing diverse chemical structure, pharmacology, and toxicology are well known to induce their own metabolism and/or that of other compounds in humans and animals. Some examples are listed in Table 7.6.

In general, there is no structure–activity relationship in the ability of these different inducers to stimulate drug metabolism, and the only common physicochemical property is their lipophilicity. With such a long list of compounds able to alter hepatic metabolism, a

Table 7.6 Inducers of drug metabolism in humans and animals.

Classification	Example
Drugs	Antipyrine Barbiturates Carbamazepine Chlorimipramine Clofibrate Griseofulvin Helofenate Nikethamide Phenylbutazone Phenytoin Pregnenolone-16α-carbonitrile Quinine Rifampin Spironolactone Testosterone Triacetyloleandomycin Vitamin C
Food additives, nutrients	5,6-Benzoflavone Butylated hydroxyanisole/hydroxytoluene Ethoxyquin Isosafrole
Pesticides	2,3,7,8-Tetrachlorodibenzo-*p*-dioxin (TCDD) 3,3,4,4-Tetrachiorobiphenyl DDT Kepone Piperonyl butoxide
Contaminants	1,2-Benzanthracene Benzo[a]pyrene Chrysene 3-Methylcholanthrene Phenanthrene
Solvents	Acetone Chloroform Ethanol Toluene Xylene

great deal of effort has been spent in recent years to understand the mechanisms behind these processes. This is important from a pharmacokinetic perspective since the intrinsic hepatic clearance of a drug will change if the enzymes responsible for metabolizing it are induced, thereby increasing metabolic capacity. This is especially important for low-extraction drugs. This is fully discussed in Chapter 10 when nonlinear pharmacokinetics is introduced. An example of the impact of enzyme induction on pharmacokinetic profiles will be illustrated in Fig. 10.10. Similarly, the patterns of phase I and phase II metabolism may be changed if one enzyme component's activity has been modified by inducers. These interactions introduce a significant complexity to pharmacokinetic models, describing the disposition of drugs extensively metabolized by the liver. However, they have also prompted research efforts aimed at elucidating the mechanisms behind these processes, which, when

understood, should provide a strategy for developing mechanistically meaningful models for simulation of drug metabolic disposition.

Of particular importance to the overall hepatic metabolic clearance of a drug is the activity of the Cyt P450 system. In the mid-1960s, both CYPs and its associated flavoprotein reductase were found to be induced by phenobarbitone pretreatment, which was accompanied by induction of drug metabolism. Induction was generally accompanied by increases in liver microsomal CYP content. Diverse drug metabolism responses to different inducers, all of which induce hepatic CYP, can be dependent on the substrate of interest (substrate specificity) with stereoselectivity and regioselectivity, suggesting that subpopulations of CYP (isoenzymes) might be present. This now widely accepted concept has had a profound influence on drug discovery, design of metabolism studies, and the resulting structure of pharmacokinetic models.

In human and veterinary drug development, the challenge is to identify which animal species are appropriate for extrapolating to human or veterinary species as well as to determine how changes in specific isoenzyme activities modify the hepatic clearance of a drug. In many cases, this may be impossible, and the only solution is to construct pharmacokinetic models capable of using data from experimental studies (*in vitro* and *in vivo*) in one or more species to extrapolate drug disposition in the target species. The liver appears to be a particularly sensitive target organ for the induction of the drug metabolism enzymes in general, and CYP in particular, whereas the responses of extrahepatic metabolism organs to induction are more variable depending on the inducing agent, drug, organ or tissue, and route of administration.

Induction of metabolism may arise as a consequence of increased synthesis (at different transcriptional/translational levels), decreased degradation, activation of preexisting components, or a combination of these processes (Fig. 7.3). Although the precise molecular mechanisms of Cyt P450 induction are not yet fully understood, much research effort (primarily in rats and rabbits) has been expended in trying to rationalize the response of the drug metabolism enzymes to inducers in liver tissue. It has been demonstrated that inducers have a variety of effects on the functional components of the MFO system, particularly on the terminal hemoprotein CYP, as described in Table 7.7. Some examples illustrate this concept.

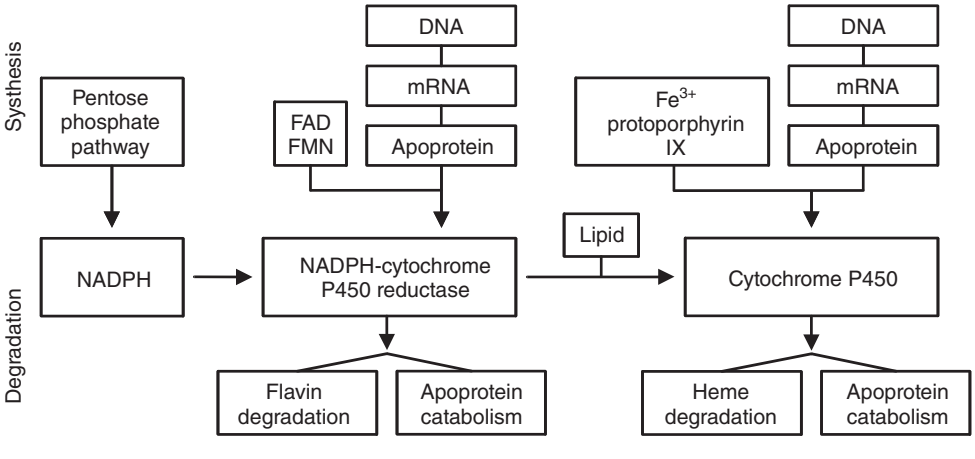

Fig. 7.3 Synthesis and degradation pathways for components of the hepatic mixed-function oxidase (MFO) system.

Table 7.7 Differences in induction mechanisms for CYP.

CYP isoenzyme	Inducer	Mechanism
1A1	Dioxin	Transcriptional activation by ligand-activated Ah receptor
1A2	3-Methylcholanthrene	mRNA stabilization
2B1/2B2	Phenobarbital	Transcriptional gene activation
2E1	Ethanol, acetone, isoniazid	Protein stabilization (in part)
3A1	Dexamethasone	Transcriptional gene activation
4A6	Clofibrate	Transcriptional activation, mediated by peroxisome proliferator-activated receptor

Table 7.8 Polycyclic aromatic hydrocarbon-related inducers of Cyt P450.

Charcoal-broiled meat
Cigarette smoke
Crude petroleum
Halogenated dibenzo-*p*-dioxins and dibenzofurans
β-Naphthoflavone and other flavones
Phenothiazines
Plant indoles (e.g., indole-3-acetonitrile, indole-3-carbinol)
Polychlorinated and polybrominated biphenyls
Polycyclic aromatic hydrocarbons (e.g., 3-methoxycholanthrene [3MC], benzo[a]pyrene, benz[a] anthracene, dibenz[a,h]anthracene)

The major inductive effect of phenobarbitone in rat liver appears to be exerted by increasing specific mRNA levels of CYP2B1 through augmented transcription, rather than stabilizing preexisting levels of protein precursors or increasing translational efficiency. No specific cytoplasmic or nuclear receptor for phenobarbitone has been identified. In contrast, induction by environmental polycyclic aromatic hydrocarbons such as 3-methylcholanthrene, benzo[a]pyrene, and 2,3,7,8-tetrachlorodibenzo-*p*-dioxin (TCDD) (Table 7.8) is recognized to be associated with a specific cytosolic receptor, termed the Ah receptor. The mechanisms are illustrated in Fig. 7.4.

The Ah receptor is likely an inducer (e.g., the ligand) -activated transcription factor. The 1A subfamily of the Cyt P450 enzymes is the major induction product for such environmental polycyclic aromatic hydrocarbons. However, ethanol and acetone can induce CYP2E1 by stabilization and inhibition of degradation of the CYP2E1 apoprotein, although multiple mechanisms may be involved depending on the induction stimulus. It is important to note the potential metabolic changes induced by ethanol and acetone since these two chemicals are often used as administration vehicles in a variety of toxicological and pharmacological studies. The impact of induction on the testing systems and resultant effects may be dramatic when multiple doses are applied in a long-term chronic experiment. Ethanol is also a substance of abuse in humans, making drug activity in alcoholics often significantly different than the normal population.

Non-Cyt P450 enzyme induction may also be relevant to altered drug metabolism. The inducers of the non-Cyt P450 enzyme induction are relatively nonspecific and thus cause a general proliferation of the hepatic ER or the enzymes themselves. Enzymes other than Cyt P450 involved in phase I and phase II reactions can be induced by various inducers, as summarized in Table 7.9. This imposes another level of control on the overall metabolic

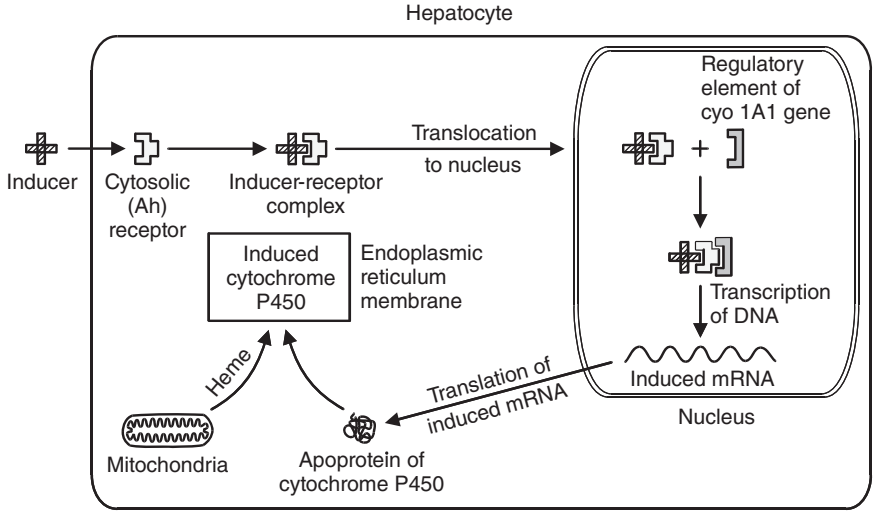

Fig. 7.4 Mechanisms of Ah receptor-mediated induction of Cyt P450 by polycyclic aromatic hydrocarbons.
Source: Adapted from Okey (1990).

Table 7.9 Inducers of non-Cyt P450 enzymes.

Enzyme	Example of inducers
Epoxide hydrolase	2-Acetylaminofluorene; aidrin; arochlor 1254; dieldrin; isosafrole; 3-methoxycholanthrene; phenobarbitone
Glucuronosyl transferase	Dieldrin; isosafrole; 3-methoxycholanthrene; phenobarbitone; 2,3,7,8-tetrachlorodibenzo-*p*-dioxin
NADPH-Cyt P450 reductase	2-Acetylaminofluorene; dieldrin; isosafrole; phenobarbitone; polychlorinated biphenyls
Glutathione-*S*-transferase	2-Acetylaminofluorene; 3-methoxycholanthrene; phenobarbitone; 2,3,7,8-tetrachlorodibenzo-*p*-dioxin
Cytochrome b5	2-Acetylaminofluorene butylated hydroxytoluene griseofulvin

fate of drugs and other relevant chemicals and adds extra complexity to metabolic modeling.

Although much progress has been made in drug metabolism induction studies, a major problem is how to assess the extent of induction of hepatic drug metabolism. The existing methods include assessing increased drug clearance, shortened drug plasma half-life, increased plasma-glutamyltransferase, increased urinary excretion of D-glucaric acid, increased urinary 61-hydroxycortisol, and increased plasma bilirubin levels. These measurements can collectively provide a reasonable indication of induction of drug metabolism in humans, although none of them can unequivocally substantiate such induction. Induction of specific liver enzymes (particularly the MFO system) may play a substantial role and have profound implications in clinical pharmacology. Inducers that modify drug metabolism, which would have the greatest effect on low-extraction drugs, would be expected to

alter drug effects. A good example of this phenomenon is the impact of phenobarbitone or benzo[a]pyrene pretreatment in rats on the metabolism and duration of action of the subsequently administered muscle relaxants (e.g., zoxazolamine).

7.2.2 Metabolism inhibition

Similar to the induction of metabolism, inhibition is a well-recognized phenomenon secondary to serial drug dosing, coadministration of drugs, endogenous compounds, environmental xenobiotics, and complex multiple-ingredient drug formulations. Many of the human drug–drug interactions involve CYP1A2, CYP2C9, CYP2D6, and CYP3A4, and the interactions may be the result of competitive inhibition or from binding to other parts of the enzyme proteins resulting in conformational changes (noncompetitive inhibition). Several mechanisms for metabolism inhibition have been noted, including the destruction of preexisting enzymes by porphyrinogenic drugs and xenobiotics containing olefinic (C=C) and acetylenic (C≡C) functions, inhibition of enzyme synthesis (by metal ions), or complexing with the hemoprotein, thereby inactivating enzymes (Table 7.10). The more clinically important inhibition interactions are associated with inhibitors that bind irreversibly to the CYP and terminate their function (suicide inhibition). In veterinary medicine, one classical example is the interaction of the macrolide antibiotic tiamulin and the ionophore coccidiostat monensin used to treat coccidia in poultry. Because tiamulin inhibits CYP3A, which results in limited monensin metabolism, poultry will develop liver and other clinical signs of monensin intoxication. The inhibitory effects of ketaconazole, erythromycin, and cimitidine have been well characterized in humans and veterinary species where there are significant increases in elimination half-lives (Fink-Gremmels, 2008).

Compounds such as porphyrinogenic drugs and xenobiotics can modify or destroy the heme component of CYP to generate alkylated or substrate-heme adducts. This results in a significant and sustained drop in the level of functional CYP and a concomitant reduction in the metabolic capacity of the liver. Inhibition of metabolism by these compounds depends not only on the structure of the drug itself but also on the prevailing complement of Cyt P450 isoenzymes and their substrate specificity. In contrast to the porphyrinogenic drugs described above, which act primarily by modifying existing CYP heme, metal ions such as cobalt exert their inhibitory effects by modulating both the synthesis and degradation of the heme prosthetic group of CYP enzymes. Formation of inactive Cyt P450-inhibitor complex is another mechanism for drug metabolism inhibition. Inhibitors are usually substrates of Cyt P450 and require metabolic conversion to exert their full inhibitory effects, in a manner similar to porphyrinogenic drugs and xenobiotics. However, inhibitors forming complexes with hemoprotein are metabolized by Cyt P450.

Table 7.10 Mechanisms of metabolism inhibitors.

Modify/destroy preexisting Cyt P450:
Acetylene, allobarbital, allylisopropylacetamide, aprobarbital, ethylene, norethindrone, secobarbital, vinyl chloride
Modulate synthesis and degradation of Cyt P450 heme prosthetic group:
Cobalt
Complexation with Cyt P450:
Amphetamine, cimetidine, diphenyhydramine, isosafrole, methadone, oleandomycin, piperonyl butoxide, safrole, sesamol, sulfanilamide, triacetyloleandomycin

These inhibitors can form metabolic intermediates or products that tightly bind to the hemoprotein, thereby preventing its further participation in drug metabolism.

Many drug–drug interactions may be explained at the level of CYP destruction, although interactions may also occur at other pharmacokinetic (absorption, distribution, and elimination, see Chapters 4, 5, and 6) and even pharmacodynamic (see Chapter 13) levels. Similarly, liver disease processes may decrease drug metabolizing efficiency, and becomes a major challenge when trying to adjust drug dosages in such patients, as fully developed in Chapter 17 of this text.

7.3 HEPATIC CLEARANCE

As presented in our discussion on renal excretion (Chapter 6), clearance of a drug by an organ (Cl_{org}) (Chapter 6, Eq. 6.2) can be ultimately defined as a function of its blood flow (Q_{org}) and its extraction ratio (E_{org}):

$$Cl_{org} = Q_{org} \cdot E_{org}. \tag{7.1}$$

The ability of the liver to remove drug from the blood, defined as hepatic clearance, is related to two variables: the intrinsic hepatic clearance (C_{int}) and hepatic blood flow rate (Q_h) as defined below:

$$Cl_{hepatic} = Q_{hepatic}[Cl_{int}/(Q_{hepatic} + Cl_{int})] = Q_{hepatic} \cdot E_{hepatic}, \tag{7.2}$$

where $Cl_{hepatic}$ is the hepatic clearance, $Q_{hepatic}$ is the hepatic blood flow, and $Cl_{int}/(Q_{hepatic} + Cl_{int})$ is the hepatic extraction ratio or $E_{hepatic}$. The intrinsic clearance Cl_{int} is conceptualized as the maximal ability of the liver to extract/metabolize drug when hepatic blood flow is not limiting. As indicated in Equation 7.2, when $Cl_{int} >> Q_{hepatic}$, hepatic extraction ratio ≈1.0 (*flow-limited or high extraction*, usually seen with $E_{hepatic} > 0.8$), $Cl_{hepatic}$ is only dependent on the blood perfusion rate, $Q_{hepatic}$. In this case, the more blood passing through the liver, the more drug molecules will be extracted by the liver for metabolic elimination. Changes in protein binding will not affect the drug's $Cl_{hepatic}$. A hepatic blood perfusion-dependent hepatic clearance will then be seen.

In contrast, if $Cl_{int} << Q_{hepatic}$, the $E_{hepatic}$ approaches zero, and thus the $Cl_{hepatic}$ is dependent only on the Cl_{int}; that is, the liver extracts as many drug molecules as it can from the blood flow presented (*metabolism-limited or low extraction*, usually with $E_{hepatic} < 0.2$). Protein binding will affect drug clearance in this case. These two extremes occur with propranolol and antipyrine, respectively. Intermediate values of extraction ratio of 0.2 to 0.8 give hepatic clearance rates that can be dependent to varying extents on both hepatic blood perfusion rate and intrinsic clearance. Therefore, to estimate hepatic drug clearance, one must consider the drug's physicochemical properties, hepatic drug metabolism enzyme activity, and the rate of hepatic blood perfusion. The reader should note the similarity of this discussion to that introduced in Chapter 6 concerning capacity or flow-limited renal tubular secretion. The concepts are identical for both organs; however, they are more often employed when hepatic clearance is modeled.

The intrinsic hepatic clearance has been shown to be related to the following enzymatic and kinetic parameters: maximal velocity of metabolism (V_{max}), Michaelis–Menten or affin-

ity constant (K_m), and drug concentration (C) following the law of mass action. These concepts will be mathematically developed and fully presented in Chapter 10 (e.g., see Eq. 10.4).

To illustrate such a high-extraction drug, we found that in our parathion metabolism modeling studies in swine, parathion can be trapped in the liver as indicated by both a very high liver/blood concentration ratio of 7 and a very high liver/perfusate distribution coefficient of 16–20. Therefore, parathion is a high hepatic extraction ratio compound, making its hepatic clearance blood flow limited. In fact, other researchers have found that the perfused liver effectively retains most of the parathion infused into it with little of the oxidation metabolite paraoxon escaping. This indicates that the liver is a very effective sink for both parathion and paraoxon.

In drug metabolism studies, the use of so-called hybrid physiological pharmacokinetic models (see Chapter 10) has gained popularity and received increasing research attention. These models are partially physiological since the organs having metabolic importance are separated out from the other tissues/organs that do not possess significant metabolic capacity for the compound being studied. A hybrid model is illustrated in Fig. 7.5, which describes the kinetics of a drug and its metabolite(s) based on their circulating concentrations. Such models apply volume terms to relate circulating drug concentration to the total amount of drug in the system (concepts introduced in Chapter 5, Eq. 5.5, and Chapter 8) and use clearance terms to relate the circulating concentration to the elimination processes of drug and metabolites (see Chapter 8, Eq. 8.17). This model is introduced at this point in order to provide a conceptual framework on which to study hepatic drug metabolism and to introduce the reader to the utility of pharmacokinetic models. Full details of model construction are presented in subsequent chapters.

Within the liver compartment, which is assumed to be the only site in the body possessing considerable metabolic elimination, the unbound drug molecules at a concentration of C_u are converted to the metabolite yielding a liver metabolite concentration of C_m according to its intrinsic metabolic clearance (Cl_{int}). The intrinsic clearance of a drug can be further conceptualized as its clearance from liver water. This removal occurs subsequent to dissociation from drug binding sites in the blood, transport into the hepatocyte, and attainment of equilibrium with intracellular binding sites. It is assumed that the final step in this

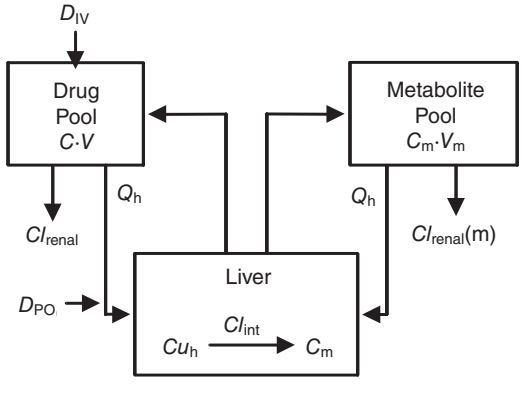

Fig. 7.5 A hybrid physiologically based pharmacokinetic model describing hepatic drug metabolism.

catenating (e.g., sequential) pathway, metabolism, is the rate-limiting process. From an enzymatic viewpoint, the intrinsic clearance of free drug may be regarded as equivalent to the ratio of V_{max} to K_m for the reaction (see Chapter 10 for relevant equations). In this model, as presented in Fig. 7.5, the extrahepatic tissues available to the parent drug and metabolite are designated as the drug central pool and metabolite central pool with volume of V and V_m and concentrations of C and C_m, respectively. The compartments are linked by the hepatic blood flow ($Q_{hepatic}$) and renal clearances of the drug and metabolite are termed Cl_{renal} and Cl_{renal}(m), respectively. The drug can be administered either intravenously or orally (via portal vein) at a dose of D_{IV} or D_{PO}.

The total body clearance of a drug relates the rate of the compound's overall elimination to the blood concentration circulating within the body, as previously defined in Chapter 6, Equation 6.1. Therefore, the fraction of the dose metabolized in the liver (f_m) can be used to estimate $Cl_{hepatic}$ from Cl_B as

$$Cl_{hepatic} = f_m \cdot Cl_B. \tag{7.3}$$

The relationship between hepatic clearance and liver blood perfusion rate for drugs with different extraction ratios can be determined according to Equation 7.2 (Fig. 7.6) using a logic that parallels the logic of partitioning renal elimination into filtered, absorbed, and secreted components, as presented at the end of Chapter 6. With a lower hepatic extraction drug, the blood perfusion rate is less important to $Cl_{hepatic}$, although for a high hepatic extraction drug, the $Cl_{hepatic}$ is proportional to the blood flow, as discussed earlier.

As two complementary parameters, intrinsic and hepatic clearance can now be used to characterize the rate of elimination of a drug. $Cl_{hepatic}$ is derived from circulating drug blood concentrations, while Cl_{int} reflects the full potential (V_{max}/K_m) of the drug metabolizing or excretory system without any other limitation/restriction and thus has no upper limit of hepatic blood flow.

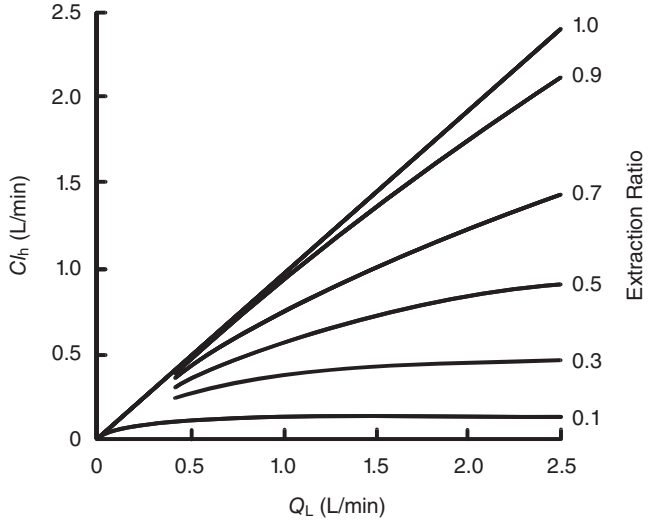

Fig. 7.6 Relationship between liver blood flow (Q_h) and hepatic clearance (Cl_h) for drugs with different hepatic extraction ratios (E_h). Extraction-ratio values are at a blood flow of 1.5 L/min.

$$Cl_{\text{int}} \approx (\text{Liver weight})[V_{\max} / K_{\text{m}}] \quad \text{zero order} \tag{7.4}$$

$$Cl_{\text{int}} \approx (\text{Liver weight})[(V_{\max} / (K_{\text{m}} + C)] \quad \text{first order} \tag{7.5}$$

The reader should note that this translation of Equations 7.4 and 7.5 is exactly the same as will be demonstrated in Chapter 10 when the pharmacokinetic implications of Michaelis–Menten kinetics on elimination rate constants are developed. Intrinsic clearance may also be expressed in terms of unbound drug fraction (f_{u}) within the liver (Cl_{int}). Therefore, intrinsic clearance is dependent on neither the drug protein binding nor the rate of hepatic blood perfusion rate, making it an independent measure of hepatocellular "potential" in drug metabolic elimination.

Drug intrinsic clearance can only be assessed directly from blood drug concentration time data when its hepatic extraction ratio is low (e.g., <0.3) and its plasma protein binding is low (e.g., <30%), using Equation 7.3. When binding is high but extraction ratio remains low, the relationship can be modified to

$$Cl_{\text{int}} = (f_m \cdot Cl_{\text{hepatic}}) / f_{\text{u}}, \tag{7.6}$$

which clearly shows how these two clearances are related. The most popular model for a drug with medium and high hepatic extraction ratio (e.g., >0.3) is

$$Cl_{\text{int}} = [f_{\text{m}} \cdot Cl_{\text{hepatic}}] / [f_{\text{u}}(1 - E_{\text{hepatic}})]. \tag{7.7}$$

These concepts will be fully developed in subsequent chapters but are presented here only to bridge hepatic physiology to the later development of kinetic models. They will be especially important when trying to adjust dosage regimens in the face of hepatic disease in Chapter 17.

Metabolite disposition kinetics can be characterized by analyzing the metabolite concentration–time data generated simultaneously with the parent drug data set. In general, metabolite distribution volume and clearance can be calculated using a similar data processing approach as that used for parent drug. More accurate parameters of metabolite kinetics can be obtained by direct administration of the metabolite to animals. An example of direct administration of metabolite (*p*-nitrophenol) via various dosing routes, to construct and verify its parent (parathion) metabolic disposition model, can be found at the end of Chapter 8.

7.4 BILIARY DRUG ELIMINATION

As an exocrine function of the liver, bile excretion is thought to be present in almost all vertebrates. The three basic physiological functions of the bile are (1) to serve as the excretory route for products of biotransformation; (2) to facilitate the intestinal absorption of ingested lipids such as fatty acids, cholesterol, lecithin, and/or monoglycerides due to the surfactant properties of bile forming mixed micelles (see Chapter 4); and (3) to serve as a major route for cholesterol elimination in order to maintain normal plasma cholesterol levels. In addition to its physiological functions, bile is also pharmacologically and toxicologically important since some heavy metals and enzymes are also excreted via the biliary system. Bile secretion is very important to chemical/drug transport and elimination

under both physiological and pathological conditions. However, bile secretion has proven difficult to study, mainly due to the inaccessibility of the biliary tree for direct sampling.

7.4.1 The mechanism of bile formation

Bile is continuously produced by liver cells and then stored in the gall bladder, except for those species (rat, horse) lacking it. The pH level of bile ranges from 5.0 to 7.5 depending mainly on the animal species. Biliary excretion is a major route for some drugs with a molecular weight greater than 300 and a high degree of polarity. This occurs by active transport of drug and metabolites into bile; thus, saturation and competition are important issues to consider. Passive diffusion of drug into bile is insignificant. Most of the compounds secreted into bile are finally excreted from the body in feces, where they may be subject to enterohepatic circulation and degradation by intestinal microflora.

Bile is formed at two sites: the ramifications of the bile duct within the portal triads and the anastomosing network of the narrow bile canaliculi in the hepatic parenchyma. The bile canaliculi are the primary secretory units of the liver. These small channels or furrows are lined by the apical membranes of the hepatocytes and thus do not have their own epithelium or basement membrane. Similar to the relationship of the nephron to the kidney, the volume and composition of canalicular bile are often determined by the activity of several cords of hepatocytes.

The overall bile flow is in the opposite direction to sinusoidal blood flow, and thus solute transfer from plasma to bile involves a counterflow process (Fig. 7.7). Such a blood–bile flow pattern reduces rediffusion of biliary solutes such as drugs and metabolites back into sinusoidal plasma in the portal area, which is richer in solute concentration, bathes peri-

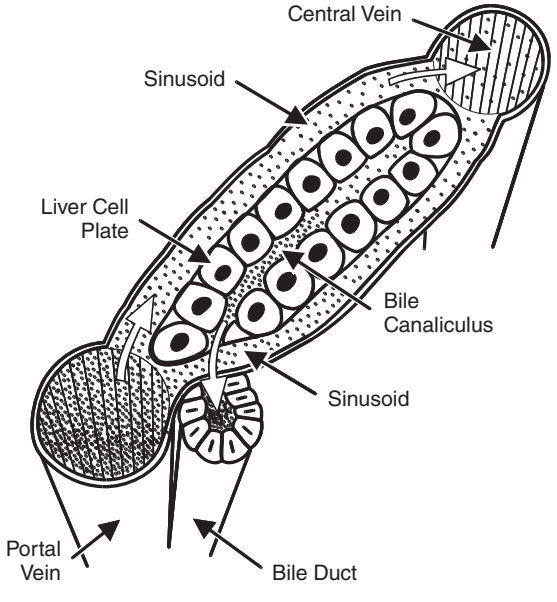

Fig. 7.7 Gradient concept of bile secretion in a liver lobule. Sinusoidal concentration of a solute (e.g., drug, metabolite, or endogenous compound) is represented by dots that progressively decrease as blood flows from the portal to central vein. Consequently, solute concentration in the bile canaliculus increases as it courses toward the bile duct.

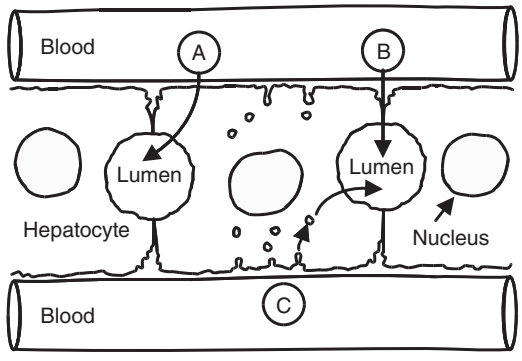

Fig. 7.8 Three transport pathways from sinusoidal to canalicular lumen are involved in biliary excretion: transcellular (A); transjunctional shunt (B); and transcytotic (C).

portal hepatocytes, and is exposed to higher canalicular concentration than any given solute (Fig. 7.7). In human liver, the canalicular space accounts for 0.4% of the liver volume and has a surface area greater than 70 cm^2 per gram of tissue. An intact microtubular network is essential for vesicular movement of receptor-mediated transcytosis and for biliary translocation of bile acids and other lipids. Microfilaments might serve as pump or pressure valves to control the ejection of the hepatocellular secretion into the biliary space. Three routes of fluid and drug transfer from the sinusoid to the bile canaliculus have been postulated and are shown in Fig. 7.8.

7.4.2 Transcellular pathway (A)

Conventionally, it was assumed that water and solutes enter (secretion) and leave (absorption) the lumen by traversing the plasma membranes of the epithelial cell (basolateral and apical regions) and the cytoplasm. Diffusive and osmotic water flow, including dissolved solutes, are recognized to enter the canalicular lumen through the lipid bilayer and/or the so-called water channels located at the protein core (polar route) of the hepatocyte plasma membrane.

7.4.3 Paracellular pathway (B)

This pathway is anatomically delineated by the structures forming the tight junctions between hepatocytes and the intercellular space. Many polar nonelectrolytes (e.g., sucrose, inulin, and polyethylene glycols) can be significantly excreted in bile although they are too large to readily pass through the hepatocyte plasma membrane. The transjunctional movement of fluid between liver cells may not simply be a leak secondary to the inability of the hepatocyte tight junction to seal off the canalicular space, but instead may play an essential role in the plasma-hepatobiliary transport of fluid and drugs.

7.4.4 Transcytotic (vesicular) pathway (C)

Water and dissolved solutes are internalized within the hepatocyte cytoplasm through acidic vesicles, most of which can return to the plasma. However, others may move either into

storage compartments or into the canalicular lumen. This is similar to the pinocytotic pathway in renal tubules illustrated in Fig. 6.5 (see Chapter 6).

7.4.5 Bile acid secretion

It has been recognized that the primary driving force for bile formation is the hepatobiliary transport of the osmotically active bile acids. Theoretically, bile acids transported across the hepatocyte allow for formation of a local osmotic gradient, which transports water by osmosis and permeable solutes by convection and/or electrochemical diffusion. This process has been traditionally referred to as bile acid-dependent bile secretion. Bile acid-dependent bile flow is a function of bile acid secretion and is regulated by both the physicochemical properties of the secreted bile acids and the factors affecting the kinetics of bile acid enterohepatic circulation. Bile acid transport mechanisms (Hagenbuch, 2010) have been determined to be very efficient and specific at both the sinusoidal and canalicular poles of the hepatocyte plasma membrane. Therefore, the pool size and intestinal reabsorption efficiency are the major determinants of bile acid entry into bile. Bile acids are the most abundant anions in bile, and a direct relationship between the excretion of bile acids in bile and canalicular secretory activity has been identified in all vertebrate species studied. Alternative mechanisms have also been proposed, including an interaction of bile acids with other solute pumps, possibly a bicarbonate transport mechanism, and/or the involvement of a vesicular transport process.

Evidence for bile acid-independent canalicular secretion has evolved mainly from studies of bile acid-induced choleresis (bile flow), which have proved that bile flow is mathematically related to bile acid excretion rate. A positive intercept can be observed in most cases when plotting the rate of bile formation against bile acid secretion, suggesting that a fraction of bile is secreted in the absence of bile acid excretion. The importance of such bile acid-independent canalicular secretion in overall bile formation rate is animal species dependent. More detailed signal transduction mechanisms regulating this phenomenon have been postulated at the cellular level. The bile flow stimulating effect of certain prostaglandins supports the involvement of cyclic adenosine monophosphate (cAMP) in the bile acid-independent mechanism. Active secretion of bicarbonate, chloride, and/or glutathione may provide the osmotic driving force for bile secretion. Na-K-ATPase and Na/H exchange have also been identified in hepatocytes and other preparations. Therefore, secretion of bile acid-independent canalicular bile flow is at least regulated by the cAMP cascade and also requires an intact microtubular system. Fig. 7.9 illustrates the comparison of bile acid-independent and total bile flow in select species.

In summary, bile formation involves an osmotic process whereby water and dissolved solutes (drug, metabolites, xenobiotics, and physiological molecules) move from sinusoidal blood into the bile canaliculus. The only well-documented driving force for this vectorial movement of fluid is the translocation of bile acids. The reader should note the parallels with renal secretion, where sodium assumes this primary role. However, another process is also involved since significant bile secretion can occur independent of bile acid secretion. Therefore, any factor or process that affects bile acid secretion, reabsorption from the intestine, or the cAMP system can potentially alter bile formation rate and thus biliary drug excretion. If the drug being modeled in a pharmacokinetic study is excreted in the bile and can influence the rate of bile formation, this change may be reflected in the value of its pharmacokinetic parameters.

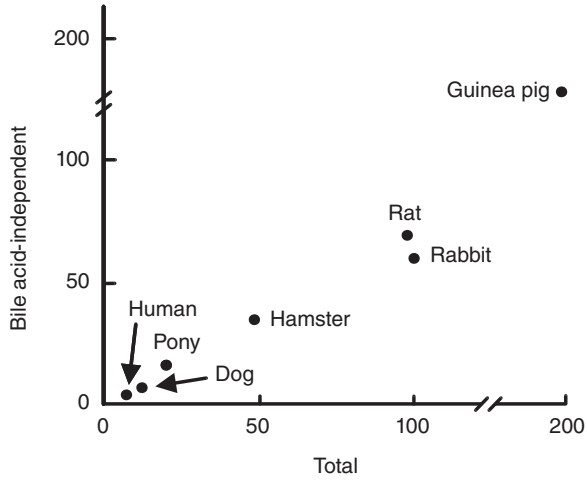

Fig. 7.9 Relationship between bile acid-independent and total bile flow in various species (μL/min/kg). Linearity of the relationship suggests that bile acid-independent canalicular bile flow is a constant fraction of the total bile formation over a wide range of different species.

7.4.6 Factors influencing biliary drug elimination and enterohepatic recycling

Uptake and elimination kinetics of various model compounds (anions, cations, neutral steroids, and metals) in isolated perfused liver and genetically altered animal models have been used to elucidate mechanisms underlying hepatobiliary drug transport. The four major processes governing hepatic drug elimination are (1) hepatocyte uptake from blood; (2) metabolism in hepatocytes; (3) hepatobiliary excretion; and (4) intestinal reabsorption resulting in enterohepatic recirculation. Drug molecules have to be transported to hepatocytes before they can be secreted into the bile. For most drugs (except polar ones), uptake into hepatocytes across the basolateral membrane efficiently occurs via passive diffusion, with minimal reliance on carrier-mediated transport systems. In contrast, Na^+-dependent hepatic uptake of alanine and bile acids as well as Na^+-independent hepatic uptake of bilirubin and tetrabromosulfophthalein are carrier-mediated processes. The reader again should recall the similarity of this process with that described in Chapter 6 for renal tubular transport. Once inside the hepatocyte, most drugs are first metabolized and subsequently translocated back across the sinusoidal membrane into blood or delivered to the canalicular membrane for transport into the bile for fecal excretion and potential reabsorption.

Drug uptake into hepatocytes by passive diffusion is so efficient that it is rate limited by the delivery of the drug to the liver (i.e., blood flow) rather than membrane transport per se, thereby exhibiting flow-dependent clearance. However, for highly polar molecules, passive diffusion is not an efficient mode of hepatocellular uptake, and there is an increased reliance on carrier-mediated transport systems. Drug metabolites, particularly conjugated metabolites (e.g., sulfates and glucuronides), are invariably more polar than their precursors and thus are more likely to experience hepatocyte membranes as diffusional barriers. With such a barrier, the hepatocellular export of a locally formed metabolite will depend on the

presence and activity of carrier-mediated transport systems for sinusoidal efflux and biliary excretion.

Transport systems of current interest (introduced in Chapter 5) include the P-glycoproteins, which are responsible for the biliary excretion of a range of organic cations, and the canalicular multispecific organic anion transporter. Intracellular trapping of metabolites formed in the liver, secondary to low membrane permeability, is clinically important as many are potentially hepatotoxic and/or capable of interfering with the hepatic transport of endogenous compounds or other drugs and metabolites. Again, this phenomenon is conceptually similar to renal tubular sequestration and has similar pharmacokinetic implications. Finally, if the metabolite is unstable, intracellular accumulation can lead to the regeneration of the precursor and so-called futile cycling within hepatocytes.

7.4.7 Biliary drug transport

Some parent drugs and numerous drug metabolites derived from hepatic metabolism are excreted in the bile into the intestinal tract. The excreted metabolites can be eliminated via feces, although, more commonly, they are subject to reabsorption into the blood and are eventually excreted from the body via urine. There are at least three different biliary transport pathways for organic anions, cations, and neutral compounds, although metals may also have their own transport carriers or systems. Both organic anions and organic cations can be actively transported into bile by carrier systems—again, similar to those involved in the renal tubule (see Chapter 6) but having different molecular weight and structural specificities. Such transport systems are nonselective, and ions with similar electrical charge may compete for the same transport mechanisms. Additionally, a third carrier system, whose activity is sex dependent, may be involved in the active transport of steroids and related compounds into bile. In contrast to renal excretion, amphipathic drugs (those having both polar and nonpolar properties) are preferentially excreted in the bile. Organic cation transport is not as important as the organic anion pathway. Neutral compounds may employ the third transport systems. Inorganic metals such as lead may be transported by different mechanisms from blood into bile. Such processes are not as important as those for weak acid drugs, as described above. However, due to the environmental importance of lead and its adverse effects, much research has been directed to this metal toxicant.

The drug (or metabolite) excreted into the small intestine can be reabsorbed into blood, forming the so-called drug *enterohepatic cycle*. This is an important factor changing the blood:liver or liver:bile drug concentration ratios during studies of the hepatobiliary transport mechanisms and hepatic drug elimination. Ouabain, a cardiac glycoside, is used as a model uncharged and nonmetabolized (by rat liver) compound in hepatobiliary transport studies.

Glucuronides of endogenous compounds and xenobiotics, including drugs, can be actively transported from hepatocytes into bile via transport systems similar to those for organic anions. Glucuronide conjugates are very important in hepatic drug metabolism and biliary excretion. The effectiveness of biliary excretion for glucuronide conjugates can be greatly limited by enzymatic hydrolysis after the bile is mixed with the small intestine contents, thereby releasing the parent drugs to be reabsorbed and enter the enterohepatic cycle. The reabsorbed drugs and metabolites can be ultimately excreted in urine. Some drug metabolites further undergo either biotransformation in the liver or other organs or are subjected to microbiological and physicochemical degradation in the small intestine before being excreted in the feces.

Table 7.11 Mean bile flow in selected species.

Species	Bile flow (mL/min/kg body weight)
Cat	11
Chicken	20
Dog	4–10
Guinea pig	200
Hamster	50
Human	5–7
Monkey	10
Mouse	78
Opossum	20
Pig	9
Pony	19
Rabbit	90
Rat	50–80
Sheep	43

Molecular weight is another key determinant of the extent to which drug/metabolite molecules are transported into bile. The molecular weight cutoff required for biliary excretion is much greater than that for renal tubular secretion. The thresholds (in daltons) are approximately: 325 ± 50 for rats, 400 ± 50 for guinea pigs, and 475 ± 50 for rabbits. If the molecular weight is lower (e.g., <325–475 Da), the compound may be preferentially excreted in urine (see Chapter 5). Molecules with weights from 325 to 850 Da may be eliminated via both the renal and biliary routes. Excretion of molecules larger than 850 Da occurs mainly via the biliary active transport system. However, molecular weight is not the sole factor determining the route of drug excretion. Physicochemical properties of the drug (polarity/lipophilicity, structure) are also very critical to the extent of biliary excretion of a drug/metabolite, with amphipathic drugs being well secreted by the biliary route.

The specific animal species being studied is also an important factor, as can be appreciated from the differences in thresholds discussed above. Table 7.11 lists species differences in bile flow rate, which may explain some of this variation. Bile composition (acids, ions, electrolytes) also varies between species and may further explain species differences in drug biliary excretion rate and thus differences in pharmacokinetic disposition.

These species differences in bile flow are intriguing since they do not follow any obvious pattern related to typical pharmacokinetic metrics such as body weight or body size. As will be discussed in Chapter 18, certain parameters are closely related to blood flow and thus scale according to body mass, with smaller species having relatively larger parameter values on a weight basis. As can be seen from this Table 7.11, this does not hold for bile production since species of similar mass have vastly different values. In all likelihood, biliary excretion is an evolutionary adaptation to dietary pressures which are very species specific. Continuing studies on transport proteins suggest such species specificity, making the ability to make broad-based extrapolations across animals difficult.

7.5 PHARMACOLOGICAL AND TOXICOLOGICAL SIGNIFICANCE

Any factor affecting drug concentration at its target site can potentially alter the intensity and duration of drug action. As discussed in this chapter, drugs or xenobiotics are

subject to pharmacological/toxicological activation and deactivation via the double-edged sword of biotransformation. In addition, numerous enzymes capable of metabolizing drugs have overlapping substrate specificities and can also metabolize endogenous compounds. This results in a sex dependency in disposition of certain drugs since endogenous hormones are also metabolized by these enzyme systems. Hepatic drug metabolism also demonstrates stereoselectivity. There is a high likelihood of competition among and between drugs and endogenous substances for the same enzyme or among enzymes for the same compound. These interactions may have profound pharmacological and toxicological.

Most drugs can be deactivated by various phase I reactions, including deamination (amphetamine), side chain hydroxylation (phenobarbitone), *N*-dealkylation (methadone), *S*-oxidation (chlorpromazine), ester hydrolysis (meperidine), and/or amide hydrolysis (procainamide). Phase II reactions generally produce pharmacologically less active metabolite(s) compared with the parent drug or to the phase I metabolite. Phase I reaction-mediated pharmacological activation, on the other hand, is the basis for prodrug design in targeted drug delivery. For example, the prodrug levodopa crosses the blood–brain barrier to become trapped by the neuron, where it is metabolically activated to dopamine, which exerts the pharmacological activity on the neuron as its target site. Dopamine cannot be effectively delivered to its target neuronal site because it cannot cross the blood–brain barrier. Obviously, there are great advantages in such prodrug development in terms of effective drug delivery and maximal therapeutic benefits. Thus, prodrugs require metabolic activation before they can exert their pharmacological action. Another classic example identified in the 1930s is the dye prontosil, which must be activated to liberate the pharmacologically active antibacterial agent, sulfanilamide, via the azoreduction pathway. Metabolic activation can overcome difficulties encountered in drug transport from the site of administration to the target site as well as reduce the chance of site-specific biodegradation and toxicity during drug absorption and distribution.

An even more complex pairing of metabolic activation and deactivation exists with the model organophosphate pesticide, parathion. If the products of such metabolic reactions modify other disposition processes of parent parathion or its metabolites, the effect on biotransformation can be even greater. Parathion can be toxicologically activated as well as deactivated through phase I metabolism. Parathion can be activated to paraoxon (the bioactive anticholinesterase moiety) by desulfuration oxidation and deactivated to *p*-nitrophenol either directly from parathion or indirectly by hydrolysis of paraoxon by A-esterases (Fig. 7.2). Phase II conjugation reactions of *p*-nitrophenol with glucuronide and sulfate can increase *p*-nitrophenol water solubility for a more rapid urinary excretion. *In vitro* parathion metabolism studies suggest that oxidation catalyzed by Cyt P450 is the first and necessary metabolic step, with about 65% of the parathion conversion into paraoxon being contributed by the liver.

7.6 THE IMPORTANCE OF EXTRACTION RATIO

The concept of high- and low-extraction drugs applied to hepatic clearance is central to a complete understanding of drug disposition. The primary factors that may influence hepatic clearance are blood flow, extent of plasma protein binding, and the inherent capacity of the liver to metabolize drug, which is reflected by Cl_{int}.

Table 7.12 Classification of drugs based on extraction ratios.

	Low	Intermediate	High
Liver	Diazepam Digitoxin Phenobarbital Phenylbutazone Procainamide Theophylline	Aspirin Codeine Quinidine	Isoproterenol Lidocaine Meperidine
Kidney	Digoxin Furosemide Aminoglycosides Tetracyclines	Procainamide Penicillins 4° Ammoniums	Most glucuronides Penicillins Sulfates

7.6.1 Low extraction

When metabolic capacity is low (low Cl_{int}), the drug is defined as being a low-extraction drug, and its clearance will be dependent on the extent of protein binding. In the example of protein binding displacement in Chapter 5, a sixfold increase in the free fraction of drug could increase hepatic metabolism by a similar amount, which paradoxically would eliminate any potential adverse effect. A low-extraction drug's clearance will be independent of hepatic blood flow. Low-extraction drugs generally have inadequate quantities of enzyme, poor biliary transport, or poor diffusion of the drug to the site of metabolism. The disposition of these drugs is also susceptible to enzyme induction (which would increase Cl_{int}) and further enzyme inhibition.

7.6.2 High extraction

In contrast, if Cl_{int} is high, the drug is considered to be a high-extraction compound, and its clearance is now limited to how much drug can be delivered to the organ, hence its hepatic blood flow. Changes in protein binding will not affect its clearance. High-extraction drugs will also have a high first-pass effect after oral administration and, in many cases, may prevent oral administration from being an effective route of dosing even if the compound is well absorbed across the gastrointestinal mucosa. For these drugs, enzyme induction will have little effect; however, enzyme inhibition may decrease Cl_{int} sufficiently to decrease the extraction ratio to the range of a moderate- to low-extraction drug.

Table 7.12 lists drugs according to extraction ratios and, for comparison, also lists drugs in a similar classification that are cleared by the kidney. These factors are important to consider when making interspecies extrapolations (Chapter 18) and when adjusting dosage regimens for renal or hepatic disease (Chapter 17).

7.7 CONCLUSION

This chapter presents an overview of some essential principles regarding the classification, cellular and molecular mechanisms, and modifying factors involved in drug metabolism. The exact mechanism of a compounds metabolism by the liver and its pathway of biliary excretion are important components of interspecies extrapolations. The remaining chapters

of this text will focus on the pharmacokinetic strategies needed to quantitate the processes presented in this review. Based on the heterogeneity of hepatic metabolism and biliary secretory processes, and the fact that drugs are often excreted by both renal and hepatic mechanisms, both of which may be characterized by linear and nonlinear processes, it is not surprising that drugs eliminated by these mechanisms often require the most complex pharmacokinetic models. In order to fully characterize and predict drug and xenobiotic effects, models must therefore be developed and parameters such as clearance subsequently estimated. This is the goal of conducting pharmacokinetic studies.

ACKNOWLEDGMENT

The authors thank GuiLin Qiao for his contributions to this chapter in the first edition of the text.

BIBLIOGRAPHY

Ballatori, N. 1991. Mechanisms of metal transport across liver cell plasma membranes. *Drug Metabolism Reviews*. 23:83–132.

Calabrese, E.J. 1991. *Principles of Animal Extrapolation*. Chelsea, MI: Lewis Publishers.

Caldwell, J., Winter, S.M., and Hutt, A.J. 1988. The pharmacological and toxicological significance of the stereochemistry of drug disposition. *Xenobiotica*. 18(Suppl. 1):59–70.

Court, M.H., and Greenblatt, D.J. 2000. Molecular genetic basis for deficient acetaminophen glucuronidation by cats. UGT1A6 is a pseudogene, and evidence for reduced diversity of expressed hepatic UGT1A isoforms. *Pharmacogenetics*. 10:355–369.

D'Argenio, D.Z. 1995. *Advanced Methods of Pharmacokinetic and Pharmacodynamic Systems Analysis*. New York: Plenum Press.

Dutczak, W.J., Clarkson, T.W., and Ballatori, N. 1991. Biliary-hepatic recycling of a xeno-biotic. *American Journal of Physiology*. 260:G873–G880.

Ekroos, M., and Sjogren, T. 2006. Structural basis for ligand promiscuity in cytochrome P450 3A4. *Proceedings of the National Academy of Sciences of the United States of America*. 103:13682–13687.

Farrell, G.C. 1994. *Drug-Induced Liver Disease*. Edinburgh: Churchill-Livingstone.

Fink-Gremmels, J. 2008. Implications of hepatic cytochrome P450-related biotransformation processes in veterinary sciences. *European Journal of Pharmacology*. 585:502–509.

Gibson, G.G., and Skett, P. 1994. *Introduction to Drug Metabolism*, 2nd Ed. New York: Blackie A&P.

Guengerich, F.P. 1997. Role of cytochrome P450 enzymes in drug-drug interactions. *Advances in Pharmacology*. 43:7–35.

Guengerich, F.P., Tang, Z., Salamanca-Pinzón, S.G., and Cheng, Q. 2010. Characterizing proteins of unknown function: orphan cytochrome P450 enzymes as a paradigm. *Journal of Molecular Intervention*. 10:153–163.

Hagenbuch, B. 2010. Drug uptake systems in liver and kidney: a historic perspective. *Clinical Pharmacology and Therapeutics*. 87:39–47.

Halpert, J.R., Guengerich, F.P., Bend, J.R., and Correia, M.A. 1994. Contemporary issues in toxicology: selective inhibitors of cytochrome P450. *Toxicology Applied Pharmacology*. 125:163–175.

Hawkins, D.R. 1988. *Biotransformations*. London: Royal Society of Chemistry.

Hodgson, E. 2010. *A Textbook of Modern Toxicology*, 4th Ed. Hoboken, NJ: John Wiley.

Hodgson, E., and Levi, P.E. 1994. *Introduction to Biochemical Toxicology*. Norwalk, CT: Appleton and Lange.

Illing, H.P.A. 1989. *Xenobiotic Metabolism and Disposition*. Boca Raton, FL: CRC Press.

Jakoby, W.B., Bend, J.R., and Caldwell, J. 1982. *Metabolic Basis of Detoxification: Metabolism of Functional Groups*. New York: Academic Press.

Jenner, P., and Testa, B. 1981. *Concepts in Drug Metabolism*. New York: Marcel Dekker.

Kalow, W. 1992. *Pharmacogenetics of Drug Metabolism*. New York: Pergamon Press.

Klaasen, C.D. 2008. *Casarett and Doull's Toxicology: The Basic Science of Poisons*, 7th Ed. New York: McGraw-Hill.

Klassen, C.D., and Watkins, J.B. 1984. Mechanisms of bile formation, hepatobiliary uptake, and biliary excretion. *Pharmacology*. 36:1–67.

Lim, Y.P., and Huang, J.D. 2008. Interplay of pregnane X receptor with other nuclear receptors on gene regulation. *Drug Metabolism and Pharmacokinetics*. 23:14–21.

Meeks, R.G., Harrison, S.D., and Bull, R.J. 1991. *Hepatotoxicology*. Boca Raton, FL: CRC Press.

Mosher, C.M., and Court, M.H. 2010. Comparative and veterinary pharmacogenomics. In: Cunningham, F., Elliott, J., and Lees, P. (eds.), *Comparative and Veterinary Pharmacology*. Heidelberg: Springer, pp. 49–78.

Nebbia, C., Dacasto, M., Rossetto-Giaccherino, A., Giuliano-Albo, A., and Carletti, M. 2003. Comparative expression of liver cytochrome P450-dependent monooxygenase in the horse and in other agricultural and laboratory species. *The Veterinary Journal*. 165:53–64.

Okey, A.B. 1990. Enzyme induction in the cytochrome P450 system. *Pharmacology and Therapeutics*. 45:241–298.

Pang, K.S., and Rowland, M. 1977. Hepatic clearance of drugs. *Journal of Pharmacokinetics and Biopharmaceutics*. 5:625–653.

Paulson, S.K., Engel, L., Reitz, B., Bolten, S., Burton, E.G., Maziasz, T.J., Yan, B., and Schoenhard, G.L. 1999. Evidence for polymorphism in the canine metabolism of the cyclooxygenase 2 inhibitor, celecoxib. *Drug Metabolism and Disposition*. 27:1133–1142.

Qiao, G.L., and Riviere, J.E. 1995. Significant effects of application site and occlusion on the pattern of cutaneous penetration and biotransformation of parathion *in vivo* in swine. *Journal of Pharmaceutical Science*. 84:425–432.

Qiao, G.L., Williams, P.L., and Riviere, J.E. 1994. Percutaneous absorption, biotransformation and systemic disposition of parathion *in vivo* in swine. I. Comprehensive pharmacokinetic model. *Drug Metabolism and Disposition*. 22:459–471.

Shah, S.S., Sanda, S., Regmi, N.L., Saski, K., and Shimoda, M. 2007. Characterization of cytochrome P450-mediated drug metabolism in cats. *Journal of Veterinary Pharmacology and Therapeutics*. 30:422–428.

Sim, E., Lack, N., Wang, C.J., Long, H., Westwood, I., Fullam, E., and Kawamura, A. 2008. Arylamine *N*-acetyltransferases: Structural and functional implications of polymorphisms. *Toxicology*. 254:170–183.

Smith, R.L. 2001. The discovery of the debrisoquine hydroxylation polymorphism: scientific and clinical impact and consequences. *Toxicology*. 168:11–19.

Tavoloni, N., and Berk, P.P. 1993. *Hepatic Transport and Bile Secretion: Physiology and Pathophysiology*. New York: Raven Press.

Vogelgesang, B.H., Echizen, H., Schmidt, E., and Eichelbaum, M. 1984. Stereoselective first-pass metabolism of highly cleared drugs: studies on the bioavailability of L- and D-verapamil examined with a stable isotope technique. *British Journal of Clinical Pharmacology*. 18:733–740.

Wainer, I.W., and Drayer, D.E. 1988. *Drug Stereochemistry: Analytical Methods and Pharmacology*. New York: Marcel Dekker.

Waterman, M.R., and Johnson, E.E. 1991. *Cytochrome P450. Methods in Enzymology, Volume 206*. New York: Academic Press.

Waxman, D.J., and Azaroff, L. 1992. Phenobarbital induction of cytochrome P450 gene expression. *Biochemistry Journal*. 281:577–592.

Wilkinson, G.R., and Rawlins, M.D. 1985. *Drug Metabolism and Disposition: Considerations in Clinical Pharmacology*. Boston: MTP Press.

Williams, P.A., Cosme, J., Ward, A., Angove, H.C., Matak-Vinkovic, D., and Jhoti, H. 2003. Crystal structure of human cytochrome P450 with bound warfarin. *Nature*. 424:464–468.

Yang, X., Schadt, E.E., Wang, S., Wang, H., Arnold, A.P., Ingram-Drake, L., Drake, T.A., and Lusis, A.J. 2006. Tissue-specific expression and regulation of sexually dimorphic genes in mice. *Genome Research*. 16:995–1004.

Yang, X., Zhang, B., Molony, C., Chudin, E., Hao, K., Zhu, J., Gaedigk, A., Suver, C., Zhong, H., Leeder, S., Guengerich, F.P., Strom, S.C., Schuetz, E., Rushmore, T.H., Ulich, R.G., Slatter, J.G., Schadt, E.E., Kasarskis, A., and Lum, P.Y. 2010. Systematic genetic and genomic analysis of cytochrome P450 enzyme activities in human liver. *Genome Research*. 20:1020–1036.

8 Compartmental Models

The initial chapters of this text presented the underlying physiology of drug fate. The processes involved in absorption, distribution, and elimination are the primary phenomena that must be quantitated to predict the fate of a drug or toxicant in an animal. The two primary characteristics needed to adequately describe these processes are their *rate* and *extent*. In fact, this can be appreciated in the origin of the word kinetic, which is defined by Webster as "*of or resulting from motion*." Many mathematical approaches to this problem have evolved over the course of the history of pharmacokinetics. In addition, hybrid as well as novel strategies are constantly being developed to quantitate these processes. However, all approaches share certain fundamental properties that are based on estimating the rates of chemical movement. These are best illustrated using the classic models that are often considered synonymous with pharmacokinetics.

The most widely used modeling paradigm in comparative and veterinary medicine is the compartmental approach. In this analysis, the body is viewed as being composed of a number of so-called equilibrium compartments, each defined as representing nonspecific body regions where the *rates of compound disappearance* are of a similar order of magnitude. Specifically, the fraction or percent of drug eliminated per unit of time from such a defined compartment is constant. Such compartments are classified and grouped on the basis of *similar rates of drug movement* within a kinetically homogeneous but anatomically and physiologically heterogeneous group of tissues. These compartments are theoretical entities that allow formulation of mathematical models to describe a chemical's behavior over time with respect to movement within and between compartments. This concept was initially introduced in Chapter 7 with the model in Fig. 7.5. Since pharmacologists and clinicians sample blood as a common and accessible biological matrix for assessing drug fate, most pharmacokinetic models are constructed with blood or plasma drug concentrations as the central reference to which other processes are related. This chapter will be restricted to the discussion of models composed of compartments defined by processes that show linear pharmacokinetic behavior, the definition of which will now be formally presented.

Comparative Pharmacokinetics: Principles, Techniques, and Applications, Second Edition. Jim E. Riviere.
 ISBN: 978-0-813-82993-7

8.1 A PRIMER ON THE LANGUAGE OF PHARMACOKINETICS

The roots of pharmacokinetics lie in the estimation of rates. The language is that of differential calculus. It is instructive to present a brief overview of the basic principles of rate determination since the logic embedded in its syntax forms the basis of pharmacokinetic terminology.

To begin, a rate in pharmacokinetics is defined as *how fast the mass of a compound changes per unit of time*, which is expressed mathematically as the change (represented by the Greek letter delta—Δ) in mass per small unit of time (Δt). This is synonymous with the flux of drug in a system. Units of rate are thus mass/time. For the sake of convenience only, we will express this in terms of mg/min. The reader should recall that $\Delta X/\Delta t$ was the symbol used in Chapter 6 to define the rate of renal drug excretion. We will begin this discussion using mass of a compound (X), which in clinical terms would be related to the dose, rather than using concentration. As will be developed shortly, mass and concentration are easily convertible using the proportionality factor of volume of distribution.

The rate of drug excretion $\Delta X/\Delta t$ actually has two components: a constant that reflects the rate of the process and the amount of compound available for transfer:

$$\Delta X / \Delta t = K \cdot X^n, \tag{8.1}$$

where K is the fractional rate constant (1/min), X (mg) is the mass or amount of a compound available for transfer by the process being studied, and n is the order of the process.

8.1.1 First-order rates

For a first-order process, $n = 1$. Since $X^1 = X$, this equation simplifies to

$$\Delta X / \Delta t = K \cdot X. \tag{8.2}$$

By definition, in first-order or linear processes, K is *constant* and thus *the actual rate of the process ($\Delta X/\Delta t$) varies in direct proportion (and hence linearly) to X*. K can be viewed as the fraction of X that moves in the system being studied (absorbed, distributed, or eliminated) per unit of time. Therefore, as X increases, $\Delta X/\Delta t$ increases in direct proportion as was graphed in Fig. 2.6 for diffusion processes. This distinction is very important, for in linear models, the rate constant is fixed, but the actual rate of the process changes in direct proportion to the mass available for movement.

As can again be appreciated by examining the equation for Fick's law of diffusion (Eq. 2.1), compounds that are absorbed, distributed, or eliminated in direct proportion to a concentration gradient are by definition first-order rate processes. The rate constants (K_n) modeled in pharmacokinetics are actually aggregate constants reflecting all of the membrane diffusion processes involved in the disposition parameter being studied. This includes pH partitioning phenomena in the body that exist when blood and a cellular or tissue compartment have a pH gradient that alters the fraction of X available for diffusion. Recall that it is only the unionized fraction of a weak acid or base that diffuses down its gradient across a lipid membrane. The rate constant also reflects the degree of plasma protein binding since only the free fraction of drug is available for distribution. The actual value of a K in a pharmacokinetic model thus reflects all of these variables, whose relationship defines the biological system we are attempting to quantitate. If the system is perturbed (e.g., acid–base abnormalities, altered protein binding), the K values determined in an analysis will also

change. Since the majority of these transmembrane fluxes are either diffusion driven or involve bulk flow through membrane "pores," the sum of all their individual rates can be described using linear pharmacokinetic models.

8.1.2 Zero-order rates

For a nonlinear or zero-order process, by definition $n = 0$. Since $X^{\circ} = 1$, the rate equation now becomes

$$\Delta X / \Delta t = K_0. \tag{8.3}$$

In this scenario, the *rate of excretion is now fixed and thus independent of the amount of compound available*, X. K_0 now has the units of rate (mg/min) and is not a mass-independent fractional rate constant. Although this would appear to simplify the situation, in reality, nonlinear kinetics actually complicates most models. Only when saturation occurs would nonlinear behavior become evident (recall again Fig. 2.6 in Chapter 2, as well as the clearance discussions on tubular secretion in Chapter 6 or biotransformation in Chapter 7, especially Eqs. 7.4 and 7.5). Chapter 10 will present this subject in more detail and discuss the scenario in which the system changes from first order to zero order. The focus of most pharmacokinetic studies is on drugs with linear pharmacokinetics since most therapeutically active compounds are described by these models. The remainder of this chapter will be limited to linear or first-order models.

8.1.3 Instantaneous rates and the derivative

The use of $\Delta X/\Delta t$ to describe the rate of a process is experimentally and mathematically cumbersome. Calculus has been used to describe these same processes using the concept of a derivative. This tremendously increases the options available to manipulate the data and, paradoxically, to simplify applications to biological systems. Instead of describing rates in terms of some small, finite time interval (Δt), differential equations express rate in terms of the change in compound mass (dX) over an infinitesimally small time interval termed dt. Equation 8.1 could now be written as

$$dX / dt = K \cdot X. \tag{8.4}$$

The biological interpretation is identical; however, now the full power of the calculus can be used to provide tools by which these rates can be reliably estimated from biological data. Note that K and X are the same in both equations, the only change is a conceptual one in that dX/dt now describes the instantaneous rate of change in mass over time. By convention, if the amount of drug is increasing, dX/dt is positive (e.g., absorption of drug into the blood), while if it is declining (e.g., elimination or distribution from the blood), then the rate is negative or $-dX/dt$.

8.1.4 Graphical representations of rates

Recalling algebra, if a plot (Cartesian graph) is made with X on the y-axis (dependent variable; ordinate or vertical axis) and t on the x-axis (independent variable; abscissa or horizontal axis), then the rate $\Delta X/\Delta t$ is depicted in Fig. 8.1. Slopes can easily be taken from straight lines described by the equation $y = mx + b$, where m is the slope ($\Delta X/\Delta t$) and b is the y-intercept. Because of this simple relationship, many of the most widely employed techniques in pharmacokinetics are simply exercises in transforming the data (e.g., taking

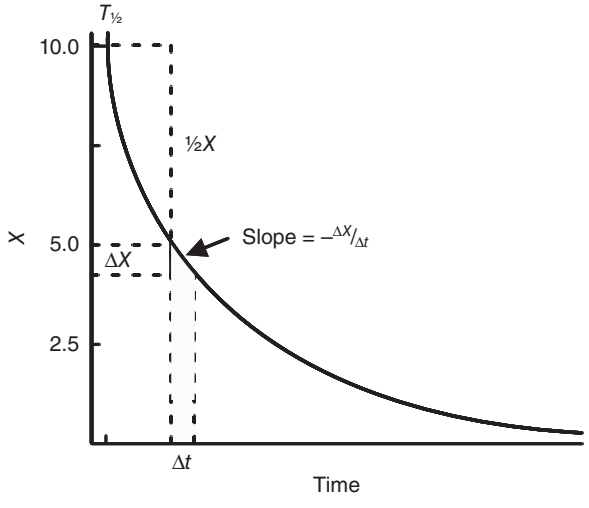

Fig. 8.1 Cartesian plot of the decay in drug (X) versus time. The $T_{½}$ is defined as the time required for X to deplete to one-half X. Slope at any time is $\Delta X/\Delta t$.

logarithms) to derive an equation in this slope–intercept form. Equations of this form will be encountered throughout this text as pharmacokinetic, pharmacodynamic, and statistical models are discussed. This approach facilitates the use of graphical techniques and is a "preprogrammed" function in most computer software packages and handheld calculators. However, for equations that cannot be linearized, obtaining the slope is difficult since it changes with time, as seen in Fig. 8.1. Although modern computational tools make this approach historical, many of the basic equations used in pharmacokinetics today are based on these earlier formulations and form the basis of the models used to analyze the data.

8.1.5 Integration

The derivative is in essence the instantaneous "slope" of any function determined by taking the tangent to the curve at the time point of interest. Thus, equations written as differentials allow instantaneous rates to be calculated. One may solve a differential equation through the process of integration denoted by the symbol $\int$, which transforms the equation back into terms of t rather than dt. Integration is, in reality, a process by which the area under the curve (AUC) defined by $\Delta X/\Delta t$, the demarcated trapezoid in Fig. 8.1, is taken. By repeatedly summing ($\sum$) these areas for the entire experimental period, the AUC will be obtained. We introduced this concept in Chapter 4 when the concept of AUC was introduced (Fig. 4.13). Analogous to the relation of a derivative to a slope, integration sums the areas under infinitesimally small regions defined by dX/dt. The fundamental theorem of integral calculus, developed by Sir Isaac Newton and Gottfried Leibnitz in the 17th century, linked integration to the related process of taking antiderivatives. In calculus, the rate equations may be solved using various mathematical techniques over specific time intervals, generally $t = 0$ through $t = x$ (definite integral), or through the end of an experiment estimated as $t = \infty$ (indefinite integral).

In summary, *defining rates with differentiation is analogous to taking slopes, while the inverse process of integration produces parameters that may often be expressed and*

numerically estimated as areas. This basic analogy simplifies many of the concepts inherent in pharmacokinetics and, in fact, is the basis for noncompartmental modeling presented in Chapter 9.

8.1.6 Solving a rate equation

The advantage of this approach is best illustrated by example. Let us assume that the process being studied is excretion, and thus X is declining over time. If one wants to determine the total amount of drug excretion using Equation 8.1, one must sum the amount excreted during each Δt interval until the proper time is reached:

$$X = \Delta X/\Delta t_1 + \Delta X/\Delta t_2 + \Delta X/\Delta t_3 + + + = \sum \Delta X/\Delta t. \tag{8.5}$$

This requires collection of discrete timed samples and determining the AUC. The problem is less straightforward if one wants to determine the rate of drug excretion. The first step required using Equation 8.1 would be to measure the rates of compound decay ($-\Delta X/\Delta t$) over time. If one plotted the data as X versus time, the plot would resemble Fig. 8.1. As one can see, a curve results and multiple samples would have to be collected to determine values for $\Delta X/\Delta t$ at different times that would allow determination of K. $\Delta X/\Delta t$ is not constant on a Cartesian plot. The X in Equation 8.1 could be determined from Equation 8.5. It is also not evident how one would easily obtain values of K, the parameter of interest.

In contrast, the situation becomes much easier if Equation 8.4 is instead used and solved for K. In this case, we are assuming decay thus the equation is $dX/dt = -KX$. We can use the technique of integration to solve this problem. We must integrate the equation from X at time zero (X_0) through X at time t (X_t) to obtain a formula for the mass of drug at any time.

$$\int (dX/dt)\, dt = \int (-KX)\, dt. \tag{8.6}$$

There are numerous techniques to accomplish this integration (e.g., Laplace transformation), and the interested reader should consult a calculus textbook for further details. The result is

$$X_t = X_0\, e^{-Kt}, \tag{8.7}$$

where e is the base of the natural logarithm ($e = 2.713$). *It is important to realize that the process of integrating the differential equation describing rate generates the exponential term found in most linear pharmacokinetic models*. In reality, any method of pharmacokinetic analysis using exponential functions to describe physiological data implicitly assumes that a linear process is operative. Exponentials can easily be eliminated from an equation by taking their natural logarithm (ln) since the logarithm is defined as the power to which a base (in this case e) is raised. Taking the natural logarithms of Equation 8.7 yields

$$\ln X = \ln X_0 - K \cdot t. \tag{8.8}$$

If one plots the data similar to Fig. 8.1, but instead uses ln$X$ rather than X, a straight line results (Fig. 8.2). Recalling the algebraic expression for a straight line on x–y coordinates, in this case the y-intercept (b) becomes $\ln X_0$ and the slope of the line (m) is $-K$. The

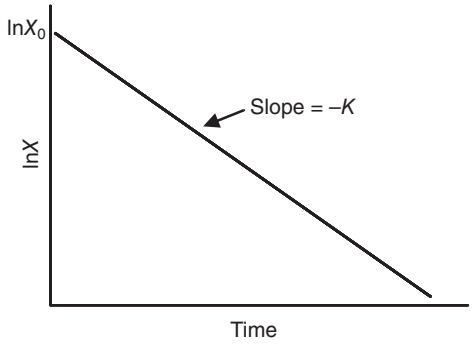

Fig. 8.2 Semilogarithmic plot of drug decay versus time with slope equal to $-K$ and intercept $\ln X_0$.

equation has been linearized providing a simple graphical method to calculate the rate constant.

The reader must realize that this equation can be linearized only because it is a first-order rate function. In theory, only two samples would have to be taken to define this line, although, statistically, a better estimate is obtained if more points are used. This type of plot, which is widely used throughout pharmacokinetics, is termed a semilogarithmic plot (in contrast to the Cartesian plot) since the logarithm of mass is plotted against time. Again, *when a straight line results on a semilogarithmic plot, one can assume that a linear first-order process is operative and the slope of the line is the exponent of an exponential equation*. Alternatively, a linear regression program on a computer or pocket calculator could be used to calculate K by regressing the $\ln X$ against time. Once again, the slope is $-K$ and the y-intercept is $\ln X_0$. More sophisticated statistical techniques to solve complex linear rate equations that are employed in practice will be presented in Chapter 14.

From an historical perspective, graphs used logarithms to the base 10 (log X) $\{10^X\}$ rather than the base e $(\ln X)\{e^X\}$, then the transformation of bases can be accomplished as

$$\text{Log } X = \ln X / 2.303, \tag{8.9}$$

which transforms Equation 8.8 to

$$\text{Log } X_t = \log X_0 - Kt / 2.303. \tag{8.10}$$

If base 10 semilogarithmic graph paper were used to plot Fig. 8.2, the slope becomes $-K/2.303$. As this technique was in widespread use before the advent of digital computers, some workers and texts still use this approach, explaining why 2.303 appears in many pharmacokinetic equations.

This brief explanation of the derivation of exponential equations is important since all pharmacokinetic models for linear processes are expressed in these terms. These equations have certain mathematical properties (such as additivity or superposition) that greatly simplify analysis of biological data. As models become more complex, so does the process of integration, but the solutions to the equations still collapse to exponential terms that are easily analyzed using modern digital computers or graphical techniques. Thus, for the remainder of this text, the derivations and analytical solutions to the equations will not be expanded, and the reader must have faith in the author. Instead, we will focus on the proper

use of the equations and the development of techniques for applying them to biological systems, the focus of this text.

8.2 THE CONCEPT OF HALF-LIFE

The exponential equations in pharmacokinetics have another property that is central to biological applications. This is the concept of half-life ($T_{½}$), whose logic is central to much of this discipline. The astute biologist reading this text will have realized that Equation 8.7 is the same as that used to describe population-doubling times in microbiology or ecology and to generate population growth curves, defined as the time needed for a population of organisms to double their total numbers when they are in their so-called logarithmic growth phase. The only difference is that since growth is described, the exponent is positive in this application. In pharmacokinetics, our perspective is a $T_{½}$, which is instead the time required for the amount of drug to decrease by one-half, or 50%. Again, we must stress that *the concept of $T_{½}$ is applicable only to first-order rate processes*.

Using Equation 8.8, we can derive a simple equation for $T_{½}$. We first rearrange terms to solve for T, which yields

$$T = (\ln X_0 - \ln X_t)/K. \tag{8.11}$$

We now solve for the time at which X is equal to ½ the initial amount X_0; that is, where $T = T_{½}$. Substituting these values above,

$$\begin{aligned} T = T_{½} &= (\ln X_0 - \ln ½ X_0)/K \\ &= \ln(X_0 / ½ X_0)/K \\ &= \ln(2)/K \\ &= 0.693/K. \end{aligned} \tag{8.12}$$

Alternatively, by algebraic rearrangement, we now have an equation for K, which is

$$K = 0.693/T_{½}. \tag{8.13}$$

It is instructive to emphasize that it is this transformation of K and $T_{½}$ that forces 0.693 to appear in many pharmacokinetic equations when first-order rate constants are converted to $T_{½}$.

What does $T_{½}$ really mean? This is best illustrated by returning to Fig. 8.1 (remember that this is plotted on Cartesian X-versus-time scales). We can determine the time required for X to decrease to ½X using the original data; that is, estimating the Δt required for ΔX to be equal to ½X. No matter where this is done on the concentration–time (C-T) plot, the same value for Δt (e.g., $T_{½}$) will be obtained even though the actual rate of drug excretion ($\Delta X/\Delta t$) is decreasing at each time interval. In addition to providing a simple means of estimating $T_{½}$ when the data correspond to intervals of 50% decrease in X, it also clearly illustrates the meaning of $T_{½}$.

Assume that we start with X, decrease it by half, and repeat this process 10 times. Table 8.1 compiles these data and lists how much drug is remaining and how much has been excreted over each Δt corresponding to one $T_{½}$. Note that if you sum these columns, as

Table 8.1 Relationship between $T_{½}$ and amount of drug (*A*) in the body.

Number of $T_{½}$s	% of drug eliminated	% of drug remaining
1	50	50
2	75	25
3	87.5	12.5
4	93.75	0.625
5	96.88	0.312
6	98.44	0.156
7	99.22	0.078
8	99.61	0.039
9	99.80	0.019
10	99.90	0.0097

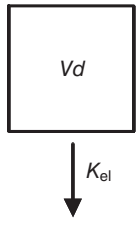

Fig. 8.3 One-compartment open pharmacokinetic model.

discussed above using Equation 8.5, one would have accounted for 99.9% of the original dose *X*. After 10 $T_{½}$s, 99.9% of the drug has been eliminated, or the rate process being studied has been essentially completed. This also illustrates the logic that must be used when dealing with doses. For example, if we doubled the dose to 2*X*, then after one $T_{½}$, we would be back to the original dose! Many "rules of thumb" used in pharmacokinetics and medicine are based on this simple fact. For therapeutic drugs, most workers assume that after five $T_{½}$s, the drug has been depleted, or the process is over since 97% of the depletion has occurred. These so-called rules will be revisited in later chapters when the design of dosage regimens is considered. It is now time to develop our first pharmacokinetic model using mathematical rather than physiological concepts.

8.3 ONE-COMPARTMENT OPEN MODEL

The simplest compartment model considers the body as consisting of a single homogeneous compartment; that is, the entire dose *X* of drug is assumed to move out of the body at a single rate. This model, depicted in Fig. 8.3, is best conceptualized as instantly dissolving and homogeneously mixing the drug in a beaker from which it is eliminated by a single rate process described by the rate constant *K*, now termed K_{el}. Since drug leaves the system, the model is termed open. Equation 8.7 is the pharmacokinetic equation for the one-compartment open model. Although expressed in terms of the amount of drug remaining in the compartment, most experiments measure concentrations.

This requires the development of one of the so-called primary pharmacokinetic parameters, the volume of distribution (*Vd*), which was introduced in Chapter 5 (recall Eq. 5.5). In terms of the one-compartment model, this would be the volume of the compartment into

which the dose of drug (D) instantaneously distributes. Vd thus becomes a *proportionality factor* relating D to the observed concentration Cp by

$$Vd\,(\mathrm{mL}) = X(\mathrm{mg}) / Cp(\mathrm{mg/mL}) = D / Cp. \tag{8.14}$$

Using this relation, we can now rewrite Equation 8.7 in terms of concentrations, which are experimentally accessible by sampling blood, instead of the total amount of drug remaining in the body:

$$Cp = (X_0 / Vd) \cdot e^{-K_{el}t} = Cp_0 \cdot e^{-K_{el}t}. \tag{8.15}$$

A semilogarithmic plot seen after intravenous administration using this model is depicted in Fig. 8.4. One can easily convert between Figs. 8.1 or 8.2 and 8.4 using the Vd relationship above. Vd quantitates the apparent volume into which a drug is dissolved since, recalling the discussion in Chapter 5, the true volume is determined by the physiology of the animal, the relative transmembrane diffusion coefficients, and the chemical properties of the drug being studied. A drug that is restricted to the vascular system will have a very small Vd, while one that distributes to total body water will have a very large Vd. In fact, it is this technique that was used to calculate the plasma and interstitial spaces quoted in Chapter 5.

From this simple analysis, and using the model in Fig. 8.3, a number of useful pharmacokinetic parameters may be defined. Assuming that an experiment such as depicted in Fig. 8.4 has been conducted using a dose of D and values for K_{el} and Vd have been determined, $T_{½}$ can easily be calculated from Equation 8.12 above.

8.3.1 Clearance

Recalling the development of clearance concepts in Chapter 6, we now can easily determine Cl_B using this information. Clearance was defined as the *volume of blood cleared of a substance by the kidney per unit of time*. If one considers the whole body, this would read as the *volume of distribution of drug in the body cleared of a substance per unit of time*. Translating this sentence to the syntax of pharmacokinetic terminology and considering whole-body elimination, Vd represents the volume and K_{el} the fractional rate constant (units of 1/time). Thus, clearance is

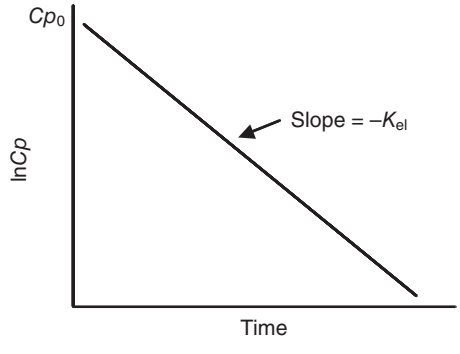

Fig. 8.4 Semilogarithmic concentration–time profile for a one-compartment drug with slope $-K_{el}$ and intercept Cp_0.

$$Cl_B\,(\text{mL/min}) = Vd\,(\text{mL}) \cdot K_{el}\,(1/\text{min}). \tag{8.16}$$

As alluded to in the discussion on renal clearance, this equation allows one to determine the glomerular filtration rate (GFR) if a glomerular filtration marker such as inulin were injected into the body and its decay plotted as in Fig. 8.4. Similar logic was applied to use clearances to describe hepatic drug metabolism.

There is another method available to calculate Cl_B. In Chapter 6, clearance was also defined in Equation 6.4 as the *rate of drug excretion relative to its plasma concentration*. We can also express this sentence in the syntax of pharmacokinetics and get the relation

$$Cl_B = (dX/dt)/Cp. \tag{8.17}$$

If we integrate both the numerator and denominator of this relation from time = 0→∞, the numerator is simply the sum of the total amount of drug that has been excreted from the body; that is, the administered dose *D*. The denominator is the integral of the plasma C-T profile. Since integration was analogous to taking the area under the function to be integrated over infinitesimally small time intervals (*dt*), the result of this operation is simply the AUC. The relation thus becomes

$$Cl_B = D/\text{AUC}. \tag{8.18}$$

There are two approaches to calculate AUC that are based on determining the area under the observed C-T profile. A common approach is to use the trapezoidal method alluded to when integration was defined. Fig. 4.13 (see Chapter 4) introduced this technique, which will be presented in much greater detail in the next chapter on noncompartmental models since this modeling approach is based completely on calculating the AUCs of different functions. However, for the one-compartment open model being discussed, which generates the semilogarithmic C-T plot depicted in Fig. 8.4, the problem is simply determining the area of the right triangle. The area of this triangle (AUC) is height divided by the slope of the hypotenuse, or

$$\text{AUC} = Cp_0 / K_{el}. \tag{8.19}$$

8.3.2 Interpretation of pharmacokinetic parameters

With these equations, we now have the *three so-called primary pharmacokinetic parameters describing drug disposition in the body*: $T_{½}$, Cl_B, *and Vd*. The data required to calculate them is a knowledge of dose and an experimental derivation of either K_{el} or $T_{½}$. Coupled with a knowledge of absorption, which estimates absorbed dose, most practical aspects of constructing a dosage regimen are at hand. These are related in the following scheme that shows how these parameters are interrelated.

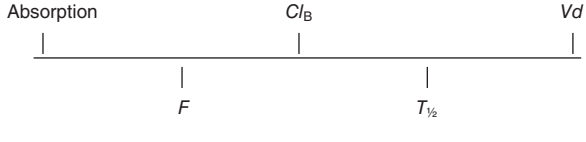

This is a good point at which to discuss the limits of calculating parameters from simple C-T profiles. Only two parameters are actually being "measured" from this analysis: the slope K_{el} and intercept Cp_0 of the semilogarithmic plot, which, using Equation 8.14, directly calculates Vd. The third parameter Cl_B is "calculated" from the two "measured" parameters. Based on the mathematical method used to calculate these, some workers suggested that K_{el} and Vd are the independent parameters in a pharmacokinetic analysis, and Cl_B is a derived parameter. This assertion is usually made when the statistical properties of the parameters are being defined since errors for these can be easily obtained. However, this belief is an artifact of the use of a compartmental model as a tool to get at values for these physiological parameters and introduces confusion when pharmacokinetic parameters are linked to physiological variables. As should be appreciated from the discussions in Chapters 5–7, physiologically, the truly independent parameters are the Vd and Cl_B, with K_{el} and thus $T_{½}$ becoming the dependent variables. This distinction is very important when the effects of either a species' physiology or an individual's disease state on pharmacokinetics are being estimated. From this biological perspective, the true relationship is

$$T_{½} = (0.693 \cdot Vd) / Cl_B. \tag{8.20}$$

The observed half-life of a drug is dependent on both the extent of a drug's distribution in the body and its rate of clearance. If the clearance of a drug is high (e.g., rapidly eliminated by the kidney), the $T_{½}$ will be relatively short. Logically, a slowly eliminated drug will have a prolonged $T_{½}$. Although not at first obvious, if a drug is extensively distributed in the body (e.g., lipid-soluble drug distributed to fat), Vd will be large and the $T_{½}$ will be relatively prolonged. In contrast, if a drug that has restricted distribution in the body (e.g., only the vascular system), the Vd will be small and thus the $T_{½}$ relatively short. In a disease state, $T_{½}$ may be prolonged by a diseased kidney; a reduced capacity for hepatic drug metabolism; or an inflammatory state, which increases capillary perfusion and permeability, thus allowing drug access to normally excluded tissue sites. *Therefore*, $T_{½}$ *is physiologically dependent on both the volume of distribution and clearance of the drug*. The basic physiological principles outlined in Chapters 5–7 are important to keep in mind since, as we build more complicated (but realistic) pharmacokinetic models, the calculation of Vd and Cl_B becomes more complex because the underlying biology dictates it.

8.3.3 Clearance from intravenous infusions

There is yet another strategy that can be used to estimate clearance in an intravenous study. This is based on the basic principle of mass balance. The strategy is to infuse a drug into the body at a constant rate R_0 (mass/time) and then measure plasma drug concentrations. By definition, when a steady-state plasma concentration is achieved, C_{ss} (mass/volume), the rate of drug input must equal the rate of clearance from the body, Cl_B:

$$R_0\ (\text{mg/min}) = C_{ss}\ (\text{mg/mL}) \cdot Cl_B\ (\text{mL/min}). \tag{8.21}$$

Rearranging this equation gives a simple formula for determining Cl_B:

$$\begin{aligned} Cl_B\ (\text{mL/min}) &= R_0\ (\text{mg/min}) / C_{ss}\ (\text{mg/mL}) \\ &= R_0 / C_{ss} \end{aligned} \tag{8.22}$$

The Cl_B calculated in this manner is identical to that determined using Equations 8.16 and 8.18 above, and only requires knowing the rate of infusion and assaying the achieved steady-state concentration. One may also calculate the *Vd* from an intravenous infusion study by the relation

$$Vd = R_0 / (C_{ss} \cdot K_{el}). \tag{8.23}$$

This line of reasoning supports Cl_B as a primary parameter since it can be calculated independently of a one-compartment analysis. In fact, as discussed in Chapter 6, this is another method to estimate GFR using markers of renal clearance. If steady-state is assumed, then R_0 must equal the rate of excretion presented in Equation 6.4 as $\Delta X/\Delta t$. Making this substitution, and using this chapter's terminology of C_{ss} in place of C_{art}, both equations are equivalent. If one knows the rate of infusion of a glomerular filtration marker such as inulin and assays the steady-state concentration, GFR can thus be estimated in a relatively robust manner since errors in time or assay will be minimized when the average C_{ss} is determined. In fact, this method holds for even more complicated pharmacokinetic models (discussed below) since as long as steady-state is achieved, the rate of infusion will always be dependent on Cl_B. As will be discussed in Chapter 12, this relationship also forms the basis of multiple-dose regimens.

8.3.4 Pharmacokinetic analysis from urine data

Many of the above pharmacokinetic parameters may be obtained by analysis of urine data alone. This is often advantageous when concentrations of the compound studied are too low for assay in the blood, or when exposure in an environmental scenario results in very low absorbed doses. In these cases, the ability of the kidney to concentrate urine is taken advantage of since the kidney thereby concentrates the excreted drug. However, to use these techniques, it is important that the concepts of Cl_B and Cl_{renal} be kept distinct. In a one-compartment open model for a drug completely eliminated by the kidney, and for which there is no extravascular administration or systemic metabolism, all injected drug will appear in the urine, and thus the total amount excreted over the course of an experiment (e.g., the sum of Eq. 8.5) is equivalent to *X* or *D*. If the drug also undergoes hepatic elimination, then $D \neq X$ since a fraction will be excreted by other routes (e.g., bile, expired, or as metabolites in urine).

Urine-based techniques all assume that some fraction of the drug is eliminated from the body by renal elimination. The compound has a C-T profile best characterized by a monoexponential decay (e.g., one-compartment open model) even though it may be eliminated by multiple organs. Recall in Chapter 6 that Cl_B is the sum of $Cl_{renal} + Cl_{hepatic} + Cl_{other}$. In an analogous fashion, since $Cl_B = K_{el}\, Vd$ and *Vd* is the same for drug excreted by the kidney or any organ, dividing this relationship by *Vd* we obtain

$$K_{el} = K_{renal} + K_{hepatic} + K_{other} = K_{renal} + K_{nonrenal}. \tag{8.24}$$

For the sake of simplicity, we will consider only renal and nonrenal routes of elimination.

In a manner analogous to analyzing the C-T profile to obtain K_{el}, we will instead analyze the rate of drug excretion in the urine. We will denote urine concentration at time *t* as U_t. *With the C-T profile, we are studying drug that has not yet been eliminated from the body,*

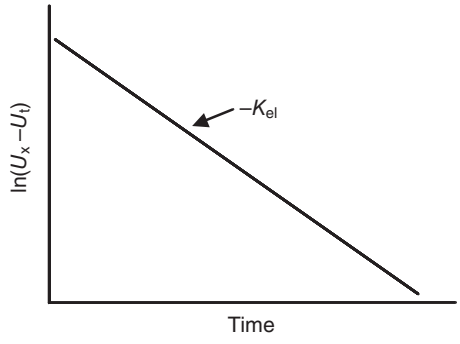

Fig. 8.5 Pharmacokinetic analysis of urinary drug concentrations using a semilogarithmic amount remaining to be excreted (ARE) plot whose slope is $-K_{el}$.

while in urine-based methods, we are examining the drug that has already been excreted. If bile were collected instead of urine, similar techniques could be used to model biliary drug excretion.

In many of these experiments, we are essentially measuring $\Delta X/\Delta t$ based on urine collection. It thus behooves the investigator to take great care in collecting urine specimens. For best results, one must have properly timed urine collections, and when rates are estimated, Δt should be less than one $T_{½}$. The assayed urine concentration is then multiplied by the collected urine volume to obtain the mass excreted in Δt, that is, U_t. When excretion plots are constructed as described below, the time plotted on the *x*-axis should be the midpoint of the Δt interval. Similarly, if a corresponding *Cp* is obtained, it should either be collected at the midpoint of collection or be calculated as the average of the time points defining Δt.

When data are analyzed in this manner, the rate of elimination K_{el}, and not K_{renal} alone, determines the slope of the $\ln U$ excretion rate profiles. Since one is measuring the rate of unchanged drug excretion into the urine, this rate will also reflect nonrenal elimination even when the drug eliminated by this route is not being excreted into the urine. This can be appreciated by examining Fig. 8.3 and substituting $(K_{renal} + K_{nonrenal})$ for K_{el}. The driving concentration for elimination by both routes is the *Cp* in this compartment. Thus, as drug is eliminated by the kidney and other routes, its concentration will decrease at a rate proportional to the total K_{el} from this compartment. What will be dependent on K_{renal} is the fraction of this eliminated dose, which is excreted into the urine and will affect the total urinary recovery U_∞. *Urine-based methods monitor the systemic rate of elimination.*

The technique termed the amount remaining to be excreted (ARE) or sigma-minus method is depicted in Fig. 8.5. The term ARE is obtained because the *y*-axis is now $(U_\infty - U_t)$ or, alternatively, the amount of drug remaining to be excreted in the urine, reflecting the fact that not all of the systemically administered dose will appear in the urine. To construct this plot, for every Δt of urine collection, one plots $[U_\infty - U_t]$ versus the time of the midpoint of the collection interval. Note that since this is a semilogarithmic plot, the excretion profile is log-linear. The slope is then equal to K_{el}. In another technique, the rate of drug excretion $(\Delta U/\Delta t)$ versus time is plotted as in Fig. 8.6. The resulting slope is again K_{el}.

What is different in Figs. 8.5 and 8.6 compared with the plasma-based plot of Fig. 8.4 is the nature of the intercept, not the rate of decay that is controlled by K_{el}. This becomes

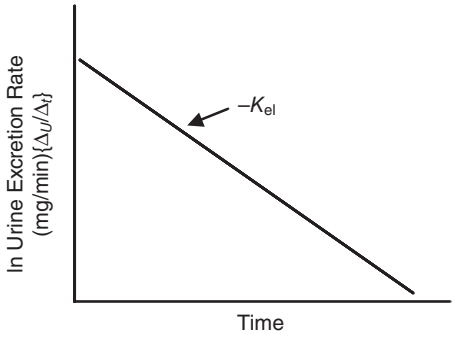

Fig. 8.6 Semilogarithmic plot of rate of drug excretion in urine versus time with a slope equal to $-K_{el}$.

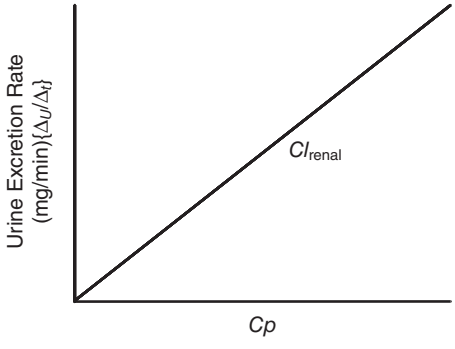

Fig. 8.7 Plot of rate of drug excretion in urine versus plasma concentration with slope equal to Cl_{renal}.

clearer from the differential rate equations for $\Delta U/\Delta t$. The formula that describes Fig. 8.6 would be similar to Equation 8.8:

$$\ln U_t = (K_{\text{renal}} \cdot U_0) - (K_{\text{el}} \cdot t). \tag{8.25}$$

The slope of the plot is the same; however, the intercept now reflects the fraction of drug excreted in the urine. Similarly, the equation for the ARE plot would be

$$\ln(U_\infty - U_t) = \ln U_\infty - K_{\text{el}} \cdot t. \tag{8.26}$$

Again, slopes are identical, but now the intercept reflects how much drug actually was excreted in the urine. As can be appreciated from studying these relationships, if the drug is totally excreted by the kidney, then $U_\infty = D$. However, if renal and nonrenal elimination routes are occurring, these data may be used to estimate the extent of nonrenal elimination since the ratio of U_∞/D is equivalent to $K_{\text{renal}}/K_{\text{el}}$ (also termed f in Chapter 17, Eqs. 17.10 and 17.11).

More information may be obtained if corresponding *Cp*-versus-time data is available for each $\Delta U/\Delta t$. A plot of rate of excretion on a Cartesian axis versus *Cp* is shown in Fig. 8.7. As defined in Chapter 6 (Eq. 6.4), the rate of excretion relative to the blood concentration is defined as the renal clearance, and thus the slope of the line in Fig. 8.7 ($\Delta U/\Delta t$ vs. *Cp*) is Cl_{renal}. In this analysis, more information is present than with the two techniques

discussed above since the rate of drug excretion in the urine is being compared with the *Cp* profile, which is declining with a rate constant of K_{el}. The *Cp* data have K_{el} information embedded within it. The clearance obtained using this technique reflects Cl_{renal} and not Cl_B. If one integrates both axes of this plot, the slope remains Cl_{renal}, but now the *y*-axis is the cumulative amount of drug excreted in urine and the *x*-axis is AUC. At any time *t*, the slope is cumulative *U* divided by AUC through time *t* (AUC_t), which provides a point estimate of Cl_{renal}.

The selection of which method to use is dependent on experimental constraints and data quality. Urine excretion data are often variable and dependent on accurate sampling. The more samples that make up an analysis, and thus the shorter Δt, the better the estimate. Theoretically, all of the above methods will result in the same rate constant and clearance estimates. However, physiological anomalies in how the kidney handles a compound (tubular reabsorption with storage, tubular secretion with subsequent metabolism) within the tubular system may make differences in these methods evident. For example, assume a drug is completely eliminated by the kidney, making any estimate of Cl_B equivalent to Cl_{renal}. However, if one of these processes occurs, Cl_B will be greater than Cl_{renal} since *Cp* cannot reflect what happens to the drug after filtration (see Chapter 5). Fig. 8.8 illustrates this phenomenon with gentamicin. When Cl_B was compared with Cl_{renal} in four separate studies, the above relation was always noted, suggesting that tubular sequestration was reducing the flux of intact drug into the urine. The same would occur if parent drug were metabolized by the kidney and excreted as an undetectable metabolite. However, this difference becomes a strength since these phenomena can be studied due to this discrepancy in clearances.

Additional urine techniques will only be briefly discussed in the remaining chapters since an extension of the logic presented above can be used to obtain many values formally presented only for C-T profiles. In some laboratory animal situations in which urine collection is easier than blood sampling, these approaches may prove particularly powerful as many pharmacokinetic parameters may be obtained from noninvasive urine monitoring.

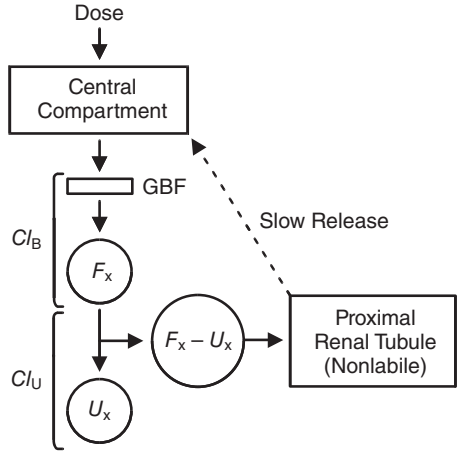

Fig. 8.8 Difference between total body clearance calculated from plasma (Cl_B) or urine (Cl_U) due to drug that was filtered by the glomeruli (GBF) but reabsorbed and stored in the renal tubules ($F_X - U_X$) rather than being excreted in the urine. F_X is filtered drug, and U_X is drug excreted in the urine.

8.4 ABSORPTION IN A ONE-COMPARTMENT OPEN MODEL

The models presented above up to this point assume that the drug was injected into the body, which behaves as a single space into which the drug is uniformly dissolved. The first real-world complication occurs when the drug is administered by one of the extravascular routes discussed in Chapter 4. In this case, the drug must be absorbed from the dosing site into the bloodstream. The resulting semilogarithmic C-T profile, depicted in Fig. 8.9, is now characterized by an initial rising component that peaks and then undergoes the same log-linear decline. The proper pharmacokinetic model for this scenario is depicted in Fig. 8.10. The rate of the drug's absorption is governed by the rate constant K_a.

When the absorption process is finally complete, elimination is still described by K_{el} as depicted in Fig. 8.2. The overall elimination half-life can still be calculated using K_{el} if this terminal slope is taken after the peak in the linear portion of the semilogarithmic plot (providing $K_a >> K_{el}$). However, calculation of Vd and Cl_B becomes more complicated since K_a is present and, unlike an intravenous injection, one is not assured that all of the drug has been absorbed into the body. In order to handle this, we must now write the differential equations to describe this process by including rate constants for absorption and elimination:

$$dX/dt = K_a \cdot D - K_{el} \cdot X, \tag{8.27}$$

Fig. 8.9 Semilogarithmic plot of plasma concentration versus time with first-order absorption.

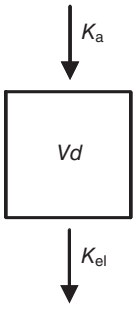

Fig. 8.10 One-compartment open pharmacokinetic model with first-order absorption.

where D is the administered dose driving the absorption process and X is now the amount of dose absorbed and available for excretion. The relationship between D and X is the absolute systemic availability F originally introduced in Chapter 4 (Eqs. 4.2 and 4.3); $\{X = FD\}$. In the language of differential equations, rates are simply additive, which allows the same data sets to be described in components reflecting the different processes. As above, integrating this equation and expressing it in terms of concentrations gives the expression that describes the profile in Fig. 8.9:

$$Cp = \frac{K_a \cdot F \cdot D}{Vd \cdot (K_a - K_{el})} \cdot \left[e^{-K_{el}t} - e^{-K_a t}\right]. \tag{8.28}$$

8.4.1 The concept of curve stripping applied to absorption

This is an excellent point in the discussion to appreciate the validity of the use of multi-exponential equations to describe blood C-T profiles, as the exponential terms, like the rates above from which they were derived, are simply additive. *A C-T profile is the sum of the underlying exponential terms describing the rate processes involved.* This property of superposition is the basis on which observed C-T profiles were once "dissected" to obtain the component rates. Although not used today to actually determine these parameters, the process is instructive and underscores the processes involved in determining the shape of a C-T profile.

Fig. 8.11 illustrates this process, in which an observed semilogarithmic profile is plotted as a composite of its absorption phase (controlled by K_a) and the elimination phase (controlled by K_{el}). In contrast to the intravenous Equation 8.15, the time zero intercept is now a more complex function, which is dependent on the fraction of administered dose that is systemically available and thus able to be acted on by the elimination process described by the rate constant K_{el}. For this procedure to work, K_a must be greater than K_{el} so that at later time points $e^{-K_a t}$ approaches zero [exponential of a large negative number approaches zero, or expressed mathematically, as $L_{t\to\infty}\ (e^{-t}) = 0$].

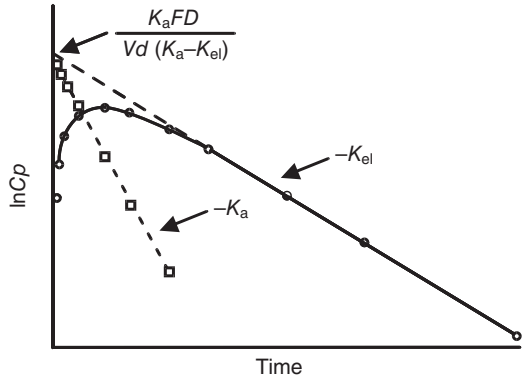

Fig. 8.11 Semilogarithmic plot of plasma concentration versus time using a one-compartment open pharmacokinetic model with first-order absorption. The profile is decomposed into two lines with slopes $-K_a$ and $-K_{el}$.

This equation reduces to

$$Cp = \frac{K_a \cdot F \cdot D}{Vd \cdot (K_a - K_{el})} \cdot \left[e^{-K_{el}t}\right], \tag{8.29}$$

which is the terminal phase of the C-T profile. If K_a were less than K_{el}, the same C-T profile as the one in Fig. 8.9 will result; however, now the terminal slope will be K_a as it is the rate-limiting process! The intercept term would be appropriate if one just flip-flopped K_a and K_{el}. In fact, recalling the discussion in Chapter 4 on slow-release dosing formulations, we termed the resulting effect on disposition of drug in the body an example of the *flip-flop* phenomenon, the origin of which is the above relation.

In any multiexponential model, in order for multiple phases of a C-T profile to become evident, the ratio of *K*s (in our example K_a and K_{el}) must be ≥3. The computational procedure of "stripping" the slower elimination process away from the observed composite C-T profile to generate the absorption profile (or any other faster exponential process, such as distribution) was the basis of many earlier software algorithms.

It is important to once again digress at this point of the discussion to stress the reason why *intravenous pharmacokinetic studies should always be conducted to define drug disposition*. If an extravascular route of administration is used, the investigator can never be certain that the C-T profile is not dependent on a slow, and thus rate-limiting, absorptive process secondary to a formulation factor. If a depot or extended-release formulation is administered such that K_a *is less than* K_{el}, the terminal slope will reflect the rate of absorption rather than the rate of elimination. $T_{½}$ may be overestimated as it will now reflect $0.693/K_a$ rather than $0.693/K_{el}$. Complete absorption also cannot be ensured (e.g., $F = 1$), thus one never truly knows the size of the absorbed dose. Accurate estimates of Cl_B and Vd, reflecting the true pharmacokinetic disposition of a drug, are required as input to determine these relations. These are best calculated after a complete intravenous injection using the equations described above.

In many cases, values for Cl_B and Vd are calculated after nonparenteral administration and reported as Cl_B/F or Vd/F. As will be discussed shortly, even when intravenous data is available, there are limits to interpretation of these parameter estimates, suggesting that great caution be used when interpreting such normalized parameter values. Using a value for F to normalize these parameters from an independently conducted study will introduce inaccuracy due to different experimental designs.

When intravenous and extravascular dosing experiments are conducted, one can estimate the absolute systemic availability F for a specific formulation by determining the ratios of AUCs. In an intravenous study in which the total mass of drug is injected, all of the drug will have had to appear in the bloodstream, and thus AUC_{IV} will reflect the maximum AUC possible. The F of the extravascular dose then is the ratio of $AUC_{extravascular}$ to AUC_{IV}, the same as Equation 4.3 (see Chapter 4 on absorption).

8.4.2 Analysis of urine data to estimate absorption parameters

As discussed above for intravenous administration, urine analysis may also be used to estimate absorption parameters. If the rate and pathway of metabolism is similar between both routes, F may also be simply calculated as $(U_\infty)_{extravascular}/(U_\infty)_{IV}$. If they are different, and the other route of elimination can be assessed (e.g., expired air, bile, feces), then abso-

lute systemic availability becomes a ratio of the total amount excreted by both routes as depicted previously in Equation 4.2 (see Chapter 4). In many cases, it is difficult to collect total urine and feces in the field, and one would like a method to assess availability (or in toxicology terms, exposure) from only one route. To accomplish this, one must know the fraction of drug that is eliminated by the route being studied. Based on our discussions of urine-based methodologies above, this is the ratio of K_{renal}/K_{el}. As shown above, this is equivalent to the ratio $(U_\infty)_{IV}/D_{IV}$. Multiplication of this ratio times the U_∞ obtained in the intravenous study corrects it to reflect the fraction of dose absorbed that could be excreted in the urine. Bioavailability by this route is then calculated as

$$F = (U_\infty)_{\text{extravascular}} / (\text{corrected } U_\infty)_{IV}. \tag{8.30}$$

The rate of absorption K_a can also be calculated from the data in Fig. 8.11, but there are more efficient techniques, which will now be briefly presented. First, urine excretion data can be used to analyze for K_a in addition to F using techniques very similar to that described in Equations 8.25 and 8.26 and depicted in Figs. 8.5 and 8.6. The "twist" now added is that the total dose is a function of F, and the rate of absorption K_a comes into play. Thus, similar to the C-T profile in Fig. 8.9, a biexponential curve in urine will result. If ARE or $\Delta U/\Delta t$ plots are used, the slopes of the line are K_a and K_{el}, with K_{el} being the terminal slope if K_a is greater than K_{el}. *Again, realize that the slope of the terminal portion of a urine excretion curve reflects overall systemic elimination and not renal excretion.* If a flip-flop situation is present, the terminal slope will be K_a. For a rapidly absorbed drug, it is often difficult to get good estimates of K_a from the "stripped" urine data since very short urine collection intervals (Δt) are almost impossible. The intercept term is also more complex as it now reflects K_{el}, K_{renal}, and K_a. However, at time infinity, the total amount excreted in urine, U_∞, reduces to $(K_{renal} \cdot F \cdot D)/K_{el}$, which is another form of the expression used to derive Equation 8.30 above.

8.4.3 Systemic bioavailability

If all of these concepts are considered, and the rate of absorption may become rate limiting, then the most widely used experimental approach for determining absolute systemic availability is based on an analysis of AUC. If different doses are applied or if the $T_{½}$ is different by the extravascular route being studied due to the route effects in clearance, then F should be calculated as

$$F = \frac{(\text{AUC}_{\text{extravascular}}) \cdot (D_{IV}) \cdot (T_{½})_{IV}}{(\text{AUC}_{IV}) \cdot (D_{\text{extravascular}}) \cdot (T_{½})_{\text{extravascular}}}. \tag{8.31}$$

It must be stressed that when a flip-flop absorption rate-limiting drug is studied, F must not be corrected for the rate-limiting absorption due to flip-flop, but must be corrected for prolonged extravascular $T_{½}$ due to altered systemic disposition by this route, otherwise F will be greater than 1.0—a value that is biologically meaningless. Such "strange" values of F may also be encountered if the injected intravenous dosage form is not soluble in blood (e.g., precipitation, too lipophilic). In this case, a fraction of the intravenous dose never is truly available for systemic distribution.

Finally, it must be stressed that F is only an estimate of systemic bioavailability since it assumes that the absorbed drug enters the central circulation in the same form; for

example, free, not bound to plasma proteins or lipids, or distributed into red blood cells, as it does after intravenous injection. For example, after oral dosing, one would assume drug would exit the portal circulation potentially bound to some blood constituent. If the time it takes for the drug to re-equilibrate is longer than, or of a similar order of magnitude to, K_{el} or other distribution rate constants in a more complex model, bioavailability could be overestimated. However, if these processes are very rapid compared with K_{el}, the estimate is accurate. These concepts are fully developed in Chapter 15 on bioequivalence.

8.4.4 Wagner–Nelson method

The final techniques employed in bioavailability studies are designed to extract data on K_a from C-T profile analysis. The techniques above assume that K_a is a first-order process and thus may be described using an exponential equation, which, due to additivity, may be stripped away from a semilogarithmic C-T profile. However, in many cases, K_a may be zero order, for example, in a sustained-release dosage form. The Wagner–Nelson method may be used in this situation. Finally, should nonlinear kinetics be operative, interpretation of AUC is more tenuous and sensitive to dose as described in Equations 10.23–10.25 in Chapter 10.

This technique is based on analyzing data based on percent absorbed plots. Simply, this method assumes that the amount of drug absorbed into the systemic circulation at any time after administration (X_S) equals the sum of the amount of drug remaining in the body (X_B) plus the cumulative amount of drug that has already been eliminated (X_E) by all routes combined $\{X_S = X_B + X_E)$. If we write a differential rate equation describing dX_S/dt, we get this rate: $dX/dt = dX_B/dt + dX_E/dt$. We see that dX_E/dt is equivalent to Equation 8.4 as X_E is the amount of drug in the body remaining to be excreted. As previously derived, this is equal to rate of drug elimination $K_{el} \cdot X$. If we express X_B in terms of Cp using the Vd relation of Equation 8.14, we get

$$dX_S / dt = Vd \cdot C / dt + K_{el} \cdot Vd \cdot C. \tag{8.32}$$

If one integrates this equation from time zero to t, we get

$$\begin{aligned} X_S(t) &= Vd \cdot C_t + K_{el} \cdot Vd \int C\, dt \\ &= Vd \cdot C_t + K_{el} \cdot Vd \cdot \mathrm{AUC}_t, \end{aligned} \tag{8.33}$$

where C_t is the concentration at time t and $\int C\,dt$ is the AUC from time zero through t, denoted as AUC_t. At time infinity, the total amount of drug absorbed could be calculated by integrating Equation 8.32 from $t = 0 \rightarrow t = \infty$. In this procedure, $C_0 = 0$ for both time points. The result is

$$X_S(\infty) = K_{el} \cdot Vd \cdot \mathrm{AUC}_\infty. \tag{8.34}$$

Note that AUC_∞ is equivalent to the AUC calculated earlier. If we take the ratio of Equations 8.33 and 8.34 and cancel common terms, we derive a relation describing the fraction of drug absorbed through time t:

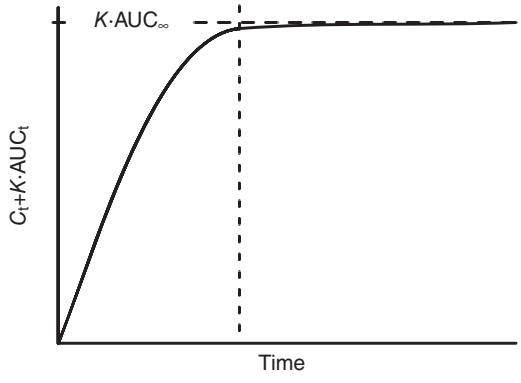

Fig. 8.12 Wagner–Nelson plot used to analyze drug absorption in a one-compartment model.

$$\frac{X_S(t)}{X_S(\infty)} = \frac{C_t + K_{el} \cdot \mathrm{AUC}_t}{K_{el} \cdot \mathrm{AUC}_\infty}. \tag{8.35}$$

This expresses the relation of the fraction of drug absorbed at any time relative to that ultimately absorbed, not the administered dose. However, from our systemic availability discussion above, $X_S(\infty) = F \cdot D$, a value that only can be derived using intravenous data.

Wagner–Nelson plots can now be obtained as follows. Fig. 8.12 shows the amount of drug absorbed as a function of time and is constructed by plotting the numerator of Equation 8.35 versus time. K_{el} is obtained by the methods discussed above using a semilogarithmic C-T plot. Although many of these calculations appear at first to be cumbersome, the key is to organize collected data by time of observation such that each calculation is straightforward, a process facilitated by using a spreadsheet program in which columns are defined as

$$\text{Time} \,|\, \text{Observed } C_t \,|\, \mathrm{AUC}_t \,|\, K_{el} \cdot \mathrm{AUC}_t \,|\, C_t + K_{el} \cdot \mathrm{AUC}_t.$$

As seen in this plot, as time increases, the value of the function approaches $K_{el} \cdot \mathrm{AUC}_\infty$. Knowing AUC_∞, a plot of the fraction absorbed calculated using Equation 8.35 is depicted in Fig. 8.13. It should be noted that this approach makes no assumptions about the order of the kinetics of the absorption process since a model is never fitted to the plots. This is the power of this approach since estimates of the rate of absorption can be made for processes with zero-order (e.g., extended-release) and even more complex kinetics.

If one were to take the same data used to generate Fig. 8.13 and instead plot 100 (1 − Percent absorbed), that is, percent of drug unabsorbed, a first-order absorption process would generate a curve on ordinal plots and a straight line on a semilogarithmic plot, as in Fig. 8.14a. In some cases where absorption is complex and described by multiexponential equations, a curve stripping approach could be used to break this plot into its constituent rates (K_x and K_y), as in Fig. 8.14b. The Wagner–Nelson approach is generally only applicable to one-compartment data, and the Loo–Riegelman technique described below should be used in multicompartmental situations.

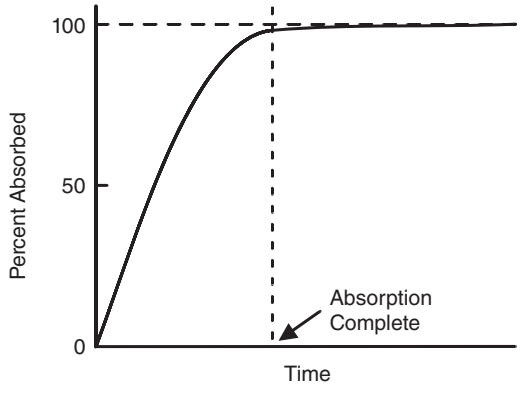

Fig. 8.13 Plot of percent absorbed versus time used to analyze drug absorption data.

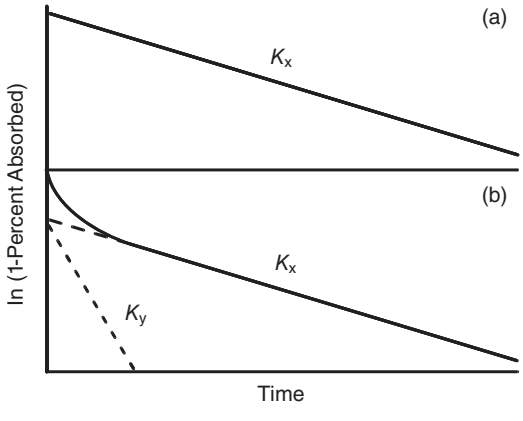

Fig. 8.14 Semilogarithmic plots of amount of 1 – percent of drug absorbed demonstrating (a) a single absorption phase and (b) a two-component absorption phase.

8.5 TWO-COMPARTMENT MODELS

Unfortunately, most drugs are not described by a simple one-compartment model since the plasma C-T profile is not a straight line. This reflects the biological reality that for many drugs, the body is not a single homogeneous compartment, but instead is composed of regions that are defined by having different *rates* of drug distribution. Such a situation is reflected in the two-compartment model depicted in Fig. 8.15. The drug initially is distributed in the central compartment and by definition is eliminated from this compartment. The difference comes because now the drug also distributes into other body regions at a rate that is different from that of the central compartment.

As presented in Chapter 5, many factors determine the rate and extent of drug distribution into a tissue (e.g., blood flow, tissue mass, blood/tissue partition coefficient). When the composite rates of these flow and diffusion processes are significantly different than K_{el}, then the C-T profile will reflect this by assuming a biexponential nature. For many

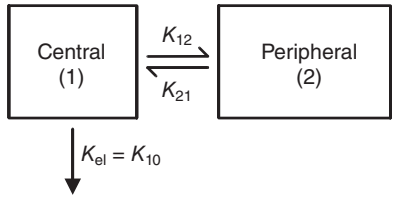

Fig. 8.15 Generalized open two-compartment pharmacokinetic model after intravenous administration with elimination (K_{el}) from the central compartment. K_{12} and K_{21} represent intercompartmental microrate constants.

drugs, the central compartment may consist of blood plasma and the extracellular fluid of highly perfused organs, such as the heart, lung, kidneys, and liver. Distribution to the remainder of the body occurs more slowly, which provides the physiological basis for a two-compartment model. Such a peripheral compartment is defined by a distribution rate constant (K_{12}) out of the central compartment and a redistribution rate constant (K_{21}) from the peripheral back into the central compartment. As discussed in Chapter 5 on distribution, depots or sinks may also occur. This is a pharmacokinetic concept whereby the distribution rate constants are significantly slower than K_{el} and thus become the rate-limiting factor defining the terminal slope of a biexponential C-T profile, a situation analogous to flip-flop in absorption studies.

We will begin the discussion of multicompartmental models with the principles of analyzing a two-compartment model after intravenous administration (Fig. 8.15). This is the most common scenario encountered in comparative medicine, and the principles translate easily to more complicated models. The fundamental principle involved is that the observed serum C-T profile is actually the result of two separate pharmacokinetic processes, which can be described by two separate exponential terms, commonly written as

$$C = Ae^{-\alpha t} + Be^{-\beta t}. \tag{8.36}$$

Note the similarity of this biexponential equation to that presented for absorption in Equation 8.28. In this case, we have terms with slopes (α and β) and corresponding intercepts (A and B). The C-T profile on semilogarithmic plots is depicted in Fig. 8.16. By definition, $\alpha >> \beta$, and thus is the terminal slope. If $\alpha = \beta$, then the slopes of the two lines would be equal and we would be back to the single line of Fig. 8.2 and a one-compartment model!

8.5.1 Nomenclature

When dealing with multicompartmental models, it becomes necessary to introduce new nomenclature to denote the intercept terms and slopes of the C-T profile because, as will be shown shortly, the observed slopes are no longer synonymous with the elimination and absorption rate constants as they were when we were analyzing absorption plots (Fig. 8.10) for K_{el} and K_a. When these models were constructed, the defining differential rate equations could be written in terms of the mass of drug in the central compartment (X). In the two-compartment model of Fig. 8.15, this equation now must describe drug movement in terms of the mass of drug in compartments one and two. As will be derived below, the solution to this differential equation are the slopes of the biexponential C-T profile giving α and β.

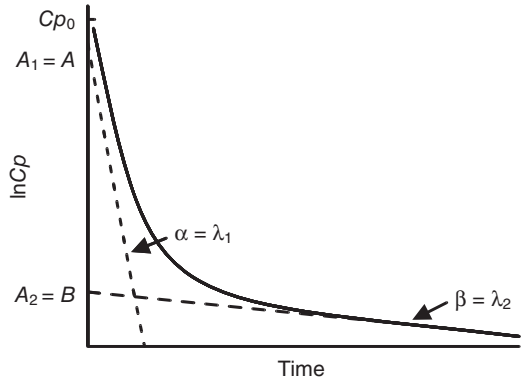

Fig. 8.16 Semilogarithmic plasma concentration versus time profile of a drug described by a two-compartment open model. Parameters are defined in the text.

Multicompartmental models thus have their own syntax: the slopes of the C-T profile are named with letters of the Greek alphabet, starting with the most rapid rate, α, for distribution, followed by β for elimination. The intercept terms are denoted using the roman alphabet, in this example *A* being related to α and *B* to β. However, this can be confusing when distribution is into a slowly equilibrating depot, where α would now reflect elimination and β distribution. This often happens when the experiment is conducted over days rather than hours, as we found in studies conducted with gentamicin as described below.

The preferred nomenclature carries less phenomenological context and uses the Greek letter λ_n, with $n = 1, 2, 3, \ldots$, progressing from the most rapid to the slowest rate process. The corresponding intercept terms are denoted as A_n. This nomenclature describes any multicompartmental model without implying a physiological basis to the underlying mechanism responsible for the different rates observed. The biexponential equation for a two-compartment model may now be written as

$$Cp = A_1 e^{-\lambda_1 t} + A_2 e^{-\lambda_2 t}. \tag{8.37}$$

The actual rate constants describing flux between compartments are now termed microrate constants and denoted by k_{xy} where compound moves from x to y. Smaller values for x and y indicate more rapid interdepartmental microrate constants. When the origin or destination of a compound is outside of the body, then x or y is denoted as 0, respectively. Thus, K_a becomes k_{01} and K_{el} becomes k_{10}. In order to avoid confusion, the microrate constants defining a multicompartmental model will be denoted as lowercase k to distinguish them from one-compartment rate constants, which are uppercase K since the latter may be obtained directly from an analysis of the C-T profile (e.g., $K_{el} = k_{10}$). Finally, the central compartment is always denoted as 1, with higher numbers assigned to more slowly equilibrating compartments.

With a two-compartment model, three *Vd*s may now be calculated: the volume of the central compartment V_c or V_1, the peripheral compartment V_p or V_2, and the total volume of distribution in the body V_t or $V_1 + V_2$. As will be seen below, the actual *Vd* calculated from the data is dependent on the method used; however, the only estimate of *Vd*, which can be broken into its component central and peripheral volumes, is the volume of distribution at steady-state Vd_{ss}.

When more complex models are presented in subsequent chapters, the K_{el} and K_a nomenclature may still be used to differentiate these first-order rate constants from other metabolic and pharmacodynamic effect parameters. Similarly, in some of these scenarios, α and β may still be used to denote the slopes of a biexponential model. However, most automated software packages utilize similar notation to λ_n and A_n to define the shapes of multiexponential C-T profiles and microconstants to define the underlying compartmental structure linked to the observed data. *When using any software package, the user should first relate the program's nomenclature to these basic parameters to ensure that the data are properly interpreted.*

8.5.2 Derivation of rate equations

Now that we have the appropriate nomenclature, it is instructive to derive the equations for λ_n and A_n based on the microconstants that define the differential rate equation. For a two-compartment model after intravenous injection of dose D with elimination occurring from the central compartment, the following differential equation describes the rate of drug disposition:

$$dC_1/dt = -(k_{12} + k_{10}) \cdot C_1 + (k_{21}) \cdot C_2. \tag{8.38}$$

Processes that remove compound from the central compartment (k_{10} and k_{12}) are grouped together and have a negative rate since they result in a descending C-T profile. The only process that adds chemical to the central compartment (k_{21}), that is, redistribution from the peripheral compartment, is assigned a positive rate and results in an ascending C-T profile. The rate of this process is driven by the concentration of compound in the peripheral compartment, C_2. Note the similarity of this equation to the differential equation for absorption in a one-compartment model (Eq. 8.27). In this model, the only process that added drug to the central compartment was K_a, which therefore was assigned a positive sign, while the only process removing drug was K_{el}. Similarly, as stressed throughout this text, the driving mass for this passive absorption process was the fraction of administered dose ($F \cdot D$) available for absorption.

The power and essence of pharmacokinetic analysis is that the physiological processes driving drug disposition can be quantitated by using differential equations describing drug flux into and out of observable compartments. Most models are structured to reflect the central compartment, which is monitored via blood sampling, as the primary point of reference. Solution of the differential equation 8.38 by integration yields Equation 8.36 or 8.37, which describe the biexponential C-T profile characteristic of a two-compartment open model.

The observed slopes λ_1 and λ_2 and intercepts A_1 and A_2 are related to the microconstants as

$$k_{21} = (A_1 \cdot \lambda_2 + A_2 \cdot \lambda_1)/(A_1 + A_2) \tag{8.39}$$

$$k_{10} = (\lambda_1 \cdot \lambda_2)/k_{21} \tag{8.40}$$

$$k_{12} = \lambda_1 + \lambda_2 - k_{21} - k_{10} \tag{8.41}$$

Each of the slopes now has a corresponding $T_{½}$ calculated as

$$T_{½}\lambda_1 = 0.693/\lambda_1 \text{ (Distribution)} \tag{8.42}$$

$$T_{½}\lambda_2 = 0.693/\lambda_2 \text{ (Elimination)} \tag{8.43}$$

The slope of the terminal phase of the C-T profile reflects the elimination $T_{½}$ and is the primary parameter used to calculate dosage regimens. Note that since $\lambda_1 >> \lambda_2$, $T_{½}\lambda_1 << T_{½}\lambda_2$, and at later time points (recall the five $T_{½}$ rule), distribution will be complete, and the biexponential Equation 8.37 collapses to the monoexponential equation $Cp = A_2e^{-\lambda_2 t}$. (Mathematically, this is true because e raised to a very small negative exponent becomes zero since the limit L of (e^{-t}) as $t \to \infty$ is 0). This equation is similar in form to the one-compartment Equation 8.15 except the intercept is now A_2 and not Cp_0, and the slope is $-\lambda_2$ and not K_{el}.

These differences are the basis for much confusion in pharmacokinetics when the data for a drug, truly described by a biexponential equation, are analyzed only at later postdistribution time points, and the monoexponential C-T profile observed is assumed to be described by a one-compartment model. As will be discussed below, the *Vd* calculated by this method erroneously uses A_2 (or B in the "αβ" nomenclature) as being equal to Cp_0 and thus overestimates the true *Vd* since A_2 or B is less than Cp_0. Dosage regimens determined using this approach will therefore administer the wrong dose since the true *Vd* is actually smaller.

This property of "disappearing" exponentials with large λs at later time points provides the basis for analyzing polyexponential C-T profiles using the curve stripping approach (technically called the method of residuals) depicted in Fig. 8.16 and discussed earlier in the context of absorption in Fig. 8.11. To derive this residual line, one subtracts the slower process $(A_2e^{-\lambda_2 t})$ from the earlier time points described by the biexponential Equation 8.37 $(Cp = A_1e^{-\lambda_1 t} + A_2e^{-\lambda_2 t})$ to reveal the rapid component $(A_1e^{-\lambda_1 t})$. The slopes and intercepts of these two lines can then be easily determined by the techniques described above for fitting monoexponential equations.

It is often difficult to accurately estimate distribution parameters when λ_1 is very rapid since early blood samples must be collected to determine the residual line. Recall that compartmental models assume that the drug is instantaneously distributed into the compartment being studied. Physiologically, for this to occur, drug must first circulate through the vascular system at a rate limited by the blood circulation time. In a large animal such as a horse or cow, this requires a few minutes, and thus very early samples (e.g., less than 5 min) will not have sufficient time for this mixing to occur. Second, small errors in sample timing result in a large percent error (1 min off for a 5-min sample; error is 20%), and thus the data obtained at very early time points are often extremely variable. In contrast, a 5 min mistake for a 6-h sample is only a 1% error, making estimates of terminal slopes much less variable.

It is important to stress that when one is fitting an equation to a plasma C-T profile for pharmacokinetic analysis, exponential-phase additivity implied by this curve stripping process is assumed. Some statisticians and mathematicians not familiar with the physiological basis of using exponential models could elect to just split the line into two parts and determine the slopes. However, the slopes determined in this manner, which may be statistically correct, are not useful for pharmacokinetic analyses, and their insertion into the equations presented is incorrect because the initial slope determined without stripping is in reality a composite of λ_1 and λ_2. This stripping concept arises directly from the principle of superposition, whereby an observed plasma concentration is the sum of all

processes (absorption, distribution, elimination) involved in its disposition. These techniques will be fully discussed when their implementation in software packages is presented in Chapter 14.

8.5.3 Volumes of distribution

There are three volumes of distributions to contend with: V_c or V_1, V_p or V_2, and $V_t = (V_1 + V_2)$. These are again calculated by a knowledge of intercepts and administered dose (assuming intravenous administration). The relevant intercept is Cp_0, which is now simply $A_1 + A_2$.

$$V_1 = D/Cp_0 = D/(A_1 + A_2) \tag{8.44}$$

$$Vd_{ss} = V_1 \cdot [(k_{12} + k_{21})/k_{21}] \tag{8.45}$$

$$V_2 = Vd_{ss} - V_1 \tag{8.46}$$

$$Vd(B) = D/B = D/A_2 \tag{8.47}$$

$$Vd_{area} = D/(\mathrm{AUC} \cdot \lambda_2) = D/(\mathrm{AUC} \cdot \beta) \tag{8.48}$$

$$= Vd_{\beta} = (k_{10} \cdot V_1)/\lambda_2 \tag{8.49}$$

There is a great deal of confusion and debate on which volume of distribution should be used in a pharmacokinetic analysis. The answer is really dependent on what the investigator wants to do with the data. The relationship between these estimates is

$$Vd(B) > Vd_{area} > Vd_{ss} > V_c. \tag{8.50}$$

The easiest to discard is $Vd(B)$, the apparent volume of distribution by extrapolation, since it is often used when a complete analysis of the curve is avoided and only the terminal slope and its intercept A_2 is determined. As discussed above, this estimate completely ignores V_1 and the earlier time points where distribution is still present. Similarly, V_1 is defined as the central compartment volume. It is the volume from which clearance can be determined using certain equations; it is used in some intravenous infusion calculations to determine maximal plasma concentration after an intravenous bolus dose of a drug such as a rapid acting anesthetic is administered, or it could be used to estimate the plasma volume when a drug restricted to the plasma is used as a physiological marker.

The volume of distribution at steady state, Vd_{ss}, is the most "robust" estimate since it is mathematically and physiologically independent of any elimination process or constant. It is the preferred Vd estimate for interspecies extrapolations and the study of the effects of altered physiology on Vd since it is independent of elimination. Theoretically, Vd_{ss} describes the Vd at only a single time point when the rate of elimination equals that of distribution. The point at which this occurs is the inflection point or bend in the C-T profile, which occurs because the more rapid tissue distribution phase has now peaked and a true equilibrium exists between distribution and elimination. This is best appreciated in Fig. 8.17 when the concentrations in the central and tissue compartments are plotted.

Vd_{area} is often used when clinical dosage regimens are constructed (see Equations 12.2, 12.6, and 12.12 in Chapter 12) because it reflects the area during the elimination phase of the curve, which predominates in any dosage regimen (see Fig. 8.17). This is absolutely

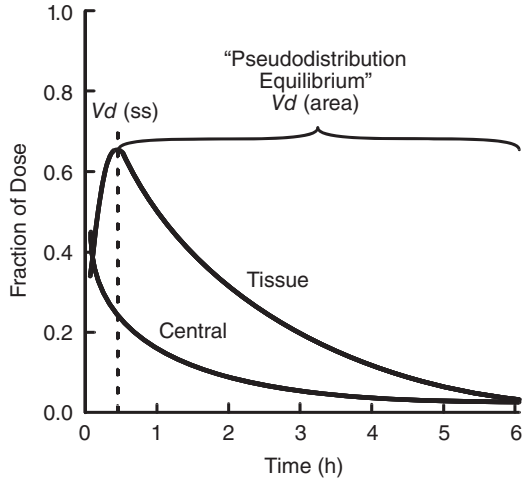

Fig. 8.17 Relationship between Vd_{ss} and Vd_{area} for a drug described by a two-compartment model. Note that Vd_{ss} is only descriptive of the volume of distribution at the peak of the tissue compartment concentration-versus-time profile (true equilibrium), while Vd_{area} describes the volume throughout the terminal elimination phase when a pseudoequilibrium is operative.

Table 8.2 Pharmacokinetic parameters for gentamicin administered intravenously in dogs with and without renal disease.

Parameter	Units	Normal values	Values in dogs with renal disease
Cl_B	(mL/min/kg)	3.66	1.55
K_{el}	(1/h)	1.45	1.01
$T_{½\lambda 2}$	(min)	75	136
V_c	(L/kg)	0.15	0.11
Vd_{ss}	(L/kg)	0.23	0.28
Vd_{area}	(L/kg)	0.40	0.29
Vd_{area}/Vd_{ss}	—	1.74	1.03

equivalent to Vd_β, the so-called volume of distribution at pseudodistribution equilibrium. At this point in the drug depletion profile, plasma concentrations are decreasing at a rate proportion to Cl_B. If the rate of elimination is very prolonged (slow), as seen in severe renal disease, then the terminal slope of the C-T profile may approach zero (plateaus; $T_{½}$ becomes very long), which effectively "stretches out" the curve's inflection due to a plateau in the peripheral tissue compartment. Under this scenario, Vd_{area} becomes equal in value to Vd_{ss}, mathematically since the limit of Vd_{area} as $K_{el} \rightarrow 0$ is Vd_{ss}.

This is illustrated in Table 8.2, which shows the various *Vd* estimates actually determined for gentamicin in dogs with different levels of renal function using a two-compartment open model. Physiologically, Vd_{ss} actually increased in renal disease in these dogs. However, the mathematical dependence of Vd_{area} confounds this as its reduced value is secondary to the reduction in K_{el} due to reduced renal function.

As is stressed throughout this text, any estimate of *Vd* is really a proportionality constant between administered dose and observed plasma concentration. It is often overinterpreted

to estimate the true extent of drug distribution into tissues. Actual distribution is dependent on many physiological factors including extent of plasma and tissue binding as discussed in Chapter 5 and depicted in Equation 5.6. The value observed for a specific drug will be also dependent on the activity of various drug transporters as to whether they are uptake or efflux pumps and what tissue bed they are primarily located in. Changes in their activity from induction or inhibition may alter *Vd*. Which *Vd* is effected is dependent on the mechanism of the transporter studied. If tissue distribution is primarily affected but elimination is not impacted, Vd_{ss} will change. If renal transporters that also augment elimination occurs, Vd_{area} may be affected. These phenomena are important for assessing pharmacological effect; they also further illustrate both the different properties of Vd_{ss} versus Vd_{area} and interaction of distribution and elimination processes on the value of pharmacokinetic parameters.

8.5.4 Clearance

Knowing V_1, one can calculate the systemic clearance since Cl_B occurs from the central compartment and is essentially the same as a one-compartment model. If Vd_{area} is known, the terminal C-T slope can be used.

$$Cl_B = K_{10} \cdot V_1 = \lambda_2 \cdot Vd_{area} \tag{8.51}$$

Alternatively, Cl_B may be calculated using the intravenous infusion Equation 8.22 presented earlier. The only difference is that with the more complex distribution kinetics presents in a multicompartmental model, the time to reach C_{ss} may be significantly longer.

Finally, Cl_B may also be determined using Equation 8.18 based on AUC. In a two-compartment model, AUC may be calculated using slopes and intercepts by the relation

$$\text{AUC} = (A_1/\lambda_1) + (A_2/\lambda_2), \tag{8.52}$$

which can be generalized for a multicompartmental model to

$$\text{AUC} = \sum A_i/\lambda_i. \tag{8.53}$$

Realize that this equation still requires fitting exponential equations to the C-T profile and, unlike other area methods discussed in Chapter 9 on noncompartmental models, first-order linear rate constants are assumed. However, this is a relatively robust technique to calculate many parameters and will be revisited where formulae for Vd_{ss} and other parameters may be determined.

8.5.5 Interpretation of parameters

Using *Vd* and Cl_B, Equation 8.20 can again be used to calculate the overall $T_{½}$ of drug in the body. This $T_{½}$ reflects both distribution and elimination processes and is very useful as input into an interspecies allometric analysis. This is not equivalent to the terminal elimination half-life, $T_{½}\lambda_2$ but instead must be calculated from the Cl_B and Vd_{ss} parameters. Again, as will be seen in Chapter 9, it is directly related to the mean residence time of drug in the body and is thus an excellent aggregate parameter for disposition.

The comparison of pharmacokinetic parameters across species brings up another concern related to parameter selection. If the elimination rate is very prolonged in a specific species (e.g., no metabolism, different type of kidneys that restricts renal clearance), or as just discussed the pharmacogenomics of drug transporters are different, the calculated Vd_{area} between two species may be very different, while the Vd_{ss} may be similar. The disposition of a drug across species should use mathematically and physiologically independent estimates of Vd_{ss} and Cl_B. The real concern in any pharmacokinetic analysis of multicompartmental systems is that the *Vd* used is *appropriate* for the equation being employed to make predictions. As will be seen in Chapter 17, this is critical in the construction of dosage regimens, especially when renal disease is present.

Finally, as was presented for a one-compartment model, all of these approaches may be analyzed using urinary excretion data. The slopes in a urinary excretion plot reflect the λs determined from the C-T profile since k_{10} and not K_{renal} is rate-limiting. However, there are severe experimental restrictions on the ability to use urine data to model rapid distribution processes; it is difficult to accurately collect urine over very short time intervals since Δt should be less than the $T_{½}$ of the rate process being studied. When the typical $T_{½}$ is only a few minutes, and the distribution process starts immediately after drug administration, it is often impossible to collect accurate urine samples.

8.5.6 Absorption in a two-compartment model

When an extravascular dose is administered as input into a two-compartment model (Fig. 8.18), the differential equation defining this model is

$$V_1 \cdot dC_1 / dt = -(k_{12} + k_{10}) \cdot C_1 \cdot V_1 + k_{21} \cdot C_2 \cdot V_2 + k_{01} \cdot X. \tag{8.54}$$

Note that the movement of drug in the central compartment is now driven by three different concentrations: C_1, C_2, and the fraction of the administered dose D that is available for absorption (X). There are a number of approaches to solve this model and various forms of the solution. An example of a plasma C-T profile for such a drug is depicted in Fig. 8.19. The solution to this differential equation in exponential form is

$$C_p = (k_{01} \cdot D / V_1) \cdot [A_1' e^{-\lambda_1 t} + A_2' e^{-\lambda_2 t} - A_3' e^{-k_{01} t}] \tag{8.55}$$

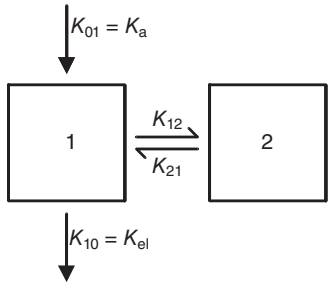

Fig. 8.18 Generalized open two-compartment pharmacokinetic model with first-order absorption (K_{01}) into and elimination (K_1) from the central compartment. K_{12} and K_{21} represent intercompartmental constants reflecting distribution.

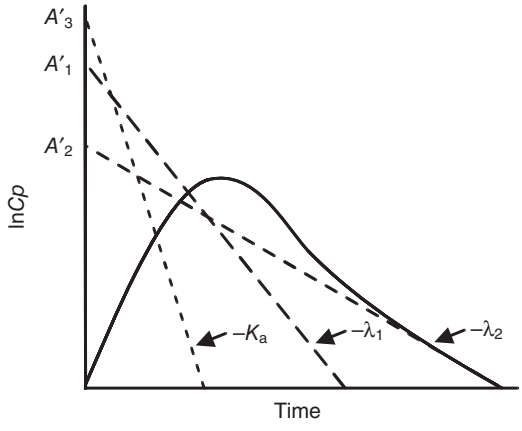

Fig. 8.19 Semilogarithmic plasma concentration-versus-time profile generated using the two-compartment model in Fig. 8.18.

In this case, the intercepts (A_n') are different from those obtained from an intravenous study (A_n) and significantly more complex since the "driving" concentrations in compartments one and two are now dependent on the fraction absorbed in a fashion analogous to the terms of Equation 8.28 seen for absorption in a one-compartment model:

$$\begin{aligned} A_1' &= (k_{21} - \lambda_1)/[(k_{01} - \lambda_1)\cdot(\lambda_2 - \lambda_1)] \\ A_2' &= (k_{21} - \lambda_2)/[(k_{01} - \lambda_2)\cdot(\lambda_1 - \lambda_2)] \\ A_3' &= (k_{21} - k_{01})/[(\lambda_1 - k_{01})\cdot(k_{01} - \lambda_2)] \end{aligned} \tag{8.56}$$

Fig. 8.19 depicts the C-T profile and the resulting residual lines that could be used to estimate the slopes and intercepts. However, a C-T profile such as this, which allows clear rectification of k_{01} from λ_1 is rare since even in this case, the two are of a similar order of magnitude, and independent values cannot be estimated. In fact, these residuals may only be determined from as few as two time points. Remembering that early points are often prone to large errors, even attempting this analysis may be futile. Depending on the ratio of rate constants, the C-T profile may even appear monoexponential. Workers have erroneously analyzed these profiles, neglecting to take into account the confounding of the absorption and distribution phases. The intercepts thus calculated would yield erroneous estimates of distribution volumes. The final complication is that absorption flip-flop may also occur, making selection of k_{01} and λs difficult. The only method to reliably address all of these problems is to conduct an independent intravenous bolus study using a two-compartment model and independently estimate λ_1 and λ_2 to arrive at an estimate of the absorbed dose. Even in this case, interindividual variability may make a unique model solution impossible for some drugs. This situation again supports the view that if the disposition of a drug is to be accurately modeled, the first step should be an intravenous injection so that the primary pharmacokinetic model may be unambiguously defined.

Similar to the situation with the one-compartment model above, a fractional absorption plot may be used to analyze these data. The approach used is the Loo–Riegelman method, which requires that both intravenous and extravascular dose studies be conducted in the same individual. In this case, k_{10} may be unambiguously determined from the intravenous study. The equation used to generate the fractional absorption plot, analogous to the Wagner–Nelson method (Eq. 8.35; Figs. 8.12 and 8.13), is

$$\frac{X_S(t)}{X_S(\infty)} = \frac{C_t + K_{10} \cdot \mathrm{AUC} + \left[\left(X_p\right)_t / V_1\right]}{K_{10} \cdot \mathrm{AUC}_\infty}, \tag{8.57}$$

where $(X_p)_t$ is the amount of drug in the peripheral compartment at time t. Calculation of this amount requires solution of both intravenous and extravascular pharmacokinetic models using various techniques beyond the scope of this text. The advantage of this approach is that, like the Wagner–Nelson method, there is no assumption to the order of the absorption rate process, and thus complex absorption processes may be modeled.

8.5.7 Data analysis and its limitations

Clearly, as pharmacokinetic models become more complex, the reader must question the wisdom of pursuing such analyses. In reality, there are mathematical limitations to the complexity of the model able to be fit to an experimental data set that is based on the "information density"; that is, how many data points are analyzed relative to how many parameters need to be calculated. This is similar to the statistical concept of degrees of freedom, which will be presented in Chapter 14 as a means of quantifying this dilemma. A primary strategy to overcome this is to simultaneously model both plasma and urine data, a process that improves estimates of all parameters. Population pharmacokinetic techniques (see Chapter 16) are also available that simultaneously can model the interindividual statistical variation.

In practice, there are better approaches to model complex absorption using noncompartmental strategies of residence times and linear system deconvolution analysis; these will be discussed in Chapter 9. The solution of differential equations into their constituent slope/intercept forms, and the definition of these in terms of the underlying microrate constant, are termed *analytical solutions* for the model. In reality, modern software packages solve complex differential equations using techniques of *numerical integration*. The user defines the model on the basis of inputs and outputs or, in some cases, graphically defines a model such as depicted in Figs. 8.3, 8.10, 8.15, and 8.18. The data are then inputted from all the sample matrices collected (e.g., plasma and urine), and the chosen model is numerically fitted to the data. Although this is easy to do, especially with modern graphical microcomputer software interfaces, one must still properly define the underlying model for the resulting analysis to make any sense.

The final consideration with two-compartmental models, and one that is even more serious for multicompartmental models, is the actual structure of the model studied. Until now, we have *assumed* that input into (absorption) and output from (elimination) the model are via the central compartment (model A) and, furthermore, that all samples are taken from this compartment and expressed as differential equations based on dC_1/dt. Fig. 8.20 illustrates other possible structures of the basic two-compartment model. Examples in which these might apply include implantation of a slow-release drug delivery device in a

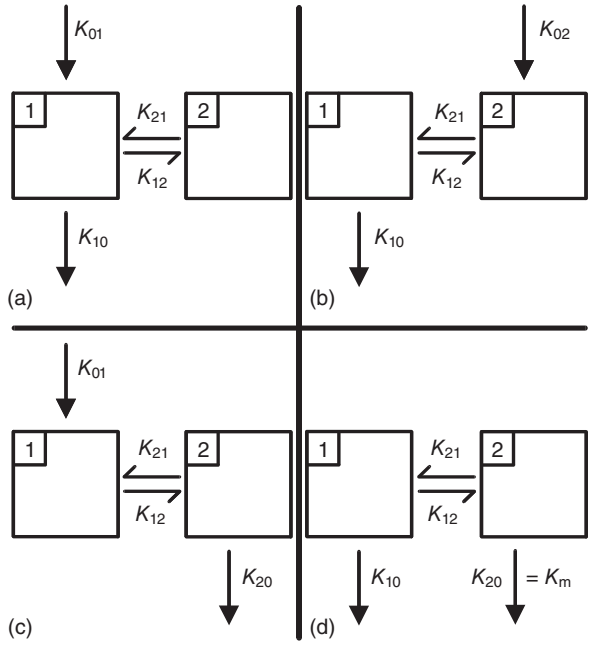

Fig. 8.20 Four different two-compartment pharmacokinetic models. (a) Absorption into and elimination from compartment 1; (b) absorption into compartment 2 and elimination from compartment 1; (c) absorption into compartment 1 and elimination from compartment 2; and (d) intravenous administration with elimination from compartment 1 and metabolism to compartment 2.

specific organ (model B) and when drug distributes to the organ before elimination (model C). The latter type of problem often occurs when the rate of distribution is actually slower than elimination, making the initial exponential term reflect elimination. For example, a very lipophilic chlorinated hydrocarbon may initially distribute extensively throughout the body and then slowly (periods of months) redistribute to the blood, where metabolism and elimination would then occur. The redistribution rate constant would be the rate-limiting process. All would generate C-T profiles described by the sum of exponential very similar to Equation 8.55; however, realize that the equations (such as Eq. 8.56) that link these fitted parameters to the underlying microrate constants would be very different and, in some cases, unsolvable using analytical solutions. As will be presented in subsequent chapters, mixed-order models may be constructed in which some of the parameters are zero-order metabolic rates. Volume of distribution using Vd_{ss} may be underestimated when elimination occurs from the peripheral rather than central compartment. Model-independent approaches discussed in the next chapter eliminate this concern since underlying model structure is not defined.

There are mathematical approaches used to quantify the uniqueness of any model relative to the data collected, that is, to determine the *structural identifiability* of the model. The reader should consult the literature to calculate the parameter (ϕ) whose value determines whether the model is uniquely identifiable, nonuniquely identifiable, or unidentifiable (Williams, 1990). This issue will be revisited for pharmacodynamic models in Chapter 13.

These considerations illustrate the assumptions inherent to constructing complex models that are too often forgotten when the results of such analyses are then analyzed. Models should be constructed using the principle of parsimony, whereby the fewest assumptions are made and the simplest models constructed.

8.6 MULTICOMPARTMENTAL MODELS

The final level of compartmental model complexity to be dealt with in this chapter is the three-compartment model depicted in Fig. 8.21, which generates the C-T profile in Fig. 8.22. The data are from studies conducted in the author's laboratory for the aminoglycoside antibiotic gentamicin in dogs, but the model is identical to that for similar work performed in horses and sheep. In this case, the drug distributes into two different compartments from the central compartment, one with rates faster (k_{12}/k_{21}) and the other with rates slower (k_{13}/k_{31}) than those for k_{10}. The slopes of the C-T profile for λ_1 primarily reflect the contribution of rapid distribution, while those for λ_3, the terminal slope, primarily reflect the

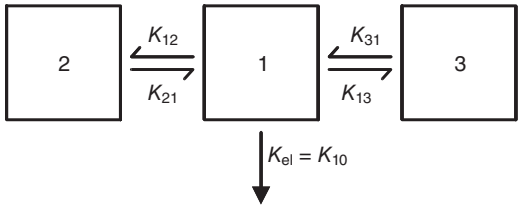

Fig. 8.21 Three-compartment pharmacokinetic model after intravenous administration. Parameters are defined in the text.

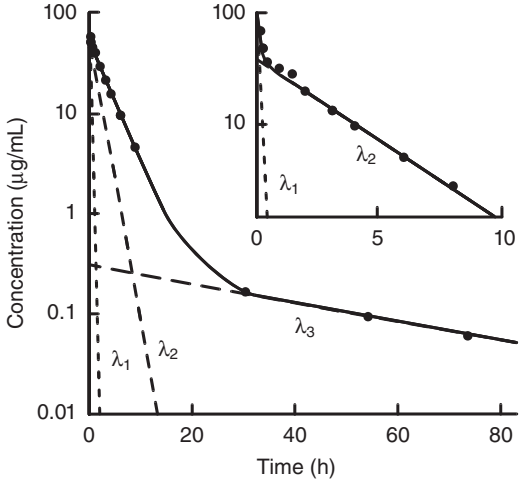

Fig. 8.22 Semilogarithmic plot of plasma concentration-versus-time for intravenous gentamicin in the dog. Disposition is described by a three-compartment model when samples are collected for 80 h and by a two-compartment model when samples are collected for only 10 h (insert).

contribution of slower distribution into the so-called deep compartment. This model is applicable to many three-compartment drugs encountered in comparative medicine (e.g., aminoglycosides, tetracyclines, persistent chlorinated hydrocarbon pesticides). Drug elimination from the central compartment is primarily reflected in λ_2 or β and through general usage is termed the β elimination phase.

These models are generally employed when experiments are conducted over long time frames and C-T profiles are monitored to low concentrations. If the data are truncated at earlier times, as shown in the insert in Fig. 8.22, a normal two-compartment model is adequate to describe the data. However, as will be discussed in Chapter 19, the goal of a study is often to describe the tissue residue depletion profile of a drug in a food-producing animal, and thus the tissue C_3-T profile is of interest since it is the tissue used in establishing legal tolerances. As can be appreciated from Fig. 8.22, each exponential phase describes the C-T profile over a specific range of concentrations and time frames. One must ensure that the appropriate parameters are used to predict the desired range of the *Cp*. If a model is misspecified and a terminal phase deleted, prediction of concentrations for a multiple-dose regimen using λ_{n-1} as the rate-limiting slope may underestimate the true λ_n controlling *Cp* since accumulation may have occurred in a deep compartment. Similarly, such misspecification will generate erroneous values for microconstants. These considerations are also important when fitting the models to the data since specific statistical weighting schemes may have to be used.

An examination of Table 8.3 reveals this relation for experiments of different time frames and concentration ranges reported in the literature for gentamicin. The β-phase elimination generates a $T_{½}$ of 0.5–2 h, depending on species, which is closely correlated to renal GFR. Therefore, if the focus of a study is to examine effects of GFR on Cl_B, the λ_n corresponding to a β of ≈1.3 to 0.3 h^{-1} should be selected. Note that one four-compartment model has been reported as a consequence of very early time samples detecting a very rapid distribution phase based on plasma–erythrocyte equilibration, requiring a model with two distribution components followed by elimination. In contrast, the second four-compartment model is constructed with one distribution, one elimination, and two slow, deep compartment redistribution components. It is little wonder that confusion in the literature has occurred!

Table 8.3 Correspondence of pharmacokinetic parameters for one-, two-, three-, and four-compartment models for intravenous gentamicin.

No. of compartments	Study duration (h)	Slopes	Intercepts
1	12	– – λ –	– – A_1 –
		– – β –	– – B –
2	12	– λ_1 λ_2 –	– A_1 A_2 –
		– α β –	– A B –
2	≥50	– – λ_1 λ_2	– – A_1 A_2
		– – β γ	– – B C
3	≥50	– λ_1 λ_2 λ_3	– A_1 A_2 A_3
		– α β λ	– A B C
3	12	λ_1 λ_2 λ_3 –	A_1 A_2 A_3 –
		π α β –	P A B –
4	≥50	λ_1 λ_2 λ_3 λ_4	A_1 A_2 A_3 A_4
		π α β λ	P A B C

Models consisting of more than three compartments for unchanged parent drug have been used when the data are of sufficient quality as was the case with the four-compartment gentamicin model discussed above. In this case, the drug exhibits sufficient distributional complexity that these models may be warranted. The polyexponential equation describing an *n*-compartment model is as follows:

$$Cp = \sum A_i \cdot e^{-\lambda_i t} \tag{8.58}$$

summed from $i = 1$ through n. The differential equations needed to link these slopes and intercepts to the microrate constants are exceedingly complex and will not be developed here. Because of the serious concern of structural identifiability for such complex models based on plasma data alone, coupled with statistical concerns of adequate degrees of freedom based on limited plasma data, determination of microconstants with any "real" meaning is suspect. Complete equations for such models can be found in the Bibliography section.

The AUC can be calculated for an *n*-compartment model using Equation 8.53, where *i* is summed from 1 to *n*. This also provides a useful method to determine how important a specific exponential phase is to overall drug disposition by dividing any component by the overall summed area ($\lambda_i/A_i \div$ AUC), which becomes the fraction of the AUC determined by that phase. This allows one to assess just how much of an effect a terminal disposition phase may have on calculated values of Cl_B or Vd_{ss}.

In some circumstances, the terminal λ may be influenced by a drug-reentry phenomenon. This is seen with drugs undergoing enterohepatic recycling (see Chapter 7) or from redistribution secondary to ion trapping (see Chapter 5). In these cases, drug input may be intermittent, resulting in discontinuous λ slopes. Use of such confounded rate parameters would bias estimates of drug accumulation after multiple dosing (see Chapter 12), prediction of steady-state plasma concentrations, and estimation of withdrawal times. Under these circumstances, more complex models that specifically take into account this continuous absorption should be employed.

Techniques are also available for solving these equations in terms of C_n, which becomes useful when tissue concentrations are studied. These models were once analyzed using analog computers; however, modern digital computers have made this a lost art and allow for construction of complex models using data collected from multiple matrices. This approach also increases model identifiability and increases degrees of freedom necessary for model solution.

The form of Equation 8.58 can also be used to develop an alternate approach to handling models that may only be fit to an equation with a large number of exponential terms. In the gentamicin studies discussed above, we often obtained data that were best fitted by three- and four-term exponential equations. If one takes the limit of Equation 8.58 as $n \to \infty$, an equation of the form results:

$$Cp = D \cdot At^{-a}. \tag{8.59}$$

This is a power function that forms the basis of the noncompartmental stochastic modeling approach. Fig. 8.23 compares the multiexponential and power function analysis of gentamicin. The power function analysis only requires estimating two parameters and is more robust from a statistical perspective. However, its link to physiological reality is

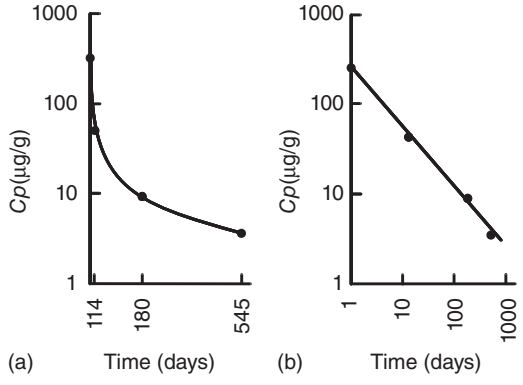

Fig. 8.23 Semilogarithmic (a) and log-log (b) plots of gentamicin concentrations in rat kidneys, representing disposition described by exponential and power function equations, respectively.

significantly different from that developed for compartmental models and is instead based on residence times (which will be introduced in Chapter 9) and the phenomenon of "random walk." Additionally, unlike the exponential models, a $T_{½}$ does not exist with a power exponent, and thus a different conceptual framework is needed to apply this to a clinical or field scenario.

When a tissue sample is taken, one is not measuring just concentrations in that tissue since its vascular and extracellular fluid components are actually part of the central compartment. Similar arguments can be made for other components. When one is looking at deep compartment disposition, this may be satisfactory since release from these depots is rate limiting, making this tissue component larger than any other phase that has already reached equilibrium. Equations are available to fractionate a tissue mass into vascular, extracellular, and cellular components based again on *Vd* estimates. Tracers such as albumin or inulin may be administered to directly derive these fractions. Protein and tissue binding may be directly assessed. Alternatively, tissue cages or microdialysis probes may be inserted into the tissue mass and extracellular kinetics directly modeled.

The dilemma facing the pharmacokineticist is determining the minimum number of exponential components to adequately describe the data. Chapter 14 will deal extensively with the statistical aspects of this curve fitting regression problem. However, in a compartmental framework, one is essentially asking: "*When are the microrate constants significantly different from one another such that the aggregate rates will affect the λs of the observed C-T profile?*" We touched on this issue earlier when absorption was discussed in a two-compartment model. The impact on the analysis is that addition of compartments will affect the magnitude of the various volumes of distributions calculated. Recall the relation of $Vd(B)$ to Vd_{area} or Vd_{ss} in a two-compartment model when the distribution phase was ignored. The ratio of $[(k_{xy}{:}k_{yx})/k_{el}]$ must generally be greater than about three for it to be distinguishable in an experiment. The construction of the actual ratio (k_{xy}/k_{yx}) or (k_{yx}/k_{xy}) determines whether the compartment could be considered rapidly versus slowly equilibrating, and thus whether it appears in the C-T profile as λ_n, greater or less than what could be called the λ_β elimination slope. In some models, a biphasic elimination process could also occur if two physiologically separate mechanisms were responsible for excretion;

however, the compartmental model would have to reflect this structure with two elimination rate constants k_{10} and k_{20} probably coming from two separate rapidly equilibrating central compartments.

There is an additional limitation inherent to the analysis of drugs with deep compartment characteristics when, over the time course of an experiment, k_{xy}/k_{yx} does not reach equilibrium. In this case, the redistribution microconstant for this compartment (k_{yx}) may be approaching zero relative to the other constants. This results in this process appearing to be the elimination from the "perspective" of the central compartment. In these cases, k_{xy} will appear as a component of k_{el} and become confounded with Cl_B. This deep compartment will not appear in Vd_{ss}. Dosage regimens that utilize these values will overestimate the Cl_B and underestimate Vd_{ss} determined from a longer experiment. This was seen with drugs or xenobiotics that strongly bind to tissues (e.g., cisplatin, gentamicin). Studies over longer time frames would detect this redistribution. The sensitivity of k_{xy} to inadequate early distribution data will be addressed in Chapter 14.

Any parameter that is dependent on the ratio of k_{el} to the distributional microrate constants will be sensitive to the model structure. These so-called hybrid parameters include the λ_n, A_n, V_n, and Vd_{area} or Vd_λ. In contrast, Cp_0, and Cl_B will be independent, as will the $T_{½}$ calculated according to Equation 8.20 using Vd_{ss} as the Vd estimate. This realization is the pharmacokinetic basis that supports the use of noncompartmental models described in the next chapter as a very powerful tool in analyzing drug disposition. As these discussions highlight, microrate constants are estimated as ratios (e.g., k_{xy}/k_{yx}). It is not appropriate to conduct simulations where only one rate constant in the ratio is varied as this would never be accurately reflected in a study. Any such change would alter the value of the ratio and affect other intercompartmental and elimination rate constants.

In many cases, very complex multicompartment models are solely used as a tool to simultaneously analyze multiple sample matrices or metabolites. Compartments are constructed specifically for metabolites (model *D* in Fig. 8.20) since a fraction of the parent drug is eliminated from the central compartment. However, the Vd for the metabolite may be different from that of the parent drug. This was the case in the model in Fig. 7.5 (see Chapter 7). Finally, as presented in subsequent chapters, when a compound is extensively bound to either plasma or tissue proteins, this binding may often be incorporated into a model since only the unbound (f_u) drug is distributed through these various compartments. Some workers have used compartments to model this, although Chapter 10 will develop other approaches. Partial differential equations would have to be written and numerical methods, as mentioned above, used to obtain parameter estimates. In fact, such models are often constructed solely to aid their input into packages in which multiple matrices, metabolites, and tissue binding are simultaneously modeled. Alternatively, they may be used to simulate C-T profiles to compare with the observed data so that a realistic model may then be used to analyze the drug under study.

8.6.1 Examples of multimatrix compartmental analysis

We will conclude this chapter by illustrating a very complex model our laboratory had utilized to describe topical application of the pesticide parathion in pigs. We employed the multicompartmental scheme depicted in Fig. 8.24 to analyze parathion and its metabolites paraoxon, *p*-nitrophenol (PNP), and PNP-glucuronide (metabolic pathway depicted in Chapter 7, Fig. 7.2) in blood, urine, feces, and tissues from intravenous and topical *in vivo*

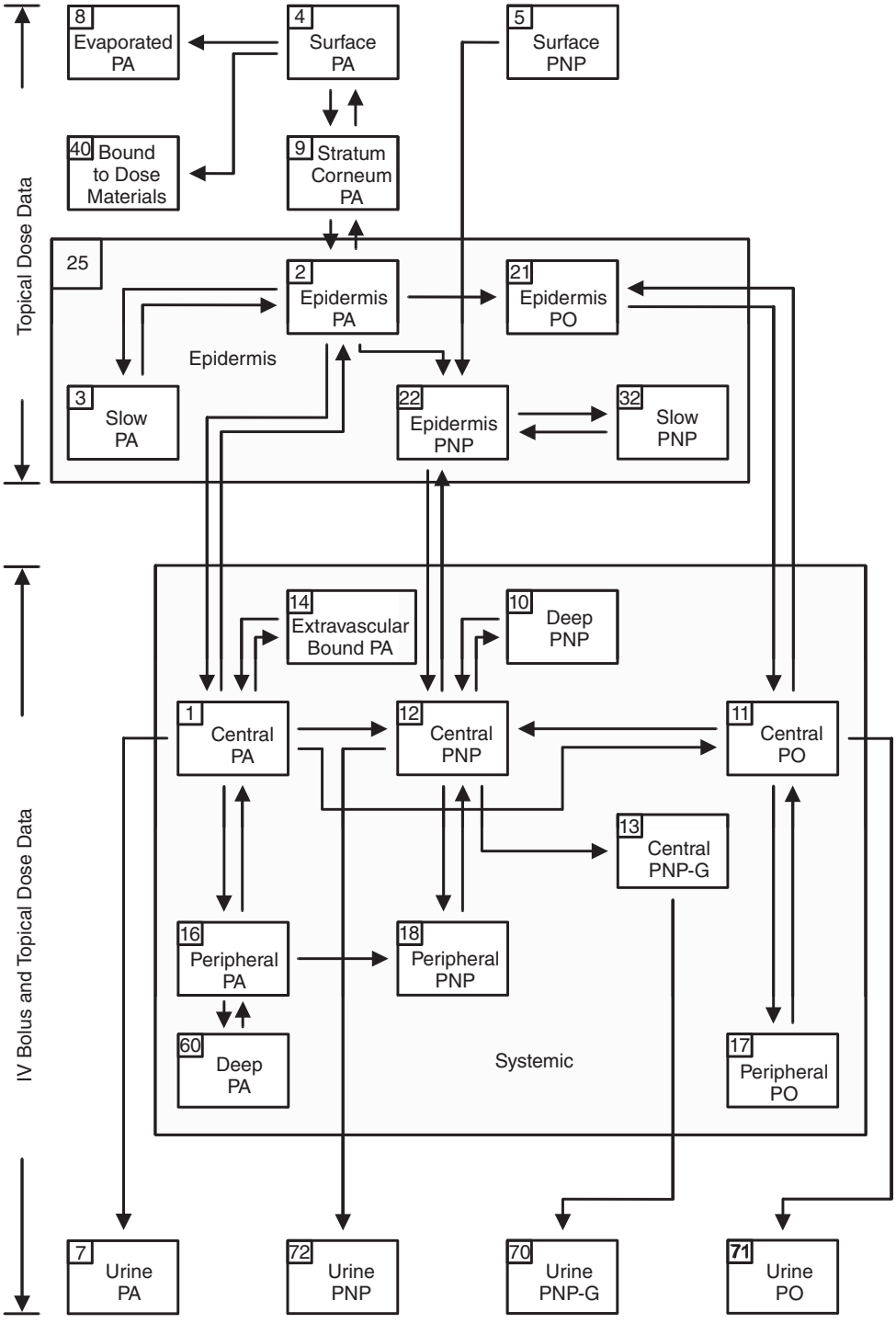

Fig. 8.24 Multicompartmental pharmacokinetic model used to study parathion and its metabolites after topical and intravenous administration to pigs. Metabolic pathway and identity of metabolites were presented in Fig. 6.2 (see Chapter 6). Topical dosing used *in vitro–in vivo* data to model absorption. Parent and metabolite concentrations were determined in plasma, urine, and tissue at termination of the experiment. PA: parathion; PO: paraoxon; PNP: *p*-nitrophenol; PNP-G: PNP-glucuronide. (For further details, see publications by Qiao et al. in the Bibliography section.)

studies using the CONSAAM software package by Qiao and coworkers (Qiao et al., 1994; Qiao and Riviere, 1995). Since low concentrations of compounds were studied, metabolic rates were first order. Additionally, we integrated these models with data from *in vitro* porcine skin models. This allowed us to probe regional absorption differences and study the effects of cutaneous metabolism on disposition and tissue residues. This modeling exercise utilized radiolabeled parathion in 20 pigs. Metabolites were separated by high-performance liquid chromatographic analysis of plasma, blood, and urine. This model is far from being mathematically unique. In order to experimentally validate this model, eight pigs were used to model intravenous and topical PNP disposition according to Fig. 8.25, which was constructed to mirror the parathion model. We assumed that since PNP is the final metabolite produced in this process, it would be most sensitive to modeling errors and structural misspecifications.

This model also illustrates many of the concepts of drug metabolism presented in Chapter 7. Metabolism in the systemic central compartments (#s 1, 11, 12, 13) was postulated on the basis of the high hepatic biotransformation capacity. It was previously demonstrated that in rat plasma, parathion was directly degraded into PNP ($k_{1,12}$ in our scheme) and was the dominant route of parathion metabolism for the first 15–30 min after intravenous administration. This is followed by activation of parathion to paraoxon and hydrolysis

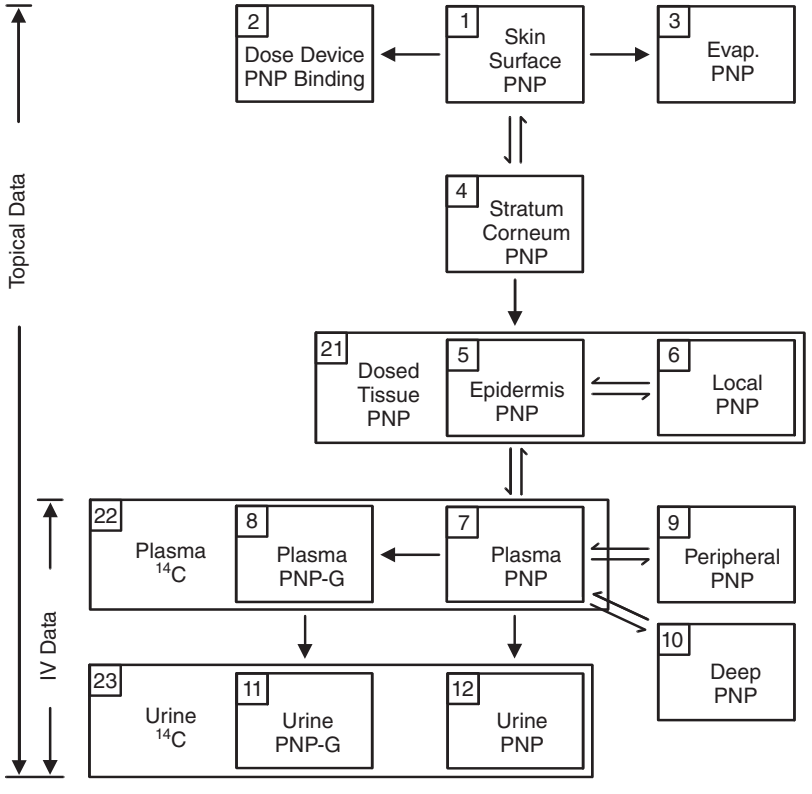

Fig. 8.25 Multicompartmental pharmacokinetic model used to study disposition of *p*-nitrophenol (PNP) after intravenous administration in pigs. These data were used to validate PNP parameters obtained from analysis described in Fig. 8.24.

of parathion. The enzymes determined to be involved in blood degradation include esterases, proteases, erythrocyte cholinesterase, serum butylcholinesterase, B-esterases, and some plasma proteins. Our compartments 17 and 60 may be partially composed of nervous tissue, such as the brain, as well as other lipophilic tissues. Previous rodent studies suggest that only parathion and paraoxon could be found in brain after intravenous administration. The pattern of cutaneous metabolism/distribution/absorption was specifically structured to reflect current understanding. Transport between compartments 2 and 1, as well as between 2 and 3, could be approximated by a one-way process since $k_{2,3} >> k_{3,2}$ and $k_{2,1} >> k_{1,2}$. Assuming this, one can calculate the relevant significance of cutaneous metabolism as compared with local skin distribution and absorption of parathion by comparing rate-constant ratios for each component. This ratio approach is a useful tool to probe the relative importance of each one-way leaving process in the overall output from a given compartment. However, if the two compartments are linked by a two-way process with similar orders of magnitude, the results may be suspect since significant back transport would affect the net flux from that compartment. This approach was also used to assess the significance of cutaneous biotransformation relative to hepatic metabolism using the ratio of the microrate constants as the relevant parameter.

Paraoxon produced by the liver will enter the systemic circulation and distribute to extrahepatic tissues. However, paraoxon will react with blood enzymes and stoichiometrically destroy paraoxon through phosphorylation of these nontarget sites. When paraoxon concentration is very low secondary to a very low parathion dose, hepatic protein phosphorylation constitutes the major route of paraoxon degradation. This emphasizes that factors such as parent compound dosage, relative rates of activation and degradation of the metabolite paraoxon, transit times through the liver, and anatomical localization of the enzymes catalyzing these sequential reactions must all be taken into account when extrapolating any pharmacokinetic model to an *in vivo* setting. This is the primary reason that a model is good only under these limiting conditions, and the biological system must be "stressed" in order to validate model predictions. This was the motivation to independently study PNP disposition since it is the terminal metabolite in the parathion → paraoxon → PNP sequence and would be exquisitely sensitive to model misspecification. Finally, systemic availability of parathion and its metabolites in all compartments was also investigated using area methods, which will be introduced in the next chapter. The original manuscripts should be consulted for details of the modeling and data analysis.

Another application of a multicompartment–multimatrix pharmacokinetic model involving topical drug exposure in veterinary medicine is the excellent work on ivermectin by Laffont et al. (2003). This model demonstrated how animal licking results in oral absorption of topical ivermectin, which causes high intra- and interindividual variability in systemic ivermectin exposure. To account for this in their model illustrated in Fig. 8.26, there are three processes removing drug from the skin after topical dosing: (1) absorption (k_{51}); (2) removal by binding, degradation, metabolism, or other processes that render the drug not bioavailable (k_{57}); and (3) licking (k_a). The licking process then serves as an input for oral absorption in the gastrointestinal track. Each of these absorption processes have been modeled with its own lag time. Both intravenous and topical experimental data was used to develop the model. Note that compartment 7 in this model is similar to compartments in the models of Figs. 8.24 and 8.25, which reflects compound bound or lost from further absorption. This model nicely illustrates the power of properly designed and parameterized compartmental models to address mechanistic issues.

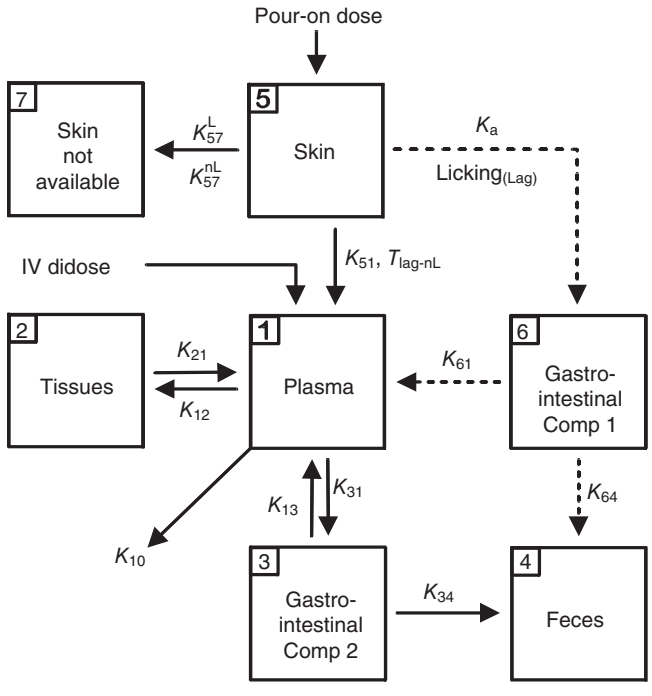

Fig. 8.26 Multicompartment multimatrix pharmacokinetic model of topical ivermectin absorption with licking. Compartments include skin, plasma tissues, and two gastrointestinal units; one to model absorption after licking and the other to model fecal elimination. Compartment 7 reflects drug that is either bound, degraded, or otherwise not available for systemic absorption or removal by licking. K_a is the oral absorption rate constant after licking modeled as a biexponential function, and K_{10} is elimination by metabolism. Each absorption process in skin is associated with their own lag time. For example, K_{57} has licking and nonlicking absorptive lag times.
Source: Adapted from Laffont et al. (2003).

8.7 CONCLUSION

Compartmental modeling concepts and techniques have defined the discipline of pharmacokinetics and continue to be extremely useful tools. One- and two-compartment analyses form the basis for most models used in human and comparative medicine. These two models also serve as the foundation on which many of the other techniques now to be developed are based. Modern computers have facilitated the analysis of these data to the point that the user no longer has to derive all of the relevant differential equations. However, when compartmental schemes are assumed, the defining model is also implied, and thus the cautious investigator must be aware of the numerous caveats presented in this chapter.

BIBLIOGRAPHY

Baggot, J.D. 1977. *Principles of Drug Disposition in Domestic Animals: The Basis of Veterinary Clinical Pharmacology*. Philadelphia: W.B. Saunders Co.

Benet, L.Z. 1972. General treatment of linear mammillary models with elimination from any compartment as used in pharmacokinetics. *Journal of Pharmaceutical Sciences*. 61:536–541.

Berezhkovsky, L.M. 2006. The influence of drug kinetics in blood on the calculation of oral bioavailability in linear pharmacokinetics: the traditional equation may considerably overestimate the true value. *Journal of Pharmaceutical Sciences*. 95:834–848.

Brown, S.A., and Riviere, J.E. 1991. Comparative pharmacokinetics of aminoglycoside antibiotics. *Journal of Veterinary Pharmacology and Therapeutics*. 14:1–35.

Brown, S.A., Coppoc, G.L., and Riviere, J.E. 1986. Effect of dose and duration of therapy on gentamicin tissue residues in sheep. *American Journal of Veterinary Research*. 47:2373–2379.

Brown, S.A., Riviere, J.E., Coppoc, G.L., and Dix, L.P. 1986. Superiority of the power function over exponential functions for prediction of renal gentamicin residues in sheep. Analysis of terminal phase gentamicin pharmacokinetic data. *Journal of Veterinary Pharmacology and Therapeutics*. 9:341–346.

Byron, P.R., and Notari, R.E. 1976. Critical analysis of "flip-flop" phenomenon in two-compartment pharmacokinetic model. *Journal of Pharmaceutical Science*. 65:1140–1144.

Chiou, W.L. 1981. The physiological significance of the apparent volume of distribution, Vdarea or Vd, in pharmacokinetic studies. *Research Communications in Chemical Pathology and Pharmacology*. 33:499–508.

De Biasi, J. 1989. Four open mammillary and caternary compartment models for pharmacokinetic study. *Journal of Biomedical Engineering*. 11:467–470.

Dhillon, A., and Kostrzewski, A. 2006. *Clinical Pharmacokinetics*. London: Pharmaceutical Press.

DiStefano, J.J., and Landaw, E.M. 1984. Multiexponential, multicompartmental, and non-compartmental modeling. I. Methodological limitations and physiological interpretations. *American Journal of Physiology*. 246:R651–R664.

Fleishakei, J.C., and Smith, R.B. 1987. Compartmental model analysis in pharmacokinetics. *Journal of Clinical Pharmacology*. 27:922–926.

Gibaldi, M., and Perrier, D. 1972. Drug elimination and apparent volume of distribution in multicompartmental systems. *Journal of Pharmaceutical Sciences*. 61:952–954.

Gibaldi, M., and Perrier, D. 1982. *Pharmacokinetics*, 2nd Ed. New York: Marcel Dekker.

Greenblat, D.J., Abernethy, D.R., and Divoll, M. 1983. Is volume of distribution at steady state a meaningful kinetic variable? *Journal of Clinical Pharmacology*. 23:391–400.

Grover, A., and Benet, L.Z. 2009. Effects of drug transporters on volume of distribution. *The AAPS Journal*. 11:250–261.

Jacobs, J.R. 1988. Analytical solution to the three-compartment pharmacokinetic model. *IEEE Transactions on Biomedical Engineering*. 35:763–765.

Jacobs, J.R., Shafer, S.L., Larsen, J.L., and Hawkins, E.D. 1990. Two equally valid interpretations of the linear multicompartment mammillary pharmacokinetic model. *Journal of Pharmaceutical Sciences*. 79:331–333.

Jusko, W.J., and Gibaldi, M. 1972. Effects of change in elimination on various parameters of the two-compartment open model. *Journal of Pharmaceutical Sciences*. 61:1270–1273.

Labat, C., Mansour, K., Malmary, M.E., Terrissol, M., and Oustrin, J. 1987. A variable reabsorption time-delay model for pharmacokinetics of drugs. *European Journal of Drug Metabolism and Pharmacokinetics*. 12:129–133.

Laffont, C.M., Bousquet-Mélou, A., Bralet, D., Alvineria, M., Fink-Gremmels, J., and Toutain, P.L. 2003. A pharmacokinetic model to document the actual disposition of topical ivermectin in cattle. *Veterinary Research*. 34:445–460.

Loo, J.C.K., and Riegelman, S. 1968. New method for calculating the intrinsic absorption rate of drugs. *Journal Pharmaceutical Science*. 57:918–928.

Notari, R.E. 1980. *Biopharmaceutics and Clinical Pharmacokinetics*, 3rd Ed. New York: Marcel Dekker.

O'Flaherty, E.J. 1981. *Toxicants and Drugs: Kinetics and Dynamics*. New York: John Wiley & Sons.

Pecile, A., and Rescigno, A. 1987. *Pharmacokinetics. Mathematical and Statistical Approaches to Metabolism and Distribution of Chemicals and Drugs*. New York: Plenum Press.

Qiao, G.L., and Riviere, J.E. 1995. Significant effects of application site and occlusion on the pharmacokinetics of cutaneous penetration and biotransformation of parathion *in vivo* in swine. *Journal of Pharmaceutical Sciences*. 84:425–432.

Qiao, G.L., Williams, P.L., and Riviere, J.E. 1994. Percutaneous absorption, biotransformation and systemic disposition of parathion *in vivo* in swine. I. Comprehensive pharmacokinetic model. *Drug Metabolism and Disposition*. 22:459–471.

Riegelman, J.L., and Rowland, M. 1968. Concept of a volume of distribution and possible errors in evaluation of this parameter. *Journal of Pharmaceutical Sciences*. 57:128–133.

Riegelman, J.L., and Rowland, M. 1968. Shortcomings in pharmacokinetic analysis by conceiving the body to exhibit properties of a single compartment. *Journal of Pharmaceutical Sciences*. 57:128–133.

Riviere, J.E. 1982. Paradoxical increase in aminoglycoside body clearance in renal disease when volume of distribution increases. *Journal of Pharmaceutical Sciences*. 71:720–721.

Riviere, J.E. 1982. Limitations on the physiologic interpretation of aminoglycoside body clearance derived from pharmacokinetic studies. *Research Communications in Chemical Pathology and Pharmacology*. 38:31–42.

Segre, G. 1982. Pharmacokinetics-compartmental representation. *Pharmacology and Therapeutics*. 17:111–127.

Segre, G. 1984. Relevance, experiences, and trends in the use of compartmental models. *Drug Metabolism Reviews*. 15:7–53.

Shargel, L., Wu-Pong, S., and Yu, A.B.C. 2005. *Applied Biopharmaceutics and Pharmacokinetics*, 5th Ed. New York: McGraw Hill.

Simon, W. 1987. *Mathematical Techniques for Biology and Medicine*. New York: Dover Press.

Toutain, P.L., and Bousquet-Melou, A. 2004. Plasma clearance. *Journal of Veterinary Pharmacology and Therapeutics*. 27:415–425.

Toutain, P.L., and Bousquet-Melou, A. 2004. Volumes of distribution. *Journal of Veterinary Pharmacology and Therapeutics*. 27:441–453.

Wagner, J.G. 1975. *Fundamentals of Clinical Pharmacokinetics*. Hamilton, IL: Drug Intelligence Publications.

Wagner, J.G. 1983. Significance of ratios of different volumes of distribution in pharmacokinetics. *Biopharmaceutics and Drug Disposition*. 4:263–270.

Wagner, J.G., and Nelson, E. 1968. Percent absorbed time plots derived from blood level and/or urinary excretion data. *Journal Pharmaceutical Sciences*. 52:610–611.

Welling, P.G., and Tse, F.L.S. 1995. *Pharmacokinetics: Regulatory, Industrial, and Academic Perspectives*. New York: Marcel Dekker.

Wijnand, H.P. 1988. Pharmacokinetic model equations for the one- and two-compartment models with first-order processes in which absorption and exponential elimination or distribution rate constants are equal. *Journal of Pharmacokinetics and Biopharmaceutics*. 16:109–127.

Williams, P.L. 1990. Structural identifiability of pharmacokinetic models—compartments and experimental design. *Journal of Veterinary Pharmacology and Therapeutics*. 13:121–131.

Williams, P.L., Thompson, D., Qiao, G.L., Monteiro-Riviere, N.A., Baynes, R.L., and Riviere, J.E. 1996. The use of mechanistically defined chemical mixtures (MDCM) to assess component effects on the percutaneous absorption and cutaneous disposition of topically-exposed chemicals. II. Development of a general dermatopharmacokinetic model for use in risk assessment. *Toxicology and Applied Pharmacology*. 141:487–496.

Yates, J.W.T., and Arundel, P.A. 2008. On the volume of distribution at steady state and its relationship with two-compartmental models. *Journal of Pharmaceutical Sciences*. 97:111–122.

Zierler, K. 1981. A critique of compartmental analysis. *Annual Reviews of Biophysics and Bioengineering*. 10:531–562.

9 Noncompartmental Models

As discussed in the last chapter, compartmental models have become the primary approach to pharmacokinetics. Only in the last few decades has there been any indication of a migration in pharmacokinetics to noncompartmental methods. Noncompartmental models were first developed and applied to radiation decay analysis and remain dominant in the physical and biological science literature for general applications. Since their first application to problems in pharmacokinetics in 1979, noncompartmental methods have grown steadily in use and are incorporated in most commercial pharmacokinetic software programs. This approach is for the most part based on classical statistical moment theory.

Technically, the term noncompartmental used in reference to classical pharmacokinetics is somewhat misleading. The data that are analyzed with statistical moments are typically plasma concentration–time (C-T) profiles, which implies that at least a one (central) compartmental model structure exists since behavior of the drug in the body is being linked to the plasma C-T profile. There is simply no way to avoid that assumption. In other words, theoretically, any "noncompartmental" analysis has a compartmental equivalent. Furthermore, when noncompartmental models are solved by fitting polyexponential equations to data, an assumption of first-order rate processes is made. In fact, some would argue that a multicompartmental structure is implied since the intercepts and slopes of the C-T profile are solutions to multicompartment differential equations. However, when the data are analyzed solely by computation of areas under curves (e.g., application of the trapezoid method), as will be presented shortly, this limitation is not present since equations are not being fitted to data. In many ways, this is the strength of this approach.

Those who prefer noncompartmental methods usually do not think of their models in terms of compartmental infrastructure, whereas those who prefer compartmental methods link their observed models to the microrate constants and different volumes (e.g., V_1, V_2) of constitutive compartments as discussed in Chapter 8. From a mathematical perspective, noncompartmental methods are somewhat limited in application for pharmacokinetics, but their advantage (i.e., that of obviating the necessity to deliberately commit to a specific model) is ample motivation for many investigators to use them. Additionally, as discussed in the previous chapter, many multicompartmental models become too complex for the data at hand since statistically sound estimates of each slope (λ_i) and intercept (A_i) must be obtained. Solution of the microrate constants and volumes for individual compartments becomes ambiguous, but is not necessary if the focus of the study is an aggregate

Comparative Pharmacokinetics: Principles, Techniques, and Applications, Second Edition. Jim E. Riviere.
 ISBN: 978-0-813-82993-7

description of drug disposition, which may be obtained with estimates of Cl_B and Vd_{ss}. There are many applications in which similar end points are required and the assumptions inherent to defining specific compartments become unnecessary. These include, among others, the design of dosage regimens and interspecies extrapolations.

9.1 STATISTICAL MOMENT THEORY

We will begin with an overview of the basic tenets of statistical moment theory, which is a component of the more general stochastic modeling approach. Suppose one could observe a single molecule, from the time it is administered into the body ($t = 0$) until it is eventually eliminated ($t = t_{el}$). Clearly, t_{el} is not predictable. This individual molecule could be eliminated during the first minute or could reside in the body for weeks. If, however, one looks at a large number of molecules collectively, their behavior appears much more regular. The collective, or mean time of residence, of all the molecules in the dose, is called the mean residence time (MRT). This is classically based on plasma concentration data but has meaning for almost any mathematical function, $f(t)$. The MRT of $f(t)$ integrated from $t = 0$ to ∞ is defined as

$$\text{MRT} = \frac{\int t \cdot f(t)\, dt}{\int f(t)\, dt}. \tag{9.1}$$

MRT can be interpreted as a mean of some variable only if $f(t)$ or $(f(t)/(\int f(t)\, dt)$ can be shown to be the *probability density function* (pdf) for that variable. By definition, pdf refers to a continuous random variable X [denoted $f(x)$]. In pharmacokinetics applications, $f(t)$ is typically a plasma concentration-versus-time curve and in this context is commonly symbolized $C(t)$ [$=p_t$]. Historically, the MRT refers to drug in plasma. If Equation 9.1 is rewritten in terms of $C(t)$,and evaluated from $t = 0$ to ∞,

$$\text{MRT} = \frac{\int t \cdot C(t)\, dt}{\int C(t)\, dt} = \frac{\text{AUMC}}{\text{AUC}}, \tag{9.2}$$

the denominator of Equation 9.1 is the area under the curve (AUC), already repeatedly encountered in this text and presented in the last chapter when the plasma C-T profile was integrated to derive Equation 8.18. The numerator is known as the area under the (first) moment curve (AUMC), which is the CT-T profile. AUC and AUMC are depicted in Fig. 9.1.

Plasma concentration may not always be a mathematically legitimate function for a pdf when the elimination flux (mass/time) is not proportional to $C(t)$, or when a significant fraction of the dose either never leaves the (plasma) space or spends time in another space before being eliminated. Technically, the MRT, calculated from samples taken following an intravenous bolus injection, addresses only those molecules that are eliminated from the body at a rate proportional to $C(t)$. Therefore, the caveat is that elimination must be at least first order, and only molecules that stay in the plasma (until elimination) and are eventually eliminated are addressed. This limitation had also applied to compartmental models previ-

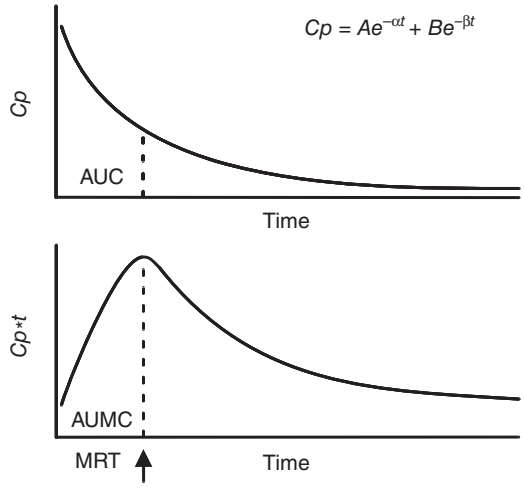

Fig. 9.1 Plasma concentration versus time (C-T) and its first-moment (CT-T) plots demonstrating AUC, AUMC, and MRT.

ously discussed, for they were defined with k_{el} being a first-order elimination rate constant from the central compartment. Such assumptions also imply that sinks and temporary reservoirs are generally not mathematically permissible. As discussed in Chapter 8, this is analogous to using an $n - 1$ compartment model when an n-compartment model really is required. It also holds when a molecule distributes and irreversibly binds to tissue as described for drugs such as gentamicin and cisplatin. In these cases, redistribution might not be detectable from the missing deep compartment, and k_{1n} would be mistakenly interpreted as being part of the elimination process. The MRT estimate will be biased unless what is measured satisfies these requirements.

As long as the above limitations are understood (many of which apply to compartmental modeling), their application remains a powerful means of practical data analysis. Furthermore, a very general (always true and applicable) definition of MRT requires only that $f(t)$ in Equation 9.1 be the elimination flux (mass transfer, mass/time). Although this quantity is not typically measurable *in vivo*, it is in *ex vivo* and *in vitro* systems, which are enjoying increasing use in the forefront of research due to recent technological advances. Despite these caveats, the MRT is a very useful parameter to describe drug disposition.

The MRT could be thought of as the statistical moment analogy to the half-life ($T_{½}$), and it is inversely related to the first-order elimination rate of a one-compartment open model:

$$\mathrm{MRT_{IV}} = 1/k_{el}. \tag{9.3}$$

Rearranging demonstrates that $k_{el} = 1/\mathrm{MRT}$. Recalling Equation 8.12 (see Chapter 8), where $T_{½} = 0.693/k_{el}$, substitution gives us

$$T_{½} = 0.693\,\mathrm{MRT}. \tag{9.4}$$

The MRT thus becomes an excellent parameter to describe the length of drug persistence in the body, much as the half-life is used in many linear pharmacokinetic models. The $T_{½}$

used in this context is the elimination $T_{½}$ in the body, and not that calculated from the terminal exponential phase as described in Chapter 8 for multicompartmental models.

The MRT represents the time point at which 63.2% of the drug has been eliminated from the body. If one takes the equation for a monoexponential C-T profile (see Chapter 8, Eq. 8.15) and solves for t = MRT, then $Cp = Cp_0\, e^{-k_{el}\,MRT}$. However, from Equation 9.3, we know that MRT = $1/k_{el}$, thus at t = MRT, $Cp = Cp_0\, e^{-k_{el}\,(1/k_{el})} = Cp_0\, e^{-1} = 0.368\ Cp_0$. Therefore, at t = MRT, 36.8% of the available dose remains in the body and 63.2% has been eliminated. MRT is always longer than $T_{½}$, a useful check of data analysis. Note that if all drug were excreted in the urine, one could simply estimate MRT as the time needed to recover 63.2% of the administered dose in the urine. MRT is also the time point at which the volume of distribution equals Vd_{ss}.

If the dose of drug is administered by intravenous infusion, the MRT_{IV} may be calculated as

$$MRT_{IV} = MRT_{infusion} - (\text{Infusion time})/2, \tag{9.5}$$

where $MRT_{infusion}$ is simply calculated from the observed data using Equation 9.2.

9.2 CALCULATION OF MOMENTS

The primary task of model-independent or noncompartmental methods is the direct estimation of the moments from data. This essentially is determining the relevant AUCs and moments from the C-T profile. *Some workers have thus referred to statistical moment analysis simply as SHAM (slopes, heights, areas, and moments) analysis to stress that these are the only data requirements for solution of these models.* However, this acronym implies that the areas are being determined using exponential-based formulae for calculating AUCs as presented in the method of Chapter 8. Other techniques ranging from trapezoidal analysis to planimetry do not require curve-fitting analysis. When the C-T profile is described by a polyexponential equation of the form $f(t) = A_i\, e^{-\lambda_i t}$, Equation 8.53 (AUC = $\sum A_i/\lambda_i$; see Chapter 8) can be generally used to determine AUC. The AUMC may then be calculated as

$$AUMC = \sum [A_i/(\lambda_i)^2]. \tag{9.6}$$

This technique requires fitting an exponential function to the C-T profile, and as alluded to earlier and in Chapter 8, this is equivalent to assuming a linear multicompartmental pharmacokinetic model.

Truly noncompartmental analysis uses geometrical techniques to estimate area. With planimetry, one simply plots the concentration-versus-time profile on regular graph paper, cuts out the profile, and weighs the paper. A modern extension of this approach is to fit a C-T and CT-T profile (Fig. 9.1) to any mathematical function (e.g., spline regression), which could determine the relevant AUC and AUMC, respectively. These techniques make no assumption about the nature of the $f(t)$ that generated the profiles; however, nuances in the statistical regression techniques used may raise some issues. Finally, numerical integration techniques may be used to directly calculate these values.

9.2.1 The trapezoidal method for estimating areas under curves

The simplest and most commonly used method for estimating area under any curve is the Trapezoidal Rule, which will be formally presented in this chapter. The application of this technique is important to master since it is the primary method used to assess bioavailability as presented in Chapter 8 as well as in the determination of bioequivalence in Chapter 15.

$$\text{AUC} = \sum \tfrac{1}{2}(C_n + C_{n+1}) \cdot (t_{n+1} - t_n), \tag{9.7}$$

where the summation is over N trapezoids, formed by $n + 1$ data points. This algorithm is quick and, if enough data points are available, relatively accurate. It is also a simple algorithm to implement on a computer. When plasma concentration (or any observed tissue data)-versus-time data are plotted on a Cartesian graph, the area under each pair of connected points describes a trapezoid (except when one of the points has zero value, in which case one of the legs of the trapezoid has zero length, making a triangle; see Chapter 4, Fig. 4.13). The area under the entire curve is then the sum of the areas of the individual trapezoids, which can easily be calculated. The estimation of moments is the summed trapezoids plotted on a CT-T graph. These techniques can be implemented in a simple spreadsheet application. A good application can produce areas as precise and accurate as the sampled data.

The data in Table 9.1 and plotted in Fig. 9.2 constitute a typical plasma concentration profile that might be obtained following a bolus intravenous injection of a drug with a biological half-life of 1 h. This particular example illustrates an ideal experiment because its duration was sufficient to ensure that the concentration would fall to zero by the end of the experiment. For drugs that have long half-lives, this is often difficult or impractical, so more typically, an observed profile is open-ended. For example, Fig. 9.3 illustrates such a case, outlining the trapezoids formed by the sampled points. Although there is important information in an AUC derived from a profile lacking closure, as a standard measure to be

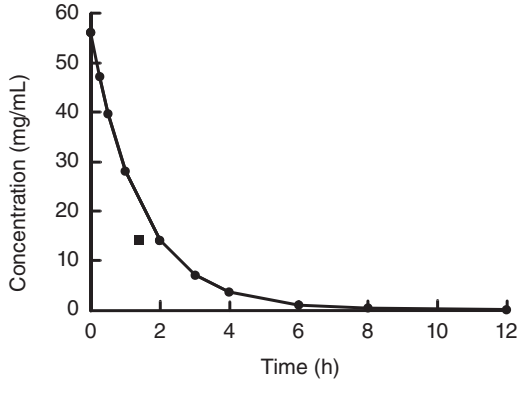

Fig. 9.2 Typical (simulated) profile of plasma concentration versus time following bolus intravenous dose (k_{el} = 0.693 h^{-1}, C_o = 56 mg/mL) used to generate the data set in Table 9.1 and area examples in this section. The actual AUC of this C-T profile is 80.79 mg/mL. The single square point at (1.44, 14.00) on the plot is the center of gravity (*Pc*) for the profile, as calculated from Equation 9.27.

Table 9.1 Statistical moment calculations.

Time (h)	C(t)	Actual trapezoid areas	Estimated trapezoid areas	Actual cumulative AUC	Estimated cumulative AUC	Actual cumulative AUMC
0.00	56.00	—	—	0.00	—	0.00
0.25	47.09	12.85	12.89	12.85	12.89	1.56
0.50	39.60	10.81	10.84	23.66	23.72	5.58
1.00	28.00	16.73	16.90	40.40	40.62	17.88
2.00	14.00	20.20	21.00	60.60	61.63	47.03
3.00	7.00	10.10	10.50	70.70	72.13	71.71
4.00	3.50	5.05	5.25	75.75	77.38	89.10
6.00	0.88	3.79	4.38	79.54	81.76	107.20
8.00	0.22	0.95	1.09	80.49	82.86	113.62
12.00	0.01	0.30	0.47	80.79	83.32	116.34

Time (h)	C(t)	Equation 9.9 cumulative AUMC	Equation 9.11 cumulative AUMC	Actual MRT (h)	Equation 9.9 MRT (h)	Equation 9.11 MRT (h)
0.00	56.00	0.00	0.00		—	—
0.25	47.09	1.61	1.56	0.12	0.13	0.12
0.50	39.60	5.67	5.59	0.24	0.24	0.24
1.00	28.00	18.35	18.02	0.44	0.45	0.44
2.00	14.00	49.86	48.36	0.78	0.81	0.78
3.00	7.00	76.12	74.04	1.01	1.06	1.03
4.00	3.50	94.50	92.13	1.18	1.22	1.19
6.00	0.88	116.39	113.14	1.35	1.42	1.38
8.00	0.22	124.05	120.59	1.41	1.50	1.46
12.00	0.01	128.71	124.97	1.44	1.54	1.50

Data columns from left to right:
- Simulated blood sample times (h)
- Drug concentrations (mg/mL)
- Simulated trapezoid area (mg·h/mL)
- Estimated trapezoid area (mg·h/mL, Eq. 9.7)
- Simulated cumulative AUC (mg·h/mL)
- Estimated cumulative AUC (mg·h/mL, Eq. 9.7)
- Simulated cumulative AUMC (mg·h^2/mL)
- Estimated cumulative AUMC (mg·h^2/mL, Eq. 9.9)
- Estimated cumulative AUMC (mg·h^2/mL, Eq. 9.11)
- Simulated MRT (h)
- Estimated MRT (h, using Eq. 9.9)
- Estimated MRT (h, using Eq. 9.11).

Although normally only calculated at the final sample point, the MRT is calculated at each sample point here for illustration of the importance of using a complete experimental data set for statistical moments.

compared among several drugs, the AUC must be calculated to infinite time. An AUC having at last 80% of AUC_∞ is the acceptable cutoff. The complete area is required for calculating plasma clearance and total absorption. In cases in which samples cannot be taken until the concentration drops to zero, the curve must be extrapolated to infinity.

The simplest and most common method to estimate this is by "end correction." This method involves calculating the area from the last sample measure, C_T, to infinite time and adding this value to the truncated area determined by the sum of the trapezoids. To calculate the terminal area from time, T, to infinity, this portion of the curve is treated as a separate

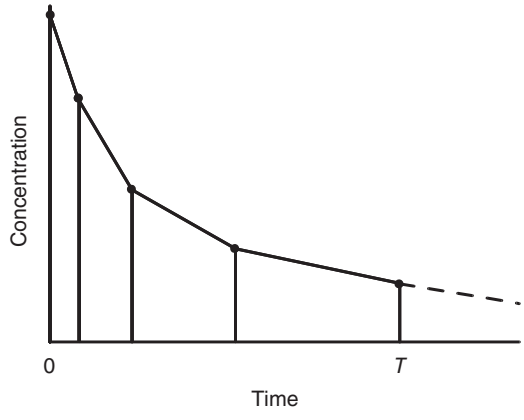

Fig. 9.3 Trapezoids formed from sampled concentration-versus-time data for calculation of areas. To estimate the total AUC, the curve must be extrapolated beyond the ultimate sample time, *T*, to infinity (dashed line).

profile (Fig. 9.4, Table 9.2). This profile is a triangle with a height of $C_0 = C_T$. The slope of the C-T profile determines the length of the base. In a monoexponential C-T situation, the elimination rate constant k_{el} is the slope, which could be calculated from these data as $\ln (C_n/C_{n+1})$. The estimate is simply $AUC_{T\to\infty} = C_T/k_{el}$. If a polyexponential equation is used, the slope of the terminal phase λ_n should be employed, where $AUC_{T\to\infty} = C_T/\lambda_n$. This, of course, assumes that concentrations have been taken for sufficient time to identify and characterize k_{el} or λ_n. Various logarithmic transformations have been employed to improve the estimate of this terminal portion of the C-T profile.

For exponentially descending data (such as plasma concentrations following bolus injection), the trapezoidal method will always overestimate the AUC because the linear trapezoid is greater than the convex exponential functions. Thus, the estimate should be regarded as an upper limit. Other routes of administration lead to data profiles that typically begin at zero, peak later, and decline back toward zero. The trapezoidal method generally underestimates the portion of the curve that is concave down (i.e., the early portion) and overestimates the portions that are concave up (i.e., the tails), so the biases tend to cancel, giving a potentially better overall estimate. There are several numerical integration alternatives to the linear trapezoidal method available, including log trapezoid, Lagrange polynomials, and spline approximations. Chapter 15 presents a discussion on the log-linear trapezoidal method used in bioequivalence studies for submission to drug regulatory agencies.

9.2.2 Estimation of area under the moment curve

The numerical procedures for estimating AUMC are less precise than those for AUC because the first moment is a weighted function of time, and where the trapezoids are of equal weight in the AUC determination, they are not for the AUMC. The greater time values carry correspondingly greater weight because their value is being multiplied by increasing *t*. Finally, the extrapolation of the terminal component of AUMC is more tenuous than that of the AUC. The area of the extrapolated curve equals $(TC_t)/\lambda + (C_T)/\lambda^2$, where λ is the terminal slope of the C-T profile and *t* is the time of the last measured concentration, C_t.

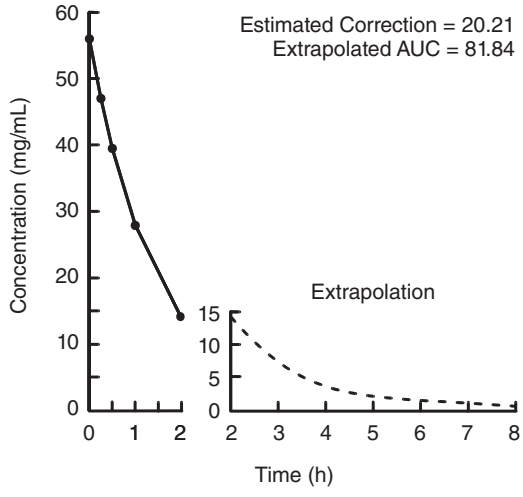

Fig. 9.4 Extrapolation of plasma concentration-time data from Fig. 9.2 terminated at 2 h (AUC = 61.63 h), showing extrapolation beyond this time. AUC analysis is shown in Table 9.2.

Table 9.2 Statistical moment calculations from a truncated 2-h data set.

Time (h)	*C*(*t*) (mg/mL)	Trapezoid areas (mg h/mL)	Cumulative AUC
0.00	56.00	0.00	0.00
0.25	47.09	12.89	12.89
0.50	39.60	10.84	23.72
1.00	28.00	16.90	40.62
2.00	14.00	21.00	61.63

Estimated end correction: 20.21.
Extrapolated AUC: 81.84.
Data are the sample points for the first 2 h, as plotted in left-hand plot of Fig. 9.4. Estimated end correction simulated profile is plotted in the right-hand plot. Extrapolated AUC and total extrapolated AUC estimates were 20.21 mg h/mL and 81.84 mg h^2/mL, respectively.

A crude but unfortunately commonly used method for calculating AUMC is to simply multiply the area of each trapezoid by the time:

$$\text{AUMC} = \sum \tfrac{1}{2}(C_n + C_{n+1}) \cdot (t_{n+1} - t_n) \cdot (t_{n+1}). \tag{9.8}$$

This algorithm can be very biased, especially for late, wide-spaced points. Using t_{n+1} overestimates the AUMC because the entire curve in the n^{th} interval is assigned the weight t_{n+1}. Conversely, using t_n instead would underestimate the AUMC (with an even greater error). A better method is to use the linear mean time within each trapezoidal interval:

$$\text{AUMC} = \sum \tfrac{1}{2}(C_n + C_{n+1}) \cdot (t_{n+1} - t_n) \cdot \tfrac{1}{2}(t_n + t_{n+1}). \tag{9.9}$$

This approach, which is actually based on the same considerations used in Chapter 8 to plot the midpoint of a urine excretion interval when analyzing excretion kinetics, is considerably more accurate than Equation 9.8 but is still biased. Looking at the data of Table 9.1, it is evident that estimated trapezoid areas (using Eq. 9.7) are in greater error for the later times. This error could be mitigated with a higher sampling frequency. Since the algorithm for estimating AUMC (Eq. 9.9 was used for Table 9.1 estimated cumulative AUMC) is dependent on the trapezoid areas (using the same expression as Eq. 9.7, with the mean time factored in), the error of Equation 9.7 carries over to the AUMC calculation. However, the AUMC error is not as proportionally great because the mean time term actually results in an underestimation of the AUMC of a given trapezoid; so again, there is a partial cancellation of errors.

The remaining bias in Equation 9.9 is in the last term, the time (t) midpoint. It is correct to use such geometry for the AUC calculation, but not for the AUMC, because time is a weight in Equation 9.8. If we substitute the equation for a straight line in the expression for AUMC (numerator of Eq. 9.1) for a single interval (segment) (from time t_n to t_{n+1}), we get

$$\text{AUMC} = \int t \cdot C(t)\, dt = C_n \cdot \int t\, dt + [(C_{n=1} - C_n)/(t_{n+1} - t_n)] \int t \cdot (t - t_n)\, dt, \quad (9.10)$$

then integration and some algebra admits,

$$\text{AUMC} = \tfrac{1}{2}[C_n \cdot (t_{n+1}^2 - t_n^2] + \tfrac{1}{6}(C_{n+1} - C_n) \cdot (2t_{n+1}^2 - t_n \cdot t_{n+1} - t^2). \quad (9.11)$$

This is an exact AUMC for a trapezoid, and thus offers a much better theoretical solution than the other methods. A similar expression can be obtained via a quadrature method. Equation 9.11 estimates of Table 9.1 are closer to the actual values for AUMC and, consequently, MRT. The reader is cautioned to remember, however, that the trapezoid itself is still a biased estimator of a curve's interval area, and the manifestation of that bias is a function of sampling frequency.

The attraction of statistical moment analysis to pharmacokinetics is implicit to the use of trapezoids to determine the relevant areas. No assumptions about the underlying mechanisms of drug disposition are made except for the two caveats introduced at the beginning of this chapter. One simply determines areas under the trapezoids formed from the $\Delta C/\Delta t$ intervals. The reader should realize that this is similar to the techniques used to analyze urine excretion data as the total amount excreted is essentially the same as determining the area of the U_t-T profile. Thus, many strategies used to improve AUC or AUMC determination are directly applicable to improve urine excretion data analysis.

When nonlinear pharmacokinetics are operative, interpretation and use of AUC in these models is more complex as discussed in Chapter 10 and illustrated in Equations 10.22–10.25.

9.3 OTHER RESIDENCE TIMES AND PARAMETERS OF INTEREST

Three other residence times that have general application in pharmacokinetics are the mean absorption time (MAT), the mean transit time (MTT), and the variance of the residence

time (VRT). MAT is technically the mean arrival time into the systemic circulation of bioavailable absorbed molecules. MAT is the statistical moment theory equivalent of estimating k_a. MAT is a computationally straightforward method to characterize the rate of drug absorption in bioavailability studies. Riegelman and Collier (1980) extended this theory using the additivity of various transit times, including the MAT, and advanced the notion that MAT is the mean time for drug molecules to remain unabsorbed:

$$\text{MAT} = \text{MRT}_{\text{ni}} - \text{MRT}_{\text{IV}}. \tag{9.12}$$

MAT is simply the difference in MRT following intravenous injection (MRT_{IV}) and another noninstantaneous administration (MRT_{ni}) by any route. Assuming absorption is described by a first-order process with an apparent rate constant of k_a,

$$k_a = 1/\text{MAT} = 1/(\text{MRT} - 1/k_{el}), \tag{9.13}$$

then the absorption half-life is, following Equation 9.4,

$$T_{½}(\text{abs}) = 0.693\,\text{MAT}. \tag{9.14}$$

On the other hand, when absorption is assumed to be a zero-order process,

$$\text{MAT} = T/2, \tag{9.15}$$

where T is the duration of the absorption. Note the similarity to the infusion Equation 9.5 above. In reality, a constant rate infusion is a zero-order absorption whose MAT is just one-half the length of the infusion. In comparisons of formulations based on intrasubject differences in MAT, the bias introduced in MRT when drug is eliminated peripherally, as noted in the caveat above, is not present in the use of MAT, but the fact remains that only those molecules that are systemically available are considered in the MAT. Workers have also calculated MRTs for different processes, including mean dissolution time of a formulation and mean distribution time.

The reader should recall that the determination of systemic availability expressed in Equation 8.31 (see Chapter 8) is a noncompartmental analysis. AUCs should be determined by the trapezoidal methods presented in this chapter. If the point of an analysis is to determine bioequivalence between two formulations, one is actually calculating relative systemic availabilities, a concept equivalent to determining whether two formulations are therapeutically interchangeable. Bioequivalence is determined as the ratio of AUCs between the two formulations. In addition, the mean time to peak concentration and peak concentration are often compared. Comparison of MATs would also shed light on the equivalence of two formulations. The reader should consult the list of selected readings for further approaches to determining bioequivalence and Chapter 15 for a discussion of its formal application in the regulation of veterinary products.

The MTT is by definition the mean time taken by drug molecules injected into the kinetic system at a given point to leave the kinetic space after first and possible subsequent entries into that space. Thus, in contrast to the MRT, which includes times spent on multiple visits of the same individual molecule to the kinetic space, MTT is the mean time spent per visit. In some stochastic modeling approaches to pharmacodynamics (Chapter 13), the MTT becomes a very useful parameter since it relates to the probability of a drug being available

for causing an effect. If all molecules exit irreversibly from a kinetic space, then MTT = MRT. Note also that this is the condition mentioned above under which the MRT is a mathematically acceptable parameter for the plasma space or any other subspace of the whole body. Statistical moment theory thus describes drug behavior based on the mean or average time an administered drug molecule spends in a kinetically homogeneous space, a concept identical to that of a compartment. The difference again is that no specific inferences are being made about the structure of these spaces.

Another parameter that has been calculated is the VRT, which is determined using the area under the second moment curve as

$$\mathrm{VRT} = \left[\int (t - \mathrm{MRT})^2 \cdot C\, dt\right] \Big/ \mathrm{AUC}. \tag{9.16}$$

VRT is used to calculate the coefficient of variation of residence times (CVRT) as

$$\mathrm{CVRT} = [\sqrt{\mathrm{VRT}}]/\mathrm{MRT}. \tag{9.17}$$

The CVRT is the dimensionless dispersion ratio and provides a measure of the dynamics and heterogeneity of drug distribution. However, as was mentioned above for determining trapezoidal areas for the AUMC, these problems are multiplied when higher moment curves are analyzed because small errors in time will be greatly magnified. This is less prone to occur with CVRT since the errors are somewhat canceled out by MRT in the denominator.

AUCs may also be used to easily estimate the fraction of a drug metabolized if the metabolite is available for a separate study. In this case, two intravenous experiments are conducted: one with the parent drug and the second with the metabolite of interest. Two C-T profiles using metabolite concentrations are then determined and the AUCs calculated. The fraction metabolized is then

$$\text{Fraction metabolized} = \mathrm{AUC}_{\text{drug}}\ (\text{metabolite data})/\mathrm{AUC}_{\text{metabolite}}\ (\text{alone}). \tag{9.18}$$

Many other types of AUC ratios may be calculated to estimate disposition when data from multiple routes are available. In the parathion example presented at the end of Chapter 8 (Fig. 8.24), AUCs and MRTs were determined for all compartments after both intravenous and topical pesticide administration in order to probe whether metabolism occurred in the skin. To aid in this analysis, parathion was also dosed topically at two different sites using either occlusive or nonocclusive applications. Recalling discussions in Chapter 4, occlusion increases the rate and extent of absorption, while the same may occur as a result of body site differences. Thus, the extent (estimated by AUCs) and rates (estimated by MRTs) of parathion in the various compartments would be reflected by these differences in input to the systemic circulation. Similarly, by comparing radiolabeled parathion absorption in the central compartment estimated using AUCs and parent drug excretion in urine (bioavailability-excretion analysis), one could probe the kinetics of biotransformation with the equation

$$\text{Percent metabolism skin} = \left(\sum \mathrm{AUC}_{\text{central}}\ (\text{top})/\sum \mathrm{AUC}_{\text{central}}\ (\text{IV})\right) - \text{Parent parathion} \cdot F, \tag{9.19}$$

where AUC is determined from the ^{14}C profile, and the parent parathion systemic availability F is calculated in the normal manner using Equation 4.3 or 8.31 (see Chapters 4 and 8). The result of this analysis yielded estimates of the ratio of cutaneous metabolism to systemic metabolism of parathion administered by these four dosing scenarios and suggested that occlusion significantly increased the amount of biotransformation occurring in the skin. These results were similar to those determined from an analysis of microrate constants using classical compartmental methods.

9.3.1 Clearance

The determination of Cl_B is easily obtained by this approach using Equation 8.18 (see Chapter 8), where $Cl_B = D/\text{AUC}$. Using the trapezoidal methods above to estimate AUC makes this a robust estimate of clearance. Cl_B can also sometimes be calculated following other routes of administration, but only if it is known that the entire dose is systemically available. For oral administration, the ratio of dose to AUC (D_{oral}/AUC) is reliably the hepatic intrinsic clearance only if the dose is known to be completely absorbed from the gastrointestinal tract and is eliminated exclusively by liver metabolism, an assumption difficult to make for most drugs. Clearances by other tissues and from temporal perspectives other than those assumed by D/AUC (e.g., first-pass vs. repetitive-pass clearance considerations) can also be determined but are beyond the scope of the present text. If one fits the initial slope of an exponential C-T profile λ_1 and estimates V_c, as described below, then a distributional clearance can be calculated as

$$Cl_D = V_c \cdot \lambda_1 - Cl_B. \tag{9.20}$$

9.3.2 Volume of distribution

The volume of the central compartment is simply Equation 8.44; $V_c = D/Cp_0 = D/\sum A_i$. The volume of distribution at steady state (Vd_{ss}), according to statistical moment theory, is simply the product of MRT and Cl_B:

$$Vd_{ss} = Cl_B \cdot \text{MRT}. \tag{9.21}$$

This, incidentally, affords an expression for half-life as a function of clearance by solving Equation 9.21 for MRT, and substitution into Equation 9.4 gives

$$T_{½} = 0.693\, Vd_{ss} / Cl_B, \tag{9.22}$$

which is the same as that derived in Equation 8.20 (see Chapter 8). Continuing our investigation of distribution volume, we note that substitution of the respective expressions for MRT (Eq. 9.2) and Cl_B (Eq. 8.18, see Chapter 8) into Equation 9.21 yields

$$Vd_{ss} = (D \cdot \text{AUMC}) / \text{AUC}^2. \tag{9.23}$$

Equation 9.21 assumes a bolus intravenous dose. With a short-term constant infusion, then

$$Vd_{ss} = [(R_0 \cdot T \cdot \text{AUMC}) / \text{AUC}^2] - [R_0 \cdot T^2 / 2 \cdot \text{AUC}], \tag{9.24}$$

Table 9.3 Noncompartmental equations for calculating common pharmacokinetic parameters.

Cl_B	$= \text{Dose}/\text{AUC}$
Cl_D	$= (V_c \cdot \lambda_1) - Cl_B$
Vd_{ss}	$= (\text{Dose} \cdot \text{AUMC})/\text{AUC}^2$
V_c	$= \text{Dose}/Cp_0$
MRT_{IV}	$= \text{AUMC}/\text{AUC} = Vd_{ss}/Cl_B$
MAT	$= \text{MRT}_{route} - \text{MRT}_{IV}$
K_a	$= 1/(\text{MRT} - 1/k_{e1})$
$T_{½}$	$= 0.693\ \text{MRT} = 0.693\ Vd_{ss}/Cl_B$
$T_{½}(\lambda)$	$= 0.693/\lambda$
F	$= [(\text{AUC}_{route})\cdot(\text{Dose}_{IV})]/[(\text{AUC}_{IV})\cdot(\text{Dose}_{route})]$
	$= [(\text{AUC}_{route})\cdot(\text{Dose}_{IV})\cdot(T_{½IV})]/[(\text{AUC}_{IV})\cdot(\text{Dose}_{route})(T_{½route})]$
AUC	$= \sum A_i/\lambda_i$
AUMC	$= \sum A_i/(\lambda_i)^2$
Cp_0	$= \sum A_i$

Note that AUC and AUMC could be calculated using trapezoidal analysis of areas.

where T is the length of infusion and R_0 is the zero-order infusion rate. In this case, for constant infusions, Vd_{ss} is independent of where drug is being eliminated. Another volume parameter also calculated using statistical moments after an intravenous dose is Vd_{area}:

$$Vd_{area} = D_{IV}/(k_{el} \cdot \text{AUC}), \tag{9.25}$$

and for a constant intravenous infusion,

$$Vd_{area} = R_0/(k_{el} \cdot C_{ss}), \tag{9.26}$$

where C_{ss} is the steady-state plasma concentration as previously defined by rearrangement of Equation 8.22 ($C_{ss} = R_0/Cl_B$; see Chapter 8). The computational advantage of Vd_{ss} over Vd_{area} is, of course, the avoidance of the need to estimate an elimination rate constant, k_{el}, but as described in Chapter 8, it is thus also independent of altered elimination. Recall that Vd_{ss} is the volume operative at the MRT.

One can appreciate that statistical moment analysis provides a powerful tool for calculating many of the common pharmacokinetic parameters that are routinely used—in the bioequivalence studies discussed above, in constructing dosage regimens (Chapter 12), in correlating disease and physiological changes to pharmacokinetic disposition (Chapter 17), and in making interspecies extrapolations (Chapter 18). As can now be even more fully appreciated, Cl_B and Vd_{ss} are truly independent parameters that quantitate distribution and excretion using computationally robust techniques based on minimal model-specific assumptions. Table 9.3 is a compilation of equations useful to calculate these parameters from an analysis of a C-T profile.

9.4 OTHER MODEL-INDEPENDENT APPROACHES

The center of gravity (or center of mass) of a curve is a single point that provides a quantitative description of a C-T profile. Veng-Pedersen defined the coordinates of this point as

$$P_c = (\text{MRT}, C_{\text{mean}}) = (\text{AUMC}/\text{AUC}, \tfrac{1}{2}\text{AUCC}/\text{AUC}), \tag{9.27}$$

where C_{mean} is the mean concentration, and AUCC is the area under the squared curve:

$$\text{AUCC} = \int [C(t)]^2 \, dt. \tag{9.28}$$

P_c is a simple yet powerful tool for comparing C-T profiles because it is sensitive to both the rate and extent of absorption or elimination. The square data point on the plot of Fig. 9.2 at (1.44, 14.00) represents the P of that profile.

Another model-independent approach to analyzing pharmacokinetic data is linear systems deconvolution analysis, which actually provides a mathematical basis for the superposition principle discussed earlier. In this approach, any observed C-T profile $\{C(t)\}$ can be broken down or deconvoluted into two mathematical functions: the characteristic function $\{F(t)\}$, which describes the disposition after intravenous bolus administration, and the input function $\{C(t)\}$, which is an equation describing drug input as a function of time after any mode of administration. This technique is also called superposition integration and uses the observed C-T profile and the characteristic profile to determine the input profile using the relations

$$C(t) = F(t) + C'(t) \,(\text{convolution}) \tag{9.29}$$

$$C'(t) = C(t) - F(t) \,(\text{deconvolution}). \tag{9.30}$$

There are numerous mathematical approaches to implement this. If one has intravenous data fit to a multicompartment model, then $F(t)$ is expressed as Equation 8.58. When an extravascular administration route is being studied, the $C(t)$ is equivalent to the shape of the absorption input profile. Thus, this approach gives an excellent quantitative description of any absorption profile resulting from any complexity of drug delivery system. It is a powerful tool for assessing absolute systemic availability. Although multiexponential equations are often used to describe both functions, this is not necessary, and equations of any mathematical form can be employed. The mathematical equations describing the resulting input profile may be complex, and their derivation is beyond the scope of this text.

We have used this approach to study the comparative nephrotoxicity of identical gentamicin C-T profiles in dogs with normal and impaired renal functions. We defined a target profile that is the sum of the input function and the characteristic response determined after intravenous dosing. Note that in renal disease, Cl_B and thus k_{el} are reduced compared to normal, making the achievement of identical C-T profiles in both groups impossible. However, if one uses deconvolution principles to solve for the input function required to achieve identical C-T profiles, this can be programmed into a computer-driven infusion pump to make the infusion rate limiting. A loading dose ($C_{ss}V_c$) was first administered to rapidly achieve steady state. A steady-state infusion (mg/kg h) was then administered for time, t, according to the equation

$$R_{ss} = (C_{ss} \cdot V_c) \cdot (k_{10} + k_{12} \cdot e^{-k_{21}t}). \tag{9.31}$$

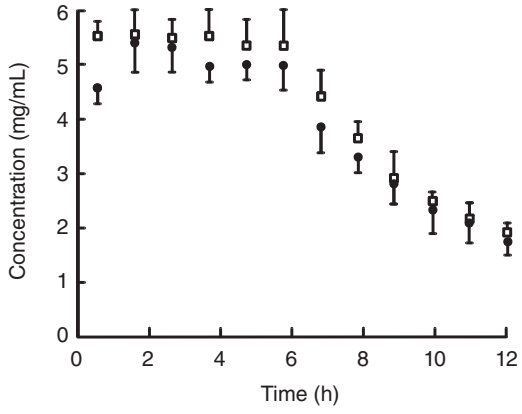

Fig. 9.5 Plasma concentration-versus-time profiles obtained after administering computer-controlled intravenous infusions of gentamicin to normal (●) and subtotal nephrectomized (□) dogs targeting a terminal slope of k in both groups at rates defined in Equations 9.31 and 9.32.

At the termination of infusion, a declining rate infusion was then administered as

$$R_{\text{decl}} = (C_{\text{ss}} \cdot V_{\text{c}}) \frac{[(\alpha - k) \cdot (\beta - k)]e^{-kt'} + k \cdot k_{12} \cdot e^{-k_{21}t'}}{(k_{21} - k)}, \tag{9.32}$$

where k is the target terminal slope and t' is the length of time in the declining phase of the infusion. Fig. 9.5 shows the resulting C-T profile for normal and subtotally nephrectomized dogs (see Chapter 8, Table 8.2 for pharmacokinetic parameters of the intravenous bolus dose) administered drug according to their calculated input functions. This method thus served as an excellent tool to probe the toxicokinetics of a nephrotoxic drug in diseased animals.

We have also employed a similar convolution technique to model the predicted C-T profile resulting from transdermal drug delivery when the input function is experimentally determined using an isolated perfused skin preparation. In this case (depicted in Fig. 9.6), the output of the skin profile could either be the experimentally observed profile or be simulated using a compartmental model to generate the terms of $C'(t)$. This skin model will be further developed in Chapter 11 (see text accompanying Figs. 11.5–11.7). The characteristic response, $\{F(t)\}$, is based on a two-compartment model determined from intravenous studies (obtained after a bolus dose or modeled better with an infusion of the same duration as the transdermal input profile) conducted in the species in which the prediction is to be made. In our laboratory, we use porcine skin as the preferred human model and obtain the intravenous data from human studies. Additionally, both the input and characteristic functions may be inputted as a confidence interval to account for interindividual differences; or a "bootstrap" or "full-space" technique can be used to assess all possible combinations of input and disposition functions. This technique accurately predicts the subsequent profiles in all drugs and pesticides studied to date.

The final stochastic approach to modeling was the power function introduced in the previous chapter for gentamicin tissue disposition. Fig. 9.7 depicts a power analysis of gentamicin renal cortex tissue concentrations in rats using this same general approach. This technique has been explored in much greater detail for general organ distribution models

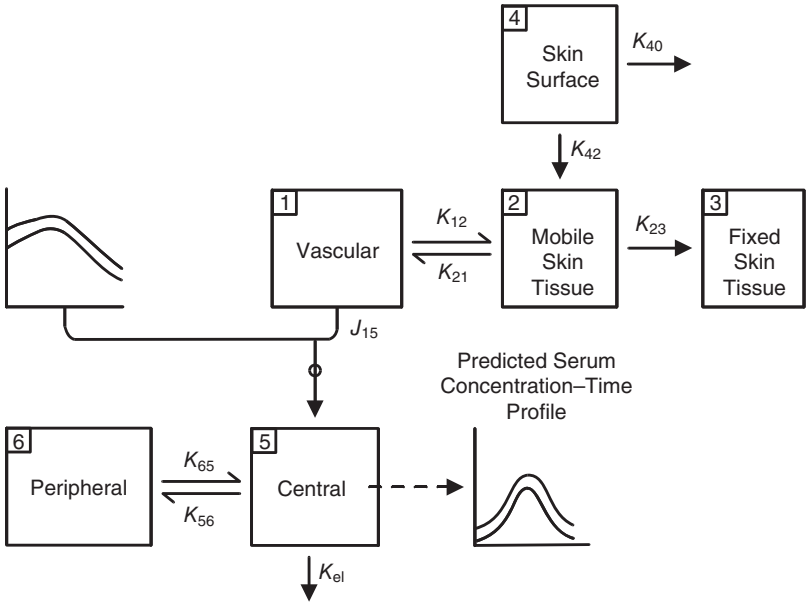

Fig. 9.6 Pharmacokinetic strategies used to extrapolate output profiles from an *in vitro* perfused skin flap model to predict *in vivo* concentration-time profiles. Compartments 1, 2, 3, and 4 constitute the *in vitro* model, whose output (now the *input function* ($C'(t)$; upper left corner) into the *in vivo* systemic pharmacokinetic model is composed of compartments 5 and 6 (*characteristic function*, $F(t)$). A derivation of a similar skin component is further developed in Fig. 10.4.

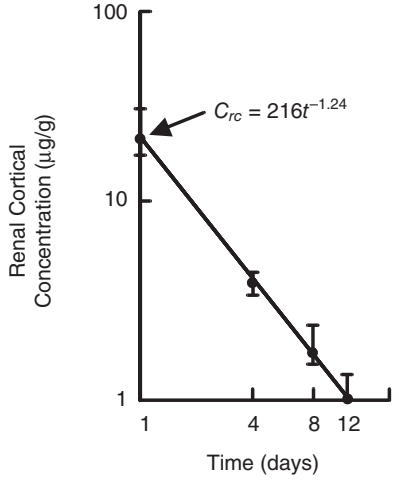

Fig. 9.7 Power function (log C vs. log T) analysis of gentamicin decay in rat renal cortex.

and is rooted in the concept of residence times. The power function arises when a drug molecule exits the rapidly equilibrating kinetic space (e.g., normal compartments) and randomly remains nonavailable for return to this compartment because of sequestration in the so-called deep compartment. Recall that this sojourn to a peripheral compartment vio-

lated one of the basic assumptions of MRT; that is, a significant fraction of the dose never spends time in another space before being eliminated, which makes the residence time no longer directly proportional to the plasma *Cp*. This can be handled by using so-called random walk principles, which generate equations taking the form of a power function (Eq. 8.59). The concept is that drugs distribute freely into tissues until they bind to a receptor, or enter a cell, for which time they no longer can randomly reenter the exchanging kinetic compartments. The distribution of the residence times for such tissues is described by a gamma function, which implies the power dependence. Additionally, if the diffusion of the compound is described by an anatomical configuration having spherical symmetry (e.g., the liver lobule), then the equations assume the form of a power function. Significant work has been done in this area, especially applied to drug distribution in the liver (spherical diffusion) and heavy metal deposition in bone (binding). The equations for this model are beyond the scope of this introductory text since nonlinear equations are also needed to describe how the drug distributes to these sites.

9.5 AN APPLICATION OF STATISTICAL MOMENT THEORY

We will close this chapter with another application from the author's laboratory using a statistical moment approach. When absorption through skin was presented in Chapter 4, the rate-limiting factor was penetration through the stratum corneum. For many compounds in skin-absorption studies, a generally critical factor is perfusion because the rate and extent of absorption into the general circulation (i.e., the bioavailability) of a topically applied compound is a function of (among other things, such as stratum corneum permeability and cutaneous metabolism) the extent to which the underlying skin is perfused. This is especially true with so-called active drug delivery systems (e.g., iontophoresis), which rapidly allow drug to pass the epidermal barrier. The capillary beds in the viable epidermis are normally in a dynamic state in the constant need to shunt or recruit as a function of thermoregulation. The MRT of a drug in skin following topical application may be described as

$$\mathrm{MRT}_{\mathrm{skin}} = P \cdot V_{\mathrm{T}} / Q_{\mathrm{skin}}, \tag{9.33}$$

where P is the skin-to-blood partition coefficient, V_{T} is the volume of distribution of drug in skin, and Q_{skin} is (theoretically) the blood flow through the space where the drug is diffusing, and can be defined as

$$Q_{\mathrm{skin}} = Q_{\mathrm{exchange}} + Q_{\mathrm{shunt}}. \tag{9.34}$$

Thus, Q_{skin} is the sum of flow through capillaries that are exchanging with the extravascular space, and flow that has been shunted, and therefore not able to exchange (i.e., not perfused). The point is that the MRT here is dependent on two independent variables (assuming P is constant): V_{T} and Q_{skin}. Historically, most models in the literature assume that V_{T} is constant, which is not generally true since V_{T} is actually a direct function of Q_{exchange}, a dynamic variable. This leads to a dynamic MRT that is difficult to measure without knowledge of the corresponding profile of Q_{skin}.

The MTT of blood through a perfused space was estimated in a model to predict the transdermal iontophoretic delivery of lidocaine. In this model, it was necessary to address

the MTT (called T_{eff} to indicate the *effective* transit time through drug exchanging capillaries) in order to develop a mathematical expression for the flux of electrically driven drug molecules into the systemic circulation:

$$T_{eff} = V_{eff} / Q_{eff}, \tag{9.35}$$

where V_{eff} and Q_{eff} are the effective vascular volume and blood flow, respectively. The subscript "eff" denotes that space through which drug diffuses in the skin, and those vessels in the proximity that have the capacity to exchange drug. This study revealed, among other things, that the state of skin vasculature is exquisitely sensitive to penetrating vasoactive compounds (i.e., tolazoline and norepinephrine as vasodilator and vasoconstrictor, respectively, in this case). Furthermore, changes in vascular state in skin have a great influence on the absorption of topically applied compounds after active delivery. In the case presented, the estimated T_{eff} for lidocaine when coadministered with tolazoline was 46 min, in contrast to 2 min when coadministered with norepinephrine (eff for lidocaine alone was 9 min).

This example illustrates the power of relatively simple pharmacokinetic techniques to probe the physiological basis of drug disposition in numerous organ and experimental systems. As stressed in the introduction of this text, pharmacokinetics is a useful tool to generate testable experimental hypotheses. There are no absolutely correct models or approaches, as many different systems may be used depending upon the availability of data and limiting assumptions.

ACKNOWLEDGMENT

The author acknowledges the contribution of Patrick Williams, who coauthored this chapter in the first edition of this text.

BIBLIOGRAPHY

Caines, P.E. 1988. *Linear Stochastic Systems*. New York: John Wiley & Sons.

Caprani, O., Sveindottir, E., and Lassen, N. 1975. SHAM, a method for biexponential curve resolution using initial slope, height, area and moment of the experimental decay type curve. *Journal of Theoretical Biology*. 52:299–315.

Chan, K.K.H., and Gilbaldi, M. 1982. Estimation of statistical moments and steady-state volume of distribution for a drug given by intravenous infusion. *Journal of Pharmacokinetics and Biopharmaceutics*. 10:551–558.

Chanter, D.O. 1985. The determination of mean residence time using statistical moments: is it correct? *Journal of Pharmacokinetics and Biopharmaceutics*. 13:93–100.

Chiou, W.L. 1978. Critical evaluation of the potential error in pharmacokinetic studies of using the linear trapezoidal rule method for the calculation of the area under the plasma level-time curve. *Journal of Pharmacokinetics and Biopharmaceutics*. 6:539–546.

Cutler, D.J. 1978. Theory of the mean absorption time, an adjunct to conventional bioavailability studies. *Journal of Pharmacy and Pharmacology*. 30:476–478.

Cutler, D.J. 1979. A linear recirculation model for drug disposition. *Journal of Pharmacokinetics and Biopharmaceutics*. 7:101–116.

DiStefano, J. III. 1982. Noncompartmental versus compartmental analysis: some bases for choice. *American Journal of Physiology. Regulatory, Integrative and Comparative Physiology*. 243:R1–R6.

Dix, L.P., Frazier, D.L., Cooperstein, M., and Riviere, J.E. 1986. Exponential intravenous infusions in toxicology studies: achieving identical serum drug concentration profiles in individuals with altered pharmacokinetic states. *Journal of Pharmaceutical Sciences*. 75:448–451.

Frazier, D.L., Dix, L.P., Bowman, K.F., Thompson, C.A., and Riviere, J.E. 1986. Increased gentamicin nephrotoxicity in normal and diseased dogs administered identical serum drug concentration profiles: increased sensitivity in subclinical renal dysfunction. *Journal of Pharmacology and Experimental Therapeutics*. 239:946–951.

Gibaldi, M., and Perrier, D. 1982. *Pharmacokinetics*, 2nd Ed. New York: Marcel Dekker.

Martinez, M.N. 1998. Article 1: noncompartmental methods of drug characterization: statistical moment theory. *Journal of the American Veterinary Medical Association*. 213:974–980.

Metzler, G.M. 1989. Bioavailability/bioequivalence: study design and statistical issues. *Journal of Clinical Pharmacology*. 29:289–292.

Nakashima, E., and Benet, L.Z. 1988. General treatment of mean residence time, clearance, and volume parameters in linear mammillary models with elimination from any compartment. *Journal of Pharmacokinetics and Biopharmaceutics*. 16:475–492.

Norwich, K.H., and Siu, S. 1982. Power functions in physiology and pharmacology. *Journal of Theoretical Biology*. 95:387–398.

Nüesch, E.A. 1984. Noncompartmental approach in pharmacokinetics using moments. *Drug Metabolism Reviews*. 15:103–131.

Pang, K.S., and Rowland, M. 1977. Hepatic clearance of drugs. I. Theoretical considerations of a "well-stirred model" and a "parallel tube" model. Influence of hepatic blood flow, plasma and blood cell binding, and the hepatocellular enzymatic activity on hepatic drug clearance. *Journal of Pharmacokinetics and Biopharmaceutics*. 5:625–653.

Pecile, A., and Rescigno, A. 1987. *Pharmacokinetics. Mathematical and Statistical Approaches to Metabolism and Distribution of Chemicals and Drugs*. New York: Plenum Press.

Purves, R.D. 1994. Numerical estimation of the noncompartmental pharmacokinetic parameters variance and coefficient of variation of residence times. *Journal of Pharmaceutical Sciences*. 83:202–205.

Qiao, G.L., and Riviere, J.E. 1995. Significant effects of application site and occlusion on the pharmacokinetics of cutaneous penetration and biotransformation of parathion *in vivo* in swine. *Journal of Pharmaceutical Sciences*. 84:425–432.

Riegelman, S., and Collier, P. 1980. The application of statistical moment theory to the evaluation of in vivo dissolution time and absorption time. *Journal of Pharmacokinetics and Biopharmaceutics*. 8:509–534.

Riviere, J.E., and Williams, P.L. 1992. Pharmacokinetic implications of changing blood flow in skin. *Journal of Pharmaceutical Sciences*. 81:601–602.

Riviere, J.E., Williams, P.L., Hillman, R., and Mishky, L. 1992. Quantitative prediction of transdermal iontophoretic delivery of arbutamine in humans using the *in vitro* isolated perfused porcine skin flap (IPPSF). *Journal of Pharmaceutical Sciences*. 81:504–507.

Riviere, J.E., Monteiro-Riviere, N.A., and Williams, P.L. 1995. Isolated perfused porcine skin flap as an *in vitro* model for predicting transdermal pharmacokinetics. *European Journal of Pharmacy and Biopharmaceutics*. 41:152–162.

Segre, G. 1988. The sojourn time and its prospective use in pharmacology. *Journal of Pharmacokinetics and Biopharmaceutics*. 16:657–666.

Shargel, L., Wu-Pong, S., and Yu, A.B.C. 2005. *Applied Biopharmaceutics and Pharmacokinetics*, 5th Ed. New York: McGraw Hill.

Toutain, P.L., and Koritz, G.D. 1997. Veterinary drug bioequivalence determination. *Journal of Veterinary Pharmacology and Therapeutics*. 20:79–90.

Veng-Pedersen, P. 1989a. Mean time parameters in pharmacokinetics: definition, computation and clinical implications (part I). *Clinical Pharmacokinetics*. 17:345–366.

Veng-Pedersen, P. 1989b. Mean time parameters in pharmacokinetics: definition, computation and clinical implications (part II). *Clinical Pharmacokinetics*. 17:424–440.

Veng-Pedersen, P. 1991. Stochastic interpretation of linear pharmacokinetics: a linear system analysis approach. *Journal of Pharmaceutical Sciences*. 80:621–631.

Veng-Pedersen, P., and Gillespie, W. 1984. Mean residence time in peripheral tissue: a linear disposition parameter useful for evaluating a drug's tissue distribution. *Journal of Pharmacokinetics and Biopharmaceutics*. 12:535–543.

Weiss, M. 1983. Use of gamma distributed residence times in pharmacokinetics. *European Journal of Clinical Pharmacology*. 25:695–702.

Williams, P.L., and Riviere, J.E. 1993. Model describing transdermal iontophoretic delivery of lidocaine incorporating consideration of cutaneous microvascular state. *Journal of Pharmaceutical Science*. 82:1080–1084.

Williams, P.L., and Riviere, J.E. 1994. A "full-space" method for predicting *in vivo* transdermal plasma drug profiles reflecting both cutaneous and systemic variability. *Journal of Pharmaceutical Sciences*. 83:1062–1064.

Yamaoka, K., Nakagawa, T., and Uno, T. 1978. Statistical moments in pharmacokinetics. *Journal of Pharmacokinetics and Biopharmaceutics*. 6:547.

Yeh, K.C., and Kwan, K.C. 1978. A comparison of numerical integrating algorithms by trapezoidal, Lagrange, and spline approximation. *Journal of Pharmacokinetics and Biopharmaceutics*. 6:79–98.

Yu, Z., and Tse, F.L.S. 1995. An evaluation of numerical integration algorithms for the estimation of area under the curve (AUC) in pharmacokinetic studies. *Biopharmaceutics and Drug Disposition*. 16:37–58.

10 Nonlinear Models

Most pharmacokinetic models incorporate the common assumption that drug elimination from the body is a first-order process, and the rate constant for elimination is assumed to be a true constant, independent of drug concentration. In such cases, the amount of drug cleared from the body per unit time is directly dose or concentration dependent, the percentage of body drug load that is cleared per unit time is constant, and the drug has a constant elimination half-life. Fortunately, first-order elimination (at least apparent first-order elimination) is typical in drug studies. First-order linear systems application greatly simplifies dosage design, bioavailability assessment, dose–response relationships, prediction of drug distribution and disposition, and virtually all quantitative aspects of pharmacokinetic simulation.

However, drugs most often are not eliminated from the body by mechanisms that are truly mathematically first order by nature. Actual first-order elimination applies only to compounds that are eliminated exclusively by mechanisms not involving enzymatic or active transport processes (i.e., processes involving energy). As presented in Chapter 2, they are primarily driven by diffusion and obey Fick's law. The subset of drugs not requiring a transfer of energy in their elimination is restricted to those that are cleared from the body by urinary and biliary excretion and, among those, only drugs that enter the renal tubules by glomerular filtration or passive tubular diffusion. Albeit there are some minor passive excretion routes, such as saliva or sweat, these elimination routes generally account for such a small fraction of total eliminated drug that they are essentially negligible. All other important elimination processes require some form of energy-consumptive metabolic activity or transport mechanism. Thus, the number of compounds that clear by truly first-order processes are very few indeed, and nonlinear elimination is therefore a potential condition for the great majority of compounds.

One might ask, then, why the elimination kinetics of so many drugs can be modeled with linear first-order processes. At clinical dosages, the majority of drugs do not reach saturation concentrations at the reaction sites, or at least not a significant fraction of the dose. One notable exception is ethanol, which is cleared from the body by oxidative metabolism at an apparent zero-order rate (indicative of a well-saturated process). There is nothing special about ethanol except its low molecular weight (46 Da) relative to most drugs (>300 Da). This means that a typical ethanol dose is actually equivalent to a relatively

Comparative Pharmacokinetics: Principles, Techniques, and Applications, Second Edition. Jim E. Riviere.
 ISBN: 978-0-813-82993-7

high molar dose that saturates metabolism. Metabolic activity operates on a molecular basis and therefore would be better expressed on the basis of the number of interacting molecules (e.g., molarity). In fact, much of the pharmacokinetic techniques already presented and their interpretation would be facilitated if molarity were employed rather than mass or concentration. However, this is rarely done.

The reason energy-involved processes are not strictly first order is that they are generally saturable or, more specifically, capacity limited. That is, as the availability of finite enzyme and/or energy sources is temporarily depressed (i.e., saturated) due to acute competition among drug molecules for reaction sites, the reaction rate slows and is no longer first order, taking on some of the properties of a zero-order process. Recalling Chapter 8 and Equation 8.2 for first-order processes, a constant percentage of remaining drug is cleared per unit time, and the drug has a discrete, concentration-independent elimination rate constant (K) and thus half-life (or multiple half-lives for multicompartment models). For drugs eliminated by zero-order kinetics or saturated pathways (Eq. 8.3), however, a constant quantity of drug is eliminated per unit of time, and this quantity is drug concentration independent, and the drug does not have a constant, characteristic elimination half-life. The potential impact of saturable elimination, leading to zero-order (vs. first-order) elimination, can be profound, and its effects include altered drug concentration profiles, scope and duration of drug activity, distribution, and disposition among tissues. As discussed in Chapter 7, saturable hepatic metabolism may markedly affect drug absorption due to altered first-pass activity.

10.1 MICHAELIS–MENTEN RATE LAWS

The primary technique used to model saturable metabolic process employ the Michaelis–Menten rate laws introduced in Chapter 7. Systematic studies of the effect of substrate concentration upon enzyme activity were begun in the late 19th century. The concept of the enzyme–substrate complex was introduced before any enzymes had even been purified. In fact, at the time, it was not even known that enzymes were proteins, but the idea of the enzyme–substrate complex served to launch the development of enzyme kinetics.

If one follows the appearance of product (or the disappearance of substrate in a reaction with 1 : 1 stoichiometry) as a function of time in an experiment, a progress curve for the reaction can be obtained (Fig. 10.1). The initial rate (V_0) of the reaction is equal to the slope of the progress curve at time zero. As the reaction continues, the product continues to accumulate, but at slower rates as the supply of substrate diminishes. If a series of these experiments are affected, starting with a corresponding series of substrate concentrations, a plot of V_0 versus substrate concentration is obtained, such as shown in Fig. 10.2 and explained below.

One of the most basic enzymatic reactions, first proposed by Michaelis and Menten (1913), involves a substrate S reacting with an enzyme E to form a complex SE, which in turn is converted into a product P and the enzyme. This can be represented schematically by

$$S + E \underset{k_{-1}}{\overset{k_1}{\longleftrightarrow}} SE, \quad SE \xrightarrow{k_2} P + E, \tag{10.1}$$

where k_1 is a second-order reaction rate constant, and k_{-1} and k_2 are first-order reaction rate constants. Michaelis and Menten proposed that the enzymatic reaction proceeds through an enzyme–substrate complex that forms rapidly (the left reaction of Eq. 10.1) and is then

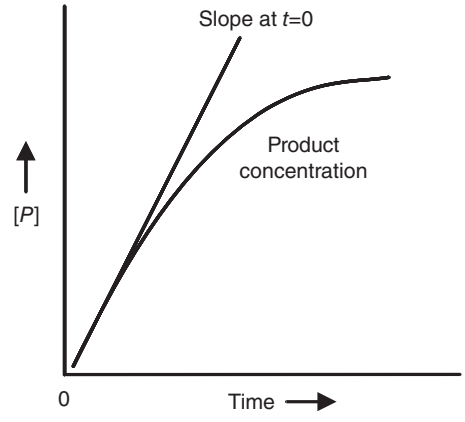

Fig. 10.1 Simulated enzyme-linked metabolite product formation progress curve. [*P*] is the concentration of product, plotted against time. The initial rate, the slope at $t = 0$ (V_0 in the text), is an important parameter for characterizing the reactions of Equation 10.1 (see Fig. 10.2).

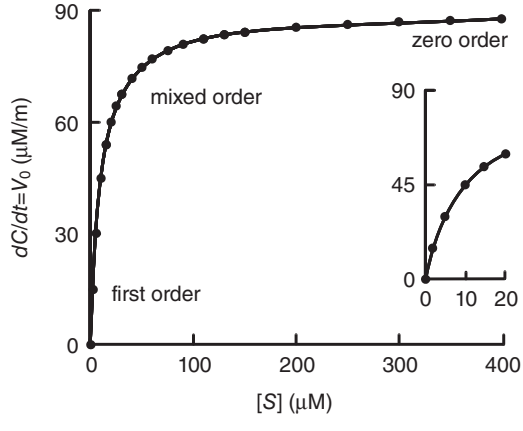

Fig. 10.2 A simulated plot of initial rates (dC/dt, or V_0) versus substrate concentration [*S*] for a reaction described by Equation 10.1. With $V_{max} = 90\,\mu M/m$, K_m is estimated to be $10\,\mu M$ at half-maximal velocity ($V_{max}/2 = 45\,\mu M/m$), as shown in inset.

slowly converted to product (metabolite) in the rate-determining step of the reaction (the right reaction in Eq. 10.1). The major assumption of Equation 10.1 that provides a logical basis for Equation 10.2 (below) is that the enzyme and the substrate remain in thermodynamic equilibrium with the enzyme–substrate complex at all times. Michaelis–Menten kinetics is formulated for initial rates, and based on the assumption that $k_{-1} >> k_2$, which implies that, provided $[E]_t << [S]$, the concentration of enzyme substrate complex will be small and constant. $[E]_t$ denotes the total concentration of enzyme, free and complexed, and [*S*] is the free substrate concentration. This is known as the *steady-state assumption*. Since only a small amount of product accumulates initially, the reverse reaction (i.e., that described by k_{-1}) can be ignored, which allows the method used to obtain the V_0-versus-[*S*] plot in Fig. 10.2. With the above assumptions and some algebra, the Michaelis–Menten rate law (Eq. 10.2) can be derived, assuming [*S*] is a function of information obtained from the experimental procedures shown in Fig. 10.2.

$$d[S]/dt = -[V_{max} \cdot [S]]/[K_m + [S]], \tag{10.2}$$

where V_{max} is the maximum velocity, or rate, of the reaction, and K_m is the Michaelis constant,

$$K_m = [k_{-1} + k_2]/k_1, \tag{10.3}$$

which represents the drug concentration at which half-maximal reaction velocity ($V_{max}/2$) occurs.

Note the similarity of Equation 10.2 to the formulation of saturable protein binding in Chapter 5, Equation 5.4, as well as the pharmacodynamic activity models developed in Chapter 13 and expressed in effect models such as Equation 13.1. The full development of these applications is covered in their respective chapters and will not be formally developed here. However, the implications of nonlinear rates discussed here on pharmacokinetic models are applicable across these other applications. The difference is also in nomenclature that often is specific to each application.

In order to present a nomenclature consistent with the majority of the pharmacokinetics literature and the rest of this text, we will use C (referred to earlier as Cp when in plasma) in place of [S] for drug or substrate concentration (i.e., C = [S]). Thus,

$$dC/dt = -[V_{max} \cdot C]/[K_m + C]. \tag{10.4}$$

The parameters V_{max} and K_m can be estimated from a plot like that shown in Fig. 10.2, but more accuracy for *in vivo* plasma data with less experimental effort can be attained utilizing other methods. Because of the potential complexity of such models, it is prudent to use simple techniques to first test one's data for dose dependency or nonlinearity.

10.1.1 Testing for nonlinearity

Fig. 10.3 depicts the simplest technique, whereby one determines if the terminal phase of the ln$C$ (or log C)–versus-time profile is a straight line using regression techniques. If this is curvilinear, then nonlinear kinetics are operative, and a plot of C versus time will often

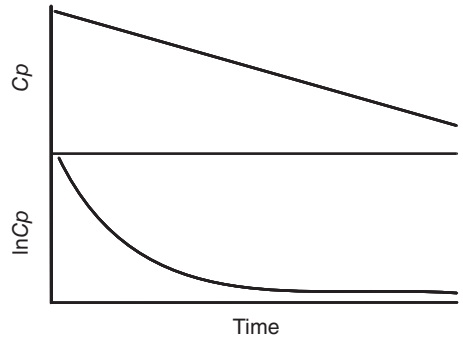

Fig. 10.3 Plot of ln concentration (ln*Cp*) versus time, and concentration (*Cp*) versus time, suggesting nonlinear kinetics. Recall that ln*Cp*-*T* plots for linear processes result in straight terminal elimination phases as shown in the figures in Chapter 8.

be straight. Alternatively, if multiple doses are used, one can determine the area under the curve (AUC) by a graphical technique discussed earlier in Chapter 9 and plot dose versus AUC as in Fig. 10.4. If this plot is linear, then dose-independent kinetics is present, and the classical compartmental exponential or noncompartmental first-order models are appropriate. If this plot is not a straight line (in its terminal segment if a multicompartment drug), nonlinear models are required.

It is important that a true area integration technique (e.g., trapezoidal method) and not an exponential fitting equation be used to calculate AUC for this purpose since the use of an exponential fitting program implies linearity. Recall that this technique was used in Table 5.1 when cisplatin tissue concentrations were normalized for systemic exposure by AUC. This was a major assumption, and the cisplatin data set was thus first tested using the approach depicted in Fig. 10.5, which demonstrated that a linear dose-versus-AUC relation was present. Alternatively, one may determine the terminal half-life for an ln$C$ versus time profile after graduated doses. If the half-life is constant, linear kinetics is operative. If it increases with dose, then dose-dependent kinetics is present. When one's data "pass" these tests of linearity and dose independence, then the relatively simpler techniques discussed in Chapters 8 and 9 are appropriate. If not, then more complex models (presented below) may be required.

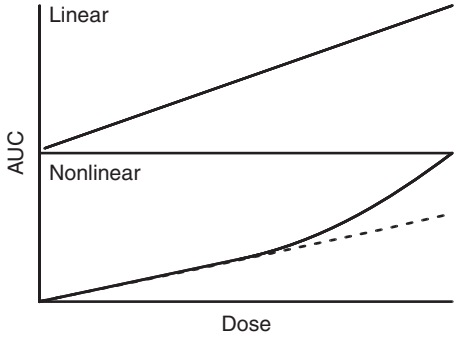

Fig. 10.4 Linearity test using dose versus area under the curve (AUC).

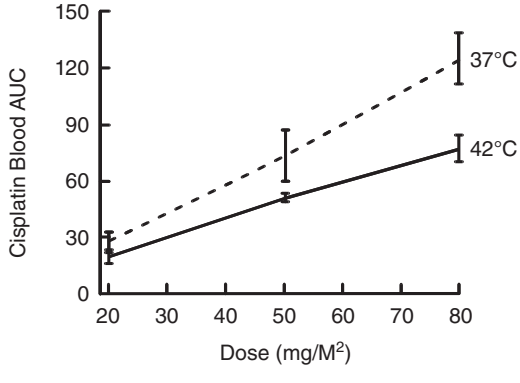

Fig. 10.5 Illustration of linear cisplatin disposition under normothermic (37°C) versus hyperthermic (42°C) conditions.

10.1.2 Estimating Michaelis–Menten parameters from concentration–time data

When nonlinearity is present, one can determine the rate of change of plasma drug concentrations between successive sampling times during the postabsorptive and postdistributive phases (e.g., terminal phase) of a plasma concentration–time profile. Then the rate of change in plasma concentration, together with the drug concentration at the midpoint of each sampling period, C_m, can be incorporated into one of several appropriate expressions to solve for V_{max} and K_m. One such expression is

$$1/[\Delta C/\Delta t] = 1/V_{max} + K_m\,[V_{max} \cdot C_m]. \tag{10.5}$$

This is the Lineweaver–Burke equation, which is a linear form of the Michaelis–Menten Equation 10.4. In this treatment, $\Delta C/\Delta t$ and C_m represent the decline in drug concentration during a time interval and the drug concentration at the midpoint of the time interval, respectively. A plot of the left-hand side of Equation 10.5 versus $1/C_m$ yields a slope of K_m/V_{max} and an intercept of $1/V_{max}$, as illustrated in Fig. 10.6.

In another method, estimates of V_{max} and K_m are obtained directly from ln$C$-versus-t data, the typical concentration-versus-time profile modeled in previous chapters. Equation 10.4 can be rearranged to

$$-dC - K_m\,dC/C = V_{max}\,dt. \tag{10.6}$$

Integration of this result and solving for $t = 0$, where $C = C_0$ results in

$$t = [(C_0 - C)/V_{max}] + [K_m/V_{max}]\ln(C_0/C). \tag{10.7}$$

Solving for ln$C$ yields

$$\ln C = (C_0 - C)/K_m + \ln C_0 - V_{max}t/K_m. \tag{10.8}$$

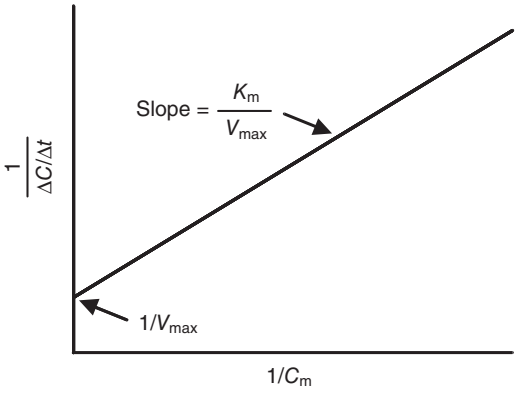

Fig. 10.6 Lineweaver–Burke plot, as defined in Equation 10.5, used for estimating Michaelis–Menten parameters K_m and V_{max}. Plotting the reciprocals of the change (decline) in drug concentrations versus the reciprocal of drug concentrations at the midpoint of the measured intervals yields a slope of K_m/V_{max} and an ordinate intercept of $1/V_{max}$. This method is appropriate for both IV and oral administration.

$\ln C$ can be plotted against t for data following a bolus intravenous (IV) dose. The terminal log-linear portion of the curve (the region where apparent first-order kinetics occur) is a straight line described by

$$\ln C = \ln C_0^{\#} - V_{\max} t / K_m, \tag{10.9}$$

where $C_0^{\#}$ is the extrapolated intercept of C on the vertical axis, exemplified by Fig. 10.7. In the log-linear region at low plasma concentrations, Equation 10.9 is identical to Equation 10.8 expressed as ln. These expressions can thus be equated

$$\ln C_0^{\#} - V_{\max} \cdot t / K_m = (C_0 - C) / K_m + \ln C_0 - V_{\max} \cdot t / K_m. \tag{10.10}$$

Simplifying and rearranging yields

$$\ln C_0^{\#} / C_0 = (C_0 - C) / K_m. \tag{10.11}$$

Then, recalling that Equation 10.10 specifically corresponds to the terminal phase of the drug profile (when $C << C_0$), the quantity $[C_0 - C]$ is approximately C_0. Substituting this in Equation 10.11 and solving for K_m gives

$$K_m = C_0 / \ln(C_0^{\#} / C_0). \tag{10.12}$$

Thus, because both C_0 and $C_0^{\#}$, the actual and extrapolated y-intercepts, respectively, can be measured, K_m can be calculated from Equation 10.12, and $V_{\max}$ can be calculated as

$$V_{\max} = -[\text{Slope}] \cdot K_m. \tag{10.13}$$

The two methods presented above are representative of the several methods presently in use for calculating Michaelis–Menten constants from plasma data. One method uses the rates of change in plasma concentrations, which may be based on either IV or oral data;

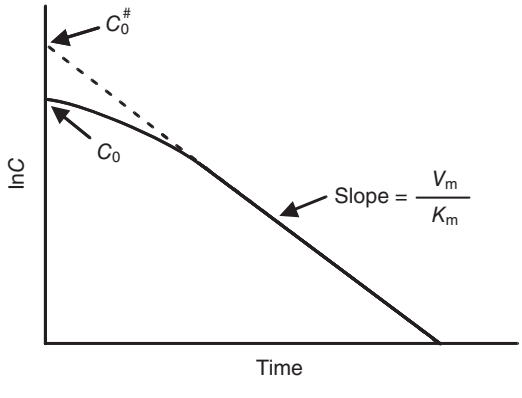

Fig. 10.7 Alternative method for estimating Michaelis–Menten parameters. Plotting ln concentration versus time, the terminal slope (from Eq. 10.9) equals $-V_{max}/K_m$. K_m is a function of C_0 (the initial in drug concentration) and $C_0^{\#}$ (the extrapolated initial in drug concentration). V_{max} is obtained from Equation 10.13. This method is appropriate for IV administrations only.

the other method is based on direct estimates from plots of ln plasma concentration-versus-time data but is restricted to IV data. However, these graphic approaches have been replaced by these equations being directly embedded in computer-based nonlinear curve-fitting programs and are an option in many commercial pharmacokinetic software packages that implement these concepts.

10.2 PHARMACOKINETIC IMPLICATIONS OF MICHAELIS–MENTEN KINETICS

There are two notable simplifying conditions of the Michaelis–Menten equation. If $K_m >> C$, then Equation 10.4 reduces to

$$dC/dt = -[V_{\max} \cdot C]/[K_m]. \tag{10.14}$$

This is equivalent to first-order elimination after IV administration in a one-compartment model, where $dC/dt = -k_{el} \cdot C$. Thus, assuming elimination by a single biotransformation process, the first-order elimination rate constant k_{el} used throughout Chapter 8 is

$$k_{el} = -V_{\max}/K_m. \tag{10.15}$$

Note the similarity of these two equations to those developed in Chapter 7 (Eqs. 7.4 and 7.5).

As suggested in the beginning of this chapter, since most drugs administered at normal dosages seem to obey first-order elimination kinetics, Equation 10.15 supports the hypothesis that typical therapeutic dose regimens lead to drug concentrations at the active site(s) in the body that are well below the K_m of the involved associated enzymology.

However, if $K_m << C$ and the concentration at the active site exceeds enzymatic capacity and saturation occurs, then Equation 10.4 collapses to

$$dC/dt = -V_{\max} = K_0. \tag{10.16}$$

The rate in this case is independent of drug concentration (i.e., a constant) and solely dependent on the rate of enzymatic activity, which describes a zero-order process and is exemplified by ethanol, as discussed above. The implication of this scenario was fully discussed in Chapter 8.

Often, drugs are found to be eliminated by both first-order and nonlinear processes in parallel. In such cases, Equation 10.4 must be expanded to include the strictly first-order elimination processes:

$$dC/dt = -[V_{\max} \cdot C]/[K_m + C] - k'_{el} \cdot C, \tag{10.17}$$

where k'_{el} is a rate constant representing one or several parallel first-order processes and, assuming one-compartment elimination, would be

$$k'_{el} = \sum k_{el}, \tag{10.18}$$

where k_{el} are the first-order elimination rate constants of the first-order elimination process from the central compartment. Similarly, we could define multiple capacity-limited processes, and the general version of Equation 10.17 would be

$$dC/dt = -\sum [V_{max} \cdot C]/[K_m + C] - k'_{el} \cdot C, \tag{10.19}$$

where all relevant saturable elimination processes defined for the central compartment are taken into account. Integration of Equations 10.17 or 10.19 do not yield an explicit general solution for C. As can be appreciated from this illustration, the presence of mixed-order kinetics rapidly complicates a pharmacokinetic study, and the statistically valid estimation of this many parameters requires a significant number of data points based on degree-of-freedom limitations (discussed in detail in Chapter 14). Such models are rarely encountered in the clinical and comparative biomedical literature. Their analytical solutions are complex and in most practical scenarios, there is not sufficient data to employ them. When such complexities occur in drug disposition, the modern approach would be to use physiologically based pharmacokinetic models as introduced in Chapter 11.

The organ in which metabolic saturation is most likely to occur is the liver since most drugs are metabolized there. The reader should review the physiological basis of hepatic biotransformation in Chapter 7. Because capacity limitation typically is important only at relatively high drug concentrations, the most likely setting for its occurrence is during absorption via the portal vein since drug concentrations are generally much higher during this first pass into the liver than after entry into the general circulation. In those cases where metabolic activity is saturated, a greater portion of the drug gains entry into the general circulation unchanged, which leads to greater systemic availability of unchanged drug. A compound that absorbs more quickly will get a greater fraction of its dose into the general circulation (hence greater systemic availability of unchanged drug) than one that absorbs more slowly, when hepatic enzymatic processes are within the saturation range. This fact must be considered when designing timed-release formulations because the resulting lower portal vein concentrations may mitigate saturation to an extent that may drastically depress systemic availability of unchanged drug.

10.3 THE IMPACT OF CAPACITY-LIMITED KINETICS AND VARIOUS PHARMACOKINETIC PARAMETERS

10.3.1 Elimination half-life

As long as blood concentrations of the drug are in the saturable range, any observed plasma half-life ($T_{½}$) will not be constant and will change continuously with drug concentration. Recall from earlier discussions in this text that half-life is a first-order concept. However, plasma concentrations are often analyzed without thinking that zero- or mixed-order kinetics may be operative. When this occurs, half-life is not stable. These issues were discussed in Chapter 8 but will be expanded upon here.

$$T_{½} = [0.693(K_m + C)]/V_{max}. \tag{10.20}$$

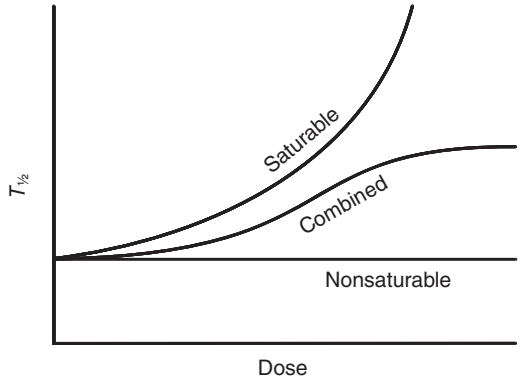

Fig. 10.8 Effects of drug concentration on half-life. When elimination proceeds exclusively by linear, nonsaturable elimination processes, $T_{½}$ is independent of dose (i.e., concentration) and $T_{½}$ is thus constant. For elimination that proceeds exclusively by saturable processes, $T_{½}$ rises without bound as a function of dose, whereas if both linear and nonlinear processes are operative, the relationship between dose and $T_{½}$ is sigmoidal.

The higher the concentration, the smaller the fraction cleared per unit time, and the longer the apparent half-life becomes. Thus, it is in the higher concentration (dose) ranges (e.g., toxic drug overdoses) where this phenomenon is particularly important. For parallel saturable and nonsaturable processes, it can be shown that

$$T_{½} = 0.693/\{[V_{\max} \cdot C]/[K_m + C] - k'_{\text{el}}C\}. \tag{10.21}$$

The extent of half-life dynamics will depend on the relative fraction of the saturable elimination pathway utilized by the drug. As drug concentrations are increased in this case, the apparent elimination half-life will tend to stabilize more or less asymptotically at a value larger than that measured at relatively low drug concentrations. The elimination half-life would ultimately become independent of concentration because the nonsaturable component becomes dominant and controls the new half-life, with negligible contribution from the saturable component. The effect of drug concentrations on the half-life of drugs that are cleared by nonsaturable, saturable, and combined parallel saturable and nonsaturable pathways is illustrated in Fig. 10.8. One potentially profound consequence of the increase in apparent half-life with increasing drug concentrations is increased and prolonged drug accumulation with repeated dosing, and an increase in time to reach steady state. As discussed in Chapter 15, the impact on the design of bioequivalence studies for such drugs is significant.

10.3.2 AUC

For a one-compartment model drug obeying linear first-order kinetics, we have seen in Chapters 8 and 9 that AUC is directly proportional to dose (Fig. 10.4):

$$\text{AUC} = D/(Vd \cdot k_{\text{el}}) = D/Cl_{\text{B}}, \tag{10.22}$$

where D is the available dose and Vd is the volume of distribution. Unfortunately, nonlinear elimination processes generally destroy this proportionality between dose and AUC. In this situation, the AUC following an IV bolus injection of a drug that is eliminated by a single capacity-limited pathway is given by

$$\text{AUC} = (C_0 / V_{\max})(K_m + C_0 / 2). \tag{10.23}$$

When the initial drug concentration, C_0, is much less than K_m, this reduces to

$$\text{AUC} = (C_0 \cdot K_m) / V_{\max} = D / (Vd \cdot k_{\text{el}}), \tag{10.24}$$

which is again identical to the nonsaturable situation of Equation 10.22. On the other hand, if $C_0 >> K_m$, then Equation 10.23 collapses to

$$\text{AUC} = C_0^2 / 2V_{\max} = D^2 / 2(Vd^2 \cdot V_{\max}) \tag{10.25}$$

since in Equation 8.14 (see Chapter 8) for a one-compartment system, C_0 is simply the IV dose (amount, D) divided by the apparent volume of distribution (Vd). Here, the AUC is proportional to the square of the dose and inversely proportional to the square of the distribution volume. Vd should remain constant and should not influence drug levels from different doses. Therefore, drug concentrations within the saturable range lead to disproportionately increasing AUC with increasing dose, as seen in the bottom of Fig. 10.4.

Systemic bioavailability is generally determined by comparing the AUC resulting from the administration of some test dosage form to the AUC from the administration of a standard. Thus, such a nonlinear change in AUC with dose becomes important and invalidates using the simple test for comparison of AUC presented in Chapter 4 (Eq. 4.3), Chapter 8 (Eq. 8.31), and many circumstances discussed in the bioequivalence determination in Chapter 15. When such behavior is present, recommendations are to use the lowest dose possible to minimize this complex response.

10.3.3 Clearance

For nonlinear elimination processes, such as Michaelis–Menten kinetics, clearance is a nonconstant function of drug concentration. In the case of a one-compartment model with elimination by Michaelis–Menten processes and first-order processes in parallel,

$$Cl_{\text{B}} = (V_{\max} \cdot Vd) / (K_m + C) + k'_{\text{el}} \cdot Vd, \tag{10.26}$$

clearance decreases as the concentration increases, until at very high drug concentrations, Cl_{B} asymptotically reaches a lower limit of $k_{\text{el}}'Vd$. Fig. 10.9 illustrates this behavior of clearance as a function of drug concentration under the influence of parallel capacity limited and noncapacity-limited elimination processes by simulating Equation 10.26.

This scenario was previously discussed in Chapters 6 and 8. Recall the discussions where renal clearance varied as tubular secretion processes became saturated, as illustrated in Fig. 6.8, and asymptotically approached renal clearance determined by glomerular filtration. In the case of the liver, when hepatic capacity is exceeded, and the drug has a low extraction ratio, total body clearance becomes independent of hepatic blood flow but sensitive to the extent of plasma protein binding. In contrast, when biotransformation is not

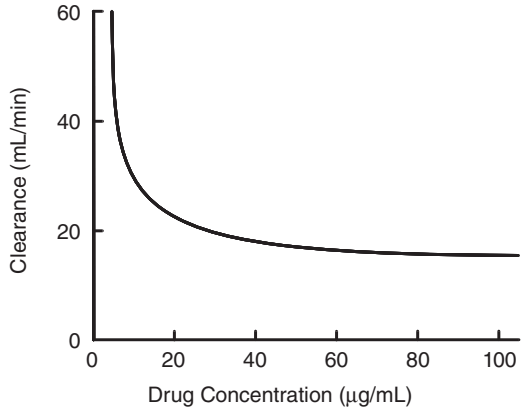

Fig. 10.9 Bimodal clearance as a function of drug concentration. As concentration increases, clearance decreases due to the nonlinear processes until, at very high concentrations, it asymptotically approaches a lower limit of $k'_{el}Vd$, which reflects the linear elimination processes. The simulation assigned the following values in Equation 10.26: $k'_{el} = 0.2\ min^{-1}$; $Vd = 60\,mL$; $K_m = 1.5\,\mu g/mL$; $V_{max} = 2\,\mu g/mL/min$.

Table 10.1 Percutaneous absorption of topical parathion on pig skin demonstrating nonlinear absorption as evidenced by decreased percent dose absorbed at higher applied surface concentrations.

Dose	**4 μg/cm²**	**40 μg/cm²**	**400 μg/cm²**
Mass (μg/cm²/h)	0.32 ± 0.02	0.77 ± 0.11	1.86 ± 0.14
Percent dose/8 h	7.91 ± 0.38	1.91 ± 0.28	0.46 ± 0.04

Data are mean ± standard deviation.

saturated, the drug has a high extraction ratio, and clearance is independent of protein binding (as all drug can be extracted and metabolized) but is dependent on hepatic blood flow. The discussion in Chapter 7 on intrinsic hepatic clearance (Cl_{int}) (Eqs. 7.2–7.7) should be revisited now that the pharmacokinetics of nonlinear elimination has been presented.

10.4 OTHER NONLINEAR ELIMINATION PROCESSES

10.4.1 Absorption

As presented in Chapter 4, there are many processes involved with extravascular drug administration in which nonlinearities may be involved, invalidating the use of linear pharmacokinetic models for data analysis. This can easily be tested by plotting percent dose absorbed after multiple dose administration. If absorption is linear, the percentage absorbed will be constant, while if saturation is present, a lower percent dose will be absorbed at higher doses, as is seen in the saturable topical absorption of parathion in pigs (Table 10.1). In such a case, pharmacokinetic models such as those described above must be employed.

Our laboratory has spent significant effort in studying topical drug and pesticide absorption, and we have constructed complex pharmacokinetic models to describe these phenom-

ena. Presentation of such models is well beyond the scope of this text; however, the interested reader should consult the Bibliography on parathion absorption and metabolism for application of many of these principles in both *in vitro* and *in vivo* systems.

10.4.2 Enzyme induction

Some drugs influence their own clearance (and that of other substrates, in some cases) by directly or indirectly activating (inducing) the gene(s) that codes for the enzyme that metabolizes them. This type of kinetic negative feedback, called enzyme induction and discussed in Chapter 7, is especially interesting because, in contrast to most pharmacokinetic parameters that are concentration dependent or dose dependent, this phenomenon is now time dependent, and results from real-time dynamic biochemical or physiological changes in the body (i.e., unscheduled protein synthesis in this case). An early model developed in 1965 by Berlin and Schimke described time-dependent enzyme concentration, $E(t)$, following induction using the following expression:

$$E(t) = S/K - [S/K - S_0/K_0] \cdot e^{-kt} \tag{10.27}$$

where S_0 = initial (steady-state, before induction) zero-order rate of enzyme synthesis, S = new (steady-state, after induction) zero-order rate of enzyme synthesis, K_0 = initial (steady-state, before induction) first-order rate constant for enzyme degradation, and K = new (steady-state, after induction) first-order rate constant for enzyme degradation.

Note that, prior to induction ($t = 0$),

$$E(0) = S_0/K_0, \tag{10.28}$$

and at the new steady-state following induction ($t = \infty$),

$$E(\infty) = S/K. \tag{10.29}$$

The pharmacokinetic implications of enzyme induction are important. It can be shown that the change in V_{max} during induction can be described as

$$V_{max}(t) = V'_{max} - [V'_{max} - V_{max}(0)] \cdot e^{-kt}, \tag{10.30}$$

where V'_{max} = the new (steady-state following induction) value at $t = \infty$ and $V_{max}(0)$ = the preinduction steady-state value at $t = 0$. Similarly, the change in systemic clearance, $Cl_B(t)$, of a drug following self-induction can be described as

$$Cl_B(t) = Cl'_B - [Cl'_B - Cl_B(0)] \cdot e^{-kt}, \tag{10.31}$$

where Cl'_B is the new (steady-state following induction) value at $t = \infty$ and $Cl_B(0)$ is the preinduction steady-state value at $t = 0$.

The plasma drug concentration profile under the influence of self-induction can be described for a one-compartment model where the drug is infused at constant rate R_0 and eliminated otherwise by first-order processes.

$$Cl_B(t) = R_0/Cl_B(0)[1 - e^{Cl_B(0)t/Vd}] \tag{10.32}$$

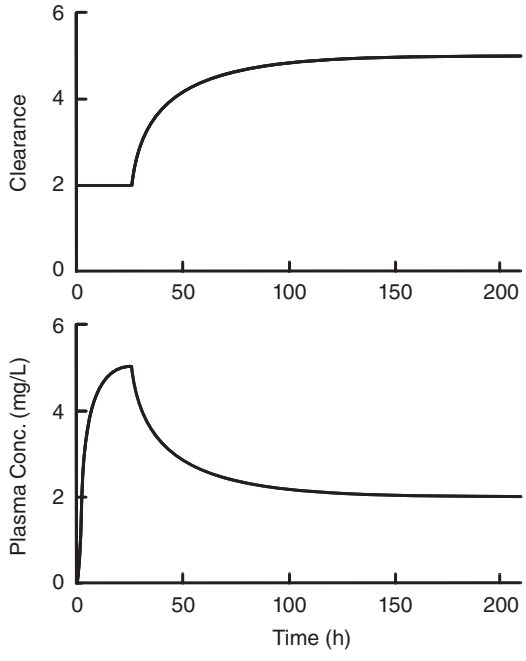

Fig. 10.10 Illustration of the influence of enzyme induction on clearance (upper plot, Eq. 10.31) and plasma concentration (lower plot, Eq. 10.32) profiles during an IV infusion. Induction occurs at $t = 20\,h$. Clearance rises and plasma concentration falls sharply at induction before asymptotically approaching new steady-state values. Values assigned were preinduction clearance = $Cl_B(0) = 2\,L/h$; drug infusion rate = $R_0 = 10\,mg/min$; $Vd = 7\,L$; postinduction steady-state clearance = $Cl'_B = 5\,L/h$; postinduction first-order enzyme degradation rate constant = $K = 0.03\,h^{-1}$.

Note that when induction begins, $Cl_B(0)$ in Equation 10.32 will be replaced by $Cl_B(t)$ (Eq. 10.31). Fig. 10.10 illustrates this by simulating Equations 10.31 and 10.32.

Enzyme induction becomes an important factor with chronic drug administration and with many examples of environmental and occupational exposure to toxicants. If experiments are conducted such that multiple pharmacokinetic trials can be done at similar doses over a prolonged period, the extent of induction can be quantitated. Examination of Equation 10.32 in the context of dosage regimens based on either infusions (see Eqs. 8.21 and 8.22) or multiple-dosage regimens discussed in Chapter 12 suggests that if Cl_B is not constant, targeted plasma concentrations will not be achieved, which could have effects on efficacy or toxicity, depending on the direction.

Other examples of time-dependent pharmacokinetic events include circadian rhythms and disease onset or chemical-induced toxicity in an organ of elimination. These events are often difficult to detect unless full metabolic studies are conducted or independent markers of toxicity are examined. Our laboratory has encountered two such cases. The first was nonlinearity in the clearance of aminoglycoside antibiotics induced by direct drug toxicity to the kidney. In this case, high doses of gentamicin resulted in decreased clearance shown by drug accumulation and nonlinear dose-versus-AUC plots. Similarly, in percutaneous absorption studies of the chemical vesicant sulfur mustard (bis(2-chloroethyl)sulfide), severe vascular damage occurred as the compound was absorbed, necessitating construct-

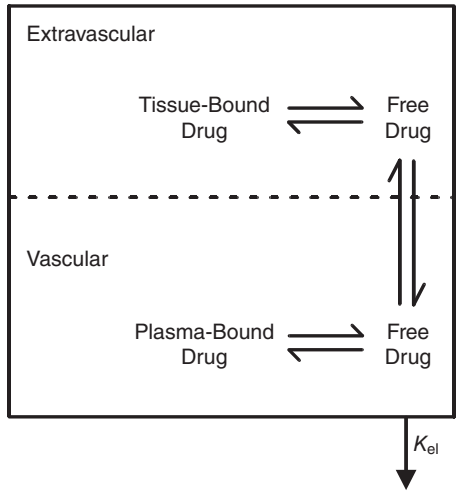

Fig. 10.11 Schematic of model of extravascular and intravascular tissue and plasma protein binding, respectively. The model assumes elimination (k_{el}) of free drug from the plasma space exclusively, and only free drug is able to traverse vascular epithelia.

ing a toxicokinetic model that specifically altered vascular volume in proportion to absorbed chemical.

10.5 PROTEIN AND TISSUE BINDING

It is typically assumed that drug binding to plasma proteins and extravascular tissues is constant and independent of concentration at the binding site. However, as presented in Chapter 5, protein binding is also saturable, and thus nonlinear pharmacokinetics may become operative. These changes have significant impact on the pharmacokinetics of drugs impacted. Fig. 10.11 depicts the two major binding sites affecting pharmacokinetic behavior: vascular plasma binding to albumin, and nonvascular tissue spaces. The mathematics of this process has been presented in Equations 5.1–5.4 and will not be further developed here. As presented in Equation 5.6, the final volume of distribution is a function of the free fractions of drug in the vascular and tissue compartments. As discussed in the development of both compartmental and noncompartmental models, one assumes that elimination exclusively occurs from the vascular space. As one can appreciate from the discussion of Michaelis–Menten kinetics, the situation when saturation occurs rapidly becomes complex.

10.6 NONLINEAR PHARMACOKINETICS: A CAVEAT

The theories developed in this chapter are based on the assumption of a one-compartment model, but it enjoys general application regardless of model structure. As can be appreciated, if multicompartmental models are operative, the mathematics becomes increasingly intractable. One caveat, however, should be raised here. In certain cases where single-

compartment kinetics is erroneously assumed, the estimation of K_m and V_{max} can be flawed. Since the elimination rate constant $k_{el} = V_{max}/K_m$, the estimate of V_{max} would be low because the estimated k_{el} would be lower than the actual value.

Sometimes it is difficult to distinguish between nonlinear processes and linear ones as they are manifested in the plasma concentration-versus-time profiles. An actual nonlinear mechanism (especially nonlinear binding) can be misinterpreted as a multiexponential or compartmental structure (e.g., an additional exponential term or compartment, respectively), or a nonlinear plasma protein binding influence could mistakenly be subsumed under in a Michaelis–Menten construct. Conversely, the distribution characteristics of a drug could be misinterpreted as one or more nonlinear phenomena. With the discovery of active drug transporters (e.g., P-glycoprotein [Pgp]) impacting both distribution and elimination, this is even more complex. Often it is prudent to invest in additional experimentation to separate and rule out certain model structures.

Normally, linear processes can be separated from nonlinear ones by analyzing various dosages with both bolus and infusion profiles, as discussed above. As will be repeatedly stressed in Chapter 14 on experimental design, it is often cost-effective to conduct pilot studies to help select the proper model. As is too often the case, the use of pharmacokinetics is judged erroneous when inconsistent results are obtained, when in reality the problem is often use of an inappropriate modeling strategy. A simple one-, two-, or noncompartmental analysis of single-dose plasma data is often not sufficient to define models for drugs that undergo extensive biotransformation or tissue binding. Thus, extrapolations using these approaches will neither be robust nor predict subsequent *in vivo* behavior. Similarly, when dealing with interspecies extrapolations, peculiarities in metabolism or binding may only occur in a single species, and without knowledge of these differences, erroneous extrapolations may be made. Simple multidose IV pilot studies may prevent these pitfalls.

ACKNOWLEDGMENT

The author acknowledges the contribution of Patrick Williams, who coauthored this chapter in the first edition of this text.

BIBLIOGRAPHY

The Bibliography listed in Chapter 7 should also be consulted for pharmacokinetic modeling of drugs undergoing nonlinear hepatic metabolism.

Berlin, C.M., and Schimke, R.T. 1965. Influence of turnover rates on the responses of enzymes to cortisone. *Molecular Pharmacology*. 1:149.

Chang, S.K., Dauterman, W.C., and Riviere, J.E. 1994. Percutaneous absorption of parathion and its metabolites paraoxon and p-nitrophenol administered alone or in combination: *in vitro* flow through diffusion cell system. *Pesticide Biochemistry and Physiology*. 48:56–62.

Cheng, H. 1991. A method for calculating the mean residence times of caternary metabolites. *Biopharmaceutics and Drug Disposition*. 12:335–342.

Cheng, H., and Jusko, W.J. 1988. Mean residence time concepts for pharmacokinetic systems with nonlinear drug elimination described by the Michaelis–Menten equation. *Pharmaceutical Research*. 5:156–164.

Cheng, H., and Jusko, W.J. 1989. Mean residence time of drugs showing simultaneous first-order and Michaelis–Menten kinetics. *Pharmaceutical Research*. 6:258–261.

Cheng, H., and Jusko, W.J. 1990. Mean residence times of multicompartmental drugs undergoing reversible metabolism. *Pharmaceutical Research*. 7:103–107.

Gibaldi, M., and Perrier, D. 1982. *Pharmacokinetics*, 2nd Ed. New York: Marcel Dekker.

Jusko, W.J., Koup, J.R., and Alvan, G. 1976. Nonlinear assessment of phenytoin bioavailability. *Journal of Pharmacokinetics and Biopharmaceutics*. 4:327–336.

Michaelis, L., and Menten, M.I. 1913. Die Kinetik der Intertinwirkung. *Biochemische Zeitschrift*. 49:333–369.

Qiao, G.L., and Riviere, J.E. 1995. Significant effects of application site and occlusion on the pharmacokinetics of cutaneous penetration and biotransformation of parathion *in vivo* in swine. *Journal of Pharmaceutical Sciences*. 84:425–432.

Qiao, G.L., Williams, P.L., and Riviere, J.E. 1994. Percutaneous absorption, biotransformation and systemic disposition of parathion *in vivo* in swine. I. Comprehensive pharmacokinetic model. *Drug Metabolism and Disposition*. 22:459–471.

Qiao, G.L., Brooks, J.D., Baynes, R.E., Monteiro-Riviere, N.A., Williams, P.L., and Riviere, J.E. 1996. The use of mechanistically defined chemical mixtures (MDCM) to assess mixture component effects on the percutaneous absorption and cutaneous disposition of topically exposed chemicals. I. Studies with parathion mixtures in isolated perfused porcine skin. *Toxicology and Applied Pharmacology*. 141:473–486.

Riviere, J.E., Brooks, J.D., Williams, P.L., and Monteiro-Riviere, N.A. 1995. Toxicokinetics of topical sulfur-mustard penetration, disposition and vascular toxicity in isolated perfused porcine skin. *Toxicology and Applied Pharmacology*. 135:25–34.

Sedman, A.J., and Wagner, J.G. 1974. Quantitative pooling of Michaelis-Menten equations in models with parallel metabolite formation paths. *Journal of Pharmacokinetics and Biopharmaceutics*. 2:149.

St-Pierre, M.V., van den Berg, D., and Pang, K.S. 1990. Physiological modeling of drug and metabolite: disposition of oxazepam and oxazepam glucuronides in the recirculating perfused mouse liver preparation. *Journal of Pharmacokinetics and Biopharmaceutics*. 18:423–448.

Williams, P.L., and Riviere, J.E. 1995. A biophysically based dermatopharmacokinetic compartment model for quantifying percutaneous penetration and absorption of topically applied agents. I. Theory. *Journal of Pharmaceutical Sciences*. 84:599–608.

Williams, P.L., Thompson, D., Qiao, G.L., Monteiro-Riviere, N.A., Baynes, R.E., and Riviere, J.E. 1996. The use of mechanistically defined chemical mixtures (MDCM) to assess mixture component effects on the percutaneous absorption and cutaneous disposition of topically exposed chemicals. II. Development of a general dermatopharmacokinetic model for use in risk assessment. *Toxicology and Applied Pharmacology*. 141:487–496.

11 Physiological Models

with Teresa Leavens

All of the pharmacokinetic modeling strategies presented up to this point have assumed that the defining criteria for a compartment or kinetic space was an anatomically heterogeneous group of tissues that could be described by single-rate equations since the disposition of drug within these areas had homogeneous rates. In compartmental terms, drug in these spaces could be characterized by a specific volume of distribution (*Vd*) and pairs of intercompartmental microrate constants (k_{xy}/k_{yx}). Noncompartmental models made no assumptions about underlying anatomy nor physiology. The infrastructure of the compartments were based on rates and were not unique (recall Fig. 8.20 in Chapter 8 for the possible configurations of a two-compartment model).

11.1 INTRODUCTION

Physiologically based pharmacokinetic (PBPK) modeling builds models based on compartments that mirror the anatomical and physiological structure of the body. A PBPK model is constructed as a parallel series of organ compartments interconnected by the circulatory system as depicted in Fig. 11.1. Specific organs are included in the model based on their relative importance in determining drug disposition for the compound being studied. Organs with similar physical and biochemical properties are often grouped together (e.g., slowly perfused organs such as muscle, skin, and bone). Compartments are connected to one another by arterial and venous blood supplies. If the lung is included in a model, it is placed in series with the plasma compartment since it receives the total of cardiac output via the right heart, while the rest of the tissues receive the output from the left heart. Thus, all drug will circulate through the pulmonary circulation before entering the systemic circulation.

The route of administration is also included as input into the relevant compartment. In the scheme depicted, the compound distributes to red blood cells (RBC), the kidney, and the liver and, furthermore, is eliminated by the latter two organs. The model is structured to handle either oral or topical administration. Inhalational administration would include a lung compartment placed in series with the blood. All other sites of compound distribution are pooled into a general tissue compartment. Each tissue is modeled as being composed of plasma and interstitial and intracellular components.

It is important to reflect on the nature of these models for they are essentially an attempt to create a mathematical structure that quantitates the processes described in Fig. 2.1

Comparative Pharmacokinetics: Principles, Techniques, and Applications, Second Edition. Jim E. Riviere.
 ISBN: 978-0-813-82993-7

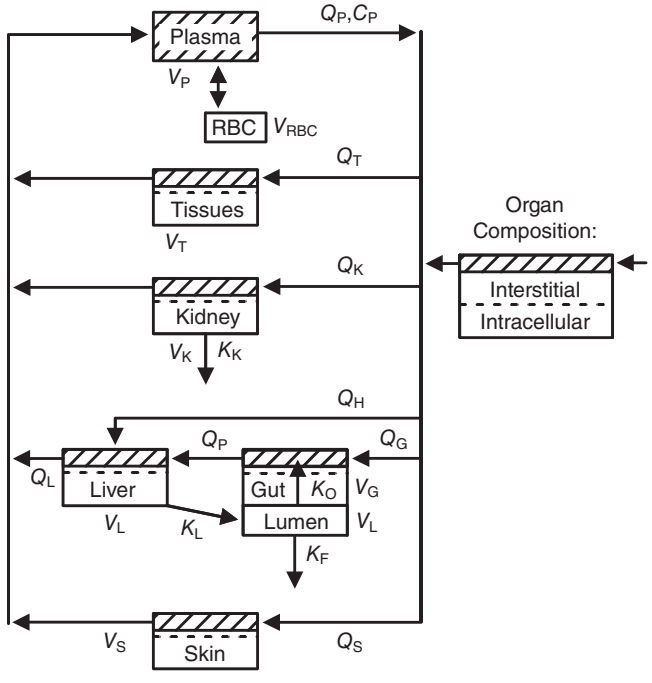

Fig. 11.1 Structure of a physiologically based pharmacokinetic (PBPK) model incorporating disposition in plasma, liver, kidney, skin, and gastrointestinal tract. Elimination from the body occurs from the kidney (K_K), liver (K_L) and gut lumen in feces (K_F). Oral absorption (K_0) is allowed. *V* refers to organ volumes of distribution and *Q* to organ plasma flows. RBC, red blood cell.

(see Chapter 2). All of the physiological factors that impact on drug distribution and elimination, discussed in Chapters 4–6, may be incorporated into the model. If a drug primarily distributes to the muscle, then it would be included as a tissue compartment. If the model were constructed to predict drug concentrations in a specific organ, that organ would be included. In most models, the liver and kidney are incorporated since their high plasma flow : tissue mass ratio coupled with their function as eliminating organs dictate that they are determining factors in predicting the overall disposition of the drug in the body.

The other major advantage of this approach is that many factors that can be experimentally assessed in a specific organ may be incorporated easily into that organ's disposition. PBPK models easily allow the incorporation of such data from *in vitro* systems. These include factors such as protein binding, active enzyme transport systems, local metabolism, and even pharmacodynamic (PD) effects on plasma flow. For example, if plasma and tissue protein binding were included, a component such as depicted in Fig. 10.11 (see Chapter 10) could be incorporated. The strategy is to describe these models on an individual organ basis and then link them, using plasma flow through the organs, to develop an overall model for disposition in the body.

11.2 MODEL CONSTRUCTION

The model is constructed by defining the rate of plasma flow (*Q*) and *Vd* of drug in each organ and then writing a mass balance equation describing the rate of drug input and output

for each organ. A common assumption for many PBPK models is that distribution between organs in the model is limited by blood flow to each organ. The basic form of these equations is based on the same principle as that of Fick's law of diffusion (described in Chapter 6) for determining the renal clearance of a drug based on blood flow and extraction ratio (E) previously introduced in Equation 6.2 (see Chapter 6). In this case, E is expressed in terms of an equilibrium ratio or partition coefficient (R) [$R = 1 - E$] as

$$R_{\text{tissue}} = R_{\text{t}} = C_{\text{tissue}} / C_{\text{blood}}, \tag{11.1}$$

where C_{tissue} (C_{t}) is the concentration of drug in the tissue and C_{blood} in the tissue venous blood at equilibrium. One uses hematocrit to convert between plasma (C_{plasma}) and blood concentrations. This is often referred to as venous concentrations (C_{ven}), and is analogous to the C_{p} encountered in previous chapters in which plasma concentrations were analyzed.

The differential equation describing the rate of change in drug concentration for any organ is simply the "rate in" minus the "rate out." For any noneliminating organ, this becomes

$$\begin{aligned} dC_{\text{t}} / dt &= (\text{Rate in}) - (\text{Rate out})\{\text{noneliminating organ}\} \\ &= [(Q_{\text{t}} \cdot C_{\text{p}}) - Q_{\text{t}} \cdot (C_{\text{t}} / R_{\text{t}})] / V_{\text{t}} \\ &= Q_{\text{t}} \cdot [C_{\text{p}} - C_{\text{t}} / R_{\text{t}}] / V_{\text{t}}, \end{aligned} \tag{11.2}$$

where V_{t} is the tissue volume that converts drug mass to concentration.

If the organ is an eliminating organ, then some fraction of drug will be removed through this process, thus reducing the venous output. This will be related to the clearance of the drug in that organ (Cl_{organ}) and C_{t}. This can be expressed as

$$dC_{\text{t}} / dt = \{Q_{\text{t}} \cdot [C_{\text{p}} - C_{\text{t}} / R_{\text{t}}] / V_{\text{t}}\} - C_{\text{t}} \cdot Cl_{\text{organ}} \{\text{eliminating organ}\}. \tag{11.3}$$

These equations describe the disposition of the drug in each organ component of the model. All that is now needed is to write an equation describing the rate of change of drug concentration in the plasma, which is the sum of the contributions of all organs:

$$dC_{\text{p}} / dt = \left[\text{Dose} + \sum Q_{\text{t}} \cdot (C_{\text{t}} / R_{\text{t}}) - \left(\sum Q_{\text{t}} \right) \cdot C_{\text{p}} \right] \Big/ V_{\text{vascular}}. \tag{11.4}$$

As discussed for distribution in Chapter 5, only free drug is distributed out of the vascular space into tissue, and thus C_{p} should ideally be expressed as the free concentration C_{f}. Equations in Chapter 5 describe plasma and tissue protein binding could be directly incorporated into these PBPK models if the drug's characteristics warrant it.

Similarly, if a drug is metabolized in an organ, the Michaelis–Menten concepts introduced in Chapter 7 and presented in Chapter 10 may be utilized in place of the Cl_{organ} term of Equation 11.3. For the liver ($t = l$), this would be

$$dC_{\text{l}} / dt = \{Q_{\text{l}}[C_{\text{p}} - C_{\text{l}} / R_{\text{l}}] - (V_{\max} \cdot C_{\text{f}}) / (K_{mf} + C_{\text{f}})\} / V_{\text{t}}, \tag{11.5}$$

where C_{f} is the free drug plasma concentration in the liver and K_{mf} is the Michaelis constant expressed in terms of free drug. Depending on the compound, the metabolite may be entered back into a parallel PBPK model that describes the metabolite's disposition in the

body; needed because the metabolite will have independent elimination and distribution characteristics from the parent or is excreted in the bile back to the gastrointestinal tract. The complexity of this compartment is dependent on how much data are available to handle biliary excretion, enterohepatic recycling, and first-pass metabolism. Some workers have modeled drug transit through the gut as a function of gastrointestinal content flow and absorption from each region of the digestive tract. This results in a more complex model, providing input into the portal vein. The physiological basis for some of these models was presented in Chapter 7, in which the hybrid PBPK model was introduced in Fig. 7.5.

In a PBPK model, the overall volume of distribution *Vd* is easily related to the sum of the *Vd* of plasma ($V_{vascular}$, V_p) and all tissues volumes (V_t), or

$$Vd_{ss} = V_p + \sum V_t \cdot R_t. \tag{11.6}$$

Finally, if absorption occurs in an organ, a term relating the administered dose to the amount and rate of absorption must also be included. When this occurs after oral absorption, the equation for the liver is often written in terms of absorption from the portal vein as a positive term adding drug input to the liver ($k_a \cdot F \cdot D$).

For topical delivery, a simple absorption rate may be added to the skin compartment, or the skin may be modeled in terms of stratum corneum (SC) penetration and dermal distribution. Our laboratory has used the output flux from the isolated perfused skin flap model to serve as the skin compartment of a PBPK model (recall Fig. 9.6 in Chapter 9), with the complexity of the skin component reflecting the design of the specific experiment. In fact, this is a strength of this modeling approach, for *in vitro* organ studies may often be directly used in a whole-body model. Isolated perfused livers are often used to define the Michaelis–Menten kinetics of a drug. Some modeling systems administer volatile drug via inhalation, obtain data on the rate of chemical uptake from the inspired air, and then collect tissue samples after equilibrium has occurred. To solve these models, air-to-tissue partition coefficients are determined.

For most tissues, equilibration among the plasma, interstitial fluid, and cellular spaces is assumed to be rapid, and thus the V_t and R become a composite estimate for that organ. This could also be assessed *in situ* by use of microdialysis probes to directly assess interstitial fluid concentrations. If diffusional barriers exist (organ is membrane limited rather than flow limited as assumed above), or if extensive tissue binding occurs (e.g., consider Chapter 10, Fig. 10.11 again), then such organs can be modeled with appropriate equations. The description of tissue concentration as being composed of vascular, extravascular, and tissue components is well handled by PBPK models for, as stressed in Chapter 8 on compartmental models, tissue concentrations may not correlate directly to a peripheral compartment prediction since they are actually composed of multiple compartments. In a PBPK model, this integration is implicit to the model. As an example of nonflow-limited behavior, if diffusion from plasma to a tissue compartment is rate limiting, the plasma and tissue concentrations are modeled as separate compartments with uptake from the plasma into the tissue as a product of permeability, diffusion surface area, and concentration driving force. Perfusion- and permeability-limited tissue distribution was conceptually introduced in Chapter 2 as illustrated in Fig. 2.7.

In most cases, only specific organs are of interest and sampled in any study; the remainder are grouped as a general tissue compartment. If tissues composing this group have heterogeneous kinetic behavior for the compound being studied, two compartments may

be added, reflecting this kinetic difference (e.g., slowly and rapidly equilibrating). In many cases, a specific tissue may be added because it is the target tissue for the drug of concern even if it has a minor influence on the total disposition of the drug in the body.

11.3 ANALYSIS

A complete PBPK model is then constructed using the differential equations for the plasma compartment and each tissue component modeled. The complete model thus consists of a series of differential equations, written in terms of C_p, that must be simultaneously solved. This allows all compartments to be linked to one another. The data required to solve these are the C_p-versus-time data, as well as estimates of organ plasma flows, organ distribution volumes, and partition coefficients for the drug in each organ. Recall that these equations assume that equilibrium has occurred within each organ, such that C_{ven} reflects C_t. One does not "curve-fit" plasma and tissue data in a PBPK model experiment; rather, one conducts experiments to estimate these components and then simulates the entire model to assess how well the predicted concentration profiles in plasma, urine, and tissues match observed data. *This is conceptually very different from all of the previous modeling approaches discussed*. The models are simulated using various software packages for solving ordinary differential equations, including ACSLX™ (Aegis Technologies Group, Inc., Huntsville, AL), Berkeley Madonna™ (University of California at Davis, CA), MATLAB® (The Mathworks, Inc., Natick, MA), and others. All of these modeling approaches use numerical integration algorithms embedded in the software to calculate time estimates of each component equation and reiterate until an optimal model solution is achieved. PBPK models had their roots in chemical engineering, and thus many approaches use software developed from this discipline.

The techniques used to obtain these parameter values are varied and determine the experimental design. Organ blood flows and volumes are usually taken from historical sources such as those tabulated in Table 11.1. The sum of all organ blood flows (excluding the lung, which, recall, is in series with the systemic circulation and thus has a total pulmonary blood flow equal to the cardiac output) must equal the overall cardiac output of the animal. In other cases, blood flows may be directly determined using microsphere, laser Doppler velocimetry (LDV), or tracer dilution techniques. In contrast, the sum of all tissue volumes may be less than total body weight since some tissues are not perfused (e.g., fur, teeth). Again, the lung is not included in these calculations. The benefit of using data collected from the same animals as in the experimental study is to reduce variability, as individual differences in any of these major parameters will confound the result. Organs with large blood flows or distribution volumes will have more influence on the overall fit to the model predictions than those with smaller flows or volumes making the overall goodness of fit of the model heavily dependent on these organs (e.g., liver, kidney). Plasma flow can be calculated from the fraction of blood as hematocrit.

One piece of data needed for a PBPK model are estimates of R_t, for which there are a number of approaches. The most robust method is to use an intravenous infusion to achieve steady-state blood concentrations. The animals are then sacrificed, and R for noneliminating organs is simply as defined in Equation 11.1 above. Alternatively, if a volatile compound is being studied, tissue : air and blood : air partition coefficients may be experimentally determined *in vitro*, with their quotient being used as the estimate of $R_t(C_t : C_a \div C_p : C_a)$, where C_t, C_p, and C_a are tissue, plasma, and air concentrations, respectively. Intravenous

Table 11.1 Representative physiological parameters for four species.[a]

Parameter	Mouse	Rat	Dog	Human
Body weight (kg)	0.025[b]	0.25[b]	10.5[c]	70.0[b]
Volume fraction (% BW)				
Adipose	7.0	7.0	15.0	21.4
Bone	10.7	7.3	8.1	14.3
Brain	1.7	0.6	0.8	2.0
Gastrointestinal tract				
Contents	5.7	5.0	4.3	1.4
Emptied	4.2	2.7	3.7	1.7
Heart	0.5	0.3	0.8	0.5
Kidneys	1.7	0.7	0.5	0.4
Liver	5.5	3.4	3.3	2.6
Lungs	0.7	0.5	0.8	0.8
Muscle	38.4	40.4	45.7	40.0
Skin	16.5	19.0	9.1	3.7
Blood	4.9	7.4	8.2	7.9
Cardiac output (L/h)	0.84	6.62	176.1	312.0
Blood flow rates (% Cardiac output)				
Adipose[d]	7.0	7.0	3.5	5.0
Bone[d]	12.2	12.2	3.77	5.0
Brain	3.3	2.0	2.0	12.0
Heart	6.6	4.9	4.6	4.0
Kidneys	9.1	14.1	17.3	19.0
Liver	16.2	17.5	29.7	25.0
Hepatic artery	2.0	2.4	4.6	19.0
Portal vein	14.1	15.1	25.1	6.0
Lungs	0.5	2.1	8.8	2.5
Muscle	15.9	27.8	21.7	17.0
Skin	5.8	5.8	6.0	5.0
Alveolar ventilation (L/h)	1.75	7.94	145.5	210.0

[a]Except for body weights, values are from Brown et al. (1997).
[b]Source of values: Arms and Travis (1988).
[c]Source of value: Andersen (1970).
[d]No data; assumed equal to rat.

dose bolus studies may also be used if simultaneous blood and tissue samples are collected for analysis after distribution pseudoequilibrium has occurred. Blood and tissue concentrations are then plotted on a Cartesian plot, and a constrained linear regression through the origin is used to fit the data. The slope of this line is used as the estimate of R_t for that tissue (Fig. 11.2). Severe deviations from linearity would be indicative of tissue binding or complex diffusion, which would require accounting for these phenomena in the differential equations for that organ. The value of R_t can also be estimated empirically from physicochemical properties of the drug and tissue (Schmitt, 2008). Finally, if no independent estimate of R_t is available, then the PBPK model itself may be used to vary R_t to determine the best fit to the data.

Many investigators use multiple doses of drugs to determine R_t to ensure that nonlinear behavior is not evident or, if it is present, to write equations that account for it. Whatever the method used to calculate ratios, R_t for an eliminating organ that has high intrinsic Cl_{organ} relative to Q_{organ} may be misleading. However, if clearance is low compared with Q_{organ}, the steady-state estimates are good approximations. Finally, R_ts calculated for one species

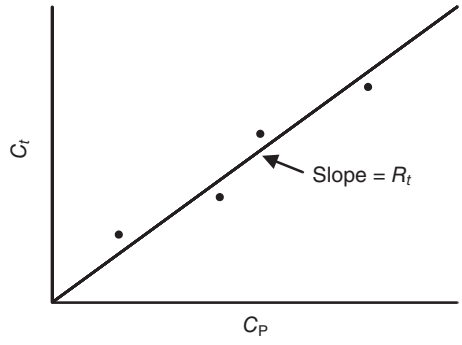

Fig. 11.2 Estimation of effective tissue : blood partition coefficients (R_t) at steady-state using a C-versus-C_p plot.

may not always be applicable to another because of species differences in tissue composition. This question may be assessed using some of the allometric principles covered in Chapter 18. The prudent investigator will determine these parameters for the species of interest to reduce extrapolation error, although PBPK modeling is probably the best approach to interspecies pharmacokinetics available at this point.

Tissue and plasma protein binding may be experimentally determined by the methods outlined in Chapter 5. As mentioned earlier, estimates of V_{max} and K_m may be efficiently determined using many *in vitro* tissue preparations. The nature of the elimination of the drug by the kidney could be assessed using many of the principles presented in Chapter 6.

The final result of a PBPK exercise is a properly parameterized model that adequately fits all of the observed data. The output of such a model is a list of *R*s and simulated versus observed concentration–time (C-T) and tissue-versus-time profiles, as simulated for a hypothetical drug in Fig. 11.3. Note that the drug concentrations vary in magnitude as a function of the tissue, with liver and kidney typically showing the highest values. In this example, there is a peak in the muscle and skin profiles, indicating the time required to reach distribution equilibrium, a slower process for skin in this example. If the model does not reasonably predict concentrations for a specific organ, the structure of the equations for that compartment must be investigated. If a lack of fit occurred in a primary organ such as the liver or kidney, the entire model would be unsatisfactory since they have such a large influence on overall disposition.

Most often the problem resides in an inappropriate or nonlinear R_t, tissue binding, or diffusion-limited distribution. Various hybrid models could be constructed to address this problem by using empirical functions for R_t obtained by fitting equation to the *C*-versus-C_p data plots. The nature of these functions could then help define the type of processes needed to be incorporated into the PBPK model. These could include nonlinear equations such as described in Chapter 10 for metabolism but instead parameterized for saturable transport processes.

11.4 ADVANTAGES

The most obvious advantage to the PBPK approach is that the model is based on both anatomical and physiological reality. It is a very powerful technique since C-T profiles can

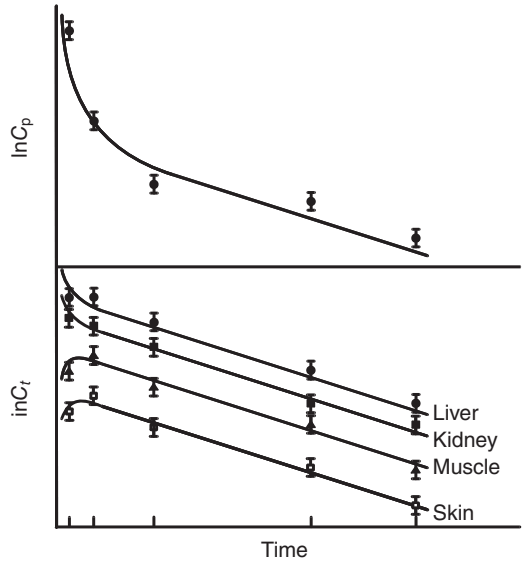

Fig. 11.3 Observed versus model-predicted (mean ± SEM) concentration-versus-time profiles of drug in all organs modeled using a PBPK model structured according to Fig. 11.1.

be simulated in different tissues of interest. It is also evident that interspecies differences in drug disposition can be easily tested by changing the organ-related parameters listed in Table 11.1, running a simulation and comparing the predictions against limited experimental data points. If the fit is reasonable, then one may be assured that no major species-specific factors are involved in the disposition process. Alternatively, one can easily incorporate *in vitro* data into the model to improve fit. These models also allow one to use experimentally simpler *in vitro* systems to assess impact on *in vivo* disposition by inserting the *in vitro* system directly into a model.

Another major advantage is that if a properly constructed PBPK model is developed, then it can serve as the pharmacokinetic component of a so-called mechanistic pharmacokinetic–pharmacodynamic (PK-PD) model for drug action as each organ compartment in a PBPK model is ideal for modeling the so-called biophase where drug action occurs.

The other major advantage to PBPK models is that the effects of altered physiology are easily simulated by just changing the organ parameters in a model. This type of modeling has been extensively used in cancer chemotherapy to target drugs specifically to tumor sites. It is also a useful tool to extrapolate rodent data to humans for toxicology risk assessment. The limitations to its widespread adoption are based on the extensive data required to adequately create a model and on difficulties with assessing statistical properties of fit and interindividual differences. Finally, these models may be linked to PD effect models (see Chapter 13) to derive PB-PK-PD models. The advantage to this approach is that the tissue in which the receptors for activity are located may be specifically modeled as the biophase or effect compartment, making PD linkages easier to construct and physiologically more realistic.

11.5 APPLICATION TO VETERINARY MEDICINE

A number of workers have begun to utilize PBPK models in problems directly relevant to veterinary medicine. Models for oxytetracycline in sheep (Craigmill, 2003), sulfamethazine in swine (Buur et al., 2005, 2006), and melamine in pigs and rats (Buur et al., 2008) have been described. This latter work illustrates the power of such models in the face of sparse data where estimates of tissue deposition were possible by using disparate data in pigs and rats to estimate oral absorption, renal deposition, and tissue withdrawal times of this toxicant. Fig. 11.4 illustrates the range of model complexity possible depending on both available data and modeling needs. The sulfamethazine model was data rich and in addition to including multiple organs, biotransformation via hepatic acetylation was also included. This model then served as the basis for including probabilistic functions to describe interanimal variability based on components of the model (e.g., independent estimates of variation in hepatic blood flow, protein binding). This model was then used to make population predictions for withdrawal time determinations. In contrast, the melamine model was designed to take into account minimal data available in the target species swine by using a PBPK model to link published rat data so that withdrawal time estimates for emergency decontamination of swine could be obtained. Since melamine is primarily cleared from the

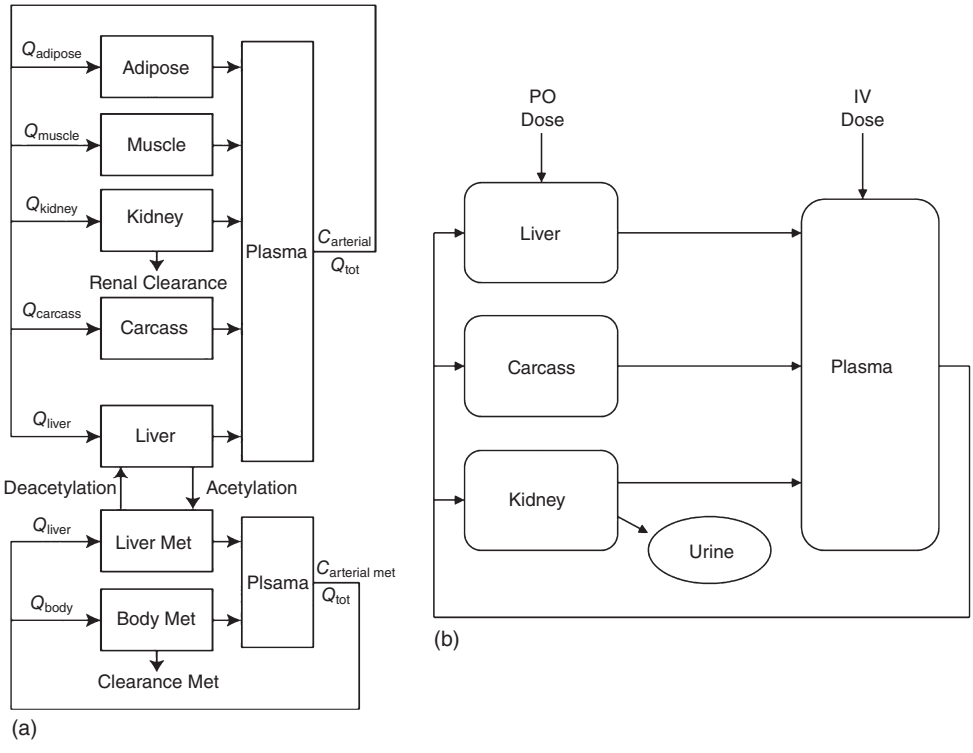

Fig. 11.4 PBPK models of sulfamethazine and melamine deposition in swine illustrating the range in levels of complexity possible depending on available data and model needs. (a) Sulfamethazine PBPK model including multiple sampled tissue compartments and metabolic biotransformation. (b) Melamine contaminant model designed to link available swine and rat data.
Source: Adapted from Buur et al. (2005, 2006, 2008).

body by the kidney, this approach was acceptable. The structure of models required to study nanomaterial deposition in the body have also begun to be studied since tissue uptake and elimination pathways are significantly different than that seen for diffusing organic chemicals (Lee et al., 2009). Such references should be consulted for further details on how such models are implemented.

These examples illustrate the underlying theme of this textbook, that pharmacokinetic models are tools to quantify biological processes. Depending on the amount of data needed and the precision of the prediction required, models can vary greatly in complexity. PBPK models are data intensive, but in some cases as for melamine, they can provide a physiologically relevant framework into which disparate data sources can be compared and integrated to solve immediate problems at hand. They also are ideal to develop biologically relevant interspecies models, a major need in comparative and veterinary pharmacology.

11.6 AN APPLICATION APPLIED TO A HYBRID MODEL

Now that the primary types of pharmacokinetic models have been presented, it is instructive to see how these various approaches can be combined using the basic construct of a PBPK model. We will close this chapter with an example of dermal absorption used by our laboratory. In the case of topical drug delivery, diffusion is the primary rate-limiting process governing drug movement across the SC and through the avascular regions of the epidermis and basement membrane zone. However, once the drug is in the dermal domain, flow-dependent vascular uptake predominates. The approach presented was necessary for certain transdermal drugs because both diffusion-limited and perfusion-limited scenarios may occur. PBPK models are better suited to describe flow-dependent processes, while compartmental schemes are often ideal to handle diffusion-limited disposition.

To follow up on the development of skin models previously presented in this book, we will describe a "hybrid" model, in which a compartmental scheme is used to describe the disposition in the epidermis, and a flow-limited physiologically based model is used to link this to the systemic circulation. We have used such a strategy (see Fig. 11.5) to describe drug disposition within isolated perfused skin flaps after arterial drug administration. A version of this model was previously presented as the "skin output" component in Fig. 9.6 (see Chapter 9). As one can see, this scheme also can be easily substituted for the skin component of Fig. 11.1 as it is constructed with arterial inputs and venous output fluxes. This model was constructed to study cisplatin disposition, which demonstrated a membrane-limited disposition within skin and extensive nonreversible covalent tissue binding, modeled here as a slowly equilibrating compartment. The volumes of the vascular compartments were independently determined using dual radiolabeled inulin/albumin infusion studies and analyzing these data using noncompartmental methods presented in Chapter 9. Similar studies were done to model drug-induced changes in capillary permeability (albumirilinulin volumes) when drugs induced vascular changes.

The absorption component may also be included to cover transdermal delivery. In this case, the output from this model assumes no arterial recirculation and thus is represented as a drug flux into the systemic model as depicted in Fig. 9.6 (see Chapter 9). Note the difference in the model structure for skin in Fig. 11.5, which is based on vascular flux into and out of the dermis, versus Fig. 9.6, which only allows unidirectional flux out of skin. However, if extensive redistribution occurs back to the skin, the elevated arterial drug concentrations may affect these processes, a scenario very difficult to account

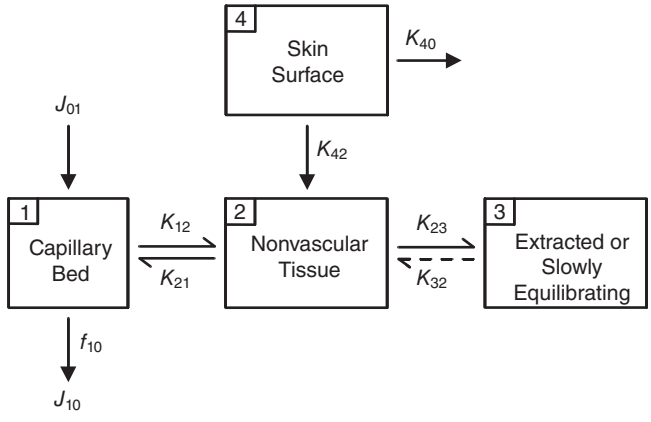

Fig. 11.5 Hybrid compartmental/PBPK model for drug absorption and distribution in the skin. Note the similarity to that presented in Fig. 9.6 (see Chapter 9) if arterial fluxes into the skin are assumed negligible ($J_{01} \cong 0$).

for in other modeling schemes. This is especially critical when drug has an affinity for the skin.

The true absorption profile of a compound is also dependent on the solvent in which it is dosed. By again using a compartmental scheme to develop this model, compound flux into and through skin may be specifically linked to relevant biophysical properties of the skin and penetrating compound, links that require some of the nonlinear models presented in Chapter 10. Such a model is structured as shown in Fig. 11.6.

The compartments on the left represent the solvent; and the rest represent the primary compound of interest. This flux is then modeled using a variant of Fick's law of diffusion (Eq. 2.1, Chapter 2) rewritten to reflect a variable diffusion "constant" and the experimental data available in our studies. Intercompartmental transfer rates are constants, except for those designated as functions of t by $k_{ij}(t)$. $J_{92}(t)$ is a mass transfer function (flux), and is defined as

$$J_{92}(t) = \{A \cdot D(t)[K_{sv} \cdot C_v(t) - K_{sw} \cdot C_T(t)]\}/L, \tag{11.7}$$

where A = area dosed; $D(t)$ = effective time-dependent diffusion coefficient that is a function of the inverses of the amounts of solvent (vehicle) (compartment 23) and solute (compartment 9) in SC; K_{sv} = SC/vehicle partition coefficient; K_{sw} = SC/water partition coefficient; $C_v(t) = M_4(t)/V_4(t)$ = surface drug concentration (compartment 4); $C_T(t) = M_2(t)/V_2(t)$ = drug concentration in viable epidermis (compartment 2); and L = length of path followed by diffusing molecules.

As presented in Chapters 3 and 4, the SC is generally the rate-limiting diffusional medium in percutaneous penetration and is kinetically very complex. A simple first-order rate constant reflecting a constant D lacks the generality to address all but very specific experimental designs. In response to this complexity, instead of a rate constant describing transfer of drug from compartment 9 (SC) to compartment 2 (viable epidermis), this model assigns a nonlinear flux. As discussed in Chapter 4, vehicles may alter intercellular lipid fluidity, which would change the drug's permeability constant. Vehicle to SC partition coefficients were determined by experimentally measuring vehicle-to-water and water-to-

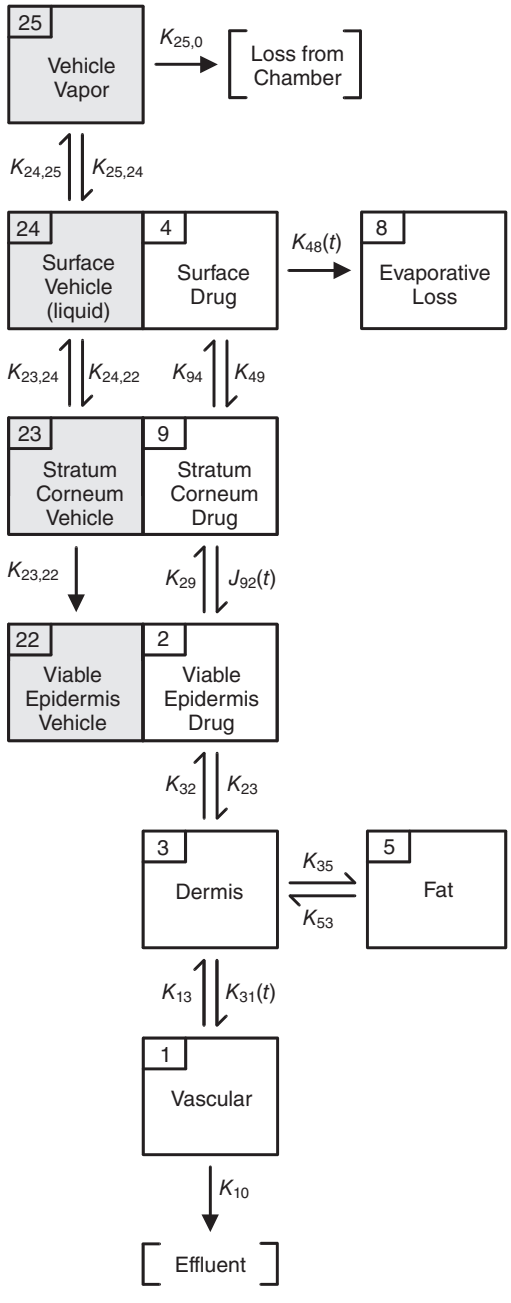

Fig. 11.6 Hybrid compartmental PBPK model for drug and vehicle absorption and distribution in the skin. The compartments on the left (shaded) represent solvent/vehicle; those on the right represent the solute or compound of interest. The k_{ij} or k_{ji}, denote intercompartmental transfer rate constants between compartment i and compartment j, while the $k_{ij}(t)$ denote nonlinear mass transfer rate functions. The two nonlinear rates defined are $k_{48}(t)$ and $k_{31}(t)$ for processes of evaporation of solute and dermal absorption of solute, respectively. $J_{92}(t)$ describes flux (mass/time) of solute from compartment 9 (stratum corneum) to compartment 2 (viable epidermis). This is a dynamic function of relative concentrations in compartments 4 (surface) and 2, and a function of the dynamic effective diffusion coefficient, which is in turn a function of amounts of solvent and solute in stratum corneum (compartments 23 and 9, respectively).

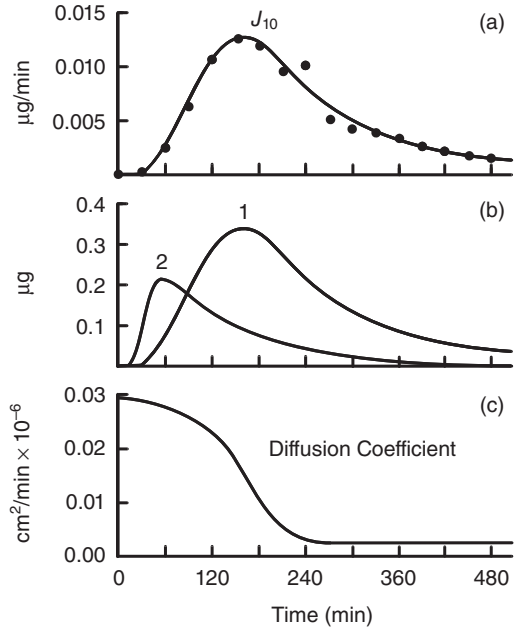

Fig. 11.7 Results of application of the model of Fig. 11.5 to data obtained from a study of percutaneous penetration and absorption of phenol following topical application of phenol in ethanol to the isolated perfused porcine skin flap. (a) Predicted (line) and measured (solid circles) venous flux (μg/mm) of phenol from the IPPSF; (b) predicted mass (μg) profiles in compartments 1 (capillary space under dosed area) and 2 (viable epidermis); (c) simulated effective diffusion coefficient (cm^2/min) profile.

SC partitioning and then applying a ratio approach similar to that earlier described for estimating the R_t from partition coefficients of volatile chemicals. Nonlinear rate functions of time were also assigned to two other intercompartmental rates in this model:

$$k_{48}(t) = s \cdot e^{-qt}, \tag{11.8}$$

where $k_{48}(t)$ is the time-dependent rate from compartment 4 (surface) to compartment 8 (surface loss, or evaporation) and s and q are constants, and

$$k_{31}(t) = \alpha \cdot p(t), \tag{11.9}$$

where $k_{31}(t)$ is the time-dependent rate from compartment 3 (dermis) to compartment 1 (vascular space or capillary beds), α is a constant, and $p(t)$ is the involved capillary surface area (i.e., the effective surface area of exchanging capillaries introduced in Chapter 9 on discussion on Eq. 9.34). The surface evaporation rates were independently estimated in separate skin experiments. Fig. 11.7 illustrates a simulation of this model with phenol in ethanol, showing calculated versus observed isolated perfused porcine skin flap (IPPSF) venous flux profiles, simulated profiles for compartments 1 and 2, and the calculated time-dependent diffusion coefficient, $D(t)$, profile.

The use of such a hybrid model allows one to probe the effects of solvent on the penetrating kinetics of a topically applied drug as well as to directly incorporate vascular changes

detected as the experiment progresses. This model is fit to the data by iterations much as was described above for PBPK models, with the goodness of fit judged by how well the model predicts drug concentrations in all compartments sampled. The use of an *in vitro* experimental tool such as the IPPSF allows cutaneous efflux profiles to be simultaneously modeled with SC concentrations, skin depth of penetration data, and complete mass balance data collected in a single experiment. The predictions of this model may then be tested in a systemic pharmacokinetic experiment based on how well the input flux matches the observed C-T profile. These models are used as tools to investigate the underlying biology of chemical disposition in skin, and to study the effects of chemical enhancers on the absorption kinetics of transdermal drugs. As is clearly seen in this example, no one approach (compartmental, noncompartmental, PBPK) is optimal for all biological situations. However, if one understands the basic assumptions, the approaches can easily be combined to facilitate the description of the underlying biology, the true goal of any pharmacokinetic study.

BIBLIOGRAPHY

Andersen, A.C. 1970. Introduction. In: Andersen, A.C. (ed.), *The Beagle as an Experimental Dog*. Ames: Iowa State University Press, pp. 309–321.

Andersen, M.E. 1989. Tissue dosimetry, physiologically based pharmacokinetic modeling, and cancer risk assessment. *Cell Biology and Toxicology*. 5:405–416.

Andersen, M.E. 1991. Physiological modelling of organic compounds. *Annals of Occupational Hygiene*. 35:309–321.

Arms, A.D., and Travis, C.C. 1988. *Reference Physiological Parameters in Pharmacokinetic Modeling*. EPA 600/6-88/004. Washington, DC: U.S. Environmental Protection Agency.

Barton, H.A., Chiu, W.A., Woodrow Setzer, R., Andersen, M.E., Bailer, A.J., Bois, F.Y., Dewoskin, R.S., Hays, S., Johanson, G., Jones, N., Loizou, G., Macphail, R.C., Portier, C.J., Spendiff, M., and Tan, Y.M. 2007. Characterizing uncertainty and variability in physiologically based pharmacokinetic models: state of the science and needs for research and implementation. *Toxicological Sciences*. 99:395–402.

Bernareggi, A., and Rowland, M. 1991. Physiologic modeling of cyclosporin kinetics in rat and man. *Journal of Pharmacokinetics and Biopharmaceutics*. 19:21–50.

Bischoff, K.B. 1980. Current applications of physiological pharmacokinetics. *Federation Proceedings*. 39:2456–2459.

Bischoff, K.B. 1986. Physiological pharmacokinetics. *Bulletin of Mathematical Biology*. 48:309–322.

Brown, R.P., Delp, M.D., Lindstedt, S.L., Rhomberg, L.R., and Beliles, R.P. 1997. Physiological parameter values for physiologically based pharmacokinetic models. *Toxicology and Industrial Health*. 13:407–484.

Buur, J.L., Baynes, R.E., Craigmill, A.L., and Riviere, J.E. 2005. Development of a physiological based pharmacokinetic model for estimating concentrations of sulfamethazine in swine and application to prediction of violative residues in edible tissues. *American Journal of Veterinary Research*. 66:1686–1693.

Buur, J., Baynes, R., Smith, G., and Riviere, J.E. 2006. The use of probabilistic modeling within a physiological based pharmacokinetic model to predict drug residue withdrawal times in edible tissue: sulfamethazine in swine. *Antimicrobial Agents Chemotherapy*. 50:2344–2351.

Buur, J.L., Baynes, R.E., and Riviere, J.E. 2008. Estimating meat withdrawal times in pigs exposed to melamine contaminated feed using a physiologically-based pharmacokinetic model. *Regulatory Toxicology and Pharmacology*. 51:324–331.

Chiu, W.A., Barton, H.A., DeWoskin, R.S., Schlosser, P., Thompson, C.M., Sonawane, B., Lipscomb, J.C., and Krishnan, K. 2007. Evaluation of physiologically based pharmacokinetic models for use in risk assessment. *Journal of Applied Toxicology*. 27:218–237.

Clewell, H.J. III, and Andersen, M.E. 1994. Physiologically based pharmacokinetic modeling and bioactivation of xenobiotics. *Journal of Toxicology and Industrial Health*. 10:1–24.

Clewell, R.A., and Clewell, H.J. III. 2008. Development and specification of physiologically based pharmacokinetic models for use in risk assessment. *Regulatory Toxicology and Pharmacology*. 50:129–143.

Colburn, W.A. 1988. Physiologic pharmacokinetic modeling. *Journal of Clinical Pharmacology*. 28:673–677.

Craigmill, A.L. 2003. A physiological based pharmacokinetic model for oxytetracycline in sheep. *Journal of Veterinary Pharmacology and Therapeutics*. 26:55–63.

EPA. 2006. *Approaches for the Application of Physiologically Based Pharmacokinetic (PBPK) Models and Supporting Data in Risk Assessment (Final Report)*. EPA/600/R-05/043F. Washington, DC: U.S. Environmental Protection Agency.

Espie, P., Tytgat, D., Sargentini-Maier, M.L., Poggesi, I., and Watelet, J.B. 2009. Physiologically based pharmacokinetics (PBPK). *Drug Metabolism Reviews*. 41:391–407.

Gargas, M.L., Andersen, M.E., and Clewell, H.J. III. 1986. A physiologically based simulation approach for determining metabolic constants from gas uptake data. *Toxicology and Applied Pharmacology*. 86:341–352.

Gargas, M.L., Burgess, R.J., Voisard, D.E., Cason, G.H., and Andersen, M.E. 1989. Partition coefficients of low-molecular-weight volatile chemicals in various liquids and tissues. *Toxicology and Applied Pharmacology*. 98:87–99.

Gearhart, J.M., Mahle, D.A., Greene, R.J., Seckel, C.S., Flemming, C.D., Fisher, J.W., and Clewell, H.J. III. 1993. Variability of physiologically based pharmacokinetic (PBPK) model parameters and their effects on PBPK model predictions in a risk assessment for perchioroethylene (PCE). *Toxicology Letters*. 68:131–144.

Gelman, A., Bois, F., and Jiang, J. 1996. Physiological pharmacokinetic analysis using population modeling and informative prior distributions. *Journal of the American Statistical Association*. 91:1400–1412.

Gerlowski, L.E., and Jam, R.K. 1983. Physiologically based pharmacokinetic modeling: principles and applications. *Journal of Pharmaceutical Sciences*. 72:1103–1126.

Jones, H.M., Gardner, I.B., and Watson, K.J. 2009. Modelling and PBPK simulation in drug discovery. *The AAPS Journal*. 11:155–166.

Lee, H.A., Leavens, T.L., Mason, S.E., Monteiro-Riviere, N.A., and Riviere, J.E. 2009. Comparison of quantum dot biodistribution with a blood-flow limited physiologically based pharmacokinetic model. *Nano Letters*. 9:794–799.

Leung, H.W. 1991. Development and utilization of physiologically based pharmacokinetic models for toxicological applications. *Journal of Toxicology and Environmental Health*. 32:247–267.

Lipscomb, J.C., and Poet, T.S. 2008. In vitro measurements of metabolism for application in pharmacokinetic modeling. *Pharmacology and Therapeutics*. 118:82–103.

Loizou, G., Spendiff, M., Barton, H.A., Bessems, J., Bois, F.Y., Yvoire, M.B., Buist, H., Clewell, H.J. III, Meek, B., Gundert-Remy, U., Goerlitz, G., and Schmitt, W. 2008. Development of good modelling practice for physiologically based pharmacokinetic models for use in risk assessment: the first steps. *Regulatory Toxicology and Pharmacology*. 50:400–411.

Luecke, R.H., Wosilait, W.D., Pearce, B.A., and Young, J.F. 1994. A physiologically based pharmacokinetic computer model for human pregnancy. *Teratology*. 49:90–103.

Marzulli, E.N., and Maibach, H.I. 1996. *Dermatotoxicology*, 2nd Ed. Washington, DC: Taylor & Francis.

Ritschel, W.A., and Banerjee, P.S. 1986. Physiological pharmacokinetic models: principles, applications, limitations and outlook. *Methods and Findings in Experimental and Clinical Pharmacology*. 8:603–614.

Rowland, M. 1984. Physiologic pharmacokinetic models: relevance, experience, and future trends. *Drug Metabolism Reviews*. 15:55–74.

Schmitt, W. 2008. General approach for the calculation of tissue to plasma partition coefficients. *Toxicology In Vitro*. 22:457–467.

Spear, R.C., and Bois, F.Y. 1994. Parameter variability and the interpretation of physiologically based pharmacokinetic modeling results. *Environmental Health Perspectives*. 102(Suppl. 11):61–66.

Theil, F.P., Guentert, T.W., Haddad, S., and Poulin, P. 2003. Utility of physiologically based pharmacokinetic models to drug development and rational drug discovery candidate selection. *Toxicology Letters*. 138:29–49.

Thompson, C.M., Sonawane, B., Barton, H.A., DeWoskin, R.S., Lipscomb, J.C., Schlosser, P., Chiu, W.A., and Krishnan, K. 2008. Approaches for applications of physiologically based pharmacokinetic models in risk assessment. *Journal of Toxicology and Environmental Health. Part B, Critical Reviews*. 11:519–547.

Van der Merwe, S., Brooks, J.D., Gehring, R., Baynes, R.E., Monteiro-Riviere, N.A., and Riviere, J.E. 2006. A physiological based pharmacokinetic model of organophosphate absorption. *Toxicological Sciences*. 89:188–204.

Verotta, D., Sheiner, L.B., Ebling, W.E., and Stanski, D.R. 1989. A semiparametric approach to physiological flow models. *Journal of Pharmacokinetics and Biopharmaceutics*. 17:463–491.

Vinegar, A., Williams, R.J., Fisher, J.W., and McDougal, J.N. 1994. Dose-dependent metabolism of 2,2-dichloro-1,1,1-trifluoroethane: a physiologically based pharmacokinetic model in the male fisher 344 rat. *Toxicology and Applied Pharmacology*. 129:103–113.

Williams, P.L., and Riviere, J.E. 1995. A biophysically based dermatopharmacokinetic compartment model for quantifying percutaneous penetration and absorption of topically applied agents. I. Theory. *Journal of Pharmaceutical Sciences*. 84:599–608.

Williams, P.L., Carver, M.P., and Riviere, J.E. 1990. A physiologically relevant pharmacokinetic model of xenobiotic percutaneous absorption utilizing the isolated perfused porcine skin flap. *Journal of Pharmaceutical Sciences*. 79:305–311.

Williams, P.L., Brooks, J.D., Inman, A.L., Monteiro-Riviere, N.A., and Riviere, J.E. 1994. Determination of physiochemical properties of phenol, paranitrophenol, acetone and ethanol relevant to quantitating their percutaneous absorption in porcine skin. *Research Communications in Chemical Pathology and Pharmacology*. 83:61–75.

12 Dosage Regimens

The primary use of pharmacokinetics in a clinical setting is to calculate safe and effective drug dosage regimens for patients. These are generally based on target plasma drug concentrations that are believed to be therapeutically effective. The dose required to achieve and then maintain these target concentrations must be calculated using knowledge of the drug's pharmacokinetic (PK) parameters in the individual animals.

12.1 DOSAGE REGIMEN DESCRIPTORS

This concept is best addressed by visualizing the drug's concentration–time (C-T) profile after multiple dose administration, as depicted in Fig. 12.1. There are two descriptors of the dosage regimen that are important to describe a multiple-dose regimen. These are the dose (D) and dosage interval (τ). The dose is further classified as the initial or loading dose (D_L) required to rapidly achieve an effective plasma concentration, and the maintenance dose (D_M) needed to sustain these concentrations. The resulting profile is characterized by peak (Cp^{max}) and trough (Cp^{min}) plasma concentrations, which result after the animal has achieved a steady-state condition.

The shape of such a multiple-dosage regimen is dependent on the relationship between the $T_{½}$ of the drug and the length of the dosage interval, τ. Assuming that a single dose of drug is administered to an animal, the resulting C-T profile after extravascular administration will resemble that depicted in Chapter 8, Fig. 8.9 (plotted on a semilog C-T axis), which (plotted on a Cartesian C-T axis) is the first shaded profile in the left of Figs. 12.1 and 12.2. The area under the curve (AUC) of this C-T segment describes the quantity of drug cleared from the body (recall Chapter 8, Eq. 8.18). If a second dose of drug were given after the first dose was completely eliminated (e.g., approximately five $T_{½}$s as seen in Table 8.1), then this profile would be repeated, as depicted in Fig. 12.2. This dosage regimen, where τ is >>5 $T_{½}$, does not result in any drug accumulation in the body.

The peak and trough plasma concentrations of this multiple-dose regimen is the same as seen after a single dose, and Equations 8.15 and 8.28 (see Chapter 8) for an intravenous and extravascular dose, respectively, may be used to describe the profile. The dose required to achieve a specific peak concentration, or Cp^{max}, after administering a very rapidly absorbed preparation is obtained by rearranging the equation for volume of distribution (Eq. 8.14), which becomes

Comparative Pharmacokinetics: Principles, Techniques, and Applications, Second Edition. Jim E. Riviere.
 ISBN: 978-0-813-82993-7

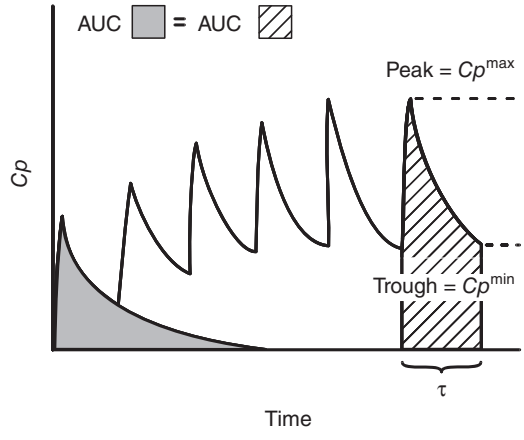

Fig. 12.1 Plasma concentration (*Cp*)-versus-time profile after multiple extravascular drug administrations demonstrating accumulation. Peak and trough concentrations represent those after achievement of steady state, at which the area under the curve (AUC) under a dosing interval τ (hatched area) is equal to that after a single dose (shaded area).

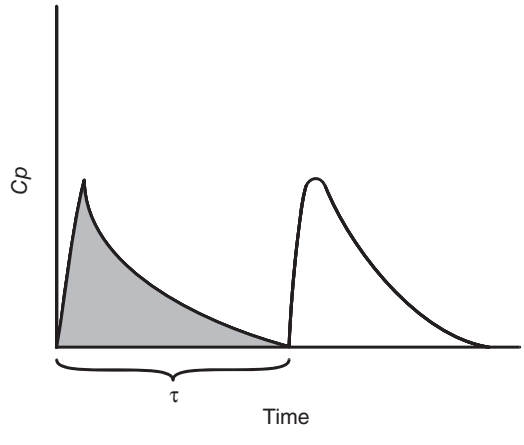

Fig. 12.2 Plasma concentration (*Cp*)-versus-time profile after multiple extravascular drug administration, with no accumulation resulting in independent pharmacokinetics described by two single-dose profiles.

$$\text{Dose} = (Cp^{\max}) \cdot Vd. \tag{12.1}$$

If the drug is not completely bioavailable (e.g., $F < 1$), then this equation is divided by the systemic availability F. For example, if 10 mg were the given intravenously (IV), and only half of this was absorbed after oral administration ($F = 0.5$), then 20 mg (D/F; 10/0.5) would be required to achieve the same plasma concentrations. Administering this dose at every τ will result in the same C-T profile characterized by Cp^{max} and a Cp^{min} of essentially zero.

However, the more likely scenario is that depicted in Fig. 12.1, in which a second dose is administered before the first dose is completely eliminated from the body. In this case, the drug concentrations will accumulate with continued dosing. This accumulation will stop or reach a steady state when the amount of drug administered at the start of each

dosing interval is equal to the amount eliminated during that interval. This can be appreciated since at steady state, the AUC under one dosing interval is equal to that after a single dose administration. In fact, steady state could be defined as the dosing interval in which the AUC for that interval is equal to the single-dose AUC. Administering repeated doses at a τ defined in this manner will continuously produce a C-T profile with the same peak and trough plasma concentrations.

12.2 PRINCIPLE OF SUPERPOSITION

This principle can be simply illustrated using a straightforward graphic approach. Fig. 12.3 illustrates this procedure. To simplify the presentation, assume that we have a drug with a *Vd* of 1 L given at a dose of 200 mg. This would result in a Cp^0 of 200 mg/L. If the $T_{½}$ is 5 h and τ also is 5 h, then 50% of the drug would be eliminated in one dosing interval, resulting in a trough concentration at 5 h equal to 100 mg/L. If a second dose is then administered, *Cp* now becomes 300 mg/L (100 + 200) and the trough after two doses becomes 150 mg/L (300/2). If this process continues, the peak and trough will approach their true steady-state values of a Cp^{max} equal to 400 and a Cp^{min} equal to 200 since at these concentrations, 200 mg would be eliminated during each dosing level, requiring 200 to be administered to replace this amount. Note that after five dosing intervals (25 h in Fig. 12.3), the peak and trough concentrations are at 98% of their steady-state levels, the expected value from Table 8.1.

This simple graphical approach, often referred to as the principle of superposition, may be used to plot the resulting C-T profile seen after any multiple dose administration. However, I believe its main strength lies in its use to visualize what actually happens after multiple drug administration. For example, if one wanted to rapidly achieve the steady-state concentrations, one could administer a loading dose (D_L) that would start this process at a *Cp* of 400 mg/L. This dose would be calculated using Equation 12.1 as

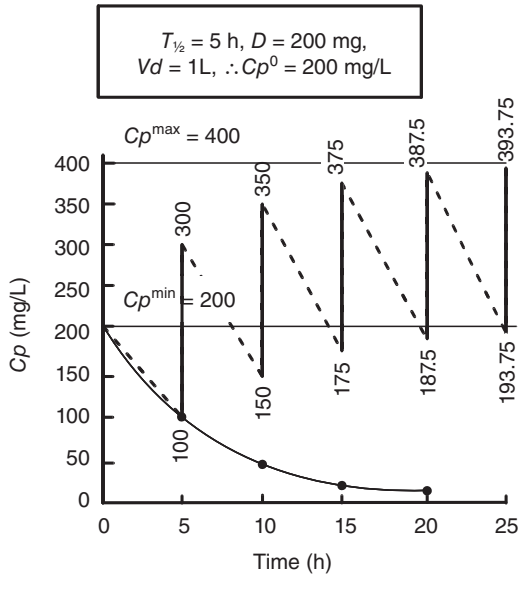

Fig. 12.3 Illustration of the principle of superposition and accumulation to steady state. (See text for full description.)

$$D_L = (400\ \text{mg/L})(1\ \text{L}) = 400\ \text{mg}$$

After one dosing interval, the trough concentration would now be 400/2 = 200 mg/L, and the maintenance dose (D_M) of 200 mg could be administered to immediately achieve the steady-state profile! The average concentration of this profile at steady state (Cp^{avg}) would be 300 mg/L ((400 + 200)/2). The final dosage regimen would be characterized as follows:

$$D_L = 400\ \text{mg}$$
$$D_M = 200\ \text{mg}$$
$$\tau = 5\ \text{h}$$
$$Cp^{max} = 400\ \text{mg/L}$$
$$Cp^{min} = 200\ \text{mg/L}$$

Recall from Chapter 8 that since log-linear decay (e.g., first-order kinetics) is governing this C-T profile, the average concentration obtained must be determined logarithmically; therefore,

$$Cp^{avg} = e^{(\ln 400 + \ln 200)/2} \cong 283\ \text{mg/L}$$

12.3 DOSAGE REGIMEN FORMULAE

This essentially is the strategy needed to calculate any multiple-dose regimen; unfortunately, in most cases, the numbers are not so easily obtained from a graphical analysis, and τ is not always equal to $T_{½}$. There are a series of simple formulae derived from the principles outlined in Chapter 8 that can be used to precisely derive these profiles. These equations are embedded into a number of software products.

The first is to determine Cp^{avg}, which is a function of Vd and the ratio $T_{½}/\tau$, where

$$\begin{aligned} Cp^{avg} &= [(1.44 \cdot F \cdot D)/Vd_{area}] \cdot [T_{½}/\tau] \\ &= [Cp^{max} - Cp^{min}]/[\ln(Cp^{max}/Cp^{min})]. \end{aligned} \tag{12.2}$$

Recalling the relationship between $T_{½}$, Cl_B, and Vd presented in Chapter 8, and rearranging Equation 8.20 ($1/Cl_B = 1.44\ T_{½}/Vd_{area}$), the first part of Equation 12.2 is now

$$Cp^{avg} = (F/Cl_B) \cdot (D/\tau). \tag{12.3}$$

The derivation of the second part of Equation 12.2 will be evident in the discussion that follows (by substituting Eqs. 12.9 and 12.12 solved for $1.44\ T_{½}/\tau$ and $F \cdot D/Vd_{area}$, respectively, in the first part of Eq. 12.2).

Another relationship becomes evident. We learned in Chapter 8 that Cl_B is D/AUC (Eq. 8.18), which allows Equation 12.3 to be algebraically expressed as $Cp^{avg} = (F) \cdot (\text{AUC})/\tau$. This relation quantitates the observation presented earlier that the AUC under any dosing

interval τ will always be the same when steady-state conditions are achieved. This is in fact the meaning of steady state.

12.3.1 Accumulation

Two factors that are important in designing dosage regimens also emerge from Equations 12.2 and 12.3. The ratio D/τ can be defined as the dosage rate and is the major determinant under the control of the clinician, which determines the amount of drug that will accumulate in the body. The ratio $T_{½}/\tau$ is a proportion relating the relative length of the dosing interval to the half-life of the drug.

If the inverse of this ratio is taken, the *relative dosage interval* ε may be defined as $\varepsilon = \tau / T_{½}$. As will be discussed later, these two ratios provide useful parameters to gauge the shape and height of the C-T profile produced by a tailored dosage regimen.

The primary factor governing the extent of drug accumulation in a multiple-dose regimen is the fraction of a dose eliminated in one dosing interval, termed f_{el}. This can be easily calculated by first determining the amount of drug remaining at the end of a dosing interval, f_r. We showed earlier that the amount of drug in the body at any time t is given by the exponential (Chapter 8, Eq. 8.7) relation $X = X_0\, e^{-kt}$. If one substitutes τ for t at the end of a dosing interval, then f_r is defined as

$$f_r = 1 - f_{el} = X_t / X_0 = e^{-k\tau} = e^{-\lambda\tau}, \tag{12.4}$$

where k is the fractional elimination constant or the relevant slope of the terminal phase (λ) of the C-T profile governing the disposition of the drug (Chapter 8, Table 8.3). Therefore,

$$f_{el} = 1 - f_r = 1 - e^{-\lambda\tau} = 1 - e^{-0.693(\tau / T_{½})} = 1 - e^{-0.693(\varepsilon)}. \tag{12.5}$$

(It is instructive when studying these relations to recall that 0.693 is the ln2, and 1.44 is 1/0.693.) Using f_{el}, the peak and trough concentrations may be calculated as

$$Cp^{max} = F \cdot D / (Vd_{area} \cdot f_{el}) \tag{12.6}$$

$$Cp^{min} = (Cp^{max}) \cdot (1 - f_{el}). \tag{12.7}$$

If these formulae are used to characterize the C-T profile in Fig. 12.3 ($D = 200$ mg, $Vd = 1$ L, $\tau = 5$ h, $T_{½} = 5$ h, $F = 1$), the following parameters could be calculated:

$$\lambda = 0.693/5 = 0.1386 \text{ h}$$

$$f_{el} = 1 - e^{-(0.1386)(5)} = 1 - e^{-0.693} = 1 - 0.5 = 0.5$$

$$Cp^{avg} = [(1.44)(200)(5)/(1)(5)] = 288 \text{ mg/L}$$

$$Cp^{max} = 200/(1)(0.5) = 400 \text{ mg/L}$$

$$Cp^{min} = (400)(1 - 0.5) = 200 \text{ mg/L}$$

The ratio of the fluctuation in Cp^{max} and Cp^{min} can be determined using an approach similar to the one used to derive Equation 12.4 from Equation 8.7 (see Chapter 8) but

instead calculate the ratio X_0/X_t, which removes the negative sign from the exponential term ($X_0/X_t = e^{\lambda t}$); therefore,

$$Cp^{\max} / Cp^{\min} = e^{0.693(\tau / T_{½})},$$

and thus

$$\ln Cp^{\max} / Cp^{\min} = 0.693\,\tau / T_{½} = 0.693\varepsilon. \tag{12.8}$$

The dosing interval (τ) required to keep *Cp* within a desired maximum and minimum window is obtained by solving for τ as

$$\tau = 1.44\,T_{½} \ln(Cp^{\max} / Cp^{\min}). \tag{12.9}$$

These extremely powerful relationships demonstrate that the magnitude of fluctuations in a C-T profile is directly related to the *relative* dosage interval ε. As either τ increases or $T_{½}$ decreases, this ratio will get larger and result in a greater fluctuation in drug concentrations. Again, using the law of exponentials ($e^{x} = 1/e^{-x}$), Equation 12.8 is equivalent to

$$Cp^{\max} / Cp^{\min} = 1 / e^{-0.0693\,\tau / T_{½}}. \tag{12.10}$$

However, we have seen from the rearrangement of Equations 12.4 and 12.5 that $e^{-0.0693\,\tau/T_{½}}$ is also equivalent to $1 - f_{el}$. Thus, this ratio can be written in a form preferred by some workers as

$$Cp^{\max} / Cp^{\min} = 1/(1 - f_{el}) = 1/f_{r}. \tag{12.11}$$

This ratio reflects the amount of accumulation that occurs in a multiple-dose regimen. In our example above, when the drug was dosed at an interval equal to the half-life, the accumulation at steady state was twofold.

12.3.2 Calculation of dosage regimens

Using these relationships, and rearranging Equation 12.6 to solve for dose, one can now derive the dosage formulae required to achieve a C-T profile with specified target peak and trough concentrations.

$$\begin{aligned} D_M &= [f_{el} \cdot Vd_{area} \cdot Cp^{\max}]/F \\ &= [Vd_{area} \cdot (Cp^{\max} - Cp^{\min})]/F \end{aligned} \tag{12.12}$$

$$\begin{aligned} D_L &= D_M / f_{el} \\ &= (Vd_{area} \cdot Cp^{\max})/F \end{aligned} \tag{12.13}$$

Equation 12.9 above is used to determine the appropriate τ. Thus, to construct a dosage regimen, the only parameters that are required are the Vd_{area} and $T_{½}$ (and hence λ or k_{el}) of the drug, which are needed to calculate f_{el}. If one is targeting only the average plasma concentration, then Equation 12.2 can be solved for dose as

$$\begin{aligned} D_M &= [(Cp^{avg} \cdot Vd_{area})/(1.44\,F)] \cdot [\tau / T_{½}] \\ &= [0.693(Cp^{avg} \cdot Vd_{area})/F)] \cdot [\tau / T_{½}] \\ &= (Cp^{avg} \cdot Cl_B \cdot \tau)/F. \end{aligned} \tag{12.14}$$

As discussed earlier, the magnitude of f_{el} is a good estimate of the degree of fluctuation that occurs between the peak and trough concentration at steady state. As the ratio of $\tau/T_{½}$ or ε approaches zero in Equation 12.5, f_{el} approaches zero, and the amount of fluctuation in a dosage interval is minimal. (This can also be seen by examining Eqs. 12.8–12.11.) In contrast, when this ratio is large, f_{el} approaches 1, and the peak and trough concentrations have a large degree of fluctuation.

When f_{el} is very small, Cp^{max} approaches Cp^{min} since f_{el} approaches zero when τ approaches zero (see Eq. 12.5 and recall that the limit of e^{-x} as $x \rightarrow 0 = 1$). The resulting C-T profile becomes characterized by Cp^{avg}. This occurs when the drug is given as an intravenous infusion. *The rate of an intravenous infusion (R_0 mg/mm) is essentially an instantaneous dose rate and is equivalent to D/τ.* When R_0 is inserted in Equation 12.3 for D/τ and F is set equal to 1 (since an intravenous dose is by definition 100% systemically available),

$$Cp^{avg} = R_0 / Cl_B \tag{12.15}$$

$$R_0\,(\text{mg/min}) = Cp^{avg} \cdot Cl_B, \tag{12.16}$$

which is identical to Equation 8.21 (see Chapter 8) for the steady-state plasma concentration (C_{ss}) obtained after administering an intravenous infusion. If one desires that concentration be achieved immediately, then a loading dose may be calculated as

$$D_L = Cp^{avg} \cdot Vd. \tag{12.17}$$

The *Vd* used in Equation 12.17 is debatable when multicompartment pharmacokinetics is operative. The discussion in Chapter 8 surrounding Fig. 8.17 is informative. For loading, Vd_{ss} would be ideal. In derivation of some equations above, $T_{½}$ is determined from the terminal slope of the C-T profile, λ. Therefore, when substituting in equations, Vd_{area} is generated. The important point is that a multiple-dose regimen is truly dependent on Cl_B as derived above, and thus as long as an accurate estimate of this crucial parameter is obtained, dose regimens will be accurate. These issues are one reason noncompartmental approaches discussed in Chapter 9 are used to estimate Cl_B and *Vd*.

Comparing Equations 12.2 and 12.15 is instructive since it demonstrates the dependence of the average steady-state concentration on the rate of drug input (R_0 or D/τ) in mass/time and the rate of drug elimination exemplified by the clearance. When constructing and comparing dosage regimens, the Cp^{avg} of any two regimens will always be the same as long as D/τ is constant. This factor becomes very important in Chapter 17, in which dosage regimens are constructed for patients with impaired clearance due to renal disease (Eqs. 17.7 through 17.11). The larger the f_{el} or ε is in a single dosage interval τ, the greater the fluctuation in plasma concentrations. To minimize fluctuation but maintain a constant Cp^{avg}, smaller maintenance doses (D_M) must be administered at shorter dosage intervals.

It is also important to stress at this point that the length of time required to achieve steady state for any dosage regimen is solely based on the rate-controlling λ or $T_{½}$ of the

drug in the clinical situation. Thus, with drugs having a prolonged half-life, a loading dose may often have to be administered to rapidly achieve therapeutically effective plasma concentrations. The more complex the distribution kinetics are, the more difficult it will be to rapidly achieve the target plasma concentration since the tissue compartment must first be loaded before the plasma compartment can reach an equilibrium (again revisit Chapter 8, Fig. 8.17). The only way to precisely counteract this is through the administration of an intravenous infusion protocol based on both distribution and elimination pharmacokinetics, as in the text discussion of Fig. 9.5 and Equations 9.31 and 9.32.

The principles presented in this chapter may be widely applied for a number of therapeutic situations. They will be revisited in Chapter 17, which discusses dosage regimens for individuals with impaired renal function. Similarly, equations developed in this chapter will form the basis for calculating the withdrawal time needed to ensure that drug is completely eliminated from a food-producing animal before its edible tissues are consumed. In this case, the problem is conceptualized as constructing a dosage regimen whereby tissue depletion data are used, the final trough or Cp^{min} is set as the legal tolerance of drug for that tissue, and the final dosage interval τ is actually the withdrawal time. Thus, Equation 12.9 in this chapter will transform to Equation 19.4 for withdrawal time determination. These equations for a multiple-dosage regimen also come into play in some situations in Chapter 15 when multiple doses and accumulation occurs. The equations presented above can be used to determine when these situations may be important.

12.3.3 Other considerations

The astute reader should realize that the equations developed above are strictly applicable only to a drug having a disposition described by a one-compartment PK model. These relations will hold if the proper set of PK parameters for the time and concentration range of the targeted C-T profile is employed (see Chapter 8, Table 8.3). For most drugs employed in a therapeutic setting, the relevant $T_{½}$ will be that governing the elimination (or so-called β phase) of the drug's C-T profile. Similarly, the slope of the C-T profile λ will often be β. This assumption is valid as long as the distribution rate constants (λ_1 or α) are much greater (more rapid, shorter $T_{½}$) than the elimination rate constants (λ_2 or β). This works since, as discussed in Chapter 8, the initial exponential term will disappear as time increases. However, when such parameters are employed, the proper volume of distribution term must be used (Vd_{area}) since the multicompartment characteristics of a drug will influence this parameter (recall relations presented in Chapter 8, Eq. 8.50). If a deep compartment (e.g., λ_3 or γ phase) exists and is not accounted for, the actual measured Cp^{min} will be greater than that predicted using λ_2 or β.

For drugs that undergo biotransformation, Chapter 10 should be consulted for equations relevant for these scenarios. The problem with drugs exhibiting nonlinear PK properties is that as drug accumulates, saturation may occur and the clearance operative at low *Cp*s may be reduced at the higher concentrations seen at steady state. When a multiple-dosage regimen is administered, $T_{½}$ will not be constant and thus, if τ is not appropriately adjusted, accumulation will occur. In contrast, if the drug induces its own metabolism, the disposition and thus the required dosage regimen may be different after chronic use.

Other considerations are operative when administering extravascular drugs with relatively slow rates of absorption. In many cases, the governing rate process may be the absorption phase (k_a), and a flip-flop situation will occur. In this case, it will take five absorption $T_{½}$s to reach steady state, but Cp^{avg} will still be predicted from Equations 12.2

and 12.3. The best approach to handle this is to use the actual equations governing the shape of the C-T profile (e.g., Eq. 8.55, see Chapter 8, if a model is available) and solve for dose. These approaches are implemented in all major clinical PK software packages available today. It must be stressed that the principles involved are identical to those presented above except for the added computation burden introduced by the multiexponential equations employed.

These approaches to constructing dosage regimens are ideally suited when PK parameters are obtained from the noncompartmental models presented in Chapter 9. In these cases, the same equations may be used. Similarly, the approaches presented above will be extensively revisited in Chapter 16 on population pharmacokinetics.

12.4 SOME COMMENTS ON EFFICACY AND SAFETY

The final point to consider is the relationship between target Cp^{max} and Cp^{min} concentrations and therapeutic or toxic effect. The precise relationship between a PK profile and pharmacodynamic (PD) or toxicodynamic (TD) effects is presented in much greater detail in Chapter 13.

The application of this to the design of clinical dosage regimens could be extrapolated from Equation 13.2, which reflects the effective dose in 50% animals (ED_{50}) to the average plasma concentration that would result as a function of Cl_B and F. Rearranging this equation yields

$$EC_{50} = (ED_{50} \cdot F)/Cl_B, \tag{12.18}$$

where EC_{50} is the predicted average plasma concentration effective in 50% of the animals. The similarity to the dosing equations previously presented (Eqs. 12.3 and 12.15) is direct. The question now at hand is how does one estimate the effective dose in the absence of the formal PK-PD models developed in Chapter 13?

It is instructive to realize that the form of a C-T profile is by itself only dependent on the dosage regimen parameters (D/τ) and the pharmacokinetics of the drug in the patient. These are the drug and patient factors which determine the PK profile. The clinician is in control of the dose and dosage interval τ.

The issue is how does the resulting C-T profile relate to drug efficacy or toxicity. This is a function of the nature of the disease being treated and the ED_{50}. Does the drug act by binding to a specific receptor, in which case the PK-PD models developed in Chapter 13 are useful if the parameters of the PD model are known. If the disease is a bacterial infection or a cancer cell in a tumor, then the relationship of drug exposure at the target site to effect must be known. Does irreversible killing occur or does the presence of drug only inhibit growth? Does drug toxicity to an eliminating organ such as the kidney or liver irreversibly alter the drug's own clearance?

In the clinical domain, rules of thumb relating descriptive parameters of the C-T profile (e.g., Cp^{max}, Cp^{min}, AUC, and time above target Cp) are often used. This concept is illustrated in Fig. 12.4, which depicts a hypothetical C-T profile versus various target Cps for efficacy and toxicity. The resulting efficacy or toxicity of the profile is dependent on the underlying pharmacology and toxicology of the drug. These biological effects are often, although not always, correlated to plasma concentrations. As will be developed in Chapter 13, the issue is actually whether the C-T profile reflects the drug concentrations at the tissue

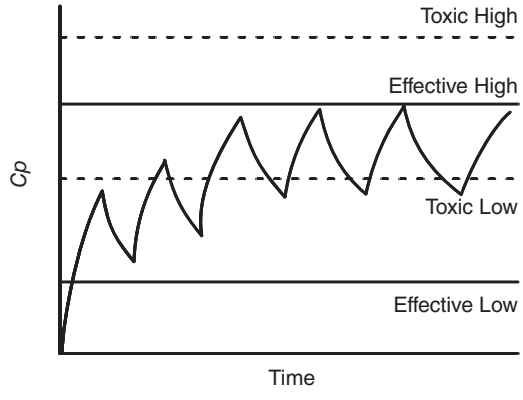

Fig. 12.4 Relationship between a multiple-dose plasma concentration-versus-time profile and thresholds for efficacy and toxicity that define the therapeutic benefit–risk ratio for the drug.

site of infection. In some cases, there is a delay, which alters this relationship. However, all agree that the C-T profile is better than correlations to dose alone since it is closer to the site of action and takes into account the drug's PK disposition.

Thus, for a specific drug, one might have data indicating that efficacy would occur when *Cp* is maintained above the effective low concentration in Figure 12.4, and toxicity would be expected to occur only if concentration exceeded the toxic high level plotted. In this case, the dosage regimen that produced this C-T profile would be considered optimal since at steady state, it is well within the *therapeutic window* defined by these two thresholds. However, if the efficacy of the drug was defined by the effective high threshold plotted, the regimen would not be therapeutically effective. Similarly, if the relevant toxicological threshold were the toxic low threshold in this figure, one would predict that this regimen would be unsafe to administer.

It is important to realize that the mechanism of action for the pharmacological and toxicological end points represented by these thresholds may be different, and thus some drugs may actually have toxic thresholds that are less than their effective levels. Such an example would be administering a nephrotoxic aminoglycoside antimicrobial drug to treat a pathogen that is moderately resistant to this drug, as indicated by a high minimum inhibitory concentration (MIC), in a patient with preexisting renal disease.

A more likely scenario often encountered in infectious disease therapy is administering a specific antibiotic regimen according to label conditions in patients infected with pathogens having different MICs. Fig. 12.5 illustrates this scenario with an antimicrobial used against pathogens with an MIC of 1 μg/mL versus one with 5 μg/mL. The steady-state C-T profiles plotted represent dosages of this drug administered (A) 6.6 mg/kg every 12 h, (B) 11 mg/kg every 6 h, (C) 15 mg/kg every 8 h, and (D) 22 mg/kg every 12 h. It is obvious that all four dosage regimens would be effective against a pathogen with a lower MIC; however, regimen (A) may not be effective against the pathogen with the higher MIC. If the drug required maintenance of effective plasma concentrations throughout a dosage interval, then one would opt for regimen (B) and, possibly, (C). If efficacy was clearly associated with high peak plasma concentrations (e.g., an aminoglycoside), then regimen (C) or (D) might be preferred. It is instructive to realize that for the latter three regimens, the total daily dose is all approximately 44–45 mg per day.

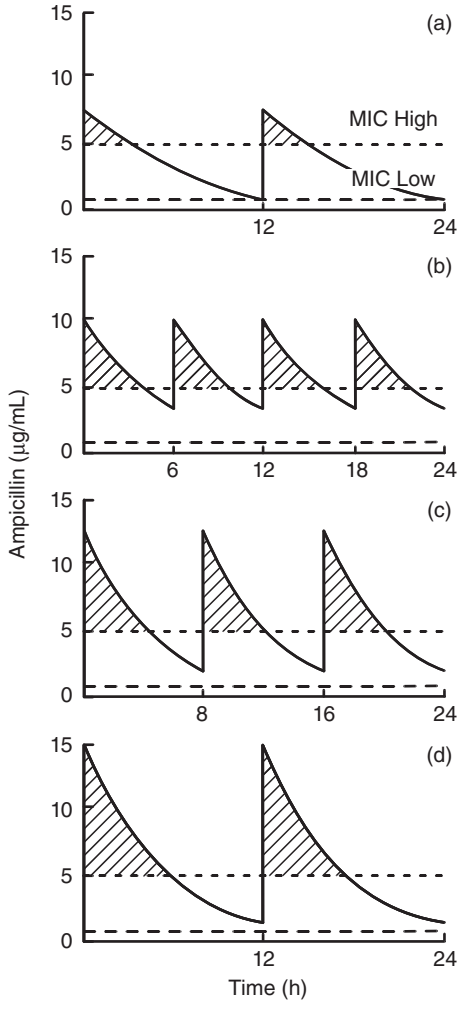

Fig. 12.5 Relationship between different antimicrobial doses and dosage intervals (τ) against a pathogen with a high or low minimum inhibitory concentration (MIC). Dosage conditions are (A) 6.6 mg/kg every 12 h, (B) 11 mg/kg every 6 h, (C) 15 mg/kg every 8 h, and (D) 22 mg/kg every 12 h. Hatched areas of the profiles are time greater than MIC.

There is an extensive amount of recent research on defining the nature of a C-T profile that correlates to efficacy for specific types of antimicrobial drugs. Aminoglycosides and quinolones have concentration-dependent killing profiles, while beta-lactam activity is dependent on duration of exposure. As will be seen in Chapter 13, these differences can be explained using the Hill equation (Eq. 13.1). As discussed in the PK-PD chapter, this work tends to suggest a few rules of thumb applicable to the clinical design of dosage regimens:

- Quinolones: Ratio of AUC/MIC
- Aminoglycosides: Cp^{max}/MIC
- Beta-lactams: % τ with Cp > MIC

These types of PK-PD activities coupled with experimental and clinical studies have developed a few rules of thumb that expand upon these relationships and allow some generalizations to be attempted. For fluoroquinolones, an AUC_{0-24}/MIC ≥ 100–125 seems optimal. For aminoglycosides, the Cp^{max}/MIC ratio ≥10 for single-dose daily administration is suggested. For beta-lactams such as the penicillins and cephalosporins, continuous exposure is desirable. This can be accomplished by relatively shorter τ to generate C-T profiles approaching an infusion. Alternatively, long-acting depository formulations could be used only if the resulting *Cp* is actually greater than the MIC as discussed in Fig. 12.5. For macrolides, glycopeptides, lincosamides, and metronidazole, time greater than MIC seems important, although precise metrics have not been agreed upon.

A problem with this approach is that MIC is not a metric related to the rate of drug bacterial kill, which might better correlate to efficacy. However, MIC is clinically available and thus is often used to quantitate effect. Similarly, the kinetics behind development of drug-induced resistance is not considered.

These *rules of thumb* are being presented here only to give an idea of how the dosage regimen equations can be used to structure C-T profiles specific to the drug, target and patient being treated. There is active work in these areas, and current literature in the specific discipline should be consulted. What will not change are the PK tools that can be used to help achieve these specific end points.

The toxicity of a regimen (e.g., an aminoglycoside) might also come into play when selecting the optimal strategy. The consensus among investigators is that aminoglycoside nephrotoxicity is best correlated to the trough (Cp^{min}) plasma concentration achieved at the end of a dosing interval, and not the peak concentration achieved (Cp^{max}) or total exposure to the substance (AUC). Such regimens are consistent with their concentration-dependent antimicrobial killing activity. In this light, regimens (A) and (D) in Fig. 12.5 would be selected based on both toxicological and pharmacological criteria. Regimen (D) may actually be the optimal approach. However, this decision is drug specific, and for those antimicrobials for which time above MIC is required for efficacy (e.g., penicillin) and peak concentrations correlate to toxicity, regimen (B) would be optimal. This could also be a function of the site of the infection (fibrous plaque in the heart vs. a renal medulla infection) and the distribution characteristics of the drug (see Chapter 5).

Similar considerations occur for other classes of drugs in which efficacy and toxicity may be dependent on the different characteristics of the C-T profile. A complete discussion of the specific approaches required for different drugs and clinical syndromes is well beyond the scope of this pharmacokinetics text. A text on clinical pharmacology should be consulted.

12.5 CONCLUSION

This chapter presented the fundamental concepts used to apply basic PK models to the selection and construction of dosage regimens. Other texts and references are available that provide equations for the more complex PK scenarios that may be encountered. However, it is the author's firm conviction that most workers in this field will use various commercially available software packages or "homegrown" spreadsheets to calculate dosage regimens. Whatever the complexity of the resulting dosage regimens obtained using these tools, the principles outlined above relating to dosage rate, accumulation, time to steady state,

and C-T fluctuations will be operative and must be taken into consideration before administering them to a clinical patient. If the desired effects or untoward adverse effects occur, then the first diagnostic technique performed should be to evaluate one's assumptions concerning the underlying pharmacokinetics before other actions are taken.

FURTHER READING

The basic pharmacokinetic texts in the Bibliography in Chapter 8 should be consulted for discussions on pharmacokinetics of multiple-dose administration and the design of clinical dosage regimens. Similarly, the Bibliography in Chapter 13 should be consulted for more detailed aspects of modeling efficacy of dosage regimens using pharmacokinetic–pharmacodynamic models.

Baggot, J.D. 1992. Clinical pharmacokinetics in veterinary medicine. *Clinical Pharmacokinetics*. 22:254–273.

Benet, L.Z., Massoud, N., and Gambertoglio, J.G. 1984. *Pharmacokinetic Basis for Drug Treatment*. New York: Raven Press.

Burton, M.E., Vasko, M.R., and Brater, D.C. 1985. Comparison of drug dosing methods. *Clinical Pharmacokinetics*. 10:1–37.

Colburn, WA., Shen, D., and Gibaldi, M. 1976. Pharmacokinetic analysis of drug concentration data obtained during repetitive drug administration. *Journal of Pharmacokinetics and Biopharmaceutics*. 4:469–486.

DeVane, C.L., and Jusko, W.J. 1982. Dosage regimen design. *Pharmacology and Therapeutics*. 17:143–163.

Frazier, D.L., and Riviere, J.E. 1987. Gentamicin dosing strategies for dogs with subclinical renal dysfunction. *Antimicrobial Agents Chemotherapy*. 31:1929–1934.

Gibaldi, M. 1991. *Biopharmaceutics and Clinical Pharmacokinetics*. Philadelphia: Lea and Febiger.

Gumbleton, M. and Sneader, W. 1994. Pharmacokinetics considerations in rational drug design. *Clinical Pharmacokinetics*. 26:161–168.

Martinez, M.N., and Riviere, J.E. 1994. Review of the 1993 veterinary drug bioequivalence workshop. *Journal of Veterinary Pharmacology and Therapeutics*. 17:85–119.

Martinez, M.N., and Silley, P. 2010. Antimicrobial drug resistance. In: Cunningham, F., Elliott, J., and Lees, P. (eds.), *Comparative and Veterinary Pharmacology*. Heidelberg: Springer, pp. 227–264.

Martinez, M.N., Riviere, J.E., and Koritz, G. 1995. Review of the first interactive work-shop on professional flexible labeling. *Journal of the American Veterinary Medical Association*. 207:865–914.

McKellar, Q.A., Sanchez Bruni, S.F., and Jones, D.G. 2004. Pharmacokinetic/pharmacodynamic relationships of antimicrobial drugs in veterinary medicine. *Journal of Veterinary Pharmacology and Therapeutics*. 27: 503–514.

Mungall, D.R. 1983. *Applied Clinical Pharmacokinetics*. New York: Raven Press.

Riviere, J.E. 1994. Influence of compounding on bioavailability. *Journal of the American Veterinary Medical Association*. 205:226–231.

Riviere, J.E., Carver, M.P., Coppoc, G.L., Carlton, W.W., Lantz, G.C., and Shy-Modjeska, J.S. 1984. Pharmacokinetics and comparative nephrotoxicity of fixed-dose versus fixed-interval reduction of gentamicin dosage in subtotal nephrectomized dogs. *Toxicology and Applied Pharmacology*. 75:496–509.

Riviere, J.E., Frazier, D.L., and Tippitt, W.L. 1988. Pharmacokinetic estimation of therapeutic dosage regimens (PETDR): a software program designed to determine drug dosage regimens for veterinary applications. *Journal of Veterinary Pharmacology and Therapeutics*. 11:390–396.

Rowland, M., and Tozer, T.N. 1995. *Clinical Pharmacokinetics: Concepts and Applications*, 3rd Ed. Baltimore, MD: Williams & Wilkins.

Ruckebusch, Y., Toutain, P.L., and Koritz, G.D. 1983. *Veterinary Pharmacology and Toxicology*. Westport, CT: Avi Publishing Co.

Shargel, L., Wu-Pong, S., and Yu, A.B.C. 2005. *Applied Biopharmaceutics and Pharmacokinetics*. 5th Ed. New York: McGraw Hill.

Toutain, P.L., and Bousquet-Mélou, A. 2004. Plasma terminal half-life. *Journal of Veterinary Pharmacology and Therapeutics*. 27:427–439.

Traver, D.S., and Riviere, J.E. 1981. Penicillin and ampicillin therapy in horses. *Journal of the American Veterinary Medical Association*. 178:1186–1189.

Vogelman, B., Gundmundsson, S., Legget, J., Turnidge, J., Ebert, S., and Craig, W.A. 1988. Correlation of antimicrobial pharmacokinetic parameters with therapeutic efficacy in an animal model. *Journal of Infectious Diseases*. 158:831–847.

Winter, M.E. 1988. *Basic Clinical Pharmacokinetics*, 2nd Ed. Spokane, WA: Applied Therapeutics.

13 Simultaneous Pharmacokinetic–Pharmacodynamic Modeling

with Pierre-Louis Toutain

The initial chapter of this text covered the pharmaceutical and pharmacokinetic phases of drug disposition encompassed in quantifying absorption, distribution, metabolism, and elimination (ADME). The final phase of modeling involves the coupling of drug concentration at the active site (pharmacokinetics, PK) to its biological (pharmacodynamics, PD) and its clinical effects (therapeutics). The present chapter will introduce the objectives, underlying concepts, methods, information, advantages as well as the limitations of the quantitative approaches to link these processes into complete models of drug disposition and action; an approach referred to as PK/PD modeling. Emphasis in this chapter will be placed on the major modeling steps for the PD components of the model. The PK approaches have been extensively discussed in Chapters 8–10. The application of PK/PD modeling to rational development of veterinary drugs will be stressed. In many ways, the material in this chapter could actually comprise a separate book focused on what could be referred to as quantitative pharmacology or pharmacometrics. As this complex area is developed, the reader will see numerous parallels to the development of pharmacokinetic models discussed throughout the text. In order to be as complete as possible, this chapter also includes a number of recent applications specifically relevant to veterinary medicine.

13.1 OVERVIEW ON PK/PD MODELING

PK/PD modeling consists of describing and explaining the time course of the drug effect (*intensity* or *frequency* of the observed response as quantified by PD) via the time course of its concentration in the plasma (PK). The primary objective of PK/PD modeling is to estimate, *in vivo*, key PD parameters of a drug to predict the time course of a drug effect under physiological and pathological conditions. Another objective of a PK/PD model is to increase the understanding of the underlying mechanisms of drug action.

PK/PD modeling is a versatile tool which is mainly used in veterinary medicine to select rational dosage regimens (dose, dosing interval) for confirmatory clinical testing. The ultimate goal in therapeutics is to control a drug response, not drug exposure. In a clinical setting, this consists of the physician applying feedback (e.g., clinical outcome) from previous drug administration to directly adjust a dosage regimen as explained in Chapter 12. This approach is efficient for some drugs such as anesthetics or opioids for which the effects

Comparative Pharmacokinetics: Principles, Techniques, and Applications, Second Edition. Jim E. Riviere.
 ISBN: 978-0-813-82993-7

are immediately observable and need to be adjusted without delay. However, for most drugs, this experience-based approach remains rather inefficient. For instance, optimizing the effect of an antibiotic in terms of efficacy (e.g., minimum inhibitory concentration [MIC]) or resistance through clinical observation of symptoms is not sufficient and the recourse to more advanced approaches is required. One should realize that systemic drug effect is mediated *via* the time-course profile of drug concentration at the site of action—referred to as the *biophase*—and for drugs acting systemically, biophase drug exposure bears a proportional relationship with plasma concentration. Thus, monitoring plasma concentrations is a way to indirectly control the response to a drug, which is the essence of the PK/PD approach, that is, considering plasma concentration as the turntable between a dosage regimen and a clinical response. This implies that PK and PD events have to be considered simultaneously and linked using a fit for the purpose model that is a PK/PD model.

13.1.1 When and why PK/PD modeling should be used

The efficiency of drug development can be greatly improved through the use of a PK/PD modeling approach, rather than by studying in parallel PK and PD data. PK/PD modeling is applicable to all phases of drug development. PK/PD can be used very early in drug development from drug target discovery to bridging *in vitro* drug action and *in vivo* drug effects as is the case for antibiotics, or to discard compounds having an initial attractive *in vitro* potency but which are unable to maintain an appropriate sustained *in vivo* exposure. Later in preclinical drug development, the primary objective of PK/PD analysis is to provide estimates of the key *in vivo* PD properties of a drug (i.e., its potency, efficacy, and selectivity) and to begin to explore the question of a dosage regimen. In veterinary medicine, the PK/PD modeling approach also offers a conceptual framework for extrapolation between species and to predict drug effects under different physiological or pathophysiological conditions. Later during clinical development, modeling clinical responses taking into account not only drug effects but also disease progression or any relevant physiopathological events on which the drug is acting or interacting may help to finalize an optimal dosage regimen.

By separating the two main sources (PK and PD) of inter- and intraindividual variability, the PK/PD modeling approach can be used during clinical trials to identify the key factors allowing a dosage regimen to be individualized, taking into account either PK- or PD-relevant covariables (population PK/PD modeling, see Chapter 16). Finally, PK/PD modeling can be used prospectively for some clinical trial simulations (CTS) to streamline their design or to explore "what-if" scenarios. Fig. 13.1 summarizes how PK/PD concepts can be used in preclinical and clinical product development in veterinary medicine.

13.1.2 Dosage regimen determination: from dose titration to PK/PD modeling

In veterinary medicine, the selection of a dose is generally based on dose-ranging studies using a simple parallel design. With parallel design, animals (healthy, experimentally infected, etc.) are randomly allocated to several dose levels and the effects are compared using a standard statistical test of the hypothesis as shown in Fig. 13.2. This design has two serious limitations: first, it is unable to provide information on the shape of the individual dose–response relationship, which is relevant to discuss the drug selectivity that is sorting out desired and undesired drug effects. Second, the dose designated as the "effective

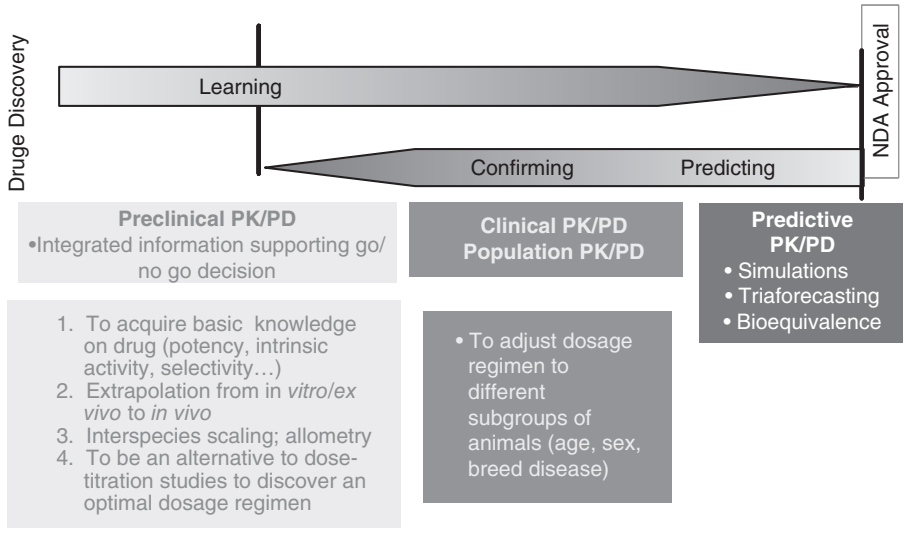

Fig. 13.1 Potential applications of PK/PD concepts during preclinical and clinical development of a veterinary product. Adapted from Meibohm and Derendorf (2002). NDA, new drug application.

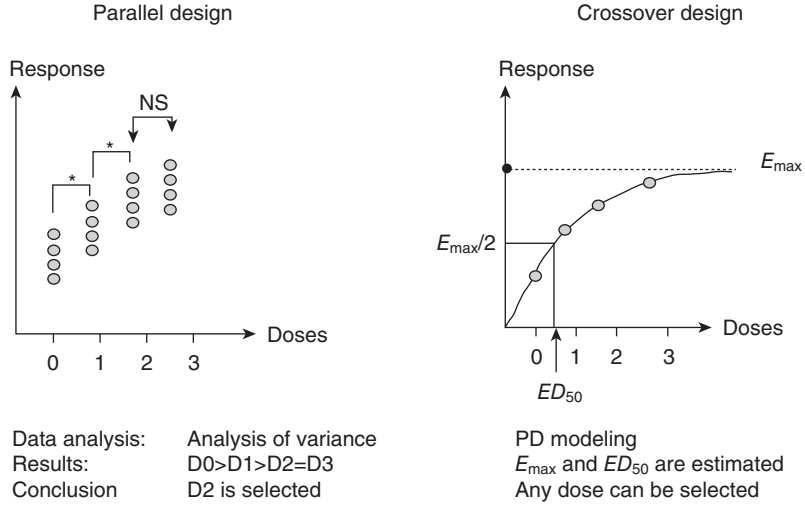

Fig. 13.2 Parallel (left) versus crossover (right) design for a dose-titration study. In a parallel design, animals (here $n = 4$ per group) are randomly assigned to one of the tested doses (0, 1, 2, or 3). Data analysis is performed by a test of the hypothesis (analysis of variance, ANOVA), the selected dose being one of the tested doses (no interpolation). Here, D2 would be selected because it gives a significantly higher response (*) than D1 but is not significantly (NS) different from D3. In a crossover design, all animals receive every dose to be tested and individual dose–effect curves are generated. For each individual curve, PD parameters (E_{max}, ED_{50}) can be computed and any dose over the tested range can be selected. Crossover but not parallel designs provide information about the shape of the dose–response relationship and the variability within the population.

dose" is not obligatorily the optimal dose. Indeed, the selected dose is highly dependent on the power of the design (number of tested animals), and trials with a small sample size generally lead to the selection of an oversized dose.

This classical parallel design remains the only usable one for antiparasitic and antibiotic drugs, because irreversible drug effects (i.e., pathogen eradication) are the pivotal outcomes. In contrast, for drugs acting reversibly on a physiological system (e.g., cardiovascular, nervous system, kidney), the most attractive design consists of using the so-called crossover design where each animal is tested with the different doses being investigated. In this way, individual dose–response curves can be generated. For a given animal, the dose–effect relationship can be described by a basic relationship of the form:

$$Effect = E_0 \pm \frac{E_{max} \cdot Dose^n}{ED_{50}^n + Dose^n} \tag{13.1}$$

where *Effect* (dependent variable) is the predicted effect for a given *Dose* (independent variable); E_0 is the effect without the drug (i.e., a placebo effect or the baseline response of the system); E_{max} is the maximum possible effect and ED_{50} is the dose producing half E_{max}. E_{max} is a measure of the drug efficacy, whereas ED_{50} is a measure of the drug potency. E_0, E_{max}, and ED_{50} are parameters. When an exponent (n) is included in the model, it reflects the slope of the dose–effect relationship and can provide information on drug selectivity for the tested effect; this equation will be fully presented and discussed later with the presentation of Equation 13.3. However, at this point, the reader should note the similarity of this nonlinear equations to those encountered in Chapter 5 for protein binding (Eq. 5.4) and in Chapter 10 (Eq. 10.4) for drug biotransformation.

When considering Equation 13.1, it should be noted that ED_{50} is not a genuine PD parameter but rather a hybrid PK/PD variable. Actually, ED_{50} incorporates three different separate determinants, as described by the following relationship:

$$ED_{50} = \frac{Clearance \cdot EC_{50}}{Bioavailability} \tag{13.2}$$

where ED_{50} is a daily dose able to maintain an average plasma concentration equal to EC_{50}; EC_{50} is the steady-state plasma concentration producing half E_{max}; *Clearance* is the daily plasma clearance (Cl_B from earlier chapters), and *Bioavailability* is the extent of the systemic bioavailability (for the extravascular route of drug administration—F) as previously defined in Chapter 8.

Fig. 13.3 shows the fundamental differences between a dose-ranging trial (also called dose-titration trial) and a PK/PD trial. Fig. 13.4 further illustrates this difference in a study designed to determine a gonadotropin-releasing hormone (GnRH) dose to reestablish estrous cycles in cows with ovarian cysts, using the pituitary luteinizing hormone (LH) response as a surrogate end point.

Both approaches aim at documenting the same relationship between dose and drug response. In a PK/PD analysis, the dose is replaced by the plasma concentration profile (or the area under the curve [AUC], i.e., the internal exposure) to explain the effect closer to the site of action independent of confounding PK factors acting on the administered dose. It enables one to estimate the drug potency in terms of an EC_{50} (or AUC_{50}) rather than ED_{50}. Unlike ED_{50}, EC_{50} is a genuine PD parameter. For a given end point, a single (steady-

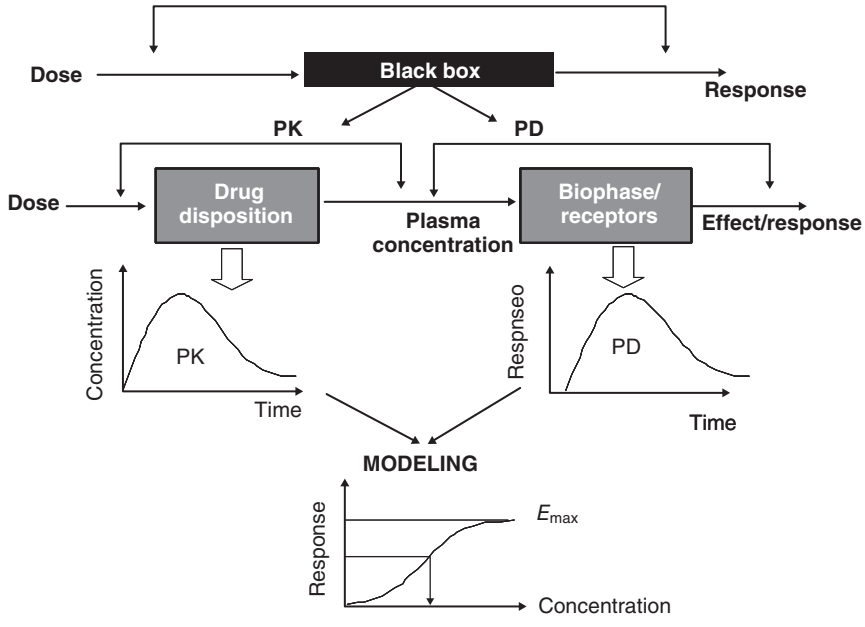

Fig. 13.3 Dose–effect relationship versus PK/PD modeling. Both approaches aim at documenting the same relationship between dose and drug response. A dose–effect relationship is a black-box approach in which the dose is the explicative variable of drug response. In a PK/PD approach, the black box is opened, thereby enabling the two primary processes that separate dose from response to be recognized. In the first step (PK), the dose is transformed into a plasma concentration profile. In the second step (PD), the plasma concentration profile becomes the variable that explains the drug response. The difficulty with the PK/PD approach is that the development of the effect and plasma concentrations over time is usually not in phase. This means that a hysteresis loop is observed when the response is plotted against plasma concentrations and data modeling is required to estimate the PD parameters (E_{max}, EC_{50}, and *slope*).

state) EC_{50} value exists, which is influenced by neither PK parameters nor the route of administration or the formulation. Moreover, because EC_{50} is a drug-dependent parameter (ED_{50} is both a drug- and formulation-dependent variable), the use of a PK/PD approach precludes the need for multiple trials as with dose-ranging. If a drug sponsor decides to develop another formulation, he will not need to perform a new PK/PD trial, but simply a new PK study to predict the influence of the bioavailability factor on the effect. For this reason, EC_{50} is much more attractive than ED_{50}, and its determination is one of the main goals of a PK/PD experiment.

13.1.3 Plasma concentration as a "driving force" for pharmaco/toxicodynamic effects

As discussed in Chapters 2 and 5, it is a tenet in pharmacology that the free plasma concentration is the driving concentration "controlling" all other local concentrations after a systemic drug administration. In addition, plasma remains the most easily accessible body compartment to measure free drug concentrations. Thus, the plasma concentration can play the genuine role of a "driving force" for a pharmacodynamic or a toxicodynamic effect, consistent with it being the central or reference compartment in both compartmental and

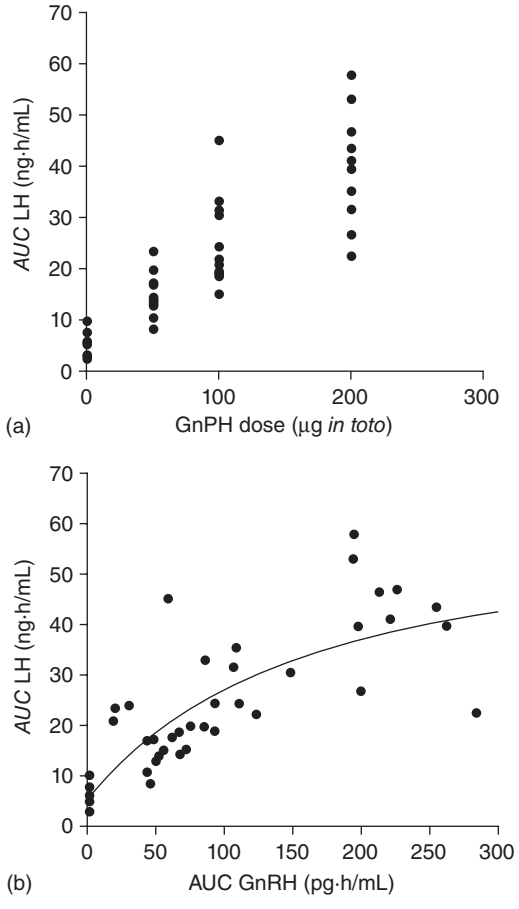

Fig. 13.4 Dose versus exposure–effect relationship. (a) The classical dose–effect relationship is plotted with the gonadotropin-releasing hormone (GnRH) dose (0, 50, 100, or 200 µg *in toto*) as the independent variable and the overall LH response (AUC LH, nanogram·hours/milliliter). When analyzed as a parallel design (i.e., ignoring that each cow was tested four times), this design is unable to provide information on the shape of the individual dose–response curves and the effective dose is imposed by the statistical analysis, that is, by testing the null hypothesis with an analysis of variance (ANOVA). (b) The dose, as an explicative variable, has been replaced by the individual GnRH exposure (GnRH AUC, picogram·hours/milliliter), which allows better characterization of the mean response curve; using a minimal PK/PD model, GnRH efficacy and potency can be computed. This approach is a "naive pooled data approach" and does not guarantee that the individual concentration–effect relationship has a similar shape to the mean shape, and a more advanced PK/PD modeling consisted of analyzing the individual time development of LH responses versus the plasma concentration versus time of GnRH (see Fig. 13.19).

stochastic PK models developed in Chapters 8 and 9. The plasma concentration profile is inherently more informative than the administered dose and in most cases the *in vivo* plasma concentration of a drug has proved to be the best predictor of the drug's effect. The dose is only a nominal mass fixed by the clinician, providing no intrinsic biological information. In contrast, the concentration versus time profile is controlled by both the dose (clinician) and the animal (through its physiological processes such as plasma clearance and distribution). In addition, plasma concentration profiles provide temporal data, allow-

ing a PK/PD trial to include time as an independent variable in a PK/PD model, enabling, for example, not only a dose, but also a dosage interval to be determined.

13.1.4 Tissue sites other than plasma concentrations to explain effects

Any biological fluid concentrations having the status of "driving force" can be considered for PK/PD modeling if the concentrations are kinetically and biologically closer to the effect. For example, all kidney loop diuretics act on the apical membrane transport of Na^+ and Cl^- of the thick ascending loop of Henle in the kidney by inhibiting Na^+-K^+-Cl^- cotransport processes that is from the urine space, not from the blood compartment. This location can be appreciated by examining Fig. 6.4 in Chapter 6. This requires that loop diuretics should gain access to the urine (filtration, secretion) to locally achieve high enough concentrations. From a PK/PD modeling perspective, the urine concentration is the relevant driving concentration to describe the diuretic effects of loop diuretics and to investigate the consequences of impaired renal function. In contrast, plasma concentration is the relevant concentration to investigate systemic effects of these agents on Na^+-K^+-Cl^- cotransport processes in nonrenal tissue and especially to investigate any side effects of loop diuretics such as deafness.

Transudate and exudate fluids inside a tissue cage or indwelling microdialysis probe can also be selected as a driving force to explain the effect of antibiotics on microorganism or the effect of nonsteroidal anti-inflammatory drugs (NSAIDs) on targeted enzyme systems. Other fluids have been used to establish a mechanistic PK/PD relationship including milk (for antibiotics), synovial fluid for NSAIDs, as well as cerebrospinal fluid for anesthetics and analgesics. Yet, plasma concentration remains the most useful biological matrix for monitoring purposes, the ultimate objective being to control this plasma concentration by an appropriate dosage regimen.

13.2 THE BUILDING OF PK/PD MODELS

13.2.1 Components

The process for building a structural PK/PD model generally involves four different submodels:

- a PK model transforming the dose into a concentrations versus time profile. These have been presented in Chapters 8–10;
- a link model describing drug transfer from plasma to the biophase;
- a system model that describes the physiological system or the pathological process on which the drug is acting;
- a PD model relating biophase concentration to an effect on the system.

In addition, any structural PK/PD model can be completed by a statistical model that describes the error component of the model and that is typically estimated in population PK/PD investigations, as presented in Chapter 16. Depending on the drug and the purpose of the modeling, the four structural submodels may or may not be involved. We will first describe the different PD models.

13.2.2 Pharmacodynamic models

There are two main types of PD models, describing either a *graded* concentration–effect relationship or a *quantal* concentration–response relationship.

A graded model is used when the response to different drug concentrations can be quantified on a scale (e.g., body temperature, survival time). In a quantal model (also known as a fixed-effect model or all-or-none effect model), the described effects are nominal (categorical) (e.g., dead or alive, parasitic cure or not, appearance of unwanted effects or not). A graded dose–effect relationship can be measured on a single animal that is exposed to a range of doses, the *intensity* of the response being related to the dose. For quantal dose–response (or exposure–response) relationships, the dose or exposure is not related to the intensity of the effect but to the *frequency* of an all-or-none effect. Thus, quantal dose–response relationships are established in a population of animals that are exposed to a range of doses. Quantal responses are often clinical end points, whereas graded responses are often biomarker concentrations or surrogates used to replace clinical end points of ultimate interest in PK/PD models.

The most general model for a graded effect relationship is the Hill model, also known as the sigmoidal E_{max} model:

$$E(t) = E_0 + \frac{E_{max} \cdot C^n(t)}{EC_{50}^n + C^n(t)} \tag{13.3}$$

where $E(t)$ is the effect observed for a given concentration at time t, that is, $C(t)$. $C(t)$ describes the PK model and explicitly introduces the variable time (t) in the model (that is the main difference with Eq. 13.1); E_{max} is the maximal effect attributable to the drug; EC_{50} is the plasma concentration producing 50% of E_{max}; and n is the Hill coefficient (no dimension), representing the slope of the concentration–effect relationship. The power function (C^n) first encountered in Chapter 8 (see Eq. 8.59) has been introduced in this equation to bring an appropriate flexibility for describing a great variety of shapes of the concentration–effect relationships seen in Fig. 13.5. Equation 13.3 was first formulated in 1910 for studying the O_2 and hemoglobin association–dissociation process and subsequently used for more complex binding processes such as drug-receptor binding. When $n = 1$, Equation 13.3 is analogous to the Michaelis–Menten equation as derived and explained in Chapter 10, Equation 10.4. Many drug effects involve modulation of a physiological variable (e.g., blood pressure) and the inclusion of the term E_0 in Equation 13.3 indicates the presence of a baseline effect. E_0 can also represent a placebo effect. E_0 may not be a constant: if the baseline is subjected to some variation, it should be modeled (see later).

The sigmoidal model shows a great degree of flexibility and other simpler models can be viewed as particular cases of the sigmoidal model. For example, when $n = 1$, the Hill model is reduced to the classical E_{max} model, which corresponds to a rectangular hyperbolic function:

$$E(t) = E_0 \pm \frac{E_{max} \cdot C(t)}{EC_{50} + C(t)} \tag{13.4}$$

The E_{max} model originates from the classical receptor theory, but in PK/PD modeling, it serves primarily as an empirical model. From this equation, the three main PD parameters can be defined (Figs. 13.6 and 13.7).

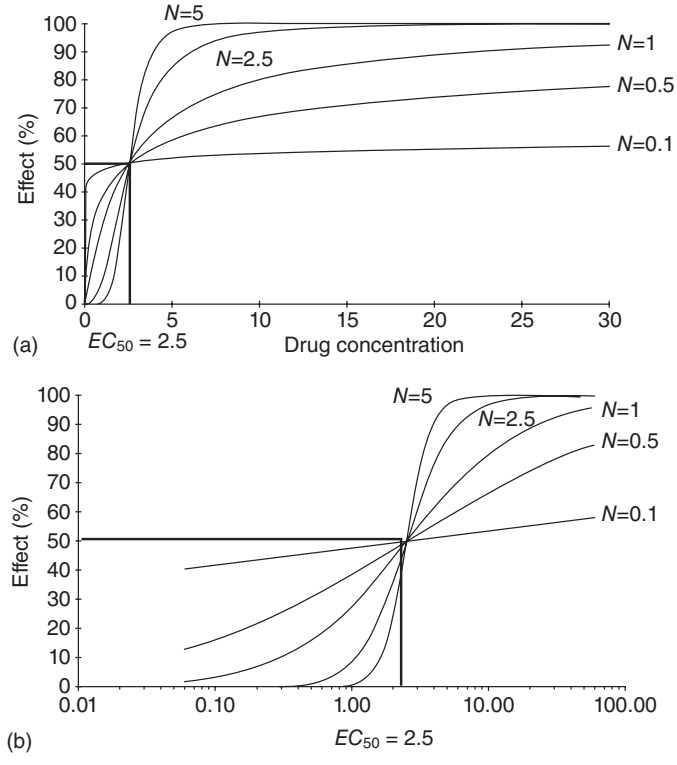

Fig. 13.5 Hill model. Influence of the Hill coefficient (*N*) on the shape of the concentration–effect relationship; simulation of the effect change (%) for $N = 0.1$, 0.5, 1, 2.5, and 5. (a) Arithmetic scale. (b) Logarithmic scale.

If $n = 1$ and if $C(t)$ is much lower than EC_{50}, then the sigmoidal model collapses to the simple linear model of Fig. 13.8:

$$E(t) = E_0 + \frac{E_{\max}}{EC_{50}} \cdot C(t) \tag{13.5}$$

with $E_{\max}/EC_{50}$ as a slope. This can be rewritten more simply as:

$$E(t) = E_0 + Slope \cdot C(t) \tag{13.6}$$

Note that this equation is written in the now all-too familiar slope–intercept form ($y = a + bx$) whose solution is similar to that presented in Chapter 8 for solving PK equations. A negative slope can be used if the drug has an inhibitory effect. Although this linear PD model is simple and easy to use, it is unsuitable for accurately predicting the baseline effect at time 0 (i.e., E_0).

If the tested $C(t)$ are of the same order of magnitude as EC_{50}, it is often observed that a simple log-linear model is sufficient to describe drug action:

$$E(t) = E_0 + Slope \cdot \log C(t) \tag{13.7}$$

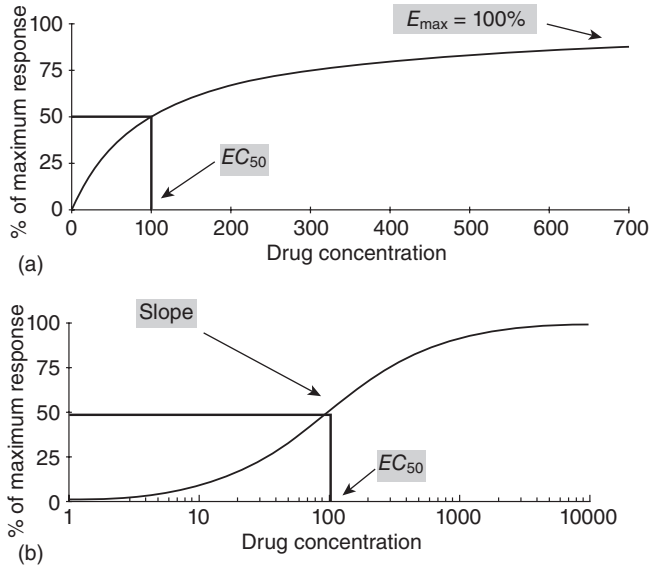

Fig. 13.6 E_{max} model plotted with arithmetic (a) and semilogarithmic scale (b). (a) When the drug response (arithmetic *y*-axis) is plotted against the tested dose (arithmetic *x*-axis), a hyperbolic relationship is often observed with a maximal effect noted E_{max}. EC_{50} is the concentration that produces an effect equal to half E_{max}. (b) When the same data are represented using a log-*X* scale, the relationship becomes sigmoidal with a more or less steep slope. The advantage is to compress the concentration scale and to visualize the slope more easily. A sigmoidal curve allows the definition of three drug parameters, namely E_{max}, EC_{50}, and the slope ($\Delta Y/\Delta X$). E_{max} describes the drug efficacy and EC_{50} describes the drug potency. The slope (measured by the *n* of the Hill equation—see Eq. 13.3 in the text) indicates the sensitivity of the dose–effect curve. The slope of the curve is involved in the drug selectivity (see Fig. 13.13).

where the *Slope* parameter can be computed by linear regression. In *in vitro* steady-state conditions, $C(t)$ is a constant (C) and Equation 13.7 has been used extensively to characterize basic *in vitro* PD drug properties such as drug potency and to test competitive versus noncompetitive antagonism between drugs. However, it should be realized that Equation 13.7 describes only a limited range of the concentration–effect relationship, namely between about 20% and 80% of the possible E_{max} as seen in Fig. 13.9. Precautions must be taken when using this model beyond this range (possible overestimation of drug effect at over 80% of E_{max} and underestimation below 20% of E_{max}) and the availability of computer software to fit by nonlinear regression data to the E_{max} or the Hill model no longer justify the use of Equation 13.7.

When the drug effect corresponds to the inhibition of a biological process, the drug effect is subtracted from the baseline (E_0) and Equation 13.3 can be rewritten as:

$$E(t) = E_0 - \frac{I_{max} \cdot C^n(t)}{IC_{50}^n + C^n(t)} \tag{13.8}$$

where IC_{50} is the concentration producing 50% of the maximum inhibition effect (I_{max}). If the drug is capable of reducing the baseline effect to zero, that is, I_{max} is equal to E_0, then Equation 13.8 can be simplified to the so-called fractional I_{max} model:

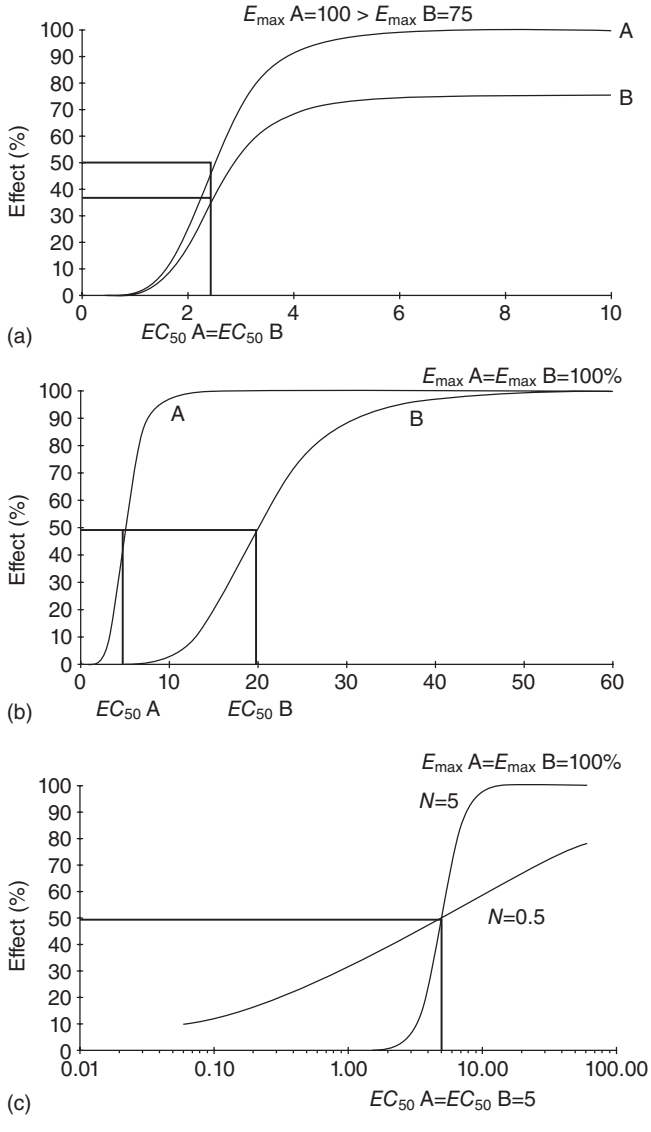

Fig. 13.7 Dose–response relationship and characterization of the three main pharmacodynamic parameters. (a) Efficacy. Drug A is more efficacious than drug B because E_{max} *A* = 100 is higher than E_{max} *B* = 75, whereas drugs A and B have the same potency (same EC_{50}). (b) Potency. Drug A is said to be more potent than drug B because EC_{50} *A* is lower than EC_{50} *B,* but drugs A and B have the same efficacy (same E_{max}). (c) Sensitivity. The sensitivity of drug A is higher than the sensitivity of drug B because the slope of the dose–concentration relationship is steeper for drug A (Hill coefficient of 5) than for drug B (Hill coefficient of 0.1), whereas they have the same potency (same EC_{50}) and efficacy (same E_{max}, not shown).

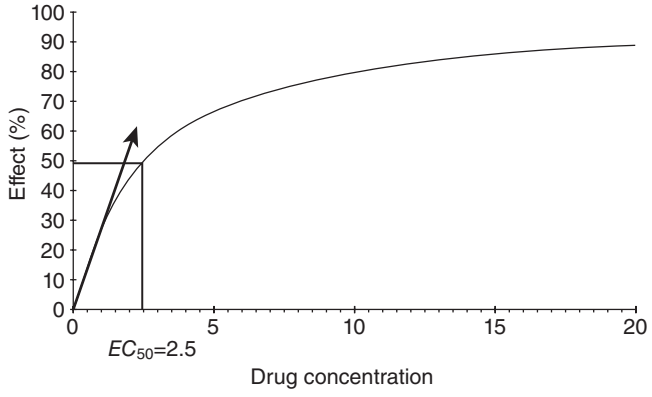

Fig. 13.8 Linear model: if the effect is measurable in the initial portion of an E_{max} model the concentration–effect relationship appears to be linear between about 0% and 20–30% of E_{max}.

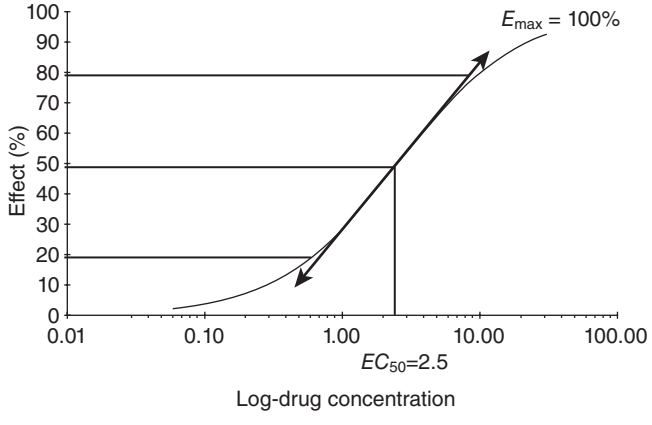

Fig. 13.9 Log-linear model: if the effect is measured around the EC_{50} of an E_{max} model, the concentration–effect relationship appears to be linear on a log-scale over a range of plasma concentrations ranging typically from 20% to 80% of E_{max}.

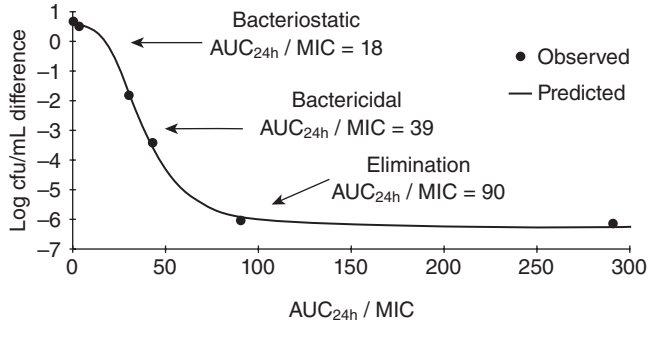

Fig. 13.10 Example of an inhibitory sigmoidal E_{max} model establishing a relationship for bacterial count versus *ex vivo* AUC_{24h}/MIC in a goat for a pathogenic strain of *M. haemolytica*. It illustrates what AUC/MIC values are required for bacteriostatic and bactericidal effects and eradication of bacteria (from Aliabadi and Lees, 2001).

$$E(t) = E_0\left(1 - \frac{C(t)^n}{IC_{50}^n + C(t)^n}\right) \tag{13.9}$$

More sophisticated E_{max}/I_{max} models can be developed to investigate combined drug action as is the case for many NSAIDs that are used as racemates in veterinary medicine. For example, a PD model including both *S*- and *R-ketoprofen* plasma concentrations was used to describe the analgesic effect of ketoprofen in piglets by Fosse et al. (2010). It was assumed that the two enantiomers produced their analgesic effect by two separate mechanisms of action and a simple additive I_{max} model was selected:

$$Effect_{R+S} = Hyperalgesia(t) \cdot \left[1 - \left(\frac{C_{pr}}{IC_{50r} + C_{pr}} + \frac{C_{ps}}{IC_{50s} + C_{ps}}\right)\right] \tag{13.10}$$

where *Hyperalgesia*(*t*) is a function describing the time-dependent hyperalgesia due to a paw kaolin administration (actually described by Eq. 13.19). C_{ps} and C_{pr} are plasma concentration of the *S*- and *R-ketoprofen*, respectively, IC_{50r} and IC_{50s} are the *R*- and *S-ketoprofen* plasma concentrations, which are capable, when acting alone, of producing half the maximum inhibitory effect on *Hyperalgesia*(*t*). Jonker et al. (2005) presented a series of PD models for combined drug action (multiple ligands, additive vs. competitive effects, stereoisomers, multiple receptors, and cascade activity).

Equations 13.3–13.10 contain several parameters (E_0, E_{max}, EC_{50} or IC_{50}, and n). The ultimate goal of PK/PD modeling is to estimate both the mean and variance of these parameters from $E(t)$ observations obtained over a range of $C(t)$ values.

When an all-or-none effect is observed due to the drug's mechanism of action (antiepileptic drug, antiarrhythmic drug, etc.), or when the selected end point is binary (cured or not cured for parasiticides), the concentration–response curve represents the *frequency* at which a concentration of a drug produces the all-or-none effect. For this kind of end point, data with exactly two possible outcomes, quantal or percent–concentration relationship (fixed-effect model), are in order. The link between the measure of a drug concentration and the corresponding probability is given by a logistic equation of the form:

$$P = \frac{e^{Logit}}{1 + e^{Logit}} = \frac{1}{1 + e^{-Logit}} \tag{13.11}$$

where P is the binary or dichotomous outcome from 0 to 1, *Logit* (L) is the natural log of the odds (relative risk):

$$L = \text{logit}(P) = \log(odds) = Ln\frac{P}{(1-P)} \tag{13.12}$$

The *Logit* can be written as a linear equation of the form:

$$Logit = \theta_1 + \theta_2(predictor1) + \theta_3(predictor2)\ldots \tag{13.13}$$

This equation allows the development of linear models describing the relationship between the success probability and various predictors. The logit bearing linearity in its parameters (θ_i) and ranging from $-\infty$ to $+\infty$, it transforms the 0–1 probability to a

continuous scale. For example, the probability of cure for an antibiotic of the quinolone family can be modeled as

$$\mathrm{POC} = \frac{1}{1 + e^{-(\theta_1 + \theta_2 X)}} \tag{13.14}$$

where POC is the probability of cure (from 0 to 1), θ_1 is a parameter for baseline (here a placebo effect) and θ_2 is an index of sensitivity (a slope). X is the independent variable and can be the AUC/MIC ratio that is classically selected for this class of antibiotic to predict efficacy or any other quantitative index predicting drug efficacy. If θ_2 equal 0, the response is independent of X and the POC corresponds to the placebo effect in Equation 13.14. Exponential θ_2 represents the change in the odds of the outcome (multiplicatively) by increasing X by 1 unit holding all other predictors constant. In this relationship, the equivalent of the EC_{50} (or ED_{50}) of Equation 13.3 is named EL_{50}; it is now the median effective level of the independent variable (e.g., dose, AUC, AUC/MIC) for which 50% of the subjects are above the threshold, and the slope of the curve now represents the dispersion (variance) of the threshold in a population. The EL_{50} can be estimated by the ratio $-\theta_1/\theta_2$, the X value associated with the steepest slope of the S-shaped logistic regression curve. When Equation 13.14 is plotted against a range of X values, this model has an S-shaped curve, approaching values of 0 and 1 gradually as shown in Fig. 13.11.

This kind of model can be extended to include qualitative indicators (e.g., gender, breed, etc.). For the development of a binary logistic model see Fiedler-Kelly (2007). When the end point is measured on an ordered categorical scale with several levels such as pain scores or adverse events (mild, moderate, severe, or life threatening) with repeated measurement and censored data, more advanced models are in order as described by Ette et al. (2007).

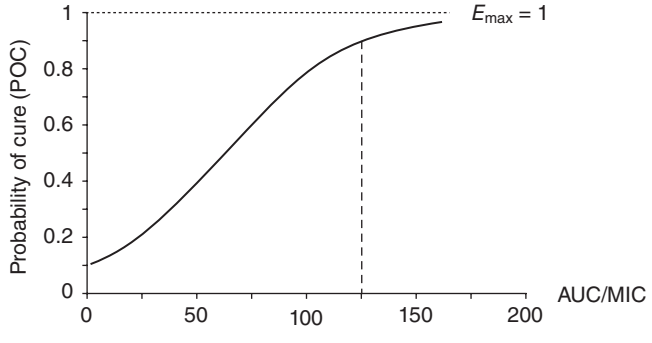

Fig. 13.11 Logistic regression. When an effect is binary (cure/no cure), a logistic curve is used to describe the relationship between the independent variable (often dose, exposure, or any explicative variable) and the dependent variable (a probability between 0 and 1). This quantal dose–response curve does not relate dose to *intensity* of effect but to the *frequency* in a population of individuals in which a drug produces an all-or-nothing effect. Here, the POC for a hypothetical concentration-dependent antibiotic has been plotted against the value of a PK/PD index generally selected for this class of antibiotics (i.e., AUC/MIC). The threshold AUC/MIC varies among individuals and the fixed effect model quantifies the likelihood or probability that a given AUC/MIC will produce a cure or not.

13.3 THE MEANING AND CLINICAL RELEVANCE OF THE DIFFERENT DEPENDENT VARIABLES OF A PD MODEL: ACTION, EFFECT, RESPONSE, BIOMARKERS, AND SURROGATES

When performing a PK/PD analysis, special attention should be paid to the nature of the dependent variable that has been selected. The dependent variable E is named after the generic term "effect." However, it can be useful to distinguish between drug action, drug effect, and drug response. For example, for an antibiotic, the "action" consists of inhibiting bacterial protein synthesis, the "effect" corresponds to the killing rate of bacteria, and the clinical "response" would be the cure of animals. When the objective of a PK/PD trial is to investigate a mechanism of action, the drug action at a primary site (bacteria, parasites, enzyme, receptor) should be measured. However, if the purpose of a PK/PD trial is to determine a dosage regimen, it is more relevant to measure the response of clinical interest. For example, to explore the pharmacological effect and selectivity of NSAIDs, the convenient dependent variables are the level of inhibition of the different COX isoenzymes. However, if the goal of the PK/PD is to establish a dosage regimen for future clinical trials, then the reduction of an experimental lameness will be more relevant.

In many situations, it is impossible or too difficult to select the most meaningful end point as a dependent variable: for example, how dogs feels under an analgesic treatment may be difficult to assess quantitatively using demeanor and the effect of an anticancer drug on the survival time of treated dogs or cats may be too delayed to be conveniently used in a PK/PD modeling strategy. For these situations, the end points of ultimate interest are replaced by so-called *biomarkers* that are assessed more easily and rapidly than definitive and more easily quantifiable clinical end points.

The role of biomarkers in PK/PD modeling is pivotal and needs to be fully understood. A biomarker, as defined by the Biomarkers Definition Working Group (Atkinson et al., 2001), is a characteristic that can be objectively measured and evaluated as an indicator of normal biological processes, pathogenic processes, or pharmacological responses to a therapeutic intervention as depicted in Fig. 13.12. Biomarkers are usually more precisely measured with validated assays or medical devices compared with clinical outcomes, thus making biomarkers attractive in preclinical PK/PD modeling. For example, biomarkers are extensively used in preclinical PK/PD modeling to assess NSAIDs' potency and selectivity by measuring the inhibition of PGE_2 formation using an appropriate *in vitro* or *ex vivo* test system (Lees et al., 2004). Angiotensin converting enzyme (ACE) inhibition has been used to evaluate the potency of ACE inhibitors in dogs (Toutain et al., 2000) and cats (King et al., 2003). When the clinical end point of ultimate interest is difficult to quantify or is much delayed in time, it may be judicious to replace the clinical end point in a PK/PD trial by a *surrogate* end point, which is a biomarker expected to predict clinical benefit (or harm) based on epidemiological, therapeutic, pathophysiological, or other scientific evidence. The most commonly used surrogate end point for regulatory purposes is the plasma concentration of drug in bioequivalence studies. Some examples of surrogates in veterinary medicine are the PK/PD indices that have been proposed for predicting the clinical success and bacteriological cure of antibiotics such as AUC/MIC or $T > \text{MIC}$, and conventional radiography for the evaluation of osteoarthritis.

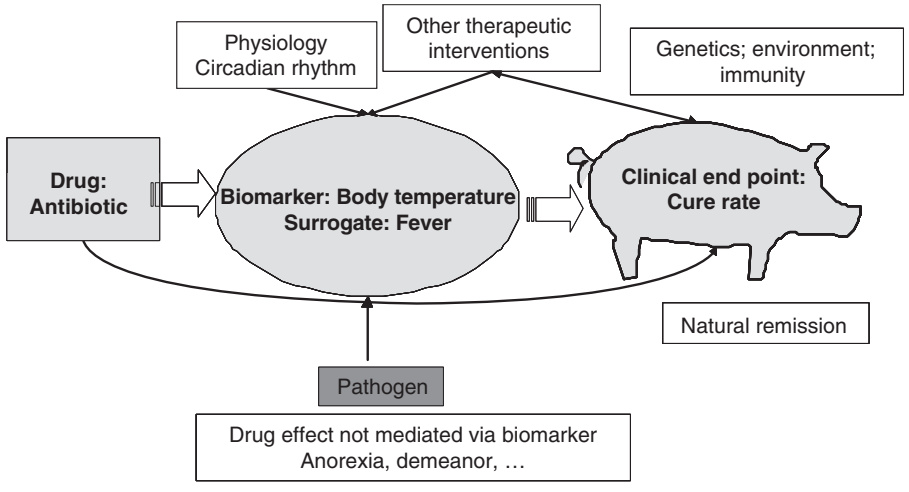

Fig. 13.12 Biomarker, surrogate, and clinical end points for an antibiotic intended to treat pneumonia in pigs. Hyperthermia should be considered as a biomarker, fever (i.e., hyperthermia, anorexia, drowsiness) should be considered as a surrogate, and the clinical cure rate should be considered as the clinical end point of ultimate interest.

Whatever the selected biomarkers, they should be carefully validated even if they appear to be directly linked to the disease of interest. Currently, few biomarkers in veterinary medicine are robust enough to serve as surrogate end points as is the case in human medicine for blood pressure and cholesterol concentrations that are accepted as surrogates for cardiovascular drugs. Indeed, a drug may have a favorable effect on a biomarker and an unfavorable effect on the disease and any biomarker believed to be a surrogate of clinical relevance must be validated. For a classification and validation of the different types of biomarker, see Williams and Ette (2007). In the future, it is likely that proteomics and metabolomics will provide some biomarkers of drug effects.

13.3.1 Hill equation parameters

Drug potency, maximal efficacy, and sensitivity are the three PD parameters that can be estimated using the Hill equation (Eq. 13.3). They have been defined in Figs. 13.6 and 13.7.

13.3.2 Potency (EC_{50})

Potency expresses the intensity of drug activity in terms of concentration. EC_{50} (for stimulation) and IC_{50} (for inhibition) are estimated directly by the Hill model. Potency varies inversely with the concentration required to produce the effect (Fig. 13.6b). It should be stressed that a drug can be more potent but less efficacious than another one as is the case of buprenorphine versus morphine. However, provided that the required dose can be conveniently administered, potency alone is relatively unimportant from a therapeutic perspective. Low potency becomes a disadvantage only when the size of the effective dose renders it difficult to administer (e.g., for spot-on drugs in pets).

13.3.3 Maximal efficacy (E_{max})

E_{max} is the maximum effect that can be generated by a particular system (e.g., the maximal possible reduction of blood pressure). It is the most important parameter for clinicians when the dependent measured variable has a clinical meaning (blood pressure, lameness score), but in most indirect effect models, E_{max} does not have a direct meaning; for example, E_{max} can be the scalar by which the modeled underlying process can be multiplied.

13.3.4 Sensitivity

In the Hill model, the shape coefficient (n) gives the slope of the concentration–effect relationship (Fig. 13.5). In receptor theory, n has a precise meaning in terms of drug binding, but *in vivo*, n should not be interpreted in mechanistic terms. n is of considerable clinical relevance when examining selectivity and drug sensitivity, that is, the range of useful concentrations (doses) for achieving a desired effect or avoiding an unwanted effect. Fig. 13.13 provides a more detailed explanation.

In vivo, for drugs with a low n (<1), the PD profile is shallow, meaning that only moderate changes in effect will be observed over a wide range of drug concentrations (several orders of magnitude). This type of relationship explains the very long-lasting action of some drugs (e.g., beta blockers for heart rate). For this kind of drug, the length of the terminal half-life can be very important for predicting the duration of an effect. In contrast, for drugs with a steep slope, minor variations in the concentrations around EC_{50} can produce

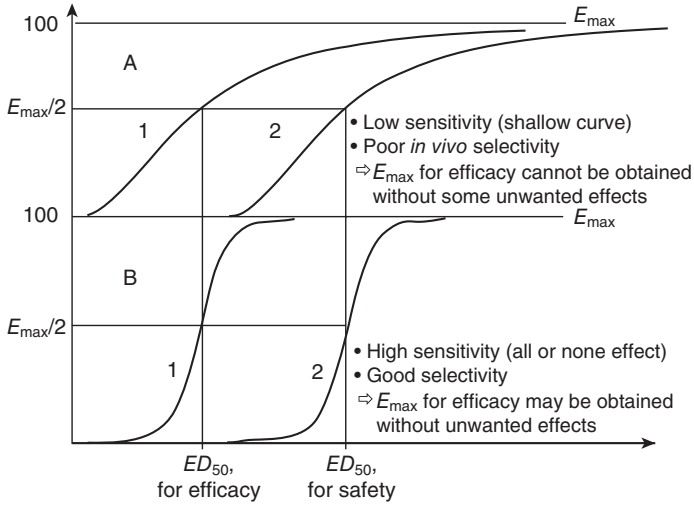

Fig. 13.13 *In vivo* drug selectivity is related to both the therapeutic index (i.e., the ratio ED_{50} safety/ED_{50} efficacy) and to the slope of the concentration effect relationship. Drugs A (top) and B (bottom) have the same potency (ED_{50}) and the same efficacy (same E_{max}) for the desired effect (curve 1) and unwanted effects (curve 2), that is, the same therapeutic index. However, they differ in terms of sensitivity (slope) (shallow for drug A and steep for drug B). Only with drug B can the full effect (i.e., E_{max}) be obtained without any significant side effects despite the fact that drugs A and B have the same ED_{50} safety/ED_{50} efficacy ratio. Definition of therapeutic index by ED_{10} safety/ED_{90} efficacy takes into account the differences in sensitivity of dose–response curves.

effects ranging from null to nearly maximal. This is the case with phenylbutazone, flunixin, and meloxicam for lameness in horses. Drugs with a high n but a low therapeutic index may require therapeutic drug monitoring to guarantee efficacy without toxicity. As n increases ($n > 5$), the concentration range diminishes to become a simple threshold (i.e., critical concentration just above EC_{50}), and the graded PD model becomes a quantal model, representing a limit of graded concentration when $n >> 1$.

13.3.5 Modeling the PD baseline

As quoted above, E_0 in Equation 13.3 may or may not be a constant. If the drug effect is investigated over a short period of time or if physiological stability of the measured effect can be assumed, E_0 is treated as a simple parameter. More generally, the baseline is subjected to some variations and it should be modeled. Many models, empirical or mechanistically based, can be selected or developed to model baseline status; the simplest is the linear model:

$$Baseline(t) = E_0 + \alpha t \tag{13.15}$$

where E_0 is the initial baseline status, α is a slope parameter, and t is the time after the initial observation.

If the baseline undergoes a circadian rhythm such as cortisol secretion from the adrenal gland, modeling the suppressive effect of exogenous glucocorticoids should not be confounded with the occurrence of a natural nadir (physiological minimal plasma cortisol concentration) and the baseline cortisol plasma concentration can be modeled as follows:

$$E_0 = E_m + E_b \cdot \cos\left[(t - t_z) \cdot 2\pi / 24\right] \tag{13.16}$$

where E_0 characterizes the circadian pattern of plasma cortisol concentrations (actually a production rate), E_m and E_b (same units as E_0) are the cosine function mesor (i.e., the adjusted mean) and amplitude, t is the clock time converted with the numeric fraction into radians t_z is the peak time (acrophase), and $2\pi/24$ is used to convert time into radians. Then a full model for the synthetic glucocorticoid suppressive effect can be developed by mitigating E_0 with an I_{max} model.

Currently, most PD models are mechanistically founded and the baseline (response in absence of drug) cannot be summarized by a single E_0 parameter but is the result of a dynamic equilibrium that can be affected not only by drug action but also by other factors including experimental challenge or spontaneous (disease) progression. This aspect will be developed later in the chapter.

13.3.6 The PK models

In a PK/PD modeling approach, a PK model is required to serve the role of the independent (or explicative) variable. The PK model (plasma, urine, or any other relevant matrix) can be a classical one (e.g., a compartmental model as developed in Chapter 8) for which parameters have been previously estimated. Its role is only to provide concentration inputs

in the PD model. Thus, it can be replaced by a noncompartmental model presented in Chapter 9 or simply a curve-smoothing procedure (e.g., cubic spline that is a special type of piecewise polynomial) if the plasma–concentration profile cannot be described adequately by a conventional PK model. This is a nonparametric approach that can be extended to the PD part of the model. In PK/PD modeling, the PK step is generally the easiest to carry out, but a more advanced PK model may be required if the predicted effect is related not only to the parent drug but also to some active metabolite(s), or if a racemate drug is administered with an enantioselective disposition. For example, to build a PK/PD model of the analgesic effect of ketoprofen, it is important to consider that both the disposition and the potency of the *R*(+) and *S*(–) enantiomers are different, so that both enantiomers must be explicitly included in the PK/PD model rather than just the total ketoprofen plasma concentration. Conversely, when no concentration data are collected and when the only information is the kinetics of the response, a so-called kinetic–pharmacodynamic model (K-PD) can be built. In this case, the plasma concentrations are unknown but the input rate function is modeled using a simple monocompartmental model and the dosing history (for details see Pillai et al., 2004).

13.4 HYSTERESIS

13.4.1 The origin of the delay in drug action for the building of a PK/PD model

For some drugs, the plasma concentration profile as generated by the PK model and the observed effects can be in phase, and the plasma concentrations can be directly incorporated into a PD model as described in Equation 13.3. Levy (1964), a pioneer of PK/PD modeling, used a monocompartmental model (first-order kinetics) to describe d-tubocurarine disposition. When introducing the plasma concentrations into a simple log-linear model (Eq. 13.7), he was able to describe correctly the time course of muscle paralysis. It can be easily shown that the effect versus time is a simple linear function of time (zero-order kinetic). Such quite simple PK/PD models were historically developed especially for cardiovascular drugs (effect of digoxin on systolic time intervals, effect of disopyramide and prolongation of the Q-T interval).

Most often plasma concentration profiles and the observed effects are not in phase, and the plasma concentrations cannot be directly incorporated into a PD model. For most drugs, the effect lags behind the plasma concentrations. This can easily be visualized by plotting the effects (*y*-axis) against the plasma concentrations (*x*-axis). When data points follow a chronological order, a loop is observed as seen in Fig. 13.14. This phenomenon is termed "hysteresis," from the Greek word meaning "coming late." The inverse situation (i.e., a lesser effect at a later time for the same plasma concentration) is termed "proteresis," a neologism meaning "coming early." This terminology is preferred to "clockwise hysteresis" and "counterclockwise hysteresis," which is often used in the literature. The actual direction of the loop depends on the direction of the effect (positive or negative).

When a hysteresis loop is observed, the cause of the delay must be identified to select a modeling strategy. Observing the time of occurrence of the maximal effect when the dose of the tested drug is progressively increased, as depicted in Fig. 13.15, may also help to select a model.

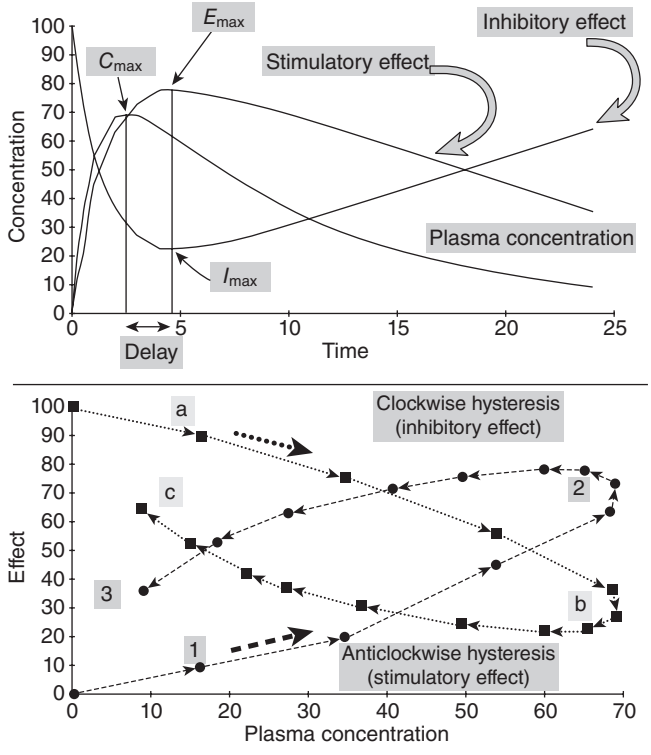

Fig. 13.14 Lack of synchronization of concentration–effect relationship and hysteresis plot. In general, plasma concentration–time and effect–time relationships are not in phase. The peak plasma concentration (C_{max}) occurs before a peak effect (E_{max} for a stimulatory effect and I_{max} for an inhibitory effect). This delay generates hysteresis that is, that for any given concentration, two different levels of effect are possible. Hysteresis is well evidenced by plotting plasma concentration versus effect in a time sequence. In this example, the plot reveals two hysteresis loops: a counterclockwise loop for the stimulatory effect (from 1 to 3) and a clockwise effect (from a to c) for the inhibitory effect.

When the delay is of PK origin (e.g., slow rate of distribution at the biophase, transformation of a prodrug into its active metabolite) and when the drug effect is directly related to the drug concentration at the biophase level, an *effect-compartment model* can be chosen with the selection of a *link model*. However, for most drugs, the measured response is not a primary drug action resulting from direct binding of the drug to its receptor. Rather, there is a cascade of time-consuming biological events between the plasma drug concentration and the final observed response (e.g., signal transduction and other processes that are discussed below). Under these conditions, the observed delay between the kinetics of the plasma concentrations and the time development of a response is not of distributional origin (i.e., of PK origin) but rather reflects the intrinsic temporal responsiveness of the system that is of PD origin. For this kind of response, so-called *indirect response models* are suitable. In the next section, we will see how to build a PK/PD model when the delay is either of PK or PD origin.

Fig. 13.16 gives the general decision tree to select a class of model according to the origin of the delay between the plasma concentration versus time and the effect.

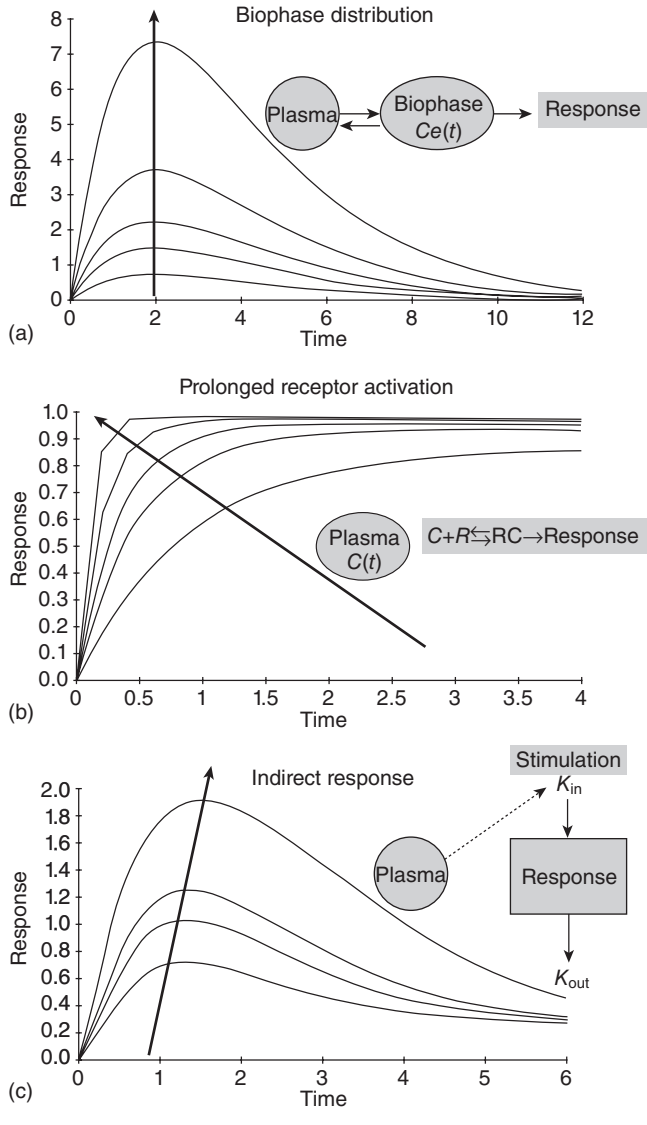

Fig. 13.15 Influence of the dose level on the time of maximal effect according to the type of the selected model. (a) For an *effect compartment model* (distributional model), the time of maximal effect is independent of the dose level. (b) For a prolonged receptor activation model (RC is the drug-receptor complex and *R* the free receptors), the time of maximum effect is observed earlier and earlier when the dose is increased. (c) The inverse phenomenon is observed with an indirect effect model, that is, a delay when the dose is increased.

13.4.2 Delay of PK origin and the link model

If it is acknowledged that the limiting step for a drug to produce its effect is of PK origin with a rather slow distributional process followed by an immediate action when the drug has gained access to its biophase, the biophase can be represented by a specific compartment named the "hypothetical effect compartment" as historically introduced by Sheiner

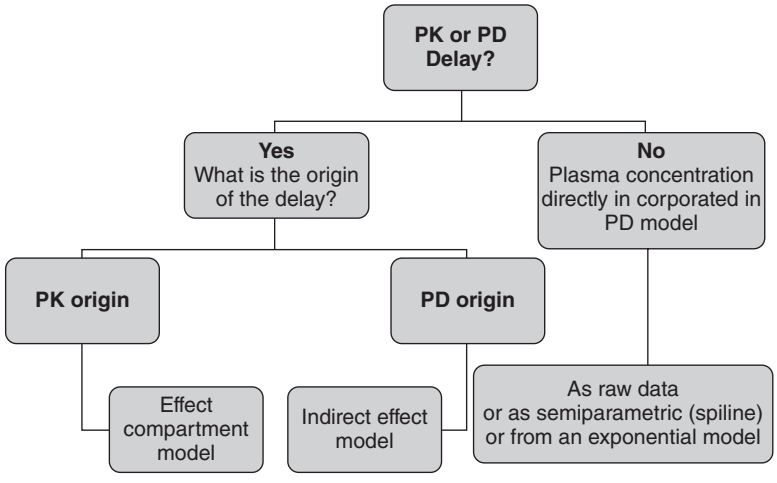

Fig. 13.16 Decision tree to select a PK/PD model according to the origin of the delay between the plasma concentration and observed effect.

et al. (1979) and shown in Fig. 13.17 describing the time development action of d-tubocurarine. Here, the hypothetical compartment was introduced as a tool to model the delayed effect by using the time course of the effect itself to define the rate of drug movement into the biophase. To accomplish this, the effect compartment should have two main features: (1) there is no hysteresis between the drug concentration in the effect compartment and the effect, meaning that the drug effect is instantaneously reversible and is a memoryless function of biophase drug concentration and (2) the amount of drug entering the compartment is negligible and does not affect the ability of the PK model to describe the time course of systemic drug concentrations. Since the amount of drug entering the effect compartment is assumed to be negligible, any drug entering the effect compartment can be eliminated directly from that compartment (according to a first-order rate constant named K_{e0}), rather than returning to the central compartment for systemic elimination. This assumption greatly simplifies the mathematical expression of the model that allows E_{max}, the plasma steady-state EC_{50} (i.e., PD parameters), and K_{e0} (the link model parameter) to be estimated from PD versus time data using nonlinear regression techniques. For a detailed description of this model, see the first edition of this book and the review by Holford and Sheiner (1982). Such a model was used to describe the effect of meperidine in goats (Qiao and Fung, 1993). Today, it is acknowledged that most delays are not of PK but are of PD origin, and this kind of model is used much less often.

13.4.3 Modeling delay of PD origin using physiological systems

It is now acknowledged that the limiting step for a drug to produce its effect is most often of a PD origin with a rather rapid distributional process followed by a slow development of the observed drug response when the drug had gained access to its biophase. This is due to the drug mechanisms of action at the cellular level and/or the drug effect on the physiological or pathophysiological system. For example, suppression of lameness by an NSAID requires inhibition of a COX isoenzyme at the biophase level (e.g., joint articulation) and

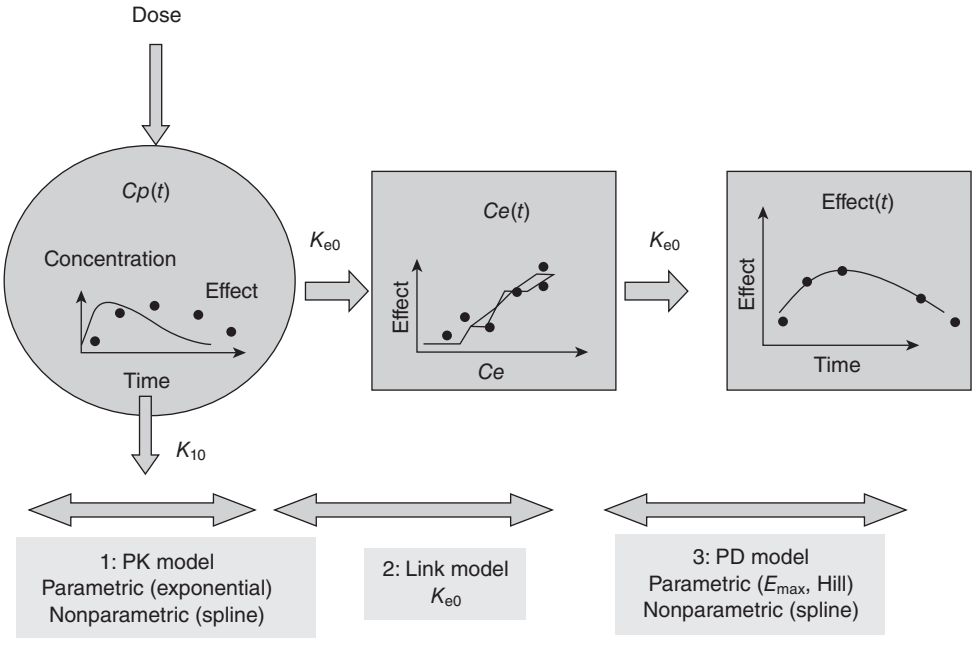

Fig. 13.17 The "effect compartment model" was proposed to model situations where the delay between plasma concentration, $C(t)$, and observed pharmacological effect, $E(t)$, are due to a distributional delay from time taken for the drug to gain access to its biophase. The model removes this delay by creating a hypothetical effect compartment in which the drug concentration $Ce(t)$ is in phase with $E(t)$. Schematically, this model is formed by three components: a classical compartmental PK model, a "hypothetical effect compartment," and a PD model. $C(t)$ and $Ce(t)$ are drug concentrations in the central and hypothetical effect compartments, respectively. The drug is administered and eliminated from the central compartment with K_{10} as the rate constant of elimination; the drug gains access to the *effect compartment* through a first-order rate constant historically called K_{1e} (but now equated to K_{e0}; see later). This "virtual effect compartment" should only receive a negligible amount of drug in order to have no influence on the overall drug disposition as described by the main compartmental model. This condition eliminates the drug directly out of the effect compartment (biophase) through a first-order rate constant that renders simpler equations describing $Ce(t)$. This exit rate constant is named K_{e0} and it controls the rate of drug equilibration in the effect compartment. K_{e0} should be selected (estimated) in order to have no hysteresis between $Ce(t)$ and the pharmacological effect. $Ce(t)$ cannot be directly measured, but rather is indirectly derived from the time course of the drug effect itself that by essence, is parallel to $Ce(t)$. K_{e0} is the link model, K_{e0} combined with $C(t)$—the plasma kinetics—enables $Ce(t)$ to be computed. In this model, K_{1e} was equated to K_{e0} not because $C(t)$ is equal to $Ce(t)$ in steady-state conditions but for identifiability reasons. The consequence is that the EC_{50} (or the IC_{50}) that is computed in the last step of the modeling is actually the steady-state plasma concentration corresponding to half the maximum effect and not the actual EC_{50} (or IC_{50}) at the biophase level. To operate, the effect compartment model should be in rapid equilibrium with $C(t)$. However, if K_{e0} is slow (compared with the other rate constant of the model), the biophase is not in equilibrium with $C(t)$ and the $Ce(t)$ profile would not be reflected by $C(t)$.The last part of the model is the PD model (E_{max}, Hill model). To use this model, one needs PD data from the rise and fall of the pharmacological effect over time to characterize correctly the time development of $Ce(t)$. From this modeling, the half-time of equilibration can be computed from K_{e0} (i.e., $0.693/K_{e0}$). A feature of this model is that the T_{max} of the observed effect is dose independent, whereas it is time dependent for the indirect effect model (see Fig. 13.15).

then, the time-consuming elimination of the proinflammatory substances present before the drug administration. For many drugs, the effect involves some protein synthesis and a cascade of different events reflecting the complexity of the targeted system. This is the so-called pharmacological transductions that govern the transduction of target activation into a final drug response *in vivo*.

When the drug concentration is directly incorporated into a PD model without specific consideration for the system under investigation, the model is said to be *empirical*: these types of models are a *model of data*. They may be able to describe properly the time course of effect when little is known about the underlying process and they can be reasonably predictive if they are used in conditions rather similar to those already studied (e.g., for interpolation). When a PK/PD model includes a submodel that is related to the biology of the system itself, independently of the drug under investigation and with its own structural parameters, the PK/PD model is said to be *semimechanistic* or *mechanistic*, depending on its level of complexity. Here, the objective is not only to describe empirically what is the output (effect) from a black box (body) for a given input (dose), but also to understand the *in vivo* pharmacology and systems biology. Hence, a suitable PK/PD model should determine not only the main pharmacodynamic parameters of the tested drug but also the major rate-limiting steps (turnover, transduction, tolerance) in the biology of the system under investigation. Fig. 13.18 depicts the current view of the different basic components that might be included in a PK/PD model.

Mechanistic models are more complex and more fully described by the different components of a system, as is the case of a physiologically based pharmacokinetic model (PBPK) as discussed in Chapter 11. For antibiotics, anticancer drugs, and parasiticides, the drug effect consists of some irreversible inactivation and to do so the natural proliferation of the target in the absence of drug should be modeled.

The most used physiological PD model is the so-called *turnover model*. This model is based on the established fact that most physiological and biochemical functions are in dynamical equilibrium with two terms: a term corresponding to the formation of the response and a term corresponding to the loss of the response. The rate of change of response over time with no drug can be expressed as follows:

$$dR/dt = K_{\text{in}} - K_{\text{out}} \cdot R \tag{13.17}$$

where dR/dt represents the rate of variation in the response variable (R). K_{in} is the rate of input, and $K_{\text{out}} \cdot R$ is the rate of loss; the model assumes that the measured response is being formed at a zero-order constant rate (K_{in}) but disappears in a first-order manner (K_{out}).

In control conditions (no drug, no pathological challenge), $dR/dt = K_{\text{in}} - K_{\text{out}}\, R = 0$, for example, there is no change in the response variable and thus $K_{\text{in}} = K_{\text{out}}\, R_0$. K_{in} can reflect the production rate of a measurable endogenous substance (hormone, mediator) with a dimension of concentration per unit of time and K_{out} is a hybrid rate time constant having a dimension of 1/time with the same meaning as K_{10} for a monocompartmental model (see Chapter 8) that is proportional to the clearance of that substance and inversely proportional to its volume of distribution. K_{in} and K_{out} may or may not have a precise meaning: when modeling the antipyretic effect of NSAIDs using body temperature as a surrogate, K_{in} (°C per time units) indirectly reflects thermogenesis (watts) and K_{out} (per time units) indirectly reflects thermolysis (watts) even if for a physiologist, thermolysis cannot be reduced to a

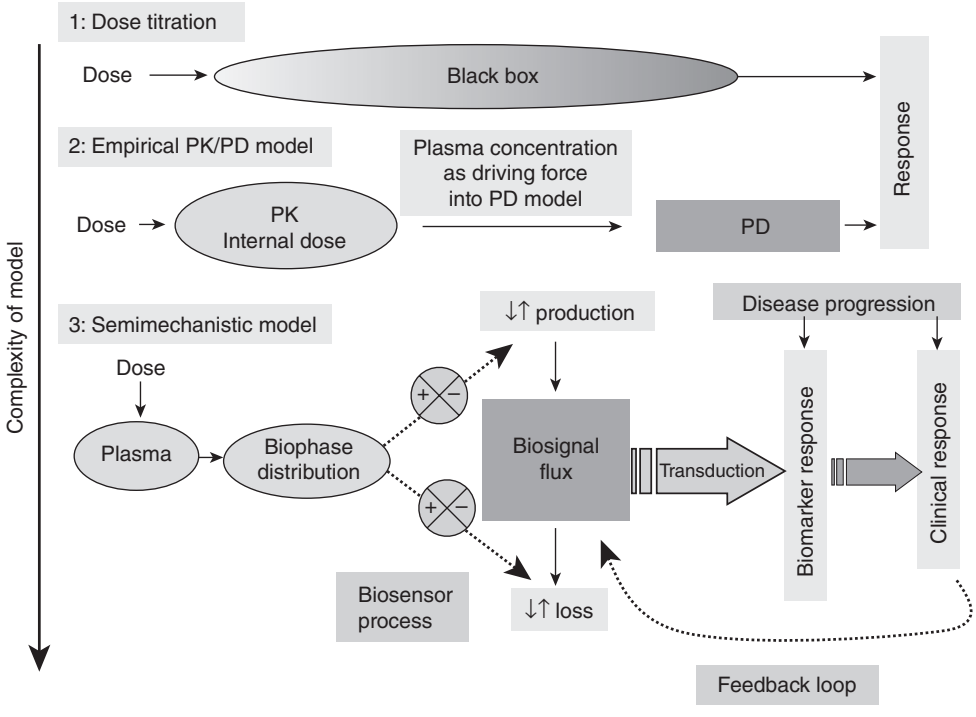

Fig. 13.18 Different levels of complexity of modeling the dose–effect relationship. The simplest model is the dose–effect relationship: it is typically a black box approach with the dose as the explicative variable and the clinical response as the dependent variable linked by a simple model (statistical or PD). The events between the dose and the response (e.g., PK and PD processes) are totally ignored. The black box can be opened to account for the two main steps separating a dose from its effect, namely a PK and a PD step. The main difference between a dose-titration model and an empirical PK/PD model is that now the plasma concentration profile is the explicative variable (the driving force) explaining effect and response. Both the PK and PD steps can be broken down further to characterize the relationship between a dose and its response in a more mechanistic way. For example, the PK step can include a distributional phase by including an effect compartment (biophase) with a link model; it is the PD step that is the most explicitly modeled. The drug acts on some biosensor process involving the reversible or irreversible interaction between the drug and its pharmacological target (receptor binding, killing pathogens) and may be described or not by various receptor occupancy models or some irreversible model of drug target interaction. Many drugs act *via* some indirect mechanisms on system-related processes and the biosensor may influence the production or loss of endogenous mediators (biosignal flux). This altered flux of mediators may not represent the observed terminal effect but rather trigger a further pharmacological transduction process (e.g., second messenger cascade), thus accounting for a further time delay. In addition, the system itself on which the drug is acting may be time variant, requiring, for example, the disease progression to be modeled or is able to trigger some feedback loop requiring additional modeling components.

passive phenomenon described by a first-order process. For this end point, the action of an NSAID will be to increase K_{out} rather than decrease K_{in} because it has been shown that NSAIDs stimulate thermolysis mechanisms. However, if the anti-inflammatory effect of the same NSAID is described using a quantitative lameness scoring as a biomarker, K_{in} will reflect more loosely all the different underlying mechanisms, triggering pain associated

with inflammation (local release of inflammation mediators, translation into pain including detection and modulation by the central nervous system of the pain signal). K_{out} will reflect every mechanism mitigating lameness (such as elimination of the inflammatory mediators, modulation of pain) and it can be more difficult in this case to decide if the NSAID is acting mainly by decreasing K_{in} and/or also by increasing K_{out}.

13.5 TURNOVER MODELS

In an empirical PK/PD model, the status of the biological system in the absence of drug is kept invariable with time, but this is not realistic when a drug is acting on a disease that deteriorates over time or when an animal is subjected to an experimental challenge as an experimental inflammation or infection. *Turnover models* are well suited to incorporate other submodel elements accounting for a placebo effect, for the time development of an experimental challenge (such as experimental inflammation) or to take into account the natural progression of a physiological process (e.g., growth) or pathological condition (e.g., diabetes, cancer). Several modeling strategies can be selected according to the type of drug action, namely purely symptomatic (no effect on the disease itself), disease-modifying effect (protective effect), or curative effect. See Mould (2007) and Post et al. (2005) for further discussions.

For a placebo effect the following equation can be used:

$$dR/dt = K_{in} + Placebo(t) - K_{out} \cdot R \tag{13.18}$$

where placebo can be modeled as:

$$Placebo(t) = \mathrm{P1}[e^{-\mathrm{P2}(time\text{-}lag)} - e^{-\mathrm{P3}(time\text{-}lag)}] \tag{13.19}$$

where P1, P2, and P3 are parameters of the input rate function allowing, after a given lag time (lag), introduction of a placebo-associated input rate that is first increasing and then decreasing if P1 is positive, or conversely, a placebo effect that is first decreasing and then increasing if P1 is negative. An example is the anticipation and habituation behavior that are observed when sequentially measuring pain responses when experimentally testing an analgesic drug in dogs.

In preclinical investigations, it is usual to use some experimental models to test new drugs; for example, experimental paw inflammation can be induced by administering a phlogogenic agent such as kaolin to assess the anti-inflammatory and antipyretic action of NSAIDs (Giraudel et al., 2005). This experimental inflammation is not steady and its time course should be typically modeled with a function able to account for its onset and its spontaneous recovery. This is normally done during the control period of a two-period crossover design in which the same animal is challenged with and without the tested drug.

For example, the time development of the inflammation or any pathophysiological response in a control period as assessed by a clinical end point such as hyperthermia, or lameness following a kaolin administration, can be modeled using an empirical biexponential equation of the same form as for a placebo:

$$Pathophysiological(t) = \mathrm{P1} \cdot [e^{-\mathrm{P2} \cdot (time\text{-}lag)} - e^{-\mathrm{P3} \cdot (time\text{-}lag)}] \tag{13.20}$$

with P1, the intercept, as a scale factor reflecting the amplitude of the inflammatory response (as measured by hyperthermia, lameness, pain); P2 (1/time unit) is the slope of the decreasing phase of kaolin phlogogenic effect; P3 (1/time unit) is the rate constant reflecting the increasing phase of the phlogogenic effect following the kaolin administration, and *lag* is the time of kaolin administration. The time development of the end point in the absence of drug during the control period is then modeled with:

$$dR/dt = K_{\mathrm{in}} + Placebo(t) + Pathophysiological(t) - K_{\mathrm{out}} \cdot R \tag{13.21}$$

In this additive equation, *Placebo*(*t*) and *Pathophysiological*(*t*) are the input rate functions and have the same dimension as K_{in}.

Finally, the drug effect can be introduced using a function mitigating *pathophysiological*(*t*) as:

$$dR/dt = K_{\mathrm{in}} + Placebo(t) + Pathophysiological(t) \cdot (1 - Drug) - K_{\mathrm{out}} \cdot R \tag{13.22}$$

where *Drug* is the PD model of drug action mitigating the inflammatory process.

To be identifiable, that is, to be in position to uniquely estimate every parameter of the model, the response has to be measured: (1) in control conditions to obtain information on K_{in} and K_{out}; (2) in a test placebo condition to get specific information on *Placebo*(*t*); (3) in a test condition but without drug to get genuine information on *Pathophysiological*(*t*); and finally, (4) in a test drug condition. This requires a relatively demanding crossover design. When all the data are collected under these different conditions, they are fitted altogether assuming that the time course of the placebo effect is the same with and without inflammation and in the presence or not of the tested drug. This assumes a good reproducibility of the end points that are measured during different periods of a crossover design or reproducibility between groups if using a parallel design.

Other additive parameterization models are possible. To test the antipyretic effect of a drug using an experimental fever triggered by injection of an endotoxin, assuming that the endotoxin stimulates thermogenesis (K_{in}), a multiplicative function can be introduced in the general turnover system and can be written as:

$$dR/dt = K_{\mathrm{in}} \cdot (1 + Pathophysiological(t)) + Placebo - K_{\mathrm{out}} \cdot R \tag{13.23}$$

For a PK/PD model developed in clinical rather than an experimental setting, the same class of equations can be used, with a model of disease progression replacing the pathophysiological function as:

$$dR/dt = K_{\mathrm{in}} + Placebo(t) + Disease(t) - K_{\mathrm{out}} \cdot R \tag{13.24}$$

Many options exist to model disease progression where different types of models are proposed for symptomatic, disease modifying, and curative drug action.

13.6 INCORPORATION OF A PD MODEL OF DRUG ACTION INTO A PHYSIOLOGICAL MODEL

The incorporation of a PD model in an existing physiological model portrays the last step of the PK/PD modeling efforts that is a PD model can be nested in the different parts of a physiological model. For the turnover model (see Eq. 13.17), it is generally assumed that indirect drug action, consisting of inhibiting or stimulating physiological factors, control production, or dissipation of the measured effect (Dayneka et al., 1993). Inhibition or stimulation of the response production (or dissipation) can be described by accounting for inhibitory or stimulatory processes:

$$dR/dt = K_{\text{in}} \cdot \{\text{stimulation or inhibition function}\} - K_{\text{out}} \cdot \{\text{stimulation or inhibition function}\} \cdot R \tag{13.25}$$

or more formally:

$$dR/dt = K_{\text{in}} \cdot \{1 + H_1(t)\} - K_{\text{out}} \cdot \{1 + H_2(t)\} \cdot R \tag{13.26}$$

where $H(t)$ is a function of time. An inhibitory process can be described by the function $I(t)$:

$$I(t) = -\frac{I_{\max} \cdot C(t)}{IC_{50} + C(t)} \tag{13.27}$$

where IC_{50} is the drug (plasma) concentration that produces 50% of the maximum inhibition; $I_{\max}$ is a number from 0 to 1 (1 for total inhibition); and $C(t)$ is the drug (plasma) concentration over time.

By incorporating this function into Equation 13.17, we get two basic inhibitory PD models, as expressed:

$$dR/dt = K_{\text{in}}\left(1 - \frac{I_{\max} \cdot C(t)}{IC_{50} + C(t)}\right) - K_{\text{out}} \cdot R \tag{13.28}$$

$$dR/dt = K_{\text{in}} - K_{\text{out}}\left(1 - \frac{I_{\max} \cdot C(t)}{IC_{50} + C(t)}\right) \cdot R \tag{13.29}$$

The model shown in Equation 13.28 stands for an inhibition of the response production rate (e.g., the action of a synthetic glucocorticoid on the secretion rate of cortisol by the adrenal gland). The model shown in Equation 13.29 stands for an inhibition of the response loss rate (e.g., the inhibition of Na^+ reabsorption by furosemide in the loop of Henle).

A stimulation process can be described as:

$$S(t) = \frac{S_{\max} \cdot C(t)}{SC_{50} + C(t)} \tag{13.30}$$

where SC_{50} is the drug plasma concentration producing 50% of the maximum stimulation that is of S_{max}; S_{max} is a positive number and $C(t)$ is the drug (plasma) concentration over time. It should be noted that S_{max} does not represent a maximum observed effect but a maximum for the stimulation of a physiological process.

Incorporating the stimulatory function in Equation 13.17 gives two basic stimulatory PD models:

$$dR/dt = K_{in}\left(1+\frac{S_{max}\cdot C(t)}{SC_{50}+C(t)}\right)-K_{out}\cdot R \tag{13.31}$$

and

$$dR/dt = K_{in}-K_{out}\left(1+\frac{S_{max}\cdot C(t)}{SC_{50}+C(t)}\right)\cdot R \tag{13.32}$$

The model shown in Equation 13.31 corresponds to the stimulation of the response production rate (e.g., production of cAMP by a bronchodilatator beta 2-agonist). Equation 13.31 was used in Fig. 13.19 to model the LH response to GnRH, the LH response being selected as a surrogate end point to determine a dose able to reestablish estrous cycles in cows with ovarian cysts. The model shown in Equation 13.32 corresponds to the stimulation of response loss (e.g., the antipyretic effect of NSAIDs with stimulation of thermolysis). These models have been used successfully for different classes of drugs (anticoagulants, corticosteroids, beta-adrenergics, antipyretics, etc).

13.7 TIME-VARIANT MODELS: TOLERANCE AND REBOUNDS

For a repeated drug administration, the PK/PD model might be able to adequately describe data for the first-dose administration, but progressively suffer some drift, that is, time dependency (nonstationarity). This is due to a physiological adaptation of the biological system with initiation of more or less complicated feedback mechanisms following repeated exposure to a drug. For instance, when a drug is given repeatedly, there can be a progressive reduction in the response to the drug due to some desensitization at the receptor level (downregulation). This phenomenon is called "tolerance" and it corresponds to the reversible decrease of the response for a given fixed plasma concentration. "Rebound" is the opposite effect that is observed at the cessation of drug administration.

Tolerance is frequently reported in human medicine but few relevant examples exist in veterinary medicine. Tolerance to opioids has been well described in animals but these drugs are seldom used for a long-enough period to have clinical consequences. Several mechanisms can explain this dampening phenomenon and they can be of a PK and/or PD origin. For phenobarbital that is extensively used as an anticonvulsant in small animals, tolerance develops rapidly, owing to the induction of hepatic enzymes increasing the phenobarbital metabolism. In addition, during a more prolonged treatment, there is a desensitization (downregulation) of GABA receptors. The formation of antagonistic metabolites competing with a drug for the same binding sites on the receptor and biofeedback regulation (counterregulation) are other tolerance mechanisms. Both empirical and more mecha-

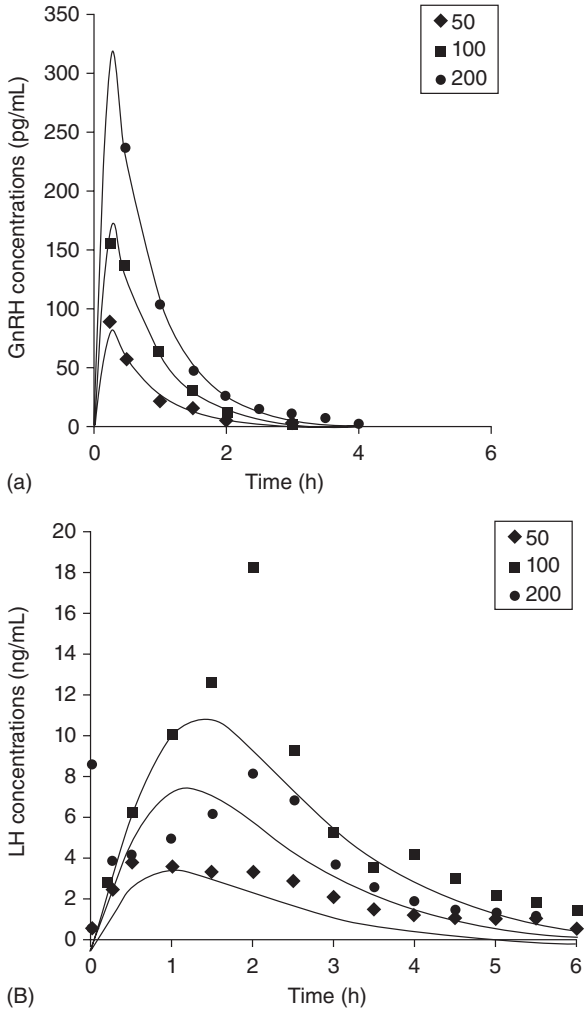

Fig. 13.19 PK/PD analysis of the luteinizing hormone (LH) response to gonadotropin-releasing hormone (GnRH) in a cow. The pharmacokinetics of GnRH and the pharmacodynamic LH response were determined after administration of GnRH at doses of 50, 100, and 200 µg *in toto* (see Fig. 13.4). The three doses were fitted together using an indirect effect PK/PD model. Observed and fitted values for GnRH (a) and plasma (LH) concentrations (b) for a representative cow. From this model, PD parameters were calculated, thus enabling a GnRH dose to be determined that reestablished estrous cycles in cows with ovarian cysts.

nistically oriented models of tolerance have been developed. For example, E_{max} or EC_{50} can be modeled to become time-dependent parameters, that is, to model a time dependency of efficacy (for a noncompetitive antagonistic inhibition) or a time dependency of drug potency (for a competitive antagonistic competition). A hypothetical tolerance counteracting compartment with its own constant can be introduced in the model to mimic the time course of tolerance. A compilation of approaches to modeling tolerance and rebound is given by Gabrielsson and Weiner (2006), though many of them are indistinguishable under different experimental conditions.

13.8 POPULATION PK/PD MODELING APPROACHES

For any given species, the sources of PK variability in veterinary medicine (e.g., breed, age, sex, dietary factors, and kidney and liver functions) have been widely discussed, but the sources of PD variability have been little considered. It is now recognized that PD variability can be more pronounced than that associated with PK. This is especially true for antibiotics, where the clinical response is affected not only by the ability of the drug to reach the site of infection but also by the PD variability (host response to the invading pathogen and bacterial susceptibility). The reader should consult Chapter 16 for development of the statistical nomenclature used in this discussion.

One of the main advances of PK/PD approaches has been to separate the two main sources (PK and PD) of variability through the use of population PK/PD approaches. Similar to the PK population model, a population PK/PD model describing a drug effect across individuals and disease subgroups can be built. Using these techniques, population analysis can explain the variation between animals (or between groups of animals) not only in terms of drug exposure but also in terms of drug responsiveness. For example, the EC_{50} of Equation 13.3 can be modeled using an exponential error model:

$$EC_{50} = \theta_2 \cdot e^{\eta_2} \tag{13.33}$$

where η is the deviation from the mean for the ith subject (intersubject variability) with zero mean and variance ω^2 enabling the interanimal variability of EC_{50} in the population to be determined.

13.8.1 Some practical considerations when building a PK/PD model

The analysis of PK/PD data can be complex and time-consuming because it requires competent modelers having both a good understanding of the general principles of modeling (i.e., statistical and computer skills) and also a broad knowledge of the underlying biology. When planning a PK/PD study, a question should be clearly raised by the intended user (generally a clinician having to design a clinical trial), keeping in mind that the generated results should be understandable in terms of scope and conclusions. For example, the question might be: what is the order of magnitude of the dose of a new analgesic to be tested in dogs in a clinical trial and what could be the clinical benefit of splitting the total daily dose into two doses at 12-h intervals? Conversely, for a given maximal dose of a time-dependent antibiotic in pigs (fixed to take into account some environmental constraints), and knowing the MIC distributions of the main pathogens involved in pig pulmonary disease, what is the target attainment rate, that is, what is the percentage of a pig population able to maintain their plasma concentration for 40% of the dosing interval above the MIC for an empirical antibiotherapy (MIC a priori unknown)? A PK/PD study can also be planned to investigate some pharmacological properties of a drug such as the COX1 versus COX2 selectivity for a new coxib or to bridge some *in vitro*/*ex vivo* results with the *in vivo* situation as is the case when using tissue cage fluid (exudate vs. transudate) to document the PD properties of antibiotics.

The selection of an experimental disease model (experimental inflammation to test an NSAID, experimental infection to test an antibiotic) or of an experimental challenge

(painful stimulus to investigate an analgesic, histamine-induced cutaneous wheal formation to test an antihistaminic drug) should be critically scrutinized regarding the intended use of the drug. Experimental models are usually severe and the estimated parameter can lead to relatively high doses compared with what is actually needed in a clinical setting. Similarly, the selection of a biomarker, a surrogate marker, or a clinical end point should be carefully determined to provide data having appropriate metrological performance (sensitive, gradual, and reproducible) and being overall meaningful. For example, a preclinical PK/PD approach was successfully used to determine a dose of GnRH, for the treatment of ovarian follicular cysts in cattle using the pituitary LH response as a surrogate end point (Monnoyer et al., 2004). This is because the GnRH may produce an LH response similar to the preovulatory LH surge and may initiate estrus cycles in cows with ovarian follicle cysts. In contrast, using ACE inhibition to determine a dosage regimen for ACE inhibitors like benazepril, ramipril, or enalapril, is more delicate because the relationship between ACE inhibition and the prolongation of survival time or the prevention of kidney failure is not direct and straightforward. The measurement of a clinical end point, for example, the latency of paw withdrawal time elicited by a painful stimulus when testing an analgesic, or the measurement of lameness using force plates when assessing an NSAID, is by essence more meaningful than a biochemical biomarker of stress such as secretion of cortisol. Here, the difficulty is to guarantee objective and reproducible measurements and this requires a long-term training of animals enrolled in a trial and also of investigators. It is wise to have the same metrological validation for end point measurements in a PK/PD trial as for analytical techniques (accuracy, intra- and inter-day precision) even for easy measurements like body temperature. In addition, all measurements should be carried out in blinded conditions for the investigators; this practically requires crossover trials to be designed with both a placebo and a test article period. Despite all these precautionary measures, PD variables are often less precisely measured than the plasma concentration with a coefficient of variation of reproducibility reaching up to 30% (Botrel et al., 1994).

Owing to the inclusion of nonlinear steps in most PK/PD models, a sufficiently wide range of drug concentration is necessary to correctly estimate E_{max} and EC_{50}. Often several dose levels (including dose 0 or placebo) are tested and fitted together to cover the entire concentration–effect relationship. When a time-dependent baseline is included in the model to reflect some natural biorhythm (e.g., a circadian rhythm for cortisol when modeling the negative feedback of glucocorticoïds on cortisol secretion) or a reversible pathological process (e.g., an experimental inflammation when testing NSAID or the natural course of a disease when modeling a tolerance phenomenon), the time development of these processes in the absence of drug needs to be carefully assessed.

Developing a PK/PD model requires not only a general knowledge of modeling but also a biological understanding of the primary system under investigation. A collection of physiological models is given by the Physiome Project (http://nsr.bioeng.washington.edu/), which can be a good starting point to develop a suitable physiologically based PK/PD model.

Most PK/PD models have to be written with sets of differential equations because they generally include several nonlinear processes, and equations are solved numerically. Then parameters of the model (drug and system related) are estimated by nonlinear regression. Several computer programs exist to build defined user-friendly PK/PD models including

Phoenix® WinNonlin® (Pharsight, Moutainview, CA), Kinetica (Innaphase, Philadelphia, PA), and Adapt II (Biomedical simulation resource, Los Angeles, CA). The modeling section of Chapter 14 should be consulted for additional details. To estimate parameters, initial values are needed. Vector of system parameters, that is, the component of the model that is independent of the tested drug, can be obtained from a priori knowledge. If system parameters are well known, they can be limited to the range of their possible physiological values (as for body temperature for a system model built to investigate the antipyretic action of NSAIDs or blood pressure for an antihypertensive drug). For drug-related parameters like EC_{50} and IC_{50}, initial values can be obtained from *in vitro* knowledge of substance potency.

The final PK/PD model should be simple enough to remain identifiable with the available experimental data. Indeed, the goal is not to achieve the best fit of observed data but to provide useful information to the end users by making accurate and precise predictions. As the number of parameters in a model increases, the goodness of fit increases but at the expense of estimating the model parameters with an appropriate precision, so the risk is to have an overparameterized model.

When the goal is only to simulate situations (as in predictive toxicology), complicated physiologically based models (PBPK) can be developed and the parameters fixed to some a priori values issuing from what is rather well known (like blood flow, organ weights) or from *in vitro* investigations. Here, the challenge relies on the accuracy of the prediction: when the goal is to estimate system- and drug-related parameters, the question of structural and numerical identifiability should be addressed. Structural identifiability, a concept introduced in Chapter 8, refers to the uniqueness of estimating the model's parameters given model and error-free data. Numerical identifiability (or estimability) refers to the possibility of accurately estimating parameters of a structurally identifiable model given real, observed data (Bonate, 2006). A convenient approach to test identifiability is to simulate data sets and then fit the model to the error-free simulated data using the parameters used to simulate the data as starting values. If a model is identifiable, convergence is achieved within a few iterations, the residual sum of the squares is very small, and the precision of estimates is excellent (small standard error). If not identifiable, the model may not converge or, if it converges, the parameters would have large standard errors despite the model having a low residual sum of squares. If the model is not identifiable, many combinations of parameter estimates can be obtained. The solution to this problem can be (1) re-parametrization of the model especially to solve problems of estimability; (2) further simplification of the model by combining several parameters; or (3) conversely keeping the model, but collecting more information to render observable every parameter (i.e., to be sure that any parameter has an influence on the collected data). Distinguishability is another similar issue where different structural models can produce exactly the same output profile as the one that was observed.

After having fitted data, the model is generally used to simulate scenarios such as the influence of different dosage regimens on the response. Mean or median parameter values obtained from a pool of individuals (two stages analysis) or typical values as given by a population modeling approach are selected to run the model. With a population model, estimates of inter- and intra-animal variability enable population data to be generated. This is of special interest for PK/PD modeling of antibiotics, where one of the objectives is to achieve a target attainment rate in a given percentile of the population. Finally, simulations are also the best way to communicate with end users.

13.8.2 Application of PK/PD concepts to *in vitro*/*in vivo* extrapolations

Extrapolation from *in vitro* to *in vivo* is another fruitful application of the PK/PD paradigm. Quantitative exposure–response relationships are often easily obtained from some *in vitro* or *ex vivo* system, for example, MIC for antibiotics, whole blood assay for NSAIDs, intact pathogenic organism in culture for anthelmintic drug discovery, and toxicological responses in tissue culture. If an effective concentration (*EC* for stimulation, *IC* for inhibition) is obtained on the basis of an *in vitro* or *ex vivo* assay, then a dose can be proposed by incorporating the *in vitro EC* directly into Equation 13.2. It should be noted that since *in vitro* concentrations are generally equivalent to free drug concentrations, corrections for drug binding to plasma proteins might be needed to estimate the corresponding *in vivo* plasma *EC* or *IC*. Chapter 5 discussed methods to accomplish this.

13.9 APPLICATION OF THE PK/PD APPROACH TO THE SELECTION OF AN EFFECTIVE DOSAGE REGIMEN

13.9.1 The case of NSAIDs

The main application of a PK/PD investigation is to document or suggest a dosage regimen for pivotal clinical trials. An initial approach consists of computing an average daily dose from Equation 13.2 using estimated PD parameters. For example, using Freund's adjuvant model in the dog, the IC_{50} of nimesulide for lameness was found to be 6.26 µg/mL (Toutain et al., 2001b). Using Equation 13.2 and considering the plasma clearance of nimesulide (15.3 mL/kg/h or 367.2 mL/kg/day) and its oral bioavailability (47%), the ED_{50} of oral nimesulide administration for the treatment of lameness can be calculated as 4.9 mg/kg/day. This is nearly equal to the recommended dose (5 mg/kg). A more advanced approach consists of simulating a previously established PK/PD model in order to allow the clinician to inspect the time course of the effect obtained at different dose levels in order to assist him or her in selecting a dose and a dosing interval for confirmatory clinical trials. For this, the relationship between plasma NSAID concentrations and a relevant clinical outcome such as body temperature for fever or a lameness score for locomotive inflammation needs to be incorporated. Different possible dosage regimens (dose, interval of administration, modalities of administration) can then be simulated as illustrated in Fig. 13.20 for a hypothetical NSAID.

The second parameter to be determined in a rational multiple-dose regimen is the time interval between administrations. Using a PK/PD model, a large number of dose and dosage interval scenarios can be simulated to select a dosage regimen having the best efficacy or safety margins. Such analysis requires no additional time or cost during drug development. For example, as seen in Fig. 13.21, it was shown that a PK/PD model predicted a better antipyretic efficacy for nimesulide at a dosage regimen of 2.5 mg/kg twice a day rather than at 5 mg/kg once per day, although both dosage regimens were equivalent in terms of lameness suppression.

Another aspect of PK/PD modeling is to document drug selectivity. Here, one of the most convenient approaches consists of documenting the differential action of the tested NSAID on COX1 and COX2 inhibition using an *ex vivo* experimental model of acute inflammation involving surgically implanted tissue cages (Lees et al., 2004). Then the ratio

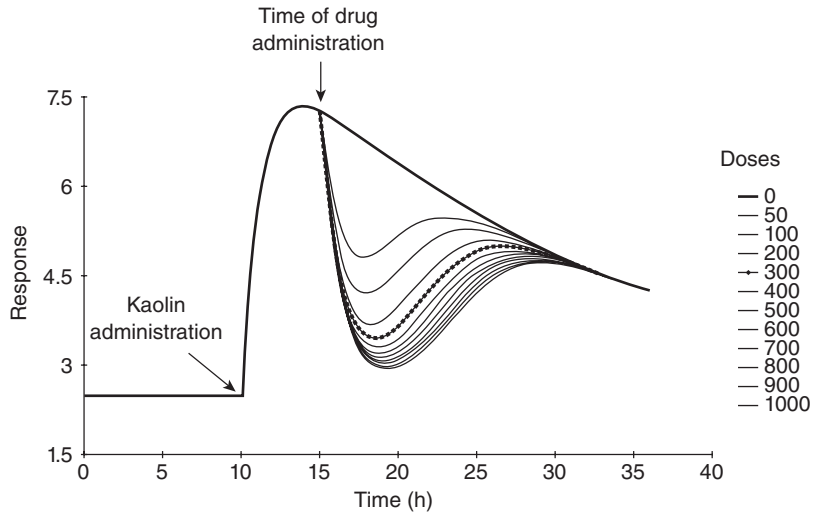

Fig. 13.20 Dose–effect relationship for a hypothetical NSAID on the reduction of lameness in experimental paw inflammation. An indirect effect model was used to simulate data. Parameters of the model were obtained from a previous experiment in which a phlogogenic agent (kaolin) was administered to create an experimental inflammation of the paw at 10 h. The drug was then administered at 15 h and the degree of lameness assessed before kaolin administration (negative control), after kaolin administration but before drug administration (positive control), and then after the NSAID administration. The experimental data were modeled with the following model:

$$dR/dt = K_{in} + Inflammation \cdot \left(1 - \frac{[Drug]}{[EC_{50} + Drug]}\right) - K_{out} \cdot R$$

where *R* is the lameness response versus time (h), and *Inflammation* is the function describing the time course of the kaolin effect on locomotion in the absence of drug. In this example, inflammation was modeled with Equation 13.20, *Inflammation* was mitigated by the NSAID through a fractional inhibitory model with *Drug*, the NSAID plasma concentration as given by the pharmacokinetic model describing the NSAID disposition (here a monocompartmental model with a phase of absorption) and EC_{50} is the NSAID plasma concentration for which the inhibitory function is at 50% of its maximum capacity. Then, using this model with the different estimated parameters, the time course of the test drug effect was simulated for doses ranging from 0 (placebo) to 1000. Visual inspection of the different curves shows that the effect increased progressively with the dose but not proportionally. With higher doses, there is a "diminishing return" because the incremental increase in effect is smaller with each incremental increase in the NSAID dose, and beyond the dose of 300 (-•-), the increase of the maximal effect becomes marginal and only the duration of effect is slightly prolonged. Therefore, it is likely that a clinician will consider the 300 dose to be a putative dose for testing in a clinical trial.

$EC_{50,COX2}/EC_{50,COX1}$ can be considered as an index to predict *in vivo* selectivity. However, it should be borne in mind that the selected end points are surrogates and not actual outcomes of direct clinical interest.

13.9.2 The case of antibiotics

PK/PD modeling was first developed for reversibly acting drugs, but it can also successfully be applied to irreversible drug effects as is the case for antibiotics. For example, the

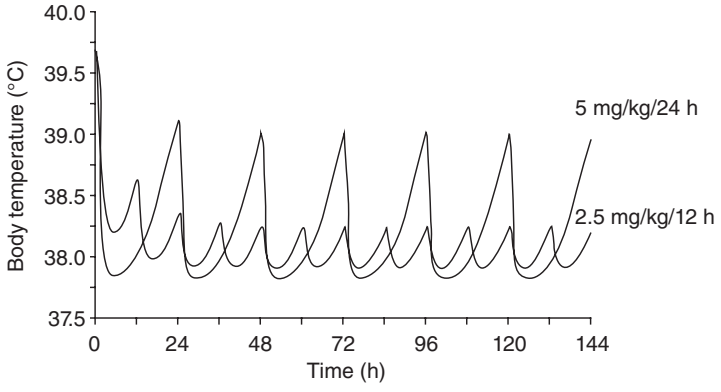

Fig. 13.21 Plot of predicted body temperature (°C) versus time (h) after administration of nimesulide in dogs at two different doses (2.5 mg/kg/12 h and 5 mg/kg/24 h, for 6 consecutive days). Visual inspection of the figure suggests the superiority of the 2.5 mg/kg/12 h dosage regimen (from Toutain et al., 2001a).

Hill equation can be used to describe the activity of an antibiotic against microorganisms as follows:

$$dN/dt = B \cdot \left(K_{\text{growth}} - \frac{K_{\text{kill\_max}} \cdot C(t)^n}{EC_{50}^n + C(t)^n} \right) \tag{13.34}$$

where B is the bacterial population size (colony-forming units/milliliter), K_{growth} is the apparent rate constant of exponential growth without exposure to the antibiotic (unit: 1/time), $K_{\text{kill\_max}}$ (1/time) is the maximum bactericidal effect, n is the Hill coefficient of sigmoidicity, $C(t)$ is the antibiotic plasma concentration at time t, and EC_{50} is the antibiotic concentration producing 50% of $E_{\max}$. From this basic model first proposed by Zhi et al. (1986), many refinements have been proposed to describe situations where growth is limited by the shortage of resources, emergence and replication of resistant subpopulations, action of antibiotics either on the replication rate or on the killing rate, and influence of immune response. Using these kinds of mechanistic models, incorporating several key factors contributing to the emergence of resistance has allowed different modalities of antibiotic administration to be simulated. For example, it was shown that the early initiation of treatment and combination therapy with two antibiotics prevented the emergence of resistant bacteria, whereas a shorter course of therapy and sequential administration of antibiotics promoted the emergence of resistance (D'Agata et al., 2008).

These PK/PD models are able to predict some general features of antibiotic/pathogen interaction. Most of the time, the so-called time-dependent antibiotics such as beta-lactams have a high Hill coefficient and a low $E_{\max}$ (low maximum killing rate) while the so-called concentration-dependent antibiotics such as quinolones and aminoglycosides are often characterized by a low Hill coefficient and a high $E_{\max}$, meaning that the same Hill equation is able to describe the action of the different antibiotic classes.

The lack of sensitivity of clinical outcomes to determine the best dosage regimen in terms of bacteriological cure opens the way for investigating the efficacy of antibiotics using surrogate PK/PD indices. Using the murine thigh and lung infection models, various empirical PK/PD indices have been proposed to predict the success or failure of a therapy. Three appear to be sufficient to predict antibiotic effectiveness: (1) the AUC/MIC ratio, an index used for quinolones; (2) the C_{max}/MIC ratio (where C_{max} is the maximum plasma concentration), an index selected for aminoglycosides; and (3) $T >$ MIC (the time during which plasma concentrations exceed MIC, expressed as a percentage of the dosage interval), an index selected for the so-called time-dependent antibiotics such as beta-lactams. These were originally discussed as targets for constructing dosage regimens in Chapter 12.

The parameter ratios AUC/MIC, $T >$ MIC, and C_{max}/MIC are said to be PK/PD indices of efficacy because they combine a PK (AUC, $T >$ MIC, C_{max}) and a common PD (MIC) parameter. These indices can be viewed as dose surrogates in a dose-titration setting (Fig. 13.2), the dose being replaced by a biomarker of exposure scaled by the MIC. Hence, they allow dual dosage individualization, that is, based on both the microbiological susceptibility and drug disposition kinetics. It should be noted that these PK/PD predictive indices of *in vivo* efficacy are again based on free, nonprotein-bound plasma concentrations of the antibiotic, not total tissue antibiotic levels.

A main goal of veterinary pharmacology is to determine breakpoint values for these three main PK/PD indices for each animal species and their pathogens. It can be done by assessing the *ex vivo* bacterial activity of an antibiotic in serum and tissue cage fluids (exudate, transudate) (e.g., Aliabadi and Lees, 2001). In this kind of experiment, the *graded* antibiotic response (expressed in terms of reduction of an initial bacterial count) is regressed against the surrogate marker (*ex vivo* AUC_{24h}/MIC) using the Hill equation:

$$\text{Antibacterial } ex\ vivo \text{ response} = \frac{[\text{maximal possible drug effect}]\cdot(surrogate)^n}{(surrogate)_{50}^n + (surrogate)^n} \quad (13.35)$$

where the antibacterial response is measured in terms of reduction of the original bacterial count. The independent variable is the surrogate (e.g., AUC_{24h}/MIC) for which a breakpoint is to be established. From Equation 13.35, it is possible to derive three parameters of clinical relevance: the maximal possible antibiotic effect (total bacterial eradication); the $(surrogate)_{50}$, the value of the surrogate associated with 50% of the maximal effect and which is equivalent to an EC_{50}, that is, a measure of antibiotic potency; and n, the Hill coefficient, which gives the slope of the concentration–effect relationship. By solving the model, different levels of the antibacterial response (bacteriostasis, bactericidal effect) can be calculated and corresponding breakpoint values for the surrogate can be computed. Another option to determine the breakpoint value of PK/PD indices is to consider the relationship between the PK/PD index and the likelihood of clinical cure, that is, a quantal response using a logistic model as described by Equation 13.14 and illustrated in Fig. 13.22.

13.10 CONCLUSIONS

This chapter provided approaches to link the concentration–time profiles described by pharmacokinetic models to biological effect. The statistical approaches used to determine PD model parameter values are the same as those used in PK models fully addressed in the next chapter.

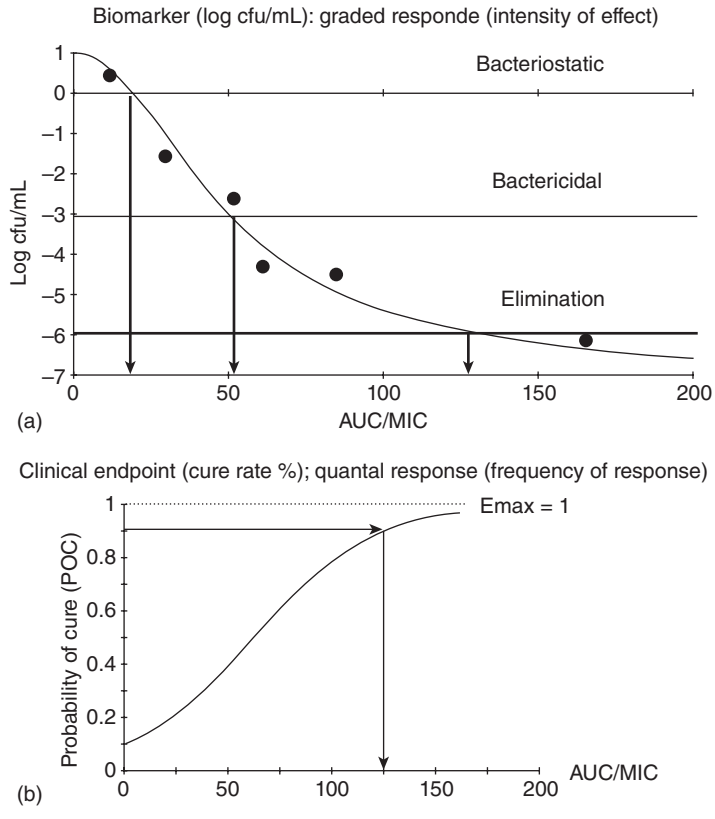

Fig. 13.22 Determination of a PK/PD breakpoint value for a quinolone (AUC/MIC). (a) *Ex vivo* approach consisting of measuring the reduction of an initial bacterial count (expressed as colony forming units [cfu] to different exposures of an antibiotic. Antibiotic exposure is scaled by the MIC of the tested pathogen allowing the AUC/MIC against the bacterial count to be regressed. From the fitted curve, the AUC/MIC corresponding to a bacteriostatic effect (no bacterial growth), bactericidal action (reduction by 3 log of the initial bacterial count) and eradication (reduction by about 6 log of the initial count) can be estimated (see also Fig. 13.10). (b) *In vivo* approach consisting of establishing a relationship between the probability of animal clinical cure and the observed AUC/MIC.

BIBLIOGRAPHY

Aliabadi, F.S., and Lees, P. 2001. Pharmacokinetics and pharmacodynamics of danofloxacin in serum and tissue fluids of goats following intravenous and intramuscular administration. *American Journal of Veterinary Research*. 62:1979–1989.

Aliabadi, F.S., and Lees, P. 2002. Pharmacokinetics and pharmacokinetic/pharmacodynamic integration of marbofloxacin in calf serum, exudate and transudate. *Journal of Veterinary Pharmacology and Therapeutics*. 25:161–174.

Atkinson, A.J., Colburn, W.A., DeGruttola, V.G., DeMets, D.L., Downing, G.J., Hoth, D.F., Oates, J.A., Peck, C.C., Schooley, R.T., Spilker, B.A., Woodcock, J., and Zeger, S.L. 2001. Biomarkers and surrogate endpoints: preferred definitions and conceptual framework. *Clinical Pharmacology and Therapeutics*. 69:89–95.

Bonate, P.L. 2006. *Pharmacokinetic-Pharmacodynamic Modeling and Simulation*. New York: Springer.

Botrel, M.A., Haak, T., Legrand, C., Concordet, D., Chevalier, R., and Toutain, P.L. 1994. Quantitative evaluation of an experimental inflammation induced with Freund's complete adjuvant in dogs. *Journal of Pharmacology and Toxicology Methods*. 32:63–71.

Czock, D., and Keller, F. 2007. Mechanism-based pharmacokinetic-pharmacodynamic modeling of antimicrobial drug effects. *Journal of Pharmacokinetics and Pharmacodynamics*. 34:727–751.

D'Agata, E.M., Dupont-Rouzeyrol, M., Magal, P., Olivier, D., and Ruan, S. 2008. The impact of different antibiotic regimens on the emergence of antimicrobial-resistant bacteria. *PLoS ONE*. 3:e4036.

Dahl, S.G., Aarons, L., Gundert-Remy, U., Karlsson, M.O., Schneider, Y.J., Steimer, J.L., and Troconiz, I.F. 2009. Incorporating physiological and biochemical mechanisms into pharmacokinetic-pharmacodynamic models: a conceptual framework. *Basic Clinical Pharmacology and Toxicology*. 106:2–12.

Danhof, M., de Lange, E.C., Della Pasqua, O.E., Ploeger, B.A., and Voskuyl, R.A. 2008. Mechanism-based pharmacokinetic-pharmacodynamic (PK-PD) modeling in translational drug research. *Trends in Pharmacological Sciences*. 29:186–191.

Dayneka, N.L., Garg, V., and Jusko, W.J. 1993. Comparison of four basic models of indirect pharmacodynamic responses. *Journal of Pharmacokinetics and Biopharmaceutics*. 21:457–478.

Ette, E.I., Roy, A., and Nandy, P. 2007. Population pharmacokinetic/pharmacodynamic modeling of ordered categorical longitudinal data. In: Ette, E.I., and Williams, P.J. (eds.), *Pharmacometrics: The Science of Quantitative Pharmacology*. Hoboken, NJ: John Wiley & Sons.

Fiedler-Kelly, B. 2007. PK/PD analysis of binary (logistic) outcome data. In: Ette, E.I., and Williams, P.J. (eds.), *Pharmacometrics: The Science of Quantitative Pharmacology*. Hoboken, NJ: John Wiley & Sons.

Fosse, T.K., Toutain, P.L., Spadavecchia, C., Haga, H.A., Horsberg, T.E., and Ranheim, B. 2010. Ketoprofen in piglets: enantioselective pharmacokinetics, pharmacodynamics and PK/PD modelling. *Journal of Veterinary Pharmacology and Therapeutics* (in press).

Frank, R., and Hargreaves, R. 2003. Clinical biomarkers in drug discovery and development. *Nature Reviews Drug Discovery*. 2:566–580.

Friedman, P.A., and Hebert, S.C. 1997. Site and mechanism of diuretic action. In: Seldin, D., and Giebisch, G. (eds.), *Diuretic Agents. Clinical Physiology and Pharmacology*. San Diego, CA: Academic Press.

Gabrielsson, J., and Weiner, D. 2006. *Pharmacokinetic and Pharmacodynamic Data Analysis: Concepts and Applications*. Stockholm, Sweden: Swedish Pharmaceutical Press.

Gardmark, M., Brynne, L., Hammarlund-Udenaes, M., and Karlsson, M.O. 1999. Interchangeability and predictive performance of empirical tolerance models. *Clinical Pharmacokinetics*. 36:145–167.

Girard, P. 2005. Clinical trial simulation: a tool for understanding study failures and preventing them. *Basic and Clinical Pharmacology and Toxicology*. 96:228–234.

Girard, P., and Boissel, J.P. 1989. Clockwise hysteresis or proteresis. *Journal of Pharmacokinetics and Biopharmaceutics*. 17:401–402.

Giraudel, J.M., Diquelou, A., Laroute, V., Lees, P., and Toutain, P.L. 2005. Pharmacokinetic/pharmacodynamic modelling of NSAIDs in a model of reversible inflammation in the cat. *British Journal of Pharmacology*. 146:642–653.

Holford, N.H., and Sheiner, L.B. 1982. Kinetics of pharmacologic response. *Pharmacology and Therapeutics*. 16:143–166.

Holford, N.H.G., and Ludden, T.M. 1994. Time course of drug effect. In: Welling, P.G., and Balant, L.P. (eds.), *Pharmacokinetics of Drugs*. Berlin: Springer-Verlag.

Jonker, D.M., Visser, S.A., van der Graaf, P.H., Voskuyl, R.A., and Danhof, M. 2005. Towards a mechanism-based analysis of pharmacodynamic drug-drug interactions *in vivo*. *Pharmacology and Therapeutics*. 106:1–18.

Jusko, W.J., and Ko, H.C. 1994. Physiologic indirect response models characterize diverse types of pharmacodynamic effects. *Clinical Pharmacology and Therapeutics*. 56:406–419.

King, J.N., Maurer, M., and Toutain, P.L. 2003. Pharmacokinetic/ pharmacodynamic modelling of the disposition and effect of benazepril and benazeprilat in cats. *Journal of Veterinary Pharmacology and Therapeutics*. 26:213–224.

KuKanich, B., and Papich, M.G. 2009. Opioid analgesic drugs. In: Riviere, J.E., and Papich, M.G. (eds.), *Veterinary Pharmacology & Therapeutics*, 9th Ed. Ames, IA: Wiley-Blackwell, pp. 301–336.

Lees, P., Giraudel, J., Landoni, M.F., and Toutain, P.L. 2004. PK-PD integration and PK-PD modelling of nonsteroidal anti-inflammatory drugs: principles and applications in veterinary pharmacology. *Journal of Veterinary Pharmacology and Therapeutics*. 27:491–502.

Levy, G. 1964. Relationship between rate of elimination of tubocurarine and rate of decline of its pharmacological activity. *British Journal of Anaesthesiology*. 36:694–695.

Levy, G. 1998. Impact of pharmacodynamic variability on drug delivery (1). *Advanced Drug Delivery Reviews*. 33:201–206.

Mager, D.E., Wyska, E., and Jusko, W.J. 2003. Diversity of mechanism-based pharmacodynamic models. *Drug Metabolism and Disposition*. 31:510–518.

Meibohm, B., and Derendorf, H. 2002. Pharmacokinetic/pharmacodynamic studies in drug product development. *Journal of Pharmaceutical Sciences*. 91:18–31.

Monnoyer, S., Guyonnet, J., and Toutain, P.L. 2004. A preclinical pharmacokinetic/pharmacodynamic approach to determine a dose of GnRH, for treatment of ovarian follicular cyst in cattle. *Journal of Veterinary Pharmacology and Therapeutics*. 27:527–535.

Mould, D.R. 2007. Developing models of disease progression. In: Ette, E.I., and Williams, P.J. (eds.), *Pharmacometrics: The Science of Quantitative Pharmacology*. Hoboken, NJ: John Wiley & Sons.

Pillai, G., Gieschke, R., Goggin, T., Jacqmin, P., Schimmer, R.C., and Steimer, J.L. 2004. A semimechanistic and mechanistic population PK-PD model for biomarker response to ibandronate, a new bisphosphonate for the treatment of osteoporosis. *British Journal of Clinical Pharmacology*. 58:618–631.

Post, T.M., Freijer, J.I., DeJongh, J., and Danhof, M. 2005. Disease system analysis: basic disease progression models in degenerative disease. *Pharmaceutical Research*. 22:1038–1049.

Qiao, G.L., and Fung, K.F.. 1993. Pharmacokinetic-pharmacodynamic modelling of meperidine in goats (I): pharmacokinetics. *Journal of Veterinary Pharmacology and Therapeutics*. 16:426–437.

Sheiner, L.B., Stanski, D.R., Vozeh, S., Miller, R.D., and Ham, J. 1979. Simultaneous modeling of pharmacokinetics and pharmacodynamics: application to d-tubocurarine. *Clinical Pharmacology and Therapeutics*. 25:358–371.

Toutain, P.L., and Cester, C.C. 2004. Pharmacokinetic-pharmacodynamic relationships and dose response to meloxicam in horses with induced arthritis in the right carpal joint. *American Journal of Veterinary Research*. 65:1533–1541.

Toutain, P.L., and Lees, P. 2004. Integration and modelling of pharmacokinetic and pharmacodynamic data to optimize dosage regimens in veterinary medicine. *Journal of Veterinary Pharmacology and Therapeutics*. 27:467–477.

Toutain, P.L., Autefage, A., Legrand, C., and Alvinerie, M. 1994. Plasma concentrations and therapeutic efficacy of phenylbutazone and flunixin meglumine in the horse: pharmacokinetic/pharmacodynamic modelling. *Journal of Veterinary Pharmacology and Therapeutics*. 17:459–469.

Toutain, P.L., Lefebvre, H.P., and King, J.N. 2000. Benazeprilat disposition and effect in dogs revisited with a pharmacokinetic/pharmacodynamic modeling approach. *Journal of Pharmacology and Experimental Therapeutics*. 292:1087–1093.

Toutain, P.L., Cester, C.C., Haak, T., and Laroute, V. 2001a. A pharmacokinetic/pharmacodynamic approach vs. a dose titration for the determination of a dosage regimen: the case of nimesulide, a Cox-2 selective nonsteroidal anti-inflammatory drug in the dog. *Journal of Veterinary Pharmacology and Therapeutics*. 24:43–55.

Toutain, P.L., Cester, C.C., Haak, T., and Metge, S. 2001b. Pharmacokinetic profile and in vitro selective cyclooxygenase-2 inhibition by nimesulide in the dog. *Journal of Veterinary Pharmacology and Therapeutics*. 24:35–42.

Williams, P.J., and Ette, E.I. 2007. Biomarkers in drug development and pharmacometric modeling. In: Ette, E.I., and Williams, P.J. (eds.), *Pharmacometrics: The Science of Quantitative Pharmacology*. Hoboken, NJ: John Wiley & Sons.

Zhi, J., Nightingale, C.H., and Quintiliani, R. 1986. A pharmacodynamic model for the activity of antibiotics against microorganisms under nonsaturable conditions. *Journal of Pharmaceutical Sciences*. 75:1063–1067.

14 Study Design and Data Analysis

with Jason Chittenden

Mastery and comprehension of curve-fitting principles may be one of the most neglected areas in pharmacokinetics. It is at this stage that the quality of the analysis is in full control of the investigator. As can be appreciated from the discussion in earlier chapters, both compartmental and noncompartmental analyses require accurate curve fitting for calculation of the parameters that describe the concentration–time (C-T) profile, namely the slopes λ_n and intercepts A_n. Errors in this stage of the process may produce parameter estimates that are wrong simply because the data were improperly analyzed and not because the underlying model was incorrectly specified. Errors introduced here will negatively effect and bias the use of these pharmacokinetic parameters in subsequent analyses or construction of dosage regimens.

There are a number of basic statistical principles that must be followed in any curve-fitting analysis. The reader is encouraged to consult a statistics text for a complete presentation of these principles and techniques. This chapter will introduce some basic concepts since it is essential to have an intuitive grasp of this process before analyzing data using automated software.

14.1 INTRODUCTION TO STATISTICAL CONCEPTS

The problem to be considered is how to fit a pharmacokinetic model to experimental data. How does one judge that the fit is correct? If a drug is reasonably well "behaved," then the curve-fitting process should be relatively easy. For illustrative purposes, we will consider a drug with linear pharmacokinetic properties. The task then is to select the proper model (e.g., one-, two-, or three-exponential equation). Numerous commercial statistical and pharmacokinetic packages are used, which all share common attributes. The principles will be presented and then an example using a popular software package will be illustrated.

The first step in understanding this process is to rewrite the basic monoexponential pharmacokinetic equation (the model to be fitted) to include statistical error components:

$$C_t = [A_1 e^{-\lambda_1 t}] + \mu_t + \varepsilon_t \tag{14.1}$$

Comparative Pharmacokinetics: Principles, Techniques, and Applications, Second Edition. Jim E. Riviere.
 ISBN: 978-0-813-82993-7

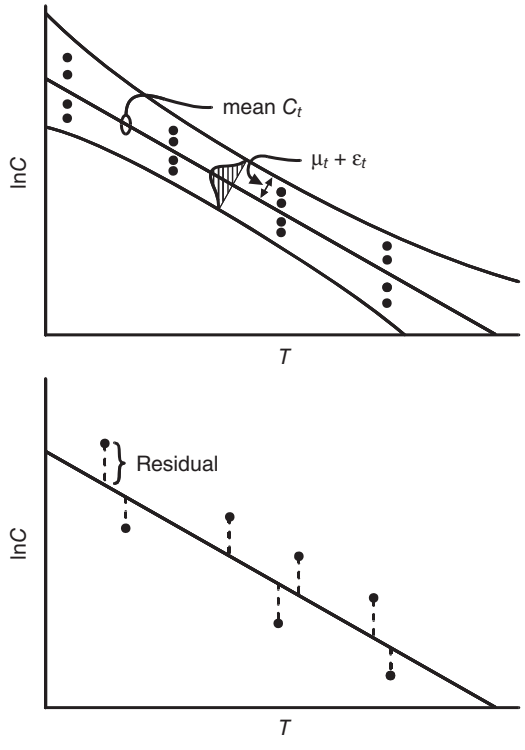

Fig. 14.1 Statistics of pharmacokinetic model-predicted concentration versus time profile. The mean predicted concentration at any time (t) is C_t. Actual data points are (•). Top panel: variance envelope characterized by $\mu_t + \varepsilon_t$, defined by the nature of its frequency distribution. Bottom panel: definition of the residual as the vertical difference between the observed and model-predicted concentration. The square of this distance is added for all data points to obtain the sums of squares, which is minimized in a regression program.

where μ_t is unexplained variation in C due to lack of model fit (model misspecification) or bias and ε_t is unexplained variation due to random error. Even if the monoexponential equation represents the optimal model to describe these data ($\mu_t = 0$), there will always be a random error component due to experimental (e.g., sample timing, analytical error) or intraindividual variation. Thus, any regression analysis will always have a degree of uncertainty, and the predictions will thus be bounded in a confidence interval that is largely defined by the magnitude of $\mu + \varepsilon$. This prediction envelope, defined by the actual statistical distribution of the error components, is illustrated in the top panel of Fig. 14.1.

One must realize that, regardless of the complexity of the model to be fitted in Equation 14.1, the identical regression process is utilized to minimize the error components. Some programs fit the exponential equations using techniques of nonlinear regression analysis, while other simpler programs linearize the exponential equations by logarithmic transformation to fit the equation in the slope-intercept form by simple linear regression (recall discussions in Chapter 8). All of the models presented earlier in this text may be fit to data using some implementation of statistical regression. Recall from Chapter 11 that these approaches are conceptually different from those employed in physiologically based pharmacokinetics (PBPK) modeling, in which the goodness of fit to the C-T data alone is not the primary constraint involved in model selection.

As will be presented in Chapter 16, population pharmacokinetic approaches essentially attempt to correlate the interindividual component of error with observable clinical parameters (termed concomitant variables or covariates), thereby improving the model-explained variation and reducing the true random error ε. Some models even remove analytical error from this term. If the statistical distribution of ε can be mathematically defined, then the overall regression analysis can be improved even further. Our focus in this chapter is on the errors resulting from the model prediction in one individual (or "pooled" individuals) and thus the error terms $\mu + \varepsilon$ are primarily related to the curve-fitting procedure. Different terminology will be employed in Chapter 16 as the aim of the modeling is different. However, conceptually, the problem is the same except that, in addition to $\mu + \varepsilon$, interindividual variance components will be included.

14.2 CURVE FITTING

In all software packages, the computer will attempt to fit the data to a number of different models, using a wide variety of statistical algorithms, and calculate various indices of goodness of fit. Pharmacokinetic curve fitting involves the use of regression techniques to fit a mathematical model to experimental data. By definition, experimental data represent a sample of the population, and in any regression program, a computer is attempting to minimize the fitting error (related to $\mu + \varepsilon$), which is based on comparing values of residuals. The residual is defined as

$$\text{Residual} = \text{Observed} - \text{Predicted} \tag{14.2}$$

which for a biexponential model is

$$\text{Residual} = \text{Observed} - (A_1 e^{-\lambda_1 t} + A_2 e^{-\lambda_2 t}) \tag{14.3}$$

As can be seen in the bottom panel of Fig. 14.1, the residual is the vertical difference between the value at time t predicted by the model and the actual experimental data point observed in the sample. The goal in a regression analysis is to reduce the overall magnitude of these residuals. The computer accomplishes this by minimizing a term called the residual sums of squares (SS), defined as

$$\text{SS} = \sum (\text{Residual})^2 \tag{14.4}$$

Squaring the residuals ensures that SS remains positive and that larger predicted deviations from observations are more greatly "punished." This could also be interpreted as a measure of variance in the data around the model predictions, so minimizing SS minimizes this variance.

Regression analysis attempts to partition the SS in an experimental sample into components that can be explained by the model and the residual which cannot. Based on the basic statistical model in Equation 14.1, this residual SS is actually composed of two components—an SS due to bias or lack of model fit and an SS due to random error. The concept that must be understood in regression analysis is that a model will explain a certain amount of variation in the experimental data. A superior model will explain more of the variation. The unexplained component of the variation (quantitated as the SS) will be due to bias and random error. The analysis attempts to reduce or eliminate the bias or lack of fit component.

There will always be a random error component, which then defines the inherent variability in the data and the nature of the prediction envelope. This random error component is then used to test the model for statistical significance and define confidence limits for the model predictions.

14.2.1 Goodness of fit

Once the parameters of a model have been estimated, one would like to assess the suitability of the model, or the "goodness of fit." Assessment of goodness of fit can involve objective and subjective measures. Subjective measures of goodness of fit involve the ability of the model to describe the observations as well as to predict new observations and possibly to interpolate and extrapolate predictions. Investigations of the model's predictability can be accomplished by re-simulation of the data, in a process called "visual predictive check." This re-simulation will involve the intraindividual error and possibly (at one's discretion) the uncertainty in the parameter estimates. The goal is to ascertain if the model is not only believable but also useful. If the prediction interval is too large, the model may not be useful at all.

Objective goodness of fit measures arises from the statistical basis of the regression. To better understand the tools at our disposal, we can look back at the SS and consider some of the tacit assumptions that have been made. First, if it is assumed that we are interested in an unbiased model, then the SS should indeed be proportional to the variance of the residuals. In that case, the residuals should be, on average, zero (i.e., the mean of the residuals is zero). But by simply summing the residuals, we have also assumed that they are independent of each other and have equal variance. As part of an objective assessment, we can examine the residuals and look for:

- clustering around a mean of zero;
- independence of consecutive values;
- equal distribution (variance), especially across different predicted values.

In practice, while it is possible to statistically test each of these assumptions, a cursory review of residual plots discussed below is usually sufficient.

The goodness of fit of a regression analysis is often assessed by the value of the correlation coefficient, R, where

$$R = f\left(\sum \text{residual} / \sqrt{\text{SS}}\right) \tag{14.5}$$

A perfect correlation has a value of $R = 1$. A more useful parameter is the coefficient of determination (R^2), which by definition is the fraction of the total variation of the data that can be explained by the fitted model. As can be seen, R and R^2 are very dependent upon the absolute magnitude of the SS and thus are completely influenced by the earlier and greater concentrations. All regression techniques operate by iteratively minimizing SS; that is, by computing different estimates of, say, A's and λ's in a model until the lowest value of SS occurs. When this occurs, statistics such as R will approach their optimal value.

Consider the influence on SS of the early (high concentrations) versus late (low concentrations) time points of a kinetic experiment. Assume that the prediction is off by 10%

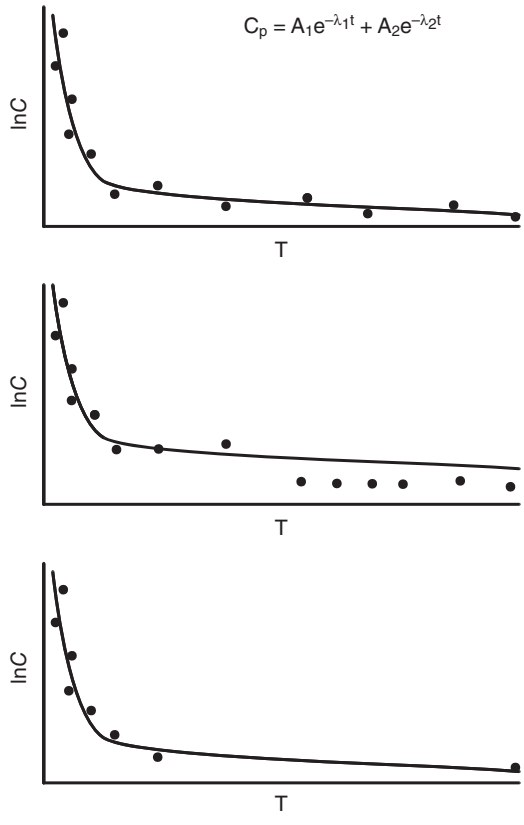

Fig. 14.2 Three biexponential plasma concentration versus time curves. Top panel: an excellent fit between observed and predicted concentrations. Middle panel: overprediction of terminal-phase concentrations. Bottom panel: An unbalanced experiment with sparse data in the terminal phase.

and the concentration data range from 20 μ/mL at 10 min to 0.1 μg/mL at 24 h. The program will try to improve the fit of the early time point since it is trying to minimize the SS generated by an error in the 20 μ/mL sample. More progress is achieved reducing the SS contribution from the earlier time points than the later ones since the concentrations (and hence residuals) vary by a factor of 200.

One of the most powerful approaches to assess goodness of fit is to graphically examine the model-predicted data versus observed data to ensure that the selected model is realistic. Numerical approaches often obscure this basic comparison. Fig. 14.2 shows several examples of actual versus predicted data generated from a two-compartment open model. The ideal fit is depicted in the top panel. The middle panel shows a terminal phase that overestimates most of the data points. This may have resulted because the minimization of SS was completely determined by the residuals of the earlier time points, as discussed above. Statistical parameters such as R^2 for this fit may be very good since both of these procedures would be heavily influenced by the good curve fit to the higher concentrations.

The fit in the middle panel of Fig. 14.2 could be corrected by weighting the regression analysis (and hence the SS for each data point) by $1/Cp$ or $1/(Cp)^2$ to give equal consideration to the lower concentrations. Practically, $1/(Cp)^2$ is often used if concentrations vary

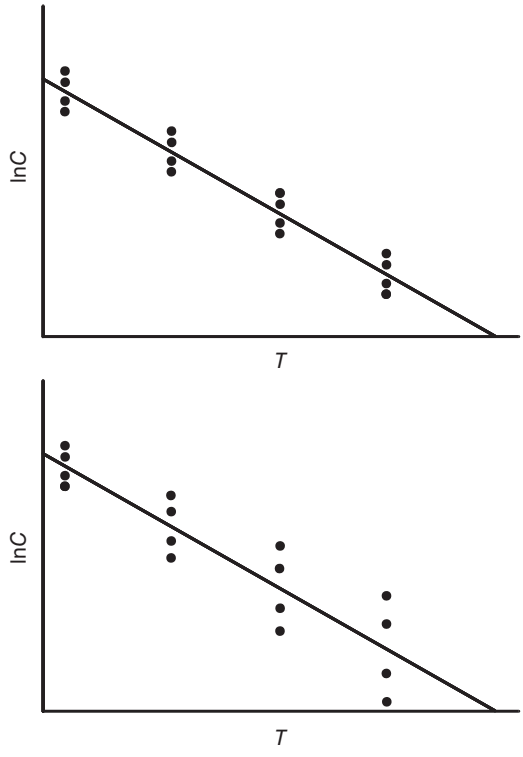

Fig. 14.3 A monoexponential model demonstrating heteroscedasticity (top panel) and one showing data with homogeneous variance (bottom panel). The former is typical of data in which intraindividual variability increases at higher concentrations. Note that the scale is logarithmic, so for an equal distribution of data, the variance is greater at higher concentrations.

over a few orders of magnitude. Recalling the concentration and time ranges presented in Table 8.3 (see Chapter 8), this approach is critical when fitting three or more exponential terms to data.

The selection of the weight is properly determined by the variance structure of the data, which is determined by the variability due to analytical, physiological, and intraindividual factors (e.g., determinants $\mu + \varepsilon$). The need for this can be appreciated by examining the data in the monoexponential C-T profile in Fig. 14.3. In the top panel, the data points have homogeneous variance (homoscedasticity) and a weighting scheme may not be necessary as it is for nonhomogeneous variance. Weighting may still be required, however, to compensate for the range of concentrations. In the bottom panel, the variance is greater at lower than higher concentrations (heteroscedasticity) and the points should be weighted by 1/variance to minimize this highly variable data from overinfluencing the final fit. The optimal approach is to select an appropriate weighting scheme to compensate for this nonhomogeneous variance structure. Depending on the nature of the pharmacokinetic model being estimated, data with nonhomogeneous variance may adversely affect the values of the parameter estimates. The need for weighting indicates a violation of the assumption that the residuals are identically distributed. This can usually be detected on a plot of the residuals versus the predicted variable, as discussed below.

This scenario is encountered in settings in which analytical methods are pushed to their limit of detection, and lower, more variable concentrations will have undue influence on the model selected. If there is a problem with assay sensitivity, a "bottoming out" of the C-T profile is typically seen. The statistics of this curve fit may be excellent as all points are predicted from this model; however, the cause of the flattening is analytical and not biological. This is often seen in veterinary medicine when withdrawal times are studied (the focus of Chapter 19). One possible solution is to only consider the early time points where the model and data appear to be good. However, if this is done, the model will only be good at predicting concentrations at early times, the inference space for this experiment (recall discussion of Fig. 1.2 in Chapter 1).

These weighting processes result in generation of weighted sums of squares (WSS), which are then employed in all subsequent statistical comparisons. Numerous approaches to generate WSS have been reported, and options for their selection are embedded in various software packages. More sophisticated approaches directly model the observed variance's statistical properties (e.g., normal or log-normal distributions) in the regression program, a process termed the extended least-squares method. The final weighting strategy is dependent upon the range of concentrations as well as the actual variability of the data. Chapter 16 should be consulted for a more in-depth discussion of these techniques. It is important to note that when different models are evaluated for goodness of fit using these criteria, the same weighting schemes must be employed when making comparisons.

Another common problem is illustrated in the bottom panel of Fig. 14.2, where there are no data in the final phase (only one point), which suggests that the estimate of the terminal phase is tenuous at best. This is typical of unbalanced experimental designs, where again the SS will be completely dominated by the points of the early phases. A similar situation can occur if the distribution phase has only a few data points.

14.2.2 Residual plots

Lack of model fit to the data can best be appreciated by examining a plot of residuals, a function present in most statistical programs. The predicted values in a residual plot are the horizontal line representing a perfect fit (residual = 0), while the actual residuals are plotted. A simple form of this plot (residual versus time) is depicted in Fig. 14.4, while a more sophisticated version (residual versus concentration) is shown in Figs. 14.6 and 14.8 in the sample data analysis section later in this chapter. As seen in the top graph of Fig. 14.4, a good fit would indicate no bias in the residuals, which suggests the model neither overpredicts nor underpredicts the actual data throughout the course of an experiment. The middle panel is a plot of the example above, where the model misses the terminal phases, with the last six points having residuals below predictions. In the lower panel, a two-compartment model was used to predict a true three-compartment drug. In this case, the model first underpredicts then overpredicts, and then underpredicts the actual data. Such a plot requires that a new model be considered. A good fit is characterized by a random pattern of residuals, which demonstrates that in general, the model is not biased.

As can be appreciated, there is a tremendous amount of information embedded in the residuals since they are plots reflecting μ and ε. Residual plots are often calculated using the WSS to more accurately present the goodness of fit obtained. Most software packages have the capacity to generate residual plots and calculate statistical indices quantitating their goodness of fit and their statistical distributions. For example, a nonbiased model ($\mu \rightarrow 0$) will have no pattern in residuals since they reflect the random error term ε. Thus,

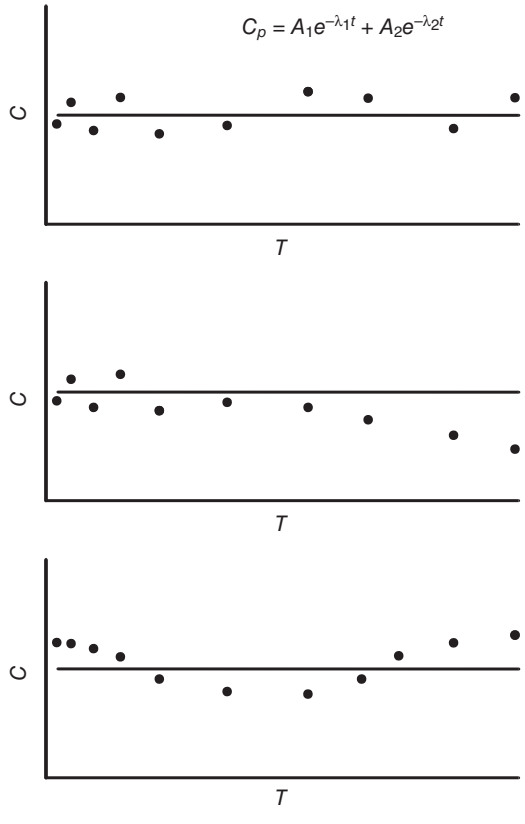

Fig. 14.4 Residual plots resulting from a two-exponential pharmacokinetic model. Top panel: a well-balanced model with random residuals. Middle panel: residuals indicate lack of model fit at late time points. Bottom panel: residuals suggest that a three-exponential equation may better describe the data.

they should alternate between plus and minus values, and their magnitude should reflect the normal Gaussian distribution of a true random error. This is seen in the top panel of Fig. 14.4, where there are eight runs of plus or minus residuals. If, however, the residuals have long runs before the residual sign changes (e.g., middle panel, five runs; and bottom panel, three runs of Fig. 14.4), then there is bias present (μ) and the model is not optimal. A large number of runs thus indicate a better model fit. Statistical tests for randomness of residuals, kurtosis, skewing, constancy of variance, and normality of residuals are included in many pharmacokinetic packages. Similarly, outliers can be easily detected in residual plots and eliminated with a known degree of statistical confidence. These assessments give the user a better idea of model fit.

14.2.3 Properties of estimates

The useful outputs of the regression are the parameter estimates. These values in combination with the model constitute the "knowledge" in the data. But not all parameter estimates are created equal. It is assumed that there is a true parameter value, but our data provide a limited window through which to view it. If the experiment were repeated, new data

would be observed and new parameter estimates would result. So, data from any given experiment will provide parameter estimates that are a sample from some distribution of the parameters. These estimates are hopefully centered on some likely value (e.g., mean or mode), but the question becomes: how much would we expect the estimate to change if the experiment were repeated? In other words, how good are the estimates?

We can imagine that if we changed a parameter value and the SS did not change at all, that parameter could take on any value and not affect the quality of the model. The SS is said to be "insensitive" to the parameter. On the other hand, if we change a parameter and see an enormous change in SS, then the SS is "sensitive" to the parameter. The sensitivity of the SS to the parameters is captured by the standard error of the parameter, a measure of the precision with which the parameter is estimated.

Regression engines output a variance–covariance matrix that is used to compute standard errors and other measures of precision such as the correlation matrix, coefficients of variation (CV, defined as parameter mean/standard error), and confidence intervals. The measures are useful in testing whether a model might be simplified, for instance if the confidence interval contains a value which would cause a term in the model to vanish. Large standard errors or correlations between parameters are indicative of an overspecified model (too many parameters, or too complicated for the amount of data collected), a poor solution (try different initial estimates), or a poor choice of weighting.

14.2.4 Model comparison

The ability to compare and select between different candidate models is enabled by the computation of various statistics of the fits. Automated pharmacokinetic packages will report out one or all of these statistics. These include R, R^2, estimated parameter CV, the F-test on a model's ability to reduce the WSS, and various criteria used to determine whether the simplest model is sufficient to fit the data (e.g., Aikake's information criterion [AIC]; Schwarz's criterion [SC or SBC]). The CV of the estimated parameters is a very robust indicator of the adequacy of the model parameter estimation since the standard error of any parameter estimate is related to the magnitude of the unexplained variation within an individual (μ and ε). The optimal model that truly describes the disposition of the drug will have a smaller CV.

The F-test is used to judge the statistical significance of the value of R^2. It is widely used in analysis of variance (ANOVA) and was used in assessing the quality of the quantitative structure permeability relationship (QSPeR) equations in Chapter 3 (Eq. 3.4). It is the comparison of SS (or WSS) between two competing models that take into account the difference in the reduction in SS between the models based on the degrees of freedom (df). Note that this will parallel the reduction in the extended least squares objective function used in population pharmacokinetic models in Chapter 16. Degrees of freedom are defined as the number of data points analyzed minus the number of parameters estimated. For a monoexponential model with 10 C-T points and two parameters being estimated (A,λ), the df_{mono} would be 8. For a biexponential model being fitted to the same 10 data points, the df_{bi} would equal 6. The greater the df, the more precise the analysis. The F-statistic is calculated as

$$F(\Delta df, df_{bi}) = \{(SS_{mono} - SS_{bi})/SS_{bi}\}\{df_{bi}/(df_{mono} - df_{bi})\} \quad (14.6)$$

The subscripts mono and bi refer to the number of exponential terms in the models being compared. In the example described, $\Delta df = 2$, and thus the appropriate F-statistic is $F(2,6)$.

The value of the calculated F is now compared with a table of F-statistics (computed directly in most software packages) for different levels of statistical significance ($\alpha = 0.05$ traditionally used). If the calculated F is greater than the reference F, then the biexponential model has resulted in a statistically significant reduction in SS and is a preferred model. In contrast, if the calculated F is less than the reference F, then the simpler model should be used.

Both the R^2 and F-tests, which are based on SS, are fairly insensitive to lack of fit for lower concentrations, and thus a weighting scheme must often be employed and then these statistics calculated using WSS values. The F-test may be used to compare any two models; as long as the weighting schemes are identical in both, and the models are "nested," a choice of a parameter value could reduce one model to the other. As can be appreciated from a consideration of df, the more data points in the analysis, the more sensitive the discrimination between models will be.

The AIC and SC are estimates of how complex a model needs to be (e.g., number of exponential phases) in order to optimally fit the models to the data. For an experiment with "n" C-T data points that estimates "p" parameters (df would now equal $n - p$)

$$\mathrm{AIC} = n(\ln \mathrm{WSS}) + 2p \tag{14.7}$$

$$\mathrm{SC} = n(\ln \mathrm{WSS}) + p \cdot (\ln n) \tag{14.8}$$

The model with the lowest value of either AIC or SC is the better model.

More recently, the corrected AIC, or $\mathrm{AIC_c}$, has been developed as an alternative to AIC to account for cases where the number of observations is low compared with the number of parameters. $\mathrm{AIC_c}$ converges to AIC as the number of observations becomes large relative to the number of parameters.

$$\mathrm{AIC_c} = n \ln(WSS) + 2p + \frac{2p(p+1)}{n-p-1} \tag{14.9}$$

When using AIC or SC to compare models, it is the difference in values between two models that is of interest. Differences of <2 are borderline, and differences of >5 are substantive. To apply AIC or SC, the models must use the same weighting and (of course) the same data, but they need not be nested as for the F-test.

We have illustrated these techniques using simple monoexponential and biexponential models. There are numerous other techniques based on correlation matrices and other statistical metrics (e.g., eigenvalue of the variance–covariance matrix) that may be used to explore complex multiparameter models. Although mathematically more complex to compute, the same indices described above may also be generated for any of the models described in previous chapters. The differences between AIC and SC in differentiating models will be based on the relative sizes of "n" and "p" that define the "df" in the experiment. If the purpose is to discriminate models, then the experiment must be designed to have a large "df" to accurately compute discriminating statistics and define mathematical identifiability. *In other words, there must be enough data collected to have sufficient df to be able to define a model.* An experiment conducted with four time points cannot be used to fit a three-compartment model to the data!

Often times, all four criteria (F-test, R or R^2, AIC, and SC) select the best model. In other cases, especially when the df are low because of either too few data points or too

many parameters being estimated, the results are not clear-cut. An example of this is provided later in this chapter. This author would strongly advise against relying on any one parameter. A final model should be selected based on an examination of all data viewed in the context of how the model will be applied.

Finally, we have only addressed the analysis of C-T profiles. Identical approaches are used when multiple matrices are sampled and concentrations in plasma, urine, and peripheral tissue versus time are modeled. An example is the parathion models depicted in Figs. 8.24 and 8.25 (see Chapter 8). In these cases, the reduction in df introduced by the addition of compartments is offset by the increased number of observations obtained by analyzing more matrices and metabolites. Similar logic applies to pharmacokinetic–pharmacodynamic (PKPD) modeling of concentration data and effect compartments, as presented in Chapter 13. Residual plots for "predicted versus observed concentration" in all these matrices or "predicted versus observed effect" can be examined and statistics calculated to obtain the best fit to all of the data. The only real difference is that more complex models are specified in the input to the programs, making selection of the proper models a critical step, especially when nonlinear data are to be studied. The fit to multiple residual plots must be simultaneously assessed. In PKPD models, it is important to start with the optimal and simplest pharmacokinetic model that adequately describes the data to ensure that, after linking to a pharmacodynamic model, all variation in the concentration versus time data is adequately predicted by the pharmacokinetic model. As alluded to in Chapter 3 and as will be seen in Chapter 18, using regression techniques to fit QSPeR data or to conduct allometric analyses are all exercises in statistical regression analysis, making the principles discussed above important.

14.3 COMPUTER CURVE-FITTING EXAMPLES

These nuances of curve fitting are best illustrated by example. The data listed in Table 14.1 are observed values obtained in the author's laboratory after an intravenous dose of 20 mg/kg of the antibiotic doxycycline to four preruminant calves. Concentrations were quantitated for total plasma doxycycline using a high-performance liquid chromatographic assay, validated with mass spectrometry as being specific for unchanged parent drug (Riond et al., 1989). These data were then analyzed using a commercially available software package, Pharsight's Phoenix® WinNonlin®. The modeling process is deconstructed and presented here with relevant discussion and graphics.

Table 14.2 and Fig. 14.5 display the parameter estimates and fitted curves, respectively, for a model with additive error (uniform weighting).

An examination of the data shows clear two-compartment behavior, so the analysis was begun with a two-compartment model. Initial estimates were obtained automatically by curve stripping (recall Fig. 8.16 in Chapter 8).

Estimation of distribution parameters is always fraught with difficulty since as discussed above, the concentrations are high and the sample times are very short. Errors in the time of sample collection will have a major impact on the parameters obtained. For example, the first sample collected was at 5 min (0.08 h). If the collection times were off by 1 min, this would be an error of 20%. In contrast, if the timing was off by 1 min for the 48-h sample, the error would only be 0.03%! In fact, at later time points, timing errors of 10–15 min have little effect on the analysis (0.3% error at 48 h). This sensitivity to sample time is a function of the slope of the fitted curve, the rate of change of concentration with respect

Table 14.1 Sample data set used as input in pharmacokinetic software packages (doxycycline plasma concentration in micrograms per milliliter after an intravenous dose of 20 mg/kg).

Time (h)	Animal 1	Animal 2	Animal 3	Animal 4
0.08	32.5	27.0	25.8	23.4
0.17	28.0	21.2	24.8	18.7
0.25	25.9	19.5	21.6	18.1
0.33	26.1	18.6	21.1	18.6
0.42	25.0	18.2	19.6	17.1
0.50	23.2	18.2	20.1	16.2
1.00	20.2	17.8	15.8	15.9
2.00	15.2	15.2	14.1	12.5
3.00	12.2	15.9	13.4	11.9
4.00	10.3	12.0	12.5	12.4
10.0	5.3	8.6	11.0	10.2
17.0	7.0	5.8	6.8	6.1
22.0	2.9	6.1	4.9	5.6
28.0	4.0	4.0	3.6	3.9
34.0	2.2	2.8	2.4	2.7
41.0	1.8	1.6	1.3	1.8
46.0	1.4	1.5	1.0	1.4
58.0	0.9	1.2	0.7	0.8
70.0	0.7	1.0	0.6	0.6

Table 14.2 Pharmacokinetic parameter output for analysis of data in Table 14.1.

Subject	A (μg/mL)	α (1/h)	B (μg/mL)	β (1/h)
Animal 1	19.93	0.79	11.17	0.04
Animal 2	18.98	9.22	17.85	0.06
Animal 3	12.43	2.42	15.84	0.05
Animal 4	10.02	3.59	14.9	0.05
Geometric mean	14.736	2.819	14.731	0.051
CI 95% lower	8.675	0.558	10.735	0.042
CI 95% upper	25.033	14.249	20.216	0.061

Confidence intervals (CI) are calculated based on geometric mean.

to time. To minimize these errors, one should record the actual time that the blood sample was collected and use this in the data analysis. Similarly, in a large animal, the blood circulation time becomes important as the drug might not have been uniformly distributed throughout the body.

One way of accounting for the increased variance in the measurements at what are typically high concentrations is to weight the residuals as discussed above. Fig. 14.6 shows the plot of the weighted residuals versus the predicted concentrations with all individuals data overlaid. A Loess regression is shown for the mean of the residuals (middle line) and mean of the absolute residuals (outer lines, mirrored). A Loess regression is a type of moving average, called a local linear regression, and is used to visualize a trend in the residual data. There is a slight trend for the residuals to increase with concentration.

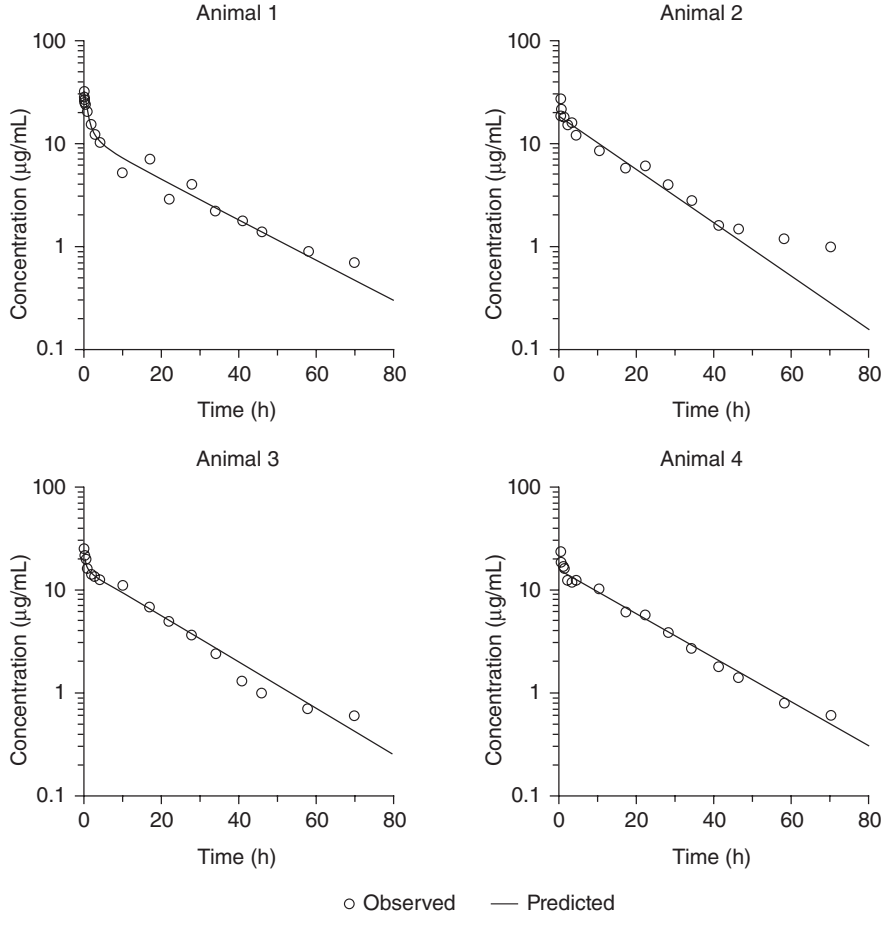

Fig. 14.5 Two-compartment unweighted model fit. Notice that the last data points are systematically underpredicted, especially for animal 2.

Weighting by the inverse predicted value produces the output in Table 14.3 and in Figs. 14.7 and 14.8. The trend in the residuals is reduced in this plot and the visual fit is improved a bit for the tails. The precision of the estimates is generally improved with the weighted model, making a further argument for it.

It is possible to fit a three-compartment model to the data. A three-compartment model could even be suggested by the consistent underprediction of the terminal points in the profiles, suggesting that maybe a third compartment would be better defined with continued sampling. Though the diagnostics related to model fit including R^2, weighted R^2, and weighted sums of squares residual (WSSR) are improved for the new model, it is indicated strongly only in animal 2, based on AIC and SBC (Table 14.4). That is, the additional parameters are not well justified by the slight improvement in model fit. In addition, the standard errors of the parameters become quite large, indicating poor estimation due to overparameterization (data not shown). When some subjects indicate the selection of a more complex model, while some indicate the selection of a less complex model, population modeling may help. This will be discussed in Chapter 16.

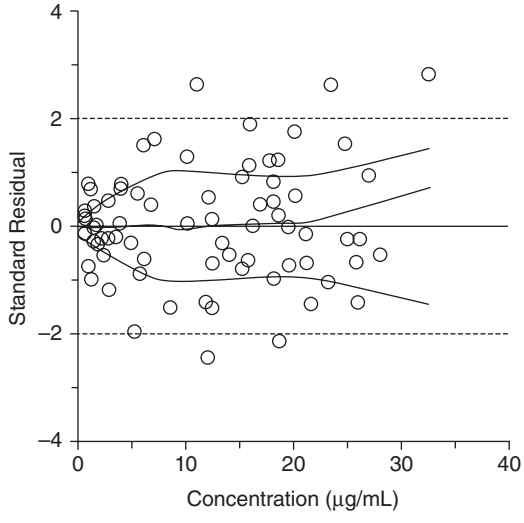

Fig. 14.6 Standardized residuals versus predicted concentration plot. There are some caveats to using this plot across individuals, but we usually find it informative. Note the pinching of the residual values at low concentrations. This indicates that the SS is being dominated by the high-concentration residuals.

Table 14.3 Pharmacokinetic parameter output for analysis of data in Table 14.1.

Subject	A (μg/mL)	α (1/h)	B(μg/mL)	β (1/h)
Animal 1	20.19	0.71	10.56	0.04
Animal 2	16.97	6.65	16.77	0.05
Animal 3	12.58	2.62	16.09	0.05
Animal 4	9.55	3.38	14.95	0.05
Geometric mean	14.241	2.545	14.368	0.049
CI 95% lower	8.415	0.575	10.272	0.041
CI 95% upper	24.102	11.271	20.097	0.058

Data is weighted by the inverse of the predicted values. Confidence intervals (CI) are calculated based on geometric mean.

Table 14.4 Model diagnostics to compare two- and three-compartment weighted models.

Subject	Source	Diagnostic				
		AIC	SBC	WSSR	R^2	R^2 weighted
Animal 1	2 comp	23.00	26.77	2.20	0.995	0.994
	3 comp	22.95	28.61	1.78	0.998	0.995
Animal 2	2 comp	21.69	25.47	2.06	0.993	0.994
	3 comp	12.47	18.13	1.02	0.997	0.997
Animal 3	2 comp	4.61	8.39	0.84	0.998	0.998
	3 comp	8.65	14.32	0.84	0.998	0.998
Animal 4	2 comp	3.97	7.75	0.81	0.995	0.997
	3 comp	1.11	6.78	0.56	0.997	0.998

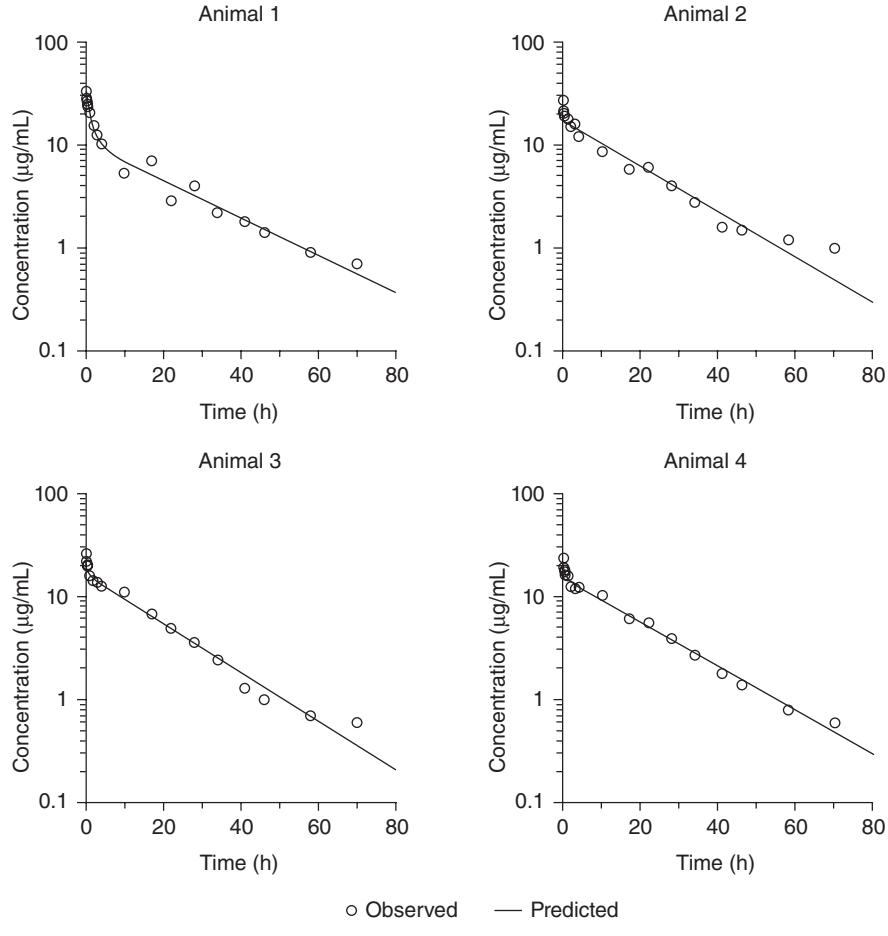

Fig. 14.7 Two-compartment, weighted (predicted^{-1}) model fit. Note that in this case, there is not much change in the predictions.

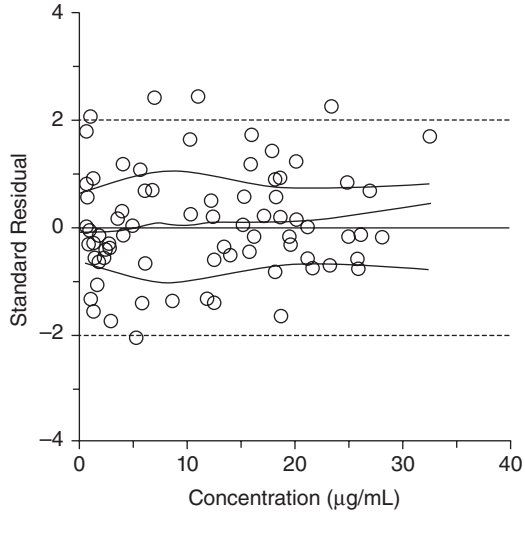

Fig. 14.8 Standardized residuals versus predicted concentration plot. The distribution of the residuals fits the assumption of identical distribution better now, as shown by the flatter trend in the residual distribution.

14.4 GENERAL CONCEPTS

To complete this discussion, we will present a personal overview of important principles of experimental design and curve fitting in the form of several rules of thumb. These should be viewed as suggestions for improving the analysis of experimental data. Independent of what type of pharmacokinetic modeling approach is to be applied, there are a few general guidelines that always should be followed, yet are often ignored, based on the author's review of numerous manuscripts in this field. These include the following:

1. Before beginning any study, it is always prudent to conduct a small pilot trial to determine what the serum C-T profile looks like. This ensures that the concentrations produced by the dose administered are in the proper range for the assay. Concentrations should always be significantly above the sensitivity of the assay, otherwise the terminal concentration profile tends to "flatten out," which erroneously suggests a long terminal half-life ($T_{½}$). Pilot studies are best conducted by taking samples at increasing time intervals to determine how long drug concentrations persist. To get an accurate estimate of a terminal $T_{½}$, one needs an experimental duration at least three to five times the actual $T_{½}$. Recall from Chapter 8 that in five $T_{½}$, 97% of that exponential phase governed by the process is over. Depending on assay methods used, this strategy also allows one to plan for appropriate dilutions.

   A pilot study begins the process of model selection since, when the data are plotted on Cartesian and semilogarithmic scales, linearity may be easily assessed (see Chapter 8, Figs. 8.1 and 8.2, and Chapter 10, Fig. 10.3) and, if appropriate, the number of exponential phases in a linear C-T profile can often be estimated. Finally, it is important to remember that when conducting an intravenous pharmacokinetic study, one must administer the drug in a different cannula from that used to collect blood samples; otherwise, residual drug left over from the high concentration injection will contaminate samples. On this point, one must also remember to discard the initial fill volume of any catheter to ensure that solution in the catheter for anticoagulation purposes will not dilute the actual sample.
2. At this point, it is important to verify that the analytical assay used is appropriate and sensitive enough for the serum concentrations observed. It is better to conduct a few pilot studies to get the concentrations in a range optimal for assay than to do a complete study only to discover that they are out of range and most samples are below the limit of detection! Unfortunately, this occurs too often. This step also helps one select the volume of blood samples needed in the final experiment. The specificity of the assay should be defined. Are any metabolites present? Does the assay measure total or free drug concentrations? Is the assay stereoselective?
3. The next phase is to determine how many samples are needed and when they should be taken. Ideally, an orthogonal sampling schedule should be selected, whereby samples are spaced at increasing time intervals, making the number of samples per exponential phase balanced (e.g., equal number of time points per phase to avoid bias in fitting any one-model component). Of course, this assumes that a log-linear C-T profile has been identified in the pilot study. The reason behind this logic is evident from our discussion of the curve-stripping procedure since essentially one is estimating the intercepts (A_n) and exponents (λ_n) of a polyexponential equation. An unbalanced experimental design that results in too many samples in one phase will give more weight to that phase (all SS determined from that phase) and therefore bias the model. If, in the actual experi-

ment, one finds that this has occurred, one might prefer to randomly delete samples from the data-rich phase to eliminate bias. The increasing time intervals between samples (every 5 min, then 15 min, then 30 min, then 1 h, 2 h, etc.) is always the best strategy to curve-fit exponential equations when the model (1, 2, or 3 terms) is not known, since this results in an equally spaced spread of data when plotted on a semilog C-T plot. A 12-time-point study would be optimally designed as collecting samples at 5, 10, 15, 30, 45, 60, 90, 120, 180, 240, 360, and 480 min. A zero-time, predosing sample should always be collected.

In contrast, if the specific model is already defined for a species, and the goal of the study is to estimate the value of the parameters (intercepts [A_n] and slopes or exponents [λ_n]) for that model, then samples should be clustered within each exponential phase since one already knows where the phases are occurring. One avoids points in the inflection areas (times between phases where the curve bends) since depending on variability, they may be assigned to the wrong phase. If a two-compartment model fits the above data, samples in such a study might be best taken at 10, 15, 20, 60, 75, 90, 240, 275, 300, 400, 440, and 480 min. To design these experiments, studies must have already been conducted in the species of interest and a model defined. In most cases, the first scenario is operative and orthogonal design is best. The reader is referred to statistical texts on experimental design and optimal sampling strategies for a discussion of the differences between model exploration and parameter estimation. A final tool is to use model simulation software (e.g., ADAPT) and assign specific statistical properties to the preliminary model to select the optimal experimental design.

4. The number of animals used for the final experiment is dependent upon the purpose of the study and the variability in drug disposition between individual animals. Standard statistical texts may be consulted to determine sample size. It is important to remember that some of the derived pharmacokinetic parameters, such as $T_{½}$ are not normally distributed, requiring transformations to be performed (e.g., use log-normal, geometric or harmonic $T_{½}$, median, or mode instead of mean) before statistical analysis. A broad examination of the comparative pharmacokinetic literature suggests that the typical size of an intravenous dose pharmacokinetic trial for a drug with normal variability in the population is approximately four to six animals.

   The statistical aspects of interindividual and intraindividual variability will be extensively discussed in Chapter 16 on population pharmacokinetic techniques. At this point, it is important to realize that any individual data point has many components of variability, including those attributed to the assay; to sample timing; to within-individual changes in drug disposition; to between-individual differences in underlying age, physiology, environment or disease states; and to an unexplained component identified as random error. The magnitude of this variability influences the sample size (number of time points and number of replicates) required to adequately fit a mathematical model to the data.

5. An allometric scaling technique could be used to arrive at the initial dose for the pilot study, assuming that a species' clearance and volume of distribution are proportional to its metabolic rate or body surface area. For example, assume that a kinetic study had already been conducted in species A at "*x*" milligrams per kilogram. You know that this dose is at least safe for use in species A. You want to know the initial dose "*y*" to use for your kinetic study in species B. This could be estimated as follows:

$$y(\text{mg/kg}) = x(\text{mg/kg})[\text{Body Weight}_A / \text{Body Weight}_B]^{0.25} \qquad (14.10)$$

The background and development of this approach is fully described in the chapter on interspecies extrapolations (see Eq. 18.3 in Chapter 18). In this case, a small animal would receive a larger dose on a per-weight basis, which would ensure that drug concentrations persist for sufficient times to get a good estimate of $T_{½}$. If a larger animal were to be studied, the dose would be reduced to ensure that one was not now overdosing the animal. If a comparative pharmacokinetic study had already been done, as described in Chapter 18, then the specific allometric exponent ("b") for that drug could be used. Of course, some drugs (especially those metabolized) do not scale, and thus this technique may not work, a situation that could result in toxicity if one was going from a large to a small animal. *This must be considered only as an initial approach to designing a pilot trial in the absence of any better data and must be tempered by any available knowledge of the pharmacology of the drug being studied.*

6. When estimating parameters, convergence (successful completion) of the regression algorithm may be sensitive to initial estimates. If bioavailability is unknown, be aware that flip-flop solutions are possible. When providing initial estimates, try to separate the exponents by an order of magnitude, especially when attempting to fit two- or three-compartment models to data that may not support them. This will help avoid degenerate solutions, where two of the compartments end up with the same exponent. It may be necessary to iterate a model in order to refine initials estimates and achieve convergence. For instance, to estimate a model with WSS, it may be necessary to use final estimates from an unweighted model as initial estimates for the weighted model.

BIBLIOGRAPHY

Any basic text in statistics or regression should be consulted for a refresher on many of the topics covered in this chapter. An excellent source of information on curve fitting can be found in the manuals accompanying many automated pharmacokinetic software packages. Finally, the Bibliography in Chapter 16 contains excellent sources on the statistics of variability in pharmacokinetic studies.

Albert, K.S. 1980. *Drug Absorption and Disposition: Statistical Considerations*. Washington, DC: American Pharmaceutical Association.

Burnham, K.P., and Anderson, D.R. 2004. Multimodel inference. *Sociological Methods and Research*. 33:261–304.

Chatterjee, S., and Price, B. 1977. *Regression Analysis by Example*. New York: John Wiley & Sons.

Daniel, C., and Wood, E.S. 1980. *Fitting Equations to Data: Computer Analysis of Multifactor Data*, 2nd Ed. New York: John Wiley & Sons.

D'Argenio, D.Z. 1981. Optimal sampling times for pharmacokinetic experiments. *Journal of Pharmacokinetics and Biopharmaceutics*. 9:739–756.

Gabrielsson, J., and Weiner, D. 1997. *Pharmacokinetic and Pharmacodynamic Data Analysis: Concepts and Applications*, 2nd Ed. Stockholm, Sweden: Swedish Pharmaceutical Society Press.

Graves, D.A., Locke, C.S., Muir, K.T., and Miller, R.P. 1989. The influence of assay variability on pharmacokinetic parameter estimation. *Journal of Pharmacokinetics and Biopharmaceutics*. 17:571–592.

Holt, J.D., and Black, W.D. 1983. On the transformation technique in pharmacokinetic curve fitting. *Journal of Pharmacokinetics and Biopharmaceutics*. 11:183–187.

Lacey, L., and Dunne, A. 1984. The design of pharmacokinetic experiments for model discrimination. *Journal of Pharmacokinetics and Biopharmaceutics*. 12:351–365.

Neter, J., Kutner, M.H., Nachtsheim, C.J., and Wasserman, W. 1996. *Applied Linear Statistical Models*, 4th Ed. New York: McGraw Hill.

Rawlings, J.O., Pantula, S.G., and Dickey, D.A. 1998. *Applied Regression Analysis: A Research Tool*, 2nd Ed. New York: Springer.

Riond, J.L., Hedeen, K.M., Tyczkowska, K., and Riviere, J.E. 1989. Determination of doxycycline in bovine tissues and body fluids by liquid chromatography using photodiode array ultraviolet-visible detection. *Journal of Pharmaceutical Sciences*. 78:44–47.

Rowland, M., Sheiner, L.B., and Steimer, J.-L. 1985. *Variability in Drug Therapy: Description, Estimation and Control*. New York: Raven.

Schwilden, H., Honerkamp, J., and Elster, C. 1993. Pharmacokinetic model identification and parameter estimation as an ill-posed problem. *European Journal of Clinical Pharmacology*. 45:545–550.

Sheiner, L.B. 1984. Analysis of pharmacokinetic data using parametric models. I. Regression models. *Journal of Pharmacokinetics and Biopharmaceutics*. 12:93–117.

Sheiner, L.B. 1985. Analysis of pharmacokinetic data using parametric models. II. Point estimates of an individual's parameters. *Journal of Pharmacokinetics and Biopharmaceutics*. 14:515–540.

Tod, M., Padoin, C., Louchahi, K., Moreau-Tod, B., Petitjean, O., and Perret, G. 1994. Application of optimal sampling theory to the determination of metacycline pharmacokinetic parameters: effect of model misspecification. *Journal of Pharmacokinetics and Biopharmaceutics*. 22:129–146.

15 Bioequivalence Studies

with Marilyn Martinez

Up through this point in the text, the focus has been to present basic principles and techniques of pharmacokinetics. There is one application in human and veterinary medicine where pharmacokinetic (PK) modeling is broadly applied and where statistical considerations are integrated into both data collection and analysis. This is the determination of product bioequivalence (BE) to be presented here from the perspective of drug regulatory agencies, primarily the US Food and Drug Administration (FDA). This chapter departs from the structure of previous ones as it will develop the basis of current regulations for determining topical BE of veterinary products. At the time of this writing, the corresponding veterinary regulations have not been published. Therefore, the human regulations adopted by the US FDA are used to illustrate these concepts. This chapter reinforces the statistical principles introduced in Chapter 14 and bridges into their further application in Chapter 16 where population pharmacostatistical models are formally introduced. In addition, it illustrates biological factors that directly influence PK parameters, especially in the area of oral drug absorption, in an attempt to reinforce these important linkages developed earlier in the text.

When evaluating the relationship between dose and response for a new active pharmaceutical ingredient (API) or for an API in a new formulation, there are numerous important PK questions to address. For example, it is important to understand clearance (Cl) mechanisms, the distributional characteristics of the compound, the presence (or absence) of active metabolites, stereospecific kinetic properties, the residence time of the drug within the body, physiological and environmental variables that can influence drug pharmacokinetics, and any processes that may lead to a lack of dose-proportional drug exposure. These concepts have been extensively presented in earlier chapters.

15.1 BIOAVAILABILITY

Another component of this PK characterization process is bioavailability. The term bioavailability, introduced in Chapter 4 (see Eqs. 4.2 and 4.3), refers to the rate and extent to which the active ingredient or active moiety is absorbed from a drug product and becomes available at the site of action. For drug products that are not intended to be

Comparative Pharmacokinetics: Principles, Techniques, and Applications, Second Edition. Jim E. Riviere.
 ISBN: 978-0-813-82993-7

absorbed into the bloodstream, bioavailability may be assessed by measurements intended to reflect the rate and extent to which the active ingredient or active moiety becomes available at the site of action (Code of Federal Regulations [CFR] §320.1). The bioavailability of a drug or of a formulation may be considered from several different perspectives, including:

Absolute bioavailability: This describes the percent of the total labeled dose that is systemically available. Most frequently, such assessments are based on the comparison of a formulation to an intravenous (IV) dose of the same active ingredient. By using the equation

$$\mathrm{AUC}_{0-\mathrm{inf}} = (D \cdot F)/Cl_{\mathrm{B}} \tag{15.1}$$

where $\mathrm{AUC}_{0-\mathrm{inf}}$ is the area under the concentration versus time curve from time zero to ∞, D is the administered dose, F is the fraction of the administered dose that is systemically available, and Cl_{B} is the systemic Cl of the drug previously defined in Chapter 8, an investigator can compare the $\mathrm{AUC}_{0-\mathrm{inf}}$ values associated with the IV dose (which, by definition, is 100% bioavailable) to the $\mathrm{AUC}_{0-\mathrm{inf}}$ associated with the formulation under question. An inherent assumption in this assessment is that Cl_{B} of the IV and non-IV formulations are identical. Furthermore, the use of $\mathrm{AUC}_{0-\mathrm{inf}}$ (or $\mathrm{AUC}_{0-\tau}$, which reflects the total AUC over a single dosing interval, τ) rather than the AUC estimated to some other time interval is necessary because the terminal elimination half-life ($T_{½}$) of the different dosage forms may not be equal. Determination of F under these circumstances was presented in Chapter 8, Equation 8.31.

Relative bioavailability: This term describes the comparison of $\mathrm{AUC}_{0-\mathrm{inf}}$ values across different formulations, instead of in reference to IV dosing.

Bioequivalence: BE describes the condition under which the relative bioavailability of two products is consistent with the absence of a significant difference in the rate and extent to which the active ingredient or active moiety in pharmaceutical equivalents or pharmaceutical alternatives becomes available at the site of drug action when administered at the same molar dose under similar conditions in an appropriately designed study (CFR § 320.1). In this regard, for two products to be considered bioequivalent, they need to contain the same API and be administered at the same molar dose.

The objective of BE studies is not to determine an appropriate dose or dosage regimen for this alternative formulation. Rather it is to determine whether or not two products will be clinically indistinguishable to the human or veterinary patient. Embodied in this assessment is the need to show a "superimposition" of respective dose–drug exposure profiles. Therefore, a determination of product BE incorporates PK, chemistry, and statistics.

BE is established on the basis of the marker that most accurately reflects potential formulation effects. As discussed later, in most cases, this marker for blood level studies is the parent compound. Prior knowledge of the API's PK characteristics is used to design a study that will discriminate between inequivalent formulations. For two products to be considered bioequivalent, parameter means and variances should also be "equivalent." For example, Fig. 15.1 illustrates three frequency distribution plots of a PK parameter (e.g., AUC). In the case of treatments A and B, the products are described by similar mean values but different variances. For treatments A and C, the magnitude of variability is similar

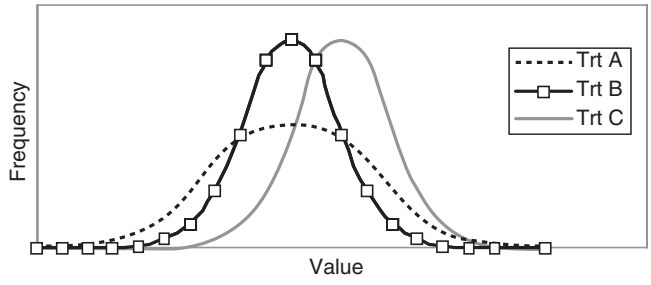

Fig. 15.1 Examples of three product profiles that fail to demonstrate product BE.

across the two formulations, but the means differ. Therefore, none of these treatments can be considered bioequivalent to the other.

Other terms associated with BE determinations include (FDA "Orange Book," 2009):

- *Chemical equivalence:* Two or more dosage forms that contain the same quantity of a particular drug.
- *Clinical equivalence:* The same drug in two or more dosage forms that provide identical *in vivo* effects as measured by some pharmacological response or by the control of the symptoms of a disease.
- *Pharmaceutical equivalents:* Drug products are considered pharmaceutical equivalents if they contain the same active ingredient(s), are of the same dosage form, route of administration, and are identical in strength or concentration. Pharmaceutically equivalent drug products are formulated to contain the same amount of active ingredient in the same dosage form and to meet the same compendial or other applicable standards (i.e., strength, quality, purity, and identity). However, they can differ in such characteristics as shape, scoring configuration, release mechanisms, packaging, excipients (including colors, flavors, preservatives), expiration time, and (within certain limits) labeling.
- *Therapeutic equivalence:* Drug products are considered to be therapeutic equivalents only if they are *pharmaceutical equivalents* and will have the same clinical effect and safety profile when administered to patients under the conditions specified in the labeling. FDA classifies therapeutically equivalent products as those formulations that meet the following general criteria: (1) they are approved as safe and effective; (2) they are pharmaceutical equivalents as just defined; (3) they are bioequivalent in that (a) they do not present a known or potential BE problem and they meet an acceptable *in vitro* standard, or (b) if they do present such a known or potential problem, they are shown to meet an appropriate BE standard; (4) they are adequately labeled; and (5) they are manufactured in compliance with Current Good Manufacturing Practice regulations.

In contrast with pharmaceutical equivalents, *pharmaceutical alternatives* are considered to be drug products that contain the same therapeutic moiety, but contain different salts, esters, or complexes of that moiety, or are different dosage forms or strengths (see Khankari and Grant, 1995, and Kumar et al., 2008, for further discussion on the relationship between salt form and API absorption characteristics). Different dosage forms and strengths within a product line by a single manufacturer are thus *pharmaceutical alternatives*, as are extended-release products when compared with immediate-release or standard-release formulations of the same API.

15.2 HISTORICAL BIOEQUIVALENCE PERSPECTIVE

In 1971, the US National Academy of Science Bioequivalence Symposium resulted in recommendations for the determination of AUC values via numerical integration and the evaluation of rate of absorption by assessing the observed peak drug concentrations (C_{max}) and the time to C_{max}, T_{max} (Ronfeld and Benet, 1977). These terms were defined and used in dosage regimen design in Chapter 12. The bounds for defining BE were set as ±20% based on consultation with physicians who concluded that this magnitude of difference would be without clinical significance. This decision was subsequently codified by publication in the Federal Register in 1977.

In the mid-1980s, the statistical test used for supporting conclusions of product BE by the FDA's Center for Drug Evaluation and Research (CDER) was the analysis of variance (ANOVA) procedure. The null hypothesis (H_0) was "no difference" between treatment means. The type I error, the risk of accepting the null hypothesis when it is in fact true, was set as $\alpha = 0.05$. From a pharmaceutical perspective, this reflects the sponsor's risk of failing to correctly confirm that two products are indeed bioequivalent. In contrast, from a patient perspective, there is the need to minimize the risk of failing to identify those products that are *not* in fact bioequivalent. This is reflective of the type II error (i.e., the probability of failing to reject the null hypothesis when it is in fact false, which was set at $\beta = 0.20$). The *power* to reject the null hypothesis when it is indeed false (the power of the test) is estimated as $1 - \beta$. A description of the type I and type II errors is provided in Table 15.1.

Initially, a statistical *F*-test (introduced in Chapter 14 when regression goodness of fit was discussed in Eq. 14.6) was used to compare product average bioavailability. If the power of the test was less than 80% and if statistically significant differences were not observed (i.e., if $p > 0.05$), then the "75/75" rule could be employed. The "75/75" rule stated that two products could be declared bioequivalent if 75% of the subjects had product ratios for AUC and C_{max} that were within the limits of 75–125% (Federal Register, 1977; Cabana, 1983).

Unfortunately, this method of data analysis presented with inherent inconsistencies. In particular, the likelihood of declaring two products as being bioequivalent increased as the standard error (SE) increased. In other words, the more variable the data, the greater was the likelihood of declaring two products bioequivalent as seen in Fig. 15.2. The upper limits of the BE boundaries were defined by *the criterion of no less than 80% power*.

In 1987, Don Schuirmann of the FDA published a landmark manuscript where he split the statistical assessment of BE into two one-sided tests procedures and applied the two-sample *t*-test for evaluating the upper and lower BE boundaries (Schuirmann, 1987). To this end, the H_0 was changed to an assessment of differences (i.e., >20% difference between treatment means) and the alternative hypothesis (H_a) was changed to a test of sameness (i.e.,

Table 15.1 Defining type I and type II error.

	Investigator accepts H_0	**Investigator rejects H_0**
When H_0 is true	Valid conclusion	Type I error (α) Sponsor risk
When H_0 is False	Type II error (β) Patient's risk	Valid conclusion

In a BE trial, α is the risk of declaring two products as being different when they in fact are bioequivalent; and β is the risk of declaring two products as being bioequivalent when they in fact are different.

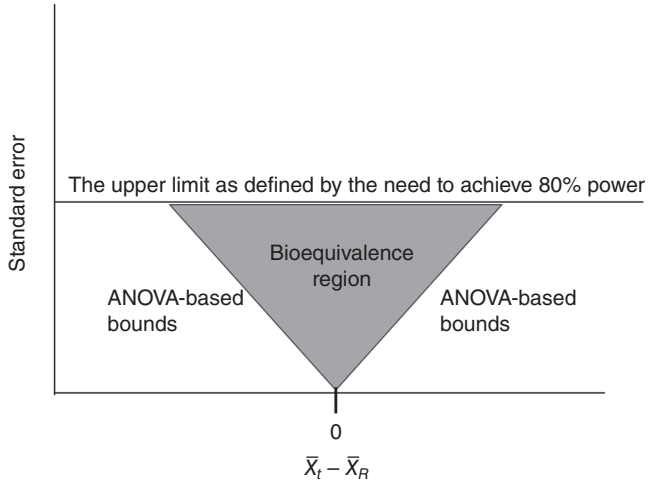

Fig. 15.2 Rejection region when using the power approach. $\bar{X}_t - \bar{X}_R$ represents the difference between the treatment means. As the SE of the estimate increases, the size of the allowable difference between the treatment means likewise increases up to a maximum difference as defined by the need to achieve no less than an 80% power of the test (based on the work of Schuirmann, 1987).

≤20% difference between treatment means). By flipping the test in this manner, an investigator needs to have the power to reject the H_0 in order to conclude that the two products are bioequivalent. Thus, Schuirmann's statistical method provided a logical approach to the assessment of product BE: the likelihood of declaring two products as bioequivalent (rejecting the H_0 that $T \neq R$) improves as statistical power increases (Fig. 15.3).

Ratification of the Generic Animal Drug Patent Term Restoration Act of 1988 (GADPTRA) provided a legal mechanism whereby the FDA's CVM could approve generic animal drug applications in the United States (Public Law 100-670, Nov. 16, 1988, 102 Stat. 3971). Following several workshops on this topic (Martinez and Riviere, 1994) the *in vivo* BE test methods were solidified into the 1996 FDA/CVM Bioequivalence Guidance (#35). This guidance has since undergone several minor revisions, with the current version having been released in November 2006. Resources are listed in the Bibliography section.

15.3 BIOEQUIVALENCE STUDY PROTOCOL CONSIDERATIONS

Although the CVM BE guidance describes several kinds of potential BE studies, this chapter will focus solely on blood level BE trials as these involve PK principles previously introduced in the text. Comparative blood level BE trials can provide a demonstration of product BE when the active molecule passes through the systemic circulation to reach its site of action. The design of these trials is predicated upon an understanding of the PK characteristics of the API. There are a number of factors that can complicate study design.

15.3.1 Nonlinear pharmacokinetics

If there are saturable absorption mechanisms, the risk of failing to detect formulation differences will increase as a function of the administered dose. In these situations, it may be

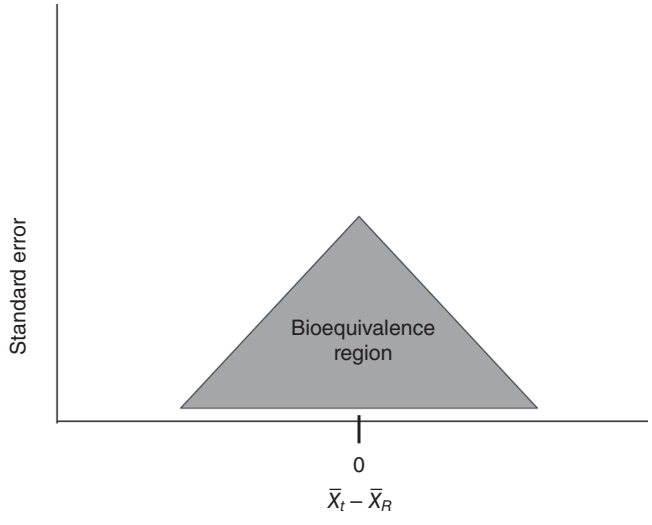

Fig. 15.3 Relationship between allowable difference between treatment means and the corresponding SE of the estimate for establishing product BE when using the two one-sided tests procedure (confidence interval approach). Note that as the SE increases, the allowable difference between product means likewise decrease (based on the work of Schuirmann, 1987).

best to design a study where the lowest, rather than the highest, label dose is administered. Conversely, if there is the risk of saturable elimination processes, small differences in drug absorption can be exaggerated under steady-state conditions. This can potentially lead to therapeutic inequivalence when the products are chronically administered (i.e., under conditions where accumulation occurs). In these situations, it may be best to conduct a steady-state BE study using the highest label dose. Profiles would be compared after the first administration to estimate the C_{max} associated with the two formulations. Comparison of the steady-state AUC values (estimated over a single dosing interval) would provide the basis for assessing the relative extents of drug exposure.

The effect of nonlinear PK behavior on AUC determination, central to some of these caveats, was discussed in Chapter 10, Equations 10.23–10.25. As is crucial in the design of any PK study, it is important to identify the sampling times needed to accurately describe potential formulation effects, and if a study is designed as a crossover investigation, it is necessary to define the duration of time needed to insure the absence of a carryover effect. This is best done in pilot trials before the final trial is started.

15.3.2 Multiple- versus single-dose studies

Even when conducting a single-dose BE trial, concomitant distribution and elimination processes influence the observed peak concentrations. This can be appreciated from discussions in Chapter 8 by examining Equation 8.55 predicting plasma concentrations in a two-compartment model after oral administration. However, this problem is greatly exaggerated in repeated dose studies when drug accumulation has occurred. In the presence of previous drug accumulation, elimination and distribution processes from preceding doses serve to further contaminate the determination of the oral input function. Therefore, product

C_{max} values are best compared following a single dose (e.g., see the FDA-CDER Guidance for Industry, 2003 Bioequivalence Guidance in the Bibliography).

Examples of when multiple-dose studies may be appropriate include drugs for which there are saturable elimination processes or when accumulation is needed to increase drug concentrations to accommodate limitations associated with the analytical method. In contrast to what some may believe, multiple-dose studies do not reduce the within-subject error associated with AUC (el-Tahtawy et al., 1998). Unless inconsistent with approved labeled dosing conditions, multiple-dose studies should be carried out to steady state (dosing for 4–7 terminal elimination half-lives) as can be appreciated from examining Table 8.1 and the definition of steady state illustrated in Fig. 12.1. In so doing, the AUC estimated over a single dosing interval ($AUC_{0-\tau}$) equals the AUC estimated to time infinity (AUC_{0-inf}) after a single dose.

15.3.3 Fed versus fasted conditions

As extensively discussed in Chapter 4, food can modify the absorption profile of many drugs, potentially having a direct effect on rate and extent of drug absorption, and thus its bioavailability. Food can increase the oral bioavailability of low solubility compounds if the drug is well absorbed throughout the gastrointestinal (GI) tract. However, food can reduce drug oral bioavailability if the compound is absorbed primarily in the upper small intestine. This decrease in drug absorption can be due to a variety of factors (Fleisher et al., 1999; Sinko et al., 1999; Jinno et al., 2008):

- An increase in the fluid volume of the GI tract decreases the concentration of drug exposed to absorptive membranes.
- An increase in the fluid viscosity of the GI tract can result in a decrease in the duration of interaction between the drug and the absorptive membrane.
- Bile salt secretion decreases intermicellar "free" drug fraction in the upper intestine, which could lead to a decrease in drug absorption. In some cases, when formulations are specifically designed to increase micelle formation, this can be a source of food-by-formulation interaction.
- There can be a physical interaction between the API and food, such as when the drug binds to fibrous food matter or to free ions, such as calcium.
- Food can affect the extent of presystemic drug metabolism (e.g., transporters or enzyme systems).
- There can be an interaction between food and components of the formulation. This potential source of food-by-formulation interaction is particularly important for modified release oral dosage forms.
- The drug may be unstable in the presence of acids, leading to an increase in the drug degradation due to food-induced increased gastric residence time. In cases where one formulation protects against exposure to gastric acids but the other formulation does not offer such protection, this can lead to a food-by-formulation interaction.
- Bioavailability may also decrease in the presence of an increase in fluid volume due to the dilution of excipients that are intended to increase drug permeability. This could be a source of food-by-formulation interaction.
- Food can increase hepatic blood flow, leading to an increase in drug metabolism as it passes through the liver (assuming that enzyme saturation does not occur).

- Food can decrease the rate of gastric emptying, which can delay drug absorption (and therefore reduce C_{max}).

Despite the multimechanistic manner in which food can alter product bioavailability, when considering the design of product BE trials, the pivotal question is *not* whether or not food influences drug absorption thereby affecting absolute bioavailability, but *rather whether there may be a food-by-drug interaction* which would affect the relative bioavaibility of two different formulations, and thus BE. Should that occur, products that are demonstrated to be equivalent in the fasted state may fail to be bioequivalent when taken with food or vice versa. Therefore, for BE investigations, the focus is on potential formulation-specific food effects (Koch et al., 1978; McLean et al., 1978; Watson, 1979; Hendeles et al., 1985; Karim et al., 1985; Watson et al., 1986; Hoppu et al., 1987; Skelly et al., 1987; Watson and Rijnberk, 1987; Tse et al., 1991; Oukessou and Toutain, 1992). Because food can increase the variability in drug absorption for monogastric species (Martinez, 1989), studies conducted in the fed state may have lower study power, rendering it more difficult to demonstrate product BE.

15.3.4 Parent drug versus the active metabolite(s)

Occasionally, BE assessments need to be based on concentrations of an active metabolite, such as when the API is administered as a prodrug. Reasons for administering the API as a prodrug include its improved solubility, intestinal stability, bioavailability, or even flavor improvement (Testa, 2009). In these situations, concentrations of the administered moiety may be too low to be adequately measured, leaving the active metabolite as the moiety upon which product BE is based.

Notwithstanding this one exception, there is an overwhelming consensus that product BE should be based on comparative concentrations of the parent compound whenever possible (Jackson et al., 2004; Midha et al., 2004; Fernández-Teruel et al., 2009; Braddy and Jackson, 2010). Since the metabolite is formed downstream from the absorption process, the concentration–time profile of the parent drug is more sensitive to changes in formulation performance than is a metabolite, even if the API undergoes extensive first-pass metabolism.

15.3.5 Chiral compounds

The importance of using stereospecific methods when evaluating the PK of chiral molecules is well recognized in human (e.g., Boulton and Fawcett, 2001; Mehvar et al., 2002) and in veterinary medicine (Landoni and Lees, 1996). However, when evaluating the BE of pharmaceutically equivalent products, the question needs to focus on whether or not the use of nonstereospecific methods would fail to detect product inequivalence for one of the enantiomers.

When using the same route of administration, the majority of drug products show no stereospecific differences in the product relative bioavailability (Midha et al., 1998b). Therefore, for most drugs with linear PK characteristics, the use of stereospecific analytical methods is not necessary (Mehvar and Jamali, 1997). However, stereospecific methods may be needed under the following conditions (Mehvar and Jamali, 1997; Srichana and Suedee, 2001; Nerurkar et al., 2005):

- When drugs exhibit nonlinear pharmacokinetics, the results of BE studies based on the total drug may differ from those based on the individual enantiomers.
- When the separate enantiomers differ substantially with regard to *Cl* and/or volume of distribution (which may lead to a bias in terms of conclusions based on C_{max} and T_{max} but not AUC).
- When the formulation contains chiral excipients.
- When the separate enantiomers exhibit markedly different solubility characteristics.

15.3.6 Selection of blood sampling times

To characterize peak drug concentrations, at least one blood sample should be taken (whenever possible) prior to the expected T_{max}. The duration of blood sampling should cover the entire time period associated with drug absorption. Once absorption is complete, the blood concentration–time profile reflects formulation-independent processes. Therefore, treatment comparison of AUC values can be adequately defined by the use of truncated profiles for long terminal elimination half-life ($T_{½}$) drugs, so long as the absorption phase has been completely captured (Lovering et al., 1975; Martinez and Jackson, 1991; Endrenyi and Tothfalusi, 1997).

A far more challenging study to design is one where the test and reference products release the API over a duration of months. This situation necessitates that subjects be enrolled in BE for an extensive duration of time, which can lead to very large within- and between-subject variability due to inherent variations in absorption, distribution, metabolism, and elimination (ADME) processes, and a high risk of subject dropout. For these reasons, the possibility of alternative study designs (e.g., a random assignment of subjects to various segments of the absorptive phase such that no one subject is enrolled for the entire duration of the study) may be worthy of consideration.

15.3.7 Defining the study population

BE studies are generally conducted in healthy animals that are representative of the species, class, gender, and physiological maturity for which the drug is approved. The BE study may also be conducted with a single gender for which the pioneer product is approved. Although aging (Ritschel, 1988, 1992; Burrows et al., 1992), disease (Ritschel and Denson, 1991; Rowland and Tozer, 1995), and maturation (Wang et al., 1990; Nouws, 1992; Schwark, 1992; Elton et al., 1993a,b) can significantly affect the PK of the API as also discussed in Chapter 17, there are only a handful of situations where these factors have been shown to bias the BE assessment. For example, in humans, an age-related increase in gastric pH was shown to alter the relative bioavailability of two diazepam formulations (Meyer, 1995). Similarly, although gender-related differences in drug pharmacokinetics are known to occur (Cleveland et al., 1995; Olling et al., 1995), statistically significant gender-by-formulation interactions have yet to be described (Chen and Williams, 1995).

15.4 PK DATA ANALYSIS

The determination of product BE is a subset of PK analysis that uses many of the approaches discussed in earlier chapters. However, there is a long and rich history of specific techniques

established to be acceptable to regulatory agencies. Issues specific to this domain will be expanded upon and illustrated below.

15.4.1 Measuring the extent of drug absorption: AUC determination

As can be appreciated, the determination of AUC is pivotal to the determination of product BE. Issues involved in accurate determination of AUC have been previously discussed in the context of noncompartmental models in the Chapter 9 section on "calculation of moments" as illustrated in Table 9.1. Topics unique to regulatory BE determination will be expanded upon here.

Depending upon the degree of curvature of the concentration versus time profile, there are several techniques that can be used for estimating the AUC (Chow, 1978; Yeh and Kwan, 1978). Most frequently, AUC is estimated by using either the trapezoidal or the log-linear trapezoidal method. It should be emphasized that log-transformed AUC values (LnAUC) are AUC values that are transformed after estimation using methods described in the example that follows. LnAUC is not the AUC based on the Ln concentration versus time profile. Furthermore, LnAUC should not be confused with the log-linear trapezoidal rule since the former refers to a population estimate and the latter refers to a method of area estimation.

When applying the trapezoidal method, each trapezoidal area is determined from Equation 9.7 [$\text{AUC} = ½(C_{ti} + C_{ti+1})(t_{i+1} - t_i)$] where t_{i+1} and t_i are the times associated with sequential blood samples and C_{ti} and C_{ti+1} are the corresponding sample concentrations. The trapezoidal method was depicted in Figs. 4.13 and 9.3 from earlier chapters. In this example, the AUC from the time of dosing (time zero) to the last concentration exceeding the assay limit of quantification ($\text{AUC}_{0\text{–last}}$ or $\text{AUC}_{0\text{–LOQ}}$), is calculated by summing ($\sum$) each of the individual trapezoidal areas. Therefore, in this case, $\text{AUC}_{0\text{–last}} = \text{AUC}_{0\text{–LOQ}} = \text{AUC}_{0\text{–24}}$. It should be noted that $\text{AUC}_{0\text{–last}}$ should never include a terminal sample whose concentration is less than the assay limit of assay quantification (LOQ). Inclusion of such triangulated areas may result in overestimation of the true $\text{AUC}_{0\text{–inf}}$.

When the decline is exponential, which we know is true for linear first-order processes, the more accurate method for calculating area is the ln-linear trapezoidal method. In this situation, the area prior to the peak concentration ($C_{\max}$) is calculated by the trapezoidal method. The area beyond $C_{\max}$ is calculated as:

$$\text{AUCC}_{\max-\text{last}} = [(C_{ti} - C_{ti+1}) \cdot (t_{i+1} - t_i)] / \ln(C_{ti} / C_{ti+1}) \tag{15.2}$$

As before, $\text{AUC}_{0\text{–last}}$ is obtained by summation of the individual trapezoids. As seen in the example in Table 15.2, minimal differences should be observed between linear and log-linear estimates unless a greater than two-fold difference occurs between consecutive concentrations during the decline portion of the curve.

15.4.2 Measuring the rate of drug absorption

Because $C_{\max}$ is not a pure estimate of absorption rate, alternative metrics have been considered. These include mean residence time (Yamaoka et al., 1978) developed extensively in Chapter 9, maximum entropy (Charter and Gull, 1987), $C_{\max}$/AUC (Endrenyi and Yan, 1993), partial AUCs (Chen, 1992), Wagner–Nelson plots (Wagner, 1974) introduced

Table 15.2 Simulated data and PK analysis: AUC estimates (μg·h/mL).

Time (h)	Concentration (mcg/mL)	Trapezoidal AUC	Log-linear trapezoidal area
0	0	Sample calculations (to three significant figures)	
0.25	4.08	0.5 · (0.25 – 0) · (0 + 4.08) = 0.510	0.5 · (0.25 – 0) · (0 + 4.078) = 0.510
0.5	5.44	0.5 · (0.5 – 0.25) · (4.08 + 5.44) = 1.70	0.5 · (0.5 – 0.25) · (4.078 + 5.443) = 1.70
0.75	5.59	0.5 · (0.75 – 0.5) · (5.44 + 5.59) = 1.38	0.5 · (0.75 – 0.5) · (5.443 + 5.587) = 1.38
1	5.24	0.5 · (1 – 0.75) · (5.59 + 5.24) = 1.35	[(5.59 – 5.24) · (1 – 0.75)]/Ln (5.59/5.24) = 1.35
2	3.36	… = 4.30	[(5.24 – 3.36) · (1 – 2)]/Ln (5.24/3.36) = 4.23
3	2.30	… = 2.83	… = 2.80
4	1.70	… = 2.00	… = 1.98
6	0.993	… = 2.69	… = 2.63
8	0.590	… = 1.58	… = 1.55
10	0.351	… = 0.941	… = 0.920
12	0.209	… = 0.560	… = 0.547
16	0.0739	… = 0.565	… = 0.519
24	0.0100	… = 0.337	… = 0.256
72	0	$AUC_{0-last} = AUC_{0-24} = 20.2$	$AUC_{0-last} = AUC_{0-24} = 19.9$

in Fig. 9.4 in Chapter 9, or center of gravity (Veng-Pedersen and Tillman, 1989) as calculated by Equation 9.27 and shown in Fig. 9.2 in Chapter 9.

However, in the majority of situations, observed C_{max} remain the metric of choice by US regulatory authorities (see FDA-CDER Guidance for Industry, 2003 Bioequivalence Guidance). Because small differences in T_{max} can lead to very small or very large test/reference ratios (e.g., 1 h/0.5 h = 2), the comparison of T_{max} values is generally based on a determination of clinical relevance.

15.5 STATISTICAL ANALYSIS OF BIOAVAILABILITY DATA

The major difference between the application of PK to BE determination compared with other applications presented in this text relate to the detailed proscribed statistical procedures that have been adopted and encoded in regulations. Although tedious to the statistically naïve reader, they illustrate sources of variability that enter into PK study design that should be taken into consideration in any PK experiment.

15.5.1 Use of the crossover design to decrease variability

Every observation contains both intended and unintended effects. These unintended effects are known as variability and are further developed in Chapter 16. Factors contributing to variability include *between-subject* factors (such as age, breed, gender, physiological attributes, mg/kg dose, and environment), *within-subject* factors (which may be due to other endogenous or exogenous factors including diurnal variability, day-to-day variability, physiological variation, and exposure to environmental and nutritional factors), and the *unexplained* random variability (ε in Chapters 14 and 16) that is due to factors such as analytical error, blood collection error (including deviation from the intended sampling time), and dosing error.

When designing a study to compare the bioavailability of two treatments, the goal is to maximize the power of the test. When using a two one-sided tests procedure, an increase in the power of the test will increase the likelihood of obtaining confidence intervals that are within the established bounds for declaring product BE.

One mechanism for increasing the power of the test is to remove the between-subject variability from the treatment comparison through the use of a *crossover study design* where each subject receives the test and the reference products. This was also discussed in Fig. 13.2 in Chapter 13 in the context of designing pharmacokinetic–pharmacodynamic (PK-PD) models. When conducting a crossover trial, the test and reference product are compared within (rather than between) individuals. The time between sequential administrations is termed the *washout period*. This is the time interval needed to insure that the drug (and any effect associated with that drug product) is absent from the body. Typically, this is estimated as 10 times the terminal elimination $T_{½}$ of the drug, where again as can be appreciated from Table 8.1, only 0.0097% of any drug remains in the body. However, other considerations also need to be factored into the duration of the washout period. These include:

- The duration of time necessary from the systemic *Cl* of any metabolite.
- The duration of time needed for any physiological effects associated with the prior drug administration to be absent from the body. For example, prior drug exposure may inhibit or induce the metabolism of the drug during subsequent exposure, and may induce an

inflammatory response that alters subsequent parenteral drug absorption, alter gastrointestinal motility, or affect blood flow.
- If there are excipients that affect subsequent absorption or *Cl* of that compound, excipient residues need to be eliminated from the body.
- If the products being compared contain multiple drug entities, the duration of the washout period should be based on the compound (or a metabolite) associated with the longest elimination $T_{½}$. This point holds true, even if only one of the multiple components is being measured within that BE trial. This is because the presence of the other compounds may affect the physiology or the kinetics of the moiety of interest, thereby biasing the data generated in period 2.

If a crossover study were designed such that each subject received treatment A (Trt A) in period 1 and Treatment B (Trt B) in period 2, then the analysis of the data would be as follows:

	Per 1	**Per 2**
Gp 1	Trt A	Trt B

where the effects associated with observations generated in the study (group = Gp 1) equals:

$$\text{Gp}\,1 = (\text{Trt B} - \text{Trt A}) + (\text{Per 2} - \text{Per 1}) + \text{Co A:B} + \varepsilon \tag{15.3}$$

where
Trt = treatment,
Per = period,
Co A:B = any carryover from Trt A to Trt B, and
ε = random error.

Therefore, when there is only one sequence group, there are other potential effects (i.e., period effects and carryover effects) that could confound our treatment comparison. To remedy this problem, a second sequence group (Gp 2) is needed where the order of drug administration is reversed. In this case, the study is designed as follows:

	Per 1	**Per 2**
Gp 1	Trt A	Trt B
Gp 2	Trt B	Trt A

For the study design to be valid, the absolute value of the data generated in Gp 2 should equal that generated in Gp 1. In other words:

$$\text{Gp}\,1 = (\text{Trt B} - \text{Trt A}) + (\text{Per 2} - \text{Per 1}) + \text{Co A:B} + \varepsilon \tag{15.4}$$

$$\text{Gp}\,2 = (\text{Trt A} - \text{Trt B}) + (\text{Per 2} - \text{Per 1}) + \text{Co B:A} + \varepsilon \tag{15.5}$$

Assuming that Gp 1 and Gp 2 are from the same population and that all other study factors are identical, then the ε associated with Gp 1 and Gp 2 should likewise be identical. In that case, our comparison would be:

$$\begin{aligned}&(\text{Trt B} - \text{Trt A}) + (\text{Per 2} - \text{Per 1}) + \text{Co A:B}\\ &\quad = (\text{Trt A} - \text{Trt B}) + (\text{Per 2} - \text{Per 1}) + \text{Co B:A}\end{aligned} \tag{15.6}$$

Since (Per 2 – Per 1) appears on both sides of the equation, it can be eliminated, simplifying to:

$$(\text{Trt B} - \text{Trt A}) + \text{Co A:B} = (\text{Trt A} - \text{Trt B}) + \text{Co B:A} \tag{15.7}$$

In other words,

$$\begin{aligned}\text{Gp 1} - \text{Gp 2} &= -[(\text{Trt B} - \text{Trt A}) - (\text{Trt A} - \text{Trt B})] + (\text{Co A:B} - \text{Co B:A})\\ &= 2(\text{Trt B} - \text{Trt A}) + (\text{Co A:B} - \text{Co B:A})\end{aligned} \tag{15.8}$$

The first point to note is that by conducting a two-sequence, two-treatment, two-period crossover trial, period effects are eliminated from the treatment comparison. Second, our comparison of Gp 1 and Gp 2 is contingent upon the two groups being described by the same random error. Third, for the difference between Gp 1 and Gp 2 to solely reflect a treatment effect, the carryover effects (Co A:B and Co B:A) need to be equal, for example, zero. If that is not the case, the resulting treatment comparison will be biased. For this reason, an important component of any crossover analysis is the confirmation that there are no statistically significant Gp (sequence) effects. Because the sequence effect is a between-subject (and not a within-subject) comparison, the error term for testing significance is subject-nested-within-sequence and *not* the residual error from the ANOVA (which will reflect the within-subject error and all unexplained error). Since sequence effects are a between-subject comparison, the level of significance (the p value) is often set as 0.1 rather than as 0.05 (Jones and Kenward, 1989).

15.5.2 Use of the ANOVA

To be statistically valid, comparisons involving the average BE (ABE) approach necessitates that certain assumptions are met. These include homogeneity of variances, normality, independence of the main effects (additivity), and the absence of a subject-by-treatment interaction (Shapiro and Wilk, 1965; Weiner, 1971; Ekbohm and Melander, 1989; Grieve, 1989).

An appropriate statistical model to describe the observations generated in a standard two-treatment, two-period, two-sequence crossover design (Weiner, 1971; Grieve, 1989; Chow and Liu, 1995) can be written as follows:

$$Y_{ijk} = \mu + \text{seq}_k + \text{subj}_{i(k)} + \text{period}_j + \text{trt}_{(j,k)} + \text{error}_{ijk} \tag{15.9}$$

where

Y_{ijk} = the observation associated with the ith subject (nested within the kth sequence) during the jth period,
μ = the population mean for the measure of interest,
seq_k = the kth sequence,
$\text{subj}_{i(k)}$ = the ith subject nested within the kth sequence,
period_j = the jth period,

$\text{trt}_{(j,k)}$ = treatment associated with the *j*th period and the *k*th sequence, and
error_{ijk} = the residual (unexplained) error associated with the *i*th subject (nested within the *k*th sequence) during the *j*th period. It is this error that determines the width of the 90% confidence interval.

If a parallel study design is used, the model reduces to:

$$Y_{im} = \mu + \text{trt}_{(m)} + \text{error}_{im} \tag{15.10}$$

where
Y_{im} = the observation associated with the *i*th subject and the *m*th treatment,
μ = the population mean for the measure of interest,
trt_m = the *m*th treatment, and
error_{im} = the unexplained variability associated with the *i*th subject and the *m*th treatment. This error estimate determines the width of the 90% confidence interval.

15.5.3 Data transformation

The use of data transformation reflects the investigator's belief that the assumptions of the ANOVA are better met when the data are presented on a transformed scale (Box and Cox, 1964). Numerous kinds of data transformations are possible (Bartlett, 1947; Draper and Hunter, 1969). However, by convention, the natural logarithmic transformation is generally used during the evaluation of PK and BE study data (Shapiro and Wilk, 1965; Schuirmann, 1989). Reasons to support this approach include PK models are multiplicative and therefore considered by some not to be in compliance with the assumption of additivity, logarithmic transformation stabilizes the variances, many biological systems are associated with log-normal distributions, BE comparisons are generally expressed as ratios rather than differences, and other types of data transformation will be very difficult to interpret.

15.5.4 The 90% confidence interval

From a statistical perspective, when using the confidence interval approach for assessing ABE, we are stating that we are 90% certain that the interval from *X* to *Y* (e.g., from 0.80 to 1.25) contains the true ratio of treatment means across the population of individuals.

If one could evaluate the test and reference product in every single patient (animal) that would potentially receive that drug, it would be possible to determine the true population mean value and the variance about that mean. However, since BE studies include only a finite number of subjects, a normal distribution of average test/reference ratios would be obtained if the study could be repeated an infinite number of times. This point is illustrated in Fig. 15.4, where a BE study (with each iteration defined by identical parameter means and variances) was simulated 10,000 times.

For any given parameter, the confidence interval about the ratio of treatment means is calculated according to FDA/CVM Bioequivalence Guidance #35 as follows:

Untransformed data: (15.11)

$$\text{Lower limit} = [(T-R) - \text{SE} \cdot t_{0.95(v)}]/R$$

$$\text{Upper limit} = [(T-R) + \text{SE} \cdot t_{0.95(v)}]/R$$

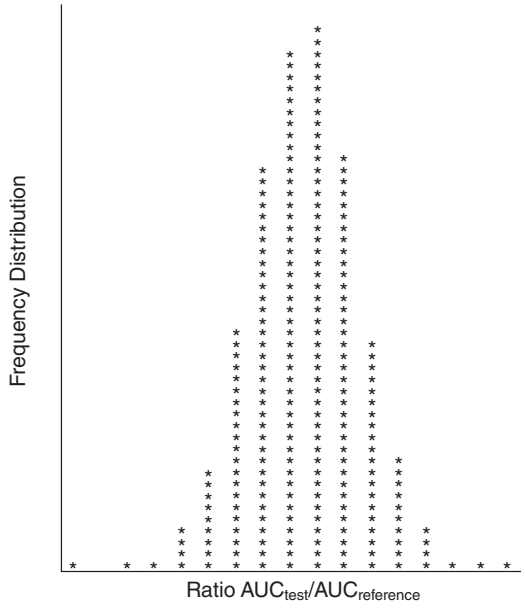

Fig. 15.4 Frequency distribution of 10,000 BE trials where the AUC values for the test and reference products were simulated with identical means and variances (mean = 150 ng·h/mL, %CV = 20, observations per treatment = 50).

$$\text{Log (Ln) transformed data:} \tag{15.12}$$

$$\text{Lower limit} = e^{[(T-R)-\text{SE}\cdot t(0.95(v))]}$$

$$\text{Upper limit} = e^{[(T-R)+\text{SE}\cdot t(0.95(v))]}$$

where

T = mean value for the test product,

R = mean value for the reference product,

SE = standard error for the estimate of the differences between the test minus reference untransformed or the ln-transformed means for the parameter of interest,

v = the error degrees of freedom, and

$t(0.95(v))$ = the t-table value corresponding with v degrees of freedom and $\alpha = 0.05$.

For a two-period, two-treatment, two-sequence crossover study, the SE is the standard error of the estimate of the difference between the r means, and is calculated as:

$$s \cdot \sqrt{\frac{1}{2}\left(\frac{1}{n_A} + \frac{1}{n_B}\right)} \tag{15.13}$$

where

s = the root mean square error (residual error) from the ANOVA,

n_A = the number of subjects in period 1 (some refer to this as the number of subjects in sequence A [Gp1]), and

n_B = the number of subjects in period 2 (some refer to this as the number of subjects in sequence B [Gp 2]). The value of ½ reflects the fact that this is a comparison of two treatments.

For extended-period crossover designs (e.g., two sequences, three periods), the SE is estimated as:

$$s \cdot \sqrt{\frac{1}{2}\left(\frac{1}{n_A}+\frac{1}{n_B}+\frac{1}{n_C}\right)} \tag{15.14}$$

where n_A, n_B, and n_C reflect the number of subjects per period. Again, the value of ½ reflects the fact that despite repeated observations, only two treatments are being compared. Additional information on alternative study designs and the statistical implications associated with these designs is provided by Jones and Kenward (1989) and by Ratkowsky et al. (1993).

15.5.5 Estimating sample size

The greater the variability in the estimate, the wider the corresponding confidence intervals. Similarly, for any magnitude of parameter variability, the width of the confidence interval decreases as the number of subjects increases (thereby providing an increasingly better approximation of the true patient population). In other words, the SE of the estimate decreases as either the variance decreases or as the number of subjects increase. *For that reason, the probability to successfully demonstrate product BE improves as the variability of the estimate decreases and as the number of subjects included in the comparison increases (even if the parameter values of the test and reference values are identical)*. This outcome, as demonstrated in Fig. 15.5, is due to a decrease in the degree of uncertainty about the BE predictions as the number of subjects increase.

With this in mind, Liu and Chow (1992) have estimated the sample size needed for Schuirmann's two one-sided tests procedure based on an untransformed data set. These estimates are a function of the variability in the estimate of the difference and the magnitude of the difference in treatment means (Table 15.3). Sample size estimates have also been developed for log-transformed data sets (Hauschke et al., 1992; Steinijans et al., 1992).

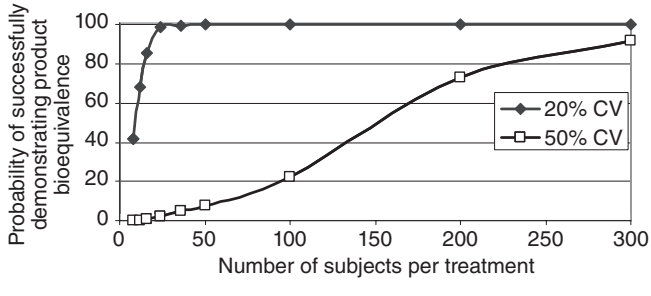

Fig. 15.5 The relationship between variability and subject number in determining the probability of declaring two products as bioequivalent.

Table 15.3 Sample sizes for Schuirmann's two one-sided tests procedure (80% power and $\nabla = 0.2 \cdot \mu_R$ at the 5% nominal level).

		Percent difference, θ			
		0	**5**	**10**	**15**
%*CV*	10	8	8	16	52
	12	8	10	20	74
	14	10	14	26	100
	16	14	16	34	126
	18	16	20	42	162
	20	20	24	52	200
	22	24	28	62	242
	24	28	34	74	288
	26	32	40	86	336
	28	36	46	100	390
	30	40	52	114	448
	32	46	58	128	508
	34	52	66	146	574
	36	58	74	162	644
	38	64	82	180	716
	40	70	90	200	794

The number of subjects provided in the table (*N*) is the total number of subjects required in a two-period crossover design (where $N = 2n$ and n = the number of subjects per sequence) to achieve a power of 80% at $\alpha = 0.05$ for a given θ between the test and reference products.

Table 15.4 Approximate sample sizes to attain a power of 80% with the multiplicative model.

		Ratio test/reference							
		0.85	**0.90**	**0.95**	**1.00**	**1.05**	**1.10**	**1.15**	**1.20**
%*CV*	5.0	12	6	4	4	4	6	8	22
	7.5	22	8	6	6	6	8	12	44
	10.0	36	12	8	6	8	10	20	76
	12.5	56	16	10	8	10	14	30	118
	15.0	78	22	12	10	12	20	42	170
	17.5	106	30	16	14	16	26	58	230
	20.0	138	38	20	16	18	32	74	300
	22.5	172	48	24	20	24	40	92	378
	25.0	212	58	28	24	28	50	114	466
	27.5	256	70	34	28	34	60	138	564
	30.0	306	82	40	34	40	70	162	670

The number of subjects provided in the table (*N*) is the total number of subjects required in a two-period crossover design (where $N = 2n$ and n = the number of subjects per sequence) to achieve a power of 80% at $\alpha = 0.05$ for a given ratio of the test/reference product.

Table 15.4 reflects the sample size estimate for ln-transformed data (the "multiplicative model").

These tables can be used to estimate the number of subjects needed in a two-period, two-treatment, two-sequence crossover study design. Each table provides the value of *N*, which equals the total number of study subjects. For the crossover study, the *%CV* pertains to the residual error, which includes within-subject and unexplained error excluding the

between-subject error. In a two-period, two-sequence, two-treatment crossover trial, n is the number of subjects within each sequence and therefore the total number of subjects, N, is $2n$. If this were applied to a parallel design, N would equal $2n$, where n is the number of subjects per treatment.

When BE is analyzed on the basis of the untransformed data, the confidence intervals are symmetric around zero. Therefore, the numbers of subjects needed to meet the upper and lower BE bounds are identical. The number of subjects needed to achieve a $1 - \beta$ power at the α nominal level is termed N, and N is $2n$, where n is the number of subjects required per sequence. If the test and reference products are truly identical (i.e., the percent difference in population means, θ = zero), then:

$$n \geq [t(\alpha, 2n-2) + t(\beta/2, 2n-2)]^2 [CV/\nabla]^2 \tag{15.15}$$

where

μ_T = the population mean for the test product,
μ_R = the population mean for the reference product,
$\theta = [(\mu_T - \mu_R)/\mu_R] \times 100$,
$CV = \left(\sqrt{MSE}/\mu_R\right) \times 100$,
$n = 2\left(\dfrac{\sigma}{0.20\mu_R}\right)^2 \left(t_{0.80(½)} + t_{0.975½}\right)^2$, and
∇ = the BE limit.

If $\theta > 0$, then

$$n \geq [t(\alpha, 2n-2) + t(\beta/2, 2n-2)]^2 [CV/(\nabla - \theta)]^2 \tag{15.16}$$

It should be noted that this is an iterative equation where the number of subjects are determined by convergence of the prior and posterior estimates.

When using a multiplicative model, the upper and lower confidence bounds are *not* symmetrical. Therefore, the number of subjects needed in a crossover study when the data are ln-transformed need to be considered from the perspective of the upper and lower bounds, respectively. For the multiplicative model, the number of subjects can be estimated as follows:

- If $\theta = 1$,
  then: $n \geq [t(\alpha, 2n - 2) + t(\beta/2, 2n - 2)]^2 [CV/\ln 1.25]^2$
- If $1 < \theta < 1.25$,
  then: $n \geq [t(\alpha, 2n - 2) + t(\beta, 2n - 2)]^2 [CV/(\ln 1.25 - \ln \theta)]^2$
- If $0.8 < \theta < 1$,
  then: $n \geq [t(\alpha, 2n - 2) + t(\beta, 2n - 2)]^2 [CV/(\ln 0.8 - \ln \theta)]^2$

Note that as with the linear model, this is an iterative equation.

In both cases, since the estimates are based on the use of a two-period, two-treatment, two-sequence crossover study design, the sample size will provide an equal number of observations with the test and the reference formulations. In other words, since each subject provides an observation for the test and reference product in a two-period, two-treatment, two-sequence crossover study design, there will be N total number of observations for both the test and reference products from each of the N subjects in the study. So, for example,

if a multiplicative model is used, where the within-subject *%CV* is 20 and the ratio of the test/reference formulations is 0.95, the equation results in an estimate of 20 subjects (10 in Gp 1, 10 in Gp 2). In this case, the estimated number of total subjects needed to declare product BE would be 20 and the total number of data points included in the BE trial would be 40 (20 observations for the test product and 20 observations for the reference product). If this were a parallel rather than a crossover study, the *%CV* would be based on the *between-subject error* rather than the *within-subject error*. For any estimated value of *N*, this is likely to result in a less powerful study. Furthermore, since there is a need for 20 observations per treatment, the study would need to employ 20 subjects that will be administered the test formulation and 20 subjects that are administered the reference formulation, that is, a total of 40 subjects. In other words, the total number of subjects that would need to be included in a parallel study would equal 2N.

15.6 INDIVIDUAL VERSUS POPULATION BIOEQUIVELANCE: ALTERNATIVE STATISTICAL DESIGNS

Up to this point, the discussion pertained to average BE, which compares the population means between the test and reference products. When using an ABE approach, only the means of the two formulations need to be sufficiently similar. However, two alternative approaches termed *individual* and *population* BE (IBE and PBE, respectively) have been proposed for consideration to include comparisons of population means and variances (FDA-CDER Guidance for Industry, 2001). While the PBE approach assesses the total variability of bioavailability measurements, the IBE approach focuses on intraindividual variability for the test and reference products, as well as on subject-by-formulation interactions. PBE and IBE approaches scale the BE criteria to the reference variability, which offers an advantage over ABE when testing highly variable drug products.

In theory, the PBE and IBE approaches reflect differences in the objectives of BE tests conducted at various stages of drug development. These differences are embodied in the concepts of *prescribability* and *switchability* (Midha et al., 1997, 1998a,b, 1999). *Prescribability* refers to the clinical setting in which a practitioner prescribes a drug product to a patient for the first time (a drug-naïve patient). In this setting, the prescriber relies on an understanding that the average performance of the drug product has been well characterized and relates in some definable way to the safety and efficacy information from clinical trials. This is in contrast to the concept of *switchability*, which refers to the setting in which a practitioner transfers a patient from one drug product to another. This latter situation arises with generic substitution, as well as with certain postapproval changes by an innovator or generic firm in the formulation and/or manufacture of a drug product. Under these circumstances, the prescriber and patient should be assured that the newly administered drug product will yield comparable safety and efficacy to that of the product for which it is being substituted. It is this concept of switchability upon which the fundamental principle of BE is based.

Due to the need for replicate study designs for obtaining the within-subject variance estimate (generally involving about four periods), PBE and IBE approaches have not been used in veterinary medicine. Furthermore, for most compounds, even within human medicine, the ABE approach has been shown to provide adequate assurance of product switchability.

15.7 ENDOGENOUS COMPOUNDS: PRODUCTS WITH NONZERO BASELINES

Many drug substances are endogenous compounds such as hormones. When evaluating the relative bioavailability of products where the active substance is an endogenous compound, the blood level data need to be corrected for background concentrations. To illustrate this point, let's say that a drug product is intended to raise the level of an endogenous hormone in the patient population, and that the average 24-h AUC for that endogenous substance is 100 ng·h/mL. Let us further state that concentrations are doubled when these subjects are administered the reference product (i.e., AUC = 200 ng·h/mL) and that it increases to only 170 ng·h/mL following administration of the test product. If evaluated on the basis of uncorrected substance concentrations, the estimated test/reference ratio would be 0.85 (which could result in declaring the products as bioequivalent if an adequate number of subjects were included in the study). However, in fact the true relative bioavailability of the test/reference formulations is 0.70, which would not be within the limits defining product BE.

A real-life example of this point was reported for the relative bioavailability evaluation of two products that deliver testosterone. The BE trial was conducted in 12 healthy human subjects (Chik et al., 2009). Without correction for endogenous concentrations, the two products met traditional BE criteria (93–120 for AUC and 88–117 for C_{max}). However, after correcting for background levels, the two products were clearly shown not to be bioequivalent with confidence intervals; 90% confidence interval for AUC was 52–106 and 50–258 based on one of the methods employed for correcting for background testosterone levels.

15.8 HUMAN FOOD SAFETY

While blood level comparisons can confirm product comparability with respect to target animal safety and efficacy, it may not accurately reflect the relative drug tissue concentrations at the innovator's approved withdrawal time, an end point fully developed in Chapter 19 of this text. In particular, analytical methods may not have the sensitivity needed to identify product differences in their respective terminal drug disposition (Wyse et al., 2003). In these situations, products could successfully meet standard blood level BE criteria despite markedly different drug concentrations within the target animal's edible tissues. Such differences may occur if, for example, a small portion of the total dose of a particular formulation is slowly released over time. This situation would be generated by the multicompartmental behavior discussed in Chapter 8 concerning PK model selection across different concentration ranges as was depicted in Fig. 8.22.

Figs. 15.6 and 15.7 provide an example of such a situation where the test product has slightly higher bioavailability (5% higher than the reference formulation) but has a small portion of the total dose (15%) that is slowly absorbed from the injection site (e.g., if a small portion of the dose precipitates at the injection site and then very slowly gets absorbed). In this example, there are minimal differences in the blood concentration versus time profiles. Therefore, these two formulations may be declared as bioequivalent. However, the differences in the terminal tissue concentrations, while of negligible therapeutic consequence, could lead to violative residues. Consequently, CVM has adopted the recommendation of the Panel on Human Food Safety at the 1993 Veterinary Drug Bioequivalence Workshop (Martinez and Riviere, 1994) that a tissue residue depletion study would generally be needed to support the approval of a generic animal drug product in food-producing animals.

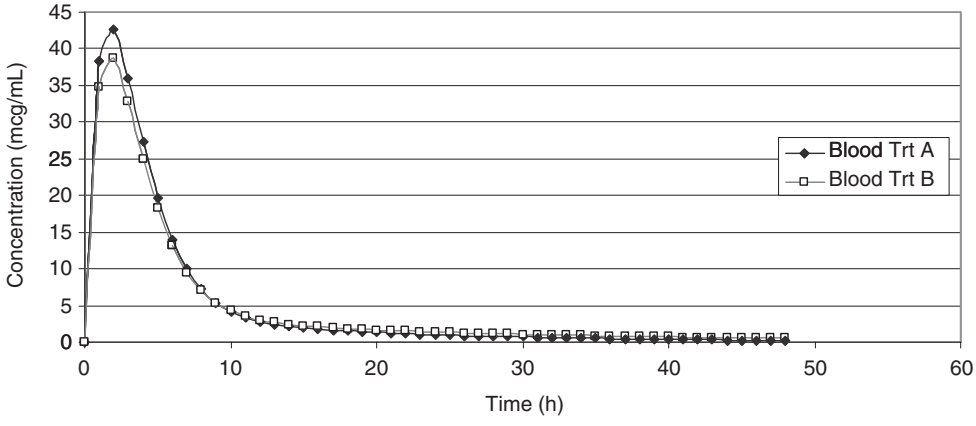

Fig. 15.6 Example of comparative blood concentration–time profiles where the test product (Trt B) that is 5% more bioavailable than the reference formulation (Trt A), but where 15% of Trt B's bioavailable dose is very slowly absorbed from the injection site.

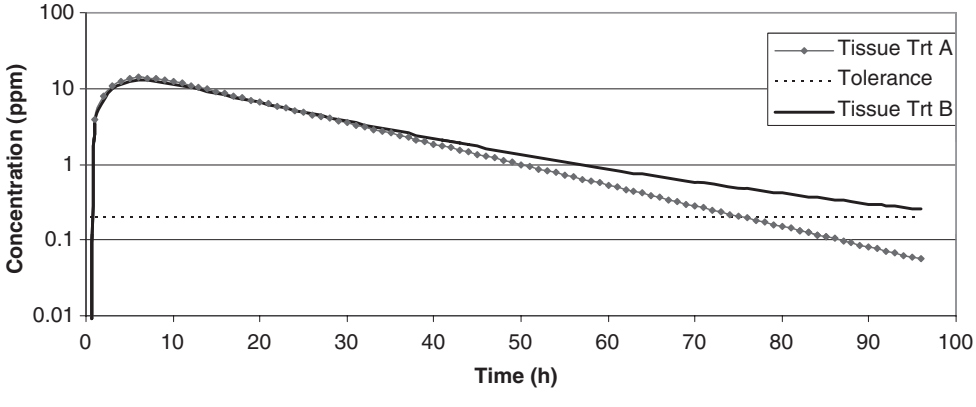

Fig. 15.7 Comparative tissue drug concentrations for the two products described in Fig. 15.4.

Certain drug products may be exempt from the requirement to conduct a tissue residue depletion study. Exemptions include products for which a waiver of *in vivo* BE testing is granted, and products for which the assay method used in the blood BE study is sensitive enough to measure blood levels of the drug for the entire withdrawal period assigned to the reference product (e.g., drug products in which the innovator is assigned a zero withdrawal time). Other requests for waiver of the tissue residue study are considered on a case-by-case basis.

15.9 *IN VITRO* TESTING AND ANALYSIS OF DISSOLUTION DATA

Drug absorption from a solid dosage form after oral administration depends on the release of the drug substance from the drug product, the dissolution or solubilization of the drug

Table 15.5 USP acceptance Table 15.1.

Stage	Number tested	Acceptance criteria
S1	6	Each unit is not less than Q + 5%.
S2	6	Average of 12 units (S1 + S2) is equal to or greater than Q, and no unit is less than Q – 15%.
S3	12	Average of 24 units (S1 + S2 + S3) is equal to or greater than Q, not more than 2 units are less than Q – 15%, and no unit is less than Q – 25%.

For additional information, see USP General Chapters <711> and <1092> (USP 27, NF 22, 2004).

under physiological conditions, and the permeability across the GI tract. Therefore, the generation of information pertaining to the *in vitro* dissolution characterization of a formulation may be relevant to the prediction of its *in vivo* performance. *In vitro* dissolution tests for solid oral dosage forms, such as tablets, suspensions, and capsules are used to (1) assess the lot-to-lot quality of a drug product; (2) guide development of new formulations; (3) ensure continuing product quality and performance after changes in formulation, manufacturing process, site of manufacture, or scale-up of the manufacturing process; and (4) support of biowaiver requests.

When used to support batch release, the US Pharmacopeia (USP) describes methods for interpreting dissolution data. They state that the specifications are met if the quantities of the API dissolved from the dosage units tested succeed in conforming to *Acceptance Table 1* presented as Table 15.5. This Acceptance Table contains three stages (S1, S2, and S3) for meeting the acceptance criteria. The quantity, Q, is the amount of dissolved active ingredient specified in the individual USP monograph, expressed as a percentage of the labeled content of the dosage unit. The 5%, 15%, and 25% values in the Acceptance Table are expressed as percentages of the labeled content, thereby allowing Q to be a unitless value.

The identification of methods to statistically compare two dissolution profiles is challenging, and numerous potential methods have been proposed (O'Hara et al., 1997). Ultimately, a method that relies on simply calculations and a limited set of assumptions was developed for comparing two dissolution profiles. This model-independent approach was used to confirm profile comparability and is termed the similarity factor (f_2). f_2 is a logarithmic reciprocal square root transformation of the sum of squared error, reflecting similarity in the percent (%) dissolution of the two curves.

The equation for the similarity factor (f_2) is:

$$f_2 = 50 \cdot \log\left\{\left[1+\left(\frac{1}{n}\right)\sum_{i=1}^{n}(R_t - T_t)^2\right]^{-0.5} \times 100\right\} \tag{15.17}$$

To understand the mathematical interpretation of this equation, we need to divide it into its separate components. The term $(1/n)\sum_{t=1}^{n}(R_t - T_t)^2$ simply reflects the average difference in the percent dissolved from two formulations. $R_t - T_t$ is the difference in the percent dissolved of the mean dissolution profile (e.g., averaged over the 12 units = n) at any sampling time, t. It is squared so that we can obtain the absolute value of the differences. When we ultimately log-transform the data, a value of zero is not acceptable. Therefore, a

value of 1 is included in the equation to allow logarithmic transformation. The negative square root allows this to be expressed as a fraction. Therefore, as the difference gets increasingly large, the size of the reciprocal gets increasingly small.

So, looking at our three examples:

$$\text{if } \sum_{i=1}^{n}(R_t - T) = 0, \text{ then } (1+0)^{-0.5} = 1/1 = 1$$

$$= 5, \text{ then } (1+25)^{-0.5} = \sqrt{\frac{1}{261}} = 0.196$$

$$= 10, \text{ then } (1+100)^{-0.5} = \sqrt{\frac{1}{101}} = 0.0995$$

$$= 30, \text{ then } (1+900)^{-0.5} = \sqrt{\frac{1}{901}} = 0.0333$$

One multiplies by 100 to express values as whole numbers.

When we take the logs of these values and multiply by 50 (see Table 15.6 for sample calculations), we obtain the following:

1. average original difference = 5%, $f_2 = 64.6$
2. average original difference = 10%, $f_2 = 49.89$
3. average original difference = 30%, $f_2 = 26.13$

Use of this model independent approach is predicated on the following stipulations (FDA-CDER Guidance for Industry, 1997):

- Twelve units each of the test and reference formulations are tested and values for each unit individually recorded.
- The dissolution measurements of the test and reference batches are made under exactly the same conditions.
- Only one measurement is considered after 85% dissolution of both products.
- To allow for the use of mean data, the percent coefficient of variation at the earlier time points (e.g., 15 min) should not be more than 20%, and at other time points should not be more than 10%.

For curves to be considered similar, f_2 values should be equal to or greater than 50. This model independent method is most suitable for dissolution profile comparison when three or more dissolution time points are available.

Table 15.6 Similarity factor (f_2).

Average original difference	(Average difference)^2	(difference)^2 + 1	√previous value	100 · previous value	50 · Log previous column
0	0	1	1	100	100
5	25	26	0.196116	19.61161	64.62567
10	100	101	0.099504	9.950372	49.89197
30	900	901	0.033315	3.331483	26.13188

In cases where *in vitro* dissolution data are to be used to support *in vivo* product BE, it is uncertain as to whether or not one set of dissolution test conditions can be used to confirm product *in vivo* comparability across all target animal species.

15.10 *IN VIVO/IN VITRO* CORRELATIONS

In the case of the f_2 test, the comparison between two products or two formulations is based solely on an assumption that if two product profiles are effectively superimposable, their corresponding rates and extent of *in vivo* drug release will likewise be identical. While there is an assumption that the *in vitro* test method is sensitive to process and manufacturing variables, the *in vivo* relevance of that test method may not have been adequately validated. Therefore, the use of the f_2 test to confirm product BE is generally limited. Oftentimes, its use is primarily in support of a biowaiver for multiple strength products when one of the dosage strengths has been confirmed to be bioequivalent to the reference formulation in an *in vivo* BE trial.

On the other hand, there are situations where there is a need to use the *in vitro* release test data to predict *in vivo* product performance. For example, if the relationship between *in vitro* drug release and product *in vivo* bioavailability were known, it would be possible to establish *in vitro* release specifications that could provide an assurance that if the product continues to meet these *in vitro* specifications, changes in product formulation or manufacturing procedure will have *in vivo* release characteristics comparable to that of the original formulation. In other words, studies have been conducted to confirm the presence of an *in vivo*/*in vitro* correlation (IVIVC).

An IVIVC implies that the *in vitro* dissolution test has *in vivo* relevance. This relevance is confirmed through validation studies that compare the *in vitro* release of several formulations, generally at least three formulations which cover rapid, slow, and intermediate rates of drug release, to the corresponding *in vivo* release characteristics of these same three formulations. The type of dissolution test criteria used to determine product comparability will depend on the level of correlation being sought (see FDA-CDER Guidance for Industry, 1997).

- *Level A:* Point-to-point relationship between *in vitro* dissolution and the *in vivo* input rate of the dosage form (i.e., *in vivo* dissolution). This is the highest category of correlation where *in vitro* data can be used to represent the complete plasma level curve.
- *Level B:* Mean *in vitro* dissolution time compared with either the mean residence time or the mean *in vivo* dissolution time. This does not reflect the actual *in vivo* plasma level curve, since several curves may produce the same mean residence time values.
- *Level C:* One dissolution time point (e.g., time to 50% dissolution) is related to one PK parameter (e.g., AUC, C_{max}, T_{max}).

IVIVCs may also be feasible for parenteral formulations. However, as parenteral dosage formulations become increasingly complex, the primary challenge will be to identify an appropriate *in vitro* release testing method (Martinez et al., 2008, 2010).

15.11 THE BIOPHARMACEUTICS CLASSIFICATION SYSTEM

The biopharmaceutical factors that determine dissolution after oral administration were reviewed in Table 4.2 in Chapter 4 of this text. By understanding the relationship between

a drug's *in vivo* oral absorption profile and its *in vitro* solubility and dissolution characteristics, or by knowing its IVIVC, it is possible to identify conditions under which the *in vitro* data can serve as a surrogate for *in vivo* BE testing (FDA Guidance for Industry, 2000). The biopharmaceutics classification system (BCS) originally introduced in Table 4.1 will now be expanded upon in the context of regulatory BE testing. The relationship can be defined by the use of the BCS, which classifies compounds in accordance with their permeability and solubility characteristics (Amidon et al., 1995):

- *Class I:* High Solubility, High Permeability: generally very well absorbed compounds.
- *Class II:* Low Solubility, High Permeability: exhibit dissolution-rate limited absorption.
- *Class III:* High Solubility, Low Permeability: exhibit permeability limited absorption.
- *Class IV:* Low Solubility, Low Permeability: very poor oral bioavailability.

For immediate release formulations, the rate of product dissolution will influence the plasma drug concentration/time profiles of class II compounds. However, for class I or III compounds, other factors influence drug absorption characteristics. For example, for class I compounds (highly soluble, highly permeable), the rate of gastric emptying rather than product performance is the rate-limiting step in determining its bioavailability characteristics. For these formulations, differences in *in vitro* dissolution profiles may occur without any resulting differences in product bioavailability (Rekhi et al., 1997; Eddington et al., 1998). Similarly, highly soluble, poorly permeable compounds (class III) dissolve rapidly. However, for these APIs, it is not the rate of drug dissolution but rather the diffusion across biological membranes that is the rate-limiting step. Therefore, for an immediate release product, the primary formulation-related question is whether or not the formulation contains components that will influence the permeability of the API. On the other hand, for high permeability, low solubility compounds (class II) or low solubility and low permeability compounds (class IV), the rate and extent of product dissolution can have a significant effect on the blood concentration/time profile (Yu, 1999). For class II compounds, this may be attributable to problems associated with either particle size (termed dissolution-limited absorption) or drug solubility (termed solubility-limited absorption).

The FDA CDER has incorporated BCS concepts into a guidance for the waiver of *in vivo* BE study requirements for high solubility/high permeability drug products (class I) based on *in vitro* dissolution data (FDA Guidance for Industry, 2000). BCS concepts have been incorporated into the CVM Guidance for the biowaiver of certain Type A medicated articles (FDA/CVM Guidance 171).

The extrapolation of human-based BCS criteria to veterinary species is not straightforward. With regard to permeability, drugs that are highly permeable in one animal species tend to be highly permeable in all animal species (Clarke and Smith, 1984; Chiou and Barve, 1998). Conversely, drugs that are absorbed via transcellular pathways or that have site-specific absorption may exhibit species-specific permeability characteristics (Ferraris and Ahearn, 1983; Karasov et al., 1985; Bijlsma et al., 1995; He et al., 1998; Johnson et al., 2001). These different types of transport pathways, discussed in Chapter 2, that could exhibit species specificity, were illustrated in Fig. 2.5. Nevertheless, interspecies differences in product bioavailability are most often the consequence of other variables such as GI transit time, *in vivo* dissolution, presystemic metabolism, physicochemical interactions

with gut contents, bacteria digestion, and site-specific differences in absorptive surface area. These differences have been extensively reviewed elsewhere (Martinez et al., 2002).

Another difference affecting BCS drug classification in veterinary species is that unlike human medications, veterinary medicines are generally dosed on a mg/kg basis. It is unlikely that the fluids to which the dosage form will be exposed (either as inherent gastric fluid volume or as volume of fluid consumed) scales linearly to body weight. Considering the size differential across breeds, this may lead to a very wide range of dose/fluid volume ratios. Thus, the use of a set volume of fluid and dosage strength for defining drug solubility may not be appropriate in veterinary medicine. Finally, it should be noted that to date, BCS characterization has been applied solely to orally administered products.

15.12 CONCLUSION

Marked changes have occurred within the therapeutic landscape. This includes the development of novel release technologies (e.g., Martinez et al., 2008, 2010), and a growing awareness of the relationship between the physicochemical characteristics of the API and the formulation effects for human (e.g., Amidon et al., 1995; Yu et al., 2002) and veterinary pharmaceuticals (e.g., Martinez et al., 2002; Fahmy et al., 2008). All of these advancements have been made using PK tools introduced in this chapter and throughout the text. There remain numerous unresolved BE challenges associated with the assessment of formulations unique to veterinary medicine (Martinez and Hunter, 2010). As these challenges evolve, the issue of product BE becomes a subject of increasing importance and an area for future research using many of the tools presented in this text.

ACKNOWLEDGMENT

The authors thank Dr. Veronica Tailor of the FDA's Center for Veterinary Medicine (CVM) for review and comment on the statistical issues presented in this chapter.

BIBLIOGRAPHY

Amidon, G.L., Lennernas, H., Shah, V.P., and Crison, J.R. 1995. A theoretical basis for a biopharmaceutic drug classification: the correlation of *in vitro* drug product dissolution and *in vivo* bioavailability. *Journal of Pharmaceutical Research*. 12:413–420.

Bartlett, M.S. 1947. The use of transformations. *Biometrics*. 3:39–52.

Bijlsma, P.B., Peeters, R.A., Groot, J.A., Dekker, P.R., Taminiau, J.A., and Van Der Meer, R. 1995. Differential *in vivo* and *in vitro* intestinal permeability to lactulose and mannitol in animals and humans: a hypothesis. *Gastroenterology*. 108:687–696.

Bois, F.Y., Tozer, T.N., Hauck, W.W., Chen, M.L., Patnaik, R., and Williams, R.L. 1994a. Bioequivalence: performance of several measures of extent of absorption. *Pharmaceutical Research*. 11:715–722.

Bois, F.Y., Tozer, T.N., Hauck, W.W., Chen, M.L., Patnaik, R., and Williams, R.L. 1994b. Bioequivalence: performance of several measures of rate of absorption. *Pharmaceutical Research*. 11:966–974.

Boulton, D.W., and Fawcett, J.P. 2001. The pharmacokinetics of levosalbutamol: what are the clinical implications? *Clinical Pharmacokinetics*. 40:23–40.

Box, G.E., and Cox, D.R. 1964. An analysis of transformations. *Journal of the Royal Statistical Society*. 26:211–252.

Braddy, A.C., and Jackson, A.J. 2010. Role of metabolites for drugs that undergo nonlinear first-pass effect: impact on bioequivalency assessment using single-dose simulations. *Journal of Pharmacuetical Science*. 99:515–523.

Bradshaw, J.W.S. 2006. The evolutionary basis for the feeding behavior of domestic dogs (*Canis familiaris*) and cats (*Felis catus*). *Journal of Nutrition*. 136:1972S–1931S.

Burrows, G.E., Macallister, C.G., Ewing, P., Stair, E., and Tripp, P.W. 1992. Rifampin disposition in the horse: effects of age and method of oral administration. *Journal of Veterinary Pharmacology and Therapeutics*. 15:124–132.

Cabana, B.E. 1983. Assessment of 75/75 rule: FDA viewpoint. *Journal of Pharmaceutical Sciences*. 72:98–100.

Charter, M.K., and Gull, S.F. 1987. Maximum entropy and its application to the calculation of drug absorption rates. *Journal of Pharmacokinetics and Biopharmaceutics*. 15:645–655.

Chen, M.L. 1992. An alternative approach for assessment of rate of absorption in bioequivalence studies. *Pharmaceutical Research*. 9:1380–1385.

Chen, M.L., and Williams, R.L. 1995. Women in bioavailability/bioequivalence trials–-a regulatory perspective. *Drug Information Journal*. 29:813–820.

Chik, Z., Johnston, A., Tucker, A.T., Kirby, K., and Alam, C.A. 2009. Correcting endogenous concentrations of testosterone influences bioequivalence and shows the superiority of TDS(R)-testosterone versus Androgel(R). *International Journal of Clinical Pharmacology and Therapy*. 47:262–268.

Chiou, W.L. 1978. Evaluation of the potential error in pharmacokinetic studies of using the linear trapezoidal rule method for the calculation of the area under the plasma level-time curve. *Journal of Pharmacokinetics and Biopharmaceutics*. 6:539–546.

Chiou, W.L., and Barve, A. 1998. Linear correlation of the fraction of oral dose absorbed of 64 drugs between humans and rats. *Pharmaceutical Research*. 15:1792–1795.

Chow, S.C., and Liu, J.P. 1995. Current issues in bioequivalence trials. *Drug Information Journal*. 29:795–804.

Chow, W.L. 1978. Critical evaluation of the potential error in pharmacokinetic studies of using the linear trapezoidal rule method for the calculation of the area under the plasma level-time curve. *Journal of Pharmaceutics and Biopharmaceutics*. 6:539–546.

Clarke, B., and Smith, D. 1984. Pharmacokinetics and toxicity testing. *Critical Reviews in Toxicology*. 12:343–385.

Cleveland, P.A., Teller, S., Kachevsky, V., Pinili, E., Evans, R., and Modi, M.W. 1995. Dose-dependent and time-dependent pharmacokinetics in the dog after intravenous administration of dextrophan. *Drug Metabolism and Disposition*. 19:245–250.

Draper, N.R., and Hunter, W.G. 1969. Transformations: some examples revisited. *Technometrics*. 11:23–40.

Eddington, N.D., Ashraf, M., Augsburger, L.L., Leslie, J.L., Fossler, M.J., Lesko, L., Shah, V.P., and Rekhi, G.S. 1998. Identification of formulation and manufacturing variables that influence *in vitro* dissolution and *in vivo* bioavailability of propranolol hydrochloride tablets. *Pharmaceutical Development and Technology*. 3:525–547.

Ekbohm, G., and Melander, H. 1989. The subject-by-formulation interaction as a criterion of interchangeability of drugs. *Biometrics*. 45:1249–1254.

el-Tahtawy, A.A., Tozer, T.N., Harrison, F., Lesko, L., and Williams, R. 1998. Evaluation of bioequivalence of highly variable drugs using clinical trial simulations. II: comparison of single and multiple-dose trials using AUC and Cmax. *Pharmaceutical Research*. 15:98–104.

Elton, S.E., Babish, J.G., and Schwark, W.S. 1993a. The postnatal development of drug-metabolizing enzymes in hepatic, pulmonary and renal tissues of the goat. *Journal of Veterinary Pharmacology and Therapeutics*. 16:152–163.

Elton, S.E., Guard, C.L., and Schwark, W.S. 1993b. The effect of age on phenylbutazone pharmacokinetics, metabolism and plasma protein binding in goats. *Journal of Veterinary Pharmacology and Therapeutics*. 16:141–151.

Endrenyi, L., and Yan, W. 1993. Variation of Cmax and Cmax/AUC in investigations of bioequivalence. *International Journal of Clinical Pharmacology, Therapy and Toxicology*. 31:184–189.

Endrenyi, L., and Tothfalusi, L. 1997. Truncated AUC evaluates effectively the bioequivalence of drugs with long half-lives. *International Journal of Clinical Pharmacology and Therapeutics.* 35:142–150.

Fahmy, R., Danielson, D., and Martinez, M. 2008. Formulation and design of veterinary tablets. In *Pharmaceutical Dosage Forms: Tablets*, Chapter 13. Informa Healthcare, 3:383–431.

FDA Approved Drug Products with Therapeutic Equivalent Evaluations. "The Orange Book." 2009. 30th edition.

FDA Guidance for Industry. 2000. Waiver of *In Vivo* Bioavailability and Bioequivalence Studies for Immediate-Release Solid Oral Dosage Forms Based on a Biopharmaceutics Classification System. www.fda.gov/downloads/Drugs/GuidanceComplianceRegulatoryInformation/Guidances/ucm070246.pdf.

FDA-CDER Guidance for Industry. 1997. Dissolution Testing of Immediate Release Solid Oral Dosage Forms. www.fda.gov/downloads/Drugs/GuidanceComplianceRegulatoryInformation/Guidances/ucm070237.pdf.

FDA-CDER Guidance for Industry. 2001. Statistical Approaches to Establishing Bioequivalence, www.fda.gov/downloads/Drugs/GuidanceComplianceRegulatoryInformation/Guidances/ucm070244.pdf.

FDA-CDER Guidance for Industry. 2003. Bioavailability and Bioequivalence Studies for Orally Administered Drug Products—General Considerations. www.fda.gov/downloads/Drugs/GuidanceComplianceRegulatoryInformation/Guidances/ucm070124.pdf.

Federal Register. 1977. Drug products, bioequivalence requirements and in vivo bioavailability procedures. *Federal Register.* 42:1634–1635.

Fernández-Teruel, C., Nalda Molina, R., González-Alvarez, I., Navarro-Fontestad, C., García-Arieta, A., Casabó, V.G., and Bermejo, M. 2009. Computer simulations of bioequivalence trials: selection of design and analyte in BCS drugs with first-pass hepatic metabolism: linear kinetics (I). *European Journal of Pharmaceutical Sciences*. 36:137–146.

Ferraris, R., and Ahearn, G. 1983. Intestinal glucose transport in carnivorous and herbivorous marine fishes. *Journal of Comparative Physiology*. 152:79–90.

Fix, A.J., Cargill, R., and Engle, K. 1993. Controlled gastric emptying: III. Gastric residence time of a nondisintegrating geometric shape in human volunteers. *Pharmaceutical Research*. 10:1087–1089.

Fleisher, D., Li, C., Zhou, Y., Pao, L.H., and Karim, A. 1999. Drug, meal and formulation interactions influencing drug absorption after oral administration. *Clinical Pharmacokinetics.* 36:233–254.

Gibaldi, M., and Perrier, D. 1982. *Pharmacokinetics*, 2nd Ed. New York: Marcel Dekker.

Grieve, A.P. 1989. Crossover versus parallel designs. In: Berry, D.A. (ed.), *Statistical Methodology in the Pharmaceutical Sciences*. New York: Marcel Dekker, pp. 239–270.

Hauschke, D., Steinijans, V.W., Diletti, E., and Burke, M. 1992. Sample size determination for bioequivalence assessment using a multiplicative model. *Journal of Pharmacokinetics and Biopharmaceutics*. 20:557–561.

He, Y., Murby, S., Warhurst, G., Gifford, L., Walker, D., Ayrton, J., Eastmond, R., and Rowland, M. 1998. Species differences in size discrimination in the paracellular pathway reflected by oral bioavailability of poly(ethylene glycol) and D-peptides. *Journal of Pharmaceutical Sciences*. 87:626–633.

Hendeles, L., Weinberger, M., Milavetz, G., Hill, M., and Vaughan, L. 1985. Food-induced "dose-dumping" from a once-a-day theophylline product as a cause of theophylline toxicity. *Chest*. 87:758–765.

Hoppu, K., Tuomisto, J., Koskimies, O., and Simell, O. 1987. Food and guar decrease absorption of trimethoprim. *European Journal of Clinical Pharmacology*. 32:427–429.

Jackson, A.J., Robbie, G., and Marroum, P. 2004. Metabolites and bioequivalence: past and present. *Clinical Pharmacokinetics*. 43:655–672.

Jinno, J., Kamada, N., Miyake, M., Yamada, K., Mukai, T., Odomi, M., Toguchi, H., Liversidge, G.G., Higaki, K., and Kimura, T. 2008. *In vitro–in vivo* correlation for wet-milled tablet of poorly water-soluble cilostazol. *Journal of Controlled Release*. 130:29–37.

Johnson, K.L., Ballevre, O.P., and Batt, R.M. 2001. Use of an orally administered combined sugar solution to evaluate intestinal absorption and permeability in cats. *American Journal of Veterinary Research*. 62:111–118.

Jones, B., and Kenward, M.G. 1989. *Design and Analysis of Cross-Over Trials*. New York: Chapman and Hall.

Karasov, W.H., Solberg, D.H., and Diamond, J.M. 1985. What transport adaptations enable mammals to absorb sugars and amino acids faster than reptiles? *American Journal of Physiology.* 249:G271–283.

Karim, A., Burns, T., Janky, D., and Hurwitz, A. 1985. Food-induced changes in theophylline absorption from controlled-release formulations. Part II: importance of meal composition and dosing time relative to meal intake in assessing changes in absorption. *Clinical Pharmacology and Therapeutics*. 38:642–647.

Khankari, R.K., and Grant, D.J.W. 1995. Pharmaceutical hydrates. *Thermochimica Acta*. 248:61–79.

Koch, P.A., Schultz, C.A., Wills, R.J., Hallquist, S.L., and Welling, P.G. 1978. Influence of food and fluid ingestion on aspirin bioavailability. *Journal of Pharmaceutical Sciences*. 67:1533–1535.

Kumar, L., Amin, A., and Bansal, A.K. 2008. Preparation and characterization of salt forms. *Pharmaceutical Development and Technology*. 13:345–357.

Landoni, M.F., and Lees, P. 1996. Chirality: a major issue in veterinary pharmacology. *Journal of Veterinary Pharmacology and Therapeutics*. 19:82–84.

Liu, J.P., and Chow, S.C. 1992. Sample size determination for the two one-sided tests procedure in bioequivalence. *Journal of Pharmacokinetics and Biopharmaceutics*. 20:101–104.

Lovering, E.G., McGilveray, I.J., McMillan, I., and Tostowaryk, W. 1975. Comparative bioavailabilities from truncated blood level curves. *Journal of Pharmaceutical Sciences.* 64:1521–1524.

Martinez, M. 1989. Food effects in bioequivalency evaluations. Proceedings of Bio-International '89—Issues in the Evaluation of Bioavailability Data. Toronto, Canada, pp. 62–63.

Martinez, M.N., and Hunter, R.P. 2010. Current challenges facing the determination of product bioequivalence in veterinary medicine. *Journal of Veterinary Pharmacology and Therapeutics.* 33:418–433.

Martinez, M.N., and Jackson, A.J. 1991. Suitability of various noninfinity area under the plasma concentration-time curve (AUC) estimates for use in bioequivalence determinations: relationship to AUC from zero to time infinity (AUC0-INF). *Pharmaceutical Research*. 8:512–517.

Martinez, M.N., and Riviere, J.E. 1994. Review of the 1993 Veterinary Drug Bioequivalence Workshop. *Journal of Veterinary Pharmacology and Therapeutics*. 17:85–119.

Martinez, M., Amidon, G., Clarke, L., Jones, W.W., Mitra, A., and Riviere, J. 2002. Applying the biopharmaceutics classification system to veterinary pharmaceutical products: part II. Physiological considerations. *Advanced Drug Delivery Reviews*. 54:825–850.

Martinez, M.N., Papich, M.G., and Riviere, J.E. 2004. Veterinary application of *in vitro* dissolution data and the biopharmaceutics classification system. *US Pharmacopeial Forum*. 30:6.

Martinez, M., Rathbone, M., Burgess, D., and Huynh, M. 2008. *In vitro* and *in vivo* considerations associated with parenteral sustained release products: a review based upon information presented and points expressed at the 2007 Controlled Release Society Annual Meeting. *Journal of Controlled Release*. 129:79–87.

Martinez, M.N., Rathbone, M.J., Burgess, D., and Huynh, M. 2010. Breakout session summary from AAPS/CRS joint workshop on critical variables in the *in vitro* and *in vivo* performance of parenteral sustained release products. *Journal of Controlled Release*. 132:2–7.

McLean, A.J., McNamara, P.J., duSouich, P., Gibaldi, M., and Lalka, S. 1978. Food, splanchnic blood flow, and bioavailability of drugs subject to first-pass metabolism. *Clinical Pharmacology and Therapeutics*. 24:5–10.

Mehvar, R., and Jamali, F. 1997. Bioequivalence of chiral drugs. Stereospecific versus non-stereospecific methods. *Clinical Pharmacokinetics*. 33:122–141.

Mehvar, R., Brocks, D.R., and Vakily, M. 2002. Impact of stereoselectivity on the pharmacokinetics and pharmacodynamics of antiarrhythmic drugs. *Clinical Pharmacokinetics.* 41:533–558.

Meyer, M. 1995. Current scientific issues regarding bioavailability/bioequivalence trials: an academic view. *Drug Information Journal*. 29:805–812.

Midha, K., Rawson, M., and Hubbard, J. 1997. Individual and average bioequivalence of highly variable drugs and drug products. *Journal of Pharmaceutical Science*. 86:1193–1197.

Midha, K., Rawson, M., and Hubbard, J. 1998a. Bioequivalence: switchability and scaling. *European Journal of Pharmaceutical Sciences*. 6:87–91.

Midha, K.K., McKay, G., Rawson, M.J., and Hubbard, J.W. 1998b. The impact of stereoisomerism in bioequivalence studies. *Journal of Pharmaceutical Sciences*. 87:797–802.

Midha, K.K., Rawson, M.J., and Hubbard, J.W. 1999. Prescribability and switchability of highly variable drugs and drug products. *Journal of Controlled Release*. 62:33–40.

Midha, K.K., Rawson, M.J., and Hubbard, J.W. 2004. The role of metabolites in bioequivalence. *Pharmaceutical Research*. 21:1331–1344.

Nerurkar, J., Beach, J.W., Park, M.O., and Jun, H.W. 2005. Solubility of (±)-ibuprofen and S(+)-ibuprofen in the presence of cosolvents and cyclodextrins. *Pharmaceutical Development and Technology*. 10:413–421.

Nouws, J.F.M. 1992. Pharmacokinetics in immature animals: a review. *Journal of Animal Science*. 70:3627–3634.

O'Hara, T., Dunne, A., Kinahan, A., Cunningham, S., Stark, P., and Devane, J. 1997. Review of methodologies for the comparison of dissolution profile data. *Advances in Experimental Medicine and Biology*. 423:167–171.

Olling, M., Van Twillert, K., Wester, P., Boink, A.B.T., and Rauws, A.G. 1995. Rabbit model for estimating relative bioavailability, residues and tissue tolerance of intramuscular products: comparison of two ampicillin products. *Journal of Veterinary Pharmacology and Therapeutics*. 18:34–37.

Oukessou, M., and Toutain, P.L. 1992. Effect of dietary nitrogen intake on gentamicin disposition in sheep. *Journal of Veterinary Pharmacology and Therapeutics*. 15:416–420.

Piscitelli, D.A., Bigora, S., Propst, C., Goskonda, S., Schwartz, P., Lesko, L.J., Augsburger, L., and Young, D. 1998. The impact of formulation and process changes on *in vitro* dissolution and bioequivalence of piroxicam capsules. *Pharmaceutical Development and Technology*. 3:443–452.

Purves, R.D. 1992. Optimum numerical integration methods for estimation of area-under-the-curve (AUC) and area-under-the-moment-curve (AUMC). *Journal of Pharmacokinetics and Biopharmaceutics*. 20:211–226.

Randell, S.C., Hill, R.C., Scott, K.C., Omori, M., and Burrows, C.F. 2001. Intestinal permeability testing using lactulose and rhamnose: a comparison between clinically normal cats and dogs and between dogs of different breeds. *Research Journal of Veterinary Science*. 71:45–49.

Ratkowsky, D.A., Evans, M.A., and Alldredge, J.R. 1993. *Cross-Over Experiments*. New York: Marcel Dekker, Inc.

Rekhi, G.S., Eddington, N.D., Fossler, M.J., Schwartz, P., Lesko, L.J., and Augsburger, L.L. 1997. Evaluation of *in vitro* release rate and *in vivo* absorption characteristics of four metoprolol tartrate immediate-release tablet formulations. *Pharmaceutical Development and Technology*. 2:11–24.

Ritschel, W.A. 1988. *Gerontokinetics: Pharmacokinetics of Drugs in the Elderly*. Caldwell, NJ: Telford Press.

Ritschel, W.A. 1992. Drug disposition in the elderly: gerontokinetics. *Methods and Findings in Experimental and Clinical Pharmacology*. 14:555–572.

Ritschel, W.A., and Denson, D.D. 1991. Influence of disease on bioavailability. In: Welling, P.G., Tse, F.L.S., and Dighe, S.V. (eds.), *Pharmaceutical Bioequivalence*. New York: Marcel Dekker, pp. 67–115.

Ronfeld, R.A., and Benet, L.Z. 1977. Interpretation of plasma concentration-time curves after oral dosing. *Journal of Pharmaceutical Sciences*. 66:178–180.

Rowland, M., and Tozer, T.N. 1995. *Clinical Pharmacokinetics: Concepts and Applications*. Philadelphia: Lea and Febiger.

Schuirmann, D.L. 1987. A comparison of the two one-sided tests procedure and the power approach for assessing the equivalence of average bioavailability. *Journal of Pharmacokinetics and Biopharmaceutics*. 15:657–690.

Schuirmann, D.J. 1989. Treatment of bioequivalence data: log transformation. Proceedings of Bio-International '89-Issues in the Evaluation of Bioavailability Data. Toronto, Canada, pp. 159–161.

Schulze, J.D.R., Peters, E.E., Vicker, A.W., Staton, J.S., Coffin, M.D., Parsons, G.E., and Basit, A.W. 2005. Excipient effects on gastrointestinal transit and drug absorption in beagle dogs. *International Journal of Pharmaceutics*. 300:67–75.

Schwark, W.S. 1992. Factors that affect drug disposition in food-producing animals during maturation. *Journal of Animal Science*. 70:3635–3645.

Shapiro, S.S., and Wilk, M.B. 1965. An analysis of variance test for normality (complete samples). *Biometrika*. 52:591–611.

Sinko, P.J., Lee, Y.H., Makhey, V., Leesman, G.D., Sutyak, J.P., Yu, H., Perry, B., Smith, C.L., Hu, P., Wagner, E.J., Falzone, L.M., McWhorter, L.T., Gilligan, J.P., and Stern, W. 1999. Biopharmaceutical approaches for developing and assessing oral peptide delivery strategies and systems: *in vitro* permeability and *in vivo* oral absorption of salmon calcitonin (sCT). *Pharmaceutical Research.* 16:527–533.

Skelly, J.P., Barr, W.H., Benet, L.Z., Doluisio, J.T., Goldberg, A.H., Levy, G., Lowenthal, D.T., Robinson, J.R., Shah, V.P., Temple, R.J., and Yacobi, A. 1987. Report of the workshop on controlled-release dosage forms: issues and controversies. *Pharmaceutical Research*. 4:75–77.

Srichana, T., and Suedee, R. 2001. Evaluation of stereoselective dissolution of racemic salbutamol matrices prepared with commonly used excipients and H-NMR study. *Drug Development and Industrial Pharmacy*. 27:457–464.

Steinijans, V.W., Hauck, W., Diletti, E., Hauschke, D., and Anderson, S. 1992. Effect of changing the bioequivalence range from (0.80, 1.20) to (0.80, 1.25) on the power and sample size. *International Journal of Clinical Pharmacology, Therapy and Toxicology*. 30:571–575.

Sutton, S.C., Evans, L.A., Fortner, J.H., McCarthy, J.M., and Sweeney, K. 2006. Dog colonoscopy model for predicting human colon absorption. *Pharmaceutical Research*. 23:1554–1563.

Testa, B. 2009. Prodrugs: bridging pharmacodynamic/pharmacokinetic gaps. *Current Opinion in Chemical Biology*. 13:338–344.

Tse, F.L., Robinson, W.T., and Choc, M.G. 1991. Study design for the assessment of bioavailability and bioequivalence. In: Welling, P.G., Tse, F.L.S., and Dighe, S.V. (eds.), *Pharmaceutical Bioequivalence*. New York: Marcel Dekker, pp. 17–34.

USP 27, NF 22. 2004. The United States Pharmacopeia and The National Formulary. General Chapter <711> Dissolution. General Chapter: <1092> The Dissolution Procedure: Development and Validation United States Pharmacopeial Convention Inc. Rockville, MD.

Veng-Pedersen, P., and Tillman, L.G. 1989. Center of gravity of drug level curves: a model-independent parameter useful in bioavailability studies. *Journal of Pharmaceutical Sciences*. 78:848–854.

Wagner, J.G. 1974. Application of the Wagner-Nelson absorption method to the two-compartment open model. *Journal of Pharmacokinetics and Biopharmaceutics*. 2:469–486.

Wang, L.H., Rudolph, A.M., and Benet, L.Z. 1990. Comparative study of acetaminophen disposition in sheep at three developmental stages: the fetal, neonatal and adult periods. *Developmental Pharmacology and Therapeutics*. 14:161–179.

Watson, A.D., Emslie, D.R., Martin, I.C.A., and Egerton, J.R. 1986. Effect of ingesta on systemic availability of penicillins administered orally in dogs. *Journal of Veterinary Pharmacology and Therapeutics*. 9:140–149.

Watson, A.D.J. 1979. Effect of ingesta on systemic availability of chloramphenicol from two oral preparations in cats. *Journal of Veterinary Pharmacology and Therapeutics*. 2:117–121.

Watson, A.D.J., and Rijnberk, A. 1987. Systemic availability of o,p'-DDD in normal dogs fasted and fed, and in dogs with hyperadrenocorticism. *Research in Veterinary Science*. 43:160–165.

Weiner, B.J. 1971. *Statistical Principles in Experimental Design*. New York: McGraw-Hill.

Wyse, C.A., McLellan, J., Dickie, A.M., Sutton, D.G., Preston, T., and Yam, P.S. 2003. A review of methods for assessment of the rate of gastric emptying in the dog and cat: 1898–2002. *Journal of Veterinary Internal Medicine*. 17:609–621.

Yamaoka, K., Nakagawa, T., and Uno, T. 1978. Statistical moments in pharmacokinetics. *Journal of Pharmacokinetics and Biopharmaceutics*. 6:547–557.

Yeh, K.C., and Kwan, K.C. 1978. A comparison of numerical integrating algorithms by trapezoidal, lagrange, and spline approximation. *Journal of Pharmaceutics and Biopharmaceutics*. 6:79–98.

Yu, L.X. 1999. An integrated model for determining causes of poor oral drug absorption. *Pharmaceutical Research*. 16:1883–1887.

Yu, L.X., Crison, J.R., Lipka, E., and Amidon, G.L. 1996. Transport approaches to the biopharmaceutical design of oral drug delivery systems: prediction of intestinal absorption. *Advanced Drug Delivery Reviews*. 19:359–376.

Yu, L.X., Amidon, G.L., Polli, J.E., Zhao, H., Mehta, M.U., Conner, D.P., Shah, W.P., Lesko, L.J., Chen, M.L., Lee, V.H., and Hussain, A.S. 2002. Biopharmaceutics classification system: the scientific basis for biowaiver extensions. *Pharmaceutical Research.* 19:921–925.

16 Population Pharmacokinetic Models

with Jason Chittenden

The goal of drug treatment in clinical medicine is to produce a therapeutic benefit in patients while reducing the incidence of side effects and adverse drug reactions and, in veterinary medicine, avoiding violative tissue residues (Fig. 1.3, see Chapter 1). Therefore, simultaneously achieving an "effective" concentration at the site of action while maintaining an "ineffective" concentration at the toxic sites of action is of paramount importance. The physiological mechanisms that control the circulation and effect of drugs in human or animal patients (processes discussed in Chapters 2, 4, 5, and 6) function at a level related to the physiological and clinical conditions of the patient. Up to this point in this text, we have assumed that these processes are constant within individuals and have constructed models based on mean parameters. However, in Chapter 14 on data analysis, it became obvious that there is significant variability present in estimated pharmacokinetic parameters due to within and between individual effects.

16.1 SOURCES OF VARIABILITY

For certain drugs and under different pathophysiological, environmental, genetic, and demographic conditions, large differences in the pharmacokinetic and/or pharmacodynamic profiles can be seen across individuals (biological variability). Other sources of unknown random variability in the concentration–time profiles and dose–effect relationships of drugs may also be present in patient populations (statistical variability). The latter may be of two kinds, namely, random interindividual variability (individual deviations from population average values according to a probability distribution) and intraindividual variability (day-to-day variation, measurement error, and model misspecification, also assumed to occur according to a probability distribution), as previously discussed in reference to Equation 14.1.

An understanding of pharmacokinetic and pharmacodynamic variability, its sources, and its influence on drug disposition and effect, is basic for rational drug therapy in target populations. Pharmacokinetic variability refers to differences in blood concentrations over time for a specific dose across individuals. As discussed in Chapters 8 and 10, this can be the consequence of differences in volume of distribution, elimination (excretion and metabolism), and rate and extent of absorption (bioavailability). Pharmacodynamic

Comparative Pharmacokinetics: Principles, Techniques, and Applications, Second Edition. Jim E. Riviere.
 ISBN: 978-0-813-82993-7

variability, as presented in Chapter 13, can be the consequence of differences in drug levels at the site of action (as inferred mostly from drug concentration in the biophase) or differences in the effect produced by a given drug concentration at the site of action (biophase, effect–compartment). Both components are important and should be taken into account when modeling the variability in the dose–effect relationships of drugs. Unfortunately, in many instances, pharmacodynamic variability is neglected by assuming that most of the variability in the pharmacologic response to a drug is due to pharmacokinetics, an unwarranted assumption. In fact, the clinical implications of interindividual variability in pharmacokinetics cannot be fully understood without a proper knowledge of the nature and the extent of variability in the relationship between the blood concentration of the drug and the pharmacologic effect.

16.2 THE STANDARD APPROACH

Traditional approaches to pharmacokinetic analysis cannot provide information that allows an adequate characterization of this variability, its sources, and its implications for drug therapy. As discussed earlier (see Chapters 8, 9, 10, and 14), studies are conducted in small homogeneous populations (from 6 to sometimes up to 30 individuals) according to a rigidly designed experimental protocol. Extensive sampling takes place (often more than 20 samples per individual), with the sampling schedule fixed and the same for each individual. Data analysis proceeds in two stages. In the first stage, the data from each individual are analyzed to obtain estimates of the individual pharmacokinetic parameters (e.g., the focus of Chapter 14). A fitting procedure, such as weighted or unweighted nonlinear regression, is used to estimate each individual's parameters. In the second stage, the individual parameter estimates are pooled to provide measures of central tendency (means) and variability (variances) for the population parameters. The association between pharmacokinetic parameters and demographic characteristics may then be assessed by independent regression techniques. This technique is termed the standard two-stage (STS) method.

Despite its straightforward nature and familiarity, the STS method presents serious limitations. The first is that intensive sampling may be required to properly determine basic features of disposition in individuals with similar physiological states. Due to this restriction, this approach can only be applied to well-defined patient subpopulations, (such as patients with renal dysfunction or within a particularly significant age range) and is not practical for the study of a population that may include a broad range of factors of potential relevance. Consequently, this method cannot be used to explore unknown relationships between population characteristics and pharmacokinetic/pharmacodynamic outcome because the variability in observed pharmacokinetic parameters becomes too great. Second, because the study population is usually small and highly homogeneous (and many times healthy), biased population parameter estimates may be obtained that are not representative of the target population. This is especially true for the estimates of interindividual and intraindividual variability. The STS method pools together both sources of variability in a unique estimate of interindividual variability. Because of this, the estimate is artificially inflated and often inadequate for valid statistical inferences. Moreover, estimates of intraindividual variability are difficult to obtain and almost never reported. Third, this type of study is quite costly, because many times it requires pathogen-free animals, special housing and confinement facilities, compliance with good laboratory practice standards, and assay of numerous samples. The strength of this approach is rooted in its experimental nature

and the fact that sufficient data are gathered from every individual so that robust individual estimates are always possible.

In summary, with the STS method it is not always possible to use routine clinical data to assess the influence of biological sources of variability on the pharmacokinetic and pharmacodynamic behavior of drugs on target patient populations. Furthermore, the estimates of statistical variability of the pharmacokinetic and pharmacodynamic parameters provided by these methods are unrealistic since they gather all sources of residual variability (essentially, interindividual and intraindividual variability) into a common variance estimate, and do not explicitly identify the nature nor source of intraindividual variability.

16.3 THE POPULATION APPROACH

In contrast, population approaches to assessing the variability in the therapeutic behavior of drugs allow for estimation of pharmacokinetic and pharmacodynamic parameters in target patient populations, accounting for the effect of concomitant pathophysiological, environmental, demographic, and genetic variables (biological variability). They also allow for an explicit estimation of the between-individual and within-individual variability in disposition or concentration–effect relationships (statistical variability).

The population approach to pharmacokinetics combines data from all individuals to fit a single model. This is in contrast to the two-stage methods that will fit one model per individual. There are several statistical advantages to the population approach. First, by fitting all of the data simultaneously one essentially increases the sample size available for estimating the model parameters. The payoff comes in the form of more precise parameter estimates. Second, the population approach allows one to account explicitly for correlation between model parameters. Third, the population approach is suitable for unbalanced data. Consider using the STS approach on data where different individuals have different numbers of samples—how should one weight the parameter estimates in determining their distribution statistics (mean, variance)? Population approaches are designed to handle this issue. Fourth, by combining all of the data, the ability to create a model that is more complicated than any individual's data could support is possible. In a simple case of naïvely pooling the data, this is obvious, but the power of the population approach allows one to account also for the correlation of the residuals, the tendency of the population mean to consistently undershoot or overshoot any given individual. Fifth, while the STS approach includes covariate modeling as a post hoc step (after the parameter estimates are obtained), the population approach includes covariate modeling in the estimation step. Estimates for covariate effects (e.g., the effect of body weight on volume of distribution) will be less biased and less correlated with other parameters. In addition, one often finds that the parameter estimates themselves may be far different with the correlation included in the estimation procedure. Finally, as the name implies, the population approach is designed to enable statistical inferences on the population rather than only the subjects of the studies being analyzed. This comes from the fact that the population approach captures information about the variability between individuals who are random samples from a population, whereas the STS approach estimates individual's parameters without reference to the population.

The population approach achieves all of this by modeling the data with a combination of "fixed" and "random" effects in a "mixed-effects" model. Fixed effects are parameters that are the same for every individual, while random effects are different for every individual. The random effects are typically assumed to come from a parametric distribution

(though there are methods that relax this constraint) and the parameters of the distribution —like a covariance matrix—define the interindividual variability within the studied population.

16.4 POPULATION VERSUS STANDARD APPROACH: AN EXAMPLE

As an example of the different results provided by the population approach, consider the doxycycline example from Chapter 14. The individual animal data was listed in Table 14.1 and pharmacokinetic analyses conducted were shown in Tables 14.2–14.4. Table 16.1 shows individual estimates of the parameters for a two-compartment model with weighting (same as Table 14.3). Table 16.2 shows the same structural model (model describing an individual's C-T profile) but with individual estimates provided by the population model. Notice that the population model's estimates are generally more "central," that is, the values have moved toward the population mean value, and the confidence intervals are shorter.

Also, the estimates of β are the same for each individual. Whereas the individual fits (Table 16.1) find a "best" estimate, which happens to show variation in all the parameters, the population model finds an overall fit that is nearly as good on an individual level, but better in the sense that the individual parameter estimates are more likely samples from the population distribution of possible parameter values. This phenomenon, where the individual parameter values in a population model collapse to a single (or nearly so) value, is called "shrinkage." Shrinkage is common with sparsity of subjects and/or data, as will be seen below.

Table 16.1 Individual estimates for a two-compartment weighted model of the doxycycline data.

Subject	A (μg/mL)	α (1/h)	B (μg/mL)	β (1/h)
Animal 1	20.19	0.71	10.56	0.04
Animal 2	16.97	6.65	16.77	0.05
Animal 3	12.58	2.62	16.09	0.05
Animal 4	9.55	3.38	14.95	0.05
Mean	14.241	2.545	14.368	0.049
CI 95% lower	8.415	0.575	10.272	0.041
CI 95% upper	24.102	11.271	20.097	0.058

Mean and 95% confidence interval (CI) of the parameters in a log-normal distribution.

Table 16.2 A population estimate of the doxycycline data.

Subject	A (μg/mL)	α (1/h)	B (μg/mL)	β (1/h)
Animal 1	18.72	0.99	12.95	0.051
Animal 2	15.96	6.47	16.99	0.051
Animal 3	12.97	2.45	15.66	0.051
Animal 4	11.96	4.82	15.22	0.051
Mean	14.672	2.945	15.131	0.051
CI 95% lower	10.626	0.779	12.626	0.051
CI 95% upper	20.259	11.137	18.133	0.051

Note the outlier values have generally moved toward the mean and the confidence intervals (CIs) are narrower.

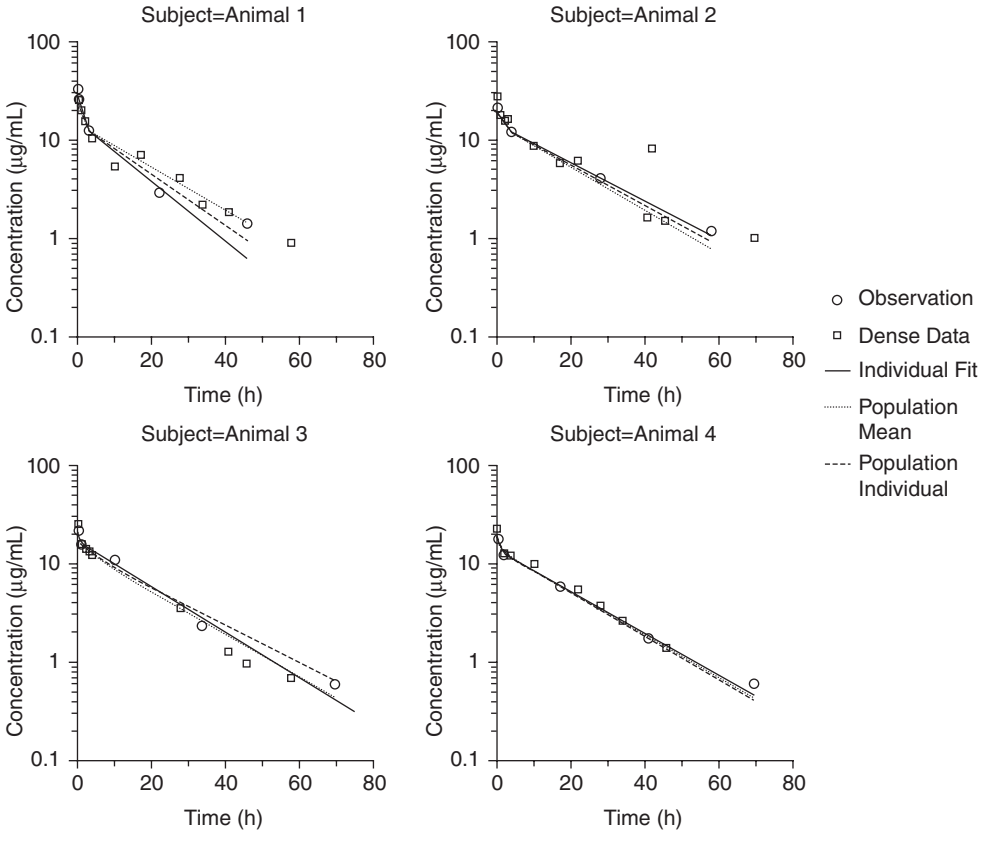

Fig. 16.1 Fitted profiles for the sparse data from Table 16.1 with an overlay of the individual and population fits. The dark lines show the individual fits, the dashed lines show the population individual predictions, and the dotted line shows the population mean (same in each panel). The original data are shown in light gray, for reference, and the sparse data are shown as dark circles.

To emphasize the ability of the population approach to handle sparse data, we have modified the doxycycline data set, as shown in Table 16.3, to reflect sparse sampling of the subject. The estimates from individual fits to the sparse data are shown in Table 16.4, and those from a population fit are shown in Table 16.5. Here, the population estimate provides much more precision in the parameter estimates and assigns almost all of the variability to one parameter (A). Fig. 16.1 shows the fitted profiles for the sparse data, with an overlay of the individual fit and population fit. The population fit consists of two curves, the population mean profile, which is the same for each individual, and the population individual fit (usually called an individual predicted profile, but we need to distinguish it from the true individual model fit). Note that animal 1 with the final two data points deleted shows the greatest difference between the various predictions, but the population mean and individual predictions are closer than the individual model fit. This is because in the population approach the data from the other subjects is informative for animal 1 as well. The terminal slope (β) is not as well identified by the data for this animal, but the population mean value for β helps to correct the population individual estimate for animal 1.

Table 16.3 Sparse doxycycline data.

Time h	Animal 1 μg/mL	Animal 2 μg/mL	Animal 3 μg/mL	Animal 4 μg/mL
0.08	32.5			
0.17		21.2		
0.25			21.6	
0.33				18.6
0.42	25			
0.5		18.2		
1			15.8	
2				12.5
3	12.2			
4		12		
10			11	
17				6.1
22	2.9			
28		4		
34			2.4	
41				1.8
46	1.4			
58		1.2		
70			0.6	0.6

Created by systematically removing three of every four points, staggering across subjects. Animal 4 has the last data point added back in to allow for individual fitting in WinNonlin®, which requires at least one more observation than parameters.

Table 16.4 Individual estimates of the sparse doxycycline data.

Subject	A (μg/mL)	α (1/h)	B (μg/mL)	β (1/h)
Animal 1	20.22	1.49	14.63	0.069
Animal 2	9.09	1.54	14.32	0.045
Animal 3	21.16	6.47	17.25	0.053
Animal 4	19.66	4.21	13.86	0.049
Mean	16.628	2.815	14.959	0.053
CI 95% lower	8.746	0.875	12.806	0.04
CI 95% upper	31.611	9.052	17.475	0.071

Data summarized to give the mean and 95% confidence interval (CI) of the parameters in a log-normal distribution.

Table 16.5 A population estimate of the doxycycline data.

Subject	A (μg/mL)	α (1/h)	B (μg/mL)	β (1/h)
Animal 1	20.79	1.58	14.33	0.059
Animal 2	9.24	1.58	14.34	0.047
Animal 3	10.78	1.58	14.45	0.044
Animal 4	8.05	1.58	14.22	0.05
Mean	11.36	1.58	14.336	0.05
CI 95% lower	5.822	1.58	14.19	0.041
CI 95% upper	22.164	1.581	14.483	0.061

Note the outlier values have generally moved toward the mean and the confidence intervals (CIs) are narrower.

Table 16.6 A population estimate of the sparse doxycycline data for a three-compartment model.

Subject	A (μg/mL)	α (1/h)	B (μg/mL)	β (1/h)	C (μg/mL)	γ (1/h)
Animal 1	–6.84	155.96	20.78	1.57	14.31	0.059
Animal 2	4.69	155.96	9.26	1.57	14.31	0.047
Animal 3	2.98	155.96	10.97	1.57	14.31	0.044
Animal 4	6.04	155.96	7.90	1.57	14.31	0.051
Mean	2.14	155.95	12.14	1.66	14.46	0.05
CI 95% lower	1.18	155.94	9.99	1.41	13.53	0.05
CI 95% upper	2.81	155.96	14.27	2.19	15.04	0.06

The mean and confidence intervals (CIs) were generated by bootstrap. The negative value for A in animal 1 is an indication of the difficulty in estimating the third compartment, where this particular solution sees it as an absorption compartment. In any case, the contribution of the first (A) compartment dampens very rapidly.

Finally, to show how all of the data can be combined to accomplish something that is nearly impossible for individual modeling, we show in Table 16.6 the results of a three-compartment fit to the sparse data. Recall in Chapter 14, Table 14.4, this model was not possible to fit with individual C-T analyses because there are not enough data points in any one profile to uniquely identify the models. However, combining data across the individuals allows for the estimation of the parameters with the population approach. The means and confidence intervals in this case come from a bootstrap analysis, which will be discussed later. The case for using a three-compartment model with the sparse data is not very convincing, given that there is only a negligible difference in AIC and SBC (between model differences within 0.1 for each). Nonetheless, the point is that the population approach enables analyses that are otherwise out of reach.

This brief introduction to the population approach has stressed some of its statistical advantages. One of those advantages, as previously mentioned, is the ability to account for variability between subjects by incorporation of covariates. When considering models, it is helpful to have some ideas about what effects the covariates may have on the pharmacokinetics of the drug, in order to better inform your efforts. We turn our attention now to some common sources of pharmacokinetic and pharmacodynamic variability.

16.5 PHARMACOKINETIC AND PHARMACODYNAMIC BIOLOGICAL VARIABILITY

It is well appreciated in pharmacology that identical doses may produce effects that vary markedly in nature, extent, and duration in different individuals. The pharmacokinetic and pharmacodynamic profiles of many drugs differ across different individuals in a population, even when the population consists only of healthy individuals with homogeneous characteristics (recall interindividual variability in doxycycline pharmacokinetic parameters above). Some of the sources of pharmacological variability have been very well studied (age, weight, disease, and breed), and for some drugs meaningful correlations have been established between pathophysiological factors and altered pharmacokinetic and pharmacodynamic parameters. Evaluation of drugs during clinical trials quantitatively assesses the influence of these factors, termed concomitants (or covariates in statistical parlance), on the therapeutic response. This allows for the design of optimal dosage regimens for specific patients or subpopulations of patients (target populations). However, assessing the influence

of concomitant factors on the mean response is not enough for proper dosage regimen design. Quantitative estimation of the unexplained part of the variability in the patient population that remains after accounting for these other factors is also essential. Once the variability in the parameters is defined in terms of concomitant factors and the unexplained variability is quantitated, the expected variability in concentration and response within the patient population associated with a specific dosage regimen can be estimated.

In this section, some of the aforementioned concomitant factors will be discussed. The next section will deal with the sources of unexplained variability and their estimation and incorporation into a population pharmacokinetic model. Demographic, pathophysiological, environmental, genetic factors (such as age, weight, sex, enzymatic make-up), health status, and concurrent use of other drugs have been reported to influence the fate and effect of drugs administered for therapeutic purposes.

16.5.1 Age

The age of an animal or human has been shown to affect the distribution and elimination of many drugs. It influences drug metabolism, excretion, distribution, and binding. In general, drug elimination seems to improve from birth to maturity and thereafter declines with advancing age. For certain drugs, younger individuals tend to exhibit larger volumes of distribution and lower protein binding and have a greater ratio of extracellular to intracellular water content. Distribution of drugs can also be altered because of the continuous replacement of lean body mass by fat and the decrease in total body water.

The variability in drug response associated with age is most significant in the very young and very old. Differences in drug metabolism between individuals of different ages are also remarkable. In general, drug metabolism enzyme capacity is lower in very young individuals than in adults, particularly for phase II glucuronidation. Renal excretion tends to be less efficient in very young individuals despite the fact that their ratio of kidney to total body weight is double that of adults, a finding suggestive of the kidney's structural and physiological immaturity early in the life of most species. The half-life of many drugs shows a remarkable trend to increase with advancing age due to a decrease in the rate of drug elimination and, for lipophilic drugs, the increase in percent body fat. Physiological functions such as cardiac output, glomerular filtration, and drug metabolism are reduced to varied degrees in the geriatric patient. Oral absorption is also affected by changes in gastrointestinal pH, surface area, motility, and blood flow that parallel age changes. In very young animals, intestinal absorption can be altered. In nursing calves, drug absorption following oral administration is often greater than in adults.

Considering all these changes, the probability of adult patients experiencing adverse drug effects seems to increase with age. This probability is further enhanced by the fact that the geriatric patient is more likely to be receiving medication to treat processes directly or indirectly related to the aging process.

16.5.2 Body weight

Most pharmacokinetic parameters are correlated to body mass. This specific relationship will be explored in Chapter 18 when allometry is presented. The apparent volume of distribution is dependent on body weight since the volumes of total body water and extracellular fluid are directly linked to weight, especially for drugs that are poorly bound to tissue. As mentioned above, differences in volume of distribution may be related to differences

in the lean/fat body mass ratio between individuals with different body weights. The degree of lipophilicity of the drug under consideration will determine the extent of change in volume of distribution under these circumstances. In contrast, hydrophilic drugs will tend to correlate to volumes of the extracellular fluid compartments. Other organ functions may also be affected by weight.

16.5.3 Gender

Differences in drug disposition between sexes are usually less important than the differences attributable to other physiological variables. One source is sex-related differences in the lean/fat mass ratio between females and males. These effects are drug dependent. In females, different levels of circulating hormones at varied stages of the reproductive cycle or status of lactation could influence the therapeutic behavior of certain drugs. Pregnancy has been associated with delayed gastric emptying and reduced gastrointestinal motility, which in turn may reduce drug absorption. Pregnancy increases the volume of distribution for many drugs due to increases in body mass, altered plasma protein concentrations, and changes in distribution of blood flow. We found significant differences in the disposition of ampicillin, with the mean peak serum ampicillin concentration in pregnant mares being 2.5 times lower than in nonpregnant mares. Similar findings have been reported for this drug in women. In the case of very lipophilic and weakly basic drugs, lactation may provide a primary route of excretion. The major gender-related differences in disposition relate to drugs metabolized by hepatic cytochrome P450 enzymes, whose function is correlated to sex steroids. This is primarily seen in some rodents. Similarly, drugs that bind to sex hormone-binding proteins will have gender-specific disposition.

16.5.4 Genetics

Differences in drug metabolism among individuals in a population may account for a large part of the observed therapeutic variability. Genetic factors contribute significantly to the intersubject variation in the metabolic clearance of certain drugs, as fully discussed in Chapter 7. Consequently, subpopulations of slow and fast acetylators as well as poor and extensive debrisoquine metabolizers have been identified. Not all drugs show the same susceptibility to genetic differences; however, the potential for variability in drug disposition and effect due to this factor has to be taken into consideration. Genetic polymorphisms have been less extensively studied in veterinary medicine, although the presence of well-defined breed phenotypes would suggest that this may be a concern.

16.5.5 Disease

Without a doubt, the factor that has the greatest potential for introducing variability in the pharmacokinetic and pharmacodynamic behavior of drugs is disease. The effects of renal and hepatic disease will be extensively discussed in Chapter 17. Because of the central role of the liver in drug metabolism and excretion, hepatic disease has a major effect on drug disposition. Pathological conditions affecting other organs, such as the gastrointestinal tract, heart, and endocrine organs, may alter drug disposition and effect. We had shown that experimentally induced thyroid dysfunction in pigs changed renal glomerular filtration, which impacted on the clearance of gentamicin. Inflammation has been documented to alter drug protein binding and concentrations of binding proteins. Diabetes in humans is well

known to alter antimicrobial drug disposition. This list could go on indefinitely; however, the point is well accepted that many disease states significantly alter drug disposition through a wide variety of pathophysiological mechanisms.

16.6 PHARMACOKINETIC AND PHARMACODYNAMIC STATISTICAL VARIABILITY

In general, disease processes may introduce changes not only in the mean values of the pharmacokinetic and pharmacodynamic parameters, but also in the nature of their population frequency distribution. Fig. 16.2 illustrates this phenomenon based on our observations of gentamicin distribution in dogs, rats, and horses with renal disease. Changes in physiology due to the above factors modify the average value of clearance in the diseased population, as well as its interindividual variability, yet are not explained by the concomitant variable (covariate) that predicts the mean response. This remaining variability is random in nature and for modeling purposes will be characterized by virtue of the so-called random effects. The average value of a pharmacokinetic parameter does not provide enough information to develop rational dosage strategies in individuals.

This important concept is better illustrated in Fig. 16.3, which represents the probability distributions of clearance for three hypothetical drugs. The three drugs depicted in this figure have a similar average value of clearance, but drug 2 exhibits larger interindividual variability than drug 1. This suggests that the level of uncertainty in individual predictions

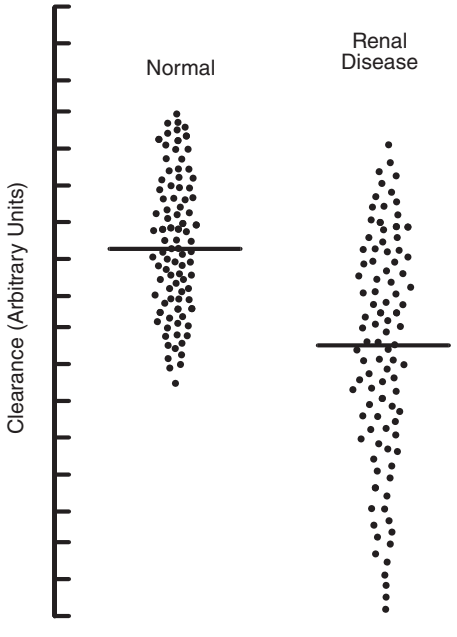

Fig. 16.2 Clearance in normal animals and those with renal disease illustrating how disease processes can change both the mean and variance of pharmacokinetic parameters in a population. When the interindividual variability is great, mean values are not representative of a large portion of the population, and individualized therapy may be required.

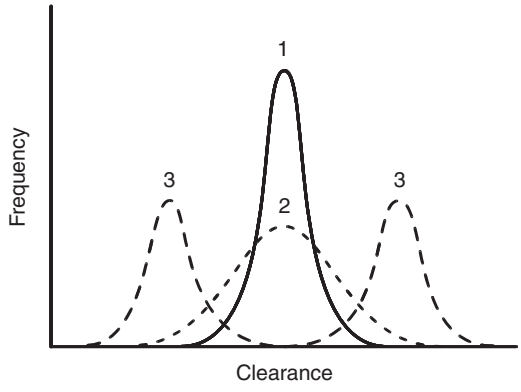

Fig. 16.3 Relationship between the average value of a pharmacokinetic parameter and its frequency distribution. For the three situations depicted, the mean clearance is constant, but the interindividual variability (and consequently the degree of uncertainty in dosage regimen determination) is wider for drug 2 than for drug 1. Drug 3 presents a population composed of two subgroups with different clearances (e.g., secondary to genetic polymorphisms or disease). In this case, it would be unlikely to find an individual in either subgroup with the average population mean. Knowledge of the probability distribution function of the parameters in a population is essential for proper dosage regimen design.

based on the average clearance will be larger for drug 2 than for drug 1. For drug 3, the situation is even more complicated, since the population is clearly represented by two separate subgroups. The population average value of clearance for this drug would not occur in any particular individual from either subgroup. These subgroups could represent populations of different ages or disease states and is typical of genetic polymorphisms in drug metabolism. A similar bimodal population was identified by our group with gentamicin in laboratory rats relative to their sensitivity to nephrotoxicity.

This simple figure illustrates how knowledge of the interindividual variability in population pharmacokinetic and/or pharmacodynamic parameters is essential, even after adjusting for the influence of concomitant variables (fixed effects) such as age or creatinine clearance as an indicator of renal disease. Different types of estimates of population pharmacokinetic and pharmacodynamic parameters are needed to characterize the remaining random interindividual variation that determines the nature of the frequency distributions in the examples presented. This relates to obtaining information about the probability distributions of deviations of individual pharmacokinetic and pharmacodynamic parameters from their population values. One also needs to know how these deviations correlate with one another. This information is provided by the variances and covariances of these probability distributions (random interindividual effect parameters).

A second issue deals with the stability (reproducibility) of the observed outcome (blood concentration, effect) after drug administration in a single individual. As depicted in Fig. 16.4, the observed outcome may vary in an individual with time. These fluctuations could represent steady-state concentrations or measurements of effect after drug administration to a patient. In the effect case, they could be the consequence of intraindividual biochemical changes, such as that which occurs in the development of tolerance, which affects the pharmacodynamic relationships between drug concentration and effect. They can also result from fluctuations in physiology that affect drug disposition, such as those due to circadian rhythms or induction of metabolism. Finally, measurement errors or temporary

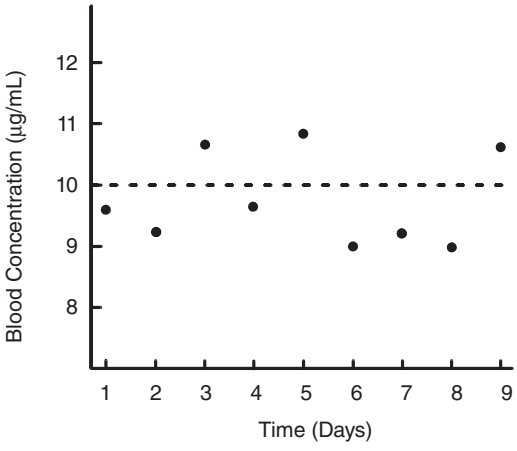

Fig. 16.4 Drug concentrations collected in an individual at the same time after administration of a nonaccumulating dosage regimen (e.g., samples taken at T_{max} in the regimen from Fig. 12.2, see Chapter 12), illustrating how the pharmacokinetic characteristics of a drug may vary within the same individual over time. Transient changes in an individual's physiology or circadian rhythms, or measurement error may be responsible for this component of variability.

changes in the underlying structural pharmacokinetic or pharmacodynamic model also contribute to this random intraindividual variability.

This source of variability is of clinical concern if its magnitude is considerable and it remains unaccounted for in the predictive model. Unknown intraindividual variability would cause an artificial overestimation of the interindividual variability and may lead investigators to erroneously accept as interindividual variability something that is in fact a reflection of methodological shortcomings. Consequently, verifying the stability and reproducibility of the observed response in an individual over time is important in order to place confidence in the estimated interindividual variability. Knowledge of the magnitude of this variability may also be used to set a reasonable threshold on dosage increments in case the observed concentrations indicate the need to increase the dose. For the intraindividual term, another random-effect population parameter is needed; in other words, another variance is needed. This variance combines the random variability afforded by intraindividual changes, as well as measurement error, sampling time recording error, and misspecification of the underlying structural (pharmacokinetic or pharmacodynamic) model fitted to the data.

16.7 PHARMACOSTATISTICAL MODELS FOR POPULATION STUDIES

Population methods encompass a series of techniques that allow the study of the pharmacokinetic and/or pharmacodynamic characteristics of a drug in a target population using sparse data obtained from the sampling of only a few plasma concentrations per subject, from a large number of subjects. Implementing this methodology allows estimation of average values of pharmacokinetic or pharmacodynamic parameters in a population with determined clinical features. More importantly, information is provided about the interin-

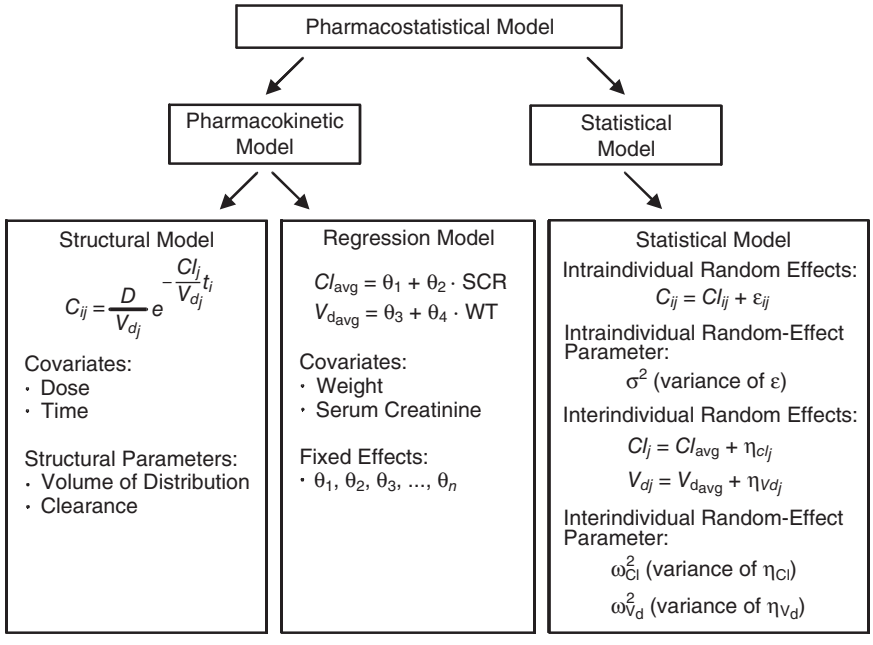

Fig. 16.5 Pharmacostatistical models can be split into a pharmacokinetic model that accounts for the influence of fixed effects (dose, time, covariates) and a statistical model that accounts for the influence of random effects (interindividual and intraindividual). In the pharmacokinetic model, the fixed-effect parameters (pharmacokinetic parameters and proportionality factors on covariates) quantitate the influence of the fixed effects on the model. In the statistical model, the random-effect parameters (variances of the random variables) quantitate the influence of the random effects on the model.

dividual and intraindividual variability of the estimated parameters. Depending on the specific method, the joint probability distribution function of the pharmacokinetic or pharmacodynamic parameters and covariates may be estimated. The joint probability distribution reflects the frequency distribution associated with two variables, and consequently provides an indication of the variance of these two variables and their degree of correlation. In the usual clinical setting, there are not enough data points per subject to fully characterize each individual's pharmacokinetic profile. This limitation is overcome by studying a larger number of clinical patients with an average of one to five samples per individual, as was simulated above with the doxycycline sparse data set. Given the sampling and design restrictions, population pharmacokinetic methods were conceived to analyze observational rather than experimental data. In order to obtain valid information from this type of data, population methods require an a priori, thorough specification of the pharmacostatistical model (Fig. 16.5). This includes specification of the pharmacokinetic or pharmacodynamic model (containing the fixed effects), as well as a complete description of the statistical model (containing the random effects).

The object of study is the entire population; therefore, the outcome of population studies is more representative of the target population than are traditional (STS) studies. One of the most advantageous characteristics of population methods is that they quantify the influence of clinical conditions on the average pharmacokinetic/pharmacodynamic characteristics of the population. Hence, one can explore possible relationships between the therapeutic

behavior of drugs and clinical features of patient populations. Another advantage is the explicit estimation of the magnitude of interindividual and intraindividual (residual) variability (parametric methods) or the direct estimation of the joint probability density function (PDF) of the structural PK parameters (nonparametric methods). This allows for adequate individual predictions to be made according to their clinical features and an assessment of the degree of uncertainty of those predictions. Furthermore, these estimates can be included as a priori information in Bayesian forecasting techniques to further improve individual predictions (see section on clinical applications).

There are two general types of population pharmacokinetic methods, known as parametric and nonparametric. A third, intermediate method is the seminonparametric approach. In parametric methods, the pharmacokinetic parameters and the error terms are assumed to come from a known probability distribution (normal or log-normal, usually) with unknown parameters (e.g., mean and variance). Parameter estimation is restricted to some structural model. Confidence intervals and standard errors are based on parametric methods. These methods, as originally implemented by the computer program NONMEM (for NONlinear Mixed Effects Modeling) developed by Beal and Sheiner in 1980 at the University of California, San Francisco, can also handle some multimodal distributions if they are accounted for in the variance model. With seminonparametric methods, the process of parameter estimation is not restricted to a specific statistical model, and alternative fitting procedures can be employed. However, estimates of uncertainty about the parameter estimations are confined to parametric procedures. In nonparametric methods, there are no restrictions regarding statistical models and distribution of interindividual and intraindividual error terms. The uncertainties about parameter estimates employ nonparametric procedures such as nonparametric confidence intervals. These methods compute the joint PDF of the pharmacokinetic parameters, which measures the variance and covariance of two parameters.

Selecting the most appropriate method depends on the original assumptions about the underlying distribution. Parametric methods are usually easier to implement from a modeling standpoint, but they cannot be used to identify evident deviations from normality in the distribution of the pharmacokinetic parameters in the population, such as bimodal or very skewed distributions.

16.7.1 Parametric methods

Among parametric methods, the main difference is typically in how the algorithm computes a rather difficult integral that provides a likelihood for each individual's data. Due to the computational complexity of the calculation, some of the first methods developed made some simplifications to the likelihood function in order to speed convergence to the solution. Beal and Sheiner (1980) first published on these "first-order" methods in reference to a computational tool (NONMEM) that was the first widely utilized population pharmacokinetic tool. The first-order approximations come in various flavors: first order (FO); first order with conditional estimates (FOCE); and FO or FOCE with interaction. Typically, FO is the fastest but least accurate while FOCE with interaction is slower but more accurate. Solution of these methods is accomplished by moving parameter values to minimize the likelihood (objective) function of the data. NONMEM optimizes the parameters with a gradient-based method, while Phoenix® NLME® from Pharsight (St. Louis, MO) provides a gradient method as well as a fixed-point (Lindstrom–Bates) method, which is usually faster though not as robust to poor initial estimates.

These methods stem from the ordinary and weighted least squares regression techniques presented in Chapter 14. In ordinary least squares, as applied to a set of individual data, parameter values are estimated that minimize the sum of squared deviations of the observations. The variances of the individual observations are assumed to be equal. If they differ but are known, then weighted least squares techniques can be used. When the differing variances are unknown, the extended least squares (ELS) method can be used. This method models the variance as a function of the pharmacokinetic parameters, a vector of independent variables (fixed effects), and some random-effect parameters (interindividual and intraindividual). The term "interaction" used above indicates that random effects are taken into account in this function. Although this method has been broadly used, and has the ability to provide adequate estimates of average parameter values and estimates of random variability, it presents some important disadvantages. First, a single set of parameters that may not be appropriate for all the individuals is fit to all of the data. Second, repeated blood drug concentration measures in an individual are treated as independent observations, and in reality they are not since they are statistically nested within an individual. The interaction between the random effects and the variance term, essentially basing the variance of the data on the individual prediction rather than the population prediction, attempts to account for these issues.

Adaptive Gaussian Quadrature (AGQ) is another technique applied to compute the likelihood integral by numerical integration. It is extremely accurate, though the computational complexity increases exponentially with the number of random effects. With the number of quadrature points (usually selectable by the user) set to one, the AGQ method becomes the "Laplacian" approximation. Both of these methods are typically slower than the first-order approximations but are extendable to non-Gaussian observations (observations that are not normally distributed) such as survival, count, and multinomial data.

Markov Chain Monte Carlo (MCMC) is a Bayesian method for estimating model parameters. MCMC works by sampling (guessing) parameter values and evaluating the likelihood function. If the likelihood is too small, the guess is rejected, otherwise the guess is stored. The guesses come from a "proposal" distribution that is specified by the modeler. The series of successful guesses converge over time to a representative sample from the parameter distribution. It is notoriously slow and tricky to work with because convergence is determined by visual inspection of the stored guesses (the Markov Chain). In addition, a poor choice of proposal distribution or prior distribution can slow convergence. The power of the method is that it enables the inclusion of information from previous studies in the form of the prior parameter distributions and performs a Bayesian update of the parameter distribution. Another advantage of MCMC is that it does not require the costly computation of the normalizing constant (the likelihood integral) that the previously discussed methods are approximating. MCMC methods are implemented in the WinBugs and PKBugs programs of the MRC Biostatistics Unit, Cambridge, U.K.

The expectation maximization (EM) algorithms provide another approach to estimating population models. They are especially good at estimating mixture models (such as situation 3 in Fig. 16.3) where classification of subjects into groups is necessary. Drawbacks of EM algorithms such as slow computation and lack of clear convergence diagnostics have curtailed their use in recent years. A new and interesting development in EM methods is the stochastic approximation to EM (SAEM) algorithm. First implemented in the Monolix (MOdèles NOn LInéaires à effets miXtes) program by the Monolix group in France, this method provides rapid convergence and accurate results. The algorithm combines MCMC sampling with a fast importance sampling computation of the likelihood. There are, as of

this writing, some constraints on the form of the structural and statistical models that can be used, but imminent developments will loosen these and make this method both easier to use and more applicable to a wide range of problems in drug development.

Fig. 16.5 depicts the full pharmacostatistical model divided into pharmacokinetic and statistical components. The pharmacokinetic model (containing the fixed effects) may, in turn, be further subdivided into structural and regression models. The statistical model contains the two types of random effects, namely, interindividual and intraindividual.

All of these parametric methods estimate parameters of mixed-effects models (MEMs), which incorporate fixed effects, random effects, and covariates. The covariates are a series of variables and constants (e.g., dose, time, age, weight, serum creatinine) assumed to be measured without error. They are linked by a structural model (e.g., $C_p = [D/Vd]\ e^{-kt}$) with the dependent variable (plasma concentration) and by a regression model with the pharmacokinetic parameters (e.g., $Cl = f$(serum creatinine) and $Vd = f$(weight)). The covariates of the structural model are dose and time. The proportionality constants (fixed-effect parameters) of the structural model are the pharmacokinetic parameters (e.g., Cl_B, Vd). For example, for the one-compartment open model with intravenous administration, the following expression applies:

$$C_p = (D/Vd) \cdot e^{-(Cl_B/Vd)t} \tag{16.1}$$

where C_p is the observation (dependent variable), D is the dose, t is the time at which the observation takes place, and Cl_B and Vd are, respectively, clearance and volume of distribution.

Note that Equation 16.1 is the basic model introduced in Equation 8.15 (see Chapter 8), where k_{el} is substituted for Cl_B/Vd derived by rearranging Equation 8.16 to allow these physiologically relevant parameters to be correlated to clinical characteristics, and C_p^0 is expressed in terms of D/Vd. Cl_B and Vd quantify the influence of the fixed effects (dose and time) on the dependent variable of the structural model (C_p). As will be seen, many of the basic models presented in earlier chapters may be employed as structural models in population analyses.

If, in turn, the pharmacokinetic parameters can be further explained in terms of patient characteristics (more covariates including age, weight, serum creatinine, and gender), then a regression model is specified in which the pharmacokinetic parameters become the dependent variables, the patient characteristics are the independent variables, and a set of fixed-effect parameters (θ_z) quantify the relationship between patient characteristics and pharmacokinetic parameters. The algorithm computes estimates of the fixed-effect parameters of the regression model. The algebraic form of the equations of the regression model (excluding the random effects) is as follows:

$$Cl_{avg} = \theta_1 + (\theta_2 \cdot Cov_1) + (\theta_3 \cdot Cov_2) + \ldots + (\theta_n \cdot Cov_{n-1}) \tag{16.2}$$

where Cov represents the covariates and θ represents the fixed-effect parameters. The intercepts of each regression equation represent the amount of the pharmacokinetic parameter value that is not due to the effect of these concomitant variables (i.e., each covariate value equals zero, for a linear relationship). For example, the term θ_1 in Fig. 16.5 represents the population average value of the nonrenal clearance. The equation itself is called a "structural parameter" equation, with Cl_{avg} being a structural parameter of the model.

Random effects are unknown quantities arising from a probability distribution whose shape is assumed to be normal or log-normal. There are two kinds of random effects,

namely interindividual and intraindividual. Interindividual random effects are associated with the pharmacokinetic parameters of the structural model (Cl_B, Vd) and reflect the between-subject variability in drug disposition. All individuals have a particular value for their pharmacokinetic parameters that will differ from those of the average population by an unknown quantity. This unknown quantity is assumed to arise from a normal or log-normal probability distribution, with a mean of zero and a certain variance ω^2 that is estimated by the algorithm. The interindividual random variable is represented in the majority of the literature by the Greek character eta (η) with a subscript relative to the pharmacokinetic parameter with which it is associated. The relationship between the random variable and the pharmacokinetic parameter is given by the statistical model similar in structure to that presented in Chapter 14 (Eq. 14.1). For example:

$$Cl_j = Cl_{\text{avg}} + \eta_{Cl_j} \tag{16.3}$$

$$Vd_j = Vd_{\text{avg}} + \eta_{Vd_j} \tag{16.4}$$

where Cl_j and Vd_j represent the clearance and volume of distribution, respectively, in the jth individual, Cl_{avg} and Vd_{avg} are the population averages for clearance and volume of distribution, and η_{Cl_j} and η_{Vd_j} represent the deviations of the individual clearance and volume of distribution, respectively, from their population averages for the jth subject. The error model can be additive (as here) or may adopt other forms (e.g., multiplicative, exponential). Intraindividual random effects represent the residual variability and arise from model misspecification (e.g., fitting a one-compartment model to data that would be better described by a two-compartment model), analytical assay error, sampling time recording error, and time variation in pharmacokinetic parameters within an individual. Formally expressed, the residual variability represents the deviation of the observed concentration from the value that would be expected were the true individual pharmacokinetic parameters known. Algebraically expressed,

$$C_{ij} = C_{ij}(\text{true}) + \varepsilon_{ij} \tag{16.5}$$

where C_{ij} is the observed concentration in individual j at time i, C_{ij} (true) is the true concentration for individual j at time i, and ε is the residual random error or difference between observation and true value for individual j at time i (introduced in Chapter 14). As in the case of the interindividual random effect, the form of this relationship may be other than additive. The random variable ε is assumed to arise from a normal or log-normal probability distribution with mean zero and variance σ^2. The algorithm computes estimates of the variances of the interindividual and intraindividual random effects, namely, ω^2_{Cl}, ω^2_{Vd}, and σ^2. Note that the parameters describing the distribution of the random effects (variance–covariance matrix, usually) are *fixed effects*; they are the same for all individuals.

Fig. 16.6 illustrates the partitioning of the variability that takes place under this mixed-effects modeling strategy. The discrepancy between the observed and predicted outcome (drug concentration in this case) arises from two distinct components. First, the *true residual variability* arises from the difference between the observed (C_{ob}) and the true (C_{true}) blood concentration. The true blood concentration is defined as the concentration that would be expected if the true values of the individual pharmacokinetic parameters were known. The intraindividual variability is a component of the residual variability. Second, the *interindividual variability* arises from the difference between the expected

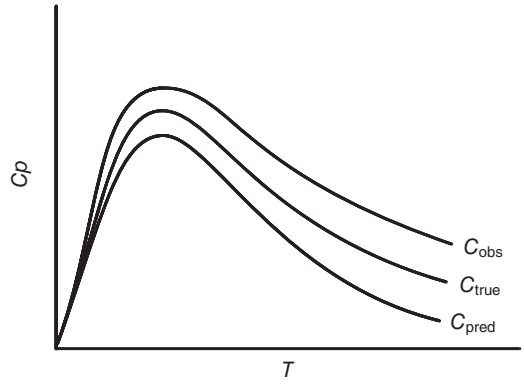

Fig. 16.6 Concentration-versus-time profile demonstrating how mixed-effects modeling partitions the *total residual error* (C_{obs}—C_{pred}) in terms of *true residual error* (C_{obs}—C_{true}), arising from the difference between the observed plasma concentration and the true concentration, and *interindividual error* (C_{true}—C_{pred}), arising from the difference between expected concentrations using the true individual pharmacokinetic parameters and those predicted using the values of parameters estimated by the regression model.

concentrations using the true individual pharmacokinetic parameters (C_{true}) and that expected using the average values of pharmacokinetic parameters estimated by the population model after accounting for the influence of the fixed effects (C_{pred}).

There are a variety of algorithms related to nonlinear regression and matrix algebra used to obtain estimates of the fixed-effect parameters, the interindividual and intraindividual random-effect parameters (variances), and the standard errors of all these parameter estimates. The covariance and inverse covariance matrices are also computed to show if parameter values are correlated. If the parameters of the model are not independent of each other, the model should be reassessed, or the correlations modeled. The correlation matrix of the parameter estimates is computed as an additional indication of the adequacy of the model, since highly correlated parameter estimates are indicative of model overparameterization. Plots of observations versus predictions, as well as plots depicting the distribution of residuals (or weighted residuals) or random effects for each parameter for different levels of a covariate, are obtained. These kinds of plots can be used to assess the necessity of including a covariate in linear MEMs and their utility extends to nonlinear MEMs as well.

Figs. 16.7 and 16.8 illustrate an example of how scatter plots can be used to develop the regression portion of the population model. Fig. 16.7a is the plot of observed versus predicted concentrations for a hypothetical set of data, which does not account for the influence of concomitant variables (covariates). The fit is generally accurate at lower concentrations but inadequate in other regions. Fig. 16.7b depicts the plot of residuals versus the covariate body weight (residual plots were introduced in Chapter 14). As we can see, the scatter of the residuals is not homogeneous, and a decreasing pattern is apparent (positive deviations in larger individuals). This suggests that weight is related to volume of distribution of the drug in the population and that it should be included in the predictive model. A plot of random effects on *Vd* versus body weight could also be examined in the same way.

We explored whether the inclusion of covariates in the regression model would improve the fit. Fig. 16.8 represents the model that includes the covariate weight in the predictive model. As one can see in Fig. 16.8a, the predictive performance improves dramatically.

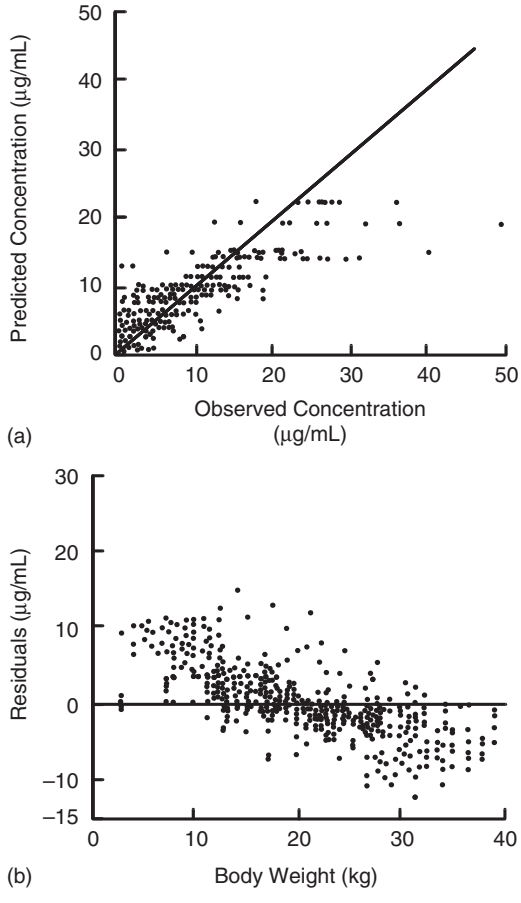

Fig. 16.7 Modeling data using a model with no covariates. (a) Plot of observed versus predicted drug blood concentrations after administration of a drug to a hypothetical population. The simplest model is one that does not account for the effect of any pathophysiological covariates. The lack of precision is considerable. (b) Plot of residuals versus the covariate body weight. A plot of the residuals (or weighted residuals) versus covariates of interest may reveal specific trends that would indicate the necessity to model the effect of such a covariate on the outcome. In this case, there is a pattern of overprediction in large individuals and underprediction in small ones.

The residual plot in Fig. 16.8b shows homogeneous scattering of the residuals as a function of weight, indicating no further variability in the data seems to be related to weight. The model has been improved.

The model-building procedure (structural and regression model) is conducted in a stepwise fashion. The statistical significance of the reduction in the minimum value of the likelihood (usually measured in log scale and called "LL") and the decrease of the interindividual and intraindividual variability when adding a new covariate to the model are assessed at every step. Each time a model is run, it minimizes the likelihood function. The minimum value of the likelihood function is an indicator of the goodness of fit of the model. This value can be used to statistically compare full-reduced regression pairs. The full model is that from which the parameter of the added covariate is estimated. Alternatively, the

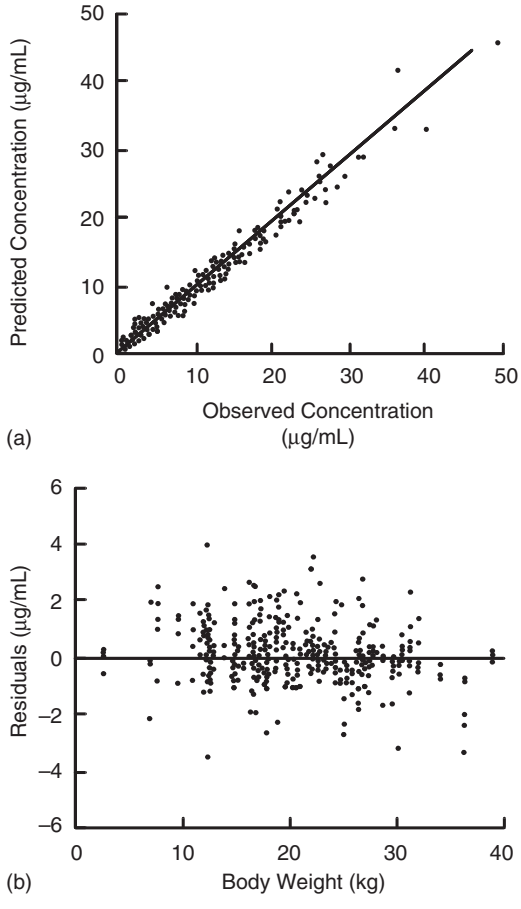

Fig. 16.8 Modeling data using a model with body weight as a covariate. (a) Inclusion of the covariate body weight considerably reduces the variability and improves the predictive performance in an observed versus predicted concentration plot compared with the plot in Fig. 14.7a. (b) Homogeneous scatter of the residuals in this plot, compared with the plot in Fig. 14.7b, indicates that the influence of body weight in the pharmacokinetic profile of this population is adequately modeled.

reduced model is that from which the parameter in question is fixed to the null value. Twice the difference between the LL of a full model and a reduced model approximates a chi-square (χ^2) distribution with degrees of freedom equal to the difference in the number of parameters between the full and the reduced model (q). Its statistical significance can be determined by comparing the difference between both LL values, with the correspondent value of the χ^2 distribution for q degrees of freedom. Note that this statistic is valid for nested models, as discussed for the F-test in Chapter 14, but not for testing variance components being equal to zero. That is, the likelihood structure as determined by the variance–covariance (omega) matrix and the residual error model (e.g., additive, multiplicative) must be the same.

The reader should note the similarity of this modeling strategy to that presented in Chapter 14. Regression plots, supported by statistical tests of fit such as R^2, F-test, AIC, and SC are compared against various models (e.g., with one, two, or three compartments)

until the proper model is selected. In the case of stepwise model building, residual plots and LL values are used to arrive at the full model, which is significantly more predictive than the reduced model.

16.7.2 Nonparametric methods

Nonparametric methods provide the opportunity for analysis without implicit assumptions as to the population distribution of the random-error terms for interindividual and residual variability. This allows one to visualize the data and determine the best function with which to represent the observed distribution. Due to this feature, nonparametric methods can handle bimodal or multimodal populations, thereby revealing unsuspected clusters of patients (e.g., drug 3 in Fig. 16.3), such as those that occur in genetic polymorphisms (e.g., slow and fast acetylators). These techniques are based on the general method known as maximum likelihood estimation. This method, as applied to regression, aims at obtaining parameter values that provide the maximum probability of producing a sample in the neighborhood of the one observed. The maximum likelihood represents a family of statistical procedures used to determine when further iterations are no longer needed to improve the fit between the observed versus the predicted values. Nonparametric methods compute the nonparametric maximum likelihood (NPML) estimate of the unknown population density function. The differences between the two main types of nonparametric methods reside in the type of algorithm that they utilize. As for the relationships between covariates and structural parameters, nonparametric methods estimate the joint distribution of the parameters (both pharmacokinetic parameters and fixed-effects parameters that describe the relationships between pharmacokinetic parameters and covariates).

16.7.3 NPML

This algorithm was first described by Mallet (1986), who showed that the joint probability distribution of parameter values in a population model is discrete as opposed to the continuous nature of a normally distributed parameter. Accordingly, it can be described by some frequency distribution. NPML computes the joint PDF of the parameter estimates. NPML states the problem of parameter estimation in terms of the probability of obtaining data similar to those actually observed. It relies on the maximum likelihood principle as applied to the estimation of pharmacokinetic parameters. In other words, given a set of unknown terms and a set of data related to the unknowns, the best estimate of the unknowns consists of the values that render the set of data most probable. In the most familiar situation, the unknowns are the pharmacokinetic parameters of an individual and the data set is the individual series of observations. The distribution of the pharmacokinetic parameters in the population can also be unknown, in which case the data are the array of such series of observations within a sample of individuals. In general, nonparametric methods require more mathematical sophistication than the parametric methods, but they allow appropriate parameter estimates to be computed when the distribution of pharmacokinetic parameters in the population departs from normality.

16.7.4 Nonparametric EM (NPEM)

This nonparametric estimator uses an iterative EM algorithm with steps utilizing both expectation and maximization. This algorithm as implemented by Schumitzky (1991)

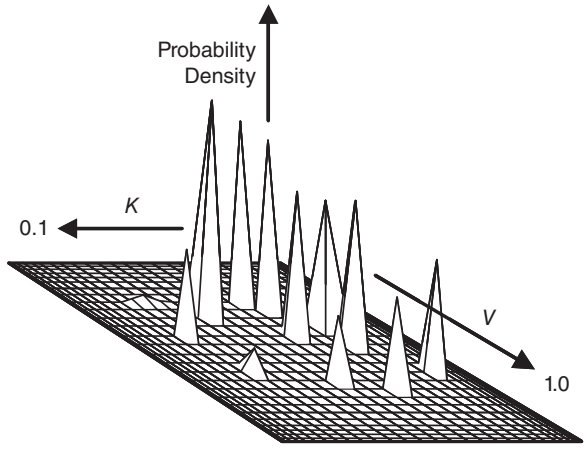

Fig. 16.9 Three-dimensional plot of the joint PDF in a population of patients treated with a drug. K = elimination rate constant (range, 0–0.1 h^{-1}). *V* = volume of distribution (range, 0–1.0 L/kg). Each spike represents the probability that a subject will have $V = x$ and $K = y$. If all true values for the population were known, this plot would be a scatter plot with a dot per individual (or overlapping dots for individuals with the same values of *V* and *K*).

computes the entire joint PDF of the parameters. During the initial phases of the estimation process, a continuous PDF is calculated. The population fit of the PDF improves with each iteration. With progressive iterations, the spikes of the joint density become narrower. At its limits, discrete distributions are obtained.

Fig. 16.9 depicts a graphical example of the joint PDF for a patient population. The joint PDF is projected as three-dimensional spikes, the location and height of which represent the estimated values and probabilities of the pharmacokinetic parameters. Together with the joint probability density, it also computes individual density functions for each parameter. This algorithm can operate with a single data point per patient. It has been integrated as a segment of the USC*PACK software package (University of South California, Los Angeles). Different studies have shown similar results when either a nonparametric method or the STS method was used to model blood sample data from populations with normal distribution of the pharmacokinetic parameters. Estimates of the means, standard deviations, modes, medians, skewness, kurtosis, correlations, and covariances between parameters can also be obtained.

16.7.5 Seminonparametric methods

The smooth nonparametric (SNP) maximum likelihood is a seminonparametric method proposed for use in population pharmacokinetic analysis by Davidian and Gallant (1992). This modeling strategy is particularly relevant for population data that can be described with nonlinear MEM strategies. For this type of data, the SNP method simultaneously estimates the fixed effects (by maximum likelihood principles) and the entire random-effects density.

16.7.6 Neural net methods

Another strategy that has been adopted for many types of modeling problems is the use of neural nets to define relations between disparate data sets. The input to these programs are

dose and any other clinical or patient variable deemed appropriate for predicting concentration and/or effect as outcomes. The data set is divided in half and the neural net is trained to predict desired outcome variables from defined input variables. The trained neural net is then tested on the other half of the input data to see whether the outcome data can be predicted. The process is repeated until convergence occurs. The major criticism of this approach is that the manner in which the neural net links the input to outcome is not known; however, its use in pharmacokinetics is being explored and no doubt will result in more mechanistically based procedures in the future.

16.8 VALIDATION OF THE RESULTS

Many population pharmacokinetic and pharmacodynamic studies are observational rather than experimental. This has led to the establishment of appropriate validation methods, to ensure that the parameter estimates obtained can be extrapolated to the general population and results are reasonable and independent of the analyst. Validation procedures are intended to assess how well a population model (obtained from a study or an index population) describes a set of data (validation set) that has not been used to develop the model itself. Whether or not validation of the population study is accomplished depends on the objective of the analysis. When a population model is developed for dosage recommendation, it must be adequately validated. Alternatively, when population models are developed for explaining variability or for providing some descriptive labeling information, validation may not be required.

It is beyond the scope of this review to discuss in detail the different validation methods that have been proposed and the statistics involved in each of them. Selection of the validation method should be justified by the ultimate goal of the population study. The interested reader should refer to the appropriate literature for more comprehensive information on each particular method.

16.8.1 Types of validation

The validation of a population model consists of the assessment of its stability and/or predictive performance using a validation data set, different from that used to develop the model. This was first introduced in Chapter 3 on QSPeR modeling where validation is an integral part of the modeling procedure. Depending on the availability of validation data, we may distinguish two types of validation, namely, external and internal. In external validation, the validation set consists of an entirely new data set obtained from another study. Alternatively, internal methods use the original data set to derive both the index and validation data sets or use resampling approaches to validate the developed model—much like the scenario described above for training neural nets. Internal validation techniques include data splitting and resampling techniques such as cross-validation and bootstrapping.

Data splitting partitions the available data set into two portions: the index data set (two-thirds) and the validation data set (one-third). Since the predictive accuracy of the model is dependent on the sample size, it is recommended that after validation of the population model, both sets are pooled together and the final model parameters estimated using this overall data set.

Cross-validation consists of repeated data splitting. Bootstrapping consists of a resampling procedure that allows the evaluation of the stability and performance of a population model by repeatedly fitting the model to the bootstrap samples. The bootstrap samples

consist of a large number (e.g., 200) of subsample replicates obtained by resampling the original data with replacement. Subsamples are distributed in a similar manner to that of the original sample and, consequently, the statistical inference of interest can be made as for the original sample. This method is computer-intensive and is an adequate alternative to external validation methods when original sample sizes are too small. Recall we employed this procedure to generate a population for the doxycycline sample above.

16.8.2 Methods of validation

16.8.2.1 *Standardized prediction errors*

This is one of the first validation methods used in population studies. This method computes the standardized mean prediction error (SMPE) and the variance for each patient. A *t*-test (actually a *z*-test) is performed to assess whether the average of SMPEs across patients is different from zero; that is, whether the prediction is, on the average, biased. Another *t*-test is conducted to test whether or not the model describes adequately the variability in the validation data set (within and between patients), by comparing the standard deviation of $SMPE_J$ (computed across *j* patients) to 1. The method has received criticism regarding its inadequacy to test the latter hypothesis and the incorrect assumption of lack of error in the estimates of population parameters.

16.8.2.2 *Concentration prediction error*

This method is based on the prediction error, which is the difference between the predicted and the observed concentrations. This method assesses the predictive performance of a population model by using the mean squared prediction error (MSPE) as an indicator of precision, and the mean prediction error (MPE) as an indicator of bias. This method is inadequate when more than one observation is obtained per subject, because in that case, prediction errors are not independent.

16.8.2.3 *Validation using model parameters*

This method accomplishes validation with the parameters of the model, hence avoiding the problems encountered in the previous method. Using the validation set, it assesses both qualitatively and quantitatively the model predictions of individual pharmacokinetic parameters, with or without covariates, and calculates the precision and bias for the predictions.

16.8.2.4 *Graphical approach*

A graphical approach to the validation of a model may be initiated by plotting the model predicted versus observed concentrations in the validation set. This plot provides one with a visual clue for the degree of agreement between model predictions and validation data. It has been argued that in judging this correlation from a clinical rather than a statistical perspective, the graphical approach may provide as much information, if not more, than that presented by standard statistical comparison approaches. A similar conclusion has been stressed throughout this book concerning the power of data inspection to determine if one's model actually describes the data at hand.

Plots of the residuals (observed minus predicted concentrations) versus some of the covariates provide additional information on the validity of the population predictions. Residuals should be conceptually viewed as the prediction error for every individual in the study. A plot of the residuals versus age may provide an indication of the clinical adequacy of the model for different age groups. Such plots could uncover "age clusters" for which the model fits the validation data with less accuracy and/or precision.

Weighted residuals can be also useful for validation purposes. Weighted residuals are obtained by normalizing the residuals by the standard deviation of the model. Use of weighted residuals is a potential source of bias if inappropriate weighting schemes are used. The weighted residuals consist of the residuals expressed in population standard deviation units. Consequently, a plot of the weighted residuals versus the individual patient identification number can be useful to assess whether the residuals follow the description established for them under the population model. If the model affords an appropriate description of the validation data, then the weighted residuals should be homogeneously scattered about the zero line on the weighted residuals axis. Similarly, plots of weighted residuals versus some of the covariates included in the model (e.g., weight, breed, creatinine clearance) may uncover situations in which the influence of the covariate has not been adequately modeled. If a trend or lack of homogeneity is observed in a plot of weighted residuals versus the covariate, instead of a homogeneous scatter, the model is not describing the variability adequately. In this case, some changes are necessary regarding the relationship between the covariate and the pharmacokinetic parameter or parameters in the population model.

Finally, a plot of the prediction interval can be invaluable in determining if a model accurately captures information about the population. The goal is to resample from the random effects in a series of replicates and record the individual predictions for each subject. Then the 95% prediction interval can be constructed, which shows the likely distribution of data if the study or studies in the analysis were repeated. Pathological over- or underpredictions can be used to disqualify a model or drive further modification to it. Fig. 16.10 shows a prediction interval for the three compartment doxycycline sparse data model discussed previously. The solid lines are the 5%, 50% (thicker), and 95% quantiles of the simulated data, and the dashed lines are the 5% and 95% observed quantiles. Ideally, one would like to have the observed and predicted quantiles agree and have the observed data fall mostly within both. Deviations from the expected behavior call a model into suspicion. In this case, the predicted values for the early times and the late times fall too low for one to be comfortable using this model.

16.9 APPLICATION OF POPULATION PHARMACOKINETICS IN VETERINARY MEDICINE

Population studies have been applied to problems in veterinary medicine. A number of recent studies of field exposure of antibiotics in feed or water to swine (del Castillo et al., 2006; Mason et al., 2008) illustrate the application of these principles to herd health dosing scenarios known to have large interindividual variability. The tools provided in this chapter can be used to define these sources of variability, and as also illustrated in the del Castillo et al. (2006) study, to assess in a highly variable population whether simultaneous administration of a second drug modifies antibiotic absorption under field, in contrast to highly controlled and artificial laboratory conditions. The works of Whittem et al. (2000), Auclair

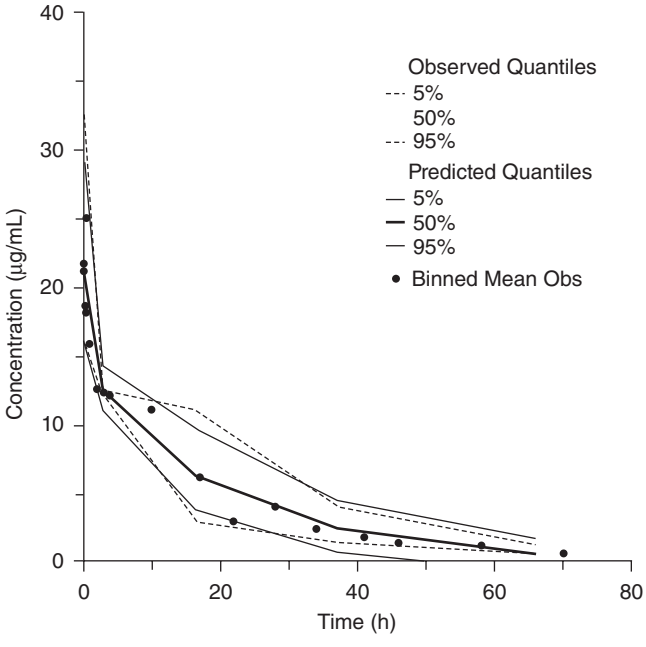

Fig. 16.10 A visual predictive check of the three compartment model of the sparse doxycycline data set. Solid lines are predicted quantiles (from resimulation) and dashed lines are observed quantiles (of the data). The data have been "binned," which is common and necessary for sparse data, so the points represent mean values in each bin for the observed data.

et al. (2002), Regnier et al. (2003), Peyrou et al. (2004), KuKanich et al. (2007), and Guo et al. (2010) should be consulted for further interesting applications. These illustrations demonstrate where population approaches are ideally suited to situations where multiple samples per individual are difficult to obtain, examples being given in wild animal work (Auclair et al., 2002 and KuKanich et al., 2007 studies) or because of the inability to do sequential sampling in an organ such as the eye (Regnier et al., 2003).

16.9.1 Clinical use

Population pharmacokinetic modeling could be used in the clinical setting in two ways. First, it can be utilized to design initial dosage regimens for new individual patients or patient clusters according to their clinical features. Second, population models can be used as prior information in Bayesian forecasting methods to further improve the accuracy of the predictions in a patient from whom only a few plasma samples can be obtained.

When a drug is used to treat a pathologic condition in a patient (human or animal), the first objective is to optimize the dose for the individual patient. This is the case particularly when the drug has a narrow therapeutic index and/or a large interindividual variability in its disposition or effect. Variability in therapeutic outcome can be partitioned into pharmacokinetic and pharmacodynamic components. Consequently, pharmacokinetic and pharmacodynamic variability in a population will dictate how confidently the clinician will be able to administer an average population dose to an individual subject. Defining the magnitude of this variability and the factors that contribute to it are the critical issues in dealing with

dose individualization. When drugs exhibit a large variability in disposition across individuals, poor correlation between plasma concentrations and dose will exist. The consequence of this will depend on the pharmacodynamic characteristics of the drug for both the therapeutic and the toxic effects. By explaining part of this variability in terms of a series of pathophysiological variables (weight, age, and renal function), dosage regimens can be designed that correlate well with serum concentrations for each particular subpopulation since the total residual variability is greatly reduced. If the inclusion of pathophysiological variables in the model reduces the interindividual variability to a relatively small magnitude and the pharmacodynamic variability is not large, one can design an optimum dose for each of these subpopulations derived from their average pharmacokinetic parameter-estimated values. This is especially valuable for subpopulations that are more prone to deviate from the general population values (e.g., very young individuals, very old individuals, subjects with impaired renal or hepatic functions).

16.9.2 Bayesian methods

The Bayesian approach to the estimation of pharmacokinetic parameters in an individual takes advantage of both the prior information derived from the population as well as the scarce information obtained from the actual patient treated with the drug. First, a population model (accounting for patient clinical conditions) is developed and validated. This model (prior probability) is used to develop an initial dosage regimen. This initial regimen will be based on the average population parameter values of the subpopulation to which the patient belongs (for example, 2-year-old beagles with a body weight of 13 kg and a serum creatinine level of 1.9). The model (including the estimates of variability) is reassessed (Bayesian feedback) with new data obtained from a few blood samples from the patient. Finally, the probability distribution of the individual parameters is adjusted (posterior probability) in light of the observed patient's plasma concentrations. Iterative fitting procedures continue, selecting those values of individual pharmacokinetic parameters (Bayesian posterior) that minimize the Bayesian objective function:

$$\left\{\left[\sum (P_{\text{pop}} - P_{\text{ind}})^2\right] \Big/ \sigma^2 P_{\text{pop}}\right\} + \{[(C_{\text{pop}} - C_{\text{ind}})^2]/\sigma^2 C_{\text{obs}} \tag{16.6}$$

where P_{pop} and P_{ind} represent the parameter values of the population pharmacokinetic model and of the patient's individualized model, respectively. C_{obs} and C_{ind} represent the observed plasma drug concentrations and the estimates of those concentrations made with the patient's individualized pharmacokinetic model (for each observation), respectively. $\sigma^2 P_{\text{pop}}$ represents the variance for the different population pharmacokinetic parameter values, and $\sigma^2 C_{\text{obs}}$ represents the variance of the observed plasma concentrations. Different studies have validated this approach to make individualized pharmacokinetic models of drugs in patients and have shown improvement of the predictive performance (future serum drug concentrations) relative to the traditional methods of linear regression when the number of samples available from each patient was small. As the number of individual samples increases, the Bayesian solution approaches that obtained by the traditional least squares method.

16.9.3 Production medicine

The use of population pharmacokinetic/pharmacodynamic methods in food animals could vastly likely improve the conditions of herd drug usage in the near future. The earlier

examples of its application to feed and water drug administration illustrate this nicely. The ability of these methods to obtain valuable information from large populations in which each individual is sparsely sampled seems ideal for studying drug therapeutics in food animals. Differences in drug disposition across individuals could be related to disease conditions, nutrition, management practices, lactation status, or breed. This knowledge, together with a better assessment of the sources and magnitude of variance, will allow a more reasonable use of drugs in these animals. Differences in disposition can be related to individual characteristics and to subpopulation characteristics, such as breed of animals or crop groups in fish. Consequently, population pharmacokinetics and pharmacodynamics in production medicine could be applied both to individual and subgroup therapeutics. Use of Bayesian approaches to incorporate existing but imprecise data to predict drug disposition in a herd environment also deserves further attention.

As pointed out previously, veterinary medicine deals not only with companion species, but also with animal species that will ultimately serve as sources for human food products. In the latter case, the importance of accurately describing the disposition of drugs in animals according to clinical or production variables without designing extensive individual pharmacokinetic studies is clearly evident. This is especially pertinent because of the influence that these variables may bear in the deposition of drug residues in those animals' tissues or food products (milk, eggs). Although there is great potential for the population approach to address drug tissue disposition and residue avoidance, adequate strategies for its implementation have yet to be explored. One of the obvious limitations of a tissue residue study is the lack of sufficient tissue samples per individual (unless biopsies are performed) to individually characterize tissue-depletion kinetics (only one sample per animal and time point is usually available).

The strength of the population approach is that data collected from a wide variety of experimental protocols (efficacy, safety, residues) can be pooled into a single model for the drug. The final objective would be to estimate the probability of violative tissue residue levels in a herd undergoing drug therapy by considering the concomitant production variables (e.g., weight, daily gain, disease) and screening a reduced number of animals in the production unit. The situation for animal food products other than those derived from animal tissues (e.g., milk or eggs) is more straightforward. Serial samples can be obtained from these "compartments," and consequently more accurate pharmacokinetic profiles can be determined for the depletion of drug from these compartments.

Another area worthy of exploration using the population approach is that of allometric interspecies scaling of pharmacokinetic parameters, given that this methodology can be used to directly model large pools of data (often unbalanced) from many individuals. A population analysis of data from several species, with body weight and enzymatic composition as covariates, has the potential to unveil allometric relationships that cannot be easily detected by other methods. Studies of this kind would provide veterinarians and comparative pharmacologists with the ability to extrapolate serum and tissue data across species, taking into account the influence of important intraspecies and interspecies clinical factors.

16.9.4 Drug development

Much can be gained from the application of population pharmacokinetic and pharmacodynamic modeling methods and concepts during the process of drug development in veterinary medicine. One of the main goals of drug development is to obtain knowledge about the pharmacokinetic–pharmacodynamic (PKPD) characteristics of a drug in populations.

This was introduced in Chapter 13. Although the clinical trial phase of the drug development process seems to be best suited to population studies, very valuable information can be derived from the implementation of this approach at earlier stages. Population kinetics would be very useful in targeting the appropriate dose for clinical trials.

The main goal of population pharmacokinetics is to identify subpopulations of patients whose responses differ with respect to either location (mean) or variability, and to correlate those differences to some measurable covariate. During field or clinical trials, population PKPD models would allow identification of subpopulations that may require a different dosage regimen. This would provide a more efficient way to determine dose ranges. Well-defined population PKPD models are useful to support supplemental applications (e.g., different dosage regimens, alternative indications, new routes of administration). Population PKPD is a useful tool for sponsors to provide the required labeling information with a minimum expenditure of resources.

Once a drug reaches the market, continued monitoring of the drug and completion of new population studies would provide additional information that, when compiled with previous information in an integrated database system, would help to define even more precisely the PKPD characteristics of drugs in clinical use. Abbreviated protocols to adjust dosages of older approved drugs could be designed and conducted in a population framework. In the case of drugs administered to food animals, this database would provide valuable information on adapting withdrawal times to specific clinical conditions. The extralabel use of drugs in food animals, as implemented by the Animal Medicinal Drug Use Clarification Act (AMDUCA) regulations in 1997, would especially benefit from this approach. Information from different sources on drug pharmacokinetics in edible tissues after different doses and clinical conditions would allow computation of better estimates of preslaughter withdrawal times. Overall, this would improve the safety of animal products destined for human consumption.

ACKNOWLEDGMENT

The authors appreciate the contribution of Tomás Martin-Jiménez, a coauthor of this chapter in the first edition of this text.

BIBLIOGRAPHY

Aarons, L. 1993. The estimation of population pharmacokinetic parameters using an EM algorithm. *Computer Methods and Programs in Biomedicine*. 41:9–16.

Auclair, B., Mikota, S.K., Peloquin, C.A., Aguilar, R., and Maslow, J.N. 2002. Population pharmacokinetics of antituberculous drugs and treatment of *Mycobacterium bovis* infections in bongo antelope (*Tragelaphus eurycerus isaaci*). *Journal of Zoo and Wildlife Medicine*. 33:193–203.

Balant, L.P., and Gex-Fabry, M. 2000. Modeling during drug development. *European Journal of Pharmaceutics and Biopharmaceutics*. 50:13–26.

Beal, S.L. 1984. Population pharmacokinetic data and parameter estimation based on their first two statistical moments. *Drug Metabolism Reviews*. 15:173–193.

Beal, S.L., and Sheiner, L.B. 1980. The NONMEM system. *American Statistician*. 34:118–119.

Beal, S.L., and Sheiner, L.B. 1988. Heteroscedastic nonlinear regression. *Technometrics*. 30:327–338.

Boeckmann, A.J., Sheiner, L.B., and Beal, S.L. 1994. *NONMEM Users Guide. Part V: Introductory Guide, Technical Report of the Division of Clinical Pharmacology*. San Francisco: University of California.

Bonate, P.L. 2005. Recommended reading in population pharmacokinetics pharmacodynamics. *The AAPS Journal*. 7:E363–E373.

Bruno, R., Vivier, N., Vergniol, J., De Phillips, S., Montay, G., and Sheiner, L. 1996. A population pharmacokinetic model for docetaxel: model building and validation. *Journal of Pharmacokinetics and Biopharmaceutics*. 24:153–172.

Chien, J.Y., Friedrich, S., Heathman, M.A., de Alwis, D.P., and Sinha, V. 2005. Pharmacokinetics/pharmacodynamics and the stages of drug development: role of modeling and simulation. *The AAPS Journal*. 7:E544–E559.

Chow, H.H., Tolle, K.M., Roe, D.J., Elsberry, V., and Chen, H. 1997. Application of neural networks to population pharmacokinetic data analysis. *Journal of Pharmaceutical Sciences*. 86:840–845.

Davidian, M., and Gallant, A.R. 1992. Smooth nonparametric maximum likelihood estimation for population pharmacokinetics, with application to quinidine. *Journal of Pharmacokinetics and Biopharmaceutics*. 20:S29–S61.

del Castillo, J.R.E., Laroute, V., Pommier, P., Zémirline, C., Keïta, A., Concordet, D., and Toutain, P.L. 2006. Interindividual variability in plasma concentrations after systemic exposure of swine to dietary doxycycline supplied with and without paracetamol: a population pharmacokinetic approach. *Journal of Animal Science*. 84:3155–3166.

Ette, E.I. 1997. Population model stability and performance. *Journal of Clinical Pharmacology*. 37:486–495.

Ette, E.I., and Ludden, T.M. 1995. Population pharmacokinetic modeling: the importance of informative graphics. *Pharmaceutical Research*. 12:1845–1855.

Frazier, D.L., Aucoin, D.P., and Riviere, J.E. 1988. Gentamicin pharmacokinetics and nephrotoxicity in naturally acquired and experimentally induced disease in dogs. *Journal of the American Veterinary Medical Association*. 192:57–63.

Grasela, T.H., and Sheiner, L.B. 1991. Pharmacostatistical modeling for observational data. *Journal of Pharmacokinetics and Biopharmaceutics*. 19:255–236.

Guo, Q.J., Huang, L.L., Fang, K., Wang, Y.L., Chen, D.M., Tao, Y.F., Dai, M.H., Liu, Z.L., and Yuan, Z.H. 2010. Population pharmacokinetics of enrofloxacin and its metabolite ciprofloxacin in chicken based on retrospective data, incorporating first-pass metabolism. *Journal of Veterinary Pharmacology and Therapeutics*. 33:84–94.

Hauck, W.W., Anderson, S., and Marcus, S.M. 1998. Should we adjust for covariates in nonlinear regression analyses of randomized trials? *Controlled Clinical Trials*. 19:249–256.

Jelliffe, R.W., Schumitzky, A., Van Guilder, M., Liu, M., Hu, L., Maire, P., Gomis, P., Barbaut, X., and Tahani, B. 1993. Individualizing drug dosage regimens: roles of population pharmacokinetic and dynamic models, Bayesian fitting and adaptive control. *Therapeutic Drug Monitoring*. 15:380–393.

Karlsson, M., Beal, S., and Sheiner, L. 1995. Three new residual error models for population PK/PD analyses. *Journal of Pharmacokinetics and Biopharmaceutics*. 23:651–672.

Kuhn, E., and Lavielle, M. 2004. Coupling a stochastic approximation version of EM with an MCMC procedure. *ESAIM: P&S*. 8:115–131.

Kuhn, E., and Lavielle, M. 2005. Maximum likelihood estimation in nonlinear mixed effects models. *Computational Statistics and Data Analysis*. 49:1020–1038.

KuKanich, B., Huff, D., Riviere, J.E., and Papich, M.G. 2007. Naïve averaged, naïve pooled, and population pharmacokinetics of orally administered marbofloxacin in juvenile harbor seals. *Journal of the American Veterinary Medical Association*. 230:390–395.

Laird, N.M., and Ware, J.H. 1982. Random-effects models for longitudinal data. *Biometrics*. 38:963–974.

Lavielle, M., and Lebarbier, E. 2001. An application of MCMC methods for the multiple change-points problem. *Signal Processing*. 81:39–53.

Lavielle, M., and Meza, C. 2007. A parameter expansion version of the SAEM algorithm. *Statistics and Computing*. 17:121–130.

Ludden, T., Beal, S., and Sheiner, L. 1994. Comparison of the Akaike information criterion, the Schwarz criterion and the F test as guides to model selection. *Journal of Pharmacokinetics and Biopharmaceutics*. 22:431–445.

Maitre, P.O., Bührer, M., Thomson, D., and Stanski, D.R. 1991. A three-step approach combining Bayesian regression and NONMEM population analysis: application to midazolam. *Journal of Pharmacokinetics and Biopharmaceutics*. 19:377–384.

Mallet, A. 1986. A maximum likelihood estimation method for random coefficient regression models. *Biometrika*. 73:645–656.

Mandema, J.W., Verotta, D., and Sheiner, L.B. 1992. Building population pharmacokinetic-pharmacodynamic models. I. Models for covariate effects. *Journal of Pharmacokinetics and Biopharmaceutics*. 20:511–528.

Martinez, M.N., Riviere, J.E., and Koritz, G.D. 1995. Review of the first interactive workshop on professional flexible labeling. *Journal of the American Veterinary Medical Association*. 207:865–914.

Martin-Jiménez, T., and Riviere, J.E. 1998. Population pharmacokinetics in veterinary medicine: potential use for therapeutic drug monitoring and prediction of tissue residues. *Journal of Veterinary Pharmacology and Therapeutics*. 21:167–189.

Martin-Jimenez, T., Papich, M., and Riviere, J.E. 1998. Population pharmacokinetics of gentamicin in horses. *American Journal of Veterinary Research*. 59:1589–1598.

Mason, S.E., Baynes, R.E., Buur, J.L., Riviere, J.E., and Almond, G.W. 2008. Sulfamethazine water medication pharmacokinetics and contamination in a commercial pig production unit. *Journal of Food Protection*. 71:584–589.

Melmon, K.L., Morrelli, H.F., Hoffman, B.F., and Nierenberg, D.W. 1992. *Melmon and Morrelli's Clinical Pharmacology: Basic Principles in Therapeutics*, 3rd Ed. New York: McGraw Hill.

Mentre, F., Mallet, A., and Baccar, D. 1997. Optimal design in random-effects regression models. *Biometrika*. 84:429–442.

Meza, C., Jaffrézic, F., and Foulley, J.L. 2007. REML estimation of variance parameters in nonlinear mixed effects models using the SAEM algorithm. *Biometrical Journal*. 49:876–888.

Panhard, X., and Samson, A. 2009. Extension of the SAEM algorithm for nonlinear mixed models with 2 levels of random effects. *Biostatistics*. 10:121–135.

Peck, C.C., Beal, S.L., Sheiner, L.B., and Nichols, A.I. 1984. Extended least squares nonlinear regression: a possible solution to the "choice of weights" problem in analysis of individual pharmacokinetic data. *Journal of Pharmacokinetics and Biopharmaceutics*. 12:545–558.

Peyrou, M., Doucet, M.Y., Vrins, A., Concordet, D., Schneider, M., and Bousquet-Mélou, A. 2004. Population pharmacokinetics of marbofloxacin in horses: preliminary analysis. *Journal of Veterinary Pharmacology and Therapeutics*. 27:283–288.

Pinheiro, J.C., Bates, D., and Bates, D.M. 2009. *Mixed-Effects Models in S and S-PLUS*. New York: Springer.

Regnier, A., Concordet, D., Schneider, M., Boisramé, B., and Toutain, P.L. 2003. Population pharmacokinetics of marbofloxacin in aqueous humor after intravenous administration in dogs. *American Journal of Veterinary Research*. 64:889–893.

Riond, J.L., Dix, L.P., and Riviere, J.E. 1986. Influence of thyroid function on the pharmacokinetics of gentamicin in pigs. *American Journal of Veterinary Research*. 47:2141–2146.

Riviere, J.E. 1988. Veterinary clinical pharmacokinetics. Part II: modeling. *Compendium Continuing Education Practicing Veterinarian*. 10:313–328.

Riviere, J.E., Dix, L.P., Carver, M.P., and Frazier, D.L. 1986. Identification of a subgroup of Sprague-Dawley rats highly sensitive to drug-induced renal toxicity. *Fundamental and Applied Toxicology*. 7:126–131.

Riviere, J.E., Martin-Jiménez, T., Sundlof, S.F., and Craigmill, A.L. 1997. Interspecies allometric analysis of the comparative pharmacokinetics of 44 drugs across veterinary and laboratory animal species. *Journal of Veterinary Pharmacology and Therapeutics*. 20:453–463.

Rosenbaum, A.E., Carter, A.A., and Dudley, M.N. 1995. Population pharmacokinetics: fundamentals, methods and applications. *Drug Development and Industrial Pharmacy*. 21:1115–1141.

Rowland, M., Sheiner, L.B., and Steimer, J.L. 1985. *Variability in Drug Therapy: Description, Estimation and Control*. New York: Raven Press.

Samson, A., Lavielle, M., and Mentré, F. 2006. Extension of the SAEM algorithm to left-censored data in nonlinear mixed-effects model: application to HIV dynamics model. *Computational Statistics and Data Analysis*. 51:1562–1574.

Samson, A., Lavielle, M., and Mentré, F. 2007. The SAEM algorithm for group comparison tests in longitudinal data analysis based on non-linear mixed-effects model. *Statistics Medicine*. 26:4860–4875.

Savic, R., and Karlsson, M. 2009. Importance of shrinkage in empirical Bayes estimates for diagnostics: problems and solutions. *The AAPS Journal*. 11:558–569.

Schumitzky, A. 1991. Nonparametric EM algorithms for estimating prior distributions. *Applied Mathematics and Computation*. 45:141–157.

Sheiner, L.B. 1994. A new approach to the analysis of analgesic drug trials, illustrated with bromfenac data. *Clinical Pharmacology and Therapeutics*. 56:309–322.

Sheiner, L.B. 1997. Learning versus confirming in clinical drug development. *Clinical Pharmacology and Therapeutics*. 61:275–291.

Sheiner, L.B., and Beal, S.L. 1980. Evaluation of methods for estimating population pharmacokinetic parameters. I. Michaelis-Menten model; routine clinical pharmacokinetic data. *Journal of Pharmacokinetics and Biopharmaceutics*. 8:553–571.

Sheiner, L.B., and Beal, S.L. 1981. Evaluation of methods for estimating population pharmacokinetic parameters. II. Biexponential model; experimental pharmacokinetic data. *Journal of Pharmacokinetics and Biopharmaceutics*. 9:635–651.

Sheiner, L.B., and Beal, S.L. 1983. Evaluation of methods for estimating population pharmacokinetic parameters. III. Monoexponential model; routine clinical pharmacokinetic data. *Journal of Pharmacokinetics and Biopharmaceutics*. 11:303–319.

Sheiner, L.B., and Beal, S.L. 1985. Pharmacokinetic parameter estimates from several least squares procedures: superiority of extended least squares. *Journal of Pharmacokinetics and Biopharmaceutics*. 13:185–201.

Sheiner, L.B., and Beal, S.L. 1987. A note on confidence intervals with extended least squares parameter estimates. *Journal of Pharmacokinetics and Biopharmaceutics*. 15:93–98.

Sheiner, L.B., and Ludden, T.M. 1992. Population pharmacokinetics/dynamics. *Annual Review of Pharmacology and Toxicology*. 32:185–209.

Sheiner, L.B., and Steimer, J.L. 2000. Pharmacokinetic/pharmacodynamic modeling in drug development. *Annual Review of Pharmacology and Toxicology*. 40:67–95.

Tornøe, C.W., Overgaard, R.V., Agersø, H., Nielsen, H.A., Madsen, H., and Jonsson, E.N. 2005. Stochastic differential equations in NONMEM®: implementation, application, and comparison with ordinary differential equations. *Pharmaceutical Research*. 22:1247–1258.

Traver, D.S., and Riviere, J.E. 1982. Ampicillin in mares: a comparison of intramuscular sodium ampicillin or sodium ampicillin-ampicillin trihydrate injection. *American Journal of Veterinary Research*. 43:402–404.

Vozeh, S., Maitre, P.O., and Stanski, D.R. 1990. Evaluation of population (NONMEM) pharmacokinetic parameter estimates. *Journal of Pharmacokinetics and Biopharmaceutics*. 18:161–173.

Vozeh, S., Steime, J.L., Rowland, M., Morselli, P., Mentré, F., Balant, L.P., and Aarons, L. 1996. The use of population pharmacokinetics in drug development. *Clinical Pharmacokinetics*. 30:81–93.

Wählby, U., Jonsson, E., and Karlsson, M. 2002. Comparison of stepwise covariate model building strategies in population pharmacokinetic-pharmacodynamic analysis. *The AAPS Journal*. 4:68–79.

Whittem, T., Hogan, D., Sisson, D., and Cooper, T. 2000. The population pharmacokinetics of digoxin in dogs with heart disease. *Journal of Veterinary Pharmacology and Therapeutics*. 23:261–263.

Yano, I., Beal, S.L., and Sheiner, L.B. 2001. The need for mixed-effects modeling with population dichotomous data. *Journal of Pharmacokinetics and Biopharmaceutics*. 28:109–128.

Yano, Y., Beal, S.L., and Sheiner, L.B. 2001. Evaluating pharmacokinetic/pharmacodynamic models using the posterior predictive check. *Journal of Pharmacokinetics and Biopharmaceutics*. 28:171–192.

Zhang, L., Beal, S.L., and Sheiner, L.B. 2003. Simultaneous vs. sequential analysis for population PK/PD data I: best-case performance. *Journal of Pharmacokinetics and Biopharmaceutics*. 30:387–404.

17 Dosage Adjustments in Disease States

with Jennifer Davis

When considering the pharmacokinetics of drugs in clinical patients, one must take into account the effects of the disease being treated on drug absorption, distribution, metabolism, and elimination. Diseases that affect the kidneys, liver, cardiovascular system, and gastrointestinal tract can all have profound consequences on drug pharmacokinetics and therefore may affect drug dosing. Unfortunately, these effects are not always predictable or consistent among patients. Therefore, the best approach to modifying drug therapy is to (1) conduct individualized pharmacokinetic studies in patients and monitor progress using therapeutic drug monitoring techniques, (2) utilize Bayesian or population strategies linking dosage regimen construction to observable concomitant physiological variables, or (3) estimate a corrected dose from commonly available organ function tests and then monitor the patient for signs of drug efficacy and toxicity. Since specific studies are not always available, particularly for veterinary patients, the latter strategy is the one most often implemented in the clinical setting. In addition to this, general guidelines can be used to predict new dosing regimens that would potentially be safe and effective in critically ill patients. The following is a review of potential alterations in drug pharmacokinetics based on specific organ dysfunction and guidelines for dosage adjustments based on those alterations.

17.1 RENAL DISEASE

One of the primary and most common factors that affect the disposition of a drug in the body is disease-induced changes in renal function. It is no surprise that renal disease has a profound impact on the disposition of a drug in the clinical setting. Many drugs are excreted primarily in urine as an unchanged pharmacologically active drug. Drugs excreted in this manner accumulate in the body during renal insufficiency as a direct result of decreased renal clearance. This must then be compensated for in clinical dosage adjustment regimens. In fact, this approach is implicit to the formulation of many population pharmacokinetic models presented in Chapter 16. Renal disease can also influence drug disposition and effect by additional mechanisms listed in Table 17.1. These effects complicate the establishment of safe and efficacious regimens for drug therapy. As presented in Fig. 16.2, a renal disease process not only will affect the mean clearance of the drug but also will often increase the interindividual variability, making treatment of the individual patient a challenge.

Comparative Pharmacokinetics: Principles, Techniques, and Applications, Second Edition. Jim E. Riviere.
 ISBN: 978-0-813-82993-7

Table 17.1 Possible effects of renal disease on drug pharmacokinetics, pharmacodynamics, and toxicity.

Decreased protein binding
Altered *Vd*
Altered electrolyte balance
Altered drug disposition and/or activity secondary to acid–base or fluid-balance abnormalities
Altered rate of biotransformation
Reduced renal clearance resulting in accumulation of parent drug and/or metabolites
Reduced activity of urinary tract antimicrobial agents secondary to reduced excretion or dilution in polyuric states
Enhanced drug activity or toxicity secondary to synergy with uremic complications

17.1.1 Drug distribution in renal failure

In renal disease, the degree of drug protein binding may be altered, which may significantly affect the disposition and activity of a drug during renal insufficiency. The pharmacologic effect of a drug is dependent on the concentration of free drug in plasma, and a marked reduction in protein binding of some drugs can occur in uremia. This may result in a significant alteration in drug disposition and activity if the fraction of total drug bound is normally greater than 90% and if the free drug has a relatively small volume of distribution (*Vd*). Examples of drugs that have decreased binding in human uremics are benzylpenicillin, clofibrate, diazoxide, diazepam, dicloxacillin, fluorescein, pentobarbital, phenobarbital, phenylbutazone, phenytom, salicylate, sulfonamides, thiopental, thyroxine, triamterene, and warfarin.

The decreased protein binding of drugs in uremia is greater than can be accounted for by the hypoalbuminemia that may accompany glomerular disease processes. A suspected mechanism is conformational change in albumin induced by the binding of "uremic toxins," endogenous metabolic by-products that accumulate in the body secondary to reduced renal clearance. These include free fatty acids, amino acids, and unidentified small dialyzable organic acids. Uremic toxins could also compete with drugs for protein-binding sites as well as alter the affinity of the receptor for the drug secondary to conformational changes. The result of this increased free-drug concentration is an increase in *Vd*. For any measured concentration of total drug in the blood, there will be an increased fraction of free drug. Variable effects on the subsequent biotransformation of free drug may also occur. Drugs cleared by glomerular filtration will show an increased clearance, although subsequent tubular reabsorption may negate this.

The concept of changes in *Vd* of drugs in renal failure has been studied. In addition to the increased *Vd* of highly protein-bound drugs in uremia, distributional changes have also been documented for drugs that are not significantly protein bound. The *Vd* of digoxin decreases, while that of some aminoglycosides has been shown to increase. The decreased *Vd* of digoxin is believed to be, in part, the result of decreased binding to kidney, liver, and myocardium. As discussed in Chapter 8 (Table 8.2), the decreased excretion of a drug may result in a decreased apparent *Vd* (Vd_{area}). This is a result of a mathematical dependence of some estimates of *Vd* on the magnitude of K_{el}. Estimates of *Vd* (i.e., Vd_{ss}) that are independent of K_{el} should be used so that true volume changes in renal disease states can be detected. The clinical significance of altered *Vd* with renal failure is not known, and dosage adjustment regimens do not generally account for it. True estimates of the magnitude of *Vd* can be obtained only through an analysis of drug concentrations in blood.

17.1.2 Drug metabolism in renal failure

Changes in the hepatic biotransformation of drugs during renal insufficiency and uremia have been documented. Sharp contrasts among species exist. Glycine conjugation, acetylation, and hydrolytic reactions are slowed in uremia. Notably, the biotransformation of cephalothin, cortisol, hydralazine, insulin, isoniazid, procaine, procainamide, salicylate, succinylcholine, and selected sulfonamides may be decreased in uremia, which could result in a decrease in the nonrenal clearance component of a drug's elimination pattern, a factor (e.g., decreased K_{nr} from Eq. 8.24, see Chapter 8) normally assumed to be unchanged in renal insufficiency. The result would be drug accumulation if the overall elimination rate constant, K_{el}, were decreased. Uremia does not appear to alter microsomal oxidation, reduction, glucuronide synthesis, sulfate conjugation, or methylation pathways. In contrast, some oxidative reactions in human uremics are accelerated. Laboratory animals show markedly different effects of uremia on the disposition of some drugs; for example, a study of pentobarbital disposition in nephrectomized dogs did not detect a different drug half-life from that measured in controls. Therefore, species differences are important, necessitating that drug therapy in diseased individuals be evaluated in each case.

An interesting effect of renal insufficiency on drugs eliminated by biotransformation is the accumulation of active metabolites. Examples of such drugs are allopurinol, cephalothin, cephapirin, chlorpropamide, clofibrate, digitoxin, doxorubicin, lidocaine, mephobarbital, primidone, procainamide, and some sulfonamides. Intoxication and enhanced drug activity have been reported to occur by this mechanism.

The prudent course of action in uremic patients is thus to titrate the dose of suspect drugs to the observed response. The clinician must assume normal rates of metabolic clearance in patients until definitive data are available for the specific drug and species being treated. The most obvious approach to accomplish this is to use pharmacokinetic principles to construct modified dosage regimens to compensate for disease-induced alterations in a drug's pharmacokinetic and pharmacodynamic profiles.

17.1.3 Drug clearance in renal failure

Current guidelines for constructing dosage regimens for renal insufficiency or failure compensate only for decreased renal clearance of the parent drug and are based on the principles of dosage regimen construction presented in Chapter 12. It is prudent to review these concepts and equations before continuing further with this discussion. There are no published guidelines recommending dosage adjustments to compensate for changes in protein binding, altered drug biotransformation, active metabolite accumulations, or altered *Vd*. This could only be accomplished using a completely defined pharmacokinetic model for the specific scenario at hand.

Recall that the total body clearance of a drug can be partitioned into renal and nonrenal parts as previously described. Therefore,

$$Cl_B(\text{mL/min}) = Cl_r + Cl_{nr} \tag{17.1}$$

where Cl_r is renal clearance and Cl_{nr} is nonrenal drug clearance. All clearances are normally expressed in terms of body weight or surface area.

The cornerstone of predicting drug disposition during renal failure in a clinical setting is based on the assumption that renal clearance is directly correlated to clinical measures

of glomerular filtration rate (GFR) as presented in Chapters 6 and 8 and incorporated as described above in the population pharmacokinetic models of Chapter 16. This assumes that the intact nephron hypothesis holds and that a relative glomerulotubular balance is present. Renal clearance is thus a linear function of GFR, whether the drug is cleared by glomerular or tubular mechanisms.

$$Cl_r(\text{mL/min}) = M \cdot \text{GFR} \tag{17.2}$$

where M is a proportionality constant. Substituting in Equation 17.1 results in this relation:

$$Cl_B(\text{mL/min}) = M \cdot \text{GFR} + Cl_{nr} \tag{17.3}$$

Total body clearance was defined in pharmacokinetic terms throughout Chapters 8 and 9. From this point onward, a one-compartment model will be assumed to simplify discussions. If Equation 17.3 is divided by Vd (recall $Cl/Vd = K_{el}$), the generally applicable relationship depicted in Equation 17.4 results:

$$K_{el}(1/\text{min}) = K_r + K_{nr} = M' \cdot \text{GFR} + K_{nr} \tag{17.4}$$

This is the equation for a straight line with slope M' and y-axis intercept K_{nr}. Remember that K_{nr} is assumed to be unchanged, as discussed previously. K_{el} represents the fraction of a drug's distribution volume cleared per unit time. Recall that for a one-compartment model, $-K_{el}$ is equivalent to $-K$, the slope of the plasma concentration–time (C-T) profile plotted on semilogarithmic paper (see Chapter 8, Fig. 8.4). The relationship defined in Equation 17.4 has been shown to hold for most drugs studied when GFR has been estimated by creatinine clearance and actually provides the basis for its use in population pharmacokinetic models.

The relationship in Equation 17.4 is graphically depicted on a Cartesian coordinate system in the top of Fig. 17.1. Three drugs are shown all having the same K_{nr}. The first is primarily cleared by nonrenal mechanisms ($K_r < K_{nr}$). As creatinine clearance decreases, K_{el} is seen to remain relatively stable. In the second drug, eliminated from the body by renal and nonrenal mechanisms ($K_r > K_{nr}$), decreases in creatinine clearance result in a steady decline in K_{el}, until $K_{el} = K_{nr}$ at a creatinine clearance of zero (anephric patient). In the third drug, primarily eliminated by renal mechanisms ($K_r >> K_{nr}$), decreases in creatinine clearance result in a great decrease in K_{el}. Note that K_{el} still approaches K_{nr}. If the drug was eliminated solely by renal mechanisms ($K = 0$), K_{el} would equal zero in the anephric patient.

A more practical approach to this problem for clinical use is to relate GFR to drug elimination half-life ($T_{½}$) in a similar fashion. However, this is not a linear relation but rather a hyperbolic function because of the inverse relationships,

$$T_{½}(\text{min}) = \frac{0.693Vd}{Cl_B} = \frac{0.693}{K_{el}} = \frac{0.693}{K_r + K_{nr}} \tag{17.5}$$

A plot of GFR versus $T_{½}$ for the same three drugs is depicted in the lower half of Fig. 17.1. This plot is clinically applicable because most dosage regimens are expressed in terms of $T_{½}$ (recall Eq. 12.14 in Chapter 12). If the drug is eliminated primarily by nonrenal mechanisms, $T_{½}$ remains relatively constant over varying degrees of renal function.

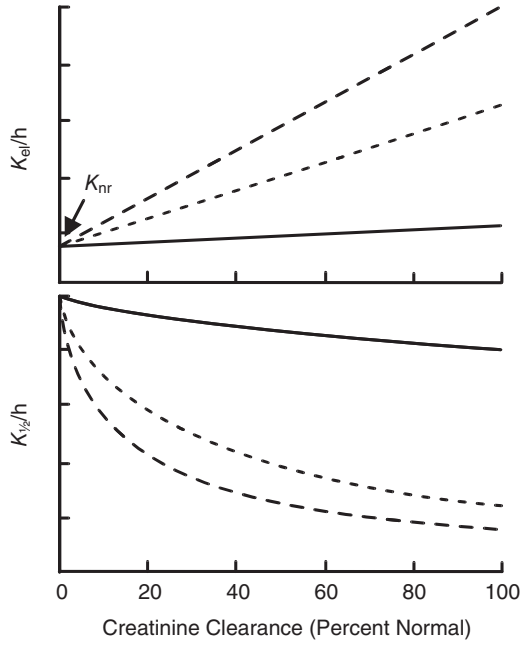

Fig. 17.1 Relationship between elimination rate constant (K_{el}) or half-life ($T_{½}$) and creatinine clearance. The three drugs depicted are dependent on renal elimination (K_r) to varying degrees (— $K_r < K_{nr}$; --- $K_r > K_{nr}$; ––– $K_r >> K_{nr}$).

However, if the drug is excreted by renal mechanisms, $T_{½}$ is stable until creatinine clearance is 30–40% of normal, at which point $T_{½}$ drastically increases. This is the basis for the general recommendation that dose adjustment in renal failure is necessary only when more than two-thirds of renal function is lost. If a drug is excreted almost entirely by the kidneys, then the $T_{½}$ approaches infinity as creatinine clearance approaches zero.

An alternative method used to relate $T_{½}$ to GFR for drugs primarily eliminated by renal mechanisms is through the use of a dose fraction, (K_f), defined as:

$$K_f = \frac{\text{Abnormal creatinine clearance}}{\text{Normal creatinine clearance}} = \frac{Cl_B(\text{abnormal})}{Cl_B(\text{normal})} \tag{17.6}$$

These relationships will now be applied to formulae designed to calculate dosage regimens in animals with renal failure.

17.1.4 Calculation of modified dosage regimens

The approach in this section will be to modify dosage regimens that are appropriate in normal animals in proportion to decreases in renal function estimated by dose fraction. This method assumes that (1) a standard loading dose is administered; (2) drug absorption, *Vd*, protein binding, extrarenal elimination, and tissue sensitivity (dose–response relation) are unchanged (major assumptions); (3) creatinine clearance is directly correlated to drug clearance; and (4) renal function is relatively constant over time.

The ultimate aim of dosage adjustment in renal disease is to fulfill the *fundamental therapeutic postulate that the C-T profile should be as similar as possible to the normal situation*. Recall from Chapter 12 that ε, the ratio $\tau/T_{½}$, determines the fluctuation in a multiple dose C-T profile based on its influence on the value of f_{el} from Equation 12.5. The dose ratio, D/τ, determines the average steady-state plasma concentration (C_p^{avg}). If τ is not adjusted in the face of an increasing $T_{½}$ in a patient with renal failure, C_p^{avg} will dramatically increase, as can be seen from revisiting Equation 12.2. This can be compensated for by either reducing D or increasing τ in this equation, which is the basis of the dose modification methods introduced below. However, the fluctuations in these regimens are a function of f_{el}, which in a renal disease patient is dependent on ε. When constructing dosage regimens for patients with renal disease that have fundamentally altered pharmacokinetic parameters, both D and τ must be modified to achieve a C_p^{avg} and f_{el}, which are similar to those parameters in patients with normal renal function.

17.1.4.1 *Dose-reduction method*

Let us assume that one has already defined a safe and effective dosage regimen for use in a normal patient. This normal dosage regimen is then adjusted according to the dose fraction by two basic procedures. The first method, termed constant-interval, dose-reduction (DR), reduces the dose (D) by a factor of the dose fraction. Dose interval (τ) is the same as that used in the healthy animal.

$$D_{\text{renal failure}} = D_{\text{normal}} \cdot K_f \qquad (17.7)$$
$$\tau_{\text{renal failure}} = \tau_{\text{normal}}$$

17.1.4.2 *Interval-extension method*

The second method, referred to as constant-dose, interval-extension (IE), extends the dosage interval by the inverse of the dose fraction, a value referred to as the dose-interval multiplier.

$$\tau_{\text{renal failure}} = \tau_{\text{normal}} \cdot (1/K_f) \qquad (17.8)$$
$$D_{\text{renal failure}} = D_{\text{normal}}$$

This type of dose adjustment strategy may also be implemented through the use of a nomogram (Fig. 17.2), in which the dosage interval multiplier for this IE regimen is simply read off a plot of creatinine clearance.

17.1.5 Implementation

The therapeutic goal is to maintain a constant product of $(T_{½} \cdot D/\tau)$ in healthy animals and those with renal failure. When this product is constant, the average steady-state plasma concentration of a drug will remain unchanged. This is the approach followed in the DR and IE methods. A constant steady-state plasma concentration is achieved by the use of the dose fraction to compensate for changes in $T_{½}$ in the following manner:

$$(T_{½} \cdot D/\tau)_{\text{normal}} = K_f (T_{½} \cdot D/\tau)_{\text{renal failure}} \qquad (17.9)$$

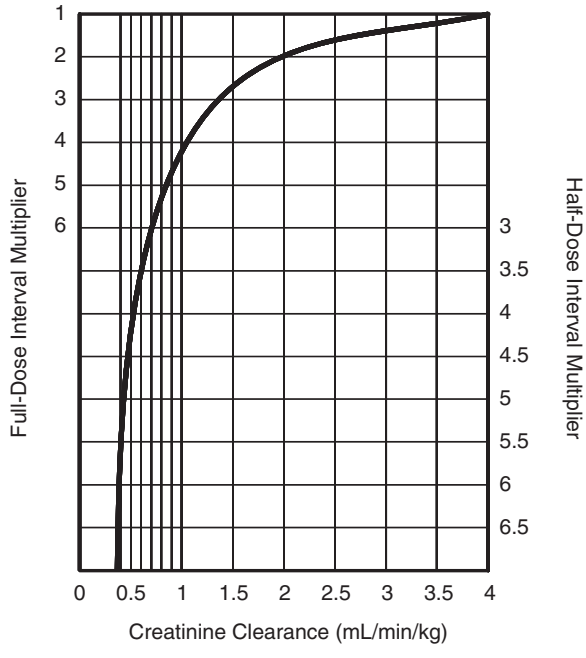

Fig. 17.2 Nomogram implementing an interval-extension dosage adjustment regimen based on creatinine clearance in the dog.

When repeated doses of a drug are administered, accumulation occurs until steady-state plasma concentrations are achieved. Recall from Chapter 12 that this takes approximately four or five $T_{½}$s. The prolonged $T_{½}$ present in patients with renal insufficiency would cause excessive delay in attaining steady-state concentration. Therefore, an appropriate loading dose should always be administered so that a therapeutic concentration of the drug is immediately attained. If the constant-interval method is employed, this can be accomplished by giving the usual dose initially, followed by the calculated reduced dose. If the constant-dose method is used, the initial two doses should be given according to the usual interval.

Equations 17.7 and 17.8 hold for drugs that are excreted solely by the kidney, since the dose fraction adjusts dosages as if K_{nr} equaled zero. For drugs undergoing biotransformation, a measure of the percent nonrenal clearance is necessary. This proportion can be estimated by knowledge of the fraction of the absorbed dose of drug excreted unchanged in the urine (f). Recall from Chapter 8 that the ratio $U_\infty/D = K_r/K_{el}$. The constant-interval method then becomes:

$$D_{\text{renal failure}} = D_{\text{normal}} \cdot [(f(K_f - 1)) + 1] \qquad (17.10)$$
$$\tau_{\text{renal failure}} = \tau_{\text{normal}}$$

For the constant-dose, increased-interval method:

$$\tau_{\text{renal failure}} = \tau_{\text{normal}} \cdot [(f(K_f - 1)) + 1] \qquad (17.11)$$
$$D_{\text{renal failure}} = D_{\text{normal}}$$

The fraction excreted unchanged in urine is not currently available for animals for most drugs. Additionally, if it is relatively small, then K is less than K_{nr}, and $T_{½}$ will remain relatively stable, avoiding the need to adjust dosages.

When creatinine clearance has not been available, the inverse of serum creatinine (mg/dL) has been substituted. Since the relationship between $T_{½}$ and serum creatinine is not linear above 4 mg/dL, adjustment formulae may not accurately predict the dose fraction.

17.1.6 Selection of the appropriate method of dosage adjustment

A great deal of controversy exists over the relative merits of the constant-dose and the constant-interval methods. These two regimens produce different C-T profiles, as is depicted in Fig. 17.3. This hypothetical drug, primarily eliminated by renal processes, is dosed every four $T_{½}$s. Creatinine clearance is one-sixth of normal (K_f = 1/6). The constant-dose regimen produces peak and trough concentrations similar to those seen in the healthy patient; however, there are prolonged periods of potentially subtherapeutic serum concentrations. This is preferred for drugs such as aminoglycoside antibiotics, whose toxicity correlates with high trough, rather than peak, concentrations. If the dose is decreased but the interval held constant, peak concentrations are lower and trough concentrations are greater than during the usual regimen. There are no periods of subtherapeutic concentrations. A compromise can be made by multiplying both the dose and the increased interval calculated in Equations 17.7 and 17.8 by a constant fraction, a procedure that does not alter the steady-state plasma concentration. An example is the half-dosage IE method in the nomogram of Fig. 17.2.

The normal drug plasma C-T profile can never be exactly duplicated in a patient with renal failure because the slopes of the elimination curves are not parallel due to different $T_{½}$s. All dosage regimens are only approximations. This inability to match C-T profiles in normal and diseased animals was the driving force behind using deconvolution techniques

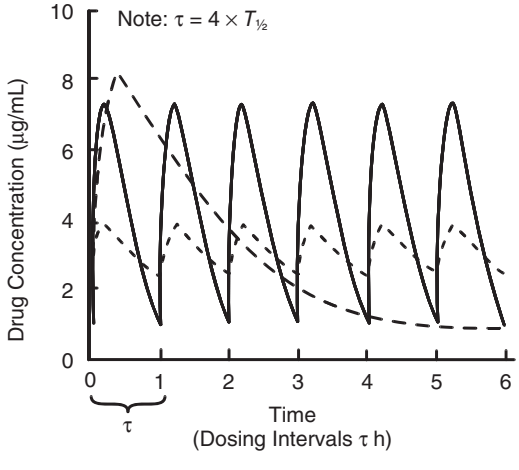

Fig. 17.3 Comparison of constant-dose (— —) and constant-interval (----) regimens in renal failure (Cl_{cr} = one-sixth usual) with a normal dosage regimen (—) in a healthy patient. τ is the dosage interval.

to develop the computer-controlled infusion profiles depicted in Fig. 9.5 (see Chapter 9). This is the only approach that allows one to assess the inherent toxicity of a drug in healthy versus diseased animals independent of accumulation secondary to a prolonged terminal elimination slope.

An advantage of the fixed-dose method is convenience. The recommended dose used in healthy animals is administered less frequently. If drugs available in fixed dosage forms are used, the constant-dose method is clearly easier to administer. As discussed in Chapter 12, the clinician should determine if drug efficacy and/or toxicity is correlated to peak, trough, or average plasma concentrations and then select a regimen balancing efficacy against potential toxicity. It should be noted that the most effective means of maintaining a constant plasma concentration of drug is by continuous infusion at a constant rate. Note that in animals with chronic renal failure whose nephrons are undergoing compensatory hypertrophy, the intact nephron hypothesis would predict that each individual surviving nephron would be exposed to a greater tubular load of drug per unit of whole kidney GFR than would a nephron in a healthy animal. Therefore, even if a drug dose is appropriately reduced according to decreased GFR, the toxic potential of a tubular nephrotoxin could be greater in the renal failure patient.

The most accurate method of adjusting a dosage regimen in renal failure is to calculate a dose, administer it, and monitor the resultant peak and trough serum concentrations by direct assay since interindividual differences in disposition cannot be accounted for using these nonpharmacokinetic approaches. A Bayesian approach can then be used to adjust subsequent drug dosage. The main advantage is that dose can be constantly adjusted so that changes in parameters assumed to be constant in the above formulae will be detected. This procedure, rooted in the principles of therapeutic drug monitoring protocols, is becoming economically feasible, even in veterinary medicine. Chapter 16 should be consulted for details. The methods discussed assume stable renal function. In clinical states in which renal function is constantly changing, drug elimination is also changing, and accurate predictions are difficult.

17.1.7 Drug clearance in dialysis

The importance of considering the effects of dialysis on drug therapy is to determine the dosage required to compensate for increased drug clearance due to peritoneal dialysis and hemodialysis. A simple way to approach this problem is to modify Equation 17.1 to include dialyzer clearance (Cl_D), allowing total body clearance to include all clearance mechanisms, both natural and artificial:

$$Cl_B = Cl_r + Cl_{nr} + Cl_D \tag{17.12}$$

The effect of increased elimination during dialysis is depicted in Fig. 17.4, in which $T_{½}$ during dialysis is a function of the elimination constant and the dialysis rate constant. This approach again assumes unchanged *Vd* and a one-compartment pharmacokinetic model. If $T_{½}$ before and during dialysis is known, the overall elimination constant can be calculated from similar blood C-T plots, and Equation 8.16 may be used to calculate total body clearance in dialysis from elimination constant and *Vd*. This value could then be used to calculate the precise amount of drug removed during dialysis by the following:

$$\text{Drug recovery} = (Cl_B) \cdot (C_{ss}) \cdot (\text{dialysis duration}) \tag{17.13}$$

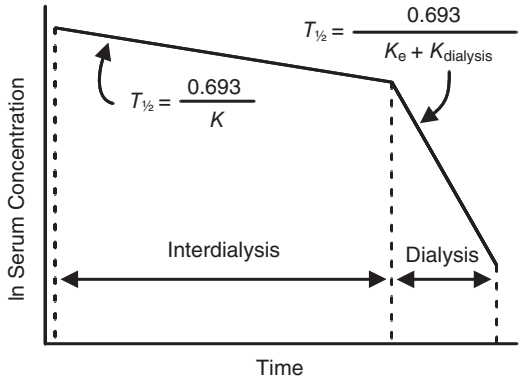

Fig. 17.4 Semilogarithmic plot of serum concentration of drug as a function of time in a patient on and off dialysis. K_e is the elimination rate constant and $K_{dialysis}$ is the dialysis rate constant.

where C_{ss} is the steady-state plasma concentration. When this estimate of total body clearance during dialysis is obtained, dose fraction is determined by the following:

$$K_f = Cl_B/\text{Normal } Cl_{\text{creatinine}} \tag{17.14}$$

If these values are calculated on a daily basis, total body clearance will be the average clearance and will reflect time on and off dialysis. Dose fraction, analogous to dose fraction in renal insufficiency without dialysis, can then be used directly in Equations 17.7 and 17.8. Alternatively, the preferred method would be to calculate the amount of drug lost during a dialysis period according to Equation 17.13, and then give this dose postdialysis. The normal dose fraction is then used for interdialysis dosing.

If *Vd* is not known, but $T_{½}$ before and after dialysis is available, the fraction of drug removed during dialysis (F) can be calculated.

$$F' = [T_{½}(\text{before}) - T_{½}(\text{dialysis})]/T_{½}(\text{before})$$
$$F = F' \cdot \left[1 - e^{-0.693/T_{½}(\text{dialysis}) \times \text{duration of dialysis}}\right] \tag{17.15}$$

Dialyzer clearance can also be calculated solely for the dialysis process independent of body clearance mechanisms. With peritoneal dialysis,

$$Cl_D = C_D \cdot V/[(C_p) \cdot (\text{dialysis duration})] \tag{17.16}$$

where C_D is the concentration of drug in the dialysate fluid after exchange, V is the total dialysate drainage volume, and C_p is the plasma concentration of drug at the midpoint of dialysis.

Hemodialysis and hemofiltration clearance can be calculated using Fick's law according to the relationship

$$Cl_D = Q \cdot [(C_{in} \cdot C_{out})/C_{in}] \tag{17.17}$$

where Q is the flow of blood through the dialyzer, C_{in} is the concentration of drug in plasma entering the dialyzer (arterial, inflow), and C_{out} is the concentration of drug in plasma

exiting the dialyzer (venous, outflow). Some discrepancies in dialyzer clearance may occur when plasma concentration of drug is not representative of total blood concentration. This results because the concentration of drug is measured for plasma while the flow is measured for blood. Adjustments based on hematocrit can be made, or blood concentrations can be separated into erythrocyte and plasma water concentrations. Equation 17.17 may be written in terms of plasma and blood. The derivation and applications of Equations 17.12–17.17 are based on an extension of the basic principles of clearance, *Vd*, and elimination rate constants developed throughout this text, and closely parallel those used to describe organ clearance in the PBPK models of Chapter 11.

17.1.8 Pharmacodynamics in renal failure

The uremic patient is in a precarious state of fluid, electrolyte, and acid–base homeostasis. For example, administration of antibiotic drugs containing sodium (ampicillin, 3 mEq/g; carbenicillin, 4.7 mEq/g; cephalothin, 2.5 mEq/g; penicillin G, 1.7 mEq/g) or potassium (penicillin G, 1.7 mEq/g) could result in serious electrolyte overload. Treatment with antacids and laxatives could result in magnesium and aluminum intoxication. Penicillin and carbenicillin, functioning as nonreabsorbable anions in the distal tubules, can cause loss of hydrogen and potassium in the urine. Acidosis of renal insufficiency favors dissociation of salicylate and phenobarbital, thereby increasing drug concentrations in the brain. Acidosis also decreases sensitivity of adrenergic receptors.

Diuretics that produce prolonged polyuric states can decrease antibiotic concentrations in urine to subtherapeutic levels. This dilution effect, coupled with decreased renal clearance of antimicrobial drugs secondary to renal insufficiency, can impair efficacy in treatment of urinary tract infections. Concentrations of antibiotics in renal parenchyma are often lower in severely diseased kidneys than in normal kidneys.

Drug toxicity may be potentiated if the drug's action is synergistic with uremic complications. An example is the administration of anticoagulants, which may induce a bleeding disorder. Untoward gastrointestinal and neurological drug reactions can be more easily elicited when uremia has caused functional changes in these systems. An altered blood–brain barrier in uremia can result in elevated drug concentrations in the cerebrospinal fluid. Sensitivity to opiates, barbiturates, and tranquilizers is increased by this mechanism, and decreased protein binding of these drugs accentuates the effect.

A number of additional complications may also occur with drug therapy in uremics. Erythrocytes collected from human patients who were in renal failure were more sensitive to development of a cephalothin-induced positive Coombs' test than were cells from healthy patients. The antianabolic activity of tetracycline and the catabolic action of corticosteroid hormones may worsen the degree of azotemia. The rate and extent of oral drug absorption can be affected by variation in gastrointestinal motility. Similarly, absorption from alimentary, muscular, and subcutaneous sites may be impaired due to decreased blood perfusion secondary to dehydration.

17.2 HEPATIC DISEASE

As discussed in Chapter 7, the liver is the major drug metabolizing organ in the body. As such, disease states involving the liver may have a profound effect on drug bioavailability, metabolism, and elimination (Table 17.2). Unfortunately, there is no endogenous marker like creatinine used in renal failure, which can be employed to estimate hepatic clearance;

Table 17.2 Possible effects of hepatic disease on drug pharmacokinetics, pharmacodynamics, and toxicity.

- Increased oral bioavailability due to reduced first-pass metabolism
- Decreased bioavailability of fats and lipophilic drugs in cholestasis
- Alterations in oral bioavailability and/or delayed drug absorption due to concurrent gastrointestinal disease
- Altered (increased) *Vd* secondary to a decrease in plasma protein binding, resulting in an increased f_u
- Altered (increased) drug disposition secondary to ascites/edema
- Reduction in hepatic clearance of high E_H drugs secondary to impaired hepatic blood flow
- Reduction in hepatic clearance of low E_H drugs secondary to impaired Cl_{int}
- Reduced biliary clearance resulting in accumulation of parent drug and/or metabolites
- Altered rate of phase I and phase II biotransformation reactions
- Reduced renal elimination of drugs (hepatorenal syndrome)
- Increased therapeutic effects of analgesics, anxiolytics, and sedatives
- Decreased therapeutic effects of diuretics and β-adrenoreceptor antagonists
- Increased toxicity of NSAIDs and ACE inhibitors

Table 17.3 Summary of dosing recommendations for patients with hepatic disease based on hepatic extraction (E_H).

E_H	Protein binding	Cl_{sys}	Dose adjustment	Example
<0.3	>90	$\approx f_u \cdot Cl_{int}$	$\downarrow D_M$ based on f_u	Clindamycin
<0.3	<90	$\approx f_u \cdot Cl_{int}$	$\downarrow D_M$ based on total drug	Metronidazole
0.3–0.7	—	$Q_H \cdot [f_u \cdot Cl_{int}/(Q_H + f_u \cdot Cl_{int})]$	Low normal D_L (oral); $\downarrow D_M$	Ciprofloxacin
>0.7	—	$\approx Q_H$	$\downarrow D_L$ (oral); $\downarrow D_M$	Morphine

Loading dose is D_L and maintenance dose is D_M.

therefore, dosage adjustments are not easily predicted. Furthermore, the degree of alteration in pharmacokinetics may differ based on the severity and type of hepatic disease process present. The effects on pharmacokinetics can be further influenced by the degree of hepatic extraction and degree of protein binding of each drug (Table 17.3). Despite these limitations, guidelines can be developed for dosing regimens in patients with hepatic disease. However, careful attention should be paid to the pharmacodynamics and toxicity in individual patients in order to provide adequate dosing.

17.2.1 Drug absorption in hepatic disease

Oral absorption and bioavailability may be affected through concurrent gastrointestinal disease, or through decreased presystemic or "first-pass" metabolism. It is well documented in human patients that gastrointestinal disease frequently accompanies liver failure. This would include portal hypertensive gastropathy, gastritis, and gastrointestinal ulceration. The effects on drug absorption with these conditions are difficult to predict. Bioavailability may increase as a result of an increase in mucosal permeability, it may decrease as a result of a loss of functional enterocytes, or there may be no significant change. One thing that is more consistent is a delayed absorption, or decreased rate of absorption, observed in liver disease patients. This is thought to be a result of delayed gastric emptying secondary

to a decrease in production of various gastrointestinal hormones including secretin, glucagon, motilin, and cholecystokinin. This may have a significant effect on drug absorption and efficacy, particularly in the case of delayed release formulations.

As discussed briefly in Chapter 2, drugs absorbed from the gastrointestinal tract (with the exception of the oral cavity and rectum) enter the portal circulation and are therefore subject to hepatic metabolism and biliary excretion prior to entering the systemic circulation. The fraction of the oral dose that is not metabolized during presystemic elimination (F_H) can be calculated by the equation:

$$F_H = (1 - f_H) \cdot E_H \tag{17.18}$$

where f_H is the fraction of mesenteric blood flow passing through the nondiseased liver and E_H is the hepatic extraction ratio. As stated in Chapter 7 (see Eq. 7.7), E_H is also a function of hepatic blood flow (Q_H), the unbound fraction of drug in the blood (f_u) and the intrinsic clearance capacity of the liver (Cl_{int}). Therefore, the equation can be rewritten as:

$$F_H = [Q_H + f_u \cdot Cl_{int}(1 - f_H)]/[Q_H + f_u \cdot Cl_{int}] \tag{17.19}$$

Liver cirrhosis can therefore affect multiple aspects of first-pass metabolism. With chronic disease, intra- and extrahepatic shunting occurs, which diminishes Q_H and f_H. The Cl_{int} is also decreased due to a decrease in hepatic drug metabolizing enzymes. This can result in a substantial increase in oral bioavailability, particularly in drugs with a moderate to high E_H, as these drugs typically have low oral bioavailability in normal individuals. Some examples of high E_H drugs with an increased oral bioavailability secondary to a decreased first-pass metabolism in liver disease include clomethiazole, carvedilol, meperidine, metoprolol, midazolam, nifedipine, pentazocine, propranolol, and morphine. When using these drugs in patients with liver cirrhosis, it is recommended that dosage adjustments be made in both the loading and maintenance oral doses. To estimate the new dose, one can assume bioavailability has increased to 100% and adjust the dose using the equation:

$$D_{\text{liver failure}} = [D_{\text{normal}} \cdot F_{\text{normal}}]/100 \tag{17.20}$$

17.2.2 Drug distribution in hepatic failure

Drug distribution in cirrhotic patients may be affected by alterations in fluid balance due to ascites/edema as well as alterations in plasma protein binding. Either of these conditions can lead to an increased *Vd*, particularly in hydrophilic drugs. Patients with ascites or edema may need an increase in the initial loading dose for hydrophilic drugs to compensate for this increased *Vd*. Maintenance doses should be calculated based on total body weight, to take into account the increased fluid volume present. It is important to remember that a drug's $T_{½}$ is also related to the *Vd*, as depicted in Equation 8.20. Therefore, an increase in *Vd* may result in an increased $T_{½}$ in patients with ascites/edema. This has been shown for drugs such as furosemide, ceftazidime, and cefprozil, but the clinical significance is questionable.

Alterations in protein binding during hepatic failure may be related to a decreased synthesis of albumin and α_1 acid glycoprotein (AAG), qualitative changes in albumin and AAG, or inhibition of protein binding by high concentrations of bilirubin. This decreased protein binding leads to an increased *Vd* and also affects the oral clearance (*Cl*/*F*) of high

E_H drugs as well as the oral and systemic clearance of low E_H drugs, as shown in Equations 7.6 and 7.7. Therefore, to accurately interpret the effect of hepatic disease on Cl_{int}, the change in f_u should be taken into account using the equation:

$$Cl/F = (Cl_u/F)/f_u \tag{17.21}$$

This is particularly important for low E_H drugs with high protein binding, since hypoalbuminemic patients may have a decreased total drug concentration, while the free (unbound) fraction remains the same. This fact necessitates therapeutic monitoring based on free drug concentrations and clinical pharmacodynamic parameters prior to dosage adjustments.

17.2.3 Drug metabolism and elimination in hepatic failure

Chronic liver disease affects the intrinsic clearance capacity of the liver independent of hepatic blood flow. The Cl_{int} is, in turn, dependent on hepatic metabolic enzyme activity and the activity of sinusoidal and canalicular transporters. In cirrhotic patients, there is a decrease in liver cell mass, and a resulting decrease in enzyme activity that leads to a decrease in drug metabolism. Additionally, uptake of drugs across the endothelium may be reduced. The resulting effects on metabolism can then affect the pharmacokinetics and pharmacodynamics of the parent drug and any metabolites.

As discussed in Chapter 7, hepatic metabolism consists of phase I (CYP-mediated) and phase II (conjugation) reactions. Of these two processes, the phase I reactions are affected the most in hepatic disease. These reactions require NADPH and molecular oxygen for proper function. Portosystemic shunting as well as sinusoidal capillarization and resulting decreased liver perfusion results in a lack of oxygen and therefore decreased enzymatic functioning. As disease severity progresses, there is a correlated decrease in enzymatic activity; however, this appears to be selectively regulated. In early hepatic disease, there is a decreased clearance of drugs metabolized by CYP2C19 (i.e., mephenytoin). With intermediate disease, other enzyme activities become affected, with CYP2C19 > CYP1A 2 > CYP2D6 > CYP2E1. In the late stages of hepatic disease, all enzymes systems are expected to be affected equally. CYP3A enzymes are extremely important in drug metabolism in humans and account for the biotransformation of up to 50% of commonly used drugs. Individual pharmacokinetics studies of drugs metabolized by CYP3A4 and CYP3A5, including midazolam, nifedipine, and everolimus, have demonstrated a decreased clearance in patients with hepatic disease.

Phase II conjugation reactions are less commonly affected by hepatic disease. This is thought to be due to a compensatory upregulation of UDP glucuronyltransferase activity by the remaining functional hepatocytes. In late stage cirrhosis, however, this compensatory mechanism is overcome, and glucuronidation reactions will become impaired.

17.2.4 Dosage adjustments in hepatic disease

Since there is currently no endogenous marker for determining the extent of reduction in hepatic clearance, determining the correct dosage in patients with hepatic dysfunction can be challenging. Serum bile acids may be useful for estimating the degree of hepatic shunting, but do not give an accurate reflection of metabolism. Other endogenous and exogenous markers have been studied (Table 17.4), but have not been found to be particularly useful,

Table 17.4 Endogenous and exogenous substances evaluated for the potential to estimate hepatic function and metabolism of drugs.

	Metabolism/clearance	**Comments**
Endogenous substances		
Serum bile acids	Phase II reactions; enterohepatic recycling	Estimate of portosystemic shunting
Serum bilirubin; serum AST/ALP		Increase with increasing severity of disease
Albumin; coagulation factors		Decrease with decreasing severity of disease
Exogenous substances		
High E_H (blood-flow limited model)		
Galactose (IV)	First-order elimination reflecting functional hepatic capacity; limiting step is phosphorylation	Undergoes extrahepatic metabolism, making interpretation difficult
Indocyanine green (IV)	Biliary excretion	Estimate of hepatic blood flow
Lidocaine (IV)	CYP3A substrate	
Propoxyphene (PO)	Metabolized to norpropoxyphene and d-propoxyphene	Ratio of AUCs of metabolites estimates portosystemic shunting and possibly hepatocyte function
Sorbitol (IV)		Estimate of hepatic blood flow
Intermediate E_H		
Erythromycin (IV)	CYP3A	CO_2 exhalation test used to estimate CYP3A activity
Low E_H (capacity-limited model)		
Aminopyrine (PO, IV)	Multiple CYPs	CO_2 exhalation test used to estimate general CYP activity
Antipyrine (PO)	Multiple CYPs	
Caffeine (PO/IV)	CYP1A2; n-acetyltransferase type 2	CO_2 exhalation test used to estimate CYP1A2 activity

AST, aspartate transaminase; ALP, alkaline phosphatase.

as they typically only test a certain aspect of the hepatic metabolism (i.e., blood flow vs. intrinsic clearance).

Clinical severity scores have also been investigated as guidelines for dosage adjustments. The Child–Pugh severity score is the one most commonly used in human medicine. This scoring system is designed to assess the prognosis in cirrhotic patients by examining multiple clinical and laboratory parameters such as bilirubin and albumin concentrations, prothrombin time or the international normalized ratio (INR) of prothrombin time, and the presence or absence of ascites and hepatoencephalopathy. Patients assigned to Child–Pugh class A (least severe) should have their maintenance doses of drugs metabolized by the liver reduced by 50%, class B patients should have maintenance doses reduced by 75%, and patients in class C should, whenever possible, not receive drugs metabolized mainly by the liver unless there are existing data demonstrating the safety of these drugs in severe hepatic failure. No such scoring system exists for veterinary species; therefore, dosing recommendations based on disease severity do not exist.

In recognition of the difficulty of determining the appropriate dose of drug in patients with liver disease, many regulatory agencies are now requiring pharmacokinetic studies on

patients with hepatic dysfunction prior to new drug approval. While this has become commonplace in human medicine, no such requirements exist in veterinary medicine, therefore data are often lacking.

Cholestatic disease may impair clearance of drugs that undergo predominantly biliary elimination. It has also been shown to decrease the activity of CYP2C and CYP2E, which may impair phase I metabolism. Despite these potentially significant effects on drug metabolism and elimination, little is known about the effects of cholestasis on drug pharmacokinetics. Perhaps the most commonly studied class of drugs is the antineoplastic class. Recommendations have been made for dosage adjustment based on serum bilirubin and ALP concentrations for drugs such as the vinca alkaloids, doxorubicin and dactinomycin in patients with cholestasis.

Renal function is often concurrently impaired in patients with cirrhosis (hepatorenal syndrome). Cirrhosis may lead to a decreased GFR and renal plasma flow in patients with or without evidence of ascites. In such patients, assessment of serum creatinine levels is not an accurate predictor of renal function, possibly due to a decreased muscle mass or decreased creatine synthesis. Creatinine clearance measured by the urinary excretion method may be more accurate, but would still tend to overestimate GFR. Other measures such as iohexal clearance or serum cystatin C may also be used. It is important to remember that renal dysfunction in cirrhosis may require dosage adjustments for drugs excreted primarily through the kidney as well as for nephrotoxic drugs.

17.2.5 Pharmacodynamics in hepatic failure

Patients with liver cirrhosis are reported to have differences in drug pharmacodynamics that appear to be unrelated to any pharmacokinetic effect. The result may be an increased or decreased sensitivity to a drug's actions and/or adverse effects. Angiotensin converting enzyme (ACE) inhibitors and nonsteroidal anti-inflammatory drugs (NSAIDs) may interfere with adaptive physiological processes induced by liver disease, such as the enhanced activity of the renin–angiotensin system in advanced liver disease. This leads to a high risk of excessive hypotension or acute renal failure with ACE inhibitors and NSAIDs, respectively. These drugs should therefore be avoided in patients with cirrhosis.

The use of morphine and benzodiazepines in cirrhotic patients may produce severe sedative effects as well as precipitate encephalopathy. With morphine, this can occur even at doses lowered to compensate for the increased oral absorption and/or decreased clearance seen in liver failure. With benzodiazepines, encephalopathy can be induced even in patients administered drugs of this class that are not metabolized extensively by the liver, including oxazepam, temazepam, and triazolam. Some proposed mechanisms of the increased sensitivity to benzodiazepines include an alteration in the blood–brain barrier leading to higher concentrations of the drug in the central nervous system (CNS), increased GABA-ergic tone, or an increased number of GABA receptors. These effects can be counteracted by the administration of the benzodiazepine antagonist flumazenil, so some clinicians still recommend their use in cirrhotic patients.

Conversely, a decreased therapeutic effect can be seen with diuretics and β-adrenoreceptor antagonists. Higher concentrations of loop diuretics, such as furosemide and bumetanide, are needed in the renal tubules to excrete the same amount of sodium as in healthy individuals. Patients with liver disease are also less sensitive to the chronotropic effects of isoproterenol, possibly due to a decreased density of β-adrenoreceptors in mononuclear cells.

There may also be pharmacologic effects that overlap with pathophysiological responses in liver disease, such as increased portal pressure with calcium antagonists, or hypoprothrombinemia due to inhibited synthesis of vitamin K-dependent clotting factors by the beta-lactam antibacterials moxalactam and cefamandole.

Reduced drug metabolism in patients with liver disease does not seem to increase the frequency of hepatotoxicity. This may be because most cases of drug-induced hepatotoxicity are idiosyncratic, rather than dose-related reactions. Dose-related hepatotoxicity can occur with methotrexate, isoniazid, and acetaminophen (paracetamol); therefore, these drugs should not be used in cirrhotic patients.

17.3 OTHER DISEASE STATES

Orally administered medications require absorption from the gastrointestinal tract prior to exerting a pharmacologic effect on the body; therefore, gastrointestinal disease can cause dramatic variability in oral drug absorption and enterohepatic recycling. Changes in luminal pH may result in ion trapping of compounds within the gut lumen, making them unavailable for systemic absorption. The majority of drugs are absorbed from the proximal small intestine, due to the increased surface area available. For this reason, any disease causing prolonged gastric emptying times, such as gastric impactions or pyloric outflow obstructions, will decrease the rate, although not necessarily the total amount of drug absorbed. Additionally, conditions leading to villus destruction will decrease the surface area available for drug absorption and affect bioavailability of orally administered drugs.

The gut is capable of biotransforming drugs through reactions similar to those found in the liver, such as acetylation and conjugation. Therefore, decreased intestinal motility may cause a decrease in the amount of drug absorbed, primarily by increasing the amount of time the drug is in contact with these metabolizing enzymes. The opposite may be true for drugs that do not undergo metabolism by these processes and the bioavailability may be higher due to an increased amount of time for absorption. Conversely, increased intestinal motility may decrease drug absorption secondary to decreased time for absorption and failure of drug dissolution. Certain drugs require metabolism by bacteria in the large colon prior to absorption. The classic example of this is sulfasalazine, a prodrug formulation used to deliver 5-amino salicylic acid directly to the colon for the treatment of inflammatory bowel disease. Gastrointestinal diseases resulting from or causing altered bacterial flora may cause a decrease in absorption of such drugs.

Cardiac dysfunction leading to circulatory failure can cause vasoconstriction in the peripheral tissues via sympathetic stimulation. Blood flow is subsequently redistributed to the brain and heart; therefore, toxic levels of drugs may be reached in these organs. In fact, the central *Vd* may be reduced by up to 90%. Absorption from extravascular routes may be impaired due to decreased perfusion in the tissues. The intravenous and intratracheal routes are therefore preferred for patients with cardiac dysfunction. Circulatory failure may also cause disruptions in drug metabolism and excretion. Reduced hepatic blood flow can decrease the clearance of highly extracted drugs and lead to hepatic hypoxia with subsequent hepatocellular dysfunction, which may further decrease the clearance of drugs metabolized by the liver. Impaired renal blood flow may result in decreased filtration and secretion as well as increased reabsorption. Careful therapeutic monitoring of patients with cardiac dysfunction should be performed until normal circulation has been reestablished.

Table 17.5 Rules of thumb.

1.	Do not use drugs unless definite therapeutic indications are present.
2.	If the dosage regimen of a drug during disease has been determined via individual clinical pharmacokinetic studies, this should be followed in preference to use of the previously discussed general guidelines.
3.	In a situation in which the drug has not been studied but some information on its characteristics are available (e.g., the percentage of its excretion in an unchanged form by the kidney, hepatic extraction ratio, protein binding), it is possible by use of the described equations to make an estimate of the proper dose.
4.	If an assay procedure for the drug is available, the periodic measurement of blood concentrations of the drug is advisable for any schedule. Consider monitoring free drug fraction in some cases.
5.	Careful clinical monitoring for toxicity and pharmacologic effect is mandatory in all cases.
6.	Whenever possible, the clinician should select a drug that is biotransformed or excreted by an organ other than that affected by disease.

The following points should serve as guidelines for drug treatment during disease states.

Chronic heart disease may also affect drug pharmacokinetics. Fluid retention and edema may occur, leading to an increased *Vd* of hydrophilic drugs. Patients with congestive heart failure often receive multiple drugs concurrently, many of which are designed to alter blood pressure and fluid balance, leading to altered disposition of other drugs.

17.4 CONCLUSIONS

Disease states can profoundly alter drug pharmacokinetics, as well as affect the pharmacodynamics and actions of the drug in the body. Whenever possible, adjustments in dosing should be made based on available data or sound pharmacologic/pharmacokinetic principles (Table 17.5), in order to avoid subtherapeutic or toxic plasma drug concentrations. Given the interindividual variability in drug pharmacokinetics in healthy and diseased patients, as well as species variations, one should never forget the importance of individual patient monitoring.

BIBLIOGRAPHY

Anderson, R.J., Gambertoglio, J.G., and Schrier, R.W. 1976. *Clinical Use of Drugs in Renal Failure*. Springfield, IL: Charles C. Thomas.

Benet, L.Z. 1976. *Effects of Disease States on Drug Pharmacokinetics*. Washington, DC: Academy of Pharmaceutical Sciences.

Bennett, W.M., Porter, G.A., Bagby, S.P., and McDonald, W.J. 1978. *Drugs and Renal Disease*. New York: Churchill Livingstone.

Bennett, W.M., Aronoff, G.R., Golper, T.A., Morrison, G., Singer, I., and Brater, D.C. 1987. *Drug Prescribing in Renal Failure. Dosing Guidelines for Adults*. Philadelphia: American College of Physicians.

Brater, D.C. 1989. *Pocket Manual of Drug Use in Clinical Medicine*, 4th Ed. Toronto: B.C. Dekker.

Brater, D.C. 2009. Drug dosing in patients with impaired renal function. *Clinical Pharmacology and Therapeutics*. 86:483–489.

Brater, D.C., Anderson, S.A., and Brown-Cartwright, D. 1986. Response to furosemide in chronic renal insufficiency. Rationale for limited doses. *Clinical Pharmacology and Therapeutics*. 40:134–139.

Bricker, N.S. 1969. On the meaning of the intact nephron hypothesis. *American Journal of Medicine*. 46:1–11.

Delcò, F., Tchambaz, L., Schlienger, R., Drewe, J., and Krähenbühl, S. 2005. Dose adjustment in patients with liver disease. *Drug Safety*. 28:529–545.

Frazier, D.L., and Riviere, J.E. 1987. Gentamicin dosing strategies for dogs with subclinical renal dysfunction. *Antimicrobial Agents Chemotherapy*. 31:1929–1934.

Frye, R.F., Zgheib, N.K., Matzke, G.R., Chaves-Gnecco, D., Rabinovitz, M., Shaikh, O.S., and Branch, R.A. 2006. Liver disease selectively modulates cytochrome P450-mediated metabolism. *Clinical Pharmacology and Therapeutics*. 80:235–245.

Gibson, T.P. 1986. Renal disease and drug metabolism: an overview. *American Journal of Kidney Disease*. 8:7–17.

Lee, C.S., Marbury, T.C., and Benet, L.Z. 1980. Clearance calculations in hemodialysis. *Journal of Pharmacokinetics and Biopharmaceutics*. 8:69–81.

Maher, J.F. 1984. Pharmacokinetics in patients with renal failure. *Clinical Nephrology*. 21:39–46.

Melmon, K.L., Morrelli, H.F., Hoffman, B.F., and Nierenberg, D.W. 1992. *Melmon and Morrelli's Clinical Pharmacology: Basic Principles in Therapeutics*, 3rd Ed. New York: McGraw Hill.

Nimmo, W.S. 1976. Drugs, diseases and altered gastric emptying. *Clinical Pharmacokinetics*. 1:189–203.

Pea, F., Pavan, F., and Furlanut, M. 2008. Clinical relevance of pharmacokinetics and pharmacodynamics in cardiac critical care patients. *Clinical Pharmacokinetics*. 47:449–462.

Pentel, P., and Benowitz, N. 1984. Pharmacokinetic and pharmacodynamic considerations in drug therapy of cardiac emergencies. *Clinical Pharmacokinetics*. 9:273–308.

Reidenberg, M.M., and Drayer, D.E. 1984. Alteration of drug protein binding in renal disease. *Clinical Pharmacokinetics*. 9(Suppl. 1):18–26.

Riviere, J.E. 1982. A possible mechanism for increased susceptibility to aminoglycoside nephrotoxicity in chronic renal disease. *New England Journal of Medicine*. 307:252–253.

Riviere, J.E. 1984. Calculation of dosage regimens of antimicrobial drugs in animals with renal and hepatic dysfunction. *Journal of the American Veterinary Medical Association*. 185:1094–1097.

Riviere, J.E., and Coppoc, G.L. 1981. Dosage of antimicrobial drugs in patients with renal insufficiency. *Journal of the American Veterinary Medical Association*. 178:70–72.

Riviere, J.E., and Vaden, S. 1995. Drug therapy during renal disease and renal failure. In: Osborne, C.A., and Finco, D.R. (eds.), *Canine and Feline Nephrology and Urology*. Baltimore, MD: Williams & Wilkins, pp. 555–572.

Riviere, J.E., Carver, M.P., Coppoc, G.L., Carlton, W.W., Lantz, G.C., and Shy-Modjeska, J.S. 1984. Pharmacokinetics and comparative nephrotoxicity of fixed-dose versus fixed-interval reduction of gentamicin dosage in subtotal nephrectomized dogs. *Toxicology and Applied Pharmacology*. 75:496–509.

Riviere, J.E., Bowman, K.F., and Rogers, R.A. 1985. Decreased fractional renal excretion of gentamicin in subtotal nephrectomized dogs. *Journal of Pharmacology and Experimental Therapeutics*. 234:90–93.

Rodighiero, V. 1999. Effects of liver disease on pharmacokinetics. An update. *Clinical Pharmacokinetics*. 37:399–431.

St. Peter, W.L., Redic-Kill, K.A., and Halstenson, C.E. 1992. Clinical pharmacokinetics of antibiotics in patients with impaired renal function. *Clinical Pharmacokinetics*. 22:169–210.

Superfin, D., Iannucci, A.A., and Davies, A.M. 2007. Commentary: oncologic drugs in patients with organ dysfunction: a summary. *The Oncologist*. 12:1070–1083.

Tegeder, I., Lötsch, J., and Geisslinger, G. 1999. Pharmacokinetics of opioids in liver disease. *Clinical Pharmacokinetics*. 37:17–40.

Verbeeck, R.K. 2008. Pharmacokinetics and dosage adjustment in patients with hepatic dysfunction. *European Journal of Clinical Pharmacology*. 64:1147–1161.

Verbeeck, R.K., and Horsmans, Y. 1998. Effect of hepatic insufficiency on pharmacokinetics and drug dosing. *Pharmacy World and Science*. 20:183–192.

Verbeeck, R.K., and Musuamba, F.T. 2009. Pharmacokinetics and dosage adjustment in patients with renal dysfunction. *European Journal of Clinical Pharmacology*. 65:757–773.

18 Interspecies Extrapolations

The purpose of this chapter is to address how pharmacokinetic data may be extrapolated across species based on coupling the basic processes of distribution and elimination to physiological factors that vary as a function of body weight (*BW*). A review of interspecies scaling could easily require multiple books; thus, this chapter will focus on basic principles and techniques that illustrate the strategies employed.

The ultimate aim of any interspecies extrapolation would be to predict drug activity or toxicity in a new species not previously studied. There are two sources of error inherent in such an extrapolation. The first is that a drug's pharmacokinetic profile (especially excretion, metabolism, and distribution) does not extrapolate across species without adjusting for some individual species characteristics. The second, which will always be problematic, is that the pharmacodynamic response of a drug may be very different between species and not at all related to pharmacokinetics. This latter concern may not be important for antimicrobial drugs since the pathogenic organisms being treated should have susceptibilities that are pathogen and host independent. However, for drugs that interact with physiological functions that have species-specific receptor types and distributions, an estimate of pharmacokinetic parameters may not be sufficient to predict pharmacodynamic response. Although this issue will be touched upon in this presentation, the emphasis will be on extrapolating pharmacokinetic parameters across species. When such an extrapolation is made, the techniques of pharmacokinetic–pharmacodynamic (PK-PD) modeling presented in Chapter 13 could then be applied using species-specific PD parameters.

The optimal strategy to make interspecies extrapolations would be to derive a physiologically based pharmacokinetic (PBPK) model for the drug in question, as discussed in Chapter 11. In this case, one models the disposition of a drug in terms of the major anatomical organs responsible for its distribution, metabolism, and excretion from the body. These organs are linked by the rate of blood flow to each organ. As can easily be appreciated, once a PBPK model is obtained for one species, knowledge of the second species' organ weights and blood flows may be input into the process and the disposition of the drug in this species simulated. This was accomplished with melamine data in pigs and rats in the model illustrated in Fig. 11.4. Likewise, differences in plasma/tissue binding or pathways of biotransformation may be accounted for and input into the model. This approach to interspecies extrapolation was shown to be reasonably successful by DeBuck et al. (2007) for predicting the disposition of 26 human drugs from rat *in vivo* pharmacokinetic as well as *in vitro* metabolism data.

Comparative Pharmacokinetics: Principles, Techniques, and Applications, Second Edition. Jim E. Riviere.
 ISBN: 978-0-813-82993-7

Factors such as interspecies differences in protein binding were important to take into consideration. A PBPK model also lends itself to straightforward pharmacodynamic coupling with *in vitro* data collected in the target species. This approach has not been widely adopted primarily because of the paucity of complete PBPK studies published to date and the overall complexity of conducting such studies at early stages of drug development. Instead, the literature is replete with descriptive compartmental and noncompartmental studies that report on classic pharmacokinetic parameters (volume of distribution [Vd], clearance [Cl_B], half-life $T_{½}$) collected from individual experiments in a species at a specific dose. How can these existing data be used to probe the differences in drug disposition across species?

18.1 PHARMACOKINETIC SCALING

There is a wealth of empirical observations that suggest that physiological functions such as O_2 consumption, renal glomerular filtration, and cardiac output, are not linearly correlated to the mass of an individual animal, both within and between species. That is, if one expresses any physiological function on a per kilogram of *BW* basis (e.g., glomerular filtration rate [GFR]/kg), an isometric relationship would suggest that the parameter is constant. However, in the case of these physiological functions, such a relationship does not hold since the parameter expressed on a milligram/kilogram basis still is species dependent and is not constant. A knowledge of *BW* does not allow one to determine the value of the parameter across species with different *BW*s. However, if these parameters are expressed on a per unit surface area (SA) basis, then many parameters, including GFR, will show less variation across species.

More refined analyses suggest that the optimal scaling factor would be to a species' basal metabolic rate (BMR). Empirical observations suggest that BMR is a function of *BW* (in kilogram) raised to the 0.75 power (BMR = $f(BW_{kg})^{0.75}$); when expressed on body SA, the exponent is 0.67. An exponent of 0.75 is also theoretically predicted if metabolic functions are based on a model in which substances in the body are transported through space-occupying fractal networks of branching tubes (e.g., the vascular system) that minimize energy dissipation and share the same size at the smallest level of structure (e.g., capillaries). Whatever the mechanism, these approaches are well suited for extrapolating drug disposition across species. The focus of our discussions will be restricted to mammals since it is known that BMR is species specific across the five Hainsworth energy groups, and separate relationships hold for different birds, mammals, marsupials, and fish.

18.1.1 Basis of allometry

Equations in which a parameter is related to a mathematical function (in this case a power function) of a metric such as *BW* is termed an allometric relationship. The extensive literature surrounding the question of how one "collapses" physiological parameters between species has created a field of study called allometry. Since most drug pharmacokinetic parameters are dependent upon some physiological function, they may also be scaled across species using these strategies. The method for doing this is to correlate the parameter of concern (e.g., GFR, Cl_B) with *BW* using the following allometric equation:

$$Y = a \cdot (BW)^b \tag{18.1}$$

where Y is the parameter of concern, a is the allometric coefficient, and b is the allometric exponent. The data are obtained using simple linear regression on $\log_{10} Y$ versus $\log_{10} BW$ as depicted in Fig. 18.1. The slope is the allometric exponent b and the intercept a.

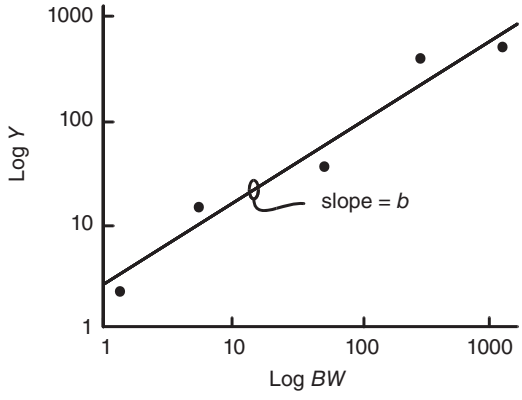

Fig. 18.1 Basic log–log allometric plot of a biological parameter (*Y*) versus *BW* with slope *b* and intercept *a*.

There is uniform agreement that for most physiological processes, the allometric exponent *b* ranges from 0.67 to 1.0. Note that if the parameter being modeled is an inverse function of a physiological process (e.g., $T_{½}$), then the exponent will be $1 - b$ for that process. The coefficient *a* is actually the value of *Y* for a 1.0 kg *BW* animal ($b = 0$). These exponents are estimates that improve if good data is available. They should not be viewed as biological constants of nature!

This is also a good point at which to consider what happens if isometry is assumed. In this case, $b = 1.0$ and the parameter is a direct function of BW^1, which equals *BW*. From this perspective, *if one adjusts dosages across species on the basis of kilogram of* BW *alone, one is implicitly assuming that* b *= 1 for the relationship between parameters*, which we know is not correct from data such as the above.

18.1.2 Scaling of half-life

An example of an allometric analysis conducted in our laboratory is shown in Fig. 18.2, with gentamicin β-elimination phase $T_{½}$ data collected after intravenous administration of 10 mg of gentamicin per kilogram of *BW* to animals ranging in size from the mouse to the horse. There is an excellent fit based on analysis of this large data set, with $T_{½\beta}(\text{min}) = 42\ BW^{0.249}$. This suggests that knowing the $T_{½\beta}$ in any species, the corresponding value of this parameter can be estimated in another. In general, the $T_{½\beta}$ will be shorter in small animals with a large BMR and ratio of SA to body mass than in larger animals, which have a smaller BMR and SA. The caveat in these types of analyses is that the pharmacokinetic parameters being estimated must have been properly determined. Points discussed in Chapter 8 on how $T_{½}$ is a function of the experimental design and pharmacokinetic model used to estimate it should be considered when conducting such analyses from widely different literature sources.

This equation has been extensively applied to numerous sets of pharmacokinetic data. The first was demonstrated by Dedrick et al. (1970), who analyzed methotrexate data and achieved results very similar to those of gentamicin depicted above. This is not surprising, since both compounds are primarily eliminated from the body by renal glomerular filtration, which scales with $b \approx 0.75$ based on BMR. Thus $T_{½}$ scales to 0.25 (1 − 0.75).

From the perspective of pharmacokinetics, the important parameters in a pharmacokinetic equation are both the Cl_B and the *Vd*. When one scales $T_{½}$, one is actually scaling to

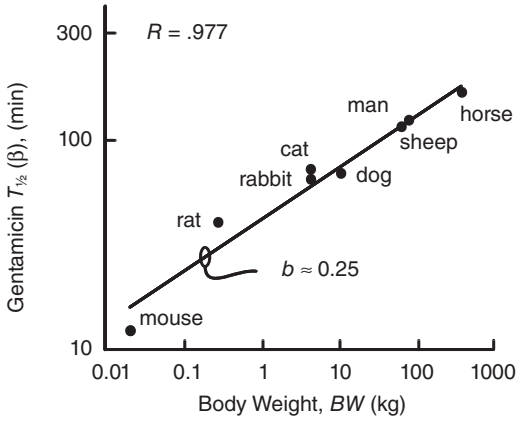

Fig. 18.2 Allometric plot of log gentamicin half-life versus log *BW* in eight species.

Vd/Cl_B in the exponent since $T_{½} = 0.693\ Vd/Cl_B$ (Eq. 8.20, see Chapter 8). If *Vd* usually scales with $b = 1$ and Cl_B to 0.75, the exponent is now $BW^{1-0.75}$, which equals 0.25. In all of these studies, intravenous dosing must be used since formulation variables and differences in absorption would completely confound the analyses. When *Vd* and Cl_B scale with significantly different parameters, this relationship to $T_{½}$ would not be expected to hold as well as it does for compounds cleared exclusively by the kidney and have a *Vd* restricted to extracellular space like gentamicin and methotrexate. For example, fluoroquinolones showed dispersity in $T_{½}$ allometric scaling (Cox, 2007). The writings by Mahmood (2005, 2010) listed in the Bibliography should be consulted for a further discussion of this point.

18.1.3 Scaling of clearance

For clearances, the situation is more straightforward. Total body clearance (Cl_B) is actually the sum of all clearances ($Cl_B = Cl_{renal} + Cl_{hepatic} + Cl_{other}$) (Eq. 6.1, see Chapter 6). Most drugs are primarily cleared by either the kidney or the liver. Overall renal and hepatic functions are determined by blood flow to these organs, which are dependent upon cardiac output. As mentioned earlier, cardiac output scales to $\approx b^{0.75}$. Thus, for drugs cleared by the kidney, renal clearance scales to $b \approx 0.75$, and thus $T_{½}$ should scale to $b \approx 0.25$. This is even true of drugs excreted by active tubular transport (unless transport is saturated) since renal blood flow governs this function.

For the liver, the hepatic clearance ($Cl_{hepatic}$) of a drug has been previously expressed in Equation 7.2 (see Chapter 7) as:

$$Cl_{hepatic} = Q_{hepatic} \cdot [Cl_{int}/(Q_{hepatic} + Cl_{int})] \tag{18.2}$$

where Cl_{int} is the intrinsic metabolic clearance of a drug and $Q_{hepatic}$ the hepatic blood flow, which is a constant fraction of cardiac output. If a drug's $Cl_{hepatic}$ is "flow limited" when the drug is a "high-extraction drug" ($Cl_{int} >> Q_{hepatic}$), its value approaches hepatic blood flow and thus scales with an allometric exponent of $b \approx 0.75$. However, if the drug is "capacity limited" and thus is a "low-extraction drug" ($Cl_{hepatic} << Q_{hepatic}$), then clearance

is a function of the intrinsic metabolic capability of the individual and species, a value that is very dependent upon isoenzyme expression and other genetic factors that, as discussed in Chapter 7, is very species specific. For these drugs, allometric scaling may not be feasible. In fact, these drugs show the greatest interindividual variation in drug disposition.

18.1.4 Scaling of volume of distribution

The *Vd* of a drug generally is related to the fraction of body mass occupied by body water (see Chapter 5). If a drug distributes primarily through body water or primarily into one tissue that is a constant fraction of total body water, the allometric exponent is ≈1.0 since body water is directly proportional to *BW*. If the drug is limited to extracellular fluid, *b* becomes ≈0.67. If one is looking at the volume of distribution at steady state (Vd_{ss}), which is a function of vascular, extracellular, and total body fluid, *b* will be between 0.67 and 1.0. If the drug is lipophilic, allometric analysis does not produce consistent predictions. Most workers in this field assume that *Vd* directly correlates to *BW* ($b = 1.0$); however, this may not be accurate. Note that if the species has relatively unique compartments into which drug may distribute and become sequestered or eliminated (e.g., rumen, equine cecum), interspecies extrapolations would fail.

18.1.5 Relationship between parameters

It is informative to illustrate scaling of all these parameters. An example for a common class of antimicrobials, the macrolides, was reported by Duthu (1985) using data from the mouse, rat, rabbit, dog, and cow. Individual allometric exponents for *Vd*, Cl_B, and $T_{½}$ were calculated as:

	Vd	Cl_B	$T_{½}$
Erythromycin	0.73	0.69	0.14
Oleandomycin	0.64	0.76	0.14
Tylosin	0.75	0.68	0.18

Note for this drug, the *b* for $Vd \neq 1.0$ (as for gentamicin), and thus the aggregate *b* was not a simple combination of the allometric exponents for *Vd* and Cl_B. By doing studies as above, more confidence can be placed in the allometric extrapolations since data for a specific drug are utilized. Also, as discussed below, allometric techniques are more effective if there is a wide range of *BW* (e.g., from mouse to cow) because of the logarithmic transformation involved. It would not be effective if data were, say, collected in pigs, goats, and sheep. Other approaches to modify these relationships are also discussed below (e.g., life span, brain weight). Finally, it cannot be overstressed that errors in estimation of pharmacokinetic parameters and model misspecification will carry into empirical techniques such as allometry.

18.2 PROTEIN BINDING

This is a good point at which to consider the extent of protein binding of the drug that was discussed earlier in Chapters 5, 7, and 10. The magnitude of protein binding may have a

significant effect on drugs cleared by "capacity limited" mechanisms if total protein binding is greater than 85–90%. Flow-limited drugs should be insensitive to protein binding, as should capacity-limited drugs with very low protein binding. Secondly, the magnitude of protein binding may also affect the *Vd*, again with significant levels of protein binding (>85–90%) having the most impact. Species-specific differences in tissue binding, an area not well studied, would further introduce variability in *Vd*, as can be appreciated from examining Equation 5.6 introduced in Chapter 5. As will be demonstrated below, whenever possible, allometric scaling should be performed using the free fraction of drug. The major problem with drug protein binding is that there is, at present, no easy way to predict the extent of interspecies binding. However, many parameters are insensitive to protein binding, and thus allometric relationships are also insensitive to changes.

Many proteins besides albumin (e.g., α_1-acid glycoproteins, lipoproteins, hormone carrier globulins) may bind to drugs, making interspecies extrapolation problematic in a limited number of cases. For example, our laboratory has studied the disposition of testosterone in pigs as a model for transdermal human drug delivery. Pigs, like rodents and carnivores, are deficient in sex hormone-binding globulin compared to humans, primates, rabbits, goats, cows, and sheep. This results in an alteration of the species' ability to metabolize testosterone to dihydrotestosterone and estradiol. This difference in metabolic disposition could not be predicted on the basis of an allometric analysis.

18.3 APPLICATIONS

There is a great deal of empirical evidence to suggest that the allometric approach of expressing drug dosage scaled to a $(BW)^b$ works. A number of workers used allometry to analyze the maximum tolerated dose (MTD) or LD_{10} of numerous antineoplastic drugs, which relates to the toxic potential of these chemicals across different species. Not surprisingly, b approximated 0.75. For these compounds, this correlation simply supports the hypothesis that drug action or toxicity is correlated to the area under the curve (AUC), as presented throughout this text. This extrapolation holds for most subacute toxicities but does not work for predicting chronic toxicity or carcinogenesis. These effect models are much more complicated and are beyond the scope of the dose extrapolation problem addressed in this chapter. Chapter 13 should be studied for a detailed discussion of effect modeling.

A similar approach was used by our laboratory to estimate isonephrotoxic doses (i.e., doses that produce the same degree of kidney damage) for gentamicin across species. In this procedure, one calculates a proportion of the dose of drugs in two species based on a ratio of their respective half-lives. In the case of gentamicin, the allometric exponent $b = 0.25$ from Fig. 18.2 was used in the following equation to estimate species-equivalent doses:

$$D_{\text{SpeciesA}} = D_{\text{SpeciesB}} \cdot [BW_B/BW_A]^{0.25} \tag{18.3}$$

where D_{SpeciesB} is a dose of known nephrotoxicity in species B. This resulted in the following isonephrotoxic doses (milligram/kilogram [species]): 20 (rat), 9 (dog), 5 (human), and 3 (horse). These are confirmed by the literature and illustrate why a large species such as the horse would appear more sensitive to a canine dose of 9 mg/kg. Equation 18.3 could be used to extrapolate the dose known to be efficacious in one species and to estimate the

therapeutically equivalent dose in another, as suggested for selecting pilot pharmacokinetic trial doses in Equation 14.10 (see Chapter 14).

18.4 THE CONCEPT OF SPECIES-EQUIVALENT TIME AND SPECIES-INDEPENDENT CONCENTRATION-VERSUS-TIME PROFILES

There is another way to view allometric scaling as simply a method of changing the time coordinates of a serum/blood/plasma concentration–time (C-T) profile from chronological or astronomical time to the more relevant physiological time. This allows one to use these relationships in more detailed pharmacokinetic models. Boxenbaum (1982) has strongly argued that physiological processes are linked to an internal biological clock that is a function of BMR and body size, as well as other species indicators including life span, length of gestation, and brain weight. These relationships are defined by the interaction of the animal with its environment, relative to energy conservation and biomechanical constraints (elasticity), which is related to the SA of interfacing membranes. Body size can be viewed as a regulating mechanism for a species' internal biological clock. Specifically, each species may have a finite number of heartbeats; thus a mouse, which has a shorter life span (because its BMR must be higher due to its small body size), will have a more rapid heart rate when measured in chronological time. Boxenbaum (1982) contends that each species has a finite quantity of "pharmacokinetic stuff" that also is consumed as a function of the species-unique "lifestyle" spread over its life span.

One approach to implement these concepts is to scale the time access of a C-T profile in units that reflect a species physiological clock. One such unit is the kallynochron, a unit of equivalent time across species equal to the amount of time any species clears the same volume of plasma per unit of BW. This equals

$$\text{Kallynochron} = (\text{time})/(BW^{1-b}) \tag{18.4}$$

What this effectively does is scale the time axis of a C-T plot by a measure of physiological time. Thus, if BW scales with $b = 0.75$, then the time axis should be plotted using the above equation. Dedrick et al. (1970) earlier demonstrated this relationship with methotrexate. Accordingly, this technique is often referred to as a Dedrick plot. However, this assumes that the y-axis (concentration) of a C-T profile also scales "properly"; that is, Vd scales to the same value of b. If this is not true, then the y-axis may also be scaled, and a "complex" Dedrick plot results. Alternatively, the time access can be scaled to account for Cl and Vd using apolysichrons as the unit of equivalent time.

Other more complex units of species-equivalent time that scale for life span (dienetichron) and brain weight (syndesichron) have been implemented for specific drugs. These have been shown to correlate to species-specific processes (e.g., life span to low capacity clearance processes, and brain weight to oxidative metabolism). This is conceptually similar to the approach suggested by Mahmood (2005, 2010), which uses life span and brain weight when scaling from small laboratory animals to humans in empirical allometric analyses. This is accomplished by modifying the basic allometric Equation 18.1 with parameters such as maximum life span and brain weight for specific drugs when indicated. A "rule of exponents" has been suggested that directs when these additional correction factors should be implemented.

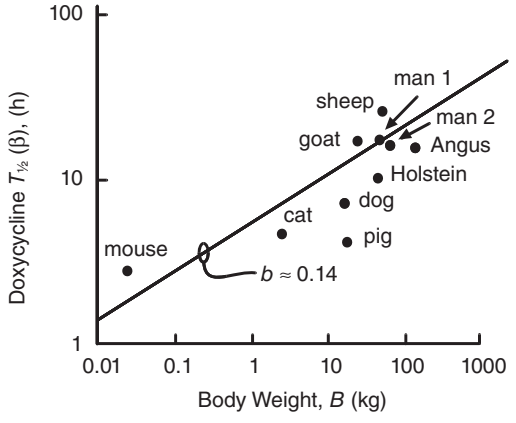

Fig. 18.3 Allometric plot of log doxycycline half-life versus log *BW* in nine species.

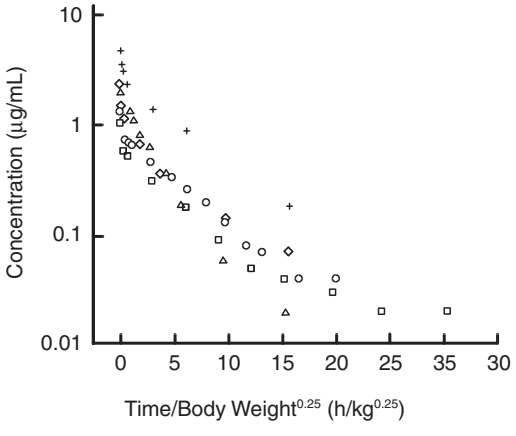

Fig. 18.4 Dedrick plot of total plasma doxycycline concentrations versus normalized *BW* in cats (+), dogs (◇), pigs (△), mature Angus (○), and immature Holstein (□) calves administered a single 10 mg/kg intravenous dose.

These approaches can be illustrated using doxycycline pharmacokinetic data generated in our laboratory. In this study, all species were given an intravenous dose of 10 mg/kg. In Fig. 18.3, $T_{½}$ is plotted against *BW* using our data and values from the literature. The typical allometric relation is demonstrated. Fig. 18.4 is a Dedrick plot of data generated solely from data in our laboratory. In this case, all samples were analyzed by the same high-performance liquid chromatographic assay, which should minimize analytical variation, and parameter estimates obtained by the same pharmacokinetic programs, which should minimize curve-fitting errors. This plot transforms the time axis to kallynochrons and adjusts the plasma concentration (*y*-axis) to observed concentration divided by dose/kilogram, thereby normalizing by dose (assumes that *b* for *Vd* equals 1.0).

The serum C-T profile is relatively tight across species except for the data from cats, which tend to produce higher normalized concentrations than calves, pigs, and dogs. If free doxycycline is plotted (Fig. 18.5) from these same five species using ultrafiltered serum to

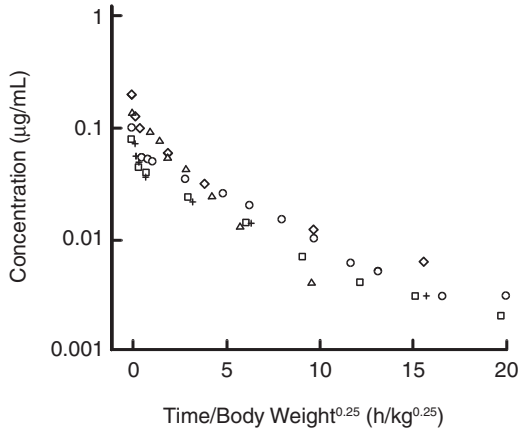

Fig. 18.5 Same plot as Fig. 18.4 except that free doxycycline concentrations were used, which resulted in better prediction of the cat data. Cats (+), dogs (◇), pigs (△), mature Angus (○), and immature Holstein (□) calves were administered a single 10 mg/kg intravenous dose.

estimate the doxycycline-free fraction, a true "species-independent" C-T profile results, which describes the data for all species. The cat is the outlier in the total C-T profile since it uniquely has a very high degree of protein binding (≅98%) compared to 90% for the other species. Thus, the concentration of free drug in the cat is fivefold higher than other species.

This technique has tremendous "conceptual impact" since it clearly indicates that if free drug concentrations are expressed in kallynochrons, one C-T profile adequately describes the disposition of drugs across widely disparate species. If one assumes that the action of a drug is correlated to some measure of its C-T profile (e.g., AUC), then if one knows the AUC in one species, one would estimate it in all species by expressing it in terms of the appropriate physiological time. This approach to interspecies scaling is thus used to define an effective AUC in species A and calculate a dose per unit BW^b, which could be used for all species. In this case, b would be determined by analyzing available experimental data. This is another way of generating the isonephrotoxic doses of gentamicin referred to above, for this strategy works if dose is linearly correlated to AUC, an expected finding when the drug has first-order pharmacokinetic properties. Similarly, for the problem of tissue residues presented in Chapter 19, if tissue C-T profiles similarly scale, then withdrawal times for "well-behaved" drugs could be normalized to physiological time and a single parameter used in all species.

18.5 EXTRAPOLATION PITFALLS

There are a number of cases, too numerous to outline here, in which simple empirical interspecies extrapolations would not be expected to work because of complex disposition processes. Our group used the extensive Food Animal Residue Avoidance Databank (FARAD) compilation of 10,300 pharmacokinetic experiments with 419 drugs to assess how well allometry could be used to extrapolate drug disposition for veterinary drugs collected in a database with a wide quality of reported data (Riviere et al., 1997). In this

analysis, 44 drugs had sufficient data (intravenous administration, at least four species per drug) to conduct the allometric regression. Three groups of drugs were identified from this meta-analysis.

Eleven of 44 drugs (≈25%) drugs (ampicillin, apramycin, carbenicillin, cephapirin, chlortetracycline, diazepam, erythromycin, gentamicin, oxytetracycline, prednisolone, and tetracycline) had statistically significant allometric regressions, with b ranging from 0.10 to 0.42. Significantly, the mean value of the allometric exponent was 0.24 ± 0.09, with 65% of the b being between 0.19 and 0.32. Thus, the rule of thumb quoted above that b for $T_{½}$ of 0.25, based on a BMR scaling factor of 0.75, is a reasonable estimate for these "well-behaved" drugs. Plots of these drugs were very similar to the idealization presented in Fig. 18.1. Drugs with this behavior are primarily antibiotics and are eliminated unchanged by the kidney. The only surprise was diazepam since it has a variable degree of protein binding and is cleared by a capacity-limited hepatic metabolic process.

Of these well-behaved drugs, the average number of species in the analysis was 6.2 ± 2.2, and the log BW ratio $[\log(BW_{\text{largest}}/BW_{\text{smallest}})]$ averaged 8. This is consistent with workers who attempt to use two-species allometry to predict human drug disposition (e.g., rat to human, dog to human) that conclude that prediction of clearance is much improved if ≥3 species are used (Goteti et al., 2010). The log BW ratio appears to be an excellent metric of how robust the data set is for analysis since a wide spread in log BWs would increase the power of a log–log allometric regression. This analysis suggests that when one has a robust data set covering multiple species of differing masses, and the drug has relatively simple linear pharmacokinetics, allometric scaling is possible even from a multiple-source data set.

Nineteen drugs, although having similarly rich data sets and robust log BW ratios, did not have significant allometric regressions. These drugs included many compounds metabolized by capacity-limited hepatic biotransformation. The remainders of the drugs produced equivocal results but were characterized by a smaller species data set. Without further data, it was not possible to determine whether these compounds actually could not be analyzed with allometric principles or if the data set was simply inadequate.

This analysis and those of other workers highlight a number of factors, touched upon in the introduction, which at this point would preclude allometric pharmacokinetic extrapolations. These will now be discussed.

18.5.1 Biotransformation

If a drug is eliminated primarily by capacity-limited hepatic biotransformation, total body clearance would be related to $Cl_{\text{intrinsic}}$, which is dependent upon the intrinsic ability of that species and individual to metabolize drug. Numerous studies have demonstrated a great deal of heterogeneity in both phase I and phase II drug metabolism reactions, as discussed in Chapter 7. For example, dogs are known to be deficient acetylators, pigs are deficient in sulfation capacity, and cats are deficient in glucuronidation. If a drug is metabolized by one of these phase II pathways, extrapolation might be problematic. However, if the only result is to produce a sulfated rather than an acetylated inactive metabolite, and the C-T profile of the parent drug and active phase I metabolites are not affected, allometry should still work. Of course, one must realize that the disposition of the parent drug between two species, if it is a flow-limited highly extracted drug, may be similar even if there are species-specific isozymes present which produce different metabolites. As mentioned above, species differences in oxidative metabolism may potentially be accounted for by including

brain weight in any allometric analysis, while low-capacity processes may be accounted for by including life span. These factors were not included in this simple analysis.

18.5.2 Genetic polymorphism

The largest and most important species differences relate to genetic differences in cytochrome P450 isoenzyme makeup. Although cytochrome content scales to *BW*, species differences in isoenzymes confound one's ability to make predictions. A substantial amount of progress has been made on studying which genes are responsible for controlling P450 expression. Chapter 7 should be consulted for specifics. For example, the P450 IIIA gene expresses isoenzymes in the rat, dog, and human, which show similar substrate specificity and inhibitor selectivity, with sex differences being expressed only in the rat. If one knew a priori that the drug in question was metabolized by an isoenzyme under control of this gene (N-demethylation, steroids undergoing 6 hydroxylation), then allometry should work on extrapolating such drugs (flunisolide, cyclosporine, dihydropyridine Ca^{++} channel blockers). However, the database for which these data are available is sparse at best and, outside of the dog, contains no veterinary species. Secondly, some of these compounds may also be metabolized by isoenzymes controlled by the P450 IIC gene which, depending on relative substrate specificities between IIIA and IIC isoenzymes, will produce a different profile of phase I metabolites. The situation becomes very complicated when other genes and noncytochrome P450 enzymes (e.g., flavin monooxygenases) are also considered, and beyond simple understanding if the species specificity in P-glycoprotein transporters are added into the equation.

18.5.3 Protein binding

As discussed with doxycycline, protein binding is almost impossible to extrapolate across species. Differences in protein binding would be expected to affect Cl_B, *Vd*, and the fraction of a drug dose that can interact with receptors (only free fraction is available). This would be especially evident for orally administered drugs as the first-pass hepatic metabolism would be different. A similar concern exists with extent of tissue binding as discussed earlier.

18.5.4 Saturation

If the effective dose in any of the species being analyzed produces concentrations that saturate elimination mechanisms, nonlinear pharmacokinetics result, which makes allometry almost impossible. This should not be a problem for most pharmacological doses except where metabolic capacity for a specific pathway is limited (e.g., cats and glucuronidation).

18.5.5 Drug induces alterations in physiology

Up to this point, we have considered drugs to be pharmacologically inert. If the drug alters physiology (e.g., renal function, hepatic blood flow) in one species and not in another, then the allometric relation of physiology to *BW* will be broken and interspecies scaling will not work. In the doxycycline example discussed above, such a situation occurred when single-dose intravenous pharmacokinetic studies were attempted in the horse (note the

absence of equine data in these plots). When two horses were injected with this 10-mg/kg dose, they immediately went into cardiac arrest and died, a phenomenon later attributed to the high lipophilicity of the doxycycline, which gave it immediate "access" to cardiac pacemaker cells. This illustrates again that pharmacokinetic data alone are not sufficient to predict pharmacodynamic effect.

18.5.6 Interspecies differences in enterohepatic recirculation

If a large fraction of a drug is cleared via the bile, and the species differences outlined in Chapter 7 result in changes in the fraction of biliary-excreted drug reabsorbed back into the circulation, pharmacokinetic parameters may not scale well across species. This does not appear to be a major problem since in the FARAD analysis discussed above, many tetracyclines potentially fall into this class, and these drugs were well behaved from the perspective of allometric regression. The same may not hold for drugs cleared primarily by this route.

18.5.7 Renal tubular reabsorption sensitive to urine pH

As discussed in Chapter 6, the clearance of some weak acids and bases may be dependent upon distal renal tubular reabsorption, a process that would be sensitive to species differences in urine pH. Carnivores tend to have an acidic urine based on their normal protein-rich diet, while ruminants tend to have an alkaline urine. Depending upon the species included in an allometric analysis and the diets of the animals being studied, one could speculate that weak organic acids with pKa values from 3 to 7 may have a decreased $T_{½}$ when urine is alkaline. The opposite would occur with weak bases.

There are probably a number of additional factors that could influence the efficacy of an allometric regression analysis. For example, *BW* could be corrected for the volume of the gastrointestinal tract when ruminants and nonruminants are compared since the rumen may represent a substantial fraction of nonavailable body mass into which drug could not distribute.

18.6 CONCLUSION

As can be appreciated, scaling pharmacokinetic parameters using allometry is a powerful empirical tool to eliminate the influence of body mass on the value of pharmacokinetic parameters. This technique is applicable to data generated using compartmental and noncompartmental models. However, as presently implemented, the resulting models lack mechanistic foundations and are an example of a purely empirical approach to data analysis. The accuracy of such predictions are very sensitive to the actual experimental design of the studies from which data are collected as well as to the techniques of pharmacokinetic modeling that were used to generate the parameters being scaled. As was discussed early in this book in the context of QSPeR modeling in Chapter 3, interlaboratory variation may be significant. In the case of allometry, differences in analytical methods, curve-fitting techniques, and pharmacokinetic model misspecification may generate large errors in the extrapolations.

These considerations underscore a major problem in the application of allometry to conduct interspecies extrapolations. Data are needed to make these analyses. It is wrong to

assume that a fixed and magical exponent of 0.25 will work in all cases. The ability to successfully use allometric scaling is a function of the underlying pharmacokinetics of the drug. Clearance and volume of distribution should be independently and properly estimated. The more detail that can be provided in the model, the more accurate is the prediction. This leads to approaches in modeling that take into account more specific pharmacokinetic models.

An optimal approach is to use PBPK techniques if the relevant experiments could be conducted to generate the necessary input parameters. An equally promising approach would be to use population-based models as presented in Chapter 16. If these models are linked to normalized data such as presented in Fig. 18.5, the power of using a properly parameterized pharmacokinetic model could be used to correlate unexplained variance to measurable physiological correlates, such as extent of protein binding, creatinine clearance, markers of hepatic blood flow, and rate of biliary secretion. This approach would also allow interindividual and intraindividual variation to be accounted for and quantitated.

BIBLIOGRAPHY

Boxenbaum, H. 1982. Interspecies scaling, allometry, physiological time, and the ground plan for pharmacokinetics. *Journal of Pharmacokinetics and Biopharmaceutics*. 10:201–227.

Boxenbaum, H., and DiLea, C. 1995. First-time-in-human dose selection: allometric thoughts and perspectives. *Journal of Clinical Pharmacology*. 35:957–966.

Boxenbaum, H., and D'Souza, R.W. 1990. Interspecies pharmacokinetic scaling, biological design, and neoteny. *Advances in Drug Research*. 19:139–196.

Brown, S.A., and Riviere, J.E. 1991. Comparative pharmacokinetics of aminoglycoside antibiotics. *Journal of Veterinary Pharmacology and Therapeutics*. 14:1–35.

Calabrese, E.J. 1983. *Principles of Animal Extrapolation*. New York: John Wiley & Sons.

Corvol, P., and Bardon, C.W. 1973. Species distribution of testosterone binding globulin. *Biology of Reproduction*. 8:277–282.

Cox, S.K. 2007. Allometric scaling of marbofloxacin, moxifloxacin, danofloxacin and difloxacin pharmacokinetics: a retrospective analysis. *Journal of Veterinary Pharmacology and Therapeutics*. 30:381–386.

Davidson, I.W.F., Parker, J.C., and Beliles, R.P. 1986. Biological basis for extrapolation across mammalian species. *Regulatory Pharmacology and Toxicology*. 6:211–237.

DeBuck, S.S., Sinha, V.K., Fenu, L.A., Nijsen, M.J., Mackie, C.E., and Gilissen, R.A.H.J. 2007. Prediction of human pharmacokinetics using physiologically based modeling: a retrospective analysis of 26 clinically tested drugs. *Drug Metabolism and Disposition*. 35:1766–1780.

Dedrick, R.L., Bischoff, K.B., and Zaharko, D.S. 1970. Interspecies correlation of plasma concentration history of methotrexate (NSC-740). *Cancer Chemotherapy Reports Part 1*. 54:95–101.

Duthu, G.S. 1985. Interspecies correlation of the pharmacokinetics of erythromycin, oleandomycin and tylosin. *Journal of Pharmaceutical Sciences*. 74:943–946.

Goteti, K., Garner, C.E., and Mahmood, I. 2010. Prediction of human drug clearance from two species: a comparison of several allometric methods. *Journal of Pharmaceutical Sciences*. 99:1601–1613.

Hayton, W.L. 1989. Pharmacokinetic parameters for interspecies scaling using allometric principles. *Health Physics*. 57:159–164.

Hunter, R.P. 2010. Interspecies allometric scaling. In: Cunningham, F., Elliott, J., and Lees, P. (eds.), *Comparative and Veterinary Pharmacology*. Heidelberg, Germany: Springer, pp. 139–158.

Mahmood, I. 2005. *Interspecies Pharmacokinetic Scaling: Principles and Applications of Allometric Scaling*. Rockville, MD: Pine House Publishers.

Mahmood, I. 2010. Theoretical versus empirical allometry: facts behind theories and application to pharmacokinetics. *Journal of Pharmaceutical Sciences*. 99:2927–2933.

Mahmood, I., Martinez, M., and Hunter, R.P. 2006. Interspecies allometric scaling. Part I. Prediction of clearance to large animals. *Journal of Veterinary Pharmacology and Therapeutics*. 29:415–423.

Mordenti, J. 1985. Pharmacokinetic scale-up: accurate prediction of human pharmacokinetic profiles from animal data. *Journal of Pharmaceutical Sciences*. 74:1097–1099.

Mordenti, J. 1986. Man versus beast. Pharmacokinetic scaling in mammals. *Journal of Pharmaceutical Sciences*. 75:1028–1039.

O'Flaherty, E.J. 1989. Interspecies conversion of kinetically equivalent doses. *Risk Analysis*. 9:587–598.

Reilly, J.J., and Workman, P. 1993. Normalisation of anti-cancer drug dosage using body weight and surface area: is it worthwhile? *Cancer Chemotherapy Pharmacology*. 32:411–418.

Riond, J.L., and Riviere, J.E. 2008. Allometric analysis of doxycycline pharmacokinetic parameters. *Journal of Veterinary Pharmacology and Therapeutics*. 13:404–407.

Riond, J.L., Riviere, J.E., Duckett, W.M., Atkins, G.E., Jernigan, A.D., Rikihisa, Y., and Spurlock, S.L. 1992. Cardiovascular effects and fatalities associated with intravenous administration of doxycycline to horses and ponies. *Equine Veterinary Journal*. 24:41–45.

Riviere, J.E. 1985. Aminoglycoside-induced toxic nephropathy. In: Ash, S.R., and Thornhill, J.A. (eds.), *Handbook of Animal Models for Renal Failure*. Boca Raton, FL: CRC Press, pp. 145–182.

Riviere, J.E., Martin-Jiménez, T., Sundlof, S.E., and Craigmill, A.L. 1997. Interspecies allometric analysis of the comparative pharmacokinetics of 44 drugs across veterinary and laboratory animal species. *Journal of Veterinary Pharmacology and Therapeutics*. 20:453463.

Sawada, Y., Hanano, M., Sugiyama, Y., Harashima, H., and Iga, T. 1984. Prediction of the volumes of distribution of basic drugs in humans based on data from animals. *Journal of Pharmacokinetics and Biopharmaceutics*. 12:587–596.

Sedwick, C.J. 1993. Allometric scaling and emergency care. In: Fowler, M.E. (ed.), *Zoo and Wild Animal Medicine*, 3rd Ed. Philadelphia: W.B. Saunders, pp. 34–37.

Toutain, P.L., Ferran, A., and Bousquet-Mélou, A. 2010. Species differences in pharmacokinetics and pharmacodynamics. In: Cunningham, F., Elliott, J., and Lees, P. (eds.), *Comparative and Veterinary Pharmacology*. Heidelberg, Germany: Springer, pp. 19–48.

United States Environmental Protection Agency. 1984. Proposed guidelines for carcinogen risk assessment. *Federal Register*. 49:46294–46301.

Voisin, E.M., Ruthsatz, M., Collins, J.M., and Hoyle, P.C. 1990. Extrapolation of animal toxicity to humans. Interspecies comparisons in drug development. *Regulatory Toxicology and Pharmacology*. 12:107–116.

West, G.B., Brown, J.H., and Enquist, B.J. 1997. A general model for the origin of allometric scaling laws in biology. *Science*. 276:122–126.

19 Tissue Residues and Withdrawal Times

with Sharon Mason

The final application of pharmacokinetic principles will be to describe the tissue disposition of drugs after administration to food-producing animals. The concept of a withdrawal time (WDT) will be developed as an extension of the concept of half-life ($T_{½}$). This topic is of importance to veterinarians working in food animal medicine and scientists employed in the pharmaceutical and regulatory sectors who are charged with assessing the fate of drugs and chemicals that enter the human food chain via edible products (meat, milk, eggs) of food-producing animals. As can be appreciated by re-examining Fig. 1.3 (see Chapter 1), there is an additional constraint besides efficacy and safety when drugs are used to treat diseases in food-producing animals. When an animal is slaughtered or its edible products collected, there is a legal requirement that drug concentrations not persist at a level greater than those established as safe by the relevant regulatory authority in the country of origin. In the United States, this level is termed the tolerance, while in many other countries it is referred to as the maximum residue level (MRL).

MRLs and tolerances are established by regulatory authorities based on many factors, including the safety of the animal product(s) to the consumer, the usage pattern of the compound in the field (e.g., pesticides in the field), and the sensitivity of the analytical methodology. The major determining factor for a tolerance level is food safety. However, from the perspective of pharmacokinetics, the method used to arrive at a tolerance or MRL is not important; rather the focus is on the length of time after discontinuation of a drug administration or chemical exposure required to allow animal tissues to deplete to a concentration below this legal limit. This time is the preslaughter meat WDT. If the matrix is milk, then the parameter of interest is the milk discard interval (MDI). Most discussion here will be focused on the WDT as the principles apply equally well to the MDI. Exceptions to this rule will be identified as required. The reader is advised to consult relevant Web sites of regulatory agencies governing drug use in their regions for determining legal WDTs. The focus of this chapter is to illustrate the pharmacokinetic concepts behind the WDT.

What is the WDT? As with all pharmacokinetic parameters, the WDT has both kinetic and statistical properties. We will initially focus our discussion on the individual animal and consider the factors that determine the rate of depletion of drug concentrations in specific tissues. There are several steps that must be considered before a safe WDT is established. These steps include an understanding of the safety of the compound, establishing a safe tolerance for each compound and finally setting the WDT for the compound in a specific animal product. The next section will discuss the method to establish a tolerance.

Comparative Pharmacokinetics: Principles, Techniques, and Applications, Second Edition. Jim E. Riviere.
 ISBN: 978-0-813-82993-7

19.1 ESTABLISHMENT OF A TISSUE TOLERANCE

The tolerance is the target concentration in a residue depletion study. It should be established purely on the basis of safety to the person consuming the tissue and has no pharmacodynamic reality in the animal to which the drug has been administered. Tissue tolerances are normally established in fat, milk, muscle, liver, kidney, and skin, or their combination in edible tissues.

The first step in calculating the tolerance of a compound is to determine the safe concentration of the total drug that could be consumed by individuals eating animal products. The way that this safe level is established is based on an acceptable daily intake (ADI) amount, which involves a risk assessment extrapolation from laboratory animal toxicology studies. The ADI is the maximum amount of chemical (mg/kg) that may be consumed daily over a lifetime without producing an adverse effect. ADI is estimated as a fraction of the no-observed-adverse-effect level (NOAEL) determined from standardized long-term laboratory animal toxicological studies conducted in at least two animal species. The NOAEL is then divided by a safety factor ranging from 100 to 1000 depending on the nature of the compound's toxicology or the strength of the data. Part of this factor is to account for the uncertainty of interspecies extrapolations (rodent to human) and to be conservative in the face of more acute and serious toxicity (e.g., teratogens, hypersensitivity). The current US Food and Drug Administration (FDA) safety factors are the following:

Type of toxicology study	Safety factor
Chronic	100
90-day	1000
Reproductive/teratology	100 (only maternal effects)
	1000 (other effects)

As can be appreciated from this tabulation, the safety factor is greater when there is evidence of teratogenic effects or when a more economical subchronic (90-day) study is submitted in place of a more complete chronic study. This latter factor alone could result in a 10-fold lower tolerance (and hence a longer WDT) being established for a product supported by 90-day studies compared to the identical formulation supported by a chronic study. Thus, a subjective bias is directly built into the analysis that is independent of the actual toxicological properties of the compound. Additional toxicology tests (e.g., neurotoxicity, immunotoxicity, hormonal activity, mutagenic) have also been accepted for assessing potential toxicity (or lack thereof) and are handled similarly to the 90-day data above. Other countries use similar approaches, although the safety factors applied at this stage of the analysis (determination of ADI) generally do not exceed 100. Recent research in the regulatory area is working to reduce the use of broad uncertainty factors and replace them with more specific uncertainty factors based on target tissue doses and mechanistic data.

If the compound is demonstrated to be a carcinogen, a "no-risk" requirement comes into effect. In this case, a risk assessment/extrapolation analysis will be done, using statistical analysis of the laboratory animal tumor data, to derive a concentration of residue (S_0) that presents *no significant risk of cancer*. If there is no information on the compound concerning the mechanism of carcinogenesis, the FDA uses a nonthreshold, linear low-dose extrapolation to determine the upper limit of the risk, which is set at 1 : 1,000,000. An exception to this rule is if the compound is a sex steroid, in which case the agents are assumed not to be genotoxic and at low residue levels do not present a risk for carcinogenesis in the

food-consuming public. Other countries adopt different policies for reproductively active compounds.

Based on the data, the ADI is established and applied to determine a safe concentration based upon the following equation:

$$\text{Safe concentration} = \frac{(\text{ADI})\ (\text{body weight})}{\text{food consumption factor}} \tag{19.1}$$

where ADI is the acceptable daily intake, body weight is the average weight of humans consuming the product (usually assumed to be 60 kg), and the food consumption factor is the amount of edible product estimated to be consumed daily by an individual. The purpose of this equation is to distribute the ADI over different edible tissues on the basis of food consumption patterns.

The food consumption factor is based upon the average individual's daily intake of different types of foods. The FDA and other regulatory agencies have tabulated food-specific consumption factors. Examples (in kilogram consumed per day) are 0.3 for muscle, 0.1 for liver, 0.05 for kidney, 0.05 for fat, and 1.5 for milk. The ADI for milk is especially high since the total diet for an infant may be entirely milk. These values calculated by FDA assume that a person were to eat all of these products with residues at the maximum safe level every day for life. Other countries use similar food consumption factors but distribute the ADI based on independent organ consumption data, specific to the eating habits of individuals living in that country. Other countries also include organs, such as the stomach, which is not frequently consumed in the United States. These factors are then used in Equation 19.1 to determine safe concentrations.

The final step in this process is to establish the tolerance. The safe concentration is based upon the total concentration of drug (e.g., total residues), which includes the parent drug and any metabolites. Some special regulations apply for covalently bound residues. Depending on the drug, bound residues may be included as either a component of the total or a fraction removed from consideration. From these metabolites, a marker residue is now selected that has a defined relationship to the total residue amount. If the drug is not metabolized, the safe concentration becomes the tolerance. If the drug is metabolized, the tolerance will be set as a fraction of the safe concentration based on the relative amount of the marker residue to the parent drug and any other metabolites formed. Equation 19.1 is then applied for each food source using the organ-specific consumption factor and tolerances established. As discussed below, the tolerance should also not be set to the analytical methods' lowest sensitivity, since if the tolerance is at or below the ability to detect the compound, the resulting WDT will be exceedingly conservative relative to food safety concerns.

The process of establishing MRLs in many other countries is very similar to the above process except that, as mentioned earlier, the safe concentration may be partitioned across various organs under the assumption that any one individual could never consume all foods with drug present at the maximum safe concentrations. There has also been movement by the Joint Expert Committee on Food Additives (JECFA) in 2006 to substitute median concentration of residues for MRL to calculate ADI, or in the European Union, the theoretical maximum daily intake (TMDI) (WHO, 2006). It must be stressed that tolerances/MRLs are based on human food safety considerations for the consuming public and not on how long a WDT is required to achieve tolerance. Therefore, the established MRL may be lower than the ADI safe concentration in some countries.

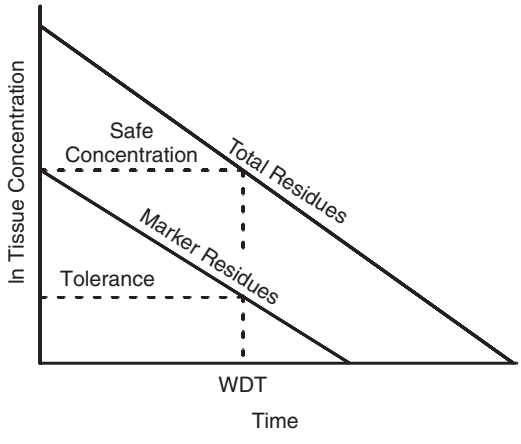

Fig. 19.1 Relationship between log-linear tissue depletion of total and marker residues and the established safe concentration and tolerance in that tissue. The WDT is the time at which total residues drop below the upper safe concentration. This establishes the legal tolerance for the monitored marker residue. Note that if the total residue equals the marker residue, the safe concentration becomes the tolerance.

19.2 ESTIMATION OF A WDT

Once the tolerance is set, a WDT necessary to ensure that the residue being monitored will fall below the established tolerance or MRL can be established. It is at this stage that pharmacokinetics comes into play. Fig. 19.1 illustrates this relationship. Note that if the total residue is the marker residue, then the safe concentration is equal to the tolerance. A WDT must be determined for each of the major organs in which safe concentrations are established, with the final WDT being set as the time at which all tissues will be below the established tolerance (i.e., the organ with the longest WDT). The FDA presently requires a repeated slaughter experiment in which groups of at least five animals per sex are slaughtered at four different time periods in the terminal part of the tissue-depletion curve closest to the established tolerance. A log-linear regression analysis is then performed on the data to determine the WDT such that *the WDT is the upper bound of the 99th percentile of the population established with 95% statistical confidence (a probability of a type I error at 5%)*. As can be appreciated from Fig. 19.2, this essentially sets the official WDT such that the 1 in 100 animals with the most persistent residue profile determine the acceptable tolerance.

Numerous experimental designs are used to establish the WDT. However, there are many assumptions behind these statistics, including a log-linear tissue depletion phase, a log-normal statistical distribution for all residue samples at each time point, homogeneous variance of residues across the various slaughter times, and statistical independence of each residue observation. The requirement for log-linear decay essentially restricts this analysis to compounds with first-order kinetics. Many sponsors will increase the number of animals collected at any time point in order to narrow the 99th percentile window, which will result in a shorter WDT.

Some discussions among regulatory authorities outside the United States have focused on nonregression-based determination of WDTs. In these situations, a WDT is established as the slaughter time at which all animals are below the MRL. The actual WDT is being tested, not the slope of the tissue depletion, which is the parameter being modeled with

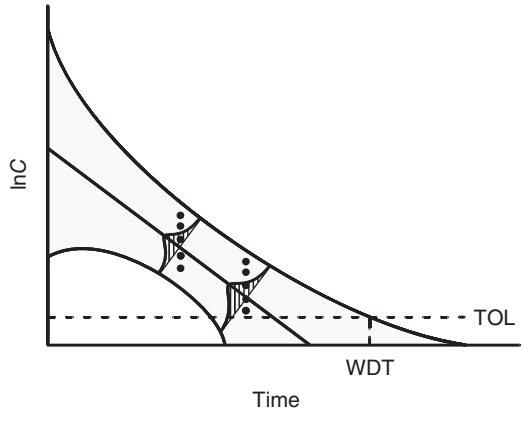

Fig. 19.2 A statistical perspective of a drug depletion curve in tissue, whereby tolerance is established based on the upper 99% percentile of the distribution centered on the mean tissue depletion profile.

parametric approaches. Other workers have proposed various nonparametric statistics to implement this practice with more statistical confidence. The factors involved in selecting the appropriate approach are actually identical to those used in selecting parametric versus nonparametric methods for population pharmacokinetic studies.

19.3 PHARMACOKINETICS APPLIED TO WDTS

Whatever the final method used to establish a WDT in an individual animal, the true WDT is closely related to the rate of elimination, and thus the $T_{½}$ of drug depletion in the specific tissue of interest. Based on linear pharmacokinetic principles developed in Chapter 8, the problem of estimating a WDT is essentially that of calculating the time for a concentration to decline to a specific target concentration, which in our case is the tolerance. One can extend the logic presented in Equation 12.8 (see Chapter 12), which was used to calculate the length of a dosage interval τ to maintain a concentration–time profile between defined peak (Cp^{max}) and trough (Cp^{min}) concentrations to calculate WDT. In this case, we assume linear first-order decay in the tissue of interest, and we will express the equations in terms of target residue concentrations (TOL). Because this relation is central to the concept of WDT, we will follow through each step of its derivation. The τ we are thus calculating is the final interval after dosing which is required to achieve a C_t^{min} equal to the established tolerance or MRL. Equation 12.8 may be originally written as

$$\ln(Cp^{max}/Cp^{min}) = (0.693/T)\cdot\tau \tag{19.2}$$

This can be algebraically rearranged to solve for τ as

$$\tau = \ln(Cp^{max}/Cp^{min})/(0.693/T_{½}) \tag{19.3}$$

If we now substitute WDT for τ, C_0 for Cp^{max}, and finally TOL for Cp^{min} (C now represents tissue concentrations), we obtain the relation

$$\begin{aligned} \text{WDT} &= \ln(C_0/\text{TOL})/(0.693/T_{½}) \\ &= 1.44\ \ln(C_0/\text{TOL}) \cdot T_{½} \end{aligned} \tag{19.4}$$

Note the similarity to Equation 12.9 for computing a dosage interval. Since we know that the slope of the tissue decay, K equals $0.693/T_{½}$, this equation can be also written as

$$\text{WDT} = \ln(C_0/\text{TOL})/K \tag{19.5}$$

Therefore, knowing the initial tissue concentration, tissue $T_{½}$ or K, and the legal target tolerance, one should be able to calculate the WDT for a specific situation. If the disposition of the drug is described by a simple pharmacokinetic model, C_0 can often be estimated from the administered dose using this data. Compilations of plasma and tissue depletion $T_{½}$ and C_0 for many drugs in species of relevance to veterinary medicine have been published most recently in the book by Craigmill et al. (2006), *Tabulation of FARAD Comparative and Veterinary Pharmacokinetic Data*, listed in the Bibliography.

The problem of using this approach in the field or a regulatory environment is that a priori knowledge of the tissue $T_{½}$ in a living animal is impossible to determine prior to slaughter. A population estimate (see Chapter 16) of tissue $T_{½}$ is required which, according to the regulatory philosophy, accurately predicts with statistical confidence of <0.05, the $T_{½}$ that would be present in the 1% of the target population that has the slowest rate of drug decay in the tolerance-limiting tissue. The reader must realize that based on this definition, the approved WDT must account for all outliers in the treated animals to ensure that the probability of a violative residue in any animal treated with a drug is vanishingly small. One is therefore not interested in the estimate of the mean value of $T_{½}$, which would be operative in the animal being treated, but rather the upper limit of 99% of the population estimated with a 95% confidence interval of this value. As discussed below, the statistical assumptions used to estimate this limit are prone to error and are heavily dependent upon the yet unknown statistical distributions used to establish the WDT in the first place.

19.4 LIMITATIONS TO CURRENT WDT DETERMINATIONS

Unfortunately, several limitations exist in the statistical and current sampling methods applied to the drug deposition data discussed above. In Chapters 14 and 16, it is obvious that many statistical assumptions may not be valid in regard to WDTs. The most obvious problem is that a homogenous sample of healthy animals is required and, further, that this sample is representative of all animals to which the drug will be administered. As was seen in the discussion of population pharmacokinetic models, most populations of animals are not homogeneous, being composed of various subpopulations based on age, breed, and multiple disease states. Withdrawal studies are performed in healthy animals, but drugs are administered to the general population and often to ill or debilitated animals, which would be expected to have a larger variability in their pharmacokinetic parameters than healthy animals. Second, most statistics are based on determining the mean parameter of a distribution, and deviations from normality near the mean are minimal due to the central limit theorem. In contrast, WDTs are estimated based on defining the 99th percentile of the distribution (upper 1% of the population), which is estimated based on a small number of individuals relative to the population. And unlike the mean, this estimate is sensitive to the nature of the underlying variance model and requires a larger sample size to fully define.

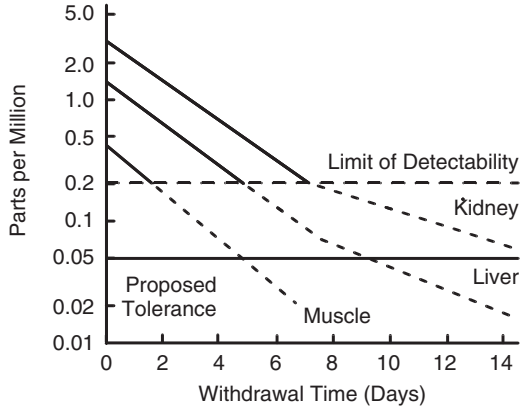

Fig. 19.3 Nonparallel tissue depletion profiles and their relationship to the limit of detectability and tolerances. Note that as in this case, if the limit of detectability is greater than the tolerance based on food safety factors, the WDT subsequently established will be conservative.

Furthermore, homogenous variance of measured residue concentrations is also unlikely because, as analytical sensitivity approaches the tolerance, coefficients of variation often become larger than those seen at more reliably assayed higher concentrations. This scenario is especially troubling when the tolerance is set near the limit of quantitation (LOQ) for the assay being used, which is commonly done. Fig. 19.3 also illustrates the dilemma present when the LOQ is greater than tolerance or MRL. Due to the greater variability at the LOQ and the tolerance being set below this, extrapolation beyond the assay is required, which adds another layer of conservatism to the WDT, extending it further.

Another complicating factor is that the slopes of drug depletion in various tissues are often not parallel, as depicted in Fig. 19.3. Log-linear terminal tissue decay is often assumed for all tissues; however, many factors, including tissue binding, redistribution and enterohepatic recycling, may change this decay rate, especially in some disease states. This is not surprising since most tissues are not in the "central compartment" and thus their depletion reflects local distribution processes. Differential rates of tissue binding, decay were discussed in the context of Fig. 5.2 (see Chapter 5), which also illustrates the relationship between drug decay in various tissues and the organ-specific tolerances set for each tissue. In this example, using gentamicin, although muscle concentrations fall below tolerance after 72 h, kidney and liver concentrations never decay in this short time frame due to the extensive tissue binding of aminoglycosides in these two organs. In this case, the typical log-linear decay is violated. Thus, the WDT must be set based on the kidney concentrations, which may require up to an 18-month preslaughter WDT. In some countries, an option termed selective condemnation has been proposed, whereby the shorter muscle-based WDTs are allowed as long as the liver and kidney are discarded at slaughter.

19.5 GUESSTIMATING WITHDRAWAL INTERVALS AFTER EXTRALABEL USE

The reason that these issues are important relates to the need to have knowledge of the tissue $T_{½}$ to modify the WDT in cases in which the drug is used in an extralabel manner.

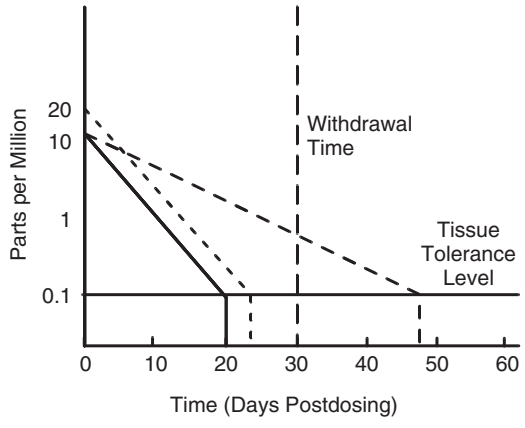

Fig. 19.4 Relationship between tolerance and tissue depletion. In a healthy animal (—), tissue depletion often occurs at a time point shorter than the WDT established for the 99th percentile of the population. In such an animal, if the dose is doubled, depletion (- - - -) should only require one more half-life and would most likely still be within the established WDT. However, if the half-life doubles due to disease, depletion (— — —) would now require double the normal WDT and probably would result in violative residues.

This practice was approved by the FDA under the Animal Medicinal Drug Use Clarification Act of 1994 (AMDUCA), which was published in 1996. In this scenario, drugs may be used in an extralabel manner if the veterinarian is able to establish a substantially extended withdrawal period prior to marketing of milk, meat, eggs, or other edible products. However, this WDT must be supported by appropriate scientific information. To accomplish this, the veterinarian must have some estimate of the relevant tissue $T_{½}$ that governs the WDT in the animal being treated and, further, how that $T_{½}$ relates to the legal WDT.

The most common field scenarios are when the dose is increased in order to improve efficacy and when a disease process is present that prolongs $T_{½}$. Fig. 19.4 illustrates these relationships, assuming that the length of the WDT is directly related to the $T_{½}$ according to Equation 19.4. If the dose is doubled, C_0 doubles, and the WDT should be increased by one $T_{½}$. However, if the $T_{½}$ doubles due to a systemic disease process, then the WDT should also be doubled. It has been estimated that for many drugs, one WDT comprises about five $T_{½}$s, allowing one to guesstimate how long a WDT should be extended to handle a doubling of dose.

One should immediately realize that the most serious threat to violative residues is when the underlying tissue $T_{½}$ changes, since this would most dramatically increase the true WDT in that animal. If such a disease process were not present in the animals in which the WDT was originally established, then the label-recommended WDT may be insufficient to guarantee residues lower than tolerance. In fact, this conclusion is supported by field residue violation data in which a significant number of violative residues are detected either in very young animals, such as veal calves or, alternatively, in culled dairy cows and other emergency slaughtered ruminants that are removed from production because of disease processes.

In the immature animal, excretory systems are often not matured, resulting in decreased systemic clearance (Cl_B), and thus a prolonged $T_{½}$ (Chapter 8, Eq. 8.20). As discussed in Chapter 5, volumes of distribution are often greater in very young animals and may be increased in certain diseased individuals, which would likewise prolong $T_{½}$. To compound this situation, culled animals are often treated with drugs to cure their underlying diseases,

and thus extralabel drug use would be expected to be greatest in these animals. In the healthy animal not receiving drugs, it is of little surprise that drug residues are not found!

These extrapolations are further complicated when the WDT is based on a marker residue and only information about the parent drug's disposition is available. Disease processes that alter the ratio of the parent drug to metabolite (in this case the marker residue) may not predict the alteration of WDT necessary to prevent residues. Processes that alter the expression of genes that modulate drug-metabolizing enzymes would have similar effects. Some disease states also change protein and/or tissue binding that alters the free fraction of the drug disproportionately to the marker residue.

The only solution, to precisely predict these effects, is to have a pharmacokinetic model that adequately predicts tissue concentrations as a function of administered dose. Based on the earlier chapters of this text, physiologically based or population pharmacokinetic models would be optimal due to their sensitivity to physiological and disease factors that might alter disposition.

For example, a physiological based pharmacokinetic (PBPK) model for sulfamethazine was developed by Buur et al. (2006), incorporating tissue-binding phenomena that produced data used to predict tissue WDTs in swine. Buur et al., in the abovementioned sulfamethazine model, used a Monte Carlo analysis to run 1000 simulations of the model with slight variations in the pharmacokinetic parameters that allowed a WDT to be calculated that complied with the FDA's criteria of the upper tail of a 95% confidence interval of the 99th percentile of the population. However, most PBPK models are generally based on relatively few individuals, thus making statistical inferences about 1% of the population problematic, and therefore, further steps must be taken to model a population, as was the case for sulfamethazine. In contrast, population pharmacokinetic models can easily integrate the statistical properties of the population and assay methodology; however, they are generally of a simpler inherent structure, which may lack good estimates of plasma to tissue transfer constants. Fortunately, this approach may allow incorporation of field residue monitoring data to improve the parameterization of the underlying model which could link clinical and production variables to the proper pharmacokinetic terms. This population-based pharmacokinetic modeling approach has been used by many sponsors to incorporate data into new drug applications from small clinical trial studies, mainly for humans. In veterinary medicine, this modeling approach could be used to tailor withdrawal estimates to specific individual or herd conditions.

Other applications of these techniques to determine WDTs include multicompartmental hybrid models using applied parametric or nonparametric population approaches. In these withdrawal-based models, however, there is a need that the low concentrations or terminal portion of the curve be most accurately predicted by the model. Some published models used a hybrid computational approach combining statistical inference and one or more of the pharmacokinetic approaches presented throughout this book, which often can be used to model compartment drug uptake or transfer rates more accurately than PBPK or population methods alone. These hybrid models may include a combination of techniques with a computational compartment or an initial uptake that is modeled differently than the rest of the body. These methods may in some situations more accurately predict tissue depletion. Such complexities in tissue depletion profiles, including nonlinearities due to tissue sequestration, extensive tissue binding, or systemic multicompartmental behavior, are projected on the individual tissue depletion profile. As discussed in Chapter 9, stochastic modeling procedures including power function analysis may collapse these more complex kinetics into scaleable models that would reduce this complexity (see Fig. 9.7). The concept of

random walk and Markov chain applications are mechanistically compatible with tissue residue modeling and should be applied in the future.

Unfortunately, the regulatory bodies are still grappling with how to apply these complex modeling techniques to their more restrictive environment. In the last 10 years, the FDA issued some guidelines on the use of population-based pharmacokinetic modeling techniques as well as pharmacodynamic applications, but only as supporting evidence for the required studies. As a result, Bayesian design techniques are now adopted for initial estimates in designing studies for regulatory agencies. However, the resulting slaughter data is still necessary to develop a safe WDT. These models do provide feedback to adjust the parameters of the original pharmacokinetic model and also provide further support for their future use in the regulatory arena. Furthermore, any drug concentrations obtained from field/clinical studies and postmarket surveillance can improve the original model and provide for extended WDT in specific situations.

If the worker has reliable tissue depletion data available, and has a good estimate of the plasma pharmacokinetic model that would allow estimation of C_0 after any therapeutic dose, Equations 19.4 or 19.5 may be directly used to calculate a safe WDT, assuming that the appropriate statistical inferences required by regulatory agencies are taken into consideration.

When an extravascular dose is being administered, an assessment must be made of the rate of absorption and bioavailability to assess whether a flip-flop scenario is occurring that would make the absorption $T_{½}$ the relevant parameter for use in the above equations. Such adjustments would be expected with extended-release formulations. Similarly, when drugs are administered continuously in feed or in water, the rate of gastrointestinal input can be considered constant and thus modeled by a zero-order rate parameter, much like an intravenous infusion. However, the systemic bioavailability would be reduced to the actual absorbed dose.

All of these techniques are more easily applied to milk depletion data because this matrix is easily obtained and is directly assayed. Therefore, the individual animal can be monitored if a reliable analytical methodology is available. Furthermore, the veterinarian can estimate a milk withholding interval and then test its validity by direct cowside sampling. There are currently a number of commercially available screening assays that are designed to detect milk drug concentrations at greater-than-tolerance levels. These assays, based on enzyme methods, binding or enzyme competition, or microbial inhibition strategies, may be applied to the individual animal, individual dairy, or milk cooperative for testing. Due to the number of tests available, one drawback is determining which test to use. Many of these tests are available for milk and urine; however, with milk, the tolerance may be substantially lower than the LOQ for the test. Furthermore, there is a risk of false positives, which have a negative economic impact on producers and may not be conducive to protecting the food supply. Tests that measure urine of treated animals are also available; however, the assumption with using these tests is that urine excretion profiles correlate to concentrations of drug in tissues. Without valid pharmacokinetic information to quantitate this relationship, extrapolation in the field is difficult.

19.6 CONCLUSION

In conclusion, there is nothing unique about the use of pharmacokinetic principles to describe tissue depletion data. The challenge comes in integrating the science with the

requirements of regulatory authorities that have preestablished experimental protocols designed to ensure food safety for the consuming public. The design of the experiments discussed above is a result of considerable effort and dialogue among government, industry, and consumer groups. In the last decade, some regulatory authorities are trying to integrate newer pharmacokinetic design techniques into their protocols and modeling schemes; however, the experimental procedures practiced are still not optimized for defining or solving these models. Fortunately, the principles of pharmacokinetics continue to describe the behavior of drugs in tissues and are fundamentally applicable to interpreting drug withdrawal information.

BIBLIOGRAPHY

Anonymous. 1994. *General Principles for Evaluating the Safety of Compounds Used in Food-Producing Animals*. Rockville, MD: Center for Veterinary Medicine, Food and Drug Administration.

Anonymous. 1999. *Guidance for Industry: Population Pharmacokinetics*. Rockville, MD: Center for Drug Evaluation and Research, Food and Drug Administration.

Anonymous. 2008. *Target Animal Safety for Veterinary Pharmaceutical Products*. Rockville, MD: Center for Veterinary Medicine, Food and Drug Administration.

Bevill, R.F. 1984. Factors influencing the occurrence of drug residues in animal tissues after the use of antimicrobial agents in animal feeds. *Journal of the American Veterinary Medical Association*. 185:1124–1126.

Buur, J., Baynes, R., Smith, S., and Riviere, J.E. 2006. Use of probabilistic modeling within a physiologically based pharmacokinetic model to predict sulfamethazine residue withdrawal times in edible tissues in swine. *Antimicrobial Agents and Chemotherapy*. 50:2344–2351.

Concordet, D., and Toutain, P.L. 1997a. The withdrawal time estimation of veterinary drugs: a nonparametric approach. *Journal of Veterinary Pharmacology and Therapeutics*. 20:374–379.

Concordet, D., and Toutain, P.L. 1997b. The withdrawal time estimation of veterinary drugs revisited. *Journal of Veterinary Pharmacology and Therapeutics*. 20:380–386.

Craigmill, A.L. 2003. A physiological based pharmacokinetic model for oxytetracycline residues in sheep. *Journal of Veterinary Pharmacology and Therapeutics*. 26:55–63.

Craigmill, A.L., Riviere, J.E., and Webb, A.I. 2006. *Tabulation of FARAD Comparative and Veterinary Pharmacokinetic Data*. Ames, IA: Blackwell.

Fitzpatrick, S.C., Brynes, S.D., and Guest, G.B. 1995. Dietary intake estimates as a means to the harmonization of maximum residue levels for veterinary drugs. *Journal of Veterinary Pharmacology and Therapeutics*. 18:325–327.

Gallo-Torres, H.E. 1990. The rat as a drug residue bioavailability model. *Drug Metabolism Reviews*. 22:707–751.

Gehring, R., Baynes, R.E., Craigmill, A.L., and Riviere, J.E. 2004. Feasibility of using half-life multipliers to estimate extended withdrawal intervals following the extralabel use of drugs in food producing animals. *Journal of Food Protection*. 67:555–560.

Lu, A.Y.H., Miwa, G.T., and Wislocki, P.G. 1988. Toxicological significance of covalently bound residues. *Reviews in Biochemical Toxicology*. 9:1–27.

Moats, W.A., and Medina, M.B. 1995. *Veterinary Drug Residues: Food Safety*. Washington, DC: American Chemical Society.

Paige, J.C., Tollefson, L., and Miller, M. 1997. Public health impact on drug residues in animal tissues. *Veterinary and Human Toxicology*. 39:162–169.

Reeves, P.T. 2010. Drug residues. In: Cunningham, F., Elliott, J., and Lees, P. (eds.), *Comparative and Veterinary Pharmacology*. Heidelberg, Germany: Springer, pp. 265–290.

Rico, A.G. 1986. *Drug Residues in Animals*. New York: Academic Press.

Riviere, J.E. 1991. Pharmacologic principles of residue avoidance for the practitioner. *Journal of the American Veterinary Medical Association*. 198:809–816.

Sundlof, S.F. 1989. Drug and chemical residues in livestock. *Veterinary Clinics of North America. Food Animal Practice*. 5:411–447.

Sundlof, S.F. 1994. Human risks associated with drug residues in animal derived food. *Journal of Agrimedicine*. 1:5–22.

Upton, R.N., and Ludbrook, G.L. 1998. A physiological model of induction of anaesthesia with propofol in sheep. 1. Structure and estimation of variables. *British Journal of Anaesthesia*. 79:497–504.

VanDresser, W.R., and Wilcke, J.R. 1989. Drug residues in food animals. *Journal of the American Veterinary Medical Association*. 194:1700–1710.

Weiss, G. 1990. The integration of pharmacological and toxicological testing of tissue residues in the evaluation of their human food safety. *Drug Metabolism Reviews*. 22:829–848.

WHO. 2006. Sixty-sixth report of the Joint FAO/WHO Expert Committee on Food Additives. WHO Technical Report Series No. 939.

Index

Note: Page numbers in *italics* refer to Figures; those in **bold** to Tables.

Comparative Pharmacokinetics: Principles, Techniques, and Applications, Second Edition. Jim E. Riviere.

ISBN: 978-0-813-82993-7